CORA Cork Open Research Archive
Cartlann Taighde Oscailte Chorcaí

| | |
|---|---|
| Title | Reconstruction of milk fat globules/membrane (MFGs/MFGM) and characterization of its physicochemical properties and techno-functionalities |
| Authors | Sun, Yanjun |
| Publication date | 2024 |
| Original Citation | Sun, Y. 2024. Reconstruction of milk fat globules/membrane (MFGs/MFGM) and characterization of its physicochemical properties and techno-functionalities. PhD Thesis, University College Cork. |
| Type of publication | Doctoral thesis |
| Rights | © 2024, Yanjun Sun. - https://creativecommons.org/licenses/by-nc-nd/4.0/ |
| Download date | 2026-10-30 11:48:52 |
| Item downloaded from | https://hdl.handle.net/10468/16925 |

UCC
University College Cork, Ireland
Coláiste na hOllscoile Corcaigh

# Teagasc Food Research Centre, Moorepark

*and*

Ollscoil na hÉireann, Corcaigh

# National University of Ireland, Cork

University College Cork, Ireland
Coláiste na hOllscoile Corcaigh

## Reconstruction of milk fat globules/membrane （MFGs/MFGM）and characterization of its physicochemical properties and techno-functionalities

Thesis presented by

**Yanjun Sun**

*MEng in Food Science (Northwest Agriculture & Forestry University University)*
*BEng in Food Quality and Safety (Henan University of Science and Technology)*

for the degree of

**Doctor of Philosophy**

**University College Cork**

**School of Food and Nutritional Sciences**

Head of School/Department: Prof. Alan L. Kelly

Supervisor(s): Prof. Dr. Song Miao (Teagasc), Prof. Dr. Yrjö H. Roos (UCC), and Dr. Maurice O′Sullivan (UCC)

June 2024

# Table of Contents

DECLARATION ..... I

DEDICATION ..... II

ACKNOWLEDGEMENTS ..... III

ABSTRACT ..... IV

LITERATURE REVIEW ..... VII

LIST OF PUBLICATIONS ..... VII

LIST OF ABBREVIATIONS ..... VIII

INTRODUCTION ..... 1

References ..... 6

CHAPTER ONE ..... 9

Literature Review ..... 9

Abstract ..... 10

1.1 Introduction ..... 11

1.2. Update on the structure and compositions of MFGs/MFGM ..... 15

1.2.1 Polar lipids ..... 16

1.2.2 Membrane proteins ..... 17

1.2.3 Other compositions ..... 18

1.3. Factors affecting the structure, compositions, and techno-functionalities of MFGs/MFGM ..... 19

1.3.1 Biosynthesis, species, lactation stage, and feeding system ..... 19

1.3.2. Effect of separation methods on the MFGs/MFGM materials ..... 21

1.3.3 The effects of dairy processes on the MFGs/MFGM materials ..... 25

1.3.4 Non-thermal treatments ..... 32

1.4 Conclusions and future perspectives ..... 38

References ..... 39

CHAPTER TWO ..... 48

Changes in milk fat globules and membrane proteins prepared from pH-adjusted bovine raw milk ..... 48

Abstract ..... 49

2.1. Introduction ..... 50

2.2. Materials and Methods ..... 53

2.2.1. Materials ..... 53

2.2.2 Preparation of Samples ..... 53

2.2.3. Compositions Analysis ..... 54

2.2.4. Particle Size Analysis ..... 55

2.2.5. Zeta (ζ) Potential ..... 55

2.2.6. Sodium Dodecyl Sulphate Polyacrylamide Gel Electrophoresis (SDS–PAGE) ..... 56

2.2.7. Confocal Laser Scanning Microscopy (CLSM) ..... 58

2.2.8. Statistical Analysis ..... 59

2.3. Results and discussion ..... 59

2.3.1. Composition Analysis ..... 59

2.3.2. Particle Size ..... 60

2.3.3. Zeta (ζ) Potential ..... 64

2.3.4. SDS-PAGE ..... 66

2.3.5. CLSM ..... 69

2.4. Conclusions ..... 72

References ..... 73

CHAPTER THREE ..... 78

Characterization of the microstructure, interfacial properties and crystallisation behaviours of milk fat globule and membrane isolated from acidified bovine milk and sweet whey ..... 78

Abstract ..... 79

3.1. Introduction ..... 80

3.2. Materials and methods ..... 82

3.2.1. Materials and reagents ..... 82

3.2.2. Samples preparation ..... 82

3.2.3. Particle size distribution ..... 84

*3.2.4.* Confocal laser scanning microscopy (CLSM) ..... 85

3.2.5. Fourier transform infrared spectroscopy (FTIR) ..... 85

3.2.6. Interfacial tension ..... 86

3.2.7. Zeta (ζ) potential ..... 86

3.2.8. X–ray diffraction (XRD) ..... 87

3.2.9. Different scanning calorimetry (DSC) ..... 88

3.2.10. Statistical analysis ..... 89

3.3. Results and discussion ..... 89

3.3.1. Particle size and microstructure of MFGs/MFGM ..... 89

3.3.2. FTIR ..... 90

3.3.3. Interfacial tension ..... 94

3.3.4. ζ-potential ..... 96

3.3.5. XRD ..... 98

3.3.6. DSC ..... 100

3.4 Conclusions ..... 103

References ..... 105

CHAPTER FOUR ..... 109

Abstract ..... 110

4.1. Introduction ..... 111

4.2. Materials and methods ..... 113

4.2.1. Materials and reagents ..... 113

4.2.2. Ultrasonic treatments ..... 113

4.2.3. Isolation of MFGs/MFGM samples ..... 115

4.2.4. Chemical compositions of the MFGs/MFGM ..... 115

4.2.5. The characterization of interfacial properties of MFGs/MFGM ... 116

4.2.6. The characterization of thermal properties of MFGs/MFGM ..... 120

4.3. Results and discussion ..... 122

4.3.1. The effect of ultrasonic treatments on the interfacial properties of MFGs/MFGM ..... 122

4.3.2. The effect on ultrasonic treatments on the thermal behaviour of MFGs/MFGM ..... 133

4.4. Conclusion ..... 139

References ..... 141

Supplementary materials ..... 145

CHAPTER FIVE ..... 146

Modifying physicochemical properties, rheology and creaming stability of milk fat globule and membrane through ultrasound treatment ..... 146

Abstract ..... 147

5.1. Introduction ..... 148

5.2. Materials and methods ..... 150

5.2.1. Materials and reagents ..... 150

5.2.2. Ultrasonic treatments ..... 151

5.2.3. Separation of MFGs/MFGM ingredients ..... 151

5.2.4. Fourier transform infrared spectroscopy (FTIR) ..... 152

5.2.5. Sodium dodecyl sulphate polyacrylamide gel electrophoresis (SDS-PAGE) ..... 152

5.2.6. Rheological analysis ..... 153

5.2.7. Accelerated emulsion stability ..... 154

5.2.8. Confocal laser scanning microscopy (CLSM) ..... 154

5.2.9. Statistical analysis ..... 155

5.3. Results and discussion ..... 156

5.3.1. General profiling of composition changes induced by ultrasonic treatments ..... 156

5.3.2. Effect of ultrasonic treatments on the distribution of milk fat globule membrane proteins ..... 161

5.3.3. Rheological properties ..... 163

5.3.4. Physical stability ..... 166

5.3.5. Microstructure ..... 170

5.3.6. Hierarchical cluster analysis ..... 171

5.4. Conclusion ..... 173

References ..... 174

Supplementary materials ..... 178

CHAPTER SIX ..... 209

Effects of high-methoxyl pectin on structure, composition, rheological properties of milk fat globules ..... 209

Abstract ..... 210

6.1. Introduction ..... 211

6.2.1. Materials and reagents ..... 213

6.2.2 Sample preparation ..... 213

6.2.3 Particle size ..... 214

6.2.4. Zeta (ζ) potential ..... 215

6.2.5. Fourier transform infrared spectroscopy (FTIR) ..... 215

6.2.6. Sodium dodecyl sulphate polyacrylamide gel electrophoresis (SDS-PAGE) ..... 216

6.2.7. Physical stability ..... 216

6.2.8. Rheological properties ..... 216

6.2.9. Statistical analysis ..... 217

6.3. Results and discussion ..... 218

6.3.1. Particle size of MFGs/MFGM ..... 218

6.3.2. ζ-potential ..... 221

6.3.3. FTIR ..... 223

6.3.4. SDS-PAGE ..... 226

6.3.5. Effect of HMP on the physical stability MFGs/MFGM materials ..... 228

6.3.6. Rheological properties ..... 231

6.3.7. Hierarchical cluster analysis (HCA) ..... 233

6.4. Conclusion ..... 234

Reference.....236

Supplementary materials.....239

CHAPTER SEVEN.....243

General discussion .....243

Reference.....252

APPENDIX.....254

**DECLARATION**

This is to certify that the work I am submitting is my own and has not been submitted for another degree, either at University College Cork or elsewhere. All external references and sources are clearly acknowledged and identified with in the contents. I have read and understood the regulations of University College Cork concerning plagiarism and intellectual property.

**DEDICATION**

*To my parents, sisters, and friends with love and gratitude*

## ACKNOWLEDGEMENTS

Time flies. It feel like I just arrived in Ireland yesterday, and three and a half years have already passed. The three and a half years of PhD study will be a very cherished memory of my life.

I would like to thank my supervisor Professor Song Miao at Teagasc Food Research Centre, Moorepark, and Professor Yrjö H. Roos from University College Cork, for hosting me to apply for the ‘China Scholarship Council’, thereby giving me the opportunity to study in Ireland. I sincerely appreciate Dr. Maurice O′Sullivan from UCC for his supervising, thesis revision, and handling all the matters related to my thesis defense. With Professor Song’s assistance and encouragement, I could carry out and accomplish my research project at Teagasc smoothly. For my thesis writing, I really appreciate Professor Yrjö H. Roos’s professional advice and meticulous revisions. They all have given me great support academically, and their help means a lot to me during my entire PhD study.

I’m really thankful for the funding providers, including 'The Open Project Program of State Key Laboratory of Dairy Biotechnology (No. SKLDB2022–007)', 'The China Scholarship Council (No.202008410212)', and 'Teagasc-The Irish Agriculture and Food Development Authority (MDDT1392)'. I sincerely appreciate the staffs and students from Teagasc or UCC for their kind help: Dr. Valentyn Maidannyk, Dr. Deirdre Kennedy, Ms. Sheila Cogan, Ms. Martina O'Brien, Dr. Norah O'Shea, Dr Prabin Lamichhane, Dr Tanweer Ziad Khalil Al-Dagamin for their help in equipment operation and instructions; Mr. John Paul Murphy, kindly providing the raw milk during my entire research.

I greatly value the friendships that have developed since coming to Ireland, especially Professor Junyi Huang, who really gave me a lot of help and care when I first came to Ireland. Also, thanks to our mutual friend- Professor Zhenmin Liu, for providing me the opportunity to attend academic meetings; friends from UCC, Shuo Wang, Xing Ouyang, Xiaohui Huang, Mei Han, Felipe Miceli de Farias, moments

hanging out with them really releasing me from the heavy studying life; friends from Lab 87,Shuyang Wang, Jie Han, Qi Tang, Lili Tian, Yichen Lin, Han Du, and Chi Zhang, the gratitude for their help academically and in life beyond words; friends Molly Kiernan, Lukasz Wojciech Wajda, and Ashling Murchy, who really help me fit into the new life in Ireland and improve my English; Fiona Clifford and her father Seamus Clifford, who treat me like a family.

At last, I'm eternally grateful for my beloved parents, sisters, and family members. They are always there, being my solid support. Especially my mother, she has always been a big fan of any of my decisions, encouraging me to pursuit the lifestyle I really want. Without their support and encouragement, I may not have had the courage to step out of my comfort zone, quit the job and leaves Shanghai, where I had stayed for more than seven years, heading to a strange country without any friends.

Thank you to all the people who have accompanied me and made me a better person during the PhD journey and my rest life.

YANJUN SUN
11/06/2024
Moorepark, Ireland

## ABSTRACT

Most commercially available infant formulas (IFs) lack phospholipids and milk fat globule membrane (MFGM) proteins. To mimic human milk's lipid profile, MFGs/MFGM ingredients from sweet whey or buttermilk are fortified in IF. Understanding the structural and compositional, and techno-functionalities changes of MFGs/MFGM is crucial for their application.

The MFGs/MFGM has been reconstructed by the mostly used processing methods in dairy industry, acidification (pH 6.30 and 5.30, 25℃), and novel non-thermal treatment, ultrasonic treatments with different intensities. Additionally, anionic polysaccharide- high-methoxyl pectin (HMP) was incorporated to the raw milk before the cream separation, examining the resulting physicochemical properties and techno-functionalities.

Results indicated that pH adjustment affected the MFGs structure and MFGM protein compositions, particularly at pH 5.30, causing protein loss such as butyrophilin (BTN) and Periodic Acid Schiff 6/7 (PAS 6/7) and particle size changes. Fourier Transform Infrared Spectroscopy (FTIR) spectra revealed more proteins compositions in MFGs/MFGM prepared from sweet whey (MFGM-C) compared to bovine raw milk, showing lower interfacial tension and ζ- potential. In addition, there were no apparent polymorphs in MFGM-C, and lower exothermic or endothermic enthalpy was needed during the heating and quenching procedures. Acidification, especially pH 6.30 conditions, led to the adsorption of non-membrane milk proteins on the MFGs or MFGM fragments and formed more types of conjugate detected by FTIR. Consequently, this induced changes in the crystal form proportion and thermal behaviour of MFGs/MFGM at pH 6.30.

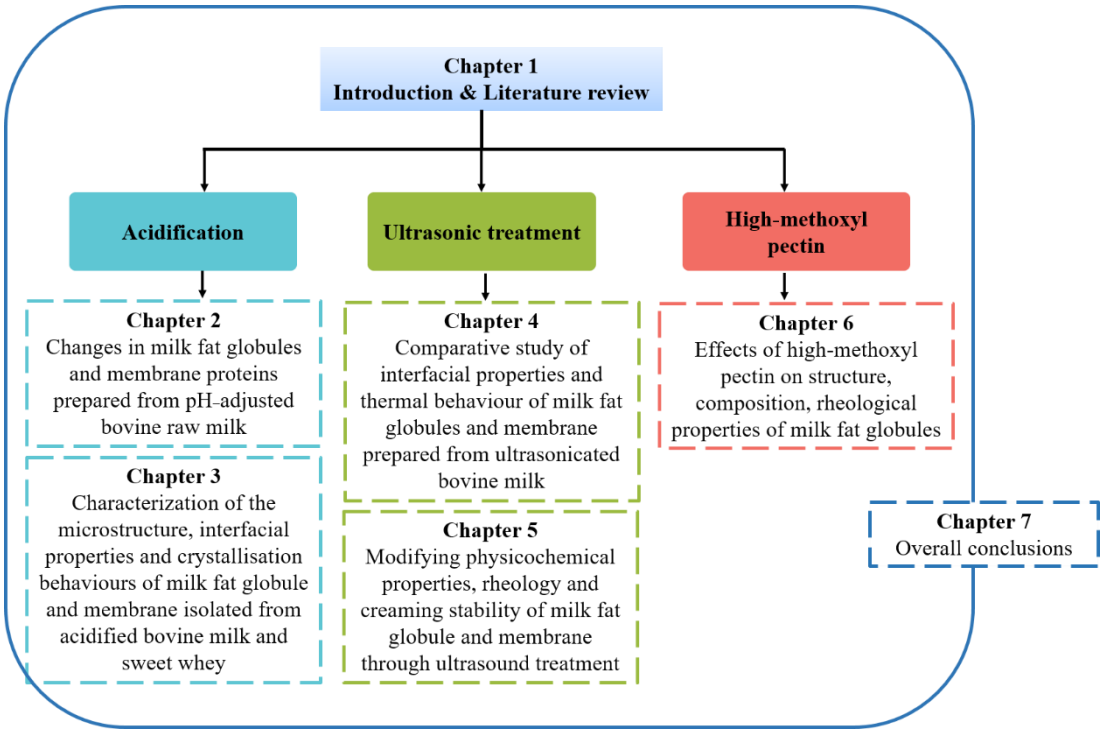
Different acoustic powers generated by the 20 kHz and 40 kHz independently or synchronously working conditions, affected the interfacial properties and thermal behaviour of MFGs/MFGM samples. 20 kHz treatments led to a relatively even particle distribution in MFGs/MFGM compared to 40 kHz and 20 + 40 kHz treated

MFGs/MFGM. Ultrasound treatment significantly resulted in the decrease of interfacial tension ($\pi$) in all MFGs/MFGM ($p<0.05$). Three typical crystal forms, α-crystal, β-form and β'-form, were observed in control and ultrasonicated 5 min MFGs/MFGM, but α-crystal disappeared in all the 15 min treated MFGs/MFGM. Ultrasonic duration has a more profound effect on the increase of β'- crystal than the intensity. Ultrasonic treatments promoted the crystallisation of MFGs/MFGM fat at higher temperature but increased the melting temperature of MFGs/MFGM. Additionally, the 15 min treatments caused more pronounced changes in the intramolecular β-sheet, random coil, and α-helix structures compared to the 5 min treatments. 20 + 40 kHz/ 15 min treatment led to aggregated membrane proteins indicated by the confocal laser scanning microscopy (CLSM) images. All the MFGs/MFGM exhibited shear-thinning behaviour, except for the 40 kHz treated MFGs/MFGM, which displayed non-Newtonian behaviour at the lower shear rate.

The preliminary investigation on the effects of HMP incorporation on the MFGs/MFGM materials showed the enhanced absorbance at the Amide I and Amide II bands and altered fingerprint regions among all the MFGs/MFGM. Larger particle sizes ranging from 10 to 100 μm presented in the 0.30% HMP MFGs/MFGM, suggesting the formation of conjugates between HMP and milk proteins. These structural and compositional changes induced by HMP affected the physical stability and rheological properties of MFGs/MFGM. Notably, MFGs/MFGM with 0.30% HMP exhibited the poorest stability, a significant increase in apparent viscosity, and shear-thinning behavior throughout the analysis.

In summary, acidification, ultrasonic treatments, and HMP incorporation significantly impact the structural, compositional, and functional properties of MFGs/MFGM ingredients.

## LITERATURE REVIEW



## LIST OF PUBLICATIONS

1. Sun, Y., Roos, Y. H., & Miao, S. (2022). Changes in Milk Fat Globules and Membrane Proteins Prepared from pH-Adjusted Bovine Raw Milk. *Foods, 11*, 4107.

2. Sun, Y., Roos, Y. H., & Miao, S. (2024). Comparative study of interfacial properties and thermal behaviour of milk fat globules and membrane prepared from ultrasonicated bovine milk. *Ultrasonics Sonochemistry*, 102.

3. Sun, Y., Roos, Y. H., & Miao, S. (2024). Characterization of the microstructure, interfacial properties and crystallisation behaviours of milk fat globule and membrane isolated from acidified bovine milk and sweet whey. *Food Hydrocolloids*, 110246.

4. Sun, Y., Roos, Y. H., & Miao, S. Modifying the physicochemical properties, rheology and emulsions stability of milk fat globule and membrane by ultrasound treatment. *Ultrasonics Sonochemistry*, 111, 107058.

5. Sun, Y., Roos, Y. H., & Miao, S. Effects of high-methoxyl pectin on structure, composition, rheological properties of milk fat globules. *Food Hydrocolloids* (Accepted).

6. Sun, Y., Roos, Y. H., & Miao, S. (2024). A review of factors affecting the structure, compositions, and the techno-functionalities of bovine milk fat globule and membrane. *Trends in Food Science & Technology*, 104570.

**Conference Presentations**

1. Sun, Y., Roos, Y. H., & Miao, S. Changes in Milk Fat Globules and Membrane Proteins Prepared from pH-Adjusted Bovine Raw Milk, 5th Food Structure and Functionality Symposium, September 2022, Cork, Ireland (Poster)

2. Sun, Y., Roos, Y. H., & Miao, S. Changes in Milk Fat Globules and Membrane Proteins Prepared from pH-Adjusted Bovine Raw Milk, Dairy Science and Technology Summer School & Symposium, June 2023, Cork, Ireland (Oral presentation).

## LIST OF ABBREVIATIONS

| | |
|---|---|
| MFGs | Milk Fat Globules |
| MFGM | Milk Fat Globule Membrane |
| ANOVA | Analysis of Variance |
| SD | Standard deviation |
| CLSM | Confocal laser scanning microscopy |
| Dv(10) | 10 percent size value below the particle size distribution |
| Dv(50) | 50 percent size value below the particle size distribution |
| Dv(90) | 90 percent size value below the particle size distribution |
| D [3, 2] | Surface-weighted mean diameter/ Sauter mean value |
| D [4, 3] | Volume-weighted mean diameter/DeBroukere mean value |
| SDS-PAGE | Sodium dodecyl sulfate-polyacrylamide gel electrophoresis |
| BTN | Butyrophilin |
| PAS 6/7 | Periodic Acid Schiff 6/7 |
| XD/XHD | The redox enzyme xanthine oxidase/dehydrogenase |
| CD 36 | Cluster of Differentiation 36 |
| PAS III | Periodic acid Schiff III |
| MUC1 | Mucin 1 |
| ADPH | Adipophilin |
| FABP | Fatty acid binding protein |
| PC | Phosphatidylcholine |
| PI | Phosphatidylinositol |
| PS | Phosphatidylserine |
| PE | Phosphatidylethanolamine |
| SM | Sphingomyelin |
| WPC | Whey protein concentrate |

| | |
|---|---|
| IF | Infant formula |
| AFM | Anhydrous milk fat |
| HMP | High-methoxyl pectin |
| TAG | Triacyglycerol |
| ARA | Arachidonic acid |
| DHA | Docosahexaenoic acid |
| FTIR | Fourier transform infrared spectroscopy |
| $T_m$ | Phase transition temperature |
| AFM | Atomic force microscopy |
| PM | Plasma membrane |
| PTMs | posttranslational modifications |
| MFD | Diet induced milk fat depression |
| CLA | Conjugated linoleic acid |
| RO | Reverse osmosis |
| NF | Nanofilration |
| UF | Ultrafiltration |
| MF | Microfiltration |
| DF | Diafiltration |
| UHT | Ultra-high temperature sterilization |
| UP | Ultra-pasteurization |
| SP | Spray drying |
| HPH | High-pressure homogenization |
| HHP | High hydrostatic pressure |
| PEF | Pulsed electric field |
| DBD | Dielectric barrier discharge plasma |
| MPL | MFGM rich in phospholipids |
| SC-$CO_2$ | Supercritical-$CO_2$ |

| | |
|---|---|
| TEM | Transmission electron microscopy |
| FA | Fatty acid |
| SSA | Specific surface area |
| TMP | Transmembrane pressure |
| SNFs | Non-fat solids |
| DTT | Dithiothreitol |
| WGA | Wheat germ agglutinin |
| FCF | Fluorescent Fast Green |
| XRD | X-ray Diffraction Spectra |
| $\Delta H_C$ | Enthalpy of crystallization |
| $\Delta H_M$ | Enthalpy of melting |
| DSC | Different scanning calorimetry |
| $\zeta$ | Zeta potential |
| ATR | Attenuated total reflectance |
| W/O | Water in oil |
| FPS | Frame per second |
| $\Phi_m$ | The measured surface fraction |
| $\Phi_e$ | The estimated surface fraction |
| $\zeta_R$ | Relative change of $\zeta$-potential |
| $T_M$ | Temperature of melting |
| $T_C$ | Temperature of crystal |
| PPP | Tripalmitoyl glycerol |
| OOO | Trioleolyl glycerol |
| POP | 1,3-dipalmitoyl-2-oleoyl-glycerol |
| POS | 1-palmitoyl-2-oleoyl-3-stearoyl-glycerol |
| $H_0$ | Surface hydrophobicity |
| $k_{diff}$ | Diffusion rate |

| | |
|---|---|
| MMF | Medium-melting fractions |
| LMF | Low-melting fractions |
| HMF | High-melting fractions |
| $\pi$ | Interfacial tension |
| $k_a$ | The first-order constant of adsorption (penetration) |
| FWHM | Full widthat half-maximum |
| ANS | 1-anilinonaphthalene-8 sulfonic acid |
| FI | Fluorescence intensity |
| PBS | Phosphate-buffered saline |
| LMF | Low-melting fractions |
| Å | d-spacing |
| PCA | Principal component analysis |
| HCA | Hierarchical cluster analysis |
| HMP | High-methoxyl pectin |
| LMP | Low-methoxyl pectin |
| SHMP | Sodium hexametaphosphate |
| NIR | Near infrared |
| n | Flow behaviour indexes |
| K (Pa $s^n$) | Consistency coefficient |

## INTRODUCTION

In mammal milk, most lipids found in milk fat globules (MFGs), which are encased in a unique tri-layer membrane known as milk fat globule membrane (MFGM) (Huang, et al., 2023). Approximately 95% of MFGs are comprised of heterogeneous triglycerides located in their inner core. MFGMs have attracted significant interest due to their multilayer structure and abundance of polar lipids and membrane proteins. The proteins in MFGM constitute about 1–4% of the total protein content in milk (Liao, Alvarado, Phinney, & Lönnerdal, 2011) but 25–70% of the MFGM composition. Research has primarily focused on eight major proteins: periodic acid Schiff III (PAS III), butyrophilin (BTN), cluster of differentiation 36 (CD 36), mucin 1 (MUC 1), the redox enzyme xanthine oxidase/dehydrogenase (XO/XDH), lactadherin or periodic acid Schiff 6/7 (PAS 6/7), adipophilin (ADPH) and fatty acid binding protein (FABP) (Fong, Norris, & MacGibbon, 2007b; Liao, et al., 2011; Holzmüller, Müller, Himbert, & Kulozik, 2016h). About 40% of the MFGM proteins are glycoproteins, with XO/XDH making up 12–13% of the total. Recent studies have highlighted that MFGM is a dynamic system containing a complex array of polar lipids, which constitute 40.6 % of each MFG. These heterogeneous polar lipids are asymmetrically distributed across the membrane surface (Lee, et al., 2018). Although polar lipids represent only 0.2 to 1% of total milk lipids, they account for 26 to 40% of the lipids in MFGM (Fong, et al., 2007b). Polar lipids are categorized into three main types based on their fatty acid structure, glycerophospholipids, sphingomyelin, and glycosphingolipids. In glycerophospholipids, two fatty acids bond with glycerol at C-1 and C-2, while the C-3 position is linked to a phosphate group that may bind to choline, inositol, serine, or ethanolamine group, forming phosphatidylcholine (PC), phosphatidylinositol (PI), phosphatidylserine (PS), and phosphatidylethanolamine (PE), respectively. Sphingomyelin (SM) is similar to PC but has a sphingosine group instead of glycerol.

Milk fat provides 50–60% of the energy necessary for a neonate's growth. The bioactive compositions of the MFGs/MFGM, such as phospholipids and glycoproteins,

are gaining attention for their crucial role in promoting brain and intelligence development in newborns (Mohamed, et al., 2022; Nieto-Ruiz, et al., 2022). The ingredients of MFGs/MFGM have been clinically confirmed as safe for inclusion in infant formula (Jiang, et al., 2022). Dairy producers, such as Fonterra, Arla and FrieslandCampina, have developed whey protein concentrate (WPC) ingredients enriched with MFGM compositions derived from cheese whey or butter milk. These commercial ingredients are added to infant formula (IF) to mimic the natural nutritional profile of human milk, addressing the deficiency of functional lipids and membrane-bound proteins in current IF products. Raza, Herzig, and Leppaluoto (2021) have extensively reviewed the physiological properties of MFGM throughout the lifespan, referring to it as a potential panacea. The bioactivity and positive effects of MFGM proteins on the defense mechanisms for breastfed infants have been extensively reviewed. Studies have shown that some MFGM glycoproteins protect immature infants against gut-derived pathogens (Timby, et al., 2015; Lopez, et al., 2017b). Defatted bovine MFGM fractions, including proteins and glycoproteins, have been reported to inhibit the adherence of *E.coli* O157:H7 strains to HT‑29 cells. Additionally, it was found that in vitro, breast cancer cell lines could be inhibited by FABP at very low concentrations (Ross, 2016). As research into the health benefits of MFGs/MFGM deepens, this ingredient is being applied in an increasing number of food products. Dairy products, such as yogurt and cheese, remain its ideal carriers.

Our literature review highlights the diverse research findings on the structure and compositions of MFGs/MFGM. Specifically, we compiled data on the most commonly used industrial dairy processing methods, including thermal treatment, homogenisation, centrifugation, membrane filtration, and emerging non-thermal treatments (Sun, Roos, & Miao, 2024). However, there is still a lack of research on how these processes affect the techno-functionalities of MFGs/MFGM. The physicochemical properties of infant formula powders are influenced not only by processing factors, such as concentration times and spray drying temperature but also

the functionality of each nutrient (Fang, Rogers, Selomulya, & Chen, 2012; Reddy, et al., 2014; Saxena, et al., 2020). Given that MFGs/MFGM are primarily used in IF powder, investigating their techno-functionalities is essential. Ren, Li, Liu, and Ma (2020) demonstrated that pasteurisation and homogenisation treatments affected the thermodynamic properties and fat polymorphs of fat globules during seven days of storage at 4 ℃. MFGs/MFGM ingredients play a significant role in the emulsifying stability of IF products (Li & Van der Meeren, 2022a). The interfacial layer of MFGs/MFGM is likely involved in emulsion formation and destabilization. MFGM fragments altered the compositions and conformational structure at the oil-water interface, thereby influencing the stability of dairy emulsions (Berton-Carabin, Sagis, & Schroën, 2018).

Commercial MFGs/MFGM ingredients are prepared from sweet whey or buttermilk, involving processes such as acidification, heating, and coagulation (Fontecha, et al., 2020). Acidification is commonly used in the production of dairy products like yogurts, cheeses, lactic fermented beverages, and acidic milk drinks with pH around 4.0. When the pH is reduced to about 4.0, the intermediate processes 5.3 and 6.30 are the two important pH condition parameters, because best working pH condition for rennet is between 5.30 and 6.30. Casein is a group name for the mixture of β, α，κ-casein which start to precipitate at pH 5.3. Previous research has shown that varying pH conditions can significantly affect the isolating efficiency of MFGM proteins from buttermilk or native MFGs from cream (Holzmüller, Gmach, Griebel, & Kulozik, 2016b; Jukkola, Partanen, Rojas, & Heino, 2018b). According to Lopez et al., the microstructure and rheology of emulsions and the stability of lipid droplets coated by MFGM are pH-dependent (Lopez, et al., 2017b).We hypothesize that acidification treatment alters the structure and compositions of MFGs/MFGM, thereby impacting their interfacial behaviour, thermodynamic properties, and fat polymorphs. To verify this hypothesis, we investigated the effect of pH conditions at 5.30 and 6.30 on the interfacial properties and fat crystallisation behaviours of MFGs/MFGM.

With the increasing consumer demand for natural and less processed foods, non-heat treatment is receiving increasing attention in food industry. Ultrasonic treatment is one of the most potentially non-thermal techniques that could be used in dairy processing. Low-frequency ultrasounds induce strong cavitation effects by forming and violently collapsing of bubbles in the solution, which can produce smaller particles, facilitate fat separation, improve emulsion properties and adjust the crystallization behaviour of anhydrous milk fat (AMF) (Martini, Suzuki, & Hartel, 2008; Juliano, et al., 2011; Leong, et al., 2014a; Leong, et al., 2014b; Krasulya, et al., 2016). Specifically, previous research has optimised the efficacy of specific ultrasonic densities for fat separation from milk (Leong, et al., 2014a). Compared to shear-homogenization, more MFGM proteins were retained after ultrasonication at 20 kHz for 30 s−180 s (Liu, Boeren, Zhang, Zhou, & Hettinga, 2021). These studies focused on the functional changes induced by ultrasonication of MFGs/MFGM in other food systems, such as cream, infant formula, or AFM, rather than in 'native and pure' MFGs/MFGM systems. Despite the positive effects of the ultrasonic treatment, there is still a lack of research on the impact of high-intensity/low-frequency ultrasound on the interfacial properties, crystal transformation, crystallization and melting characteristics of the MFGs/MFGM materials.

In acidified dairy products, pectin is commonly used to in acidified dairy products such as yogurt and acidified milk drinks to prevent milk protein flocculation and enhance the stability of the products. Additionally, pectin has been used to form coacervates with caseins or whey protein, enhancing their techno-functionalities. The previous research has primarily focused on the coacervates formation between caseins or whey proteins and pectin to enhance their techno-functionalities. For instance, in fat-reduced products, whey protein-pectin complexes produced by thermomechanical treatment act as fat replacers, improving the creaminess of the products (Filla & Hinrichs, 2023b). The interactions between casein micelles and pectin are complex and have been extensively studied (Wusigale, Liang, & Luo, 2020). The interactions

between pectin and MFGM proteins, which may also influence the stabilization of food systems, have not yet been thoroughly investigated.

Given the crucial role of tri-layer structure of MFGM in its physiological properties, maintaining the natural membrane state during the isolation and processing is vital. In summary, the factors affecting the structure, compositions, and techno-functionalities of MFGs/MFGM requires deeper exploration, especially from an industrial application perspective, to fully harness their potential in food science and nutrition. To address these issues and bridge the research gap, this thesis aims to explore the following aspects:

(i) MFGs/MFGM ingredients were isolated from acidified bovine raw milk (pH 5.30 and pH 6.30) using cream separator, followed by centrifugation for further enrichment. The physicochemical properties and the microstructure of MFGs and MFGM proteins before and after cream separation were investigated **(Chapter 2)**. Additionally, MFGs/MFGM from the sweet whey were prepared to mimic industrial MFGs/MFGM production, allowing for a comparative analysis of their interfacial properties and thermal behaviors **(Chapter 3)**.

(ii) Low-frequency sonication at 20 kHz and 40 kHz was applied independently or synchronously to bovine milk before MFGs/MFGM separation. We conducted a comparative analysis of the changes in interfacial properties and thermal behaviour of MFGs/MFGM prepared from ultrasonicated bovine milk **(Chapter 4)**. Follow-up research examined the physicochemical and rheological properties, as well as the emulsions stability of MFGs/MFGM. To deepen our understanding of the physicochemical properties and technical functionalities of natural MFGs and MFGM, bovine raw milk was used as the primary raw material **(Chapter 5)**.

(iii) The effect of high-methoxyl pectin (HMP) addition to raw milk on the structural and compositional changes of MFGs or MFGM during the cream separation process was explored. Additionally, the techno-functionalities, including physical

stability and rheological property, were investigated to provide support and a theoretical basis for industrial applications **(Chapter 6)**.

## References

Berton-Carabin, C. C., Sagis, L., & Schroën, K. (2018). Formation, structure, and functionality of interfacial layers in food emulsions. *Annual review of food science and technology, 9*, 551-587.

Fang, Y., Rogers, S., Selomulya, C., & Chen, X. D. (2012). Functionality of milk protein concentrate: Effect of spray drying temperature. *Biochemical Engineering Journal, 62*, 101-105.

Filla, J. M., & Hinrichs, J. (2023). Processing of whey protein-pectin complexes: Upscaling from batch lab scale experiments to a continuous technical scale process. *Journal of Food Engineering, 347*, 111437.

Fong, B. Y., Norris, C. S., & MacGibbon, A. K. H. (2007). Protein and lipid composition of bovine milk-fat-globule membrane. *International Dairy Journal, 17*(4), 275-288.

Fontecha, J., Brink, L., Wu, S., Pouliot, Y., Visioli, F., & Jimenez-Flores, R. (2020). Sources, Production, and Clinical Treatments of Milk Fat Globule Membrane for Infant Nutrition and Well-Being. *Nutrients*, *12*(6), 1607.

Holzmüller, W., Gmach, O., Griebel, A., & Kulozik, U. (2016). Casein precipitation by acid and rennet coagulation of buttermilk: Impact of pH and temperature on the isolation of milk fat globule membrane proteins. *International Dairy Journal, 63*, 115-123.

Holzmüller, W., Müller, M., Himbert, D., & Kulozik, U. (2016). Impact of cream washing on fat globules and milk fat globule membrane proteins. *International Dairy Journal, 59*, 52-61.

Huang, Y., Wei, T., Chen, F., Tan, C., Gong, Z., Wang, F., et al. (2023). Effects of various thermal treatments on interfacial composition and physical properties of bovine milk fat globules. *Food Research International, 167*, 112580.

Jiang, B., Xia, Y., Zhou, L., Liang, X., Chen, X., Chen, M., et al. (2022). Safety and Tolerance Assessment of Milk Fat Globule Membrane- enriched Infant Formulas in Healthy Term Chinese Infants: A Randomised Multicenter Controlled Trial. *BMC pediatrics, 22*(1), 465.

Jukkola, A., Partanen, R., Rojas, O. J., & Heino, A. (2018). Effect of heat treatment and pH on the efficiency of micro-diafiltration for the separation of native fat

globules from cream in butter production. *Journal of Membrane Science, 548*, 99-107.

Juliano, P., Kutter, A., Cheng, L. J., Swiergon, P., Mawson, R., & Augustin, M. A. (2011). Enhanced creaming of milk fat globules in milk emulsions by the application of ultrasound and detection by means of optical methods. *Ultrasonic Sonochemistry, 18*(5), 963-973.

Krasulya, O., Bogush, V., Trishina, V., Potoroko, I., Khmelev, S., Sivashanmugam, P., et al. (2016). Impact of acoustic cavitation on food emulsions. *Ultrasonic Sonochemistry, 30*, 98-102.

Lee, H., Padhi, E., Hasegawa, Y., Larke, J., Parenti, M., Wang, A., et al. (2018). Compositional Dynamics of the Milk Fat Globule and Its Role in Infant Development. *Frontiers in Pediatrics, 6*, 313.

Leong, T., Johansson, L., Juliano, P., Mawson, R., McArthur, S., & Manasseh, R. (2014a). Design parameters for the separation of fat from natural whole milk in an ultrasonic litre-scale vessel. *Ultrasonic Sonochemistry, 21*(4), 1289-1298.

Leong, T., Juliano, P., Johansson, L., Mawson, R., McArthur, S. L., & Manasseh, R. (2014b). Temperature effects on the ultrasonic separation of fat from natural whole milk. *Ultrasonic Sonochemistry, 21*(6), 2092-2098.

Li, H., & Van der Meeren, P. (2022). Sequential adsorption of whey proteins and low methoxy pectin at the oil-water interface: An interfacial rheology study. *Food Hydrocolloids, 128*, 107570.

Liao, Y., Alvarado, R., Phinney, B., & Lönnerdal, B. (2011). Proteomic Characterization of Human Milk Fat Globule Membrane Proteins during a 12 Month Lactation Period. *Journal of Proteome Research, 10*(8), 3530-3541.

Liu, Y., Boeren, S., Zhang, L., Zhou, P., & Hettinga, K. (2021). Ultrasonication retains more milk fat globule membrane proteins compared to equivalent shear-homogenization. *Innovative Food Science & Emerging Technologies, 70*, 102703.

Lopez, C., Cauty, C., Rousseau, F., Blot, M., Margolis, A., & Famelart, M. H. (2017). Lipid droplets coated with milk fat globule membrane fragments: Microstructure and functional properties as a function of pH. *Food Research International, 91*, 26-37.

Martini, S., Suzuki, A. H., & Hartel, R. W. (2008). Effect of High Intensity Ultrasound on Crystallization Behavior of Anhydrous Milk Fat. *Journal of the American Oil Chemists' Society, 85*(7), 621-628.

Mohamed, H. J. J., Lee, E. K. H., Woo, K. C. K., Sarvananthan, R., Lee, Y. Y., & Mohd Hussin, Z. A. (2022). Brain-immune-gut benefits with early life supplementation of milk fat globule membrane. *JGH Open, 6*(7), 454-461.

Nieto-Ruiz, A., Garcia-Santos, J. A., Verdejo-Roman, J., Dieguez, E., Sepulveda-Valbuena, N., Herrmann, F., et al. (2022). Infant Formula Supplemented With Milk Fat Globule Membrane, Long-Chain Polyunsaturated Fatty Acids, and Synbiotics Is Associated With Neurocognitive Function and Brain Structure of

Healthy Children Aged 6 Years: The COGNIS Study. *Front Nutrition, 9*, 820224.

Raza, G. S., Herzig, K. H., & Leppaluoto, J. (2021). Invited review: Milk fat globule membrane-A possible panacea for neurodevelopment, infections, cardiometabolic diseases, and frailty. *Journal of Dairy Science, 104*, 19649.

Reddy, R. S., Ramachandra, C. T., Hiregoudar, S., Nidoni, U., Ram, J., & Kammar, M. (2014). Influence of processing conditions on functional and reconstitution properties of milk powder made from Osmanabadi goat milk by spray drying. *Small Ruminant Research, 119*(1-3), 130-137.

Ren, Q., Li, Q., Liu, H., & Ma, Y. (2020). Thermal and storage properties of milk fat globules treated with different homogenisation pressures. *International Dairy Journal, 110*, 104725.

Ross, S. (2016). *Targeting the glycome of the milk fat globule membrane for antiinfective properties.* National University of Ireland, Galway, Galway.

Saxena, J., Adhikari, B., Brkljaca, R., Huppertz, T., Chandrapala, J., & Zisu, B. (2020). Inter-relationship between lactose crystallization and surface free fat during storage of infant formula. *Food Chemistry, 322*, 126636.

Sun, Y., Roos, Y. H., & Miao, S. (2024). A review of factors affecting the structure, compositions, and the techno-functionalities of bovine milk fat globule and membrane. *Trends in Food Science & Technology*, 104570.

Timby, N., Hernell, O., Vaarala, O., Melin, M., Lonnerdal, B., & Domellof, M. (2015). Infections in infants fed formula supplemented with bovine milk fat globule membranes. *Journal of Pediatric Gastroenterology and Nutrition, 60*(3), 384-389.

Wusigale, Liang, L., & Luo, Y. (2020). Casein and pectin: Structures, interactions, and applications. *Trends in Food Science & Technology*, *97*, 391-403.

# CHAPTER ONE

## Literature Review

Chapter 1 ‘A review of factors affecting the structure, compositions, and the techno-functionalities of bovine milk fat globule and membrane’ was published in:

Sun, Y., Roos, Y. H., & Miao, S. (2024). A review of factors affecting the structure, compositions, and the techno-functionalities of bovine milk fat globule and membrane. *Trends in Food Science & Technology*, 104570

Yanjun Sun: Conceptualization, Methodology, Writing-original draft, Visualization. Yrjö H. Roos: Supervision, Writing review & editing. Song Miao: Supervision, Conceptualization, Writing-review & editing, Funding acquisition, Project administration.

**Abstract**

*Background:* Dairy powders enriched with milk fat globules (MFGs) and milk fat globule membrane (MFGM) materials are gaining interest in food industry due to their bioactive benefits, including the promotion of brain development and cognitive functions, as well as improvements in gut health and immunity. MFGs/MFGM ingredients have been incorporated into infant formula (IF) to bridge the nutritional gap between formula and breast milk. The structure and composition of MFGs/MFGM ingredients significantly influence their functionalities and physiological properties.

*Scope and approach:* This review provides an update on recent research concerning the factors influencing the structure, composition, and functionalities of MFGs/MFGM ingredients, including the species, lactation stage and feeding methods. Additionally, conventional separation methods are discussed versus novel membrane filtration techniques. The main part of this review covers the recent progress and trends arising from the influence of the industrial dairy produce units, including thermal treatment and low temperature storage, homogenization, and non-thermal processes.

*Key findings and conclusions:* Variability in reports on the structure and composition of MFGs/MFGM across studies poses challenges in discerning whether these differences arise from varied processing techniques or analytical methods. Establishing standard analytical methods remains an ongoing research topic. By-products such as cheese whey or buttermilk continue to serve as primary raw materials for the preparation of MFGs/MFGM ingredients in the industry. Studies on the preparation of MFGs/MFGM materials while maintaining their natural state are relatively limited. Further research into the structural and compositional changes of MFGs/MFGM during food processes is essential, as it has the potential to provide the key information on their physiological properties and tech-functionalities.

**Keywords:** Milk fat globule; Milk fat globule membrane structure; Membrane compositions; Heating treatment; Homogenization; Non-thermal processing

## 1.1 Introduction

Raw milk is a complex oil-in-water emulsion where milk fat is dispersed as globules, termed milk fat globules (MFGs). The diameter of MFGs in untreated raw milk ranges from 0.2 to 15 μm, with an average of 3−4 μm. MFGs are biosynthesised by encapsulating triacylglycerol (TAG) within lipid droplets, which are surrounded by a tri-layered membrane known as the milk fat globule membrane (MFGM) (Heid & Keenan, 2005).

Recent studies have proposed MFGs/MFGM ingredients as potential nutraceuticals in infant formula (IF), particularly due to their enrichment with phospholipid, ganglioside, and glycoprotein. Extensive research has demonstrated their health benefits in the food and pharmaceutical industries. Raza, et al. (2021) provided a comprehensive review of the clinical and physiological impacts of MFGM components throughout the lifespan, highlighting their roles in neurodevelopment, cardio-metabolic health, and frailty in older adults. The technological functionalities of MFGM, such as emulsification and probiotics encapsulation, are also gaining research interest (Fontecha, et al., 2020). For instance, MFGM glycoproteins have been used in the encapsulation of *Lactobacillus*, with the size of the bacteria being a critical consideration in liposome designing to ensure complete encapsulation (Guerin, Burgain, Gomand, Scher, & Gaiani, 2019). Additionally, the glycoconjugates in milk are the primary macromolecules that prevent the adhesion of enteropathogens, known as the anti-adhesive ability. Conventional milk processing techniques, including heating and homogenisation, can modify the adhesive properties of MFGM by regulating the release and conformation of its glycoconjugates (Douellou, Montel, & Thevenot Sergentet, 2017).

Bridging the nutritional gap between IF and breast milk remains a priority for dairy enterprises. Fat is a crucial nutritional component in IF, contributing approximately 50% of the energy required for the infants' growth and development. Human milk contains around 200 types of fatty acids, ranging from C4:0 to C26:0 (Mansson, 2008).

Industrially, whole fat milk, anhydrous milk fat, or cream, serves as excellent fat sources for IF nutritional fortification. The polar lipid profile of bovine milk has been reported to be more similar to human milk than that in soybean and sunflower kernels (van Nieuwenhuyzen & Tomás, 2008), eggs (Blesso, 2015) (Fig.1-1). However, compared with human milk, bovine milk contains higher levels of saturated fatty acid (De Bhowmick, Guieysse, Everett, Reis, & Thum, 2023). To compensate for the nutritional shortcomings of milk fat with low levels of unsaturated fatty acids, vegetable oil with various chains of fatty acids are supplemented in IF products. According to the labels of IFs sold in the markets, these commonly include coconut oil, corn oil, soybean oil, canola oil, palm olein oil, and high oleic sunflower oil. In addition, *Moretierella* alpine oil and *Schizochytrium* sp. oil are also noted in a few IF products, which are sources for arachidonic acid (ARA) and docosahexaenoic acid (DHA), respectively. Efforts to develop IF that is nutritionally close to breast milk have led to significant improvements, although some challenges remain, such as the deficiency in biogenically important compositions like MFGM-phospholipids or glycoproteins.

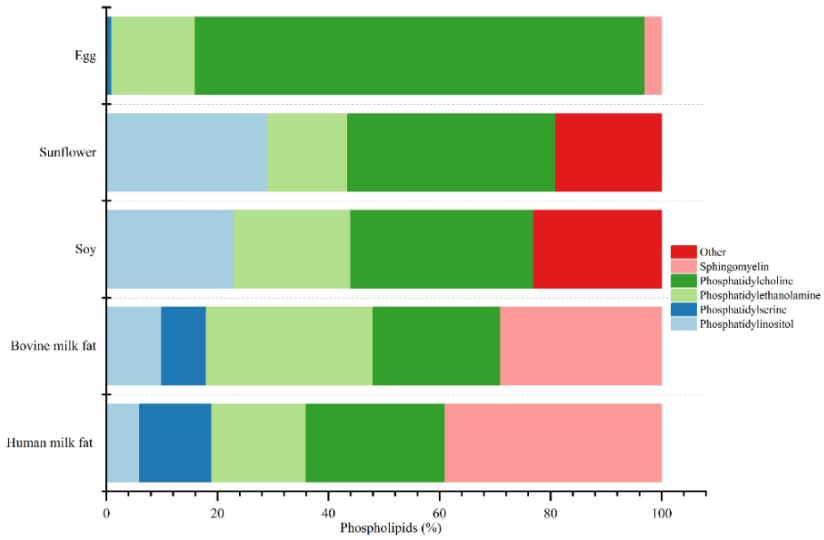



**Figure 1-1.** Relative proportion of polar lipids (% of polar lipids) from human and bovine milk (Baars, et al., 2016; Cilla, Diego Quintaes, Barberá, & Alegría, 2016), soybean and sunflower kernels (van Nieuwenhuyzen, et al., 2008), eggs (Blesso, 2015).

To date, several dairy giants like Fonterra, Arla, Hilmar, and FrieslandCampina, have introduced whey protein concentrate (WPC) enriched with MFGM components, emphasizing mainly the bioactive phospholipids. The typical components of commercial WPC ingredients produced by Arla (MFGM-10) and Friesland (Vivinal) are shown in Table 1-1. Total phospholipids in both products are approximately 6−10 %, and most of the compositions, about 65−76 %, are proteins. These WPC products, derived from cheese whey or butter milk (Fig. 1-2), are extensively applied in IF and yogurts targeted at the children's market. In China, a leading consumer of IF products, ongoing research efforts aim to address the imperfect quality standards for MFGM ingredients manufacturers and resolve the discrepancies in composition resulting from different processing methods, as noted in the 'Scientific consensus on milk fat globule membrane and its ingredients' (Wang, et al., 2022). The consensus also points out the unsound analytical method for glycoproteins analysis. As outlined in the consensus, current research predominately explores the physiological properties of MFGs/MFGM. However, the specific functional components linked to health benefits are still unclear. Bioactive proteins or lipids in MFGs/MFGM are crucial not only for their health benefits but also for their techno-functional properties. A comparative analysis of their physiological and processing characteristics is essential to better understand their composition and structure. Nevertheless, the variability in the research results on MFGs/MFGM structure and compositions complicates the comparison between studies. Holzmüller and Kulozik (2016e) suggest that the inconsistent reports on the MFGs/MFGM might be due to varied separation techniques. Moreover, natural variables such as cow's age, diet, breeds, health condition, as well as lactation stage, significantly affect the characterisation of MFGs/MFGM (Li, Delger, Dave, Singh, & Ye, 2022b), as do the methods used in sample preparation and analysis (Wang, Qiao, Gao, Jiang, & Mu, 2021a).

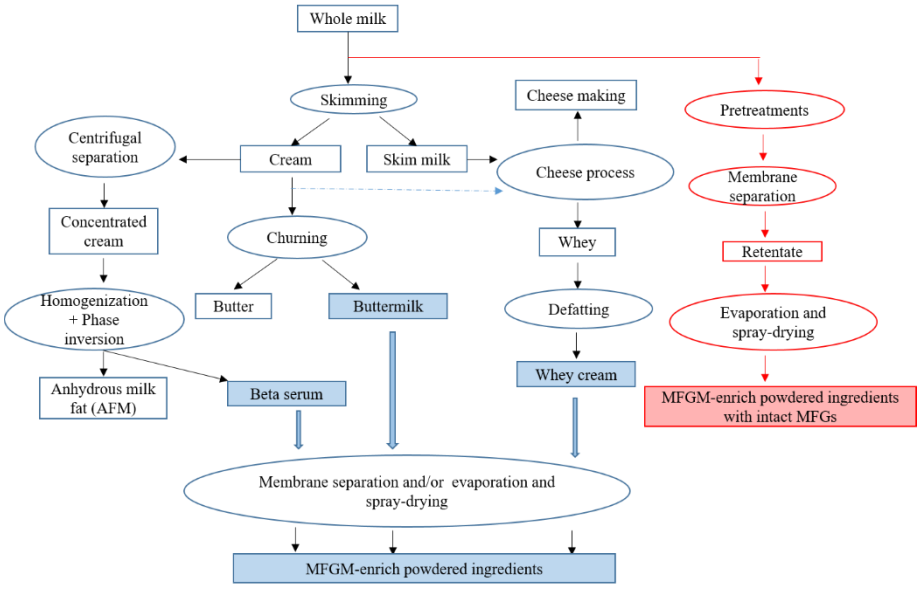



**Figure 1-2.** Schematic processing of MFGM-enrich powdered ingredients from whole milk, beta serum, buttermilk and whey cream.

In summary, this review underscores the diverse research results on structure and compositions of MFGs/MFGM. There is a growing focus on their nutritional and techno-functional properties, particularly in infant and children products. Consequently, it is necessary to critically review both past and recent studies on the factors influencing MFGs/MFGM. In particular, the most frequently used industrial dairy processing units were compiled, including thermal treatment, homogenisation, centrifugation, membrane filtration, and emerging non-thermal treatments. Additionally, this review provides an updated overview of other influential factors, such as animal species, feeding system, and the lactation stage. Before the aforementioned discussion, this review begins with a short update on the identification of the structure and compositions of MFGs/MFGM.

**Table 1-1** Typical compositions of commercial whey protein concentrate (WPC) enriched with phospholipids

| Indicative values (w/w, %) | MFGM-10 (Arla) | Vivinal (Friesland) |
|---|---|---|

| | | |
|---|---|---|
| Protein (N*6.38) | 69-76 | 65-72 |
| Fat | 16-22 | 15-21 |
| Phospholipids | 6-10 | 6-10 |
| Phosphatidyl ehtanolamine (PE) | 1.9 | 2.4 |
| Phosphatidyl choline (PC) | 1.8 | 2.2 |
| Phosphatidyl inositol (PI) | 0.5 | 0.5 |
| Phosphatidyl serine (PS) | 0.8 | 0.8 |
| Sphingomyelin （SM） | 1.9 | 2.1 |

### 1.2. Update on the structure and compositions of MFGs/MFGM

In this review, the discussion of the structure of MFGs is primarily focused on the membrane, as the core of MFGs mainly consists of triglycerides containing different fatty acids. The typical structure of MFGs and MFGM is shown in the schematic diagram Fig.1-3. Each MFG contains about 96 % triglycerides, enveloped by a three-layered membrane with outer double layers and an inner monolayer. Approximately 2 to 6% mass of MFG is the membrane in which 90% of the dry weight is proteins and polar lipids (Singh, 2006b). Each MFG contains a complex mixture of lipids (30–75%) and proteins (25–70%). Lipids represent the major building components of MFGM and include neutral lipids and polar lipids (Senorans, Gallo, Calvo, & Fontecha, 2023).

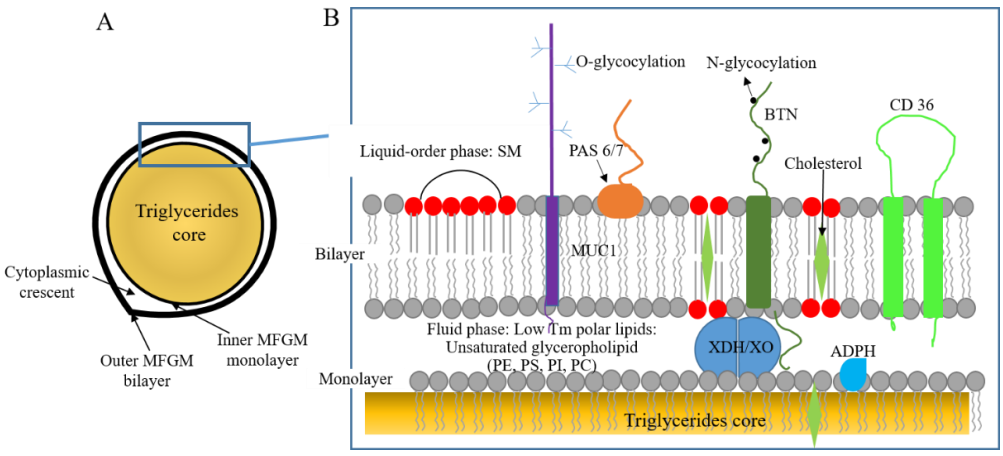


**Figure 1-3.** Three-dimensional structure of milk fat globule (A) (Chai, Oh, & Imm, 2022); Schematic diagram of fat globule with arrangement of lipids and membrane proteins (B) (Dewettinck, et al., 2008; Lopez, Cauty, & Guyomarc'h, 2015; Holzmüller, et al., 2016e).

### 1.2.1 Polar lipids

Recent studies have highlighted that MFGM is a dynamic system containing complex types of polar lipids (40.6 % of each MFG). These heterogeneous polar lipids are distributed asymmetrically across the surface of the membrane (Lee, et al., 2018). Although they represent only 0.2 to 1% of total milk lipids, they accounts for 26 to 40% of the lipids in MFGM (Fong, et al., 2007b). Polar lipids are categorized into three main types based on the structure of their fatty acid: glycerophospholipids, sphingomyelin, and glycosphingolipids. In glycerophospholipids, two fatty acids bond with glycerol at C-1 and C-2, while the C-3 position is linked to a phosphate group that may be bound to choline, inositol, serine, or ethanolamine group, forming phosphatidylcholine (PC), phosphatidylinositol (PI), phosphatidylserine (PS), and phosphatidylethanolamine (PE), respectively. Sphingomyelin (SM) is similar in structure to PC, replacing glycerol with a sphingosine group.

Both SM and PC are zwitterionic, contributing to their localization primarily in the outer layer of the membrane, whereas PI, PE, and PS, which are anionic, are predominantly found on the inner membrane surface (Deeth, 1997). Cholesterol is interspersed within both the triacylglycerol phase and the bilayer membrane. Additionally, glycolipids and glycoproteins are randomly distributed on the outer membrane surface, rather than being confined to lipid crafts (Lopez, Madec, & Jimenez-Flores, 2010b) (Fig.1-3). The membrane encompasses two coexisting lipids phases: a fluid matrix in a liquid disorder phase and a liquid-order phase. SM and saturated glycerol-phospholipids are the main components in the liquid order phase, contributing to its higher phase transition temperature ($T_m$). Conversely, the liquid disorder phase comprises glycerol phospholipids, which required less energy to

undergo conformational changes due to their lower $T_m$ and less breakthrough force is needed to change conformation (Lopez, 2011).

The distribution of fatty acids within the MFGs varies, with palmitic acids (C16:0) and stearic acids (C18:0) found predominantly in the monolayer structure of MFGM. Major fatty acids associated with glycerol phospholipids include C16:0, C18:0, C18:1, and C18:2. Additionally, a significant amount of long-chain fatty acids (C20:0, C22:0, C23:0, C24:0, and C24:1) are present in SM, explaining its higher melting point and interaction with the cholesterol rigid domains in the bilayer membrane (Fong, et al., 2007b). .

### 1.2.2 Membrane proteins

Membrane proteins account for approximately 25 to 70% of the mass of MFMG materials and about 1% of the total protein mass in milk (Holzmüller, et al., 2016e). In the early 1980s, the Milk Protein Nomenclature Committee published a proposal on the MFGM proteins classification scheme based on the molecular weight, staining characteristics, and protein mobility observed in sodium dodecyl sulphate polyacrylamide gel electrophoresis (SDS-PAGE) bands (Basch, Greenberg, & Farrell, 1985). Mather (2000) summarised the identities, characteristics, and sequences of the major MFGM-associated proteins. Currently, eight major proteins are commonly used to characterise the MFGM proteins, including mucin 1 (MUC1), periodic acid Shciff 3 (PAS3), cluster of differentiation 36 (CD36), butyrophilin (BTN), lactadherin or periodic acid Schiff 6/7 (PAS6/7), the redox enzyme xanthin oxidase/ dehydrogenase (XO/XDH), adipophilin (ADPH) and fatty acid binding protein (FABP).

Utilizing a 1-dimensional SDS-PAGE combined with micro-capillary high-performance liquid chromatography equipped with a nanospray-tandem mass spectrometer, Reinhardt and Lippolis (2006) identified up to 120 membrane proteins. More recently, proteomic techniques have enabled the identification of as many as 616 types of membrane protein in bovine MFG (Wang, et al., 2021b). These membrane

proteins are highly glycosylated and are distributed at specific locations within the MFGM through various group bindings. BTN and CD 36 are integral or transmembrane proteins that span the bilayers, whereas PAS 6/7 is a periphery protein loosely attached to the outer surface of the bilayers; ADPH is located on the monolayer surface, and XDH/XO is positioned between the bilayers and monolayer (Mather, 2000; Evers, 2004b) (Fig.1-3).

More non-invasive analytical techniques have been applied to describe the lipid and protein domains of MFGM, such as confocal laser scanning microscopy (CLSM), Fourier transform infrared spectroscopy (Sun, Roos, & Miao, 2022b), and atomic force microscopy (AFM) (Obeid, et al., 2019). These techniques, alongside proteomics and lipidomics, facilitate qualitative and quantitative analyses of MFGM compositions. Despite the technical advancements, variations in analysis techniques and sample preparation methods continue to introduce uncertainties in the structural and conformational analysis of MFGs/MFGM.

### 1.2.3 Other compositions

Various saccharides such as protein-bound N-acetylglucosamin, manose, and fucose form glycosylation complexes by bonding with membrane proteins and lipids.. These saccharides constitute critical bioactive components in MFGM and significantly contribute to its physiological effects. Oligosaccharides such as galactose, glucose, and sialic acid have been identified in glycolipids (Smoczyński, Staniewski, & Kiełczewska, 2014). Additionally, trace amounts of lipid-soluble vitamins and β-carotene are present in the triglyceride phase. Furthermore, several bioactive compounds found in milk, such as phosphodiesterase, 5’-nucelotidase, immunoglobulins, casein, or whey protein, have also been detected in MFGM. However, their presence may be attributed to the contamination during the separation and preparation process (Mather, 2000).

## 1.3. Factors affecting the structure, compositions, and techno-functionalities of MFGs/MFGM

### 1.3.1 Biosynthesis, species, lactation stage, and feeding system

- Biosynthesis

The biosynthesis of MFGM is primarily initiated on the plasma membrane (PM) because of its remarkably similar compositions to PM (Keenan, Morré, Olson, Yunghans, & Patton, 1970). However, subsequent studies in the 1980s, such as those by Kanno, Hattori, and Yamauchi (1987), identified membrane proteins and polypeptides in MFGM that were absent in PM, suggesting that PM is not the solely origin source.

The structure of MFGs/MFGM begins to alter during the secretion process (Holzmüller, et al., 2016e). Following the biosynthesis on PM, most MFGM proteins undergo posttranslational modifications (PTMs), which refers to the amino acid side chain modifications. PTMs are critical for regulating diverse cellular activities due to their regulatory impact at the molecular level. In addition, phosphorylation plays a vital role in regulating enzyme activities, membrane channels, and various proteins (Ramazi & Zahiri, 2021). Phosphorylation involves the transfers of a phosphate group from adenosine triphosphate to receptor residues, a reaction catalysed by kinase enzymes.

- Species and lactation stage

MFGs/MFGM exhibit significant variations across different mammalian species and lactation stages. Thum, Roy, Everett, and McNabb (2021) provided a detailed comparison of milk compositions from humans, bovines, caprine, and ovine, noting that bioactive compositions correlate with MFG sizes. Selecting herds based on specific MFG sizes could be an effect way to enrich bioactive proteins and lipids. Lactation and metabolic stages have a more significant influence on MFGs size than

genetic or diet factors. The MFGM proteins in Murrah, Nili-Ravi and Mediterranean buffaloes have been identified using the tandem mass tag proteomic method by Li, et al. (2021). A total of 1250 types of MFGM proteins were detected, with 103 being differentially expressed across various breeds. Moreover, Nili-Ravi milk contained more endoplasmic reticulum resident protein 29, and Murrah milk was characterized by an abundance of uromodulin. The immunological implications of species-specific MFGM compositions were explored by Felice, Owens, Kennedy, Hogan, and Lane (2021), who studied the impact of MFGM protein sources from cow, goat, sheep and buffalo (*Bubalus bubalis*) on immune system functionalities including antigen processing and presentation, immune response activity and molecular mediator of immune response productivity.

Additionally, the proteins and lipids in MFGs of different species were analysed by proteomic and lipidomic techniques. The number of proteins involved in the antigen processing differed among various species with cow, buffalo, goat and sheep containing 21, 23, 19 and 23, respectively. Goat milk fat was found to contain the highest proportion of phospholipids at 0.42%, followed by cow (0.35%), sheep (0.34%), and buffalo (0.27%), according to 31P-NMR spectroscopy results. It is important to note that variations in phospholipid content could also be partly attributed to differences in extraction methods.

Yang, et al. (2020) quantitatively and qualitatively compared the MFGM phosphoproteomics between colostrum and mature breast milk using label-free quantitative technique. Their findings indicated that colostrum contained more phosphorylation sites. Additionally, the investigation of the metabolism of fatty acid in the core MFGs revealed distinct variations in fatty acid profiles among cows with different MFGs sizes. Notably, a higher concentration of unsaturated fatty acid was detected in the milk of cow with smaller MFG phenotype, despite all the cows being subjected to the same standardized diet (Walter, Shrestha, Fry, Leury, & Logan, 2020).

- Feeding system

The milk fat profile is the highly variable and is markedly affected by diets and feeding systems. Diet-induced milk fat depression (MFD) syndrome represents a challenge in the milk fat content and yield, as well as the changes in milk fatty acids. This syndrome was initially reported by Baumgard, Corl, Dwyer, Sæbø, and Bauman (2000) in dairy cows consuming diets rich in fermentable or plant oils, primarily driven by the rumen metabolite *trans*-10, *cis*-12 conjugated linoleic acid (CLA). CLA gains interest because of its anti-carcinogenic properties, and the most common natural form of CLA identified in milk is the *cis*-9, *trans*-11 isomer (Bauman & Griinari, 2001). A negative correlation between the fat concentration and the *trans*-10, *cis*-12 CLA in dairy ewes has been reported by Toral, Gervais, Hervás, Létourneau-Montminy, and Frutos (2020). Different forms of CLA have different effects on milk yield. Perfield, et al. (2007) found that *trans*-9, *cis*-11 CLA had no effect on the milk fat yield whereas *trans*-10, *cis*-12 was responsible for the reduction in the milk fat synthesis. Additionally, *trans*-10, *cis*-12 and *cis*-9, *trans*-11 CLA supplementation in the feed did not affect milk yield compared to control MFGs/MFGM but reduced both protein and fat content, especially the relative content of PC and PE. Moreover, CLA supplementation was found to decrease the particle size of MFGs, resulting in a higher specific surface area (Zhang, Xing, Huang, & Han, 2021). A study by Argov-Argaman, et al. (2021) revealed that the phospholipid content in goat milk was lower when the goats were fed hey and confined, compared to those grazing brushland.

### 1.3.2. Effect of separation methods on the MFGs/MFGM materials

#### *1.3.2.1 Centrifugation and cream separator*

MFGs/MFGM can be separated from milk using the cream separation/ washing or centrifugation, mainly due to the density difference between the fat and skim milk phases. Holzmüller, et al. (2016e) comprehensively reviewed the effect of centrifugation and washing conditions on the MFGs/MFGM. The efficiency of MFGs/MFGM isolation using lab-scale centrifugation and cream separation was compared. Specifically, the effects of each centrifugation step have been summarized,

including the washing steps, washing solvents, temperature, dilution proportion, and centrifugation force (g). During the butter production, churning causes the breakage of MFGs, releasing MFGM fragments into buttermilk phase. A label-free proteomic approach was employed to investigate the impact of varying cream churning duration (2, 4, 6, and 8 min) on the MFGM compositions. It was found that churning for 6 min resulted in the detection of 60 unique proteins, significantly more than those identified in the 2, 4, and 8 min churning groups (Zheng, et al., 2020). Sun, et al. (2022b) demonstrated the effect of cream separation on the MFGs structure and MFGM proteins prepared from acidified bovine milk (pH 5.30 and 6.30). A profound reduction in BTN and PAS 6/7 has been reported at pH 5.30 following cream separation. Meanwhile, pH 5.30 induced a smaller particle size and lower ζ-potential of MFGs compared to the control and MFGs/MFGM at pH 6.30 during cream preparation. The particle size of MFGs can be effectively regulated by modifying the separation techniques employed, significantly impacting fat-related functionalities within food products. On an industrial scale, a two-stage centrifugal method was used by Dhungana, Truong, Bansal, and Bhandari (2021) to increase the size distribution of MFGs in milk. Critical parameters such as the size of top separating cone, feed rate and rotating rate of the bowls were optimised to maximally preserve the MFGs/MFGM in their natural state. This research provides valuable insights for scaling up the production of cream fractions with specific size distributions. Further, MFGs fractions ranging in size from millimetres to micrometres were layered and incorporated into an acid gel (induced by Glucono-δ-lactone), which exhibited superior oral tribological properties compared to control MFGs/MFGM containing naturally-sized MFGs (Cheng, et al., 2021). This pivotal discovery provides key information for regulating of MFGs size in gel emulsion systems such as yogurt and cheese. Modulating the structure and distribution of MFGs within food system is of paramount interest to food industry, as it can influence the sensory properties and functionalities of the final products.

*1.3.2.2 Membrane separation*

Membrane processing is a gentle processing method with a sustainable production system that has promising market prospects in the food and beverage industry. Membrane technology is extensively used in the dairy industry for various purposes such as spore removal, purification of active ingredients, optimization of milk proteins components, and processing of by-products. Cross-flow membrane filtration has replaced the traditional dead-end filtration in industry due to its higher efficiency and suitability for continuous production. Membranes are categorized based on the minimum molecular weight threshold that cannot pass through, including reverse osmosis (RO), nanofiltration (NF), ultrafiltration (UF) and microfiltration (MF).

Membrane filtration has been used for the fractionation of MFGs/ MFGM materials. Membrane fouling and the similar particle sizes of casein and MFGs are two major challenges in membrane separation. Efforts to address these issues have included strategies like removing or dissociating casein prior to membrane filtration. For instance, Wang, et al. (2021b) utilized membranes with varying pore sizes (30, 50 and 100 kDa) to enrich MFGM proteins from butter serum. To enhance separation efficiency, the casein micelles in the buttermilk were precipitated through acidification before undergoing membrane filtration. This process allowed for the identification of approximately 395 to 399 MFGM proteins in the retentates using label-free proteomic analysis. Notably, fewer MFGM proteins were detected in the 100 kDa permeate, indicating that a 100 kDa cutoff was more effective for MFGM proteins enrichment compared to 30 kDa and 50 kDa membranes (Wang, et al., 2021b). In addition to acidification, the application of chelating salts such as sodium citrate, sodium phosphate and sodium pyrophosphate has proven effective in removing casein by dissociating casein micelles into smaller fragments, thereby facilitating the isolation of MFGs/MFGM from buttermilk (Sun, et al., 2017). Conversely, Holzmüller, et al. (2016b) explored an alternative method by inducing gel formation from casein in buttermilk through acidification or rennet addition, rather than fragmenting the casein.

Zinc acetate and calcium acetate have been used to precipitate total lipid from the β-stream efficiently. Price, Fei, Clark, and Wang (2020) optimized the temperature and pH conditions, finding that calcium acetate precipitation at either 30 ℃ or 60 ℃ was most effective for recovering SM and PS. Although calcium acetate precipitation shows great potential for phospholipids recovery from the β-stream, it is less effective for MFGM proteins, as they were found predominantly in the supernatants after calcium acetate treatment (Price, et al., 2020).In dairy research, the primary focus has shifted towards maintaining the integrity of MFGs/MFGM during isolation processes. In the studies mentioned above, by-products like cheese whey and buttermilk, in which MFGs/MFGM is often in a fragmented state, have served as the main source for isolation. Fresh raw milk, however, presents a more ideal starting materials for preserving the natural state of MFGs or MFGM.

Hansen, et al. (2018) explored the impact of the sequence of pasteurization relative to MF on the enrichment of the MFGM proteins from raw milk. Their findings indicated that conducting pasteurization after microfiltration did not significantly alter MFGM proteins. However, pasteurizing before filtration led to a reduction in PAS 6/7. Subsequent research by Hansen, et al. (2020a) focused on optimizing membrane pore size and filtration parameters to enhance the purity of MFGs/MFGM. They also adopted a milder pasteurization temperature of 72 ℃ for 15 seconds to minimize the protein denaturation instead of 80−85 ℃/ 15 s in their previous research.

While many studies have endeavoured to isolate MFGs/MFGM from fresh milk, industrially, by-products remain the primary raw materials. Jukkola, et al. (2018b) introduced an 'ideal butter' process, where cream samples undergo MF/diafiltration (DF) before being churned into butter. This method effectively reduces serum protein drainage into buttermilk during churning, without compromising butter quality. However, the presence of small lipid droplets and MFGM fragments in the wash fluid during MF/ DF stages raises questions about the ease of separating MFGs/MFGM from buttermilk. Another study by Hokkanen, Partanen, Jukkola, Frey, and Rojas

(2021) profiled the proteins, lipids, fatty acids, and thermal behaviours of MFGM in the buttermilk or butter serum derived from microfiltrated cream. Their results revealed a lower detection of phospholipids in buttermilk during the microfiltration process, alongside variations in the phospholipids-fat ratio and melting behaviour between buttermilk and butter serum.

Comparative analyses of centrifugation and membrane filtration for isolating MFGs/MFGM have been conducted by Holzmüller, et al. (2016b) and Jukkola, et al. (2019a). The diafiltration of sweet buttermilk whey or buttermilk from whey cream offers a preferable method with fewer losses of MFGs/MFGM compositions. Although both centrifugation and MF tend to fragment MFGs, MF causes less damage, leading to higher MFGM yields and improved separation efficiency (Jukkola, et al., 2019a).

### 1.3.3 The effects of dairy processes on the MFGs/MFGM materials

#### *1.3.3.1 Heat treatments and storage temperature*

Heat treatment and refrigeration are commonly used in the dairy industry to inhibit microbial growth and ensure food safety throughout the products' shelf life. Heating or cooling treatments significantly affect the crystalline state of lipids, particularly the triglycerides in the core of MFGs, and can induce the agglutination or coalescence of MFGs as well as the attenuation and rupture of MFGM. Understanding the effect of temperature on the compositions and structure of MFGs/MFGM is of significant guidance for its practical industrial application.

- Size and lipid profile of MFGs/MFGM

Heating treatment has been reported to cause the loss of phospholipids in MFGs/MFGM by Wei, et al. (2023). Their study noted that heating at 90 ℃ for 20 min significantly accelerated the loss of SM and cholesterol in the MFGM comparting to heating at 60 ℃ for the same duration. Moreover, both 90 ℃ and 60 ℃ treatments

induced an increase in the size of MFGs and a decrease in their ζ-potential, likely due to the coalescence of MFGs and the rupture of MFGM (Wei, et al., 2023). Additionally, pasteurization and fermentation have been reported to decrease the PS levels to 1.5- and 2-fold compared to those in the untreated goat milk from confinement or gazing fed system, respectively (Argov-Argaman, et al., 2021).

- Interaction with serum protein

Heating induces the denaturation and conformational change of whey proteins, mainly α-lactalbumin (α-LA), β-lactoglobulin (β-LG) and bovine serum albumin (BSA). The denatured and unfolded structure of β-LG has been reported to more readily bind to the MFGM layer (Wiking, Gregersen, Hansen, & Hammershøj, 2022). The interaction is largely attributed to $Cys^{121}$, which facilitates the formation of β-LG self-aggregates or complexes with other milk components through thiol-disulfide interchange. Hansen, Nielsen, Rasmusen, Larsen, and Wiking (2020b) further verified that noncovalent bindings, including hydrophobic interaction and hydrogen bonding, were paramount to the association between β-LG and MFGM, beyond the simple thiol-disulfide interaction model. Even with the use of thiol-blocking agents to inhibit the $Cys^{12}$ forming disulfide bonds with MFGM proteins, conjugates between MFGM and β-LG were still observed in the SDS-PAGE results. However, the exact type of MFGM proteins that β-LG specially formed non-covalent bonds with were not identified in their study.

Caprine or goat milk is a popular alternative to bovine milk in IF products due to its easier digestion and low allergic protein content ($\alpha_{S1}$-casein) and absence of A1 β-casein. Daomin (2022) investigated various heat treatments on MFGM proteins using label-free proteomics technique, including ultra-pasteurization (85 ℃/ 30 min, UP), ultra-high temperature sterilization (135 ℃/ 5 s, UHT) and spray drying (inlet 160 ℃ and outlet 80 ℃, SP). The results showed that UP and UHT treatment reduced MFGM protein levels, whereas SP had a less significant effect on the number and abundance of MFGM proteins. Proteomic analysis and non-reduced SDS-PAGE revealed that β-

LG and α-LA were likely to bind with XDH/XO and BTN. Recombined milk, prepared by mixing skim milk and milk fat to simulate whole milk, serves as an alternative in regions where fresh milk is scarce. The process of recombined milk impacts MFGM composition containing native MFGM constituents which are replaced by casein and whey on the surface of MFGs (Ji, Lee, & Anema, 2011). The preparation methods of recombined milk affected surface compositions of MFGM and thus its gelation property. Anantawat, Loveday, Singh, and Anema (2022) investigated how the sequence of heating and homogenisation affects the composition of MFGM and its gelation properties. The results showed that homogenising milk fat with heat-treated skim milk (HEHO) resulted in lower proportion of κ-casein and denatured whey proteins on the fat globules. Nevertheless, higher amount of $\alpha_s$-casein and β-casein were present in HEHO than samples prepared by heating the blends of homogenising milk fat and skim milk (HOHE).

- Elasticity of MFGM

Quantitatively analyzing the interfacial components of MFGM presents significant challenges when using traditional analysis methods, such as solvent extraction and chromatography (Lopez, 2011). Non-destructive analytical methods have been developed to characterise the MFGs/MFGM. Atomic force microscopy (AFM) technique has emerged as a powerful tool for this purpose. Huang, et al. (2023) employed AFM, combined with Young's modulus, to quantitatively analyse the elasticity of MFGM and its binding with serum proteins after being treated by different dairy units. Young's modulus can be used to reflect the rigidity of milk samples. Young's modulus E is calculated by fitting the force curve by Hertz model:

$$F = \frac{4}{3}\frac{E\delta^{\frac{3}{2}}\sqrt{R_{tip}}}{(1-\nu^2)} \quad (1\text{-}1)$$

where F: force, $R_{tip}$: tip radius (20 nm), δ: the indentation distance and ν the Poisson ratio, taken as 0.5 (Marsh, 2006).

Homogenisation increased the Young's modulus (kPa) of raw milk more significantly compared to that in control raw milk, cream, UF retentate and standardized milk (Fig. 1-4A), indicating the increase of MFGM stiffness after homogenisation (Balasuriya, Ong, Gras, & Dagastine, 2012). Moreover, AFM images have shown that the MFGM inultra-pasteurized milk (121 ℃/ 15 s) exhibits a smoother surface compared to both control and those treated at lower temperatures (63℃ and 84 ℃) (Fig. 1-4B), indicating ultra-pasteurized milk damaged MFGM more than pasteurization (Huang, et al., 2023). Additionally, AFM has been performed to quantitatively analyze the effect of acidification (pH 4.50) and UHT treatment on the binding of MFGs with milk proteins. The results indicate an increase in the interaction force from 176 pN to 296 pN following UHT treatment, suggesting the adsorption of denatured whey protein on the surface of MFGs or casein. This treatment results in more compact and stiffer milk acid gels in UHT-treated milk compared to those formed by untreated milk samples (Obeid, et al., 2020).

- Low temperature

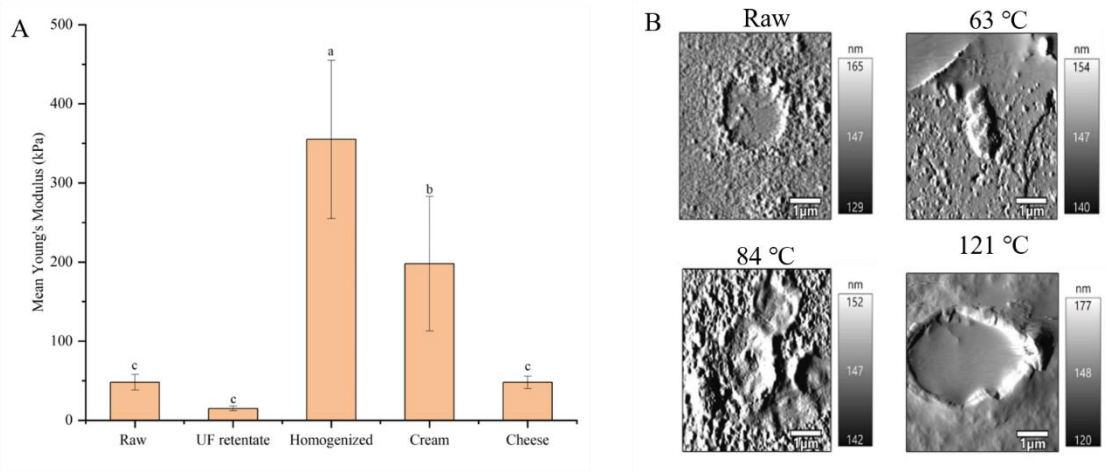



**Figure 1-4.** (A) Value of the mean Young's modulus of the milk fat globule membrane of different milk samples. Different letters above the bars indicated statistically different ($p$<0.05) (Balasuriya, et al., 2012). (B) Atomic force microscopy (AFM) images of milk fat globules in raw and heating treated milk (Huang, et al., 2023)

Low temperature is a standard practice for preserving milk products, but it also affect the structural and compositional aspects of MFGs/MFGM since milk fat

fractions start to solidify at temperatures lower than 37 ℃ (Sherbon, 1974). A study conducted by Wei, et al. (2021) demonstrated the impact of cold storage temperature and shelf life (4 ℃, −20 ℃ and −80℃ for 30, 60, 90 and 120 days) on the phospholipid composition and fat globule structure in human milk. Quantitative analysis using $^{31}P$ NMR showed a decrease in the total phospholipid of all samples after 120 days of storage. The degradation of phospholipid led to the release of inner triglyceride and subsequent flocculation of MFGs.

In brief, we conclude that different heating intensities affect the MFGs/MFMG structure, lead to the loss of interfacial compositions, influence the elasticity of MFGM, and promote the binding of MFGM with serum proteins. Nevertheless, it is worth noting that heating methods and conditions differ across the referenced studies, including variations in heating facilities, temperature and duration. In addition, the raw materials used for the MFGs/MFGM preparation and investigation also vary, such as goat or bovine milk, raw milk, cream or buttermilk, and human milk. It is evident that heating is not the sole process used in dairy production. Previous researches on the combination of thermal treatments with other dairy processes like homogenization, acidification, and membrane separation have already been reported but are not included in this review (Hansen, et al., 2018; Ren, et al., 2020; Jash & Rizvi, 2022). Consequently, a comprehensive review focusing on the combined effects of these dairy processing units on MFGs/MFGM would be both necessary and beneficial.

*1.3.3.2 Homogenisation*

Homogenisation, first developed in 1899, has become a fundamental process in the dairy industry. This technique reduces the MFGs size by forcing milk through a narrow gap at high velocity, enhancing the stability of milk emulsion. Typically, the temperature and pressure for homogenisation are set as 50−70 ℃ and 10−25 MPa (100−250 bar) to optimize the efficiency and effectiveness of the process (Gösta Bylund, 1995). Apart from reducing the size of MFGs, homogenisation also influences various chemical reactions on the newly formed MFGs, such as enzymatic hydrolysis,

increased susceptibility to Cu ion-induced oxidation, light-induced flavour deterioration, and changes in colour.

In this review, we discuss two main types of homogenization treatments: conventional homogenization (0–100 MPa) and novel high-pressure homogenization (HPH) (>100 MPa). It should be noted that HPH differs from high hydrostatic pressure (HHP). While HHP processes samples in batches and is perceived as a non-thermal processing. HPH is a continuous processing operation. Details on HHP and its applications are further explored in part 3.3.3.3 of this review.

1.3.3.2.1 Conventional homogenisation

- MFGM protein and fatty acid

Previous researches have explored the effect of homogenisation pressure and temperature on the MFGM proteins and fatty acid of milk (Wang, et al., 2019; Reis, et al., 2020). Research conducted by Reis, et al. (2020) highlights that increasing homogenization pressure (20−45 MPa) and preheating temperature (50−70 °C) before homogenization result in a reduction of MFGM proteins, especially CD36, FABP and PAS 6/7. Furthermore, more significant β-LG was observed on the surface of MFGs when subjected to homogenization at higher pressure, while preheating facilitated the interaction between α-LA and MFGM (Wang, et al., 2019). Heterogeneous fatty acids serve as primary sources of volatile compounds in milk. Homogenisation has been reported to induce the degradation of milk composition, particularly lipids, adversely affecting milk flavour. As the homogenisation pressure escalates from 0 bar to 350 bar (at 45 or 65 °C), there is a significant increase in the concentration of methyl butanoate, dimethyl sulphide, dimethyl disulphide and carbon disulphide in milk samples. In comparison, an increase in homogenisation pressure at 80 °C leads to greater formation of methyl ketones (Reis, et al., 2020). In addition, Cohen, Shamay, and Argov-Argaman (2015) have identified a correlation between the sizes of MFGs and the fatty acids/ phospholipids contents within them.

- Crystallization

Apart from the change of structure and compositions, particle size, thermal property, and emulsifying ability of MFGs/MFGM are critical in food application. Studies by Ren, et al. (2020) indicate that homogenisation at pressure of 20, 30, and 40 MPa promotes the crystallisation of MFGs at elevated temperature (20.6 ℃), attributed to the increased presence of saturated lipids in newly formed MFGs.. Compared to control samples, homogenisation inhibits the polymorphic transformation and reduces the β crystals proportion in the MFGs/MFGM (Ren, et al., 2020).

- Creaming

While homogenization enhances the stability of milk and prevents the formation of a top cream layer, the addition of food additives is essential for long shelf life products in commercial products. Research by Lu, et al. (2021) demonstrated that, in comparison to homogenized milk (20 MPa at 53 ℃) without any additives, the incorporation of soybean lecithin efficiently enhanced the storage stability of milk before homogenization. In milk enriched with soybean lecithin, the surface area of MFGs closely resembles that of control raw milk, with fewer serum protein adhering to the MFGM, thereby preserving more native MFGM proteins (Lu, et al., 2021).

1.3.3.2.2 High-pressure homogenisation (HPH)

HPH is an innovative technology employed in liquid food processing that uses high pressure to eliminate pathogenic microorganisms, enhance emulsify stability, and prolong the shelf life of food products (Zamora & Guamis, 2014). Kiełczewska, Ambroziak, Krzykowska, and Aljewicz (2021) compared the effects of HPH (100 MPa, 4-60 ℃) and conventional homogenization (20 MPa, 60 ℃) on the particle size of MFGs, MFGM proteins and phospholipids in untreated raw milk, buttermilk and their mixtures (1:1). The finding indicated a significant increase in SM and a decrease of

PS in samples treated with HPH. Correspondingly, more adsorption of serum proteins was found on the surface of MFGs after HPH treatments. Buttermilk powder has been highlighted as a natural emulsifier for enriching food products with MFGM fragments and serum in the food industry. Further research by Garczewska-Murzyn, Kiełczewska, and Smoczyński (2022) compared the effects of HPH (100MPa at 4, 20, 40, and 60 ℃) and conventional homogenization (20MPa at 60 ℃) on emulsions formed by mixing raw milk with varying concentrations of buttermilk powder (0.3−1.5%, w/v). The study demonstrated that a stable emulsion and colloidal phase were achieved after treatment at 100 MPa/20 ℃, which is attributed to the reduction of volume weighted mean diameter D [4, 3].

### 1.3.4 Non-thermal treatments

The nutrient degradation and sensory decline associated with thermal treatment are well-documented challenges in contemporary dairy processing. These thermal methods often result in the loss of heat-sensitive nutrients, as well as undesirable changes in taste and texture. In response, the food industry has increasingly adopted non-thermal technologies, driven by consumer demand for products that are perceived as natural and minimally processed. Innovative non-thermal techniques include sonication, high hydrostatic pressure (HHP), pulsed electric field (PEF), dielectric barrier discharge plasma (DBD) and ultraviolet radiation. These methods strive to preserve the natural and nutritional qualities of food while ensuring food safety, and can also modify the techno-functionalities of food materials (Sun, et al., 2014). Further research into the effect of non-thermal treatments on the MFGs/MFGM is helpful for preserving heat-sensitive components like phospholipids and glycoproteins.

#### *1.3.4.1 Ultrasound treatment*

Ultrasounds are acoustic waves in the range of 20 kHz and 1 GHz, which are classified into high-intensity (<1 W/cm$^2$) and low-intensity (10−1000 W/cm$^2$ ) based on their intensities (Mason, 1998). Research has shown that ultrasound treatments can

reduce the size of MFGs and serve as an alternative method to traditional homogenization (Chambers, 1937). For instance, MFGs in raw milk samples treated by ultrasound at 35 kJ/L and shear-homogenization at 20 MPa presented similar size distributions. Moreover, more MFGM proteins were retained in ultrasound treated samples compared to shear-homogenization (Liu, et al., 2021).

Ultrasound treatment (20 kHz, 10−50W) facilitates the formation of MFGs-protein complexes, which promotes the acid-gel formation. Moreover, a strong gel was formed due to the denaturation of whey protein and the generation of casein-MFGs complexes (Gregersen, Wiking, & Hammershøj, 2019). In addition, ultrasound processing not only reduced the average particle size of MFGM fragments but also induced the compositional reorganisation on the surface of MFGs. Emulsions stabilised by ultrasound modified MFGM exhibited higher surface tension, enhancing the emulsifying capacity of MFGM (Chen, Sagis, & Sun, 2020).

Model emulsions enriched with MFGM materials have been designed to mimic breast milk, providing critical insights for IF production. For milk powder enriched with MFGs/MFGM ingredients, it is essential that milk or soy proteins envelop the MFGs to ensure a stable emulsion upon rehydration. Ultrasonic treatment has been shown to improve the solubility and emulsifying capacity of these ingredients. For instance, the solubility of MFGM rich in phospholipids (MPL, purchased from Hilmar USA) increased from 36% to 85.88% following ultrasonic treatment (20 kHz, 43 ± 3.4 $W/cm^2$), and the emulsifying stability of mimicking human fat emulsions fortified with ultrasonic treated MPL was significantly improved (Sun, et al., 2022a). Furthermore, ultrasound treatment can influence the thermal behaviour and interfacial properties of MFGs/MFGM ingredients. Research by Sergeev, et al. (2021) on the changes of thermal properties of goat lipids treated by 45 Hz ultrasound for 30 minutes revealed that butter made from ultrasound-treated goat milk exhibited lower crystallization temperature and higher melting enthalpies, due to the formation of β'-form crystals. This is supported by Sun, Roos, and Miao (2024c) who found that raw milk treated

independently or synchronously with ultrasound at 20 kHz and 40 kHz for 15 min induced the disappearance of α-crystals in MFGs/MFGM, with only β-form and β'-form detected. In addition, a significant decrease in the interfacial tension (π) between the air and MFGs/MFGM liquid phase was noted after 20 kHz treatment for 15 minutes.

*1.3.4.2 Supercritical-$CO_2$ (SC-$CO_2$)*

SC-$CO_2$ processing has gained prominence in recent years due to its high efficiency and environmental sustainability. This technique involves exposing a substrate to specific pressure-temperature conditions, transforming it into a supercritical solvent capable of selectively dissolving target compounds from the substrates (Sahena, et al., 2009).

Research into the application of SC-$CO_2$ for purifying lipids/fatty acid was conducted by Friedrich (1984) in the early 1980s, focusing on optimizing the temperature and pressure of SC-$CO_2$ to increase the solubility of soybean oil triglycerides. Buttermilk powder with a good creamy flavor is rich in phospholipids, and is widely used in desserts, ice cream and yogurt processing. The combination of membrane filtration technology and SC-$CO_2$ has been reported to effectively extract phospholipids from buttermilk powder, resulting in a 5-time increase in the phospholipids than the original samples (Spence, Jimenez-Flores, Qian, & Goddik, 2009). This process involved hydrolyzing the buttermilk powder and then being ultrafiltered by 50 kDa membrane, followed by SC-$CO_2$ extraction that enriched the phospholipid content to 56.24 % on a dry matter basis (Barry, Dinan, & Kelly, 2017). Phospholipids are excellent materials for liposome synthesis. A novel approach combing SC-$CO_2$ and ethanol-modified method has facilitated the extraction of phospholipids with a concentration up to 75%. The phospholipids were subsequently used in a venture-based system (Vent-RESS) for the synthesis of liposomes. This system proved effective in encapsulating Vitamins E and C within the MFGM-derived liposomes, serving as models to assess the heating stability and encapsulation

efficiency (Apratim Jash, 2020). Despite these advancements, there remains a gap in research concerning the effects of SC-$CO_2$ on the structural change and specific types of phospholipids.

*1.3.4.3 High hydrostatic pressure (HHP)*

HHP involves generating pressure ranging from 100 to 900 MPa by reducing the volume of treatment chamber or pumping a pressurizing medium into the chamber. HHP applies pressure uniformly and statically to samples without altering their shape (San Martin, Barbosa-Canovas, & Swanson, 2002). This technique has been extensively studied for its effects on the structure and functionalities of MFGs/MFGM.

HHP treatment has been verified to affect the MFGs size, free fatty acid content, the interaction between MFGM and milk proteins, and the creaming ability of MFGs/MFGM in the emulsion. The impact of high pressure (200−500 MPa) and storage (4 ℃) on the particle size, protein distribution, colour, and fatty acid profile of caprine milk was analysed by Kiełczewska, Jankowska, Dąbrowska, Wachowska, and Ziajka (2020). The results showed that high pressure facilitated the agglomeration of MFGs, leading to an increase in particle size of MFGs. Notably, while the fatty acid profile remained stable under pressure, there were observable changes in the colour parameters of the milk.

Furthermore, the polymorphic behaviour of triglycerides, influenced by the types of fatty acid, was also examined under high-pressure conditions. This behaviour significantly affects the melting and crystallization properties of lipids. Vella, et al. (2021) investigated the effects of high pressure on triglyceride polymorphism in milk fat. Small-angel X-ray scattering with pressure up to1430 and 1480 MPa was used to treat and observe the samples. Their results showed that tilted β’ 2L1 and α 3L1 structures were more susceptible to compression under high pressure. In anhydrous milk fat samples, triglyceride remained in a liquid state and predominantly formed α 3L structures after HHP treatment.

*1.3.4.4 Pulsed electric field (PEF)*

PEF is a promising non-thermal treatment increasingly applied in the processing of liquid foodstuffs. The core component of PEF is the high-voltage pulse generator, which produces electric pulses from the rapid discharge of electric energy within a short period of time (Blahovec, Vorobiev, & Lebovka, 2017).

In a comprehensive review, Sharma, Oey, and Everett (2014) summarized studies on the effects of PEF treatment on MFGs/MFGM between 2000 and 2014. This review highlighted significant findings related to changes in MFGs size and interfacial ζ-potential induced by PEF while noting a scarcity of reports on the compositional and structural changes. Transmission electron microscopy (TEM) has been employed to observe the effect of PEF treatment on the surface coverage of MFGM with plasma protein. Notably, PEF-treated milk (20 kV $cm^{-1}$ for 34 μs) exhibited increased adsorption of casein micelles on the interface of MFGs compared to untreated raw milk. The increase in surface hydrophobicity of MFGs/MFGM after PEF treatment samples was further confirmed in subsequent studies (Sharma, Oey, & Everett, 2016). Comparative studies by the same researchers in 2015 found that pre-heating at 55 °C for 24 s more significantly altered the plasma proteins on the surface of MFGs than PEF treatment, indicating that thermal treatment causes more serious surface damage to native MFGs (Sharma, Oey, & Everett, 2015b). Interestingly, xanthine oxidase denaturation was approximately 13% lower in PEF-treated samples compared to those subjected to thermal treatment. Furthermore, Yang, Suwal, Andersen, Otte, and Ahrné (2021) investigated the relationship between the particle size of MFGs and changes in MFGM proteins induced by PEF treatment. It turned out that a more pronounced effect on MFGM proteins was observed in small MFGs after PEF treatment due to significant protein adsorption. Moreover, the phospholipids in MFGs remained unchanged in cream samples treated with PEF (37 kV/cm field strength, 65 °C). Additionally, increased interactions between β-lactoglobulin and MFGM proteins were evidenced by SDS-PAGE results. Another significant advantage of PEF is its ability to maintain

the original biological activities of food components. For instance, PEF-treated cream exhibited similar antiproliferative activity to untreated samples, while pasteurisation induced the loss of antiproliferative activity in cream samples. Further investigation is required to elucidate the specific components responsible for the antiproliferative activity observed in these samples (Xu, Walkling-Ribeiro, Griffiths, & Corredig, 2015).

Additionally, Mohamad, Shah, Sulaiman, Mohd Adzahan, and Aadil (2020) reported that PEF treatment led to a reduction in total saturated fatty acids and polyunsaturated fatty acids in goat milk (1 kHz, 8 μs, electrode gap distance 4.7 mm, chamber diameter 3.5 mm, and flow rate 2.5 L/h), while total monounsaturated fatty acids increased (Mohamad, et al., 2020). Moreover, moderate PEF at intensities (9 and 16 $kV \cdot cm^{-1}$, 30 μs) modified the MFGs structure accompanied by changes in lipase activity and fatty acid (FA) profile (Yang, et al., 2021).

*1.3.4.5 Dielectric barrier discharge (DBD) plasma reactor*

Cold plasma is particularly suitable for treating heat-sensitive food, as it maintains the samples at a relatively low temperature (30-60 ℃) throughout the treatment process (Coutinho, et al., 2018). However, there are scarce studies focused on the effect of DBD treatment on the compositions, structure and functionalities of food. One such study by Kim, et al. (2015) showed that indirect plasma treatment, where plasma is generated near but not in direct contact with the sample, did not alter the concentration of the various fatty acids, except for butyric acid and caprylic acid. Further research by Sarangapani, Ryan Keogh, Dunne, Bourke, and Cullen (2017) found that DBD (60−80 V for 30 min) induced lipid oxidation, leading to the formation of oxidation byproducts, such as ozonides, aldehydes, and carboxylic acids, as identified by FTIR. Meanwhile, hydroperoxides of oleic acid and linoleic acid were detected for the first time by $^{1}H$ NMR, suggesting a fatty acid transformation following the Criegee mechanism after DBD treatment (Sarangapani, et al., 2017).

Ali (2021) investigated the effects of DBD treatment (at 100 V and 1.5 A for duration of 10, 20, 30 and 40 min) on the MFGM, using pasteurization samples (68 ℃ for 30 minutes) as a control. The finding indicated an increase in saturated fatty acids in DBD-treated MFGM samples. Moreover, an interaction between non-membrane proteins and MFGM was evident in DBD-treated samples, as demonstrated by the weak bonding between casein and whey protein. The particle size of MFGs increased with prolonged plasma treatment time, likely due to the accumulation of smaller MFGs on the surface of larger MFGs, forming large aggregates.

### 1.4 Conclusions and future perspectives

The structural, compositional, and tech-functional characteristics of MFGs/MFGM reported in various studies exhibit significant variation, attributable to a complex array of factors. Dairy processing techniques that involve shearing, for instance, have been shown to alter MFGs size and form new membranes, while more intensive treatments can disintegrate the globules into membrane fragments. Conversely, milder techniques such as membrane filtration and various non-thermal treatments may partly preserve the natural state of MFGs/MFGM after processing. The effects of thermal treatments and homogenization on the MFGs/MFGM under diverse conditions have been extensively investigated. This review, however, only broadly addresses the effect of various factors on the lipids, MFGM proteins, thermal properties, and interactions between MFGs/MFGM and serum proteins. There remains a significant need to compile and update knowledge on other functionalities, including emulsification and encapsulation within delivery system. WPC enriched with MFGs/MFGM has already been utilized in infant formula design. The establishment of standardized analytical methods for assessing the compositions of MFGs/MFGM is urgently required, particularly non-invasive techniques that minimize discrepancies caused by sample preparations.

Some researchers have been working on the bioactivities of MFGs/MFGM and attempting to pinpoint the specific compositions responsible for certain bioactivities,

the results have yet to fully determine these relationships. Lab-scale centrifugation or ultracentrifugation, commonly employed in the isolation of MFGs/MFGM materials, may not adequately reflect industrial processes, suggesting a need for research methods that better simulate industrial production. Given the crucial role of tri-layer structure of MFGM in physiological properties, maintaining the natural membrane state during isolation and processing is vital. In summary, the factors affecting the structure, compositions, and techno-functionalities of MFGs/MFGM requires deeper exploration, particularly from an industrial application standpoint, to harness their full potential in food science and nutrition.

**Declaration of competing interest**

All authors declare no conflict of interest.

**Author Contributions**

Yanjun Sun: Conceptualization, Methodology, Writing-original draft, Visualization. Yrjö H. Roos: Supervision, Writing review & editing. Song Miao: Supervision, Conceptualization, Writing-review & editing, Funding acquisition, Project administration.

**Acknowledgements**

The project was founded by 'The China Scholarship Council (No.202008410212)' and 'Teagasc-The Irish Agriculture and Food Development Authority (MDDT1392)'.

**References**

Ali, F. (2021). Nonthermal and thermal treatments impact the structure and microstructure of milk fat globule membrane. *International Journal of Dairy Technology, 0*, 1-10.

Anantawat, V., Loveday, S. M., Singh, H., & Anema, S. G. (2022). Acid gelation of heat-treated recombined milk: Fat globule membrane composition and gelation functionality. *International Dairy Journal, 125*, 105243.

Apratim Jash, A. U., and Syed S.H. Rizvi. (2020). Synthesis of multivitamin-loaded heat stable liposomes from milk fat globule membrane phospholipids by using a supercritical-CO2 based system. *Green Chemistry 22 (16)*, 5345-5356.

Argov-Argaman, N., Glasser, T., Muklada, H., Hadaya, O., Mesilati-Stahy, R., Raz, C., et al. (2021). Lipidome changes, with a focus on phospholipids, due to feeding systems and processing in goat milk. *Food Chemistry, 340*, 127938.

Baars, A., Oosting, A., Engels, E., Kegler, D., Kodde, A., Schipper, L., et al. (2016). Milk fat globule membrane coating of large lipid droplets in the diet of young mice prevents body fat accumulation in adulthood. *British Journal of Nutrition 115*, 1930-1937.

Balasuriya, T. S., Ong, L., Gras, S. L., & Dagastine, R. R. (2012). Changes in morphological and nano-mechanical properties of the milk fat globule membrane during processing. *RSC Advances, 2*, 2384–2394.

Barry, K. M., Dinan, T. G., & Kelly, P. M. (2017). Pilot scale production of a phospholipid-enriched dairy ingredient by means of an optimised integrated process employing enzymatic hydrolysis, ultrafiltration and super-critical fluid extraction. *Innovative Food Science & Emerging Technologies, 41*, 301-306.

Basch, J. J., Greenberg, R., & Farrell, H. M., Jr. (1985). Identification of the milk fat globule membrane proteins. II. Isolation of major proteins from electrophoretic gels and comparison of their amino acid compositions. *Biochimica et Biophysica Acta, 830*, 127-135.

Bauman, D. E., & Griinari, J. M. (2001). Regulation and nutritional manipulation of milk fat: low-fat milk syndrome. *Livestock Production Science, 70*, 15-29.

Baumgard, L. H., Corl, B. A., Dwyer, D. A., Sæbø, A., & Bauman, D. E. (2000). Identification of the conjugated linoleic acid isomer that inhibits milk fat synthesis. *American Journal of Physiology-Regulatory, Integrative and Comparative Physiology, 278*, R179-R184.

Blahovec, J., Vorobiev, E., & Lebovka, N. (2017). Pulsed Electric Fields Pretreatments for the Cooking of Foods. *Food Engineering Reviews, 9*, 71-81.

Blesso, C. N. (2015). Egg phospholipids and cardiovascular health. *Nutrients, 7*, 2731-2747.

Chai, C., Oh, S., & Imm, J. Y. (2022). Roles of Milk Fat Globule Membrane on Fat Digestion and Infant Nutrition. *Food Science of Animal Resources, 42*, 351-371.

Chambers, L. (1937). Sonic homogenization of milk and ice cream mix. *Journal of Dairy Science, 20*, 450-451.

Chen, M., Sagis, L. M. C., & Sun, Q. (2020). Emulsification and dilatational surface rheology of ultrasonicated milk fat globule membrane (MFGM) materials. *LWT, 133*, 110094.

Cheng, W., Liu, H., Shen, Q., Liu, C., Zhou, H., & Luo, J. (2021). A novel approach for modulating the spatial distribution of fat globules in acid milk gel and its effect on the perception of fat-related attributes. *Food Research International, 140*, 109990.

Cilla, A., Diego Quintaes, K., Barberá, R., & Alegría, A. (2016). Phospholipids in Human Milk and Infant Formulas: Benefits and Needs for Correct Infant Nutrition. *Critical Reviews in Food Science and Nutrition, 56*, 1880-1892.

Cohen, B. C., Shamay, A., & Argov-Argaman, N. (2015). Regulation of lipid droplet size in mammary epithelial cells by remodeling of membrane lipid composition—A potential mechanism. *PloS one, 10*, 0121645.

Coutinho, N. M., Silveira, M. R., Rocha, R. S., Moraes, J., Ferreira, M. V. S., Pimentel, T. C., et al. (2018). Cold plasma processing of milk and dairy products. *Trends in Food Science & Technology*, *74*, 56-68.

Daomin, Y., Lina Z., Yixuan, Z., Mengyu, H., Yancong, W., Jun T. and Peng, Z. (2022). Changes in Caprine Milk Fat Globule Membrane Proteins after Heat Treatment Using a Label-Free Proteomics Technique. *Foods, 11*, 2705.

De Bhowmick, G., Guieysse, B., Everett, D. W., Reis, M. G., & Thum, C. (2023). Novel source of microalgal lipids for infant formula. *Trends in Food Science & Technology, 135*, 1-13.

Deeth, H. C. (1997). The role of phospholipids in the stability of milk fat globules. *Australian Journal of Dairy Technology*, *52*, 44–46.

Dewettinck, K., Rombaut, R., Thienpont, N., Le, T. T., Messens, K., & Van Camp, J. (2008). Nutritional and technological aspects of milk fat globule membrane material. *International Dairy Journal, 18*, 436-457.

Dhungana, P., Truong, T., Bansal, N., & Bhandari, B. (2021). A novel continuous method for size-based fractionation of natural milk fat globules by modifying the cream separator. *International Dairy Journal, 125*, 105209.

Douellou, T., Montel, M. C., & Thevenot Sergentet, D. (2017). Invited review: Anti-adhesive properties of bovine oligosaccharides and bovine milk fat globule membrane-associated glycoconjugates against bacterial food enteropathogens. *Journal of Dairy Science, 100*, 3348-3359.

Evers, J. M. (2004). The milkfat globule membrane—methodologies for measuring milkfat globule (membrane) damage. *International Dairy Journal, 14*, 747-760.

Felice, V. D., Owens, R. A., Kennedy, D., Hogan, S. A., & Lane, J. A. (2021). Comparative Structural and Compositional Analyses of Cow, Buffalo, Goat and Sheep Cream. *Foods, 10*, 2643.

Fong, B. Y., Norris, C. S., & MacGibbon, A. K. H. (2007). Protein and lipid composition of bovine milk-fat-globule membrane. *International Dairy Journal, 17*, 275-288.

Fontecha, J., Brink, L., Wu, S., Pouliot, Y., Visioli, F., & Jimenez-Flores, R. (2020). Sources, Production, and Clinical Treatments of Milk Fat Globule Membrane for Infant Nutrition and Well-Being. *Nutrients, 12*, 1607.

Friedrich, J. P., Pryde, E.H. (1984). Supercritical CO2 extraction of lipid-bearing materials and characterization of the products. *Journal of American Oil Chemists Society 61*, 223–228.

Garczewska-Murzyn, A., Kiełczewska, K., & Smoczyński, M. (2022). The influence of buttermilk powder on the stability of emulsion and colloidal phases of

homogenized milk. *European Food Research and Technology, 248*, 2629-2636.

Gösta Bylund, M. S. (1995). *Dairy Processing Handbook*. Lund, Sweden: Tetra Pak Processing Systems AB.

Gregersen, S. B., Wiking, L., & Hammershøj, M. (2019). Acceleration of acid gel formation by high intensity ultrasound is linked to whey protein denaturation and formation of functional milk fat globule-protein complexes. *Journal of Food Engineering, 254*, 17-24.

Guerin, J., Burgain, J., Gomand, F., Scher, J., & Gaiani, C. (2019). Milk fat globule membrane glycoproteins: Valuable ingredients for lactic acid bacteria encapsulation? *Critical Reviews in Food Science and Nutrition, 59*, 639-651.

Hansen, S. F., Hogan, S. A., Tobin, J., Rasmussen, J. T., Larsen, L. B., & Wiking, L. (2020a). Microfiltration of raw milk for production of high-purity milk fat globule membrane material. *Journal of Food Engineering, 276*, 109887.

Hansen, S. F., Nielsen, S. D., Rasmusen, J. T., Larsen, L. B., & Wiking, L. (2020b). Disulfide bond formation is not crucial for the heat-induced interaction between beta-lactoglobulin and milk fat globule membrane proteins. *Journal of Dairy Science, 103*, 5874-5881.

Hansen, S. F., Petrat-Melin, B., Rasmussen, J. T., Larsen, L. B., Ostenfeld, M. S., & Wiking, L. (2018). Placing pasteurisation before or after microfiltration impacts the protein composition of milk fat globule membrane material. *International Dairy Journal, 81*, 35-41.

Heid, H. W., & Keenan, T. W. (2005). Intracellular origin and secretion of milk fat globules. *European Journal of Cell Biology, 84*, 245-258.

Hokkanen, S. P., Partanen, R., Jukkola, A., Frey, A. D., & Rojas, O. J. (2021). Partitioning of the milk fat globule membrane between buttermilk and butter serum is determined by the thermal behaviour of the fat globules. *International Dairy Journal, 112*, 104863.

Holzmüller, W., Gmach, O., Griebel, A., & Kulozik, U. (2016). Casein precipitation by acid and rennet coagulation of buttermilk: Impact of pH and temperature on the isolation of milk fat globule membrane proteins. *International Dairy Journal, 63*, 115-123.

Holzmüller, W., & Kulozik, U. (2016). Technical difficulties and future challenges in isolating membrane material from milk fat globules in industrial settings – A critical review. *International Dairy Journal, 61*, 51-66.

Huang, Y., Wei, T., Chen, F., Tan, C., Gong, Z., Wang, F., et al. (2023). Effects of various thermal treatments on interfacial composition and physical properties of bovine milk fat globules. *Food Research International, 167*, 112580.

Jash, A., & Rizvi, S. S. H. (2022). Heat-stable liposomes from milk fat globule membrane phospholipids for pH-triggered delivery of hydrophilic and lipophilic bioactives. *Innovative Food Science & Emerging Technologies, 79*.

Ji, Y. D., Lee, S. K., & Anema, S. G. (2011). Effect of heat treatments and homogenisation pressure on the acid gelation properties of recombined whole milk. *Food Chemistry, 129*, 463-471.

Jukkola, A., Hokkanen, S., Kämäräinen, T., Partanen, R., Heino, A., & Rojas, O. J. (2019). Changes in milk fat globules and membrane lipids under the shear fields of microfiltration and centrifugation. *Journal of Membrane Science, 573*, 218-225.

Jukkola, A., Partanen, R., Rojas, O. J., & Heino, A. (2018). Effect of heat treatment and pH on the efficiency of micro-diafiltration for the separation of native fat globules from cream in butter production. *Journal of Membrane Science, 548*, 99-107.

Kanno, C., Hattori, H., & Yamauchi, K. (1987). Lipid Composition of Plasma Membranes Isolated from Lactating Bovine MammaryGlan. *Agricultural and Biological Chemistry, 51 (ll)*, 2995-3001.

Keenan, T., Morré, D. J., Olson, D. E., Yunghans, W., & Patton, S. (1970). Biochemical and morphological comparison of plasma membrane and milk fat globule membrane from bovine mammary gland. *The journal of cell biology, 44*, 80-93.

Kiełczewska, K., Ambroziak, K., Krzykowska, D., & Aljewicz, M. (2021). The effect of high-pressure homogenisation on the size of milk fat globules and MFGM composition in sweet buttermilk and milk. *International Dairy Journal, 113*, 104898.

Kiełczewska, K., Jankowska, A., Dąbrowska, A., Wachowska, M., & Ziajka, J. (2020). The effect of high pressure treatment on the dispersion of fat globules and the fatty acid profile of caprine milk. *International Dairy Journal, 102*, 104607.

Kim, H.-J., Yong, H. I., Park, S., Kim, K., Choe, W., & Jo, C. (2015). Microbial safety and quality attributes of milk following treatment with atmospheric pressure encapsulated dielectric barrier discharge plasma. *Food Control, 47*, 451-456.

Lee, H., Padhi, E., Hasegawa, Y., Larke, J., Parenti, M., Wang, A., et al. (2018). Compositional Dynamics of the Milk Fat Globule and Its Role in Infant Development. *Frontiers in Pediatrics, 6*, 313.

Li, S., Delger, M., Dave, A., Singh, H., & Ye, A. (2022). Seasonal Variations in the Composition and Physicochemical Characteristics of Sheep and Goat Milks. *Foods, 11*.

Li, S., Yang, Y., Chen, C., Li, L., Valencak, T. G., & Ren, D. (2021). Differences in milk fat globule membrane proteins among Murrah, Nili-Ravi and Mediterranean buffaloes revealed by a TMT proteomic approach. *Food Research International, 139*, 109847.

Liu, Y., Boeren, S., Zhang, L., Zhou, P., & Hettinga, K. (2021). Ultrasonication retains more milk fat globule membrane proteins compared to equivalent shear-homogenization. *Innovative Food Science & Emerging Technologies, 70*, 102703.

Lopez, C. (2011). Milk fat globules enveloped by their biological membrane: Unique colloidal assemblies with a specific composition and structure. *Current Opinion in Colloid & Interface Science, 16*, 391-404.

Lopez, C., Cauty, C., & Guyomarc'h, F. (2015). Organization of lipids in milks, infant milk formulas and various dairy products: role of technological processes and potential impacts. *Dairy Science and Technology, 95*, 863-893.

Lopez, C., Madec, M.-N., & Jimenez-Flores, R. (2010). Lipid rafts in the bovine milk fat globule membrane revealed by the lateral segregation of phospholipids and heterogeneous distribution of glycoproteins. *Food Chemistry, 120*, 22-33.

Lu, N., Wang, J., Chen, Z., Zhang, X., Chen, C., & Wang, S. (2021). The effect of adding phospholipids before homogenization on the properties of milk fat globules. *LWT, 146*, 111659.

Mansson, H. L. (2008). Fatty acids in bovine milk fat. *Food & Nutrition Research, 52*, 1821.

Marsh, D. (2006). Elastic curvature constants of lipid monolayers and bilayers. *Chemistry and Physics of Lipids, 144*, 146-159.

Mason, T. (1998). Power ultrasound in food processing–the way forward. *Ultrasound in food processing*, 105-126.

Mather, I. H. (2000). A Review and Proposed Nomenclature for Major Proteins of the Milk-Fat Globule Membrane. *Journal of Dairy Science, 83*, 203–247.

Mohamad, A., Shah, N. N. A. K., Sulaiman, A., Mohd Adzahan, N., & Aadil, R. M. (2020). Impact of the pulsed electric field on physicochemical properties, fatty acid profiling, and metal migration of goat milk. *Journal of Food Processing and Preservation, 44*, 14940.

Obeid, S., Guyomarc'h, F., David-Briand, E., Gaucheron, F., Riaublanc, A., & Lopez, C. (2019). The phase and charge of milk polar lipid membrane bilayers govern their selective interactions with proteins as demonstrated with casein micelles. *Journal of Colloid and Interface Science, 534*, 279-290.

Obeid, S., Guyomarc'h, F., Tanguy, G., Leconte, N., Rousseau, F., Dolivet, A., et al. (2020). The adhesion of homogenized fat globules to proteins is increased by milk heat treatment and acidic pH: Quantitative insights provided by AFM force spectroscopy. *Food Research International 129*, 108847.

Perfield, J. W., 2nd, Lock, A. L., Griinari, J. M., Saebo, A., Delmonte, P., Dwyer, D. A., et al. (2007). Trans-9, cis-11 conjugated linoleic acid reduces milk fat synthesis in lactating dairy cows. *Journal of Dairy Science, 90*, 2211-2218.

Price, N., Fei, T., Clark, S., & Wang, T. (2020). Application of zinc and calcium acetate to precipitate milk fat globule membrane components from a dairy by-product. *Journal of Dairy Science, 103*, 1303-1314.

Ramazi, S., & Zahiri, J. (2021). Posttranslational modifications in proteins: resources, tools and prediction methods. *Database (Oxford), 2021*.

Raza, G. S., Herzig, K. H., & Leppaluoto, J. (2021). Invited review: Milk fat globule membrane-A possible panacea for neurodevelopment, infections, cardiometabolic diseases, and frailty. *Journal of Dairy Science, 104*, 19649.

Reinhardt, T. A., & Lippolis, J. D. (2006). Bovine milk fat globule membrane proteome. *Journal of Dairy Research, 73*, 406-416.

Reis, M. G., Harris, P., Berry, C., Nguyen, H., Maclean, P., & Weeks, M. (2020). Tracking changes in volatile components and lipids after homogenisation and thermal processing of milk. *International Dairy Journal, 103*, 104624.

Ren, Q., Li, Q., Liu, H., & Ma, Y. (2020). Thermal and storage properties of milk fat globules treated with different homogenisation pressures. *International Dairy Journal, 110*, 104725.

Sahena, F., Zaidul, I. S. M., Jinap, S., Karim, A. A., Abbas, K. A., Norulaini, N. A. N., et al. (2009). Application of supercritical CO2 in lipid extraction – A review. *Journal of Food Engineering, 95*, 240-253.

San Martin, M. F., Barbosa-Canovas, G. V., & Swanson, B. G. (2002). Food processing by high hydrostatic pressure. *Critical Reviews in Food Science and Nutrition, 42*, 627-645.

Sarangapani, C., Ryan Keogh, D., Dunne, J., Bourke, P., & Cullen, P. J. (2017). Characterisation of cold plasma treated beef and dairy lipids using spectroscopic and chromatographic methods. *Food Chemistry, 235*, 324-333.

Senorans, M., Gallo, V., Calvo, M. V., & Fontecha, J. (2023). Lipidomic and Proteomic Profiling of the Milk Fat Globule Membrane from Different Industrial By-Products of the Butter and Butter Oil Manufacturing Process. *Foods, 12*(4), 750.

Sergeev, A., Shilkina, N., Motyakin, M., Barashkova, I., Zaborova, V., Kanina, K., et al. (2021). Anhydrous fat crystallization of ultrasonic treated goat milk: DSC and NMR relaxation studies. *Ultrasonics Sonochemistry, 78*, 105751.

Sharma, P., Oey, I., & Everett, D. W. (2014). Effect of pulsed electric field processing on the functional properties of bovine milk. *Trends in Food Science & Technology, 35*, 87-101.

Sharma, P., Oey, I., & Everett, D. W. (2015). Interfacial properties and transmission electron microscopy revealing damage to the milk fat globule system after pulsed electric field treatment. *Food Hydrocolloids, 47*, 99-107.

Sharma, P., Oey, I., & Everett, D. W. (2016). Thermal properties of milk fat, xanthine oxidase, caseins and whey proteins in pulsed electric field-treated bovine whole milk. *Food Chemistry, 207*, 34-42.

Sherbon, J. W. (1974). Crystallization and fractionation of milk fat. In J. o. t. A. O. C. Society (Ed.), *Symposium "Milk Lipids," AOCS Fall Meeting* (Vol. 51, pp. 22-25). Ottawa, Ontario, Canad.

Singh, H. (2006). The milk fat globule membrane—A biophysical system for food applications. *Current Opinion in Colloid & Interface Science, 11*, 154-163.

Smoczyński, M., Staniewski, B., & Kiełczewska, K. (2014). Composition and Structure of the Bovine Milk Fat Globule Membrane—Some Nutritional and Technological Implications. *Food Reviews International, 28*, 188-202.

Spence, A. J., Jimenez-Flores, R., Qian, M., & Goddik, L. (2009). Phospholipid enrichment in sweet and whey cream buttermilk powders using supercritical fluid extraction. *Journal of Dairy Science, 92*, 2373-2381.

Sun, Y., Chen, J., Zhang, S., Li, H., Lu, J., Liu, L., et al. (2014). Effect of power ultrasound pre-treatment on the physical and functional properties of

reconstituted milk protein concentrate. *Journal of Food Engineering, 124*, 11-18.

Sun, Y., Liu, Z., Li, H., Li, S., Mo, B., & Lv, J. (2017). Functionality of milk protein concentrate 80 with emulsifying salts and its applications in analogue cheeses. *International Journal of Food Properties, 20*, 2594-2607.

Sun, Y., Roos, Y. H., & Miao, S. (2022b). Changes in Milk Fat Globules and Membrane Proteins Prepared from pH-Adjusted Bovine Raw Milk. *Foods, 11*, 4107.

Sun, Y., Roos, Y. H., & Miao, S. (2024c). Comparative study of interfacial properties and thermal behaviour of milk fat globules and membrane prepared from ultrasonicated bovine milk. *Ultrasonics Sonochemistry, 102*, 106755.

Sun, Y., Yu, X., Hussain, M., Li, X., Liu, L., Liu, Y., et al. (2022a). Influence of milk fat globule membrane and milk protein concentrate treated by ultrasound on the structural and emulsifying stability of mimicking human fat emulsions. *Ultrasonics Sonochemistry, 82*, 105881.

Thum, C., Roy, N. C., Everett, D. W., & McNabb, W. C. (2021). Variation in milk fat globule size and composition: A source of bioactives for human health. *Critical Reviews in Food Science and Nutrition* 1-27.

Toral, P. G., Gervais, R., Hervás, G., Létourneau-Montminy, M. P., & Frutos, P. (2020). Relationships between trans-10 shift indicators and milk fat traits in dairy ewes: Insights into milk fat depression. *Animal Feed Science and Technology, 261*, 114389.

van Nieuwenhuyzen, W., & Tomás, M. C. (2008). Update on vegetable lecithin and phospholipid technologies. *European Journal of Lipid Science and Technology, 110*, 472-486.

Vella, J., Hemar, Y., Gu, Q., Wu, Z. R., Li, N., & Söhnel, T. (2021). In-situ SAXS investigation of high-pressure triglyceride polymorphism in milk cream and anhydrous milk fat. *LWT, 135*, 110174.

Walter, L., Shrestha, P., Fry, R., Leury, B. J., & Logan, A. (2020). Lipid metabolic differences in cows producing small or large milk fat globules: Fatty acid origin and degree of saturation. *Journal of Dairy Science, 103*, 1920-1930.

Wang, C., Qiao, X., Gao, Z., Jiang, L., & Mu, Z. (2021a). Advancement on Milk Fat Globule Membrane: Separation, Identification, and Functional Properties. *Front in Nutrition, 8*, 807284.

Wang, M., Cao, C., Wang, Y., Li, H., Li, H., & Yu, J. (2021b). Comparison of bovine milk fat globule membrane protein retention by different ultrafiltration membranes using a label-free proteomic approach. *LWT, 144*, 111219.

Wang, X., Wei, W., Wu, R., Zhu, X., Ren, F., Liu, L., et al. (2022). Scientific Consensus on Milk Fat Globule Membrane and Its Ingredients. *Journal of Chinese Institute of Food Science and Technology*, 1-6.

Wang, Y., Liu, M., Qu, X., Wang, S., Ma, Z., Zhang, R., et al. (2019). Changes in the fat globule membrane protein components of pasteurized milk caused by different homogenization conditions determined using a label-free proteomic approach. *LWT, 115*, 108430.

Wei, T., Huang, Y., Weng, C., Chen, F., Tan, C., Liu, W., et al. (2023). Lipid rafts may affect the coalescence of milk fat globules through phase transition after thermal treatment. *Food Chemistry, 399*, 133867.

Wei, W., Cheng, J., Yang, J., Chen, C., Jin, Q., Song, J., et al. (2021). Phospholipid composition and fat globule structure change during low temperature storage of human milk. *LWT, 150*, 1-7.

Wiking, L., Gregersen, S. B., Hansen, S. F., & Hammershøj, M. (2022). Heat-induced changes in milk fat and milk fat globules and its derived effects on acid dairy gelation – A review. *International Dairy Journal, 127*, 105213.

Xu, S., Walkling-Ribeiro, M., Griffiths, M. W., & Corredig, M. (2015). Pulsed electric field processing preserves the antiproliferative activity of the milk fat globule membrane on colon carcinoma cells. *Journal of Dairy Science, 98*, 2867-2874.

Yang, M., Deng, W., Cao, X., Wang, L., Yu, N., Zheng, Y., et al. (2020). Quantitative Phosphoproteomics of Milk Fat Globule Membrane in Human Colostrum and Mature Milk: New Insights into Changes in Protein Phosphorylation during Lactation. *Journal of Agricultural and Food Chemistry, 68*, 4546-4556.

Yang, S., Suwal, S., Andersen, U., Otte, J., & Ahrné, L. (2021). Effects of pulsed electric field on fat globule structure, lipase activity, and fatty acid composition in raw milk and milk with different fat globule sizes. *Innovative Food Science & Emerging Technologies, 67*, 102548.

Zamora, A., & Guamis, B. (2014). Opportunities for Ultra-High-Pressure Homogenisation (UHPH) for the Food Industry. *Food Engineering Reviews, 7*, 130-142.

Zhang, M., Xing, Z., Huang, Q., & Han, L. (2021). Effect of conjugated linoleic acid supplementation on fat globule size in raw milk. *International Dairy Journal, 115*, 1-7.

Zheng, S., Wang, M., Yang, F., Li, H., Li, H., & Yu, J. (2020). Changes in bovine milk fat globule membrane protein components of cream caused by different extent of churning using a label-free proteomic approach. *LWT, 134*, 110058.

# CHAPTER TWO

## Changes in milk fat globules and membrane proteins prepared from pH-adjusted bovine raw milk

Chapter 2 was published in:

Sun, Y., Roos, Y. H., & Miao, S. (2022). Changes in Milk Fat Globules and Membrane Proteins Prepared from pH-Adjusted Bovine Raw Milk. *Foods, 11*, 4107.

Author Contributions: Conceptualization, YanJun Sun and Song Miao; Data curation, YanJun Sun; Formal analysis, YanJun Sun; Funding acquisition, Song Miao; Investigation, YanJun Sun; Methodology, YanJun Sun; Project administration, Song Miao; Supervision, Yrjö H. Roos and Song Miao; Validation, YanJun Sun; Visualization, YanJun Sun; Writing – original draft, YanJun Sun; Writing – review & editing, Yrjö H. Roos and Song Miao. All authors approved publication of the manuscript.

**Abstract**

Milk fat globules (MFGs) with tri-layer biological membrane structure and their com-positions are gaining more interest for the physiological benefits. In this study, the changes of MFGs and milk fat globule membrane (MFGM) proteins after cream separation from different pH bovine raw milk were investigated. Raw milk samples were adjusted to pH 5.30 and 6.30 using citric acid at 25℃. The effect of pH and centrifugation on the structure of MFGs were evaluated by means of particle size, ζ-potential and confocal laser scanning microscopy (CLSM). Sodium dodecyl sulfate-polyacrylamide gel electrophoresis (SDS-PAGE) was used to analyze the proteins in the obtained fractions. It was found that both pH and centrifugation could affect the particle size of all samples. As the volume distribution (Dv) (Dv (10), Dv(50) and Dv (90)) decreased, the corresponding specific surface area (SSA) increased and span and uniformity values showed the same trend. The decrease in ζ-potential of MFG correlated with the Dv(50) which was further confirmed by CLSM observation. More amount of butyrophilin (BTN) and periodic acid Schiff 6/7 (PAS 6/7) lost in cream samples at pH 5.30. The findings could provide valuable knowledge for the application of MFGs in the food industry since their structures and compositions could affect their potential functional and physiological properties.

**Keywords:** Milk fat globules; Membrane proteins; Compositions; structure

## 2.1. Introduction

Bovine milk is an O/W emulsion at 37 °C or above in which lipids are present in the state of microscopic globules called milk fat globules (MFGs). Approximately 95% of MFGs are comprised of heterogeneous triglycerides, which locate in the inner core of MFGs. Milk fat globule membranes (MFGMs) enclose MFGs in a three-layer biological membrane (Liao, et al., 2011). MFGMs have gained much interest due to their multilayer structure and variety amounts of polar lipids and membrane proteins. MFGM acts as a natural emulsifying agent, preventing the flocculation and coalescence of the MFGs in milk (Singh & Gallier, 2017). Besides, it could protect the fat against enzymatic action.

The MFGM proteins account for approximately 1–4% of the total protein fraction in milk (Liao, et al., 2011) but 25–70% of the MFGM compositions. Up-to-date proteomic techniques, including two-dimensional gel electrophoresis and mass spectrometry, revealed over 100 MFG-associated proteins (Caroline Vanderghem 2010). Many of these proteins present at the interface of MFGM and the aqueous phase are heavily glycosylated. Most studies have focused on eight major proteins: periodic acid Schiff III (PAS III), butyrophilin (BTN), cluster of differentiation 36 (CD 36), mucin 1 (MUC 1), the redox enzyme xanthine oxidase/dehydrogenase (XO/XDH), lactadherin or periodic acid Schiff 6/7 (PAS 6/7), adipophilin (ADPH) and fatty acid binding protein (FABP) (Fong, et al., 2007b; Liao, et al., 2011; Holzmüller, et al., 2016h). About 40% of the MFGM proteins are glycoproteins, and XO/XDH constitutes 12–13% of the total. Each of the other proteins in MFGM is at or below 5% (Gorewit, 2002; Mana, et al., 2004).

MFGM proteins have been reviewed for their bioactivity and positive effects on defense mechanisms for breastfed infants. Research has demonstrated that some MFGM glycoproteins have been shown to protect immature infants against gut-derived pathogens (Timby, et al., 2015; Lopez, et al., 2017b). BTN, lactadherin and MUC1 in both the human and the bovine present antimicrobial effects(Peterson,

Patton, & Hamosh, 1998). Defatted bovine MFGM fractions, including proteins and glycoproteins, were reported to inhibit *E.coli* O157:H7 strains adhering to HT-29 cells. Their result also showed that in vitro, breast cancer cell lines could be inhibited by FABP at extremely low concentrations (Ross, 2016). MUC1 may play immune-protective roles in the suckling neonate by binding to and sequestering pathogenic microorganisms within the gut lumen. Mana et al. treated C57BL/6 mice with BTN either before or after immunization with oligodendrocyte glycoprotein. Their results showed that experimental autoimmune encephalomyelitis associated with multiple sclerosis can be prevented or suppressed by BTN (Mana, et al., 2004; Spitsberg, 2005).

It is assumed that the compositions and structure of MFGs change during secretion, storage, isolation and application. The MFG structure was affected by different isolation methods and conditions. Holzmüller et al. (Holzmüller & Kulozik, 2016d) reviewed the most advancing front in the MFGs composition separation and respective results. Research on the compositional and structural variation between MFGs was evaluated and consolidated. In the end, they suggested a new definition of MFGM proteins regarding the isolation method. Effect of different unit operations used in the processing on the MFGs (e.g., agitation, homogenization, heating treatment, concentration, drying and freezing.) have been investigated (Murthy, Guyomarc'h, & Lopez, 2016; Lopez, Blot, Briard-Bion, Cirie, & Graulet, 2017a; Singh, et al., 2017).

Acidification-induced coagulation of milk protein has been extensively used in the dairy industry. In order to reduce the loss of MFGM proteins into the casein curd, Holzmüller et al. investigated the effects of buttermilk's pH, temperature and preheating on the rennet- and acid-induced coagulation of buttermilk (Holzmüller, Gmach, Griebel, & Kulozik, 2016a). According to Lopez et al., the microstructure and rheology of emulsions, as well as the stability of lipid droplets coated by MFGM, were shown to be pH-dependent (Lopez, et al., 2017b). MFGM-rich emulsions were prepared from butter serum using a process described in Gassi et al.'s study (Gassi, et

al., 2016). Under pH 5.5, lipid droplets aggregated and gels formed in the emulsions, which could affect the droplets' microstructures (Lopez, et al., 2017b).

Commercial MFGM products are usually made from dairy by-products, including whey and buttermilk. Membrane separation and cream washing are the two most typical operations in MFG compositions preparation. Membrane filtration systems are being exploited by the dairy industry for the fractionation of milk proteins. Because milk-fat-rich dairy fluid contributes to membrane fouling, skim milk is frequently utilized for membrane filtration. Higher cross-flow velocities, which produce a higher shear and transmembrane pressure (TMP) and permeate flux, could minimize fouling and prevent particle deposition. In addition, interactions between MFGM components and the size similarity with casein micelles remain problems on which some researchers are still working. Cream separator is the easiest way to separate milk into cream and skimmed milk. Before the membrane treatment, cream separation is a commonly used method to concentrate the MFGs compositions from either whey or buttermilk.

Dairy companies have been working on preparing natural MFGs and their compositions with more intact structures. Raw milk is now considering the original material to isolate MFGs because most MFGs in whey or buttermilk are fragments. The most stable and best-working pH for rennet is 5.30–6.30. Casein is a group name for the mixture of β, α and κ-casein (CN) which starts to precipitate at pH 5.30 (De Kruif, 1999). However, just several studies are available on the effect of pH on MFGs and their membranes compositions before and after cream separation (Sharma, et al., 2015b; Jukkola, Partanen, Rojas, & Heino, 2016b; Singh, et al., 2017). Two of the commonly used pH conditions in dairy processing, with pH values of 6.30 and 5.30, were investigated in this research. Furthermore, it is still unclear how to differentiate MFGs from MFGM damage, as well as how proteins are released during MFGM fragment disruptions.

Therefore, this study examines the changes in MFGs and MFGM proteins during cream separation from bovine milk at different pH conditions. The physicochemical properties and the microstructure of MFGs and MFGM proteins before and after cream separation are investigated. Meanwhile, the results are discussed in comparison with untreated raw milk. This study could provide technical information for a better understanding of the effect of dairy operation units on the structure and composition changes of MFGs and MFGMs. This is crucial for future studies on the physiological properties of MFGs and related compositions.

## 2.2. Materials and Methods

### 2.2.1. Materials

Raw bovine milk (fat 4.08 ± 0.02%, protein 3.57 ± 0.01%, dry matter 13.03 ± 0.02%, pH 6.74 ± 0.04) was collected from the Teagasc dairy herd (Moorepark, Fermoy, Co. Cork, Ireland). The raw bovine milk was untreated by any other unit operation except for the rapid chilling from 37 to 4 °C with a plate heat exchanger (UK Exchangers Ltd., Buckinghamshire, UK).

Chemicals for gel electrophoresis were bought from Thermo Scientific Inc. (Thermo Fisher Scientific Inc., Cork, Ireland). Food grade citric acid was purchased from Maven Wholefoods (Maven Wholefoods Ltd, Ramsgate, UK). All solutions were prepared using MilliQ water except as otherwise noted.

### 2.2.2 Preparation of Samples

Centrifugal separation was performed using a disk bowl centrifugal separator (FT 15 Disc Bowl Centrifuge, Armfield co., Ringwood, UK) equipped with 19 disks. Firstly, 3 batches of raw milk collected from a 4 °C refrigerator, each of 5 kg, were preheated to 25–30 °C in a water bath (GFL 1012, Gesellschaft fuer Labortec, Burgwedel, Germany). Before the raw milk was separated into cream and skim fractions by a centrifugal separator, 2 batches of 5 kg raw milk were adjusted to pH

5.30 and 6.30, respectively. Citric acid solution (30%, w/w) was used to acidify the pH of milk. During the whole acidification treatment, the raw milk was stirred at the constant speed of 600 rpm to ensure the full dispersion of citric acid and avoid the protein denaturation. Batches of pH 6.74 ± 0.04 were taken as the control reference. Secondly, we continued to heat all batches of raw milk to 50–55 °C and incubated them during the whole separation process. The skim milk phase was added back into the separator one more time to maximally defat the skim milk. The cream and skim milk phases of each batch were collected separately and kept at 4 °C before analysis. The collected samples were named 6.74 R (raw milk pH 6.74), 6.30 R (raw milk pH 6.30), 5.30 R (raw milk pH 5.30), 6.74 C (cream pH 6.74), 6.30 C (cream pH 6.30), 5.30 C (cream pH 5.30), 6.74 S (skim milk pH 6.74), 6.30 S (skim milk pH 6.30) and 5.30 S (skim milk pH 5.30). Throughout the heating and pH adjustment process, all batches of samples were stirred gently to avoid part denaturation of the proteins induced by uneven temperature and excessive acidification, and 0.02% (*g*/*g*) azide sodium was added to prevent microbiological growth. For each treatment, the material preparation procedures were repeated three times.

### 2.2.3. Compositions Analysis

Fat, protein and non-fat solids (SNFs) were analyzed with DairySpec FT‑15 (Bentley Instruments Inc., Chaska, MN, USA). 30 mL of liquid sample was mixed thoroughly before analysis to avoid uneven sampling. All samples from the 4 °C storage were preheated to 25 °C in a water bath. For fat content analysis, cream samples needed to be diluted 10 times with MilliQ water. After the dilution of cream samples, the protein content is close to the detection limit (0-50%) of DairySpec FT-15, so that Kjeldahl method (ISO, 2001) was used to quantitatively analyze the protein content of cream samples (N × 6.38).

### 2.2.4. Particle Size Analysis

Particle size distributions of different pH samples were measured using a Mastersizer 3000 (Malvern Instruments, Malvern, UK) equipped with a laser light scattering. The refractive index for milk fat and water was set to 1.456 and 1.333, respectively. Particle sizes were recorded after at least 30 s of stabilization after adding samples to the measurement device. The amount of samples depends on if the obscuration could reach the range of 3–20% (Michalski, Briard, & Michel, 2001; Holzmüller, et al., 2016h). The data were calculated according to Mie theory.

Samples were analyzed 3 times, and the data are expressed as volume distributions. Dv (10) and Dv (90) stand for the size of particles below which 10%/90% of the sample lies. Dv (50) means the size in microns at which 50% of the sample is smaller and 50% is larger, also known as the median of the volume distribution. Span is the measurement of the width of the distribution. The narrower the distribution, the smaller the span becomes. Uniformity is a measure of the absolute deviation from the median. Uniformity could demonstrate the degree of particle size distribution and the gradient of the distribution curve (Mercan, Sert, & Akın, 2018). The value of the specific surface area (SSA) of all samples was calculated as the surface area of the particles per unit weight. The equation is as follows:

$$SSA = 6/pD\ \ [3,2] \qquad (2\text{-}1)$$

where p is the particle density, and D [3, 2] is the surface-weighted mean.

### 2.2.5. Zeta (ζ) Potential

The ζ-potential, as an indicator for the change of the milk fat globule surface, was analyzed by a dynamic light scattering instrument (Nano‐ZS, Malvern Instruments Ltd., Worcestershire, UK) (Michalski, et al., 2001). The Z sizer software version 7.12 (Malvern Instruments Ltd.) was used to collect and analyze data. ζ-potential is

evaluated by measuring the electrophoresis mobility and then calculated by the Henry equation. The Henry equation is:

$$U_E = 2\varepsilon z f(\mathrm{Ka})/3\eta \qquad (2\text{-}2)$$

where: z: ζ-potential; $U_E$ : Electrophoretic mobility; ε: Dielectric constant; η: Viscosity; *f*(Ka): Henry's function, in this case, is 1.5 and is referred to as the Smoluchowski approximation since the double layer κ-1 of MFGs (around 1.1 nm) is smaller than their radius (Van Oss, 1996).

The electrophoretic mobility is obtained by performing an electrophoresis experiment on the sample and measuring the velocity of the particles using laser Doppler velocimetry. Samples were diluted by MilliQ water and analyzed in a Malvern Dip Cell at 25 °C. The requirement that ζ-potential tests should be performed on diluted dispersion, which modifies the samples' structural characteristics, is a drawback. Additionally, dilution times and diluent types have a significant impact on the outcomes. In order to reduce the diluent-type effect, MilliQ water was used as the diluent. In preliminary experiments, the effect of MilliQ water dilution times (50, 100 and 1000 times) on the ζ-potential was tested, and there was no significant difference between 100 and 1000 times. Thus, all samples were diluted 100 times in this research, and a 2-min equilibrium time was allowed before each measurement. Three readings were collected from each sample.

### 2.2.6. Sodium Dodecyl Sulphate Polyacrylamide Gel Electrophoresis (SDS–PAGE)

SDS-PAGE was conducted according to the method described by Ye, A. et al. with revised (Ye, Singh, Taylor, & Anema, 2004b).

A Mini–PROTEIN Tetra cell was used for the protein analysis (Bio-Rad, Laboratories, inc. USA). Proteins in the raw milk, skim milk and cream were analyzed by reducing SDS–PAGE. Under reducing conditions, both non-covalently–linked and

disulfide-linked complexes were dispersed and migrated into the resolving gel. The NuPAGE MOPS SDS Running Buffer (20×; 50 mM MOPS, 50 mM Tris Base, 0.1% SDS, 1 mM EDTA, pH 7.7) was purchased from Thermo Fisher Scientific Inc., which is used with NuPAGE Novex Bis-Tris Gels (Thermo Fisher Scientific Inc., Cork, Ireland) to resolve mid-size proteins. For electrophoresis, dilute this buffer to 1× with MilliQ water. The NuPAGE Antioxidant (Thermo Fisher Scientific Inc., Cork Ireland) was used to avoid reoxidization.

MilliQ water was used to dilute the samples to a protein concentration of 40 μg/mL, then mixed with 4× NuPAGE LDS sample buffer (106 mM Tris–HCl, 141 mM Tris Base, 2% LDS, 10% glycerol, 0.51 mM EDTA, 0.22 mM SERVA Coomassie blue G250, 0.175 mM phenol red, pH 8.5). The NuPAGE Reducing Agent (10×; Thermo Fisher Scientific Inc., Cork, Ireland) contained 500 mM dithiothreitol (DTT) and was added to the samples at least one hour before loading the samples to prevent reoxidation during storage and producing inconsistent results.

A criterion 12% NuPAGE Novex Bis-Tris Gels (Thermo Fisher Scientific Inc., Cork, Ireland) was used to separate proteins. All samples were heated to 70 °C and inoculated for 5 min to denature the proteins. Before being loaded into the gels, denatured samples needed to cool down to room temperature and centrifuged. A marker with a molecular weight between 10–200 kDa (Thermo Fisher Scientific Inc., Ireland) was used.

Gels were run at 120 V for 45 min and then dyed the proteins with Coomassie blue for more than 60 min with gentle shaking. A solution containing 45% ethanol and 5% acetic acid was used to destain the gels. After being destained for 50 min, the solution was changed to remove the stain overnight. Typical MFGM proteins (PAS 6/7, BTN and XO) and milk serum proteins (α-LA, β-LG and caseins) were selected to relatively quantify the analysis. The relative density of representative proteins was analyzed using ImageJ software 1.36 b (Wayne Rasband, National Institutes of Health, Bethesda, USA) and normalized to 100%.

### 2.2.7. Confocal Laser Scanning Microscopy (CLSM)

CLSM could be used to qualitatively analyze different types of proteins adsorbed on the surface of MFGs, which demonstrates the effect of treatment on the reconstruction of protein and fat globules. Non-polar lipids, which were mostly triglyceride, were labeled with Nile Red (9‑ (diethylamino)‑5 H‑benzo[*a*]phenoxazin‑5‑one, Sigma–Aldrich®, Merck Life Science Ltd., Cork, Ireland), and serum protein and glycoproteins with fluorescent Fast Green (FCF; N‑ethyl‑N‑[4‑[[4‑[ethyl[(3‑sulfophenyl)methyl]amino]phenyl](4‑hydroxy‑2‑sulfophenyl)methylene]‑2,5‑cyclohexadien‑1‑ylidene]‑3‑sulfo‑benzenemethanaminium, disodium salt, Cayman Chemical, Ann Arbor, Michigan, USA) and wheat germ agglutinin (WGA; Alexa Fluro® 488 conjugate, Invitrogen, Ltd., Paisley, Europe), respectively (Lopez, Madec, & Jimenez-Flores, 2010a; Jukkola, Partanen, Rojas, & Heino, 2018a). Considering the low fat content of the skim milk, only the raw milk and cream samples (80 μL) were dual‑stained with a 10 μL mixture of Nile red (0.1%, *w*/*v*, in polyethylene glycol‑200) and FCF (0.1%, w/v, in distilled water; FCF: Nile red = 3:1 *v*/*v*). In addition, WGA (50μL, 1 mg/mL in PBS) was mixed with Nile red in a proportion of 1:1 (*v*/*v*). All dyed samples were kept in the dark for 30 min at room temperature to ensure complete staining. The proportion between the sample and stain was optimized in the pre-experiment to take account of the variation of pH and incomplete dyeing.

Leica TCS SP5 microscope (Leica Microsystems GmbH, Wetzlar, Germany) was used to detect at room temperature (25 ± 2 °C). Nile red, FCF and WGA were excited using a He‑Ne laser, and emission wavelengths were detected between 565–625 nm, 632–719 nm and 493–550 nm, respectively. A 63×oil‑immersion lens was used to observe the samples. Two channels—FCF or WGA channel 1 and Nile red channel 2—were used for CLSM observation. Dual-stain images were obtained by merging images produced in 2 different channels. No less than 10 images were recorded for each sample. Of all the images, the representative 1 for each experiment was chosen.

Leica application suite X (3.7.5.24914; Leica Microsystem CMS GmbH, Wetzlar, Germany) was used for image processing and analysis. Two-dimensional images presented a resolution of 512 × 512 pixels, and a scaling factor was used to convert the pixel scale values into micrometers.

### 2.2.8. Statistical Analysis

There was triplication of each experiment. Each value represents the mean of at least 3 measurements, and values are expressed as means ± standard deviations. A 1-way ANOVA was used to calculate significant differences (95.0% confidence level) between the samples using Minitab 17 Statistical Software (Minitab Inc. State College, PA, USA).

## 2.3. Results and discussion

### 2.3.1. Composition Analysis

The fat, protein and SNF contents of all samples are shown in Table 2-1. The amount of protein included serum proteins and MFGM proteins. After cream separation, the fat in all cream samples was between 39.90–40.5% ignoring the pH variation, but the protein content significantly varied with different pH values. 6.30 C had the most proteins (2.01 ± 0.02%), followed by 5.30 C and 6.74 C (1.76 ± 0.03% and 1.50 ± 0.01%). There was no significant difference in the amount of fat, proteins and SNF in raw milk samples ($p > 0.05$) as a function of pH decrease. For skim milk samples, 6.74 S and 6.30 S presented a similar protein amount, while 5.30 S had a higher content of fat and protein. From the data analysis above, we could speculate that the pH 5.30 condition was the main reason for the difference. The pH 5.3 condition is close to the pI of some proteins. Partial aggregates of proteins in raw milk are easy to get into the skim milk phase during the cream separation process.

**Table 2-1.** Composition analysis of raw milk, skim milk and cream samples at different pH.

| Samples | Fat (w/w, %) | Protein (w/w, %) | SNF (Solid Non-Fat; w/w, %) |
|---|---|---|---|
| 6.74 R | 4.85 ± 0.04 [a] | 3.55 ± 0.00 [a] | 12.36 ± 0.10 [a] |
| 6.30 R | 4.83 ± 0.02 [a] | 3.66 ± 0.04 [a] | 12.33 ± 0.12 [a] |
| 5.30 R | 4.90 ± 0.01 [a] | 3.63 ± 0.00 [a] | 12.23 ± 0.01 [a] |
| 6.74 S | 0.14 ± 0.00 [b] | 3.74 ± 0.03 [b] | 12.79 ± 0.06 [a] |
| 6.30 S | 0.23 ± 0.02 [a] | 3.76 ± 0.05 [b] | 12.84 ± 0.07 [a] |
| 5.30 S | 0.27 ± 0.01 [a] | 3.82 ± 0.01 [a] | 12.76 ± 0.02 [a] |
| 6.74 C | 40.50 ± 0.80 [a] | 1.50 ± 0.01 [c] | 0.40 ± 0.01 [a] |
| 6.30 C | 40.40 ± 1.02 [b] | 2.01 ± 0.02 [a] | 0.49 ± 0.02 [a] |
| 5.30 C | 39.90 ± 1.01 [b] | 1.76 ± 0.03 [b] | 0.43 ± 0.01 [a] |

Data in the table represent the mean ± SD of three replicates; Different superscript letters among the same types of samples (raw milk, skim milk and cream) in the same column refer to statistically significant differences ($p < 0.05$); 6.74 R (raw milk pH 6.74), 6.30 R (raw milk pH 6.30), 5.30 R (raw milk pH 5.30), 6.74 C (cream pH 6.74), 6.30 C (cream pH 6.30), 5.30 C (cream pH 5.30), 6.74 S (skim milk pH 6.74), 6.30 S (skim milk pH 6.30) and 5.30 S (skim milk pH 5.30).

### 2.3.2. Particle Size

The Dv(10), Dv(50) and Dv(90) of cream samples are significantly higher than those of raw milk and skim milk samples ($p < 0.05$) except for skim milk under the pH 5.3 condition (Table 2-2). This result could be explained by the fact that the fat globules present bigger particle sizes than milk proteins. According to the results of composition analysis in Section 2.3.1, fat content in cream samples was significantly higher than that in raw milk and skim milk samples. It was reported that the size of milk fat globules in untreated milk varied from 0.2–15 μm, with a mean diameter of 3–4 μm (Smoczyński, 2017). Native casein micelles which exist as the particles in milk, consist of casein proteins and calcium phosphate (De Kruif, 1999).

**Table 2-2.** Fat globule size, SSA, span and uniformity of raw milk, cream and skim milk samples with different pH.

| Samples | Dv(10) (µm) | Dv(50) (µm) | Dv(90) (µm) | Specific Surface Area ($cm^2/g$) | Span | Uniformity |
|---|---|---|---|---|---|---|
| 6.74 R | 0.03 ± 0.00 $^{e}$ | 0.65 ± 0.21 $^{f}$ | 7.65 ± 0.06 $^{e}$ | 65.41 ± 1.06 $^{c}$ | 5.51 ± 0.81 $^{d}$ | 2.14 ± 0.23 $^{b}$ |
| 6.30 R | 0.04 ± 0.00 $^{e}$ | 2.52 ± 0.19 $^{e}$ | 12.37 ± 2.13 $^{d}$ | 56.96 ± 2.03 $^{d}$ | 6.41 ± 0.55 $^{c}$ | 2.49 ± 0.11 $^{b}$ |
| 5.30 R | 0.04 ± 0.00 $^{e}$ | 2.96 ± 0.20 $^{e}$ | 10.53 ± 0.07 $^{c}$ | 47.68 ± 4.11 $^{e}$ | 8.05 ± 0.29 $^{b}$ | 4.41 ± 0.30 $^{a}$ |
| 6.74 C | 2.16 ± 0.00 $^{a}$ | 8.93 ± 0.11 $^{a}$ | 51.42 ± 0.73 $^{a}$ | 1.69 ± 0.13 $^{h}$ | 3.62 ± 0.31 $^{d}$ | 1.67 ± 0.01 $^{d}$ |
| 6.30 C | 1.57 ± 0.02 $^{b}$ | 7.28 ± 0.10 $^{b}$ | 48.21 ± 2.10 $^{b}$ | 2.04 ± 0.05 $^{g}$ | 4.88 ± 0.20 $^{e}$ | 1.78 ± 0.09 $^{d}$ |
| 5.30 C | 0.97 ± 0.04 $^{c}$ | 5.86 ± 0.26 $^{c}$ | 48.14 ± 8.50 $^{b}$ | 2.28 ± 0.02 $^{g}$ | 12.65 ± 0.41 $^{a}$ | 2.43 ± 0.25 $^{b}$ |
| 6.74 S | 0.02 ± 0.00 $^{e}$ | 0.07 ± 0.01 $^{g}$ | 0.25 ± 0.01 $^{f}$ | 110.10 ± 2.35 $^{a}$ | 3.06 ± 0.06 $^{f}$ | 1.97 ± 0.24 $^{c}$ |
| 6.30 S | 0.02 ± 0.00 $^{e}$ | 0.08 ± 0.02 $^{g}$ | 0.28 ± 0.00 $^{f}$ | 103.62 ± 10.24 $^{b}$ | 3.15 ± 0.13 $^{f}$ | 2.57 ± 0.07 $^{b}$ |
| 5.30 S | 0.81 ± 0.02 $^{d}$ | 5.29 ± 0.52 $^{d}$ | 9.18 ± 0.24 $^{c}$ | 8.32 ± 0.21 $^{f}$ | 1.59 ± 0.08 $^{g}$ | 0.43 ± 0.00 $^{e}$ |

Data in the table represent the mean ± SD of three replicates; Different superscript letters in the same column refer to statistically significant differences ($p < 0.05$); 6.74 R (raw milk pH 6.74), 6.30 R (raw milk pH 6.30), 5.30 R (raw milk pH 5.30), 6.74 C (cream pH 6.74), 6.30 C (cream pH 6.30), 5.30 C (cream pH 5.30), 6.74 S (skim milk pH 6.74), 6.30 S (skim milk pH 6.30) and 5.30 S (skim milk pH 5.30).

Native bovine milk is a semi-stable emulsion at 37 °C or above in which casein micelles at pH 6.70 are generally assumed to remain in suspension due to the hairy layer of κ-casein providing steric and electrostatic repulsion (Wong, Camirand, Pavlath, Parris, & Friedman, 1996). Hydrophobic and hydrophilic radicals on the surface of MFGs, acting as natural emulsifying agents, play an important role in preventing the flocculation and coalescence of the globules and keeping the charge balance between milk protein and fat globules. Acid induced an increased attachment of milk protein to the surface of MFGs due to the charge change of MFGs and serum protein. This could be the reason for the slight increase of Dv(10), Dv(50) and Dv(90) in raw milk samples with the pH decrease. Cream samples presented the opposite trend to raw milk with the smallest Dv(10), Dv(50) and Dv(90) at pH 5.30, which were between 0.97 ± 0.04 and 48.14 ± 8.50 μm. This is inconsistent with Holzmüller et al. (Holzmüller, et al., 2016a), who reported larger particles with decreasing pH. The shear force in the disc stack of the cream separator resulted in MFGs disruption, which led to the coalescence of the fat globules and then contributed to the increase of particle size (Evers, 2004a).

No effect of pH on Dv(10), Dv(50) and Dv(90) of skim milk samples was detected between 6.74 and 6.30, but there was a sharp increase as the pH continually decreased to 5.30. Casein, with an isoelectric point at pH 4.6, tended to coalesce and precipitate from milk with lower pH, at which condition particle size values moved towards large ones (Table 2-2 and Figure 2-1C).

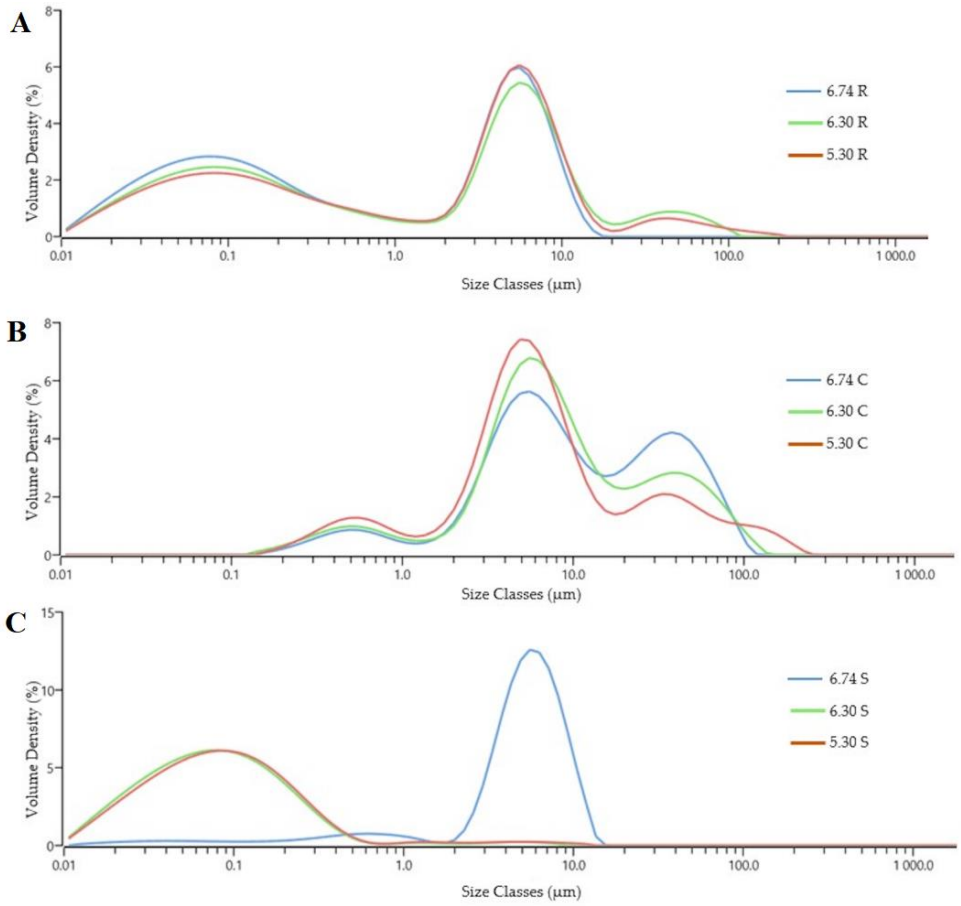



**Figure 2-1.** Volume density (%) of raw milk, skim milk and cream samples at different pH. 6.74 R (raw milk pH 6.74), 6.30 R (raw milk pH 6.30), 5.30 R (raw milk pH 5.30), 6.74 C (cream pH 6.74), 6.30 C (cream pH 6.30), 5.30 C (cream pH 5.30), 6.74 S (skim milk pH 6.74), 6.30 S (skim milk pH 6.30) and 5.30 S (skim milk pH 5.30).

Data in Table 2-2 showed that as the Dv(10), Dv(50) and Dv(90) decreased, the corresponding SSA increased. This accords with P. Sharma et al.'s report, which showed that the D [3,2] of untreated whole milk decreased with the intensity of pulsed electric field treatment (Sharma, Oey, & Everett, 2015a), while the corresponding SSA increased. The trends for span and uniformity were comparable. It was shown that more homogenous particle sizes in samples presented smaller uniformity (Mercan, et al., 2018). Cream samples presented higher span and uniformity values than raw milk and skim milk samples. Accordingly, particle size in cream samples was wider and more multitudinous (Figure 2-1B). Generally, the main particle size of raw milk samples was between 0.01 and 174 µm (Figure 2-1A), while skim milk samples with

pH 6.74 and 6.30 present the narrowest size distribution, between 0.01 and 9.98 μm (Figure 2-1C).

According to these results, we speculated that under the same pH condition, the change in particle size of fat globules could be attributed to the shear force produced by the separator. It could be due to the coalescence or damage of MFGs and the loss of MFGM materials (Zheng, Jimenez-Flores, & Everett, 2013). Besides, most of the presumed stabilizing materials (caseins and whey proteins) are lost during the cream separation. However, in this and Holzmüller et al.'s (Holzmüller, Müller, Himbert, & Kulozik, 2016f) previous research, the shear force of the cream separator was not quantitatively analyzed, and the relation between the extent of shear force and fat globules damage was not confirmed. Thus, the effect of shear force on the integrity of MFGs still needs to be further investigated. In addition, we could conclude that the pH variation could be an important factor in changing the particle size of all samples. Either because the change of proteins on the surface of MFGs, or the attachment of casein or whey proteins on MFGMs.

### 2.3.3. Zeta (ζ) Potential

The stability of casein micelles and milk fat has been associated with ζ-potential value. The measured ζ-potentials of all samples are illustrated in Figure 2-2. All of the samples showed a negative ζ-potential. According to Michalski et al. (Michalski, Cariou, Michel, & Garnier, 2002a), casein micelles and MFGs both have negative charges between pH 6.60–6.70 at 25 °C, and their apparent ζ-potential is negative. Thus, it should be noted that the description of the increase or decrease of ζ-potential in this study is not used algebraically but refer to their absolute values. Hence, it should be understood that algebra is not used in this research to describe how the ζ-potential increases or decreases; rather, it refers to the absolute magnitude of the ζ potential.

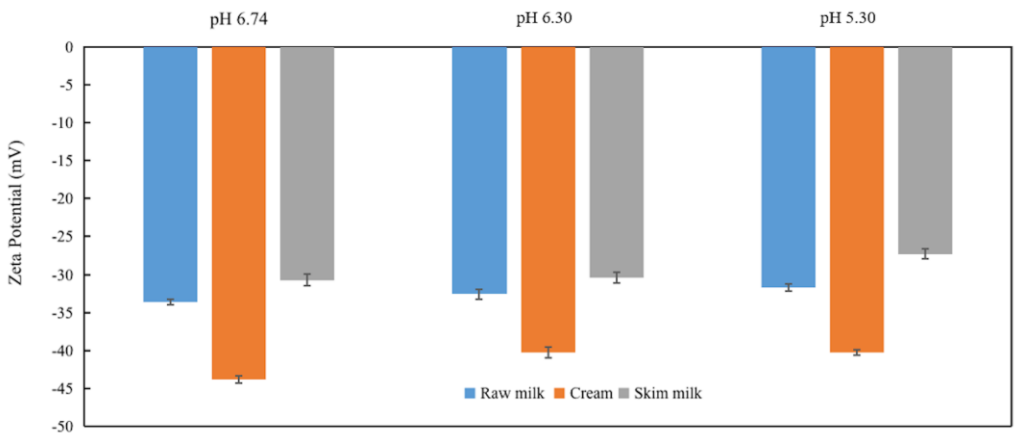



**Figure 2-2.** Zeta-potential of raw milk, cream and skim milk as a function of pH.

The ζ-potential of raw milk with pH 6.74, when measured at 25 °C, was −33.60 mV (Figure 2-2), which was much higher than the previously published reports. P. Sharma et al.(Sharma, et al., 2015a) and Michalski et al. (Michalski, Michel, Sainmont, & Briard, 2002b) showed that the ζ-potential value of whole milk at physiological pH (6.60–7.0) was −13.7 ± 0.1 mV. Some other researchers published −22 mV for whole milk at pH 6.67 (Gülseren, Alexander, & Corredig, 2010; Kühnl, et al., 2010). Jukkola et al. investigated the effect of diafiltration media on the separation of MFGs via microfiltration (Jukkola, Partanen, Rojas, & Heino, 2016a). The ζ-potential values for the feed milk were −30 mV, which is quite close to our results. Comparing ζ-potential results of different research is challenging since many factors greatly influence the obtained value. Michalski, Michel et al. (Michalski, et al., 2002b) found that different analysis techniques, including laser Doppler electrophoresis (particularly the scattered light angle) or electroacoustic methods, could affect the ζ-potential (Sharma, et al., 2015b). Other experimental conditions (e.g., diluent and temperature) could also significantly affect the ζ-potential value (Anderson & Cawston, 1975) and hence the ζ potential. There was no significant difference in the ζ-potential of raw milk between pH 6.74 and 5.30 (25 °C; $p > 0.05$)

The ζ-potential of skim samples of different pH varied from −27.3 to −30.7 mV, which was relatively lower than that of cream and raw milk samples. At a pH of 6.7–6.8 (25 °C), reconstituted skim milk was found to have a ζ-potential of −34.6 ± 3.6

mV (Sejersen, et al., 2007). The charge of casein switches from negative to positive as the pH decrease (Tuinier & De Kruif, 2002). This could explain why the ζ-potential of skim milk samples at pH 5.30 (−27.3 mV) was significantly ($p < 0.05$) lower than that of pH 6.74 (−30.7 mV). At lower pH, there was more adsorption of caseins and whey proteins on the MFGs surface in raw milk samples. However, after mechanical treatment in the centrifugation process, the amount of the adsorbing serum proteins decreased, thus decreasing the ζ-potential in skim samples.

pH 5.30 condition further decreased the ζ-potential of cream samples to −40.3 mV. This might be a result of a modification to the MFGM protein, which leads to an increase in the exposure of negatively charged and/or hydrophobic areas (Sejersen, et al., 2007). The findings for ζ-potential were consistent with those for particle size at pH 5.30, leading to the smaller particle size of cream samples. For conducting particles, the ζ-potential value generally depends on their particle size (Roy, Gallardo, & Estelrich, 1998; Michalski, et al., 2002b).

### 2.3.4. SDS-PAGE

The change in serum and MFGM protein with the pH variation was determined by SDS-PAGE under reducing condition (Figure 2-3). Meanwhile, relative protein content was quantified by combining densitometry with the total lane signal intensity (Figure 2-4). The electrophoresis mobility of proteins was used to define their molecular weight as well as numerous published literatures: caseins 19–34 kDa, β-LG 18 kDa, α-LA 14 kDa, XO 146–155 kDa, BTN 66–67 kDa and PAS 6/7 47–59 kDa (Singh, 2006a; Fong, Norris, & MacGibbon, 2007a; Dewettinck, et al., 2008; Jiménez-Flores & Brisson, 2008; Smoczyński, Staniewski, & Kiełczewska, 2012).

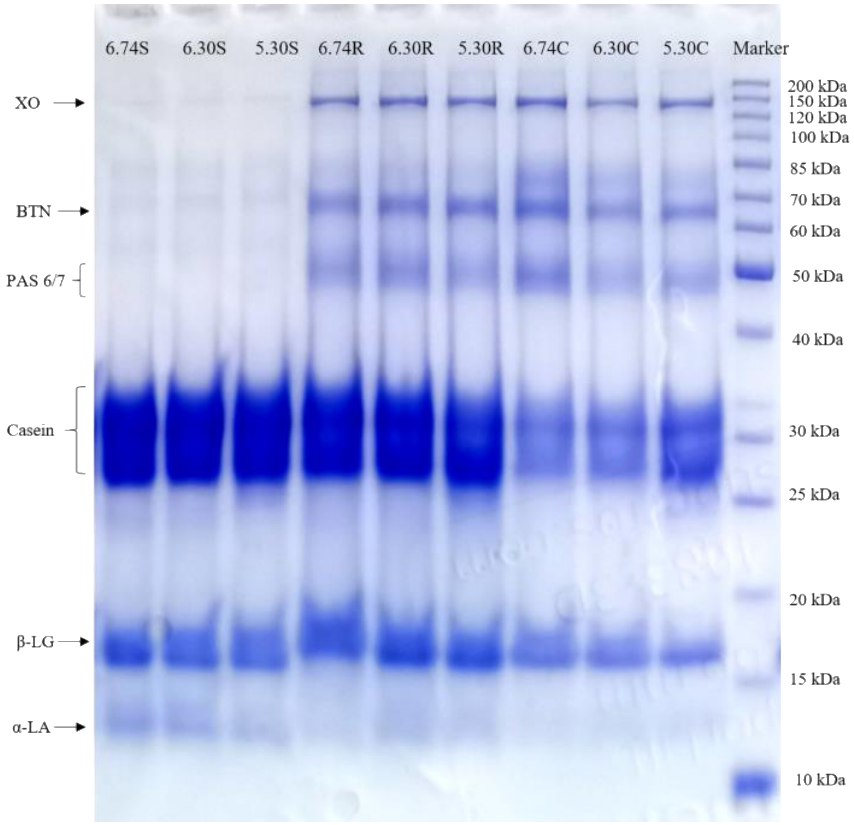



**Figure 2-3.** SDS-PAGE shows the predominant proteins presenting in raw milk, cream and skim milk with different pH. 6.74 R (raw milk pH 6.74), 6.30 R (raw milk pH 6.30), 5.30 R (raw milk pH 5.30), 6.74 C (cream pH 6.74), 6.30 C (cream pH 6.30), 5.30 C (cream pH 5.30), 6.74 S (skim milk pH 6.74), 6.30 S (skim milk pH 6.30) and 5.30 S (skim milk pH 5.30). PAS 6/7, periodic acid Schiff 6 and 7; BTN, butyrophilin; XO, xanthine oxidase; α-LA, α-lactalbumin; β-LG, β-lactoglobulin.

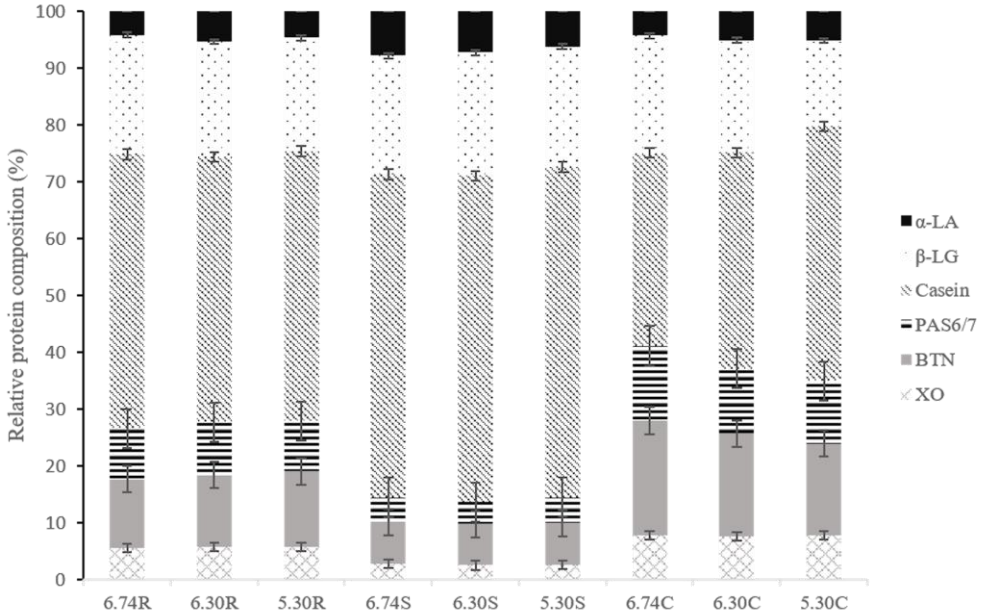


**Figure 2-4.** Relative protein compositions of raw milk, cream and skim milk samples derived from densitometry measurements of bands in a representative SDS-PAGE gel; 6.74 R (raw milk pH 6.74), 6.30 R (raw milk pH 6.30), 5.30 R (raw milk pH 5.30), 6.74 C (cream pH 6.74), 6.30 C (cream pH 6.30), 5.30 C (cream pH 5.30), 6.74 S (skim milk pH 6.74), 6.30 S (skim milk pH 6.30) and 5.30 S (skim milk pH 5.30).

Qualitative differences between the individual samples depend on the intensity of the protein bands. Higher relative intensities typically denote a higher protein content. A loss of XO, BTN and PAS 6/7 in skim milk samples was observed in Figure 2-3. The protein profile of cream samples differed from that of the skim milk, with more dominant MFGM proteins at the expense of casein, β-LG and α-LA.

It was more prominent in the incorporation of α-LA in cream samples at lower pH during centrifugal separation. The relative content of α -LA in cream samples at pH 5.30 increased by 19.18% than that in 6.74 C samples (Figure 2-4). However, at pH 5.30, the levels of α-LA in both the raw milk and the skim samples were reduced, which was predicted based on the influence of charge on the solubility of α-LA in casein micelles. The solubility of α-LA decreased by a higher calcium quantity in the aqueous phase caused by the release of calcium phosphate from micelles under acidic conditions (Dalgleish & Corredig, 2012)**.**

β-LG was reported to interchangeably interact with MFGM proteins via sulfhydryl-disulfide, then bound to the casein micelles through κ-casein (Ye, Singh, Taylor, & Anema, 2004a). A lower pH condition apparently is not helpful for this interaction since either raw milk or cream samples showed less β-LG amounts at pH 5.30.

Regarding BTN, PAS 6/7 and XO, both Figures 2-3 and 2-4 showed the lower pH led to a higher BTN and PAS 6/7 loss in cream samples. However, the relative content of XO in all samples had no significant variation as pH decreased ($p > 0.05$). The theoretical pI of BTN is 5.32 (Dewettinck, et al., 2008; Holzmüller, Gmach, Griebel, & Kulozik, 2016c), this protein tends to precipitate at pH 5.30. This could explain the more intense BTN bands in raw milk samples at pH 5.30 since BTN was released from

the MFGM and formed purer aggregates. BTN is typically referred to as an integral protein, whereas PAS 6/7 is classified as a periphery protein (Holzmüller, et al., 2016h). BTN and part of XO were reported to strongly attach to MFGM after the extracted pre-treatment with Triton X-100, sodium deoxycholate and guanidine hydrochloride(Yamauchi, Shimizu, & Kanno, 1978). The amount of PAS 6/7 in the 6.74 S samples was reduced by 51.90% more than that in the 6.74 R samples, with a relative intensity of only 7.34 and 4.29% for BTN and XO in 6.74 S, respectively (Figure 2-4). This outcome was inconsistent with the binding of MFGM proteins previously mentioned. It was positive to find that cream samples contained a more significant amount of MFGM proteins than skim and raw milk samples ($p < 0.05$), with a range of 7.59–88%, 16.09–20.12% and 10.98–13.14 %, respectively. This confirmed that not only loosely-bound membrane components but also integral proteins were lost during cream separation(Le, Van Camp, Rombaut, van Leeckwyck, & Dewettinck, 2009). The results above are consistent with the particle size shift in Section 2.3.2, which shows that cream samples present higher Dv (10), Dv (50) and Dv (90) values than skim and raw milk.

Overall, shear force plus the pH decreasing during the cream separation process did change the protein compositions of MFGM. Probably due to fat globule damage, parts of MFGM materials are released from the fat globule and partitioned into the serum phase or associated with the serum proteins.

### 2.3.5. CLSM

The CLSM technique was developed to detect the MFGs in their native or specific environments (i.e., certain pH conditions) in a non-destructive manner. In our research, the samples were dual-stained by combining Nile Red with FCF or WGA.

The microstructural comparison of raw milk and cream samples with different pH are shown in Figures 2-5 and 2-6. Just as the conclusions from amounts of previous research, milk fat existed in the state of regular spheres (Waninge, Nylander, Paulsson,

& Bergenståhl, 2003; Lopez, et al., 2010a; Nguyen, et al., 2015). Triglyceride was the main composition of MFGs and could be observed in the core of MFGs, which showed green (Figure 2-5) or red fluorescence (Figure 2-6). Serum proteins including casein and whey protein were stained using FCF and presented red color, as shown in Figure 2-5. MFGs were covered by MFGM that consisted of heterogeneous glycoproteins stained by fluorescent green color (Figure 2-6).

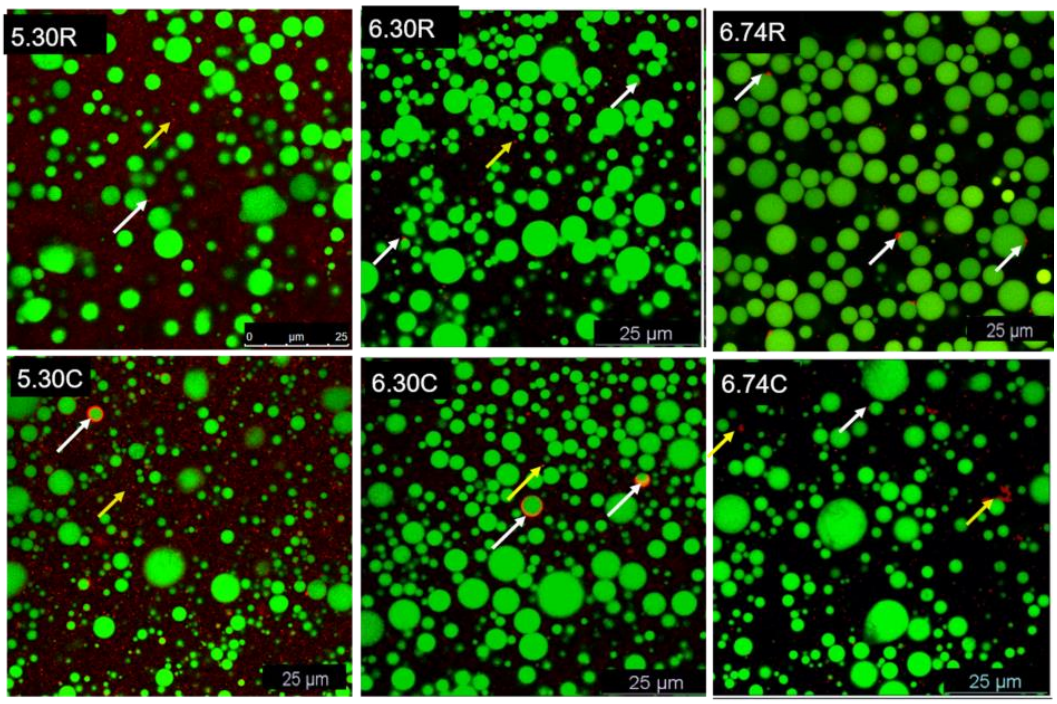



**Figure 2-5.** Confocal images of dual-stained milk fat globules in raw milk and cream at different pH. White and yellow arrows mark the serum proteins attaching on the surface of MFGs and drifting in the liquid phase, respectively. MFGs stained with Nile Red (green), and serum proteins stained with fluorescent Fast Green. 6.74 R (raw milk pH 6.74), 6.30 R (raw milk pH 6.30), 5.30 R (raw milk pH 5.30), 6.74 C (cream pH 6.74), 6.30 C (cream pH 6.30), 5.30 C (cream pH 5.30), 6.74 S (skim milk pH 6.74), 6.30 S (skim milk pH 6.30) and 5.30 S (skim milk pH 5.30).

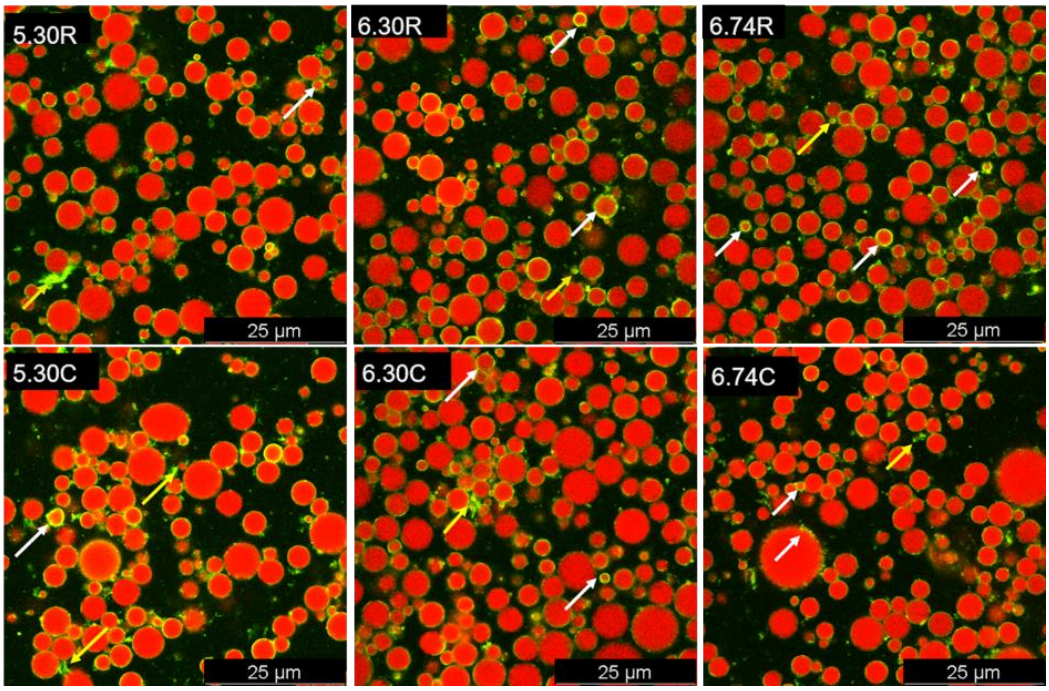



**Figure 2-6.** Confocal micrographs of double-stained milk fat globules in raw milk and cream at different pH. White arrows mark the glycoproteins attaching to the surface of MFGs, while yellow arrows mark the coalescent glycoproteins. MFGs were dyed with Nile Red (red), and glycoproteins were dyed with wheat germ agglutinin (WGA; yellow-green. 6.74 R (raw milk pH 6.74), 6.30 R (raw milk pH 6.30), 5.30 R (raw milk pH 5.30), 6.74 C (cream pH 6.74), 6.30 C (cream pH 6.30), 5.30 C (cream pH 5.30), 6.74 S (skim milk pH 6.74), 6.30 S (skim milk pH 6.30) and 5.30 S (skim milk pH 5.30).

Cream samples contained fewer serum proteins than raw milk samples, which was confirmed by the weaker fluorescent signal (red color). This could be identified by the results of the composition analysis in Section 2.3.1. Serum proteins, especially caseins, tended to form network structures at pH 5.30. In comparison with pH 6.30 and 6.74, either 5.30 R or 5.30 C samples showed the evident network structure formed by serum proteins (Figures 2-5 and 2-6. Cream samples showed bigger MFGs than raw milk samples, and this result is in accordance with the particle size analysis in Section 2.3.2.

CLSM images demonstrated that pH adjustment promoted serum protein adsorption on the outer layer of fat globules (Figure 2-5). Compared to cream samples, protein adsorption was more pronounced in raw milk samples, perhaps due to the lower protein content of cream samples or the desorption from the surface of MFGs

during centrifugation. As for the glycoproteins, the fluorescent signals on the surface of cream samples were more discontinuous than that for the raw milk samples (Figure 2-6). Meanwhile, at pH 5.30, more flocculation and coalescence of MFGM proteins were observed on the surface or in the serum phase of raw milk and cream samples. This result is in contrast to the SDS–PAGE analysis that showed the more amounts of MFGM proteins in cream samples and lower pH value further exacerbated this phenomenon. We speculated that SDS–PAGE samples preparation in this research could not tell the exact location of MFGM proteins which were either on the surface of the MFGs or in the serum phase. Since the CLSM is only a qualitative analysis method, it is impossible to accurately calculate the total MFGM proteins in the observing views. Thus, non-invasive and quantitative methods are expected to be developed in further research.

## 2.4. Conclusions

In spite of the functionality and physiology of MFGs being widely researched in recent years, the effect of dairy processing on these processing aspects is poorly understood. This research unprecedentedly demonstrated the implication of pH adjusting on the structure of MFGs and MFGM protein compositions during the cream separation. SDS-PAGE images and relative quantitative data showed that a loss of MFGM proteins after cream separation was inevitable, especially the BTN and PAS 6/7 at pH 5.30. Meanwhile, casein and whey protein tended to absorb on the surface of MFGs or form networks under the pH 5.30 condition, but mechanical force during centrifugation could desorb the attached serum proteins or the intrinsic glycoproteins. Thus, this led to the particle size change of MFGs and the rearrangement of MFGM compositions. Particle size (Dv (10), Dv(50) and Dv (90)) and ζ-potential of cream samples decrease at lower pH 5.30.

Only two typical pH conditions (pH 5.30 and 6.30) were investigated in the present study, and how the pH variation and centrifugation affected the lipids of MFGMs and their physiological properties was not studied. Considering some analysis methods

probably bringing about the structure or compositional changes of MFGs, more non-invasive methods need to be developed to conduct the real in situ observation.

**Author Contributions:** Conceptualization, Y.S. and S.M.; Data curation, Y.S.; Formal analysis, Y.S.; Funding acquisition, S.M.; Investigation, Y.S.; Methodology, Y.S.; Project administration, S.M.; Supervision, Y.H.R. and S.M.; Validation, Y.S.; Visualization, Y.S.; Writing–original draft, Y.S.; Writing–review & editing, Y.H.R. and S.M. All authors have read and agreed to the published version of the manuscript.

**Funding:** the Open Project Program of State Key Laboratory of Dairy Biotechnology (No. SKLDB2022-007) and the China Scholarship Council (No.202008410212).

**Data Availability Statement:** Data generated during the study are available from the corresponding author upon request.

**Conflicts of Interest:** The authors declare no conflict of interest.

**References**

Anderson, M., & Cawston, T. (1975). The milk-fat globule membrane. *Journal of Dairy Research*, *42*(3), 459-483.

Caroline Vanderghem , P. B., Claude Deroanne , Christophe Blecker. (2010). Milk fat globule membrane and buttermilks from composition to valorization. *Biotechnology, Agronomy, Society, and Environment., 14(3),*, 485-500.

Dalgleish, D. G., & Corredig, M. (2012). The structure of the casein micelle of milk and its changes during processing. *Annual review of food science and technology, 3*, 449-467.

De Kruif, C. (1999). Casein micelle interactions. *International Dairy Journal, 9*(3-6), 183-188.

Dewettinck, K., Rombaut, R., Thienpont, N., Le, T. T., Messens, K., & Van Camp, J. (2008). Nutritional and technological aspects of milk fat globule membrane material. *International Dairy Journal, 18*(5), 436-457.

Evers, J. M. (2004). The milkfat globule membrane—compositional and structural changes post secretion by the mammary secretory cell. *International Dairy Journal, 14*(8), 661-674.

Fong, B. Y., Norris, C. S., & MacGibbon, A. K. H. (2007a). 12 Protein and lipid composition of bovine milk-fat-globule membrane. *International Dairy Journal, 17*(4), 275-288.

Fong, B. Y., Norris, C. S., & MacGibbon, A. K. H. (2007b). Protein and lipid composition of bovine milk-fat-globule membrane. *International Dairy Journal, 17*(4), 275-288.

Gassi, J. Y., Blot, M., Beaucher, E., Robert, B., Leconte, N., Camier, B., et al. (2016). Preparation and characterisation of a milk polar lipids enriched ingredient from fresh industrial liquid butter serum: Combination of physico-chemical modifications and technological treatments. *International Dairy Journal, 52*, 26-34.

Gorewit, V. L. S. a. R. C. (2002). Isolation, Purification and Characterization of Fatty-Acid-Binding Protein from Milk. *Pakistan Journal of Nutrition, 1(1)* 43-48.

Gülseren, İ., Alexander, M., & Corredig, M. (2010). Probing the colloidal properties of skim milk using acoustic and electroacoustic spectroscopy. Effect of concentration, heating and acidification. *Journal of colloid and interface science, 351*(2), 493-500.

Holzmüller, W., Gmach, O., Griebel, A., & Kulozik, U. (2016a). 14 Casein precipitation by acid and rennet coagulation of buttermilk: Impact of pH and temperature on the isolation of milk fat globule membrane proteins. *International Dairy Journal, 63*, 115-123.

Holzmüller, W., Gmach, O., Griebel, A., & Kulozik, U. (2016b). Casein precipitation by acid and rennet coagulation of buttermilk: Impact of pH and temperature on the isolation of milk fat globule membrane proteins. *International Dairy Journal, 63*, 115-123.

Holzmüller, W., & Kulozik, U. (2016c). 6 Technical difficulties and future challenges in isolating membrane material from milk fat globules in industrial settings – A critical review. *International Dairy Journal, 61*, 51-66.

Holzmüller, W., Müller, M., Himbert, D., & Kulozik, U. (2016d). 7 (SDS PAGE/particle size) Impact of cream washing on fat globules and milk fat globule membrane proteins *International Dairy Journal, 59*, 52-61.

Holzmüller, W., Müller, M., Himbert, D., & Kulozik, U. (2016e). Impact of cream washing on fat globules and milk fat globule membrane proteins. *International Dairy Journal, 59*, 52-61.

ISO. (2001). ISO 8968-1: 2001 Milk–Determination of Nitrogen Content–Part 1: Kjeldahl Method. In: International Organization for Standardization Geneva.

Jiménez-Flores, R., & Brisson, G. (2008). The milk fat globule membrane as an ingredient: why, how, when? *Dairy Science and Technology, 88*(1), 5-18.

Jukkola, A., Partanen, R., Rojas, O. J., & Heino, A. (2016a). 4 (particle, ζ, creaming lumisizer)Separation of milk fat globules via microfiltration: Effect of diafiltration media and opportunities for stream valorization. *Journal of Dairy Science, 99*(11), 8644-8654.

Jukkola, A., Partanen, R., Rojas, O. J., & Heino, A. (2016b). Separation of milk fat globules via microfiltration: Effect of diafiltration media and opportunities for stream valorization. *Journal of Dairy Science, 99*(11), 8644-8654.

Jukkola, A., Partanen, R., Rojas, O. J., & Heino, A. (2018). 4-2(CLSM)Effect of heat treatment and pH on the efficiency of micro-diafiltration for the separation of

native fat globules from cream in butter production. *Journal of Membrane Science, 548*, 99-107.

Kühnl, W., Piry, A., Kaufmann, V., Grein, T., Ripperger, S., & Kulozik, U. (2010). Impact of colloidal interactions on the flux in cross-flow microfiltration of milk at different pH values: A surface energy approach. *Journal of Membrane Science, 352*(1-2), 107-115.

Le, T. T., Van Camp, J., Rombaut, R., van Leeckwyck, F., & Dewettinck, K. (2009). 26 Effect of washing conditions on the recovery of milk fat globule membrane proteins during the isolation of milk fat globule membrane from milk. *Journal of Dairy Science, 92*(8), 3592-3603.

Liao, Y., Alvarado, R., Phinney, B., & Lönnerdal, B. (2011). Proteomic Characterization of Human Milk Fat Globule Membrane Proteins during a 12 Month Lactation Period. *Journal of Proteome Research, 10*(8), 3530-3541.

Lopez, C., Blot, M., Briard-Bion, V., Cirie, C., & Graulet, B. (2017a). Butter serums and buttermilks as sources of bioactive lipids from the milk fat globule membrane: Differences in their lipid composition and potentialities of cow diet to increase n-3 PUFA. *Food Research International, 100*(Pt 1), 864-872.

Lopez, C., Cauty, C., Rousseau, F., Blot, M., Margolis, A., & Famelart, M. H. (2017b). Lipid droplets coated with milk fat globule membrane fragments: Microstructure and functional properties as a function of pH. *Food Research International, 91*, 26-37.

Lopez, C., Madec, M.-N., & Jimenez-Flores, R. (2010). 13 Lipid rafts in the bovine milk fat globule membrane revealed by the lateral segregation of phospholipids and heterogeneous distribution of glycoproteins. *Food Chemistry, 120*(1), 22-33.

Mana, P., Goodyear, M., Bernard, C., Tomioka, R., Freire-Garabal, M., & Linares, D. (2004). Tolerance induction by molecular mimicry: prevention and suppression of experimental autoimmune encephalomyelitis with the milk protein butyrophilin. *Internal Immunology, 16*(3), 489-499.

Mercan, E., Sert, D., & Akın, N. (2018). Effect of high-pressure homogenisation on viscosity, particle size and microbiological characteristics of skim and whole milk concentrates. *International Dairy Journal, 87*, 93-99.

Michalski, M.-C., Briard, V., & Michel, F. (2001). Optical parameters of milk fat globules for laser light scattering measurements. *Le Lait, 81*(6), 787-796.

Michalski, M.-C., Cariou, R., Michel, F., & Garnier, C. (2002a). Native vs. damaged milk fat globules: membrane properties affect the viscoelasticity of milk gels. *Journal of Dairy Science, 85*(10), 2451-2461.

Michalski, M.-C., Michel, F., Sainmont, D., & Briard, V. (2002b). Apparent ζ-potential as a tool to assess mechanical damages to the milk fat globule membrane. *Colloids and Surfaces B: Biointerfaces, 23*(1), 23-30.

Murthy, A. V. R., Guyomarc'h, F., & Lopez, C. (2016). The temperature-dependent physical state of polar lipids and their miscibility impact the topography and mechanical properties of bilayer models of the milk fat globule membrane. *Biochimica et Biophysica Acta (BBA)-Biomembranes, 1858*(9), 2181-2190.

Nguyen, H. T. H., Ong, L., Beaucher, E., Madec, M.-N., Kentish, S. E., Gras, S. L., et al. (2015). Buffalo milk fat globules and their biological membrane: in situ structural investigations. *Food Research International, 67*, 35-43.

Peterson, J. A., Patton, S., & Hamosh, M. (1998). Glycoproteins of the human milk fat globule in the protection of the breast-fed infant against infections. *Neonatology, 74*(2), 143-162.

Ross, S. (2016). *Targeting the glycome of the milk fat globule membrane for antiinfective properties.* National University of Ireland, Galway, Galway.

Roy, M. T., Gallardo, M., & Estelrich, J. (1998). Influence of size on electrokinetic behavior of phosphatidylserine and phosphatidylethanolamine lipid vesicles. *Journal of colloid and interface science, 206*(2), 512-517.

Sejersen, M. T., Salomonsen, T., Ipsen, R., Clark, R., Rolin, C., & Engelsen, S. B. (2007). Z-potential of pectin-stabilised casein aggregates in acidified milk drinks. *International Dairy Journal, 17*(4), 302-307.

Sharma, P., Oey, I., & Everett, D. W. (2015a). 6 Interfacial properties and transmission electron microscopy revealing damage to the milk fat globule system after pulsed electric field treatment. *Food Hydrocolloids, 47*, 99-107.

Sharma, P., Oey, I., & Everett, D. W. (2015b). Interfacial properties and transmission electron microscopy revealing damage to the milk fat globule system after pulsed electric field treatment. *Food Hydrocolloids, 47*, 99-107.

Singh, H. (2006). The milk fat globule membrane—A biophysical system for food applications. *Current Opinion in Colloid & Interface Science, 11*(2-3), 154-163.

Singh, H., & Gallier, S. (2017). Nature's complex emulsion: The fat globules of milk. *Food Hydrocolloids, 68*, 81-89.

Smoczyński, M. (2017). Role of phospholipid flux during milk secretion in the mammary gland. *Journal of mammary gland biology and neoplasia, 22*(2), 117-129.

Smoczyński, M., Staniewski, B., & Kiełczewska, K. (2012). Composition and Structure of the Bovine Milk Fat Globule Membrane—Some Nutritional and Technological Implications. *Food Reviews International, 28*(2), 188-202.

Spitsberg, V. L. (2005). Invited Review: Bovine Milk Fat Globule Membrane as a Potential Nutraceutical. *Journal of Dairy Science, 88*, 2289–2294.

Timby, N., Hernell, O., Vaarala, O., Melin, M., Lonnerdal, B., & Domellof, M. (2015). Infections in infants fed formula supplemented with bovine milk fat globule membranes. *Journal of Pediatric Gastroenterology and Nutrition, 60*(3), 384-389.

Tuinier, R., & De Kruif, C. (2002). Stability of casein micelles in milk. *The Journal of Chemical Physics, 117*(3), 1290-1295.

Van Oss, C. J. (1996). *Forces interfaciales en milieux aqueux*: Masson.

Waninge, R., Nylander, T., Paulsson, M., & Bergenståhl, B. (2003). 5 Milk membrane lipid vesicle structures studied with Cryo-TEM. *Colloids and Surfaces B: Biointerfaces, 31*(1-4), 257-264.

Wong, D. W., Camirand, W. M., Pavlath, A. E., Parris, N., & Friedman, M. (1996). Structures and functionalities of milk proteins. *Critical Reviews in Food Science & Nutrition, 36*(8), 807-844.

Yamauchi, K., Shimizu, M., & Kanno, C. (1978). Effect of preparation on properties of a soluble glycoprotein fraction of milk fat globule membrane. *Journal of Dairy Science, 61*(6), 688-696.

Ye, A., Singh, H., Taylor, M. W., & Anema, S. (2004a). 51.1 Interactions of whey proteins with milk fat globule membrane proteins during heat treatment of whole milk. *Lait, 84*(3), 269-283.

Ye, A., Singh, H., Taylor, M. W., & Anema, S. (2004b). Interactions of whey proteins with milk fat globule membrane proteins during heat treatment of whole milk. *Lait, 84*(3), 269-283.

Zheng, H., Jimenez-Flores, R., & Everett, D. W. (2013). 9 Bovine milk fat globule membrane proteins are affected by centrifugal washing processes. *Journal of Agricultture and Food Chemistry, 61*(35), 8403-8411.

# CHAPTER THREE

## Characterization of the microstructure, interfacial properties and crystallisation behaviours of milk fat globule and membrane isolated from acidified bovine milk and sweet whey

Chapter 3 was published in:

Sun, Y., Roos, Y. H., & Miao, S. (2024). Characterization of the microstructure, interfacial properties and crystallisation behaviours of milk fat globule and membrane isolated from acidified bovine milk and sweet whey. *Food Hydrocolloids*, 110246.

Yanjun Sun: Conceptualization, Methodology, Writing-original draft, Data curation, Investigation, Funding acquisition. Yrjö H. Roos: Supervision, Writing review & editing. Song Miao: Supervision, Conceptualization, Writing-review & editing, Funding acquisition, Project administration, Investigation.

**Abstract**

Milk fat globule and membrane (MFGs/MFGM) ingredients are the main source of the phospholipid supplementation in the dairy industry. Their physicochemical properties and functionalities play important roles for their application. This study investigated the effect of the acidification (pH 6.30 and pH 5.30) on the microstructure, interfacial and thermal properties of MFGs/MFGM sourced from bovine milk (control pH 6.70). Meanwhile, sweet whey was prepared to mimic the raw material used in industrial production of MFGs/MFGM (MFGM-C). The study revealed a broad particle size distribution of MFGs/MFGM at pH 5.30, while smaller particles were found in MFGM-C. This was confirmed by confocal scanning microscopy (CLSM) images, which showed that rare intact MFGs existed in the MFGM-C. Fourier Transform Infrared Spectroscopy (FTIR) indicated more peaks belonging to the protein-lipids associations presented at pH 6.30. Additionally, the interfacial tension of MFGs/MFGM at pH 6.30 was significantly lower than at pH 6.70 and 5.30. X-ray Diffraction Spectra (XRD) showed that the fat in MFGM-C exhibited no detectable crystalline structures, and fewer α and β' crystals appeared at pH 6.30. All MFGs/MFGM from bovine milk or whey exhibited both exothermic and endothermal events. The smallest heat enthalpy of crystallization ($\Delta H_C$) and melting ($\Delta H_M$) was observed in MFGM-C, followed by those at pH 6.30. Compared to MFGs/MFGM at pH 6.70, pH 6.30 induced more profound effects on the interfacial and thermal properties of MFGs/MFGM than pH 5.30. Acidification and the use of different raw materials lead to differentiation in the physicochemical and techno-functionalities of MFGs/MFGM.

**Keywords:** Milk fat globules/milk fat globule membrane; Acidified bovine milk; Physicochemical properties; Interfacial tension; Different Scanning Calorimetry (DSC); X-ray Diffraction (XRD)

## 3.1. Introduction

In mammal milk, most lipids exist in milk fat globules (MFGs) wrapped by the unique tri-layer membrane-milk fat globule membrane (MFGM) (Huang, et al., 2023). Milk fat provides 50–60% of the energy required for the neonate's growth. The bioactive compositions of the MFGs/MFGM, such as phospholipids and glycoproteins, are gaining significant interest for their important role in promoting new-borns' brain and intelligence development (Mohamed, et al., 2022; Nieto-Ruiz, et al., 2022). Infant formula (IF) is an essential nutrient for neonates having no adequate source of breast milk. Dairy ingredients rich in MFGs/MFGM sourced from buttermilk or whey cream have been applied in IF products to mimic breast milk nutrition (Mohan, O'Callaghan, Kelly, & Hogan, 2020).

Structural and compositional changes of MFGs/MFGM during dairy processing have been investigated in many studies, including MFGs/MFGM separation methods, heating treatments or storage temperature, homogenisation, and non-thermal treatments (Ren, et al., 2020; Kiełczewska, et al., 2021; Liu, et al., 2021; Wei, et al., 2021; Huang, et al., 2023). However, the research on the effect of these processes on the techno-functionalities of MFGs/MFGM is still lacking. Different sizes of native fat globules (NFG) separated from raw milk by a modified commercial cream separator affected the foamability of milk. The size of air bubbles in foam increased with the increase in NFG size, while the foam ability was not affected by the NFG size (Ho, Dhungana, Bhandari, & Bansal, 2021). Reconstructing MFG (RMFG) with different-melting-temperature triacylglycerols (TAG) was prepared by Ren, Guo, Teng, and Ma (2021) to improve its techno-functionalities and nutritional properties. Additionally, Ren, et al. (2020) demonstrated that pasteurisation and homogenisation treatments affected the thermodynamic properties and fat polymorphs of fat globules during seven days of storage at 4 °C. MFGs/MFGM ingredients play an important role in the emulsifying stability of IF products (Li, et al., 2022a). The interfacial layer of

MFGs/MFGM is more likely to be involved with the emulsion formation and destabilization.

The commercial MFGs/MFGM ingredients have been prepared from sweet whey or buttermilk. The processes for the MFGs/MFGM ingredients production involve acidification, heating, and coagulation (Fontecha, et al., 2020). Acidification is one of the mostly used processing methods in dairy products, such as yogurts, cheeses, and lactic fermented beverages or acidic milk drinks. Specifically, pH conditions at 5.30 and 6.30 are involved in the processing of these products. According to previous research, different pH conditions have been proven to affect the isolating efficiency of MFGM proteins from buttermilk or native MFGs from cream (Holzmüller, et al., 2016b; Jukkola, et al., 2018b). We hypothesise that the acidification treatment may change the structure and compositions of MFGs/MFGM, which further affects the interfacial behaviour, thermodynamic properties, and fat polymorphs in MFGs/MFGM materials. To verify this hypothesis, we investigated the effect of pH conditions at 5.30 and 6.30 on the interfacial properties and fat crystallisation behaviours of MFGs/MFGM.

Herein, MFGs/MFGM ingredients were isolated from acidified bovine raw milk (pH 5.30 and pH 6.30) by cream separator, followed by centrifugation to make a further enrichment. Meanwhile, MFGs/MFGM materials from the sweet whey were prepared to mimic the industrial MFGs/MFGM preparation and make the comparative analysis. Compositions of collected MFGs/MFGM ingredients were profiled by Fourier transform infrared spectroscopy (FTIR) and the microstructure was observed by confocal laser scanning microscopy (CLSM). We investigated the effect of acidification on the surface charges and air/ liquid interfacial properties of MFGs/MFGM by determining the Zeta (ζ) potential and interface tension respectively. Combined Different Scanning Calorimetry (DSC) with X-ray diffraction (XRD), the evolution of milk fat polymorphs and crystal types in MFGs/MFGM was investigated, and also the crystallization and melting behaviours. By these analytical methods, we

aimed at gaining more information on the pH-dependent properties of MFGs/MFGM. Meanwhile, the effect of different raw sources on the techno-functionalities of MFGs/MFGM was investigate by using the whey and bovine milk as the raw materials for the MFGs/MFGM preparation. MFGs/MFGM ingredients are the main source of the phospholipids supplement in dairy products. The information acquired by this study may be beneficial for the industrial MFGs/MFGM preparation and their application in dairy products.

## 3.2. Materials and methods

### 3.2.1. Materials and reagents

Fresh bovine milk (fat 4.13 ± 0.03%, protein 3.37 ± 0.02%, dry matter 13.10 ± 0.02%, pH 6.70 ± 0.04) was collected from the Teagasc dairy herd (Moorepark, Fermoy, Co. Cork, Ireland) and stored in the 4 ℃ refrigerator instantly after milking.

Nile Red (9- (diethylamino)-5 H-benzo[a]phenoxazin-5-one), Fast Green FCF (disodium 2-[[4-[ethyl-[(3-sulfonatophenyl)methyl]amino]phenyl]-[4-[ethyl-[(3-sulfonatophenyl) methyl] azaniumylidene] cyclohexa-2,5-dien-1-ylidene]methyl]-5-hydroxybenzenesulfonate), Polyethylene glycol 200, azide sodium and PBS tablets were purchased from Sigma-Aldrich®, Merck Life Science Ltd., Cork, Ireland. Starters (DVS, EASY-SET 3000), and rennet (CHY-MAX Supreme) were obtained from Chr. Hansen Inc., Copenhagen, Demark. Food grade $CaCl_2$ was purchased from Occidental Chemical Corporation, Michigan, USA.

### 3.2.2. Samples preparation

*3.2.2.1. Separation of cream samples from acidified bovine milk*

Pre-heated bovine raw milk (30–43 ℃) was separated into cream and skim milk using a disk bowl centrifugal separator (FT 15 Disc Bowl Centrifuge, Armfield Co., Ringwood, UK) at a rated throughput of 125L/h. Centrifugation speed was kept at 8500 rpm by controlling the motor housing. Before cream separation, two batches of

raw milk were adjusted to pH 6.30 and 5.30 respectively while the third batch without pH adjustment (6.70 ± 0.03) was used as the control. Each pH adjustment was repeated with three bathes. During the cream separation, skim milk was added back into the separating bowl again to be maximally defatted. The cream phase of all samples was collected and cooled down to 4 ℃ for further isolation.

*3.2.2.2. Preparation of sweet whey from the cheddar cheese drainage*

Pilot-scale cheddar whey was produced and used as raw materials to isolate MFGs/MFGM. Cheddar was manufactured using the standard procedure described by Voigt, Donaghy, Patterson, Stephan, and Kelly (2010) with some modifications. Pasteurized (70–72 ℃, 15–20 s) bovine milk 10 L was cooled down and kept at 30–35 ℃, which is the most suitable condition for starter growth (DVS, EASY-SET 3000, Chr. Hansen Inc., Copenhagen, Demark) and rennet coagulation (CHY-MAX Supreme, Chr. Hansen Inc., Copenhagen, Demark). Starters were added to acidify the milk from pH 6.70 ± 0.03 to 6.30 ± 0.02. After that, pre-dispersed rennet (40 IMCU/L) and food grade $CaCl_2$ (Occidental Chemical Corporation, Michigan, USA) (0.01 %, w/w) were added into the pasteurized milk. The formed curd was cut into $1cm^3$ grains. Subsequently, the tank was continually heated and kept at 45℃ for 15 min to facilitate the curd shrinkage and whey drainage. A sieve with a mesh number of 0.5 cm was used to filter the collected whey (pH 6.25 ± 0.03) until no visible curd grains were observed. The cheese-making process was repeated three times, and the three batches of whey were collected.

*3.2.2.3. Isolation of MFGs/MFGM materials*

Ultra-centrifugation (10000 ×g, 15 min at 4 ℃) was applied to further enrich the MFGs/MFGM compositions from the cream or whey (Zamora, Ferragut, Guamis, & Trujillo, 2012). Specifically, the upper layer was collected and mixed with an equivalent volume of PBS buffer. The mixture was dispersed in a water bath (35−40 ℃)

for 10 min and vortexed thoroughly before the second centrifugation. The centrifugation and supernatant rinse were repeated three times. The collected upper layers from the third time were freeze-dried for 72 h for further analysis. 0.03% (g/g) azide sodium was added to the supernatant to prevent microbiological growth. The freeze-dried samples were named after pH conditions: pH 6.70, pH 6.30, and pH 5.30. The samples made from whey were named MFGM-C. For each treatment, the material preparation procedures were repeated three times. The compositions of all samples were analysed by DairySpec FT-15 (Bentley Instruments Inc., Chaska, MN, USA) (Table 3-1).

**Table 3-1** The composition of freeze-dried MFGs/MFGM isolated from acidified bovine milk and sweet whey

| Samples | Protein (%, w/w) | Fat (%, w/w) | Lactose(%, w/w) |
|---|---|---|---|
| MFGM-C | 14.23±0.05$^{a}$ | 23.44±0.19$^{b}$ | 0.23±0.01$^{b}$ |
| pH 6.70 | 2.99±0.02$^{b}$ | 74.97±0.25$^{a}$ | 0.14±0.00$^{c}$ |
| pH 6.30 | 1.10±0.01$^{c}$ | 75.29±1.15$^{a}$ | 0.29±0.03$^{a}$ |
| pH 5.30 | 0.72±0.00$^{d}$ | 74.62±1.64$^{a}$ | – |

Notes: Different superscript letters in the same column indicate the significant ($p < 0.05$) differences between the samples. '–' means not detection.

### 3.2.3. Particle size distribution

Mastersizer 3000 (Malvern Instruments, Malvern, UK) equipped with a laser light scattering was performed to investigate the particle size distribution of MFGM-C and MFGs/MFGM with different pH. The measurement method was carried out according to the previous research with modifications (Sun, Roos, & Miao, 2022). Samples were heated in a water bath (30–35℃) until they completely melted before being analysed. The statistics of the particle distribution were calculated from the Mastersizer–v 3.7.1 software.

### *3.2.4.* Confocal laser scanning microscopy (CLSM)

The microstructure of lipid droplets and milk protein in MFGs/MFGM was measured by Leica TCS SP5 microscope (Leica Microsystems GmbH, Wetzlar, Germany). Neutral lipids (mainly refers to triglycerides) and milk proteins were labelled by Nile Red and Fast Green FCF, respectively. Samples were dual-stained, and the preparation method referred to the previous research with slight modifications (Pan, et al., 2024). Specifically, 0.1% (w/v) Nile Red was made in polyethylene glycol-200 solvent, and distilled water was used to dissolve FCF to a concentration of 0.1% (w/v). 50 µL MFGs/MFGM samples, 30 µL Nile Red, and 10 µL FCF were added into the 1.5 mL Eppendorf and mixed thoroughly. Stained samples were kept in the dark for 30 min at room temperature. The equipment setting and operation for the Leica TCS SP5 microscope followed our previous report (Sun, et al., 2022).

### 3.2.5. Fourier transform infrared spectroscopy (FTIR)

FTIR spectroscopy (Bruker Tensor 27, Bruker Optik GmbH, Ettlingen, Germany) equipped with an Optics Platinum Attenuated Total Reflectance (ATR) cell (Pike Technology Inc., Madison, WI, USA) was used to acquire the IR spectra of MFGs/MFGM samples. The freeze-dried sample was gently ground into a fine powder before evenly spreading down on the aperture. IR spectra were recorded at room temperature (20–25℃) from 900 to 4000 $cm^{-1}$ with an average of 120 scans at a resolution of 4 $cm^{-1}$. Background measurement was performed with consistent instrumental settings with the sample spectra acquisition. Spectral data recording, atmosphere compensation (removing the presence of atmospheric vapour and carbon dioxide from the spectra), and vector normalization were conducted by OPUS 7.5 software (Bruker Optik GmbH, Ettlingen, Germany). Each experiment was repeated three times.

Peak fitting and deconvolution were applied with OriginPro 2023 (OriginLab Corporation, Northampton, US) to pull apart and sharpen the overlapping hidden peaks

in the range of 1200–900 $cm^{-1}$. The second derivative (zero) method was used to find the baseline anchor points and detect the baseline. Peak finding was performed using the second derivation (searching hidden peaks), and only positive direction peaks were found. Savityzky–Golay function was used to perform the smooth derivative with the 10–20 points of window and polynomial order of 2. Peaking fitting was conducted using the Gaussian function, and all peak widths and centre, baseline parameters were fixed or released until the best fit was achieved ($R^2$> 0.996, reduced chi-square < $1\times10^{-6}$).

### 3.2.6. Interfacial tension

Freeze-dried MFGs/MFGM were heated in a water bath (30–35 ℃), and the melted liquid samples were deemed as a W/O emulsion used to perform the interfacial tension and Zeta (ζ) potential measurements. An optical tensiometer (Oneattension Theta lite, Biolin Scientific, Espoo, Finland) was applied to comparatively assess the impact of acidification and different raw materials on the interfacial tension of MFGs/MFGM collections. Pendant drop method and 'Advanced (two phases frame per second (FPS)' mode were set during the analysis. The hooked needle was used, which, according to the manual, was described as the higher stability for the measurement due to the minor effect from the airflow and negligible losses of evaporation. Young-Laplace equation was used to calculate the interfacial tension. Around 5−7 μL liquid sample droplet was squeezed out of the needle until its volume kept steady. During the test, images were recorded at 0.1 % frame per second FPS and, the total duration was 20 s. The resulting data were collected and analysed by Oneattension software (Version 4.1.6, Biolin Scientific, Espoo, Finland).

### 3.2.7. Zeta (ζ) potential

The dynamic light scatting instrument (Nano–ZS, Malvern Instruments Ltd., Worcestershire, UK) was performed to measure electrophoretic mobility which was used to calculate the ζ-potential by application of the Henry equation (Michalski,

Michel, Sainmont, & Briard, 2002d). The melted liquid samples were diluted 100 times with MiliQ water. Before each analysis, all diluted samples were kept still at room temperature and equilibrated for 2 minutes. The ζ-potential of each sample was read three times automatically. The fraction of MFGs/MFGM surface covered with non-membrane milk protein (Φ) was calculated from an estimative model based on the relative change in ζ-potential:

$$\Phi = 1 - \exp\left(-1.802 \times 10^{-3} \zeta_R^2\right) \qquad (3\text{-}1)$$

where, $\zeta_R$ was the relative change of ζ–potential of samples compared to the unprocessed raw milk which was assumed that Φ=0.

### 3.2.8. X–ray diffraction (XRD)

XRD analysis of the freeze-dried MFGs/MFGM was performed on a powder diffractometer STOE STAID MP (STOE, Darmstadt, Germany) equipped with Cu radiation (λ=1.5406 nm; current, 40 mA; voltage, 40 kV). The diffraction patterns were recorded in a diffraction range of 2θ from 5˚ to 30˚ with a scanning speed of 1˚/min. Freeze-dried powder samples were placed on the metal plates with film on both sides to seal the samples in.

The collected raw data were smoothened using the adjacent-averaging method, and the points of the window were set to 20. Meanwhile, baseline subtraction (Asymmetric least squares mode with asymmetric factor 0.001, threshold 0.05, smoothing factor 4, and number of literation 10) was performed using Originpro 2023.

Bragg Equation was used to characterize the short space (d) of the milk fat crystal as a function of scattering angle (Pope, 1997):

$$d = n\lambda / 2\sin\theta \qquad (3\text{-}2)$$

where d=interplanar spacing or d-spacing (Å); n=1 (order of diffraction); λ=1.5406 nm; θ=peak position (In radians) .

The typical crystalline forms in milk fat, α, β and β', were identified by the reported corresponding d-spacing: α =4.15 Å (2θ=21.41˚), β'1= 3.8 Å (2θ=23.41˚), β'2= 4.2Å (2θ=21.15˚), β= 4.6 Å (2θ=19.30˚) (D'Souza, deMan, & deMan, 1990; Han et al., 2014). In addition, the relative degree of crystallinity of α, β, and β' was calculated by integrating the area under the curve using Originpro 2023 (OriginLab Corporation, US) according to the following equation:

Crystallinity= Area of crystalline peaks/ (Area of crystalline and amorphous peaks)×100 (3-3)

### 3.2.9. Different scanning calorimetry (DSC)

The thermal behaviour of MFGs/MFGM materials separated from cream and sweet whey samples was investigated using DSC (DSC Q2000, TA Instruments, Crawley, UK). 10 –15 mg of each freeze-dried powder sample was hermetically sealed in an aluminium pan while an empty sealed pan was used as reference. Nitrogen was used as the shielding gas and purged the system at 50 mL/min. The time-temperature program was: Cycle 1: Equilibrate at 4 ℃; Cycle 2–3: Ramp 10 ℃/min to 60 ℃ and isothermal for 15 min; Cycle 4–5: Ramp 10 ℃/min to –60 ℃ and isothermal for 5 min; Cycle 6: Ramp 10 ℃/min to 60 ℃. The purpose of 1–3 cycles was to eliminate the crystal and melting history differentiation during the sample preparation. The thermal parameters of all the thermograms were exported through Universal Analysis 2000 (TA Instruments–Waters LLC, New Castle, US). The peaks for melting ($T_M$) /crystal ($T_C$), and the corresponding endothermic ($\Delta H_M$)/exothermic ($\Delta H_C$) enthalpy (J $g^{-1}$) were analysed in the OriginPro 2023 system.

### 3.2.10. Statistical analysis

All measurements were performed in triplicate unless otherwise indicated. Each value represented the mean of three measurements and was presented in mean ± standard deviation (SD). One-way ANOVA was conducted for all the analyses at the significance level of $p < 0.05$, except for interfacial tension as more strict levels of $p < 0.01$ and $p < 0.001$ were used. The ANOVA was performed in the OriginPro 2023 software, which was also used to plot all the figures.

## 3.3. Results and discussion

### 3.3.1. Particle size and microstructure of MFGs/MFGM

Most of the particles in MFGs/MFGM at pH 5.30 distributed in the range of 10−1000 μm with the highest volume density of 109.91 μm, followed by pH 6.30 (53.09 μm) and pH 6.70 samples (19.87 μm) (Fig. 3-1A). This observation may be due to more non-membrane milk proteins associated with the MFGs/MFGM fragments at pH 5.30, which may not be washed away during the MFGs/MFGM enrichment by centrifugation. Comparatively, MFGs/MFGM isolated from cheese whey presented the smallest size distribution than samples prepared from bovine raw milk. Particles in MFGM-C were mainly distributed over the range of 0.01−1 μm and 5−50 μm. The intact MFGs may break down into fragments because of the mechanical shearing treatment during the whey drainage process, which induced the increased distribution of smaller particle size (Zhou, et al., 2021b).

CLSM images visually displayed particle size differentiation mentioned above (Fig. 3-1B). From Fig. 3-1B, more attached non-membrane milk proteins were observed on the MFGs surface at pH 5.30 than at pH 6.30 and 6.70. Furthermore, at pH 5.30, non-membrane milk proteins formed network structures with intact MFGs embedded in them. In comparison, rare intact MFGs were observed and MFGs/MFGM fragments mainly existed in MFGM-C. In addition, more pronounced non-membrane milk proteins were observed adsorbing around the MFGs/MFGM fragments in

MFGM-C than MFGs/MFGM with different pH conditions. This may be attributed to coagulation in the MFGM-C preparation, which promoted the interaction of non-membrane proteins with MFGs/MFGM or fragments.

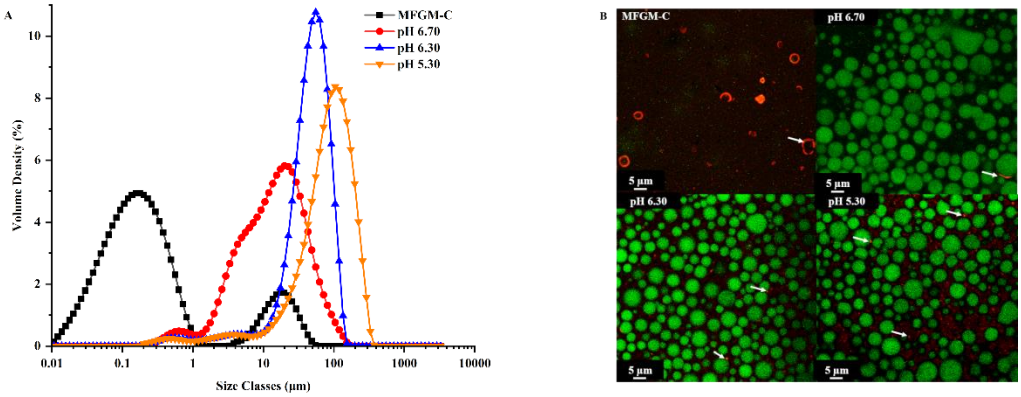



**Figure 3-1.** Particle size distribution (A) and microstructure (B) of MFGs/MFGM isolated from acidified bovine raw milk and sweet whey (MFGM-C). Confocal laser scanning microscopy (CLSM) was used to observe and capture the images. Neutral lipids (mainly triglyceride) and non-membrane milk protein were stained with Nile red and fast green FCF (white arrows pointing at the adsorbed non-membrane milk proteins on the MFGs). Scale bar=5 μm

### 3.3.2. FTIR

Fig. 3-2A shows the FTIR spectra of MFGM-C and MFGs/MFGM at different pH conditions. The full wavenumbers (4000–900 $cm^{-1}$) were divided into six different regions according to the functional groups, and the corresponding milk components associated with each region were listed in Table 3-2. The second derivative (Fig.3-2 B) and peaks deconvolution were further applied between 1200–900 $cm^{-1}$ (Fig.3-3) to separate the overlapping peaks and make a complete comparison of the spectra (Hong Bui, Cozzolino, Zisu, & Chandrapala, 2021).

Peaks at 2925 and 2852 $cm^{-1}$ in region 1 were observed in all samples which may be assigned to asymmetric and symmetric stretching modes of $–CH_2$ groups of acyl chains in TGAs or phospholipids, respectively (Fig. 3-2A). Peak positioned at 2963 $cm^{-1}$ became more obvious in the 2$^{nd}$ derivation spectra (Fig. 3-2B), which was associated

with the C−H bending of $-CH_3$ (Grewal, et al., 2017). An apparent peak with intense absorbance at 1945 $cm^{-1}$ in region 2 was detected which may mainly relate to the C=O stretching vibrations in lipid-protein conjugates or ester bonds of lipids (Nicolaou, et al., 2008) (Fig. 3-2A). Peaks over the range of 3000−2800 $cm^{-1}$ and 1800−1700 $cm^{-1}$ were observed in all spectra, combined with Table 3-2, it was concluded that all MFGs/MFGM presented a similar lipids fingerprint.

**Table 3-2** Six regions of different FTIR spectra correspond to specific milk components

| Region No. | FTIR wavenumbers ($cm^{-1}$) | Milk components | Reference |
|---|---|---|---|
| 1 | 3000–2800 | Asymmetric and symmetric stretching modes of $CH_2$ groups of acyl chains of triglycerides or phospholipids | (Nicolaou & Goodacre, 2008; Grewal, et al., 2017) |
| 2 | 1800–1700 | C=O stretching vibrations of ester, aldehydes and ketones | (Vongsvivut, et al., 2012) |
| 3 | 1700–1600 | Amide I protein | (Kher, Udabage, McKinnon, McNaughton, & Augustin, 2007) |
| 4 | 1600–1500 | Amide II protein | |
| 5 | 1500–1200 | Amide III protein | (Grewal, et al., 2017) |
| 6 | 1200–900 | Membrane lipids, protein–lipid associations, lactose | (Zhou, et al., 2006b) |

The wavenumbers from regions 3 to 5 were used to characterize protein groups, which were attributed to amide I (1700–1600 $cm^{-1}$), amide II (1600–1500 $cm^{-1}$), and amide III (1500–1200 $cm^{-1}$). None of the samples showed obvious absorbance peaks in amide I and amide II regions except MFGM-C. This finding was due to a higher amount of protein in MFGM-C (Table 3-1). According to compositional analysis results in Table 3-1, the protein content in MFGM-C was 14.23 % (w/w), significantly higher than that in cream-sourced MFGs/MFGM (0.72−2.99 %, w/w). It can be inferred that high-speed centrifugation during the isolation of MFGs/MFGM from the acidified milk removed most of the non-membrane milk proteins in the cream. Casein structure was changed by chymosin during the cheese rennet stage, which made its association with MFGs/MFGM fragments and more difficult to be removed by centrifugation. Typical β-sheet protein structure at 1635 $cm^{-1}$ was only detected in MFGM-C (Fig. 3-2 B). In addition, hidden peaks in MFGM-C at 1550 $cm^{-1}$ and 1518

$cm^{-1}$ corresponding to C–N or N–H stretching and tyrosine in free amino acid were presented in the second derivation spectra (Yang, Yang, Kong, Dong, & Yu, 2015; Sadat & Joye, 2020; De Meutter & Goormaghtigh, 2021).

A weak signal of protein secondary structure was detected in MFGs/MFGM within the amide III range (region 5, 1500–1200 $cm^{-1}$), which mainly may be the co-existence of MFGM proteins and conjugation of non-membrane milk proteins with MFGs/ MFGM. The spectra between 1500 and 1200 $cm^{-1}$ showed no significant difference among the different pH conditions by comparing the original and second derivative spectra. It may be because of the weak absorbance and high noise signal in this range. In addition, it is difficult to distinguish MFGs/MFGM materials at different pH between 1200 and 900 $cm^{-1}$ because of the multimodal. Hence, peak deconvolution was applied to this region to search for the hidden peaks. Two separated peaks, 1175 $cm^{-1}$ and 1148 $cm^{-1}$, were observed between 1200 $cm^{-1}$ and 1135 $cm^{-1}$ at all pH conditions (Fig. 3-3 A, B, and C) except for MFGM-C (Fig. 3-3 D) in which only one central peak at 1166 $cm^{-1}$ was detected. Peaks detected at 1175 $cm^{-1}$ and 1148 $cm^{-1}$ were used to characterize the stretching vibration of C–O–C in the ester bond of TGAs or fatty acids. The stretching of C–O at 1166 $cm^{-1}$ was reported to relate to the ester group due to asymmetric vibrations of C–C(=O)–O (Mekonnen, 2023). More hidden peaks were brought out after curve fitting within 1135−900 $cm^{-1}$ at the lower pH than the control (pH 6.70), especially at pH 6.30, in which three more peaks were found. According to Table 3-2, different components, such as membrane lipids, protein–lipid associations, and lactose, had absorbance signals within spectra 1200−900 $cm^{-1}$. Since the preparation methods removed most lactose (Table 3-1), we speculated that the different spectra may be attributed to the different degrees of association between non-membrane milk protein and milk fat. The change of non-membrane milk protein conformation at different pH conditions may affect their bonding ability with the MFGs/MFGM fragments. This result was supported by the formation of partially folded intermediate casein structure induced by the pH variation (Chakraborty & Basak, 2007). It can be inferred that more types of conjugates were formed between

non-membrane milk proteins and MFGs/MFGM at pH 6.30 condition verified by the more corresponding observable peaks.

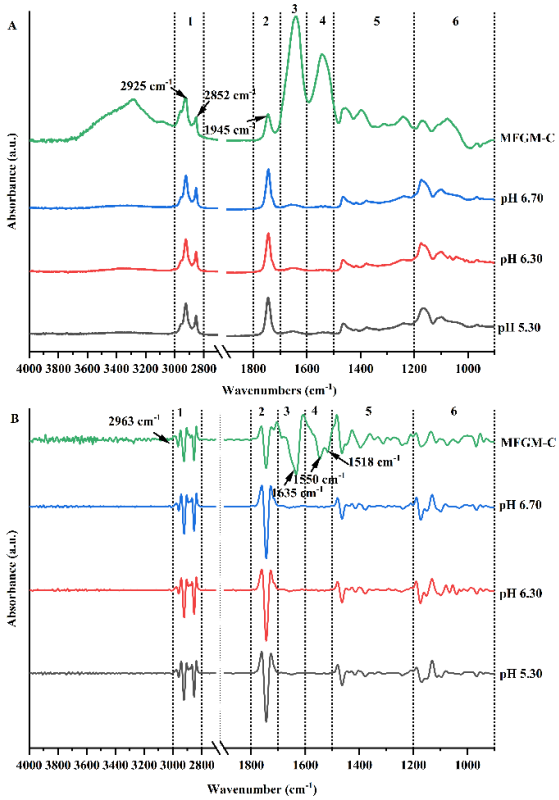



**Figure 3-2.** Original (A) and representative second derivation (B) FTIR spectra of MFGs/MFGM from acidified bovine milk and sweet whey (MFGM-C) (Spectra between 2700 and 1900 $cm^{-1}$ did not be shown because there was no peak was detected for all samples, and all the spectra exhibited the similar flat plots)

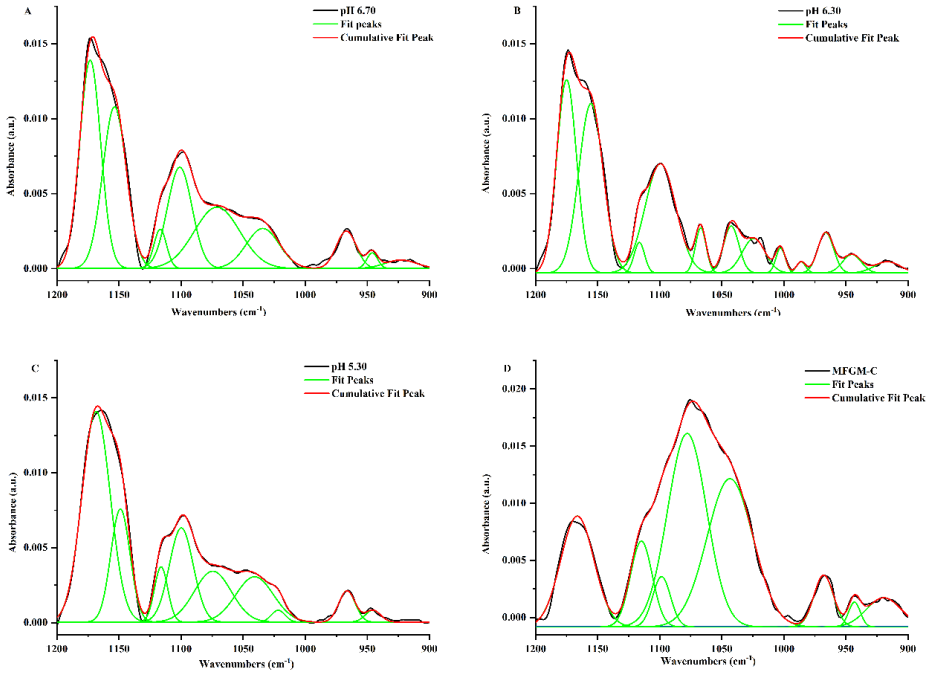



**Figure 3-3.** Curve fitted regions (1200–900 $cm^{-1}$) in FITR spectra of MFGs/MFGM separated from pH 6.70 (A), pH 6.30 (B), pH 5.30 (C) bovine milk and MFGM-C (D)

### 3.3.3. Interfacial tension

The change of composition and structural rearrangement on the surface of MFGs/MFGM can be reflected by analysing the interfacial tension between air and liquid emulsion droplets. In our pre-experiment (data not shown), the recording time was set as 600 s, but the results showed relatively stable during the entire analysis. There was no significant difference from the initial recording to the final reading at 600 s. Therefore, the recording time in this study only lasted 20 s. It can be argued that the interfacial compositions of MFGs completed rearrangement during the preparation stage and interfacial tension remained constant during the entire analysis.

As shown in Fig.3-4, the interfacial tension of MFGs/MFGM at pH 6.70 (41.00±1.00 mN/m) was significantly higher than MFGs/MFGM at pH 6.30 and 5.30

($p$<0.05), while the lowest interfacial tension magnitude was MFGM-C (24.67±0.58 mN/m). Interfacial tension of MFGM-C was significantly lower than pH 6.70 and pH 5.30 at the significant level of 0.001 ($p$<0.001) while at the 0.05 level ($p$<0.05) of the MFGs/MFGM at pH 6.30. The adsorption of non-membrane milk proteins on the surface of MFGs has been reported to be inversely proportional to the interfacial tension (Michalski, et al., 2002d). This result was consistent with the images of CLSM in Fig.3-1B, in which, visually, more non-membrane milk proteins were observed surrounding MFGs at pH 5.30 than at pH 6.70 and 6.30. In addition, interfacial tension has been reported to positively correlate with particle size (Ho, et al., 2021). This finding confirmed the particle size results of MFGM-C in Fig.3-1A. Fig.3-1A shows that less volume density (%) of bigger particles was detected in MFGM-C, which, shows the lowest interfacial tension. However, MFGs/MFGM at pH 6.70 presented the opposite trend, which shows the lower volume density (%) of bigger particle size (19.87 μm) but higher interfacial tension than MFGs/MFGM at pH 6.30 and 5.30. Most intact MFGs were crushed into fragments during the MFGM-C preparation, which was confirmed by the CLSM images (Fig. 3-1B). It can be speculated that particle size and the compositions on the surface of MFGs played an important role in the interfacial tension. Perhaps there were more exposed hydrophilic and hydrophobic groups in the MFGM-C, which were easy to adsorb on the interface of oil and air, thus forming a more stable droplet structure with the lower interfacial tension.

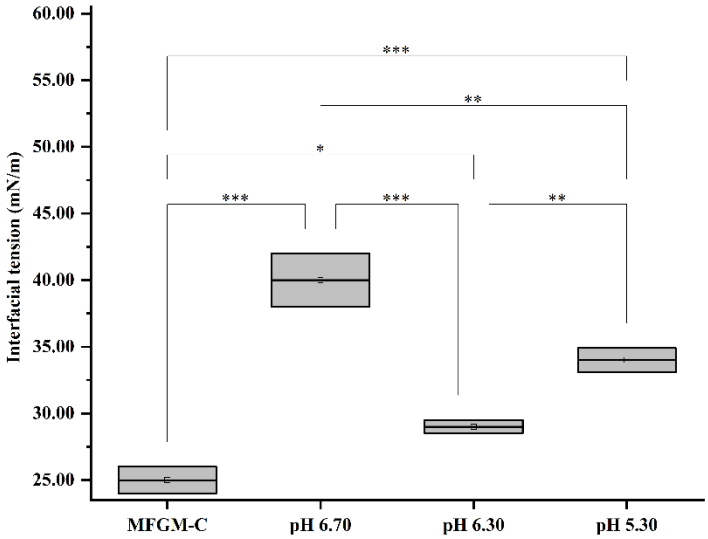



**Figure 3-4** Interfacial tension of MFGs/MFGM isolated from acidified bovine milk and sweet whey (MFGM-C). *, ** and *** represent $p < 0.05$, $p < 0.01$ and $p < 0.001$, respectively.

### 3.3.4. ζ-potential

The ζ-potential indicates the change of MFGs structure and the interfacial composition. It indirectly predicts the potential emulsifying ability of MFGs/MFGM in the emulsion. As the MFGs and casein micelles carry the negative net charge, thus MFGs/MFGM in this research exhibited negative ζ-potential. Herein, ζ-potential variation refers to the absolute value change.

The ζ-potential of MFGs/MFGM at pH 6.70 was −37.6 ± 0.11 mV (Table. 3-3), and pH decrease resulted in a significant increase of the ζ–potential to −39.4 ± 0.24 mV at pH 6.30 and −40.6 ± 0.18 mV at pH 5.30 samples ($p$<0.05). This result may be explained by the preferential adsorption of non-membrane milk protein on the MFGs at lower pH conditions. The adsorption of casein micellar on the MFGs attributed to more detected negative charges at pH 5.30. The ζ-potential of MFGM-C (–28.30±0.30 mV) was significantly lower than that of MFGs/MFGM sourced from acidified bovine

milk, even though the pH of MFGM-C was close to pH 6.30. Combined with the unique MFGs/MFGM fragments structure in MFGM-C (Fig. 3-1B), it may be inferred that intact MFGs/ MFGM structure facilitated the movement of negatively charged particles or molecules, and the velocity is positively proportional to ζ-potential.

It has been reported that surface weighted mean-D [3, 2] of MFGs/MFGM presented an opposite change tendency with the ζ-potential (Michalski, et al., 2002d). On the contrary, the results of ζ-potential of MFGs/MFGM in this study presented a similar trend to the change in particle size. The opposite results may be due to the different mechanical shear intensities. Because homogenisation has been applied by Michalski et al. (2021), a more stringent treatment than the centrifugation used in this study. The ζ-potential of unprocessed raw milk was −32.10±0.10 mV, which was used as the reference to calculate the MFGs surface fraction (Φ). There was a significant increase of Φ in MFGs/MFGM as a function of pH decrease. This finding confirmed the CLSM results in 3.2.4 which showed more attached non-membrane milk protein on the surface of MFGs at pH 5.30.

It is worth noting that the ζ-potential of unprocessed raw milk in this research is inconsistent with previous research in which the ζ-potential of untreated whole milk has been reported between −13.10±0.50 mV and −13.70±0.10 mV (Michalski, et al., 2002d; Sharma, et al., 2015b). However, it was in agreement with the results from Jukkola, Partanen, Rojas, and Heino (2016c), who reported that the ζ-potential of MFGs separated via microfiltration was −30.10±0.10 mV. Many variables, such as diet, lactation, and processing units, affected the composition and structure of raw milk. All these factors would alter the surface charge of MFGs/MFGM, thus the ζ-potential. Therefore, this research mainly focused on the comparative analysis of ζ-potential between MFGs/MFGM at different pH and sourced from different materials. In addition, all the MFGs/MFGM in this study were isolated from the same batch of raw bovine milk and were analysed with the same method.

**Table 3-3** The effect of acidification and different sources of MFGs/MFGM on the ζ-potential and surface coverage (Φ) of globules.

| | ζ–potential (mV) | $\zeta_R$ (%) | Φ |
|---|---|---|---|
| Unprocessed raw milk | –32.17±0.12$^{e}$ | – | – |
| MFGM–C | –28.30±0.30$^{d}$ | –11.84±0.93$^{d}$ | 0.14±0.02$^{d}$ |
| pH 6.70 | –37.60±0.11$^{c}$ | 17.14±0.31$^{c}$ | 0.27±0.01$^{c}$ |
| pH 6.30 | –39.40±0.24$^{b}$ | 22.74±0.62$^{b}$ | 0.43±0.02$^{b}$ |
| pH 5.30 | –40.60±0.18$^{a}$ | 26.48±1.56 $^{a}$ | 0.53±0.04$^{a}$ |

Notes: Different superscript letters in the same column indicate significant ($p < 0.05$) differences among the samples.

### 3.3.5. XRD

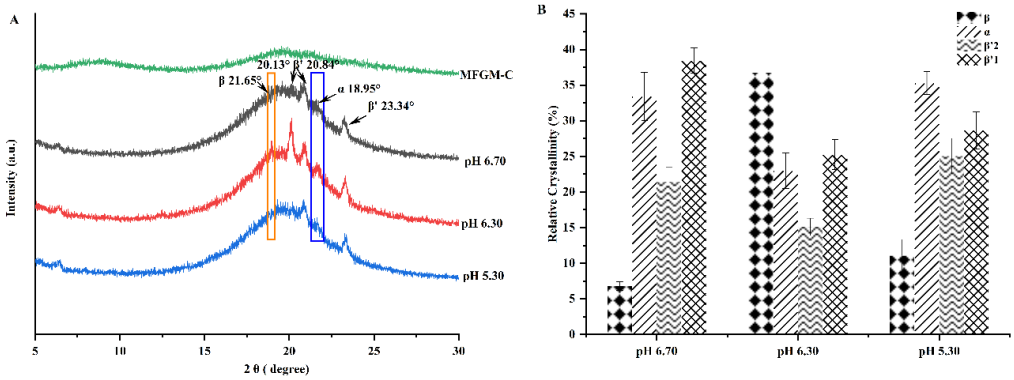



**Figure 3-5.** XRD patterns (A) and the relative crystallinity (B) of β, α, β'2, and β'1 crystals in MFGs/MFGM isolated from different pH bovine milk or sweet whey. Relative crystallinity in MFGM-C was not shown because no crystal peaks were detected during the integration process.

The polymorphic structure of MFGs/MFGM materials prepared from acidified bovine milk and sweet whey was acquired by wide angle X-ray scattering configuration (Fig. 3-5A). The typical polymorphs, β' crystal form, were identified in all acidified MFGs/MFGM materials at 20.13˚, 20.84˚ and 23.34˚. In addition, apparent peaks at 18.95˚ and 21.65˚ were identified, which were related to α and β arrangement, respectively (Ren, et al., 2020). However, broad peaks instead of sharp crystal peaks were observed in MFGM-C. It may be attributed to the different existing

state of triglyceride in MFGM-C from MFGs/MFGM isolated from acidified bovine raw milk (Fig. 3-1B).

According to Fig. 3-5B, the relative crystallinity of β' crystal ($\beta'_1$+ $\beta'_2$) in all samples is significantly higher than α and β forms. This result was supported by Wright and Marangoni (2006a), who has reported that the major polymorph in milk fat is β' crystal and milk fat is defined as β' fat. Specifically, more than 50 % of crystal type in pH 6.70 and 5.30 cream were β' crystal, while at pH 6.30, that was only 40.32 % due to the lower proportion of $\beta'_2$. The differences might be associated with the difference in MFGs interfacial curvature. It has been reported that the surface curvature of MFGs may change the crystalline characteristic because the formation of crystals started between the lipid droplets and the inner monolayer membrane (Murthy, Guyomarc'h, Paboeuf, Vie, & Lopez, 2015).

Furthermore, MFGs size has been proven to play an important role in the formation of different crystalline types (Ren, et al., 2020). Smaller particle sizes of MFGs could inhibit the polymorphism transition, and it is easy to form the small-sized polymorphs, such as α and β' forms. The results of this study contradict this theory. pH 5.30 presented a higher volume density (8.37%) for bigger particles (105.83 μm) but contained higher amounts of α and β' crystals than β crystals compared to MFGs/MFGM at pH 6.30 and 6.70.

The amount of β crystal (36.72%) in MFGs/MFGM at pH 6.30 was significantly higher than that in control (6.79%) and at pH 5.30 (11.05%). β crystal has been reported to be the most stable crystal form in milk fat (Ren, et al., 2020). In addition, β crystals melted at a higher temperature than α and β' crystals because of their densest triclinic sub-cell packing (Wright, et al., 2006a).

This study shows that decreased pH from 6.70 to 6.30 promoted a lower relative intensity of α crystals (22.96%) in MFGs/MFGM. Acidification and shearing treatment may cause changes in the types of fatty acids and TGA in MFGs/MFGM,

which would affect the MFGs diffraction patterns. Tripalmitoyl glycerol (PPP) and trioleolyl glycerol (OOO) tends to form β crystals, while 1,3–dipalmitoyl–2–oleoyl–glycerol (POP) and 1–palmitoyl–2–oleoyl–3–stearoyl–glycerol (POS) typically forms α and β' crystals (Zhang, et al., 2014). Based on this theory, we speculated that MFGs/MFGM at pH 6.70 and 5.30 may have more POP and POS than those at pH 6.30. Further investigation is needed to quantify and profile the fatty acid and TGA in MFGs/MFGM materials prepared from acidified raw milk or sweet whey.

### 3.3.6. DSC

DSC coupled with XRD has been used to elucidate the correlation between the polymorphism and thermal properties of milk fat (Lopez, Bourgaux, Lesieur, & Ollivon, 2007). Two main exothermic events were detected during the cooling stage in all cases (Fig. 3-6A), which was in good agreement with the previous research (Lopez, Lesieur, Bourgaux, Keller, & Ollivon, 2001; Lambert, et al., 2018). The exothermal curves were more complicated, with more peaks and curves than the endothermal thermograms. This finding indicated that sub-stable crystals melted firstly during the endothermic phase. Meanwhile, the un-melted crystals continually rearranged and formed more stable structures, which eventually melted at higher temperatures (Bootello, et al., 2013).

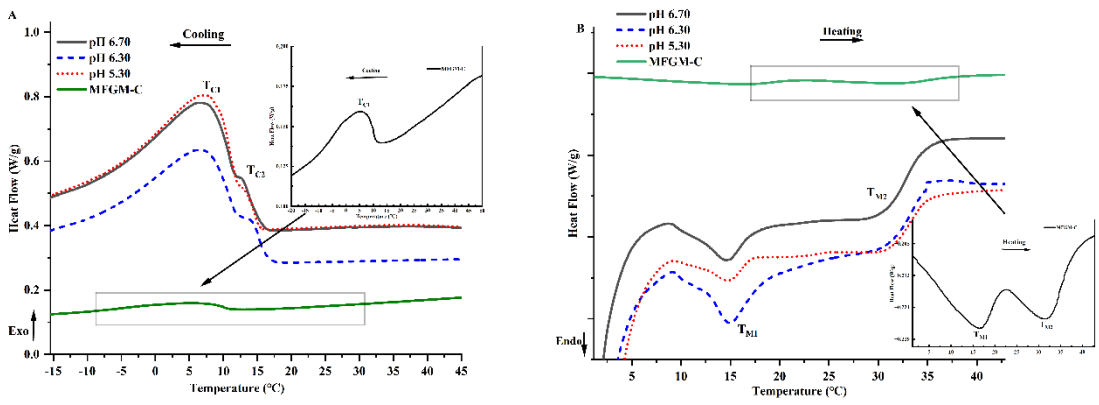



**Figure 3-6.** Crystallization (A) and melting (B) thermograms of MFGs/MFGM prepared from different pH bovine milk and sweet whey.

At pH 6.70, the first exothermic event started at 19.11℃, with the maximum exothermic heat flow at 11.94 ℃, followed by the second maximum at 6.83 ℃ (Fig.3-6A). In comparison, the first crystallisation peaks for MFGs/MFGM at pH 6.30 and 5.30 occurred at 12.74 ℃ and 12.49 ℃, which were significantly higher than that at pH 6.70 (Table 3-4). Subsequently, the second exothermal event in MFGs/MFGM at pH 5.30 occurred at 7.14 ℃, followed by 6.83 ℃ and 6.17 ℃ at pH 6.70 and 6.30, respectively. There is no correlation and consistency for the change of crystallization temperature of MFGs/MFGM as pH decreases. Regarding MFGM-C, the higher crystallization temperature peaks positioned around 12 ℃ did not appear, and only one exothermic peak with the maximum peak value at 5.48 ℃ was detected. According to the previous XRD results on anhydrous milk fat, spectra at 12 ℃ were assigned to unstable α crystals and coexisted with relatively stable β' crystals (Lambert, et al., 2018). This result confirmed the undetected crystal forms in the MFGM-C resulting from XRD.

It has been reported that the decrease in MFGs size is attributed to the delay of the crystallisation because more time was needed to form the nucleus in smaller MFGs (Michalski, Ollivon, Briard, Leconte, & Lopez, 2004). This finding explained the lower crystallisation temperature of MFGs/MFGM at pH 6.70, which have higher volume density (%) of smaller particle size than at pH 6.30 and 5.30 according to 3.1.3 results.

Similarly, two major endothermic events were observed in the MFGs/MFGM at different pH and MFGM-C during the heating stage. In all cases, the first significant heat absorption maximum peak was close to 15 ℃, and the second was between 30 ℃ and 35 ℃ (Fig. 3-6 B). These two heat flows were attributed to the medium-melting-temperature fractions and high-melting-temperature fractions. respectively (Sert & Mercan, 2020). In addition, the endotherm at 15 ℃ and around 33.8 ℃ may be associated with the transferring from α to β' form and the melting of β' form, respectively (Timms, 1980). MFGs/MFGM at pH 6.30 melted at a higher temperature

(14.77℃−14.95 ℃) than at pH 5.30 and control. Compared with MFGs/MFGM at different pH, the first endothermic event for MFGM-C occurred at a higher temperature (16.84 ℃). According to the particle size and microstructure results, MFGM-C presented rare intact MFGs structure and smaller particle size than MFGs/MFGM at different pH conditions. In addition, the preparation of MFGM-C from whey involved more severe heating treatments, during which the crystals were re-formed and glycerol recrystallized. These findings may have been attributed to the lower crystallization and higher melting temperature of MFGM-C (Wright & Marangoni, 2006b).

The enthalpy for crystal formation ($\Delta H_C$) and melting ($\Delta H_M$) in MFGM-C was significantly lower than control and acidified MFGs/MFGM ($p<0.05$) (Table 3-4). There was no significant difference in the $\Delta H_C$ between MFGs/MFGM at pH 6.70 and 5.30 ($p>0.05$), while MFGs/MFGM at pH 6.30 exhibited the lowest $\Delta H_C$. Moreover, less $\Delta H_M$ was detected in MFGs/MFGM at pH 6.30 than at 6.70 during the melting stage. This result contradicts to the XRD results, from which β crystals had the highest proportion in MFGs/MFGM at pH 6.30. As β crystal has a more stable structure than that of α and β' crystals, more energy should be needed for the crystal formation and melting at pH 6.30. It may be inferred that except for the crystal forms, the different associations between non-membrane milk protein and MFGs/MFGM demonstrated by the FTIR results (Fig.3-3) may be attributed to the lower $\Delta H_C$ and $\Delta H_M$ of MFGs/MFGM at pH 6.30.

**Table 3-4** Enthalpy, crystallization and melting temperature of MFGs/MFGM isolated from bovine milk and sweet whey

| | Crystallization | | | Melting | | |
|---|---|---|---|---|---|---|
| | $T_{C1}$ (℃) | $T_{C2}$ (℃) | $\Delta H_C$ (J $g^{-1}$) | $T_{M1}$(℃) | $T_{M2}$(℃) | $\Delta H_M$(J $g^{-1}$) |
| MFGM-C | – | 5.48±0.01$^{d}$ | 0.73±0.00$^{c}$ | 16.93±0.13$^{a}$ | 32.37±0.24$^{a}$ | 0.10±0.01$^{c}$ |
| pH 6.70 | 11.94±0.03$^{c}$ | 6.83±0.04$^{b}$ | 8.18±0.01$^{a}$ | 14.71±0.08$^{c}$ | 30.23±0.04$^{b}$ | 0.63±0.04$^{a}$ |
| pH 6.30 | 12.74±0.01$^{a}$ | 6.17±0.03$^{c}$ | 6.56±0.05$^{b}$ | 14.95±0.02$^{b}$ | 30.71±0.36$^{b}$ | 0.31±0.00$^{b}$ |
| pH 5.30 | 12.49±0.11$^{b}$ | 7.14±0.06$^{a}$ | 8.33±0.02$^{a}$ | 14.77±0.03$^{bc}$ | 30.82±0.22$^{b}$ | 0.27±0.03$^{b}$ |

Notes: 1. Abbreviations are: $T_{C1}$ and $T_{C2}$, the points of crystallisation for the first and second peaks, $\Delta H_C$, enthalpy of crystallisation; $T_{M1}$ and $T_{M2}$, the temperature of melting for the first and second peaks, $\Delta H_M$, enthalpy of melting. 2. Different superscript letters in the same column indicate significant ($p < 0.05$) differences among the samples.

## 3.4 Conclusions

Our results demonstrated that MFGs/MFGM ingredients prepared from pH 6.30 and 5.30 bovine milk presented significantly different physicochemical properties, microstructure, surface charges, interfacial tension, crystal forms, and thermal properties from those of control (pH 6.70). In contrast, MFGs/MFGM derived from

sweet whey exhibited significantly different techno-functional properties compared to those sourced from bovine milk. MFGM-C prepared from sweet whey contained rare intact globule structures and exhibited more protein compositions, as identified by FTIR spectra in the ranges of 1700–1600 $cm^{-1}$ (Amide I protein) and 1600–1500 $cm^{-1}$ (Amide II protein). Additionally, MFGM-C presented lower interfacial tension and ζ-potential than MFGs/MFGM from bovine raw milk. No apparent polymorphs were observed in MFGM-C, and lower exothermic or endothermic enthalpy was required during the heating and quenching procedures. Acidification, especially pH 6.30 conditions, led to the adsorption of non-membrane milk proteins on the MFGs or MFGM fragments, forming more types of conjugate detected by FTIR. Consequently, this induced changes in the proportion of fat crystal form and thermal behaviour of MFGs/MFGM at pH 6.30.

In conclusion, this study provides critical information for developing MFGs/MFGM ingredients and their application in the food industry. However, this study is only a preliminary exploration of the influence of industrial MFGs/MFGM processing units on its properties. Further studies can be conducted to systematically track the effect of cheese processing on the physicochemical properties and functionalities of MFGs/MFGM. There is currently little research on this topic. Future studies could simulate parameters such as heat treatment, curding, acidification, and whey removal during actual industrial cheese production to investigate their impact on MFGs/MFGM.

**Declaration of competing interest**

All authors declare no conflict of interest.

**Author Statements**

Yanjun Sun: Conceptualization, Methodology, Writing-original draft, Data curation, Investigation, Funding acquisition. Yrjö H. Roos: Supervision, Writing

review & editing. Song Miao: Supervision, Conceptualization, Writing-review & editing, Funding acquisition, Project administration, Investigation.

## Data availability

Data will be made available on request.

## Acknowledgements

The project was founded by 'The Open Project Program of State Key Laboratory of Dairy Biotechnology (No. SKLDB2022–007)' and 'The China Scholarship Council (No.202008410212)'.

## References

Bootello, M. A., Hartel, R. W., Levin, M., Martinez-Blanes, J. M., Real, C., Garces, R., et al. (2013). Studies of isothermal crystallisation kinetics of sunflower hard stearin-based confectionery fats. *Food Chemistry, 139*(1-4), 184-195.

Chakraborty, A., & Basak, S. (2007). pH-induced structural transitions of caseins. *Journal of Photochemistry and Photobiology B: Biology, 87*(3), 191-199.

De Meutter, J., & Goormaghtigh, E. (2021). Amino acid side chain contribution to protein FTIR spectra: impact on secondary structure evaluation. *European Biophysics Journal, 50*(3-4), 641-651.

Fontecha, J., Brink, L., Wu, S., Pouliot, Y., Visioli, F., & Jimenez-Flores, R. (2020). Sources, Production, and Clinical Treatments of Milk Fat Globule Membrane for Infant Nutrition and Well-Being. *Nutrients, 12*(6), 1607.

Grewal, M. K., Chandrapala, J., Donkor, O., Apostolopoulos, V., Stojanovska, L., & Vasiljevic, T. (2017). Fourier transform infrared spectroscopy analysis of physicochemical changes in UHT milk during accelerated storage. *International Dairy Journal, 66*, 99-107.

Ho, T. M., Dhungana, P., Bhandari, B., & Bansal, N. (2021). Effect of the native fat globule size on foaming properties and foam structure of milk. *Journal of Food Engineering, 291*, 110227.

Holzmüller, W., Gmach, O., Griebel, A., & Kulozik, U. (2016). Casein precipitation by acid and rennet coagulation of buttermilk: Impact of pH and temperature on the isolation of milk fat globule membrane proteins. *International Dairy Journal, 63*, 115-123.

Hong Bui, A. T., Cozzolino, D., Zisu, B., & Chandrapala, J. (2021). Infrared analysis of ultrasound treated milk systems with different levels of caseins, whey proteins and fat. *International Dairy Journal, 117*, 104983.

Huang, Y., Wei, T., Chen, F., Tan, C., Gong, Z., Wang, F., et al. (2023). Effects of various thermal treatments on interfacial composition and physical properties of bovine milk fat globules. *Food Research International, 167*, 112580.

Jukkola, A., Partanen, R., Rojas, O. J., & Heino, A. (2016). Separation of milk fat globules via microfiltration: Effect of diafiltration media and opportunities for stream valorization. *Journal of Dairy Science, 99*(11), 8644-8654.

Jukkola, A., Partanen, R., Rojas, O. J., & Heino, A. (2018). Effect of heat treatment and pH on the efficiency of micro-diafiltration for the separation of native fat globules from cream in butter production. *Journal of Membrane Science, 548*, 99-107.

Kher, A., Udabage, P., McKinnon, I., McNaughton, D., & Augustin, M. A. (2007). FTIR investigation of spray-dried milk protein concentrate powders. *Vibrational Spectroscopy, 44*(2), 375-381.

Kiełczewska, K., Ambroziak, K., Krzykowska, D., & Aljewicz, M. (2021). The effect of high-pressure homogenisation on the size of milk fat globules and MFGM composition in sweet buttermilk and milk. *International Dairy Journal, 113*, 104898.

Lambert, A., Bougrioua, F., Abbas, O., Courty, M., El Marssi, M., Faivre, V., et al. (2018). Temperature dependent Raman and X-ray diffraction studies of anhydrous milk fat. *Food Chemistry, 267*, 187-195.

Li, H., & Van der Meeren, P. (2022). Sequential adsorption of whey proteins and low methoxy pectin at the oil-water interface: An interfacial rheology study. *Food Hydrocolloids, 128*, 107570.

Liu, Y., Boeren, S., Zhang, L., Zhou, P., & Hettinga, K. (2021). Ultrasonication retains more milk fat globule membrane proteins compared to equivalent shear-homogenization. *Innovative Food Science & Emerging Technologies, 70*, 102703.

Lopez, C., Bourgaux, C., Lesieur, P., & Ollivon, M. (2007). Coupling of time-resolved synchrotron X-ray diffraction and DSC to elucidate the crystallisation properties and polymorphism of triglycerides in milk fat globules. *Le Lait, 87*(4-5), 459-480.

Lopez, C., Lesieur, P., Bourgaux, C., Keller, G., & Ollivon, M. (2001). Thermal and Structural Behavior of Milk Fat. *Journal of Colloid and Interface Science, 240*(1), 150-161.

Mekonnen, K. D. (2023). Fourier transform infrared spectroscopy as a tool for identifying the unique characteristic bands of lipid in oilseed components: Confirmed via Ethiopian indigenous desert date fruit. *Heliyon, 9*(4), 14699.

Michalski, M. C., Michel, F., Sainmont, D., & Briard, V. (2002). Apparent ζ-potential as a tool to assess mechanical damages to the milk fat globule membrane. *Colloids and Surfaces B: Biointerfaces, 23*(1), 23-30.

Michalski, M. C., Ollivon, M., Briard, V., Leconte, N., & Lopez, C. (2004). Native fat globules of different sizes selected from raw milk: thermal and structural behavior. *Chemistry and Physics of Lipids, 132*(2), 247-261.

Mohamed, H. J. J., Lee, E. K. H., Woo, K. C. K., Sarvananthan, R., Lee, Y. Y., & Mohd Hussin, Z. A. (2022). Brain-immune-gut benefits with early life supplementation of milk fat globule membrane. *JGH Open, 6*(7), 454-461.

Mohan, M. S., O'Callaghan, T. F., Kelly, P., & Hogan, S. A. (2020). Milk fat: opportunities, challenges and innovation. *Critical Reviews in Food Science and Nutrition*, 1-33.

Murthy, A. V., Guyomarc'h, F., Paboeuf, G., Vie, V., & Lopez, C. (2015). Cholesterol strongly affects the organization of lipid monolayers studied as models of the milk fat globule membrane: Condensing effect and change in the lipid domain morphology. *Biochimica et Biophysica Acta (BBA), 1848*, 2308-2316.

Nicolaou, N., & Goodacre, R. (2008). Rapid and quantitative detection of the microbial spoilage in milk using Fourier transform infrared spectroscopy and chemometrics. *Analyst, 133*(10), 1424-1431.

Nieto-Ruiz, A., Garcia-Santos, J. A., Verdejo-Roman, J., Dieguez, E., Sepulveda-Valbuena, N., Herrmann, F., et al. (2022). Infant Formula Supplemented With Milk Fat Globule Membrane, Long-Chain Polyunsaturated Fatty Acids, and Synbiotics Is Associated With Neurocognitive Function and Brain Structure of Healthy Children Aged 6 Years: The COGNIS Study. *Front Nutrition, 9*, 820224.

Pan, Y., Liu, S., Li, J., Hussain, M., Bora, A. F. M., Li, X., et al. (2024). Regulating the lipid droplet interface based on milk fat globule membrane and milk proteins to improve lipid digestion of model infant formula emulsion. *Food Hydrocolloids, 146*.

Pope, C. G. (1997). X-Ray Diffraction and the Bragg Equation. *Journal of Chemical Education, 74*(1), 129.

Ren, Q., Guo, F., Teng, F., & Ma, Y. (2021). A novel approach for the reconstitution of bovine milk fat globules with different-melting-temperature triacylglycerol cores. *Food Chemistry, 345*, 128563.

Ren, Q., Li, Q., Liu, H., & Ma, Y. (2020). Thermal and storage properties of milk fat globules treated with different homogenisation pressures. *International Dairy Journal, 110*, 104725.

Sadat, A., & Joye, I. J. (2020). Peak Fitting Applied to Fourier Transform Infrared and Raman Spectroscopic Analysis of Proteins. *Applied Sciences, 10*(17).

Sert, D., & Mercan, E. (2020). Characterisation of physicochemical, microbiological, thermal, oxidation properties and fatty acid composition of butter produced from thermosonicated cream. *International Dairy Journal, 109*, 104777.

Sharma, P., Oey, I., & Everett, D. W. (2015). Interfacial properties and transmission electron microscopy revealing damage to the milk fat globule system after pulsed electric field treatment. *Food Hydrocolloids, 47*, 99-107.

Sun, Y., Roos, Y. H., & Miao, S. (2022). Changes in Milk Fat Globules and Membrane Proteins Prepared from pH-Adjusted Bovine Raw Milk. *Foods, 11*(24), 4107.

Timms, R. (1980). The phase behaviour and polymorphism of milk fat, milk fat fractions and fully hardened milk fat. *Australian Journal of Dairy Technology, 35*(2), 47.

Voigt, D. D., Donaghy, J. A., Patterson, M. F., Stephan, S., & Kelly, A. L. (2010). Manufacture of Cheddar cheese from high-pressure-treated whole milk. *Innovative Food Science & Emerging Technologies, 11*(4), 574-579.

Vongsvivut, J., Heraud, P., Zhang, W., Kralovec, J. A., McNaughton, D., & Barrow, C. J. (2012). Quantitative determination of fatty acid compositions in micro-encapsulated fish-oil supplements using Fourier transform infrared (FTIR) spectroscopy. *Food Chemistry, 135*(2), 603-609.

Wei, W., Cheng, J., Yang, J., Chen, C., Jin, Q., Song, J., et al. (2021). Phospholipid composition and fat globule structure change during low temperature storage of human milk. *Lwt, 150*, 1-7.

Wright, A. J., & Marangoni, A. G. (2006a). Crystallization and rheological properties of milk fat. In P. L. H. M. E. A. d. c. p. In P. F. Fox (Ed.), *Advanced Dairy Chemistry* (Vol. lipids, pp. 245-291). Boston: Springer.

Wright, A. J., & Marangoni, A. G. (2006b). Formation, structure, and rheological properties of ricinelaidic acid-vegetable oil organogels. *Journal of the American Oil Chemists' Society, 83*(6), 497-503.

Yang, H., Yang, S., Kong, J., Dong, A., & Yu, S. (2015). Obtaining information about protein secondary structures in aqueous solution using Fourier transform IR spectroscopy. *Nature protocols, 10*(3), 382-396.

Zamora, A., Ferragut, V., Guamis, B., & Trujillo, A. J. (2012). Changes in the surface protein of the fat globules during ultra-high pressure homogenisation and conventional treatments of milk. *Food Hydrocolloids, 29*(1), 135-143.

Zhang, X., Li, L., Xie, H., Liang, Z., Su, J., Liu, G., et al. (2014). Effect of temperature on the crystalline form and fat crystal network of two model palm oil-based shortenings during storage. *Food and bioprocess technology, 7*, 887-900.

Zhou, Q., Sun, S. Q., Yu, L., Xu, C.-H., Noda, I., & Zhang, X.-R. (2006). Sequential changes of main components in different kinds of milk powders using two-dimensional infrared correlation analysis. *Journal of Molecular Structure, 799*(1), 77-84.

Zhou, X., Hadiatullah, H., Guo, T., Yao, Y., Li, C., & Wang, X. (2021). Dairy Processing Affects the Gut Digestion and Microecology by Changing the Structure and Composition of Milk Fat Globules. *Journal of Agricultural and Food Chemistry, 69*(35), 10194-10205.

# CHAPTER FOUR

## Comparative study of interfacial properties and thermal behaviour of milk fat globules and membrane prepared from ultrasonicated bovine milk

Chapter 4 was published in:

Sun, Y., Roos, Y. H., & Miao, S. (2024c). Comparative study of interfacial properties and thermal behaviour of milk fat globules and membrane prepared from ultrasonicated bovine milk. *Ultrasonics Sonochemistry*, *102*, 106755

Yanjun Sun: Conceptualization, Methodology, Writing-original draft, Data curation, Investigation, Funding acquisition. Yrjö H. Roos: Supervision, Writing review & editing. Song Miao: Supervision, Conceptualization, Writing-review & editing, Funding acquisition, Project administration, Investigation.

**Abstract**

Milk fat globules or milk fat globule membranes (MFGs/MFGM) have been added in the infant formula to fortify the phospholipids and narrow down the nutritional gap from breast milk. The main aim of this study was to profile the interfacial and thermal properties of MFGs/MFGM prepared from ultrasonicated bovine milk. Bovine milk was sonicated at ultrasonic intensities of 20 kHz and 40 kHz independently or synchronously with the duration time of 0 min (control), 5 min, 10 min and 15 min (work/rest cycles= 5 s: 3 s). Ultrasonic treatments at 20 kHz/ 5 min and 20 + 40 kHz/ 5 min improved the volume density (%) of smaller particles (1-10 μm), while significantly decreased the surface hydrophobicity ($H_0$) ($p<0.05$). 40 kHz/5 min samples showed significantly higher ζ- potential than the other samples ($p<0.05$), which might be because more negative charges were detected. In comparison with control samples, ultrasonic treatments decreased the interfacial tension (π) between the air and MFGs/MFGM liquid phase. 20 kHz ultra-sonicated treatments decreased the diffusion rate ($k_{diff}$) of MFGs/MFGM interfacial compositions significantly as the duration prolonged from 5 min to 15 min ($p<0.05$) but did not affect the adsorption or penetration rate ($k_a$) ($p>0.05$). X-ray diffraction (XRD) results showed that α-crystal peaks only existed in control and ultrasonicated 5 min samples, but disappeared in all 15 min samples. According to the different scanning calorimetry (DSC), one or two new exothermic events (in the range of 17.29 – 18.81 ℃ and 22.14 – 25.21 ℃) appeared after ultrasonic treatments which, however, were not found in control samples. Ultrasonic treatments resulted in the low-melting fractions (LMF) ($T_{M1}$) peaks undetectable in MFGs/MFGM samples in which only peaks of medium-melting fractions (MMF) ($T_{M2}$) and high-melting fractions (HMF) ($T_{M3}$) were detected. Compared with the control, both enthalpy of crystallisation ($\Delta H_C$) and melting ($\Delta H_M$) decreased in ultrasonicated samples. In conclusion, ultrasonic treatment affects the interfacial and thermal properties of MFGs/MFGM.

**Keywords:** Milk fat globules, Ultrasonic treatment, Interfacial properties, X-ray diffraction, DSC

## 4.1. Introduction

Infant formulas are the essential food source for new-borns in the first half-year of their lives when breast milk is not available. Milk fat in infant formulas could supply energy and vital lipophilic nutrients for infants. Milk fat globules/membrane (MFGs/MFGM) ingredients have been clinically documented to be safe for the enrichment in infant formula, and also be associated with benefits for the infant neurocognitive development, brain structure and body growth (Jiang, et al., 2022; Nieto-Ruiz, et al., 2022). Commercially produced whey protein concentrate (WPC) enriched with MFGs/MFGM ingredients has been used in the infant formula to narrow the nutritional differences from breast milk. In addition to the health benefits, the effects of MFGs/MFGM ingredients supplement on the physicochemical properties and functionality of infant formula have been examined, but only in a small number of studies. MFGs/MFGM was proved to induce the interfacial composition and microstructure changes of fat globules in infant formula by reducing the thicknesses of the MFGM (Pan, et al., 2022). The combination of the homogenization process and buttermilk powder addition resulted in the decreased fat globule diameter of infant formula, but the improved colloidal stability of milk proteins (Garczewska-Murzyn, et al., 2022).

Industrially, MFGs/MFGM ingredient is added to infant formula by wetly mixing with other nutrients, followed by homogenization, concentration and spray drying. The physicochemical properties of infant formula powders are not only affected by the processing units, such as concentration times and spray drying temperature but also the functionality of each nutrient (Fang, et al., 2012; Reddy, et al., 2014; Saxena, et al., 2020). The glass transition temperature ($T_g$), interfacial compositions and lactose crystallization play an important role in minimizing deteriorative changes during infant formula storage. However, MFGs/MFGM, as a newly developed dairy

ingredient, to date, the knowledge on its interfacial and thermal properties is limited. Homogenization was reported to affect the thermodynamics of fat crystals and the polymorphs during storage (Ren, et al., 2020). The effect of pasteurization on the crystallization, melting properties and the crystal polymorphism of MFGs/ MFGM was characterized in previous research (Ren, Li, Dudu, & Ma, 2019).

Ultrasonic treatment is one of the most potent techniques that could be used in dairy processing. According to the frequency ranges, ultrasonic frequencies can be classified into three categories: Low frequency (20 kHz−100 kHz), medium frequency (100 kHz −1 MHz) and high frequency (1 MHz−10 MHz). Meanwhile, based on intensity, different frequency ultrasound could also be divided into high- intensity (>1W/ $cm^2$) and low-intensity ultrasound (below 1W/ $cm^2$) (Bhaskaracharya, Kentish, & Ashokkumar, 2009). Low-frequency ultrasounds induce strong cavitation effects by forming and violent collapsing of bubbles in the solution, which is usually used to produce smaller particles, facilitate fat separation, improve the emulsion properties and adjust the crystallization behaviour of anhydrous milk fat (AMF) (Martini, et al., 2008; Juliano, et al., 2011; Leong, et al., 2014a; Leong, et al., 2014b; Krasulya, et al., 2016). Specifically, the efficacy of specific ultrasonic density on the separation of fat from milk was optimized in the previous investigation (Leong, et al., 2014a). Comparing with shear-homogenization, more MFGM proteins were retained after being ultrasonicated at 20 kHz for 30 s−180 s (Liu, et al., 2021). These researchers focused on the ultrasonication induced functionality change of MFGs/MFGM in other food systems, including cream, infant formula, or AFM, other than the 'native and pure' MFGs/MFGM systems. In spite of the positive effects induced by the ultrasonic treatment, we are still unaware of any studies on the impact of high-intensity/low-frequency ultrasound on the interfacial properties, crystal transformation, crystallization and melting characteristics of the MFGs/MFGM materials.

In this study, we prepared the MFGs/MFGM samples from ultrasonicated bovine milk. Low-frequency sonication, 20 kHz and 40 kHz, was applied independently or

synchronously on the bovine milk before the MFGs/MFGM separation. Subsequently, particle characterization, interfacial tension, surface charges and the surface hydrophobicity of MFGs/MFGM were analysed to evaluate the interfacial properties. In addition, crystal forms, crystallization and melting of MFGs/ MFGM samples were investigated using the XRD and DSC. Understanding the interfacial and thermal behaviours of the MFGs/MFGM separated from ultrasonicated bovine milk would be useful for the development of MFGs/MFGM enriched dairy ingredients and their application in infant formula or other food.

## 4.2. Materials and methods

### 4.2.1. Materials and reagents

Raw bovine milk (fat 4.08 ± 0.02%, protein 3.57 ± 0.01%, dry matter 13.03 ± 0.02%, pH 6.67 ± 0.04) was collected from the Teagasc dairy herd (Moorepark, Fermoy, Co. Cork, Ireland). After milking, the raw bovine milk was not processed by any other unit operation except for the rapid chilling from 37 ℃ to 4 ℃using a plate heat exchanger (UK Exchangers Ltd., Buckinghamshire, UK).

Azide sodium, 1-anilinonaphthalene-8 sulfonic acid (ANS) and Phosphate-buffered saline (PBS) tablets, Nile Red (9- (diethylamino)-5 H-benzo[a]phenoxazin-5-one), Fast Green FCF (disodium 2-[[4-[ethyl-[(3-sulfonatophenyl)methyl]amino]phenyl]-[4-[ethyl-[(3-sulfonatophenyl) methyl] azaniumylidene] cyclohexa-2,5-dien-1-ylidene]methyl]-5-hydroxybenzenesulfonate) were purchased from Sigma–Aldrich®, Merck Life Science Ltd., Cork, Ireland. All solutions were prepared using MilliQ water except as otherwise noted.

### 4.2.2. Ultrasonic treatments

Ultrasonic treatments with different intensities were applied to the bovine milk following the methods described by Zhao et al. and Sun et al. with modifications (Sun, et al., 2014; Zhao, et al., 2022). Bovine milk at 4℃ was preheated to 30 − 35 ℃ in a

water bath to make sure that the milk fat was in a liquid state. After that, the preheated milk was divided into 10 aliquots for testing and each aliquot was 10 kg. One of the aliquots was used as control and the other 9 aliquots were sonicated at different conditions by the ultrasonic facility fitted with a cooling jacket and the double frequency ultrasonic reactors (WKS1200/2J, Jiangsu Jiangda Wukesong Biotechnology Co., LT, Zhejiang, China). The independent working model at frequency 20 kHz or 40 kHz, and synchronous models (20 kHz and 40 kHz probes working together) were applied with different durations (5 min, 10 min and 15 min in 5 s: 3 s work/rest cycles). The temperature of each sample was instantly recorded at the end of the ultrasonic treatment for any variation (as shown in Table S1). Ultrasound energy would be partly lost due to the heat and sound generated during the treatment. To estimate the dissipated acoustic power (*P*) in the liquid, the equation (Eq.) 1 was applied, which was expressed as watts per unit volume of sonicated liquid (W $cm^{-3}$):

$$P=mCdT/dt \quad (4\text{-}1)$$

Where *m* stands for the mass of the sample for each treatment (in g), and *C* is the heat capacity of the sample (in J $g^{-1}$ °$C^{-1}$). *dT/dt* is the temperature change of samples as the ultrasound exposure (°C/ s). The calculated results of ultrasound acoustic power (*P*) after all treatments are shown in Table 4-1.

**Table 4-1** Acoustic power (*P*) generated by different ultrasonic intensities and durations in bovine milk

| Samples | *P* (W) |
|---|---|
| 20 kHz/ 5 min | $78.49\pm1.76^{c}$ |
| 20 kHz/ 10 min | $98.96\pm7.66^{b}$ |
| 20 kHz/ 15 min | $145.28\pm3.52^{a}$ |
| 40 kHz/ 5 min | $19.66\pm0.74^{f}$ |
| 40 kHz/ 10 min | $29.25\pm0.49^{ef}$ |

| | |
|---|---|
| 40 kHz/ 15 min | 29.25±0.49$^{ef}$ |
| 20+40 kHz/ 5 min | 25.03±2.03$^{f}$ |
| 20+40 kHz/ 10 min | 39.33±1.49$^{e}$ |
| 20+40 kHz/ 15 min | 51.68±7.28$^{d}$ |

Notes: Different superscript letters in the same column indicate significant ($p < 0.05$) differences between the samples.

### 4.2.3. Isolation of MFGs/MFGM samples

MFGs/MFGM samples were enriched from ultrasonicated bovine milk using ultracentrifugation (10000 × g, 15 min at 4 ℃) (Kendro Laboratory Products, Asheville, NC) following the methods in previous researches with modifications (Zamora, et al., 2012; Huang, et al., 2023). Specifically, 25 ml ultrasonicated milk was centrifuged, and the serum phase was carefully discarded (lower layer). The collected top layer was mixed with a triple volume of PBS buffer (volume of sample: buffer =1:3). The mixture of sample with buffer was pre-heated in a 30 − 35 ℃ water bath until melted into liquid state, then thoroughly mixed it by the vortex. The centrifugation and rinse steps were repeated on two more times. The supernatant from the third time was freeze-dried for 72 h for further analysis. The collected samples were named as the ultrasonic conditions: 20 kHz/5 min, 20 kHz/10 min, 20 kHz/15 min, 40 kHz/5 min, 40 kHz/10 min, 40 kHz/15 min, 20 + 40 kHz/5 min, 20 + 40 kHz/10 min and 20 + 40 kHz/15 min. For each treatment, the material preparation procedures were repeated three times.

### 4.2.4. Chemical compositions of the MFGs/MFGM

The compositions of all collected freeze-dried MFGs/MFGM materials were analysed by DairySpec FT–15 (Bentley Instruments Inc., Chaska, MN, USA). Before the analysis, the samples were diluted 5 times by MiliQ water and then heated at 30 – 35 ℃ to make the even solutions. The protein and fat content of all samples are given in Table 4-2.

**Table 4-2** The compositions of freeze-dried MFGs/MFGM samples isolated from control and ultrasonicated bovine milk

| Samples | Protein (%, w/w) | Fat (%, w/w) |
|---|---|---|
| Control | 3.05±0.05$^{a}$ | 73.45±0.01$^{ns}$ |
| 20 kHz/ 5 min | 1.96±0.03$^{d}$ | 74.62±2.99 |
| 20 kHz/ 10 min | 1.54±0.01$^{e}$ | 75.29±0.25 |
| 20 kHz/ 15 min | 1.25±0.02$^{f}$ | 74.97±3.35 |
| 40 kHz/ 5 min | 1.72±0.01$^{e}$ | 74.32±2.55 |
| 40 kHz/ 10 min | 2.99±0.00$^{a}$ | 73.42±1.53 |
| 40 kHz/ 15 min | 2.78±0.11$^{b}$ | 76.49±4.76 |
| 20 +40 kHz/ 5 min | 2.1±0.07$^{d}$ | 74.14±1.47 |
| 20 +40 kHz/ 10 min | 2.65±0.14$^{b}$ | 75.24±2.96 |
| 20 +40 kHz/ 15 min | 2.44±0.04$^{c}$ | 73.56±0.73 |

Notes: Different superscript letters in the same column indicate significant ($p < 0.05$) differences between the samples. 'ns' means no significant difference ($p > 0.05$).

### 4.2.5. The characterization of interfacial properties of MFGs/MFGM

#### *4.2.5.1 Particle size determination*

The particle size of MFGs/MFGM samples was analysed using Mastersizer 3000 (Malvern Instruments, Malvern, UK) equipped with a laser light scattering, and Mie theory was used to calculate the results. The refractive index of milk fat and water were taken to be 1.456 and 1.333, respectively. Sample droplets were dropped into the sampling vessel containing deionised water until the obscuration reading came into the range of 3 – 20%. In addition, each sample was equilibrated 30 s before the recording, and the stirring speed was set to 2000 rpm throughout the entire analysis. Volume density (%) at different particle size distributions was recorded. Meanwhile, the span was reported which was used to assess the width of the particle size

distribution, and the narrower span reflected the more even distribution (Sun, et al., 2022).

On the assumption that most particles in all samples were spherical and non-porous, specific surface area (SSA) was employed to calculate the surface area of the particles per unit weight according to the following Eq. (4-2):

$$SSA= 6/\rho D[3,2] \quad (4\text{-}2)$$

Where ρ stands for the particle density (Sun, et al., 2022). Additionally, the extent of MFGs/MFGM wrapped by proteins was calculated by the surface fraction ($\Phi_m$) model according to Eq. (4-3)

$$\Phi_m=(S_t - S_o)/S_o \quad (4\text{-}3)$$

Where $S_o$ is the original surface area of MFGs/MFGM in control raw milk, and $S_t$ is the surface area of MFGs/MFGM in ultrasonicated samples.

*4.2.5.2. Zeta (ζ) potential*

The ζ– potential was analysed by the dynamic light scattering instrument (Nano–ZS, Malvern Instruments Ltd., Worcestershire, UK). It has been reported that the un-adsorbed compositions, such as casein micelles, showed no significant effect on the result of ζ– potential of fat globules (Sharma, et al., 2015b). The sample preparation method referred to our previous research with modifications (Sun, et al., 2022). Specifically, the pre-melted (30 – 35 °C) samples were diluted to 100 times with MiliQ water, and then mixed thoroughly by the vortex. All samples were analysed at room temperature, and three runs were conducted automatically for each analysis. In addition, based on the relative change of ζ– potential ($\zeta_R$), an estimative model was applied to assess the fraction of MFGs/MFGM surface change:

$$\Phi_e=1-\exp\left(-1.802\times10^{-3}\zeta_R^2\right) \quad (4\text{-}4)$$

where $\zeta_R$ was the relative change of ζ–potential of MFGs/MFGM samples after ultrasonic treatment in comparison with the control which was assumed that $\Phi_e=0$.

*4.2.5.3. Surface hydrophobicity ($H_0$)*

The $H_0$ determination referred to the method described by Sun et al.(Sun, et al., 2014) in which ANS was used as a fluorescent probe. The control and ultrasonicated samples were preheated at 30 – 35 ℃ until milk fat was completely melted, and the melted samples were diluted with PBS buffer (0.1 M, pH 7.0) to a series of protein concentrations ranging from 0.01 % to 0.06 % mg $mL^{-1}$. Before the dilution, LECO FP 628 (LECO Corp., Benton Harbor, MI, USA) was used to quantify the protein content of each sample with a nitrogen conversion factor of 6.38.

40 μL of stock solution of 8 mM ANS (in PBS buffer 0.1 M, pH 7.0) was mixed with the above diluted samples and incubated for 15 min in the dark at room temperature. The fluorescence intensity (FI) was analysed by a fluorescence spectrometer (Varian Cary Eclipse, New Jersey, USA) at 390 nm (excitation wavelength) and 470 nm (emission wavelength), with a slit width of 2.5 nm and scanning speed of 5 nm $s^{-1}$. The initial slope of the FI as a function of protein concentration was calculated and defined as the $H_0$.

*4.2.5.4. Interfacial tension (π)*

Dynamic interfacial tension (π) between the air and liquid droplet of MFGs/MFGM samples was determined by a optical tensiometer (Oneattension Theta lite, Biolin Scientific, Espoo, Finland) equipped with a pendant drop apparatus. The π measurement was performed in a temperature- controlled room (25 ℃). A drop of the liquid sample with a volume between 6 – 8 μL was pushed out of a glass syringe. The profile of the droplet was captured by a built-in high-resolution camera. Young-Laplace equation was used to fit the drop shape and calculate the π in Oneattension software (Version 4.1.6, Biolin Scientific, Finland). In our preliminary experiment,

the recording time was optimised and 15 s was chosen because π values started to fluctuate greatly after 15 s. Therefore, in the current study, the analysis lasted 15 seconds with a recording rate of 0.1% frame per second (FPS). All the results were expressed in the unit of mN/ m.

Kinetic parameters were used to characterize MFGs/MFGM interfacial protein change. According to previous researches, the main processes for the adsorption of proteins within the different layers were: (i) diffusion or migration of proteins to the interface, (ii) adsorption (penetration), (iii) unfolding and rearrangement of proteins (Graham & Phillips, 1979; Seta, Baldino, Gabriele, Lupi, & de Cindio, 2012). The diffusion or migration step (i) can be fitted by the Ward–Tordai equation to model the change of π as a function of time (t) (Eq. (4-5)).

$$\pi=2C_0KT(Dt/3.14)^{0.5} \qquad (4\text{-}5)$$

where $C_0$ is the protein concentration, $K$ is the Boltzmann constant and $T$ is the temperature, $D$ is the diffusion coefficient and $t$ is the adsorption time. The diffusion or migration process was reported to be mainly controlled by protein diffusion (Graham, et al., 1979). It was possible to obtain the diffusion rate ($k_{diff}$) of the protein by calculating the slope of π versus $t^{0.5}$ plot by the linear fitting.

The adsorption (penetration), unfolding or rearrangement rate of molecules between the interface of air and oil can be analysed by the first-order equation proposed by Graham and Philips (Graham, et al., 1979) (Eq. (4-6)):

$$\ln\ [(\pi_f\ -\ \pi_t/\ (\pi_f - \pi_0)] = -k_i t \qquad (4\text{-}6)$$

where $\pi_f$ and $\pi_0$ are interfacial tension at the final and starting measurement points respectively, and $\pi_t$ is the initial point. $k_i$ is the first-order rate constant. Two linear regions were monitored yielding from the plot of $\ln [(\pi_f - \pi_t/ (\pi_f - \pi_0)]$ versus time (s). The first and second slopes were taken as the first-order constant of adsorption

(penetration) ($k_a$) and rearrangement ($k_r$) of molecules between the air and oil interface (Camino, Pérez, Sanchez, Rodriguez Patino, & Pilosof, 2009).

*4.2.5.5. Confocal laser scanning microscopy (CLSM)*

A Leica TCS SP5 microscope (Leica Microsystems GmbH, Wetzlar, Germany) was used to observe the serum proteins and lipids in the MFGs/MFGM samples. All the samples were dual-stained by Nile Red and Fast Green FCF. A concentration of 0.1% (w/v) Nile Red and FCF was used to dye neutral lipids and serum proteins respectively. 1.5 mL of the sample was mixed with 30 μL Nile Red and 10 μL FCF. The prepared samples was observed on the microscope referring to our previous report(Sun, et al., 2022).

### 4.2.6. The characterization of thermal properties of MFGs/MFGM

*4.2.6.1. X–ray diffraction (XRD)*

XRD can be used to characterize the change of polymorphs in milk fat by monitoring the intensity and position of the spectra peaks. In this study, the polymorphic forms of ultrasonicated samples were determined by a powder diffractometer STOE STAID MP (STOE, Darmstadt, Germany) mounted with Cu radiation (λ=1.5406 nm; current, 40 mA; voltage, 40 kV). All the freeze-dried samples were carefully ground into fine powder using a cleaned mortar and pestle. The ground powder was sealed in a custom metal plate with films covered on both sides. XRD patterns were recorded with a scanning speed of 1˚/ min in the range of 2θ = 5˚ −30˚.

The normalization, smooth and the calculation of full width at half-maximum (FWHM) of the crystal peaks were performed in Origin software (Originpro 2021, OriginLab Corporation, Northampton, US). Savitzky–Golay method was used to smooth the spectra with points of windows 5 and polynomial order 2. The peak analyser in Origin was used to calculate the relative crystallinity (%) by integrating the corresponding peak areas. The baseline mode was set as ‘constant Y=Minimum

value', and only positive peaks with threshold weight (%) higher than 20 were found using the 'Local Maximum' method.

Typical crystalline forms, α, β and β', were identified by the conversion of each diffraction peak to the unique corresponding d-spacing. According to the previous reports, the short spacing positions used to fingerprint the crystals in milk fats are α =4.14 − 4.16 Å (2θ=21.32˚ − 21.46˚), $\beta'_1$ =3.80 − 3.85 Å (2θ=23.06˚ − 23.70˚) and 4.20 − 4.25 Å (2θ=20.86 − 21.39˚), $\beta'_2$= 4.30 − 4.37Å (2θ=20.29 − 20.88˚), β= 4.52 −4.65 Å (2θ=19.05 − 19.64˚) (Lambert, et al., 2018; Lopez, Cheng, & Perez, 2018; Ren, et al., 2019; Ren, et al., 2020; Logan, et al., 2021).

The relative crystallinity of α, β and β' polymorphs was the percentage of each crystal peak area in the total peak area which was set as 100% (Eq.4-7).

Crystallinity= (Area of crystalline peaks) × 100/Area of all peaks (Crystalline +Amorphous) (4-7)

*4.2.6.2. Different scanning calorimetry (DSC)*

The thermal behaviour of MFGs/MFGM samples was investigated on a DSC (DSC Q2000, TA Instruments, Crawley, UK). Sample preparation and analysis method referred to the reported researches on goat milk and MFGs with modifications (Ren, et al., 2021; Sergeev, et al., 2021). Each 10 − 15 mg ground powder was hermetically sealed into an aluminium pan (tolerable temperature from −180 to 600 ℃), and the powder should evenly cover the whole bottom of the pan. Meanwhile, a hermetically sealed aluminium pan without sample was used as a reference. Nitrogen was used to purge the system at 50 mL/min. All the DSC measurements were carried out with the same time-temperature program: Cycle 1: Equilibrate at 4℃; Cycle 2–3: Ramp 10℃/min to 60℃ and keep the isothermal temperature for 15 min; Cycle 4–5: Ramp 10℃/min to –60℃ and keep the isothermal temperature for 5 min; Cycle 6: Ramp 10℃/min to 60℃. The equilibration at 4℃ (Cycle1) and isothermal stabilization at 60 ℃ for 15 min (Cycle 2–3) were used to erase the crystal and melting

history of all the samples. The crystallization and melting profiles were obtained during the cooling (Cycle 4–5) and heating (Cycle 6) procedures respectively. All the thermograms were collected and exported by Universal Analysis 2000 (TA Instruments–Waters LLC, New castle, US). The curves of heat flow (W/g) as the function of temperature were plotted in the Origin software system (Originpro 2021, OriginLab Corporation, Northampton, US). The peak analyzer function in the Origin system was used to find the peak values. The endothermic ($\Delta H_M$) and exothermic ($\Delta H_C$) enthalpy (J $g^{-1}$) for each sample were calculated by integrating the area of the corresponding peaks.

#### 4.2.7. Statistical analysis

All experiments and measurements were performed three times unless otherwise indicated. Data were expressed as the mean value ± standard deviation (SD). To evaluate the significant differences between samples, the resulting data were submitted to the OriginPro 2023 software system (OriginPro 2023, OriginLab Corporation, Northampton, USA). The variant analysis was performed (ANOVA) to test the differences between the groups at the significance level of $p < 0.05$, except for interfacial tension for which a more strict level of $p < 0.01$ and $p < 0.001$ were used.

### 4.3. Results and discussion

#### 4.3.1. The effect of ultrasonic treatments on the interfacial properties of MFGs/MFGM

*4.3.1.1 Particle size distribution*

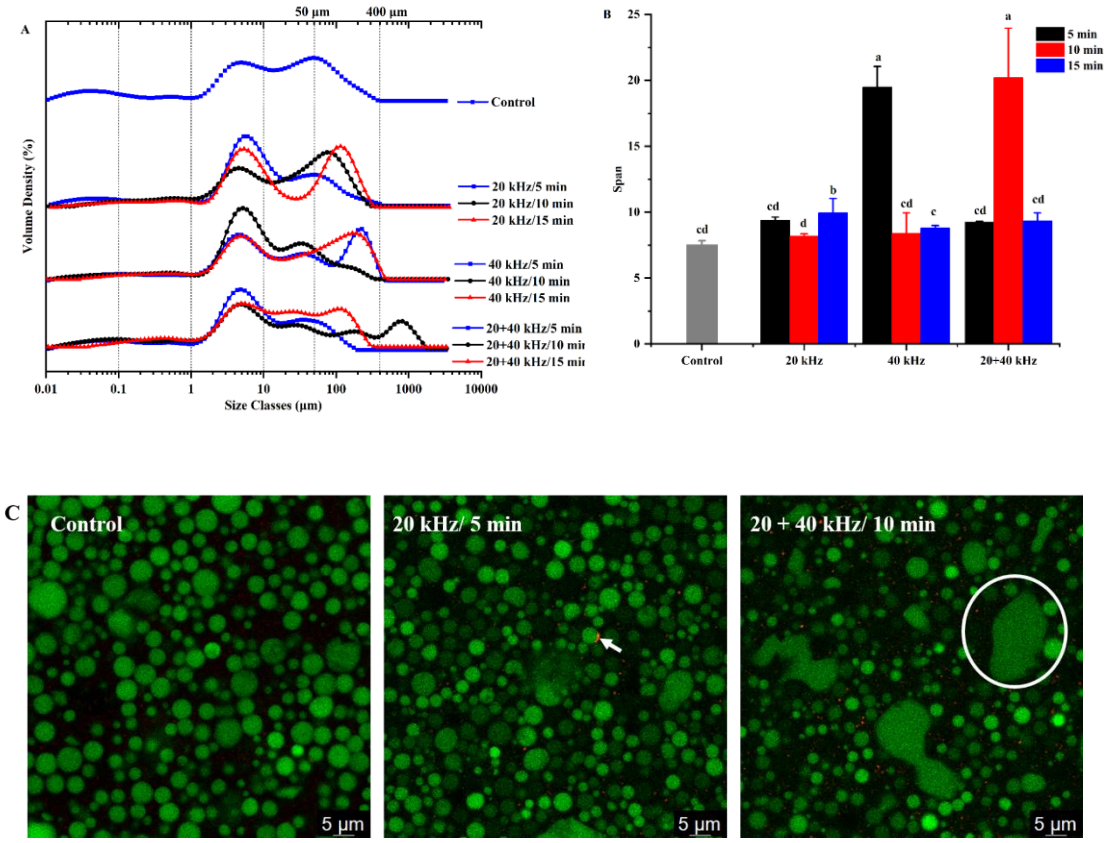



**Figure 4-1.** Particle size distribution (A) and span (B) of MFGs/MFGM samples prepared from control and bovine milk treated by different intensities of ultrasound. The different letters indicate that each sample has significant difference ($p < 0.05$). Confocal laser scanning microscopy images of control and ultrasonic treated MFGs/MFGM samples (20 kHz/ 5min and 20 + 40 kHz/10 min) (C). Neutral lipids and serum plasma protein were stained with Nile red and fast green FCF (white arrows pointing at the plasma proteins on the surface of MFGs/MFGM; aggregated MFGs/MFGM fragments in white circle). Scale bar=5 µm.

Particle size distribution of MFGs/MFGM samples prepared from ultrasonicated bovine milk is shown in Fig.4-1A. Similar to control samples, most MFGs/MFGM particles in ultrasonicated samples are distributed in the range of 1−10 µm and 10−400 µm. Small amounts of particles distributed between 0.01 µm and 0.1 µm were only identified in control and 20 kHz/ 5 min samples while these small particles were not observed in other samples.

As the ultrasound duration time prolonged, there was an apparent movement of particle size distribution from 50 µm towards 400 µm for 20 kHz treated samples. The same trend was observed for samples treated at 20 + 40 kHz, which, meanwhile,

presented multimodal distribution, especially samples treated at 20 + 40 kHz/ 10 min. This may be due to the formation of aggregates by MFG fragments or the adsorption of plasma proteins on the surface of MFGs/MFGM (Fig. 4-1C). This was inconsistent with the findings of previous researchers who reported that ultrasonic treatment would decrease the particle size of milk protein dispersion, milk phospholipid solution or emulsions (Liu, et al., 2021; Sun, et al., 2022a). Ultrasonic treatment at a certain intensity had the same impact as the shear homogenisation. The acoustic cavitation could be generated by ultrasound with results corresponding to mechanical shearing by the continual forming and collapsing of bubbles (Liu, et al., 2021). In comparison with control samples, 20 kHz independently or synchronously with 40 kHz ultrasonic treatment for 5 min exhibited a lower volume density (%) of 10 – 100 μm at the expense of higher 1 – 10 μm particles. Therefore, these two ultrasonic conditions presented corresponding effects on the decrease of the particle size as homogenisation shearing.

Generally, as a function of acoustic power, the volume density (%) of particle size distribution increases firstly followed by a decreasing trend. Regarding the increased volume density (%) of bigger particles under 40 kHz conditions, it may be because intact MFGs broke into fragments which aggregated into bigger particles. As the treatment duration was prolonged, or the increase in ultrasonic intensity, the formed big size aggregates dispersed into multimodal distribution, as shown for the 20 + 40 kHz treated samples. In addition, excessive shearing induced by a higher intensity of ultrasound at 20 kHz conditions further dispersed the different sizes of particles and facilitated less multimodal particle distribution. That result may explain why samples treated at 20 kHz displayed more even particle distribution than the lower acoustic power treated samples.

According to Fig.4-1B, the span of 20 + 40 kHz/ 10 min samples was significantly higher than other samples ($p<0.05$), followed by 40 kHz/ 5 min and 20 kHz/15 min samples. This was in accordance with the particle size distribution results in Fig. 4-

1A. The surface change of MFGs/MFGM induced by the acoustic wave was characterised by the surface fraction ($\Phi_m$) model (Table.4-3). Table 4-+3 showed that both 40 kHz *and* 20 + 40 kHz treated 15 min samples have higher $\Phi_m$ value which could be due to the increase of plasma proteins adsorption on the surface of MFGs/MFGM. This agreed with the size distribution results in Fig. 4-1A which showed that more particles with a higher volume density (%) were detected in 40 kHz/ 15 min and 20 + 40 kHz/ 15 min samples.

**Table 4-3** Effect of different ultrasonic intensities on surface change of MFGs/MFGM calculated by the surface fraction ($\Phi_m$) model

| Samples | $\Phi_m$ |
|---|---|
| 20 kHz/ 5 min | $0.27\pm0.02^{d}$ |
| 20 kHz/ 10 min | $0.79\pm0.01^{a}$ |
| 20 kHz/ 15 min | $0.61\pm0.05^{b}$ |
| 40 kHz/ 5 min | $0.56\pm0.04^{b}$ |
| 40 kHz/ 10 min | $0.48\pm0.02^{c}$ |
| 40 kHz/ 15 min | $0.81\pm0.01^{a}$ |
| 20+40 kHz/ 5 min | $0.16\pm0.02^{e}$ |
| 20+40 kHz/ 10 min | $0.17\pm0.01^{e}$ |
| 20+40 kHz/ 15 min | $0.81\pm0.01^{a}$ |

Notes: Different superscript letters in the same column indicate significant ($p < 0.05$) differences between samples.

*4.3.1.2. Zeta (ζ) potential*

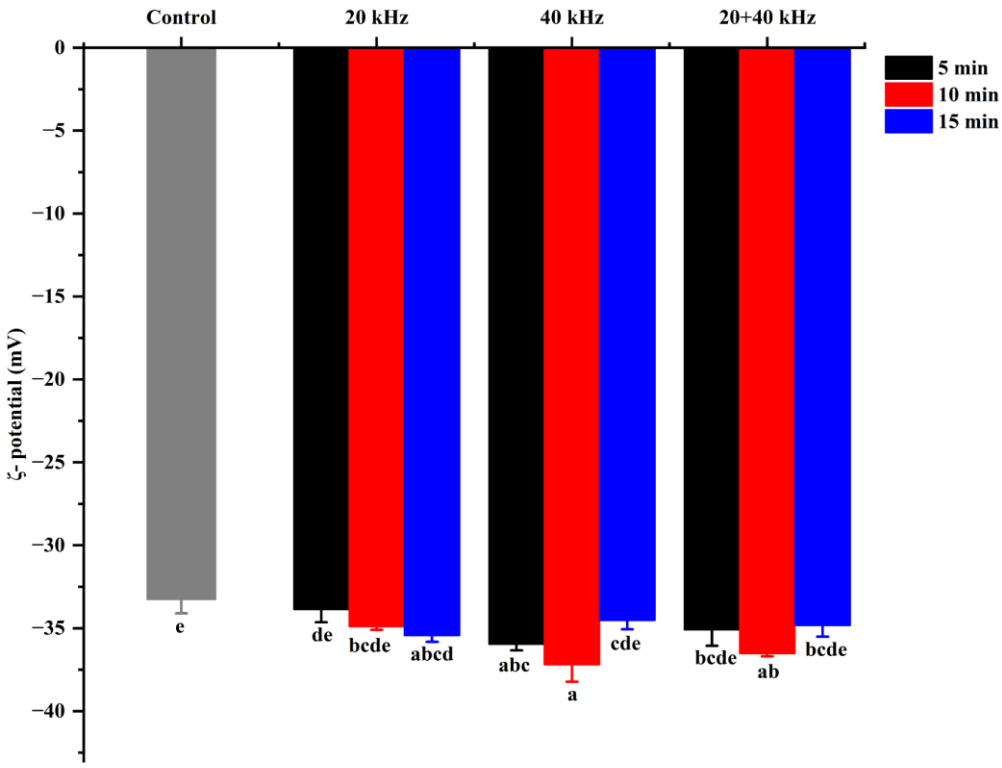



**Figure 4-2.** ζ– potential of control and MFGs/MFGM prepared from ultrasonicated bovine milk. Different superscript letters mean the significant difference between samples ($p$<0.05).

The effect of ultrasonic treatments on the ζ– potential of MFGs/MFGM is presented in Fig.4-2. In agreement with the previous research, the ζ– potential of all samples exhibited negative values which indicated that negative charges were present (Jukkola, et al., 2016c). The change of ζ– potential in this study referred to the comparison of the absolute values. According to Fig.4-2, ultrasound treatments at 20 kHz/ 15 min, 40 kHz/ 5 min, 40 kHz/10 min and 20 + 40 kHz/ 10 min significantly increased the ζ– potential to varying degrees ($p$<0.05). This was in contrast with the previous research which reported that ζ– potential of the raw milk decreased after treatment by 475 W ultrasound with energy densities of 7 kJ /mL (Kurup, Adhikari, & Zisu, 2020). However, Scudino et al. (2020) reported an increase of ζ– potential in raw milk after 100 W ultrasonic treatment and presented a similar effect to our study (Scudino, et al., 2020). In this study, 40 kHz treated samples with a duration 5 min

showed the highest ζ– potential which increased by 14.20% in comparison to the control samples, followed by the 20+40 kHz/10 min samples with an increase of 10.80%. It can be inferred that these ultrasonication conditions may cause the rupture of MFGs followed by the reconfiguration of the membrane with more negative charge exposure, consequently, causing the increased ζ– potential.

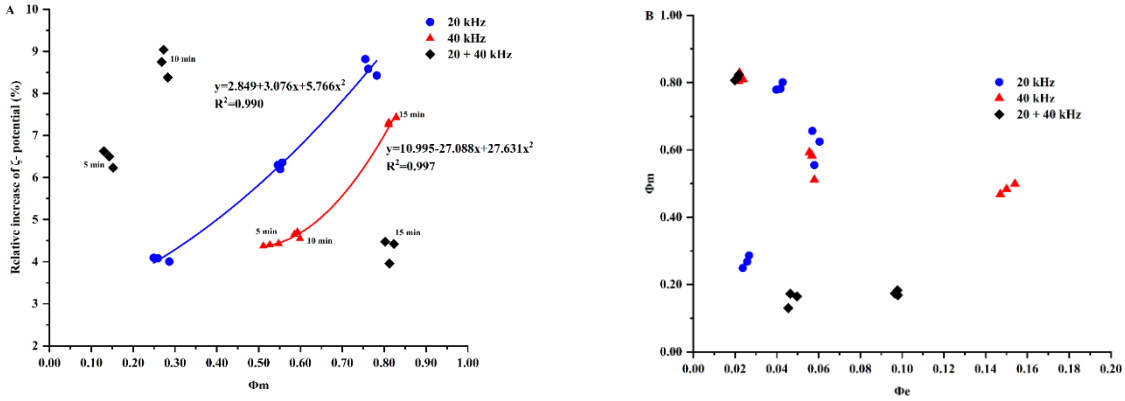



**Figure 4-3.** The relative increase of ζ– potential ($\zeta_R$) for control and ultrasonicated samples as a function of measured surface fraction ($\Phi_m$) of MFGs/MFGM samples (A). Scatters of $\Phi$ values by Mastersizer measurement ($\Phi_m$) and the predictive model estimated ($\Phi_e$) (Eq. (4)) (B).

The correlation between $\zeta_R$ and $\Phi_m$ was fitted by polynomial regression (Fig. 4-3). Fig. 4-3 A showed nonlinear relationships between the $\zeta_R$ and $\Phi_m$ for 20 kHz and 40 kHz treated samples with $R^2$=0.990 and $R^2$=0.997, respectively. This is in accordance with the results from Michalski et al. (2002) (Michalski, Cariou, Michel, & Garnier, 2002c) and Sharma et al. (2015) (Sharma, et al., 2015b). In their studies, $\zeta_R$ and $\Phi_m$ of MFGs followed a nonlinear trend after different mechanical treatments, including homogenisation, ultra-sonication, high-shear mixing (Marie-Caroline Michalski & Briard, 2001), and pulsed electric field treatment (Sharma, et al., 2015b). According to the fitted curves, in both 20 kHz and 40 Hz samples, $\zeta_R$ and $\Phi_m$ exhibited a positive correlation as the ultrasonic duration time was prolonged. However, it is worth noting that 20 + 40 kHz ultrasonicated samples with different duration times did not follow a nonlinear or linear correlation between the $\zeta_R$ and $\Phi_m$

(Fig.4-3A). In 20 + 40 kHz treated samples, there was a significant increase in both $\zeta_R$ *and* $\Phi_m$ values for 10 min treated compared to 5 min duration samples ($p < 0.05$), whereas the 15 min samples displayed the lowest $\zeta_R$ and $\Phi_m$.

The previous researches proved a good correlation fitted by a quadratic regression model between the estimated $\Phi_e$ and the measured $\Phi_m$ with a co-efficient square ($R^2$) higher than 0.960 (Marie-Caroline Michalski , et al., 2001; Sharma, et al., 2015b). This means that $\zeta_R$ values can be used to predict the surface coverage fraction of MFGs/MFGM by plasma proteins. However, in our research, there was no statistical correlation for $\Phi_e$ versus measured $\Phi_m$ in terms of ultrasonic intensity and duration time (Fig. 4-3B). Factors attributed to the different results could be the acoustic power difference or the MFGs samples preparation methods, which needs to be verified in the further investigation.

*4.3.1.3. Surface hydrophobicity (H0)*

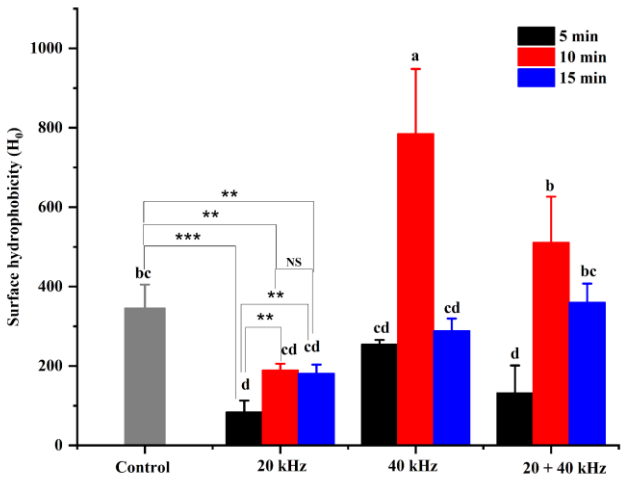



**Figure 4-4.** Surface hydrophobicity ($H_0$) of control and MFGs/MFGM samples prepared from bovine milk treated by ultrasound at different intensities. Different superscript letters mean the significant difference between samples ($p<0.05$). *, ** and *** represent $p < 0.05$, $p < 0.01$ and $p < 0.001$, respectively.

The change of the hydrophobic group has been used to reflect the protein structure change. ANS displayed high affinity to hydrophobic groups, which could be used to determine the exposed protein hydrophobic sites (Meng, et al., 2021).

As shown in Fig.4-4, different letters above each column mean the significant difference between samples resulting from ANOVA conducted on all the samples together. In comparison with control samples, 40 kHz with a duration of 10 min significantly increased $H_0$ while there was a significant decrease of $H_0$ for 20 kHz/ 5 min and 20 + 40 kHz/ 5 min samples ($p < 0.05$). Samples treated at other ultrasonic conditions showed insignificant differences from control samples ($p > 0.05$). Ultrasound may facilitate the exposure of hydrophobic protein domains or amino acid residues buried in the molecules, and then induce the increase of $H_0$ in 40 kHz/ 10 min samples (Meng, et al., 2021). In addition, it was reported that the bigger size of particles improved the $H_0$, which was related to the higher contact area for the connection of hydrophobic domains with the ANS probe (Song, et al., 2022). However, this theory was in contrast with the results in Fig.4-1. A bigger particle distribution ranging from 400−1000 μm was detected in the 20 + 40 kHz/ 10 min samples which, however, displayed no significant difference of $H_0$ with control samples ($p>0.05$).

To further compare the effect of ultrasonic frequency on the $H_0$, ANOVA was conducted between the 20 kHz and control groups, and also within the 20 kHz groups. Within the 20 kHz treated group, ultrasound with a duration of 10 min and 15 min resulted in a significantly higher $H_0$ than that of 5 min samples ($p<0.01$). This could be due to more hydrophobic regions being exposed as the treatment time was prolonged at 20 kHz frequency. In addition, more hydrophobic groups were detected in control groups than ultrasound at 20 kHz groups (Fig.4-4). This may be because the higher ultrasonic acoustic power was produced at 20 kHz conditions (Table 4-1). The excessive mechanical shearing induced by the higher energy ultrasonic treatment may lead to the unfolding of protein molecules which causes the extension of non-

covalent bonds, consequently, masking the hydrophobic regions and preventing their reaction with ANS probe (Tomé Constantino & Garcia-Rojas, 2020). Herein,

**Table 4-4** Diffusion ($k_{diff}$), adsorption ($k_a$) and rearrangement rate ($k_r$) of MFG/MFGM samples treated by ultrasound with different intensities

| Samples | $k_{diff}$ | $R^2$ | $k_a$ | $R^2$ | $k_r$ | $R^2$ |
|---|---|---|---|---|---|---|
| Control | - | - | - | - | - | - |
| 20 kHz/ 5 min | -0.728±0.004$^{g}$ | 0.994 | -0.177±0.002$^{b}$ | 0.982 | - | - |
| 20 kHz/ 10 min | - | - | - | - | - | - |
| 20 kHz/ 15 min | -0.139±0.003$^{a}$ | 0.985 | -0.175±0.002$^{b}$ | 0.989 | - | - |
| 40 kHz/ 5 min | -0.488±0.008$^{d}$ | 0.960 | -0.121±0.002$^{a}$ | 0.970 | - | - |
| 40 kHz/ 10 min | -0.562±0.016$^{e}$ | 0.947 | -0.133±0.003$^{a}$ | 0.937 | - | - |
| 40 kHz/ 15 min | -0.273±0.006$^{b}$ | 0.950 | -0.191±0.022$^{b}$ | 0.958 | - | - |
| 20+40 kHz/ 5 min | -0.679±0.006$^{f}$ | 0.983 | -0.177±0.003$^{b}$ | 0.968 | - | - |
| 20+40 kHz/ 10 min | -0.491±0.005$^{d}$ | 0.981 | -0.131±0.002$^{a}$ | 0.983 | - | - |
| 20+40 kHz/ 15 min | -0.443±0.005$^{c}$ | 0.981 | -0.134±0.001$^{a}$ | 0.979 | 0.551±0.019 | 0.965 |

Notes: $k_{diff}$ is the initial diffusion rate calculated by linear fitting of the π versus $t^{0.5}$ plot. $k_a$ and $k_r$ are the adsorption (penetration) and rearrangement rate, the slope obtained by linearly fitting the plot of ln $[(\pi_f - \pi_t / (\pi_f - \pi_0)]$ versus time (s). $R^2$ is the coefficient of determination (COD). Different superscript letters in the same column indicate significant ($p < 0.05$) difference between samples.'-' means not calculated.

compared with the control samples, $H_0$ did not change regularly with the ultrasonic intensities, duration time or the acoustic powder.

*4.3.1.4. Interfacial tension (π)*

Interfacial tension (π) has been reported to indicate the dynamic information of molecule adsorption at the gas/ liquid and liquid/ liquid interfaces (Seta, et al., 2012). In this study, the effect of ultrasound treatments on the rearrangement of MFGs/MFGM interfacial compositions was investigated by comparatively analysing the π between the air and liquid droplets.

Fig. 4-5A showed the π decreased as a function of time ($t^{0.5}$) irrespective of ultrasound intensity and durations, and there was a significant decrease in the decrease rate of π with time. This might be explained by the increase of electrostatic energy on the surface of MFGs/ MFGM droplets with the analysis time, which would prevent the further adsorption of protein (Li, et al., 2022a). In this study, the π values of all the samples ranged from 46.520 to 36.250 mN/ m, which was similar to the previous research on cream samples with different particle sizes (Ho, et al., 2021).

In comparison with control samples, ultrasonic treatment significantly resulted in the decrease of π ($p<0.05$). Meanwhile, as the ultrasonic duration was prolonged, a more profound decrease in π than control samples was observed with the same ultrasonic intensity. Comparatively, 40 kHz ultrasonic treatments decreased π less efficiently than the other frequencies, and at the end of the monitoring point (15 s), the π of 40 kHz/ 15 min treated samples was 38.890 mN/ m which was 16.095% lower than the control samples. By comparison, 20 kHz presented a more profound decrease in π, especially with 15 min treatment which was 29.877% lower than control. This may be attributed to the higher energy intensity and output power of 20 kHz frequency than the other conditions (Table 4-1). It can be inferred that the intenser mechanical shearing facilitated the interfacial tension change of MFGs/MFGM more efficiently.

The diffusion ($k_{diff}$), adsorption (penetration) ($k_a$) and rearrangement ($k_r$) rate of interfacial compositions in MFGs/MFGM were calculated by linear fitting of the curves plotted according to the Eq. (5) and Eq. (6), respectively (Table 4-4). The $k_{diff}$, $k_a$ and $k_r$ for control and 20 kHz/ 10 min samples were not included in Table 4-4, because π changed continuously during the whole analysis process which made it impossible to do the linear fitting. The initial π value of control and 20 kHz/ 10 min in this research was 46.520 and 36.68 mN/ m. According to previous researches, $k_{diff}$ could not be properly detected by the pendant drop method if the $\pi > 10$ mN/ m, because the diffusion step was too fast to be captured (Seta, et al., 2012; Zhou, Tobin, Drusch, & Hogan, 2021a). However, in this study, good linear fits for plots π versus $t^{0.5}$ were obtained for all the other samples except for control and 20 kHz/ 10 min samples. The π values of all samples at the beginning were between 32.990 and 45.505 mN/ m which were well above 10 mN/ m. The contradiction in these results could be due to the interfaces between different phases. The interfaces in current research referred to the contact surface of the air/water while the abovementioned reports investigated the interfaces between the oil and water.

Regarding the effect of ultrasound frequency and duration on the $k_{diff}$, $k_a$ and $k_r$ of MFGs/MFGM, 40 kHz treated for10 min promoted the protein diffusion more efficiently than 5 min at the same frequency. 20 kHz treatment with 5 min duration reduced the diffusion rate of MFGs/MFGM interfacial compositions more significantly compared with 20 kHz/ 15 min treatment ($p<0.05$) but had no significant effect on the adsorption or penetration rate ($p>0.05$). The increase in hydrophobicity has been reported to speed up the diffusion rate of whey protein at the oil-water interfaces (Zhou, et al., 2021a). This confirmed the hydrophobicity results in 3.3, which showed that 20 kHz/ 15 min displayed significantly higher $H_0$ than that of 20 kHz/ 5 min according to the ANOVA within the 20 Hz groups. Contrarily, $k_{diff}$ and $k_a$ results of samples synchronously treated by 20 kHz and 40 kHz treatment showed an opposite trend to the hydrophobicity results from 3.3. Except for the hydrophobicity, protein conformation, molecular dimensions and electrostatic state

could also affect the diffusion and adsorption rate of proteins at different interfaces (Seta, et al., 2012; Zhou, et al., 2021a).

Another interesting finding was that, during the adsorption or penetration step, only one linear region was fitted and $k_a$ was calculated for all samples. The $k_r$ of MFGs/MFGM interfacial compositions in all the samples could not be calculated by linear fitting the plot of ln $[(\pi_f - \pi_t / (\pi_f - \pi_0)]$ versus time (s), except for 20 + 40 kHz/15 min samples (Fig. 4-5B). It may be because the surface evaporation of sample droplets during the analysis. The mechanism behind this phenomenon is still not clear and further research needs to be conducted to investigate.

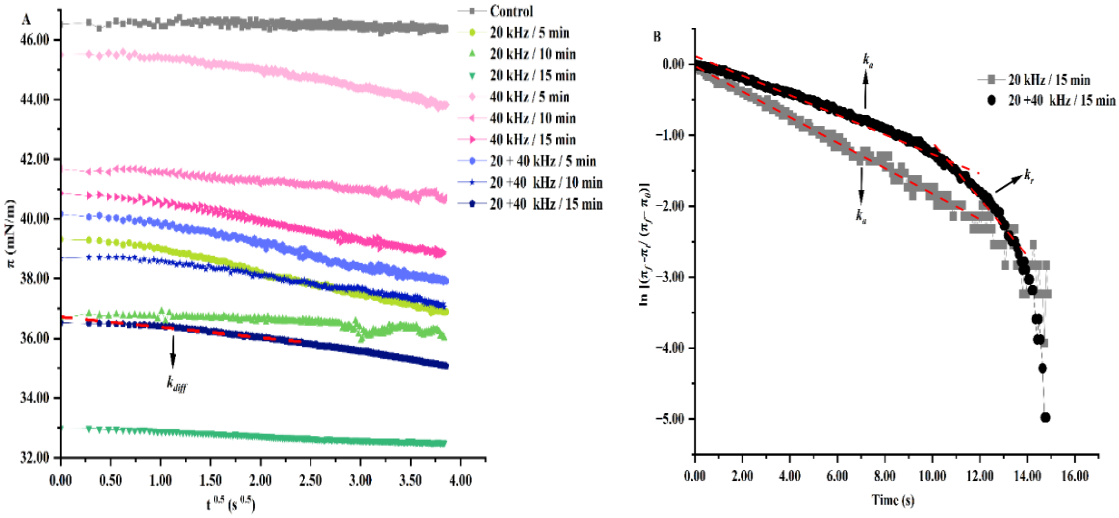



**Figure 4-5.** (A) Interfacial tension (π) as a function of time ($t^{0.5}$) at the surface of sample droplets (control and samples treated at different ultrasonic intensities), $k_{diff}$ is the diffusion rate; (B) The profile rate of protein adsorption and rearrangement for 20 kHz/ 15 min and 20 + 40 kHz/ 15 min samples, $k_a$ and $k_r$ are the first-order rate of adsorption (penetration) and rearrangement, respectively.

### 4.3.2. The effect on ultrasonic treatments on the thermal behaviour of MFGs/MFGM

*4.3.2.1. XRD*

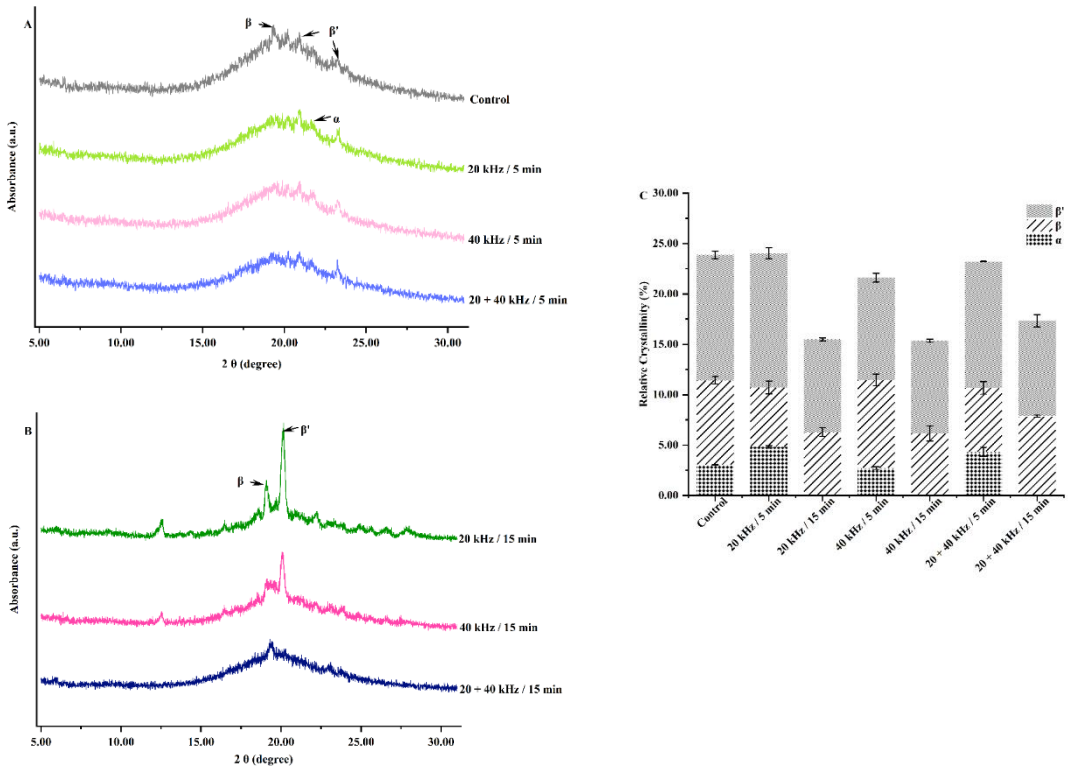



**Figure 4-6.** X-ray spectra of control and ultrasonicated 5 min samples (A) and 15 min duration MFGs/MFGM samples (B); (C) relative crystallinity of α, β, and β' crystals in MFGs/MFGM samples

XRD has been used to identify the polymorphic forms in milk fat by characterizing the crystal types measured by the d-spacing (Å) (ten Grotenhuis, van Aken, van Malssen, & Schenk, 1999).

The spectra of XRD patterns for control and ultrasonicated samples with the duration of 5 min and 15 min were shown in Fig. 4-6A and 6B. No significant difference was detected between the 5 min and 10 min treated samples (data for 10 min treatment not shown) at the same ultrasonic intensity ($p>0.05$). Fig. 4-6A showed that three typical crystals, α-crystal, β-form and β'-form, coexisted in the control and 20 kHz, 40 kHz and 20 + 40 kHz treated for 5min samples. However, peaks for α-crystal disappeared as treatment time was prolonged to 15 min, while only β-form and β'-form were detected in all 15 min treated samples. In addition, ultrasound treatment

did not shift the polymorphs position but only affected the intensity of the corresponding peaks (Fig. 4-6A and 6B). The identified polymorphs were relatively quantified by integrating the corresponding peak areas (Fig. 4-6C). In all cases, β' form was the major crystal, supported by previous researches which classified milk fat as β'-fat (Wright, et al., 2006a; Ren, et al., 2020). In comparison with control samples, 20 kHz or 20 kHz synchronized with 40 kHz treatment for 5 min significantly increased the α-crystal content, and also impeded the transition of metastable β'-crystals to stable β-form. Limited change was detected for the peak area of α-crystals in 40 kHz/ 5 min samples than that in control samples, which may be related to an unobvious effect induced by the lower acoustic power (*P*) at 40 kHz/ 5 min condition.

It appears from Fig. 4-6C that prolonged ultrasonic time decreased the β'-forms more profoundly than the increase in ultrasonic intensity. Especially in the 40 kHz/ 15 min samples, only 9.21% of β'-form was detected which was 26.01% less than that in control samples. However, treatment at 40 kHz for 5 min resulted in 18.41% less β'-crystals than control samples. 15 min duration at all ultrasound intensity significantly promoted the transition of unstable α-forms into the metastable β'-crystals. Of these, treatments of 20 kHz/ 15 min and 40 kHz/ 15 min were the most efficient treatments in facilitating the formation of stable β-form polymorphs in the MFGs/ MFGM, however, in which the major polymorph was still β'-form. This finding was supported by previous studies on MFG samples treated with different homogenised pressures (Ren, et al., 2020). 20 kHz/5 min samples contained the least amount of stable β-form polymorphs than the other samples, meanwhile, from the abovementioned results in 3.1, a higher percentage of MFGs/MFGM particles in 20 kHz/ 5 min presented in the lower particle size range (Fig. 4-1A).This is inconsistent with the research reporting that smaller MFGs constrained the formation of larger sized β-polymorphs on the surface of droplets (Lopez, et al., 2002).

The type of fat crystals plays an important role in the application of milk fat. In this research, 40 kHz treated MFGs/MFMG samples contained the most β crystals

while more β'-crystals were detected in 20 kHz/ 5 min treated samples. It was reported that β crystals with large sizes and higher melting temperatures are suitable for hard consistency texture application, while β'-crystals help improve the spreadability of fat by forming the fine crystal network (Toro-Vazquez, Briceño-Montelongo, Dibildox-Alvarado, Charó-Alonso, & Reyes-Hernández, 2000).

*4.3.2.2. DSC*

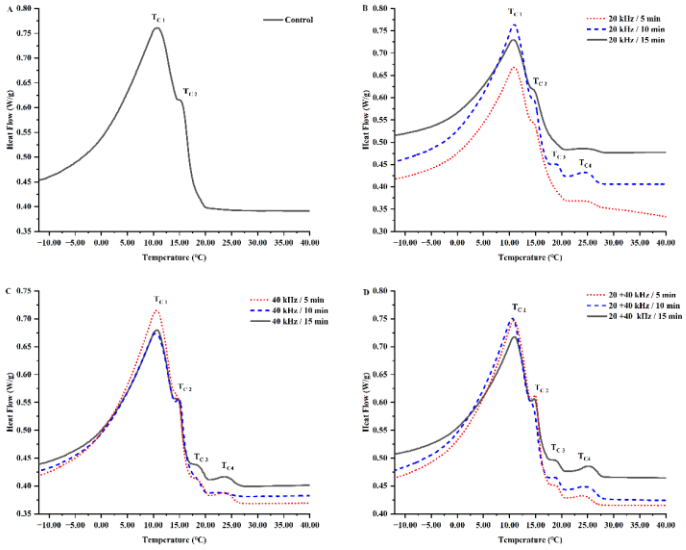



**Figure 4-7.** DSC crystallization thermograms of MFGs/MFGM samples separated from the control and ultrasonicated bovine milk, $T_{C1}$-$T_{C4}$ are crystallization temperatures

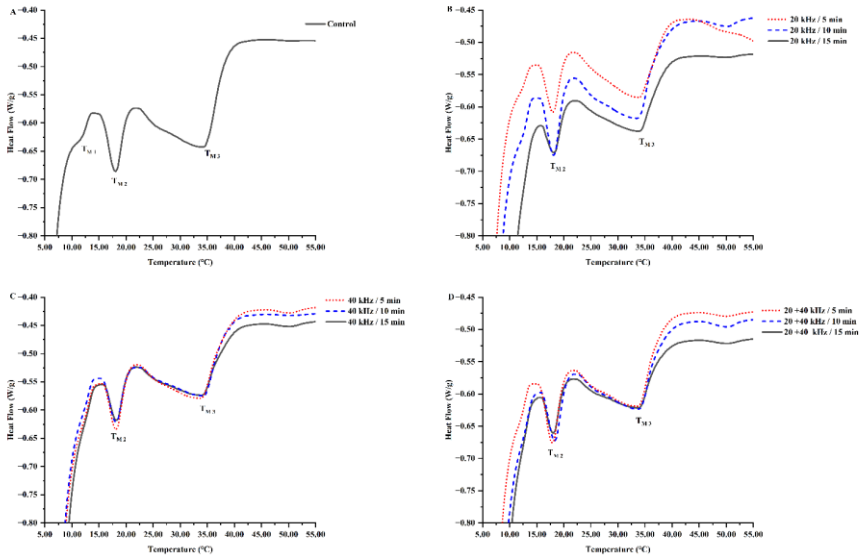



**Figure 4-8.** DSC melting thermograms of MFGs/MFGM samples separated from the control and ultrasonicated bovine milk, $T_{M1}$-$T_{M3}$ are melting temperatures.

The crystallization and melting thermograms of MFGs/MFGM samples prepared from the control and ultrasonic bovine milk are shown in Fig. 4-7 and 4-8, respectively.

According to Fig. 4-7 (A-D), two crystallization peaks were detected in all samples at approximate values of 10.50 °C ($T_{C1}$) and 14.00 °C ($T_{C2}$). There was no significant difference between the $T_{C1}$ and $T_{C2}$ of all samples ($p<0.05$). Comparatively, except for the peaks at $T_{C1}$ and $T_{C2}$, one or two new exothermic events appeared in the range of 17.29 – 18.81 °C ($T_{C3}$) and 22.14 – 25.21 °C ($T_{C4}$) in ultrasonicated samples, but not in control samples. In other words, ultrasonic treatment improved the crystallisation of MFGs/MFGM at higher temperature, supported by Martini, et al. (2008). This may be because cavitation generated by the ultrasound facilitated the nucleation (Sert, et al., 2020). Only a slight difference was observed for the $T_{C3}$ and $T_{C4}$ in ultrasonicated MFGs/MFGM samples, of which 20 + 40 kHz/ 15 min treatment promoted the crystallization more efficiently than other treatments because of the significantly higher $T_{C4}$ (Table 4-5).

Ultrasonic treatments induced the decrease of $\Delta H_C$ (J $g^{-1}$) in MFGs/MFGM samples in different degrees compared with the control samples. There was a decrease

in the $\Delta H_C$ (J $g^{-1}$) of MFGs/MFGM samples as the treating time was prolonged at the same ultrasonic intensity. 15 min ultrasonicated MFGs/MFGM samples at different intensities of 20 kHz, 40 kHz or 20 + 40 kHz showed no significant difference in $\Delta H_C$ (J $g^{-1}$) (Table 4-5). This indicated that ultrasonic duration time presented a more profound effect on the decrease of $\Delta H_C$ (J $g^{-1}$) than the intensity.

In agreement with the previous researches, three melting peaks were detected in control sample at 10.23±0.19 ℃, 18.08±0.07℃ and 34.10±0.84℃, which indicated the existence of low-melting fraction (LMF) ($T_{M1}$), medium-melting fraction (MMF) ($T_{M2}$) and high-melting fraction (HMF) ($T_{M3}$) (Fig. 4-8 A) (Sert, et al., 2020; Sergeev, et al., 2021). However, LMF peaks disappeared in all ultrasonicated samples, while only the MMF and HMF peaks were observed (Fig. 4-8 B-D). Table 4-5 showed that there was no significant difference of $T_{M2}$ and $T_{M3}$ between control and ultrasonic samples. Furthermore, different ultrasonic intensities and duration time did not affect the melting temperature of all MFGs/MFGM samples. This was supported by the previous finding on the butter produced from thermos-sonicated cream (20 kHz, 85 ℃ with the duration of 5, 10 and 15 min) (Sert, et al., 2020). However, Sergeev et al. (2021) reported that melting peaks in anhydrous fat prepared from goat milk presented unimodal distribution after the ultrasonic treatment with operating frequency at 45 kHz and output power of 12.30±1.8 W for 120 s (Sergeev, et al., 2021). It can be inferred that the crystal formation and melting probably happened during the MFGs/MFGM samples preparation stage, which may not be observed during the DSC process.

Within the same ultrasonic frequency group, $\Delta H_M$ values of all the ultrasonicated 15 min samples decreased significantly than the 5 min and 10 min duration treatments except for 20 kHz groups ($p<0.05$). This was similar to the results on $\Delta H_C$. In other words, less enthalpy was needed to melt the fat crystals in 15 min ultrasonicated samples than for 5 min and 10 min samples. This confirmed the results on the XRD in which more unstable and metastable β' were detected in the 15 min ultrasonicated samples than the amount of stale β crystals. Less energy was needed for the

deformation and melting of metastable β' than stable β crystal. However, this differed from the study on the butter which displayed an increase of the energy required to melt after thermos-sonication (20 kHz, 85 ℃ for 10 min) (Buldo, Kirkensgaard, & Wiking, 2013).

### 4.4. Conclusion

In this study, different acoustic powers generated by the 20 kHz and 40 kHz independently or synchronously working conditions, have been shown to affect the interfacial properties and thermal behaviour of MFGs/MFGM samples.

**Table 4-5** Characteristic enthalpy, crystallization and melting temperature of MFGs/MFGM separated from bovine milk with and without ultrasonic treatment

| | Crystallization | | | | | Melting | | | |
|---|---|---|---|---|---|---|---|---|---|
| | $T_{C1}$(℃) | $T_{C2}$(℃) | $T_{C3}$(℃) | $T_{C4}$(℃) | $\Delta H_C$(J g$^{-1}$) | $T_{M1}$(℃) | $T_{M2}$(℃) | $T_{M3}$(℃) | $\Delta H_M$(J g$^{-1}$) |
| Control | 10.73±0.07$^{ns}$ | 14.58±0.49$^{ns}$ | - | - | 5.53±0.72$^{ab}$ | 10.23±0.19 | 18.08±0.07$^{ns}$ | 34.10±0.84$^{ns}$ | 3.34±0.02$^{a}$ |
| 20 kHz/ 5 min | 10.86±0.84 | 14.10±0.52 | - | 23.37±0.44$^{bc}$ | 5.63±0.97$^{a}$ | - | 18.01±0.11 | 33.82±0.38 | 1.96±0.76$^{b}$ |
| 20 kHz/ 10 min | 10.98±0.59 | 13.94±0.08 | 18.81±0.77$^{a}$ | 24.26±0.25$^{ab}$ | 4.79±0.66$^{abc}$ | - | 18.09±0.46 | 33.45±0.06 | 2.41±0.35$^{ab}$ |
| 20 kHz/ 15 min | 10.87±0.96 | 14.18±0.35 | - | 23.90±0.06$^{ab}$ | 3.51±0.05$^{c}$ | - | 18.08±0.07 | 34.10±0.84 | 1.94±0.44$^{b}$ |
| 40 kHz/ 5 min | 10.52±0.05 | 13.97±0.44 | 17.28±0.52$^{c}$ | 23.35±0.98$^{bc}$ | 4.85±0.44$^{abc}$ | - | 18.08±0.97 | 33.55±0.81 | 2.68±0.08$^{ab}$ |
| 40 kHz/ 10 min | 10.44±0.19 | 14.77±0.78 | 17.29±0.51$^{bc}$ | 22.14±0.28$^{c}$ | 4.21±0.16$^{abc}$ | - | 18.07±0.03 | 34.13±0.22 | 2.38±0.03$^{ab}$ |
| 40 kHz/ 15 min | 10.68±0.29 | 14.25±0.26 | 17.29±0.25$^{bc}$ | 23.53±0.36$^{bc}$ | 3.88±0.99$^{bc}$ | - | 18.09±0.19 | 33.92±0.76 | 2.29±0.44$^{b}$ |
| 20+40 kHz/ 5 min | 10.79±0.34 | 14.88±0.76 | 17.62±0.38$^{abc}$ | 23.71±0.84$^{b}$ | 4.56±0.29$^{abc}$ | - | 17.89±0.16 | 33.52±0.15 | 2.47±0.13$^{ab}$ |
| 20+40 kHz/ 10 min | 10.54±0.97 | 13.89±0.85 | 18.57±0.06$^{ab}$ | 24.22±0.04$^{ab}$ | 4.58±0.52$^{abc}$ | - | 18.31±0.91 | 33.75±0.48 | 2.47±0.24$^{ab}$ |
| 20+40 kHz/ 15 min | 11.05±0.97 | 14.72±0.65 | 17.63±0.38$^{abc}$ | 25.21±0.49$^{a}$ | 3.48±0.34$^{c}$ | - | 18.04±0.07 | 33.71±0.52 | 1.92±0.04$^{b}$ |

Notes: Abbreviations are: $T_{C1} - T_{C4}$, the temperature of crystallisation peaks, $\Delta H_C$, enthalpy of crystallisation; $T_{M1} - T_{M4}$, the temperature of melting peaks, $\Delta H_M$, enthalpy of melting. Different superscript letters in the same column indicate significant ($p < 0.05$) differences between samples. 'ns' means no significant difference ($p > 0.05$).

20 kHz treatments led to a relatively even particle distribution in MFGs/MFGM than that of 40 kHz and 20 + 40 kHz treated samples. The relative ζ– potential ($\zeta_R$) could not be used to predict the surface change of MFGs/MFGM after ultrasonic treatments because there was no statistical correlation between estimated ($\Phi_e$) and the measured surface fraction ($\Phi_m$). Ultrasound treatment significantly resulted in the decrease of π in all samples ($p<0.05$). Three typical crystal forms, α-crystal, β-form and β'-form, were observed in control and ultrasonicated 5 min samples, but α-crystal disappeared in all the 15 min treated samples. Ultrasonic duration has a more profound effect on the increase of β'- crystal than the intensity. Ultrasonic treatments promoted the crystallisation of MFGs/MFGM fat at higher temperature but increased the melting temperature of MFGs/MFGM.

In summary, interfacial properties and thermal behaviour of MFGs/MFGM samples were affected by ultrasonic treatments, which, however, did not display a consistent correlation with the ultrasonic acoustic energy. MFGs/MFGM is a complicated mixture. Therefore, specific ultrasonic conditions should be optimised according to the different functionalities and applications.

**Declaration of competing interest**

All authors declare no conflict of interest.

**Acknowledgements**

The project was supported by 'The Open Project Program of State Key Laboratory of Dairy Biotechnology (No. SKLDB2022–007)' and 'The China Scholarship Council (No.202008410212)'.

**References**

Bhaskaracharya, R. K., Kentish, S., & Ashokkumar, M. (2009). Selected Applications of Ultrasonics in Food Processing. *Food Engineering Reviews, 1*(1), 31-49.

Buldo, P., Kirkensgaard, J. J. K., & Wiking, L. (2013). Crystallization mechanisms in cream during ripening and initial butter churning. *Journal of Dairy Science, 96*(11), 6782-6791.

Camino, N. A., Pérez, O. E., Sanchez, C. C., Rodriguez Patino, J. M., & Pilosof, A. M. R. (2009). Hydroxypropylmethylcellulose surface activity at equilibrium and adsorption dynamics at the air–water and oil–water interfaces. *Food Hydrocolloids, 23*(8), 2359-2368.

Fang, Y., Rogers, S., Selomulya, C., & Chen, X. D. (2012). Functionality of milk protein concentrate: Effect of spray drying temperature. *Biochemical Engineering Journal, 62*, 101-105.

Garczewska-Murzyn, A., Kiełczewska, K., & Smoczyński, M. (2022). The influence of buttermilk powder on the stability of emulsion and colloidal phases of homogenized milk. *European Food Research and Technology, 248*(10), 2629-2636.

Graham, D. E., & Phillips, M. C. (1979). Proteins at liquid interfaces: III. Molecular structures of adsorbed films. *Journal of Colloid and Interface Science, 70*(3), 427-439.

Ho, T. M., Dhungana, P., Bhandari, B., & Bansal, N. (2021). Effect of the native fat globule size on foaming properties and foam structure of milk. *Journal of Food Engineering, 291*, 110227.

Huang, Y., Wei, T., Chen, F., Tan, C., Gong, Z., Wang, F., et al. (2023). Effects of various thermal treatments on interfacial composition and physical properties of bovine milk fat globules. *Food Research International, 167*, 112580.

Jiang, B., Xia, Y., Zhou, L., Liang, X., Chen, X., Chen, M., et al. (2022). Safety and Tolerance Assessment of Milk Fat Globule Membrane- enriched Infant Formulas in Healthy Term Chinese Infants: A Randomised Multicenter Controlled Trial. *BMC pediatrics, 22*(1), 465.

Jukkola, A., Partanen, R., Rojas, O. J., & Heino, A. (2016). Separation of milk fat globules via microfiltration: Effect of diafiltration media and opportunities for stream valorization. *Journal of Dairy Science, 99*(11), 8644-8654.

Juliano, P., Kutter, A., Cheng, L. J., Swiergon, P., Mawson, R., & Augustin, M. A. (2011). Enhanced creaming of milk fat globules in milk emulsions by the application of ultrasound and detection by means of optical methods. *Ultrasonic Sonochemistry, 18*(5), 963-973.

Krasulya, O., Bogush, V., Trishina, V., Potoroko, I., Khmelev, S., Sivashanmugam, P., et al. (2016). Impact of acoustic cavitation on food emulsions. *Ultrasonic Sonochemistry, 30*, 98-102.

Kurup, G. G., Adhikari, B., & Zisu, B. (2020). Application of high-frequency ultrasound standing waves for the recovery of lipids from high-fat dairy effluent. *Ultrasonic Sonochemistry, 63*, 104944.

Lambert, A., Bougrioua, F., Abbas, O., Courty, M., El Marssi, M., Faivre, V., et al. (2018). Temperature dependent Raman and X-ray diffraction studies of anhydrous milk fat. *Food Chemistry, 267*, 187-195.

Leong, T., Johansson, L., Juliano, P., Mawson, R., McArthur, S., & Manasseh, R. (2014a). Design parameters for the separation of fat from natural whole milk in an ultrasonic litre-scale vessel. *Ultrasonic Sonochemistry, 21*(4), 1289-1298.

Leong, T., Juliano, P., Johansson, L., Mawson, R., McArthur, S. L., & Manasseh, R. (2014b). Temperature effects on the ultrasonic separation of fat from natural whole milk. *Ultrasonic Sonochemistry, 21*(6), 2092-2098.

Li, H., & Van der Meeren, P. (2022). Sequential adsorption of whey proteins and low methoxy pectin at the oil-water interface: An interfacial rheology study. *Food Hydrocolloids, 128*, 107570.

Liu, Y., Boeren, S., Zhang, L., Zhou, P., & Hettinga, K. (2021). Ultrasonication retains more milk fat globule membrane proteins compared to equivalent shear-homogenization. *Innovative Food Science & Emerging Technologies, 70*, 102703.

Logan, A., Lopez, C., Xu, M., Day, L., Oiseth, S., & Augustin, M. A. (2021). Tempering governs the milk fat crystallisation and viscoelastic behaviour of unprocessed and homogenised creams. *Food Research International, 147*, 110557.

Lopez, C., Bourgaux, C., Lesieur, P., Bernadou, S., Keller, G., & Ollivon, M. (2002). Thermal and Structural Behavior of Milk Fat. *Journal of Colloid and Interface Science, 254*(1), 64-78.

Lopez, C., Cheng, K., & Perez, J. (2018). Thermotropic phase behavior of milk sphingomyelin and role of cholesterol in the formation of the liquid ordered phase examined using SR-XRD and DSC. *Chem Phys Lipids, 215*, 46-55.

Marie-Caroline Michalski , F. o. M., Damien Sainmont,, & Briard, V. r. (2001). Apparent $\zeta$ -potential as a tool to assess mechanical damages to the milk fat globule membrane. *Colloids and Surfaces B: Biointerfaces 23, 23*, 23–30.

Martini, S., Suzuki, A. H., & Hartel, R. W. (2008). Effect of High Intensity Ultrasound on Crystallization Behavior of Anhydrous Milk Fat. *Journal of the American Oil Chemists' Society, 85*(7), 621-628.

Meng, Y., Liang, Z., Zhang, C., Hao, S., Han, H., Du, P., et al. (2021). Ultrasonic modification of whey protein isolate: Implications for the structural and functional properties. *Lwt, 152*.

Michalski, M. C., Cariou, R., Michel, F., & Garnier, C. (2002). Native vs. Damaged Milk Fat Globules: Membrane Properties Affect the Viscoelasticity of Milk Gels. *Journal of Dairy Science, 85:2451–2461*.

Nieto-Ruiz, A., Garcia-Santos, J. A., Verdejo-Roman, J., Dieguez, E., Sepulveda-Valbuena, N., Herrmann, F., et al. (2022). Infant Formula Supplemented With Milk Fat Globule Membrane, Long-Chain Polyunsaturated Fatty Acids, and Synbiotics Is Associated With Neurocognitive Function and Brain Structure of Healthy Children Aged 6 Years: The COGNIS Study. *Front Nutrition, 9*, 820224.

Pan, Y., Liu, L., Tian, S., Li, X., Hussain, M., Li, C., et al. (2022). Comparative analysis of interfacial composition and structure of fat globules in human milk and infant formulas. *Food Hydrocolloids, 124*, 107290.

Reddy, R. S., Ramachandra, C. T., Hiregoudar, S., Nidoni, U., Ram, J., & Kammar, M. (2014). Influence of processing conditions on functional and reconstitution properties of milk powder made from Osmanabadi goat milk by spray drying. *Small Ruminant Research, 119*(1-3), 130-137.

Ren, Q., Guo, F., Teng, F., & Ma, Y. (2021). A novel approach for the reconstitution of bovine milk fat globules with different-melting-temperature triacylglycerol cores. *Food Chemistry, 345*, 128563.

Ren, Q., Li, L., Dudu, O. E., & Ma, Y. (2019). Thermal and structural changes of pasteurized milk fat globules during storage. *Food Bioscience, 28*, 27-35.

Ren, Q., Li, Q., Liu, H., & Ma, Y. (2020). Thermal and storage properties of milk fat globules treated with different homogenisation pressures. *International Dairy Journal, 110*, 104725.

Saxena, J., Adhikari, B., Brkljaca, R., Huppertz, T., Chandrapala, J., & Zisu, B. (2020). Inter-relationship between lactose crystallization and surface free fat during storage of infant formula. *Food Chemistry, 322*, 126636.

Scudino, H., Silva, E. K., Gomes, A., Guimaraes, J. T., Cunha, R. L., Sant'Ana, A. S., et al. (2020). Ultrasound stabilization of raw milk: Microbial and enzymatic inactivation, physicochemical properties and kinetic stability. *Ultrasonic Sonochemistry, 67*, 105185.

Sergeev, A., Shilkina, N., Motyakin, M., Barashkova, I., Zaborova, V., Kanina, K., et al. (2021). Anhydrous fat crystallization of ultrasonic treated goat milk: DSC and NMR relaxation studies. *Ultrasonics Sonochemistry, 78*, 105751.

Sert, D., & Mercan, E. (2020). Characterisation of physicochemical, microbiological, thermal, oxidation properties and fatty acid composition of butter produced from thermosonicated cream. *International Dairy Journal, 109*, 104777.

Seta, L., Baldino, N., Gabriele, D., Lupi, F. R., & de Cindio, B. (2012). The effect of surfactant type on the rheology of ovalbumin layers at the air/water and oil/water interfaces. *Food Hydrocolloids, 29*(2), 247-257.

Sharma, P., Oey, I., & Everett, D. W. (2015). Interfacial properties and transmission electron microscopy revealing damage to the milk fat globule system after pulsed electric field treatment. *Food Hydrocolloids, 47*, 99-107.

Song, B., Yao, P., Zhang, Y., Pang, X., Zhang, S., & Lv, J. (2022). Ultrasound pretreatment prior to spray drying improve the flowability and water sorption properties of micellar casein concentrate. *Ultrasonic Sonochemistry, 87*, 106049.

Sun, Y., Chen, J., Zhang, S., Li, H., Lu, J., Liu, L., et al. (2014). Effect of power ultrasound pre-treatment on the physical and functional properties of reconstituted milk protein concentrate. *Journal of Food Engineering, 124*, 11-18.

Sun, Y., Roos, Y. H., & Miao, S. (2022b). Changes in Milk Fat Globules and Membrane Proteins Prepared from pH-Adjusted Bovine Raw Milk. *Foods, 11*(24), 4107.

Sun, Y., Yu, X., Hussain, M., Li, X., Liu, L., Liu, Y., et al. (2022a). Influence of milk fat globule membrane and milk protein concentrate treated by ultrasound on the structural and emulsifying stability of mimicking human fat emulsions. *Ultrasonics Sonochemistry, 82*, 105881.

ten Grotenhuis, E., van Aken, G. A., van Malssen, K. F., & Schenk, H. (1999). Polymorphism of milk fat studied by differential scanning calorimetry and real-time X-ray powder diffraction. *Journal of the American Oil Chemists' Society, 76*(9), 1031-1039.

Tomé Constantino, A. B., & Garcia-Rojas, E. E. (2020). Modifications of physicochemical and functional properties of amaranth protein isolate (Amaranthus cruentus BRS Alegria) treated with high-intensity ultrasound. *Journal of Cereal Science, 95*.

Toro-Vazquez, J. F., Briceño-Montelongo, M., Dibildox-Alvarado, E., Charó-Alonso, M., & Reyes-Hernández, J. (2000). Crystallization kinetics of palm stearin in blends with sesame seed oil. *Journal of the American Oil Chemists' Society, 77*(3), 297-310.

Wright, A. J., & Marangoni, A. G. (2006). Crystallization and rheological properties of milk fat. In P. L. H. M. E. A. d. c. p. In P. F. Fox (Ed.), *Advanced Dairy Chemistry* (Vol. lipids, pp. 245-291). Boston: Springer.

Zamora, A., Ferragut, V., Guamis, B., & Trujillo, A. J. (2012). Changes in the surface protein of the fat globules during ultra-high pressure homogenisation and conventional treatments of milk. *Food Hydrocolloids, 29*(1), 135-143.

Zhao, X., Fan, X., Shao, X., Cheng, M., Wang, C., Jiang, H., et al. (2022). Modifying the physicochemical properties, solubility and foaming capacity of milk proteins by ultrasound-assisted alkaline pH-shifting treatment. *Ultrasonic Sonochemistry, 88*, 106089.

Zhou, B., Tobin, J. T., Drusch, S., & Hogan, S. A. (2021). Dynamic adsorption and interfacial rheology of whey protein isolate at oil-water interfaces: Effects of protein concentration, pH and heat treatment. *Food Hydrocolloids, 116*.

## Supplementary materials

### Table S-1

Temperature variation induced by different ultrasonic intensities and durations in bovine milk

| Samples | *dT/dt* |
|---|---|
| 20 kHz/ 5 min | 0.0161±0.0004$^{b}$ |
| 20 kHz/ 10 min | 0.0203±0.0016$^{a}$ |
| 20 kHz/ 15 min | 0.0223±0.0004$^{a}$ |
| 40 kHz/ 5 min | 0.0040±0.0002$^{e}$ |
| 40 kHz/ 10 min | 0.0060±0.0001$^{de}$ |
| 40 kHz/ 15 min | 0.0060±0.0001$^{de}$ |
| 20+40 kHz/ 5 min | 0.0051±0.0004$^{e}$ |
| 20+40 kHz/ 10 min | 0.0081±0.0003$^{d}$ |
| 20+40 kHz/ 15 min | 0.0106±0.0015$^{c}$ |

Notes:

Different superscript letters in the same column indicate significant ($p < 0.05$) differences between the samples

# CHAPTER FIVE

## Modifying physicochemical properties, rheology and creaming stability of milk fat globule and membrane through ultrasound treatment

**Abstract**

The healthy benefits of milk fat globules and membrane (MFGs/MFGM) The healthy benefits of milk fat globules and membrane (MFGs/MFGM) ingredients are increasingly recognized in the dairy industry. In this research, we examined the effects of ultrasonic treatment on the physicochemical and rheological properties, as well as the emulsions stability of MFGs/MFGM derived from bovine raw milk. Fresh milk was subjected to sonication at frequencies of 20 kHz and 40 kHz, either individually or simultaneously, for durations of 5 min or 15 min, using work/rest cycles of 5 s on and 3 s off. Bovine milk, without any treatment, served as the control. Regardless of the intensity difference, ultrasonic treatment for 5 min resulted in more pronounced changes in the regions of Amide II (1600−1500 $cm^{-1}$), Amide III (1500−1200 $cm^{-1}$), and fingerprint region (1200−1900 $cm^{-1}$) compared to both the 15 min treatments and control MFGs/MFGM. Principal component analysis (PCA) conducted on the entire spectra, as well as in the regions of Amide I, Amide II, and the fingerprint spectra, clustered the 5 min treatment distinctly from the control and MFGs/MFGM ultrasonically treated for 15 min. MFGs/MFGM samples following 20 kHz and 40 kHz synchronously treatment for 15 min exhibited lower absorbance bands at 1727−1726 $cm^{-1}$ whereas higher content of 1740 $cm^{-1}$ compared to control MFGs/MFGM. Additionally, a more significant reduction in the intramolecular β-sheet content in 20 + 40 kHz/ 15 min treatment was observed. According to the sodium dodecyl sulphate polyacrylamide gel electrophoresis (SDS-PAGE) patterns, a diminished intensity of Periodic Acid Schiff 6/7 (PAS 6/7) bands was observed across all the MFGs/MFGM. Ultrasonic treatment retains more caseins while reducing the β –LG levels compared to controls, enhancing the stability of MFGs/MFGM, except in MFGs/ MFGM subjected to 20 and 40 kHz simultaneously treated for 15 min. The irregular sphericity of fat globules was noted particularly in MFGs/MFGM treated at 20 kHz independently or combined with 40 kHz for 15 min. According to the confocal laser scanning microscopy (CLSM), ultrasonic treatment facilitated the binding of caseins or whey proteins onto the MFGs surface and induced flocculation of

membrane proteins. Hierarchical cluster analysis (HCA) heat map further underscored the impact of ultrasonic treatments on the structural and compositional changes, as well as rheology and emulsions stability of MFGs/MFGM.

**Keywords:** Milk fat globules; Ultrasonic treatment; FTIR; Rheological property; Physical instability

## 5.1. Introduction

Milk fat primarily exists in the form of globules (MFG) characterized by a core of triacylglycerol enveloped by a tri-layer structure known as milk fat globule membrane (MFGM). The MFGM is rich in phospholipids and glycoproteins, which are crucial for the neurocognitive function and confer brain-immune-gut benefits (Jiang et al., 2022; Mohamed et al., 2022). Dairy producers, such as Fonterra, Arla, and Friesland Campina, have developed whey protein concentrate (WPC) ingredients enriched with MFGM compositions derived from cheese whey or butter milk (Sun, Roos, & Miao, 2024). These commercial ingredients are used to fortify infant formula (IF) to mimic the natural nutritional profile of human milk, addressing the deficiency of functional lipids and membrane-bound proteins in existing IF products. Despite these advancements, the industry lacks standardized quality regulations to oversee the production of MFGM ingredients, and analytical methods for MFGM proteins remain undeveloped (Wang et al., 2022). Consequently, the compositions of the MFGM ingredients vary significantly between different manufacturers, leading to heterogeneous outcomes. Whey proteins predominate in these formulations, with phospholipid content typically ranging from 6−10%; however, membrane proteins are often not specified in product labels (Sun, Roos, & Miao, 2024).

In addition to nutritional enhancement, the role of MFGM fragments in improving the technical functionalities of IFs and emulsions has been extensively studied. This includes investigation into the interfacial composition and structure of MFGs within IF products (Pan et al., 2022), as well as the stability of emulsion and colloidal phases in homogenized milk (Garczewska-Murzyn, Kiełczewska, & Smoczyński, 2022).

MFGM fragments have been shown to alter the compositions and conformational structure at the oil-water interface, thereby influencing the stability of dairy emulsions (Berton-Carabin, Sagis, & Schroën, 2018). MFGM ingredients are employed as a natural emulsifier in dairy industry due to the amphipathic nature of polar lipids and glycoproteins.

Moreover, the rheological properties of milk system are critical for processing efficiency in the dairy industry. An in-depth understanding of the rheological behaviour of milk liquids is essential for the design and evaluation of process units and operational equipment, such as the heat exchangers, heating and cooling rates, and the pressure losses in pipelines (Velez-Ruiz & Barbosa-Canovas, 1997). The rheological behaviour of milk products is complex, significantly affected by temperature and the concentration of dispersed phases (Kristensen et al., 1997). For instance, the viscosity of the concentred skim milk must be strictly controlled to avoid the detrimental effects on the properties of milk powder (Bienvenue, Jiménez-Flores, & Singh, 2003).

The structure, composition, and techno-functionalities of MFGs or MFGM have been documented in previous reviews (Wiking et al., 2022). There is a compelling need to explore the impact of various preparation steps of MFGM ingredients on their functionalities, including heating, membrane filtration, mechanical shearing, and non-thermal treatments like ultrasonic processing. Ultrasound induces physical and chemical effects in foods due to acoustic cavitation, characterized by the continuous formation and implosion of microbubbles (Patist & Bates, 2008). Research has shown that ultrasonic treatment can enhance the solubility of MFGM (rich in phospholipids, MPL), improve the emulsifying stability of MPL-based emulsions (Sun et al., 2022a), and retain more MFGM proteins compared to shear homogenisation (Liu et al., 2021). These studies predominantly utilized commercial MFGM materials, where the native structure of fat globules was disrupted and MFGM existed in fragmented form. However, studies examining the impact of dairy processing units on MFGM from derived raw milk are limited. The gap underscores the importance of further

investigations to better understand and optimize the processing of MFGs or MFGM ingredients in their most natural state.

In our previous study, we undertook a comparative analysis on the changes of interfacial properties and thermal-dynamic behaviour of MFGs/MFGM isolated from fresh milk exposed to ultrasound at varying intensities (Sun, Roos, & Miao, 2024c). For this study, a follow-up research on the physicochemical and rheological properties, as well as the emulsions stability of MFGs/MFGM was conducted. Additionally, to deepen our understanding of the technical functionalities of natural MFGs and MFGM, bovine raw milk was used as the raw material. Prior to the isolation of MFGs/MFGM materials, ultrasound at varying intensities was applied to the raw milk. The changes in MFGM proteins and their interactions with non-membrane proteins were assessed using a combination of analytical techniques, including sodium dodecyl sulfate polyacrylamide gel electrophoresis (SDS-PAGE), Fourier transform infrared spectroscopy (FTIR), and confocal laser scanning microscopy (CLSM). Furthermore, shearing scanning was performed on all the MFGs/MFGM to characterize their rheological properties, while an accelerated centrifugation method was used to evaluate the stability of emulsion stabilized by MFGs/MFGM. The findings from this research may provide valuable insights into the innovative development of MFGs/MFGM products and their prospective uses in the dairy field.

## 5.2. Materials and methods

### 5.2.1. Materials and reagents

Fresh bovine milk samples were obtained from Teagasc animal & grassland research and innovation centre (Moorepark, Fermoy, Co. Cork, Ireland). Immediately after milking, the fresh milk samples were cooled down to 4 ℃ by plate heater exchanger and maintained at this temperature until further analysis. The compositions of the collected milk was analysed using the DairySpec FT–15 (Bentley Instruments Inc., Chaska, MN, USA), revealing the mean values of fat 4.09 ± 0.01%, protein 3.36 ± 0.03%, dry matter 12.94 ± 0.03%, pH 6.68 ± 0.02.

Nile Red, Fast Green FCF, wheat germ agglutinin (WGA), Polyethylene glycol 200, and phosphate buffer saline (PBS) were purchased from Sigma–Aldrich® (Merck Life Science Ltd., Cork, Ireland). Thermo Scientific Inc. (Thermo Fisher Scientific Inc., Cork, Ireland) was the supplier of all the chemicals for gel electrophoresis.

### 5.2.2. Ultrasonic treatments

Bovine raw milk was subjected to ultrasonic treatments of different intensities referring to the methodologies detailed in our previous research (Sun, et al., 2024c). The procedure involved preheating the raw milk to 30–35 ℃ before subjecting it to sonication at frequencies of 20 kHz and 40 kHz, using both independent and synchronous operating models. An ultrasonic processor (WKS1200/2J, Jiangsu Jiangda Wukesong Biotechnology Co., LT, Zhenjiang, China) was employed, featuring a 2-cm diameter titanium probe. The durations of the ultrasonic treatment treatments were 5 and 15 min using the 5 s: 3 s work/rest cycles model. Raw milk did not undergo ultrasonic treatment served as the control groups.

### 5.2.3. Separation of MFGs/MFGM ingredients

The separation of MFGs/MFGM fractions was carried out using ultra-centrifugation (10000 ×g, 15min at 4 ℃) (Kendro Laboratory Products, Asheville, NC) following the method of Ren, Guo, Teng, and Ma (2021) with some modifications. The upper cream layer was collected and washed with 3 volumes of phosphate buffered saline (PBS, 0.1 mol/L, pH 6.80). This rinsing procedure was repeated 3 times. Subsequently, the upper layer obtained from the final centrifugation was freeze-dried for 72 h. The MFGs/MFGM were individually labelled according to the ultrasonic conditions: 20 kHz/ 5 min, 20 kHz/ 15 min, 40 kHz/ 5 min, 40 kHz/ 15 min, 20 + 40 kHz/ 5 min, and 20 + 40 kHz/ 15 min. The resulted total protein and fat content were noted in our previous study (Sun, et al., 2024c). For each treatment, the material preparation procedures were repeated three times.

### 5.2.4. Fourier transform infrared spectroscopy (FTIR)

FTIR spectra was acquired using a Bruker Tensor 27 (Bruker Optik GmbH, Ettlingen, Germany) equipped with an Optics Platinum Attenuated Total Reflectance (ATR) cell (Pike Technology Inc., Madison, WI, USA). For the analysis, 20 mg of each sample was placed on the zinc ATR crystal aperture. Spectra were captured within the spectral range of 4000 to 900 $cm^{-1}$, averaging 120 scans at a resolution of 4 $cm^{-1}$. Each sample was analysed in triplicate. Prior to each determination, a background measurement was conducted under identical conditions. The collected spectral data was initially pre-processed using OPUS 7.5 software (Bruker Optik GmbH, Ettlingen, Germany) to eliminate the atmospheric vapour and carbon dioxide interference, and vector normalization was applied to mitigate scaling effects.

Noise reduction, baseline subtraction, second derivation, and peaks fitting and deconvolution were performed using OriginPro 2023 (OriginLab, Northampton, MA, USA) to reveal hidden and overlapping bands. The Savityzky–Golay function was utilized for smoothing, and the baseline points were anchored with the 2nd derivative method. The fitting of peaks was carried out using Gaussian, Voigt, or Lorentz functions across various spectral regions to achieve the optimal fit. Parameters such as peaks widths and centres, along with baseline parameter, were adjusted until achieving a fit with $R^2 > 0.996$. Finally, unsupervised chemometric analysis, principal component analysis (PCA), was used to visually depict the variation within and between the spectra of all MFGs/MFGM and to classify samples according to treatments. Namely, loading plots highlighted differentiated wavenumbers, and PCA plots illustrated distinct groups based on their spectral profiles.

### 5.2.5. Sodium dodecyl sulphate polyacrylamide gel electrophoresis (SDS-PAGE)

The protein profiles of control and ultrasonically-treated MFGs/MFGM isolates were characterized by SDS-PAGE with a modified method described by Sun, Roos, and Miao (2022). The non-reducing SDS-PAGE was performed at 120 V for a duration

of 45 min, after which the proteins were stained with Coomassie Blue. Subsequently, the gels were detained using a blend of 45% ethanol and 5% acetic acid until a clear background was achieved. Relative quantification of caseins, whey proteins, and specific MFGM proteins was performed to assess the impact of ultrasonic treatments. The densities of protein bands were analysed by ImageJ software 1.36 b (Wayne Rasband, National Institutes of Health, Bethesda, MD, USA), and the results were normalized to a total of 100%.

### 5.2.6. Rheological analysis

The rheological properties of both control and ultrasound-treated MFGs/MFGM were evaluated using an ARG 2 Rheometer (TA Instruments, Crawley, UK). Before analysis, the freeze-dried MFGs/MFGM was kept at 35−40 ℃ until melting into the liquid state. The measuring geometry consists a 60 mm diameter aluminium parallel plate. The gaps size was set to 300 μm during the analysis. The shear rate was increased from 0.1 $s^{-1}$ to 1000 $s^{-1}$, during which both shear (apparent) viscosity and normal stress were recorded as a function of shear rate. All measurements were conducted at a constant temperature of 25 °C. A lid was used to cover the MFGs/MFGM during the rheological analysis to reduce the moisture evaporation. Each analysis was replicated three times. Given that raw milk and cream predominantly exhibit Non-Newtonian behaviour under conditions with temperature <40 ℃ and at low shear rate, the experimental data were fitted using the power law model and Herschel-Bulkley to characterize the nonlinear behaviour of the MFGs/MFGM samples (Randhahn, 1973).

Power law,

$$\sigma = K\ddot{Y}^{n} \qquad (5\text{-}1)$$

and Herschel-Bulkley,

$$\sigma = \sigma_0 + K\ddot{Y}^{n} \qquad (5\text{-}2)$$

where σ is the shear stress (Pa), while Ÿ denotes the shear rate (1/s). The parameter *K* (Pa $s^n$) serves as the consistency index, and n is the flow behavior index. Additionally, $\sigma_0$ refers to the yield stress (Pa). The power-law model is utilized to predict the rheological behaviour of fluids, characterizing them as shear-thinning for $0 < n < 1$, Newtonian for $n = 1$, and shear-thickening for $n > 1$.

### 5.2.7. Accelerated emulsion stability

Lumisizer was employed (LUM GmbH, Berlin, Germany) to investigate the impact of ultrasonic treatments on the physical stability of MFGs/MFGM. Freeze-dried MFGs/MFGM materials were initially pre-heated to a liquid phase at temperatures ranging from 35℃ to 40℃. Subsequently, 400 μL of these liquid samples were loaded into a polyamide cell (2 mm light path) and subjected to a centrifugal force of 3000 rpm for 45 min at a controlled temperature of 37±2℃. The intensity of near-infrared (NIR) light (wavelength at 865 nm) transmitted through the length of samples was recorded every 10 s intervals during the centrifugation. The SEP View software (SepView 4.1, LUM GmbH) was used for the data recording and instability calculation. To calculate the instability index, the clarity of the emulsion caused by phase separation was measured and then divided by the maximum possible transmission at the given centrifugal force. This dimensionless index spans from 0 to 1, where 0 means no alteration in NIR transmission and 1 means complete phase separation (Yerramilli & Ghosh, 2017).

### 5.2.8. Confocal laser scanning microscopy (CLSM)

CLSM, as reported in the literature, provides reliable qualitative identification of protein adsorption on the surfaces of MFGs and has demonstrated the aggregation of protein and fat globules (Jukkola, Partanen, Rojas, & Heino, 2018). In this study, CLSM (Leica TCS SP5, Leica Microsystems, Germany) was used to examine the ultrasound-induced structural and surface compositional changes of the fat globules. Samples preparation and the instrument settings were based on our published report

with modifications (Sun, et al., 2022). Generally, non-polar lipids, predominantly triglycerides, were stained with Nile Red, while non-membrane proteins and glycoproteins were labelled using Fast Green FCF and wheat germ agglutinin (WGA), respectively. All the MFGs/MFGM underwent dual staining by 10 µL mixture comprising 0.1% (w/v) Nile Red in polyethylene glycol-200 and 0.1% (w/v) Fast Green FCF in distilled water, at a ratio of 3:1 (v/v) (FCF: Nile Red). Additionally, 50 µL of 1 mg/mL WGA in PBS was combined with Nile Red at a 1:1 (v/v) ratio. All MFGs/MFGM were subsequently incubated in darkness for half an hour to ensure thorough staining. The excitation of Nile Red, Fast Green FCF, and WGA were performed with a helium-neon (He-Ne) laser at 565–625 nm, 632–719 nm, and 493–550 nm, respectively. For each sample, a minimum of 10 images were recorded, from which one representative image was selected for each experiment.

### 5.2.9. Statistical analysis

All analyses were conducted in triplicate, unless otherwise indicated. The tested results were expressed as mean value ± standard deviation (SD). The variant analysis was performed using Analysis of Varian (ANOVA), and the significance of mean differences was assessed using Fisher's test ($p < 0.05$). Additionally, Multivariate Statistical Analysis was undertaken with OriginPro, the results of which were visually represented through a heat map, derived from the Hierarchical Cluster analysis (HCA). All these statistical evaluations were conducted using the OriginPro 2023 software system (OriginPro 2023, OriginLab Corporation, Northampton, USA).

## 5.3. Results and discussion

### 5.3.1. General profiling of composition changes induced by ultrasonic treatments

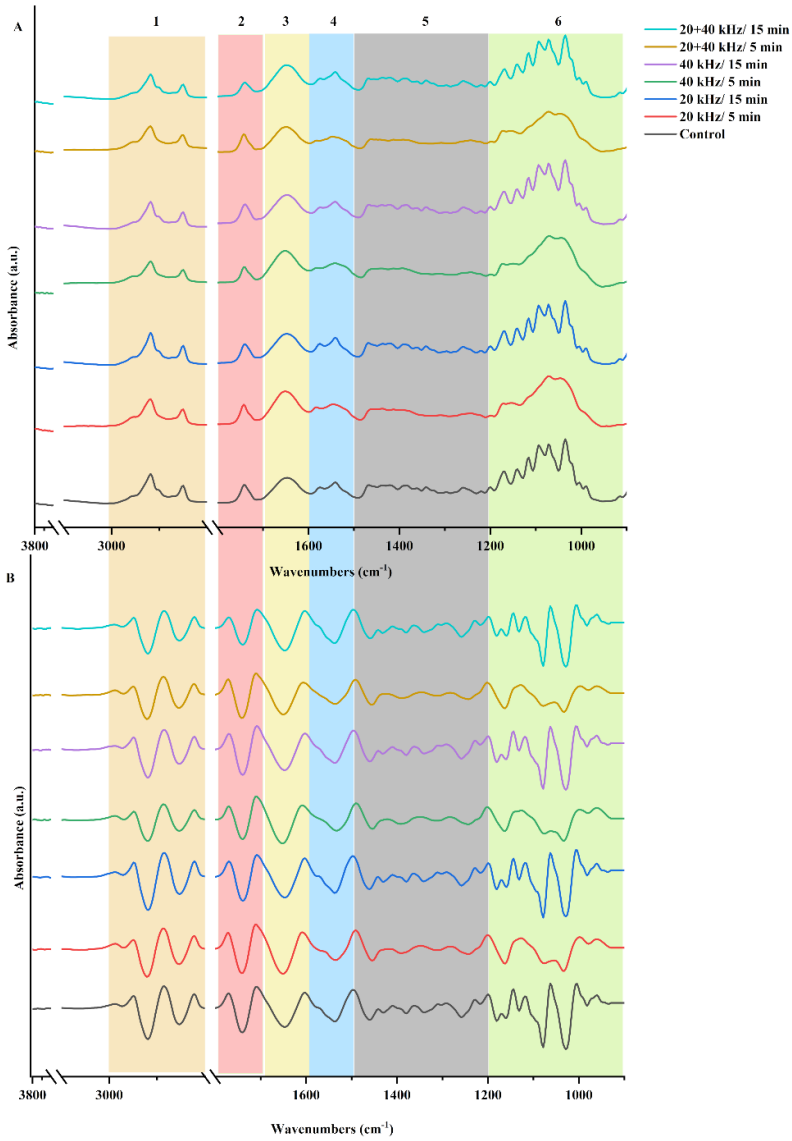



**Figure 5-1.** FTIR spectra for MFGs/MFGM materials: original (A) and 2nd derivative (B). (Spectra between 2800 and 1800 $cm^{-1}$ are not shown as no peak was detected for any of the samples, with all spectra displaying similar flat profiles). Numbers 1−6 above the figure indicate different wavenumber ranges: 1: 3000−2800 $cm^{-1}$; 2: 1800−1700 $cm^{-1}$; 3: Amide I, 1700−1600 $cm^{-1}$; 4: Amide II, 1600−1500 $cm^{-1}$; 5: Amide III, 1500−1200 $cm^{-1}$; 6: Fingerprint region, 1200−1900 $cm^{-1}$.

The averaged FTIR spectra of MFGs/MFGM fractions extracted from bovine raw milk treated with ultrasound at varying intensities are depicted in Fig. 5-1A. Additionally, a second derivative analysis was conducted to search for the hidden peaks within each spectrum (Fig. 5-1B). The entire spectral range between 4000 and 900 $cm^{-1}$ has been classified into six regions based on different milk components referring to published articles. In particular, the region from 3000−2800 $cm^{-1}$ are attributed to the stretching modes of $CH_2$ groups of acyl chains in triglycerides and phospholipids (Grewal et al., 2017) (Region 1); 1800−1700 $cm^{-1}$ represents the C=O stretching vibrations of ester, aldehydes and ketones (Vongsvivut et al., 2012) (Region 2); Protein secondary structure is commonly described by the Amide I (1700−1600 $cm^{-1}$) (Region 3), Amide II (1600−1500 $cm^{-1}$) (Region 4) and Amide III (1500−1200 $cm^{-1}$) (Kher et al., 2007) (Region 5); and the 1200−900 $cm^{-1}$, known as the fingerprint region, corresponds to the lipid components of membranes, protein-lipid complexes, and lactose groups (Zhou et al., 2006b) (Region 6).

The original and 2$^{nd}$ deprivation spectra in the regions numbered as 1−3 show no noticeable differences, whereas more pronounced changes are observed in the regions of 4−6 for MFGs/MFGM treated for 5 min compared to those treated for 15 min and the control (Fig. 5-1A and 5-1B).

PCA conducted on the full spectra range from 4000−900 $cm^{-1}$ grouped the MFGs/MFGM into two distinct categories along the axis of Principle Component 1 (PC1), which accounts for 44.30% of the variance (Fig. S1A). MFGs/MFGM treated for 5 min were differentiated from both control and 15 min ultrasonic treatment samples. This division is mainly due to the different loadings for wavenumber ranges of 3000−2800 $cm^{-1}$ and 1700−900 $cm^{-1}$ (Fig. S1B). Further PCA was performed on these specific wavenumber regions to explore the effects of ultrasonic treatments on the lipids, proteins, and the interactions of membrane proteins in the MFGs/MFGM materials. For the first region between 3000 $cm^{-1}$ and 2800 $cm^{-1}$, the control, 20 kHz/ 15 min, and 40 kHz/ 15min MFGs/MFGM were separated from the 20 + 40 kHz/

15min and the 40 kHz/ 5 min ultra-sonicated MFGs/MFGM along the PC2 (Fig. S2A) with a variation of 9.2%. This separation is due to peaks at 2916/2850 $cm^{-1}$ and 2900 $cm^{-1}$, which are ascribed to the methylene groups and C−H stretching of lipids, respectively (Fig. S2B) (Grewal et al., 2017).

In the region of 1800−1700 $cm^{-1}$, the 20 + 40 kHz/ 15 min MFGs/MFGM were distinctly separated from other treatments along the direction of PC2 (9.1%) (Fig. S3A). This division is primarily due to the differences in wavenumber at 1742 $cm^{-1}$, which is assigned to the ester functional group of lipids and their interactions with proteins via C=O stretching vibrations (Fig.S3B) (Vongsvivut et al., 2012). In addition, hidden peaks at the wavenumber of 1726 $cm^{-1}$ in each sample were searched by using a peak fitting function (Fig. S4A-G). The band at 1726 $cm^{-1}$ is typically indicative of the presence of hydrogen bonded carbonyl groups in esters (Dufour & Riaublanc, 1997). Quantitative assessments of the respective corresponding groups at band of 1740 $cm^{-1}$ and 1727 $cm^{-1}$ in each MFGs/MFGM were calculated to elaborate the changes in lipids groups (Table 5-1). Bands between 1727−1726 $cm^{-1}$ in control MFGs/MFGM were significantly higher than those in the MFGs/MFGM fractions treated by 20 and 40 kHz for 15 min ($p<0.05$), whereas the opposite trend was observed at 1742−1739 $cm^{-1}$, where a stronger spectrum was noted in the MFGs/MFGM sourced from 20 and 40 kHz ultra-sonicated raw milk for 15 min MFGs/MFGM compared to the control.

**Table 5-1** Quantitative estimation of the functional ester group of lipids at the band of 1727−1726 $cm^{-1}$ and 1740−1739 $cm^{-1}$ in all MFGs/MFGM materials prepared from bovine raw milk treated by ultrasound (1800−1700 $cm^{-1}$)

| | 1727−1726 $cm^{-1}$ | 1740−1739 $cm^{-1}$ |
|---|---|---|
| Control | $94.29\pm0.22^{a}$ | $5.71\pm0.22^{b}$ |
| 20 kHz/ 5 min | $91.37\pm0.52^{ab}$ | $8.63\pm0.52^{ab}$ |
| 20 kHz/ 15 min | $87.41\pm0.10^{ab}$ | $12.59\pm0.10^{ab}$ |

| | | |
|---|---|---|
| 40 kHz/ 5 min | 86.22±4.25$^{ab}$ | 13.78±4.25$^{ab}$ |
| 40 kHz/ 15 min | 91.94±0.92$^{ab}$ | 8.06±0.92$^{ab}$ |
| 20+40 kHz/ 5 min | 91.92±1.45$^{ab}$ | 8.08±1.45$^{ab}$ |
| 20+40 kHz/ 15 min | 81.38±17.19$^{b}$ | 18.62±17.19$^{a}$ |

Superscript letters that differ in the same column denote significant differences between samples ($p < 0.05$). 'ns' stands for no significant difference ($p > 0.05$).

For the Amide I and Amide II, PC2 classified all of the MFGs/MFGM into two separate groups, respectively (Fig. 5-S5B and 5-S6B). MFGs/MFGM treated at 20 kHz/ 5min and 40 kHz/ 5 min exhibited similar distributions, while control and those treated for 15 min clustered to another group. Notably, MFGs/MFGM from the 20 + 40 kHz/ 5min treatments demonstrated poor repeatability, as indicated by their dispersed distribution in both Fig. S5A and S6A. The separation observed in the Amide I region is due to the loading for the wavenumber at 1654 $cm^{-1}$, which can be associated with the changes in the α-helix content of proteins. The loading for 1573 $cm^{-1}$ and 1540 $cm^{-1}$ is responsible for the group separation in the Amide II band, which has been reported to associate with the –COO-asymmetric stretching vibration of Asp and Glu residues and C−N and N−H stretching, respectively (Grelet et al., 2015).

Peak fitting was applied in Amide I regions (Fig. 5-S7 A-G), the results of which demonstrated that the ultrasonic treatment has no significant effect on the structure of β-turn and side chain in all MFGs/MFGM ($p>0.05$) (Table 5-2). Comparing with control, MFGs/MFGM exposed to 20 + 40 kHz for a duration of 15 min significantly reduced the intramolecular β-sheet content ($p<0.05$). Additionally, more random coil structures were identified in MFGs/MFGM ingredients subjected to 40 kHz for 15 min than that in control, and under the same ultrasonic conditions, 15 min treatments significantly enhanced the random coil structure compared to 5 min treatments except for 20 kHz and 40 kHz concurrent treatment ($p < 0.05$). Conversely, α-helix structures were more prevalent in MFGs/MFGM treated for 5 min compared to those treated for

15 min. This finding is inconsistent with the PCA results in the band of Amide I, where differences in α-helix were the primary factor in grouping 5 min treated MFGs/MFGM from control and 15 treatments. Peak fitting in the spectrum of Amide II indicated an apparent band migration from 1582−1584 $cm^{-1}$ to 1572−1573 $cm^{-1}$ as the duration of ultrasonic treatment prolonged to 15 min (Fig. 5-S8 A-G). This supports the previous PCA results that distinguished 5 min MFGs/MFGM from those treated for 15 min and control along the PC2 at the band at 1573 $cm^{-1}$.

**Table 5-2** Relative content of secondary structures in Amide I region (1700−1600 $cm^{-1}$) in all MFGs/MFGM materials prepared from bovine raw milk treated by ultrasound

| | Intramolecular β-sheet | Random coil | α-helix | β-turn | Side chain |
|---|---|---|---|---|---|
| Control | $11.08\pm0.35^{a}$ | $36.26\pm6.00^{bcd}$ | $26.96\pm3.48^{b}$ | $17.78\pm7.70^{ns}$ | $7.92\pm1.82^{ns}$ |
| 20 kHz/ 5 min | $9.99\pm1.18^{ab}$ | $28.60\pm7.10^{d}$ | $43.13\pm10.46^{a}$ | $12.32\pm3.52$ | $5.96\pm1.07$ |
| 20 kHz/ 15 min | $8.69\pm4.53^{ab}$ | $41.18\pm6.77^{abc}$ | $26.90\pm3.37^{b}$ | $14.68\pm2.32$ | $8.54\pm1.86$ |
| 40 kHz/ 5 min | $7.39\pm2.87^{ab}$ | $31.67\pm5.46^{cd}$ | $40.00\pm6.32^{a}$ | $12.05\pm3.72$ | $8.88\pm2.56$ |
| 40 kHz/ 15 min | $6.24\pm2.85^{b}$ | $49.95\pm6.54^{a}$ | $20.18\pm5.88^{b}$ | $15.60\pm0.62$ | $8.03\pm3.64$ |
| 20+40 kHz/ 5 min | $8.53\pm3.09^{ab}$ | $35.62\pm10.68^{bcd}$ | $28.26\pm0.22^{b}$ | $17.19\pm2.69$ | $8.81\pm2.34$ |
| 20+40 kHz/ 15 min | $6.34\pm1.62^{b}$ | $45.70\pm2.59^{ab}$ | $23.72\pm2.52^{b}$ | $16.13\pm1.83$ | $8.11\pm1.20$ |

Superscript letters that differ in the same column denote significant differences between samples ($p < 0.05$). 'ns' stands for no significant difference ($p > 0.05$).

Similar group distinctions observed in the Amide I and Amide II regions were also noted when analysing the fingerprint region of 1200−900 $cm^{-1}$ via PCA. The analysis demonstrated that MFGs/MFGM treated for 5 min were differentiated from control and 15 min treatment MFGs/MFGM (Fig. S9A). This differentiation was largely attributed to absorbance peaks at 987 $cm^{-1}$, 1035 $cm^{-1}$, and 1153 $cm^{-1}$ along the PC2 axis, which represented 80.40 % of the observed variance.

The band at 987 $cm^{-1}$ has been reported to be related to the release of colloidal calcium phosphate (CCP) from the phosphate residues due to pressure effects (Gebhardt et al., 2011). The bands around 1035 $cm^{-1}$ ascribes to $–CH_2$ bending, and peak around 1159 $cm^{-1}$ represents the C−O group (esters) (Zhou et al., 2006a). Further insights were gained through peak fitting analysis of the region between 1200−900 $cm^{-1}$ (Fig. 5-S10 A-G), where peaks at bands 1003 $cm^{-1}$ and 1058 $cm^{-1}$ were absent

in 5 min treatment MFGs/MFGM. Meanwhile, absorbance peaks positioned at 1035 $cm^{-1}$ and 1141 $cm^{-1}$ in both control and 15 min treatment MFGs/MFGM shifted to 1043 $cm^{-1}$ and 1153 $cm^{-1}$, respectively, in 5 min treatment MFGs/MFGM.

In summary, PCA analysis of the spectral bands from Amide I (1700−1600 $cm^{-1}$), Amide II (1600−1500 $cm_{-1}$), and 1200−900 $cm^{-1}$ revealed that all treatments could be categorized into two distinct groups: one compromising the 5 min treatment, and another encompassing the control and 15 min treatment, a finding further substantiated by the peak fitting results.

### 5.3.2. Effect of ultrasonic treatments on the distribution of milk fat globule membrane proteins

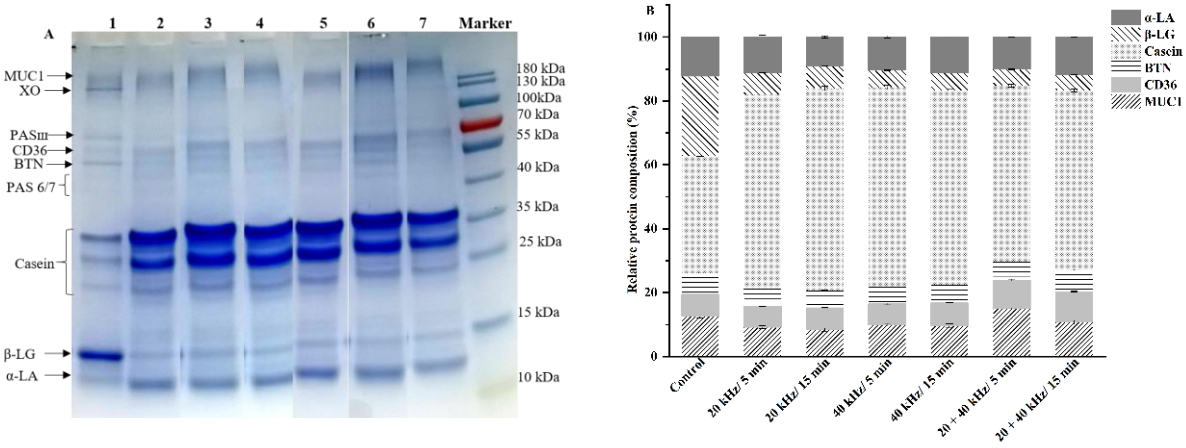



**Figure 5-2.** SDS-PAGE patterns obtained under non-reducing conditions of fat globule materials from control and ultra-sonicated raw milk. (A) Lane 1-7, control, processed at 20 kHz for 5 min and 15 min, 40 kHz for 5 min and 15 min, 20 + 40 kHz for 5 min and 15 min.

Non-reducing SDS-PAGE was conducted to illustrate the impact of varying ultrasound intensities on the MFGs/MFGM proteins, with the resulting SDS-PAGE patterns depicted in Fig.5-2A. Notable non-membrane proteins identified included casein, β-lactoglobulin (β-LG), α-lactalbumin (α-LA), and six key membrane proteins: MUC1, the redox enzyme xanthin oxidase (XO), periodic acid Shciff 3 (PAS III), CD 36, BTN, and periodic acid Schiff 6/7 (PAS 6/7). Generally, the intensity of PAS 6/7

bands was observed to be lower compared to other proteins, likely due to its classification as the peripheral protein which is more susceptible to removal through mechanical shearing during sample preparation (Sun, Roos, & Miao, 2022). In contrast, casein, β-LG, and α-LA were distinctly present in control, persisting through the centrifugation and rinsing processes (Fig. 5-2A), contrary to findings by Zhao, Du, and Mao (2019) where more intensive centrifugation and rinsing were applied, resulting in the removal of most caseins and whey proteins during centrifugation. The concentration of MFGM proteins in the MFGs/MFGM can further be improved by washing with SDS, followed by sonication (Lu et al., 2021).

The intensity of caseins in ultrasonically treated MFGs/MFGM increased dramatically, whereas a reduced intensity of β –LG bands was identified compared to control. From the quantitative analysis results in Fig. 5-2 B, 20 kHz and 40 kHz treatments retained 55.44−63.28% of caseins, compared to 36.53 % in control. With prolonged ultrasonic durations, a higher retention of caseins was observed, except in the 40 kHz treatments, consistent with the study by Lu et al. (2021) which reported that homogenization damages MFGM while aqueous phase proteins like caseins and whey proteins adsorb onto the newly formed MFGM. Conversely, the reduction of β –LG intensity in ultrasonic MFGs/MFGM may be attributed to the formation of aggregates between β –LG and MFGM proteins via disulphide bands (Hansen et al., 2020). Subsequent centrifugation aided in the removal of these aggregates, concurrently removing the PAS III and XO. This accounts for the observed reductions in the intensities of PAS III and XO bands. Notably, treating at 20 + 40 kHz ultrasound for 15 min most efficiently facilitated the removal of β –LG in MFGs/MFGM ingredients, followed by 5-min treatments at 20 + 40 kHz, then 40 kHz, and lastly 20 kHz.

Additionally, in ultrasonic MFGs/MFGM, the intensity of CD 36 increased, particularly in the 20 + 40 kHz treatments, suggesting that ultrasonic treatment enhances the transferring of CD 36 into the rinsing phase from the MFGM structure.

In contrast, lower amounts of BTN and MUC1 were detected in MFGs/MFGM after ultrasonic treatment compared to control. This variability in the effects of ultrasonic treatments on CD36, BTN, and MUC1 levels may be due to their distinct localizations within the three layers of membrane: CD 36 primarily localizes in the apical membrane (Spitsberg, Matitashvili, & Gorewit, 1995), MUC1, characterized by its extended rod-like structure, forms part of the glycocalyx on various epithelial cell surfaces and milk membranes (Peterson et al., 2001), and BTN is mainly found in a 'peripheral' cytoskeletal-like component (Banghart et al., 1998). Comparatively, the 20 kHz/ 15 min MFGs/MFGM contained fewer MFGM proteins but higher levels of non-membrane proteins than other MFGs/MFGM, indicating that more intensive ultrasonic treatment promotes greater loss of MFGM proteins.

### 5.3.3. Rheological properties

As shown in Fig.5-3, the apparent viscosity of MFGs/MFGM consistently decreased with an increase in shear rate (0.1 $s^{-1}$ to 1000 $s^{-1}$) across all MFGs/MFGM, demonstrating shear-thinning behaviour (non-Newtonian), regardless of the ultrasonic treating intensities. There was a dramatic decrease in viscosity observed in the control, 20 kHz, and 20 + 40 kHz MFGs/MFGM within the shear rate range of 0.1 to 2 $s^{-1}$, with the exception of those treated at 40 kHz, suggesting a more pronounced degree of Newtonian behavior at the higher shear rates. This observation of shear-thinning behaviour in control in disagreement with findings from Ayyash et al. (2022). They demonstrated that non-fermented raw milk exhibited little or no shear-thinning behavior. This discrepancy of the magnitudes of viscosity could be due to the differences in experimental conditions, particularly the higher shear rate range (10−1000 $s^{-1}$) used in their study.

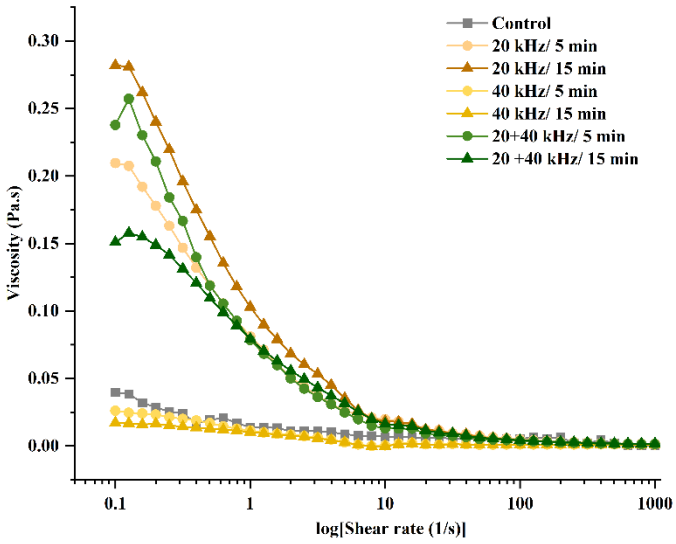



**Figure 5-3** Apparent viscosity of MFGs/MFGM prepared from bovine raw milk treated by ultrasound with different intensities

The initial viscosity of control was significantly lower compared to those treated at 20 kHz and 20 + 40 kHz, while the 40 kHz MFGs/MFGM presented the lowest viscosity. Additionally, a slight variation of the viscosity for 40 kHz MFGs/MFGM was observed throughout the analysis. This trend is accordance with the regression results in Table 5-3. The flow behavior indexes (n) for the 40 kHz MFGs/MFGM, derived from both the power law and Herschel-Bulkley models, are 1 or close to 1, indicating Newtonian or shear thickening behaviour. This characteristic may be attributed to the increase in volume density (%) of larger particles observed at 40 kHz, as noted in the prior research (Sun, Roos, & Miao, 2024c). A heterogeneous distribution of the particles, induced by higher stresses, may lead to the shear thickening behavior observed in skim milk and 3.5 % fat milk at temperature of 25 and 40 ℃ (Kristensen et al., 1997). Furthermore, the flow behavior indexes (n) of the control fitted from power law were higher than those exposed to 20 kHz or 20 kHz and 40 kHz combination treatment, indicating that ultrasonic treatment may enhance the shear thickening behaviour of MFGs/MFGM materials. Notably, ultra-sonicated treatment at 20 kHz for 15 min showed the highest consistency indexes (K, Pa $s^n$)

among all ultrasonic treatments. As reported in our previous research MFGs/MFGM isolates sourced from the bovine milk treated at 20 kHz with a duration of 15 min samples presented more protein content than other treatments (Sun, Roos, & Miao, 2024c). This observation is opposite to Kieferle et al. (2019), they reported the consistency indexes in fresh or reconstituted milk protein concentrates increased with rising protein content.

**Table 5-3** Regressed parameters of the power law and Herschel-Bulkley models used to describe the flow curve of MFGs/MFGM prepared from bovine raw milk treated by different ultrasonic intensities.

| Samples | Power law | | | Herschel-Bulkley | | | |
|---|---|---|---|---|---|---|---|
| | *K* (Pa $s^n$) | n | $R^2$ | $\sigma_0$ (Pa) | *K*(Pa $s^n$) | n | $R^2$ |
| Control | 0.003 | 0.921 | 0.998 | 0.013 | 0.002 | 0.950 | 0.999 |
| 20 kHz/ 5 min | 0.062 | 0.428 | 0.997 | 0.016 | 0.054 | 0.448 | 0.997 |
| 20 kHz/ 15 min | 0.066 | 0.426 | 0.982 | 0.070 | 0.032 | 0.529 | 0.990 |
| 40 kHz/ 5 min | 0.001 | 1.000 | 0.998 | 0.007 | 0.001 | 1.022 | 0.999 |
| 40 kHz/ 15 min | 0.001 | 1.061 | 0.998 | 0.008 | 0.000 | 1.096 | 0.999 |
| 20 + 40 kHz/ 5 min | 0.043 | 0.481 | 0.988 | 0.053 | 0.023 | 0.571 | 0.995 |
| 20 + 40 kHz/ 15 min | 0.043 | 0.506 | 0.988 | 0.064 | 0.021 | 0.608 | 0.988 |

The flow curves of control and MFGs/MFGM treated at 40 kHz exhibited the best fits with the $R^2$ =0.999, followed by the 20 kHz/ 5 min MFGs/MFGM followed with an $R^2$ of 0.997 (Table 5-3). Our preliminary results showed that the Herschel-Bulkley model provided a better fit than the power law model across all MFGs/MFGM, with the higher $R^2$ values ranging from 0.988 to 0.999. The predicted shear stress values from both the power law and Herschel-Bulkey models were higher than the expreimental values across the shear rate of 0−600 $s^{-1}$(Fig. 5-4). Notably, the shear stress predicted by power law was higher than those from Herschel-Bulkey model in the shear rate of 0−600 $s^{-1}$, but lower when the shear rate > 600 $s^{-1}$ (Fig. S11). The differentiation of the predicted shear stress between these models can be explained by the absence of yield stress ($\sigma_0$) in power law model (Develi Isikli et al., 2015).

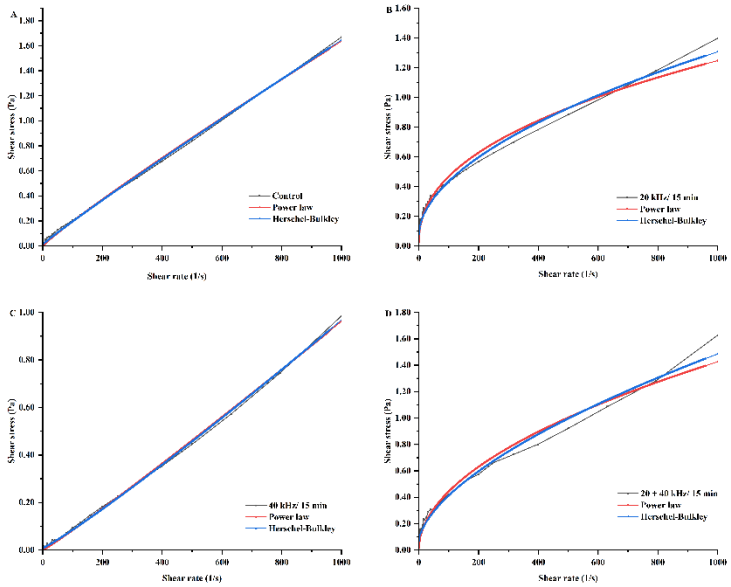



**Fig. 5-4** Rheogram of MFGs/MFGM isolated from control (A), 20 kHz/ 15 min (B), 40 kHz/ 15 min (C), and 20 + 40 kHz/ 15 min (D) treated bovine milk showing the fitting by power law and Herschel-Bulkley models.

### 5.3.4. Physical stability

Fig. 5-5 illustrates the transmission profiles of MFGs/MFGM as a function of time and space during an accelerated emulsion stability test. The red profile at the bottom of the image indicates the initial recorded profile, while the green profile layered on top shows the final transmitted profile. A noticeable shift from red to green profiles suggests the occurrence of creaming, characterized by the migration of the fat phase to the top of the cell, which implies phase separation in all MFGs/MFGM (Lin et al., 2023). In the control, the larger and more distinct separation between the initial and final profiles indicates a poorer cream stability compared to other MFGs/MFGM (Ahn et al., 2022). This observation is further confirmed by the visual evidence images in Fig. 5-6 A, where a more pronounced cream layer was observed on the top of control. Additionally, the final transmission profile of the control tended to be more horizontal, whereas ultrasonic treated MFGs/MFGM gradually inclined (Fig. 5-5 C-H). This inferred that ultrasonic treatments decelerated the phase separation and resulted in a thinner cream layer at the top of the cell (Dammak & Sobral, 2018).

By comparison, the transmission profile area of 40 kHz treated MFGs/MFGM (Fig. 5-5 E and 5-5 F) was smaller than the control and MFGs/MFGM treated by other ultrasonic intensities. This suggested that 40 kHz treatments facilitated phase stability during the centrifugal process. This effect might be associated with decreased volume density (%) of particles sizes between 1 and 10 μm in 40 kHz treated MFGMs/MFGM as found in previous research (Sun, Roos, & Miao, 2024c). The 40 kHz treatment likely causes the MFGs/MFGM to fragment into larger aggregates, decelerating their migration towards the top of the cell. Furthermore, the maximum transmission percentage in control was 60%, which decreased to 40 % following the 40 kHz treatments, reflecting lower droplet concentrations and improved cream stability. The duration of ultrasonic treatments did not significantly affect the transmission profile for 20 kHz and 40 kHz treatments, highlighting the impact of treatment intensity rather than duration.

Except for the overall transmission profile, the emulsion stability was quantitatively analysed and expressed as instability index. The instability index is the slope of the integrated transmission time plots and is a dimensionless number between 0 and 1. A value 0 signifies no change in NIR transmission whereas 1 indicates total phase separation (Yerramilli & Ghosh, 2017). A significant decrease of instability index for MFGs/MFGM treated at 40 kHz (0.099−0.143) by the end of the measurement period was observed compared to control (Fig. 5-6B). This result underscored the finding that 40 kHz treatments enhanced the emulsion stability under applied centrifugal forces, as evidenced by the reduced spacing between NIR transmission profile bands of 40 kHz treated MFGs/MFGM. This was in consist with the lower viscosity and Newtonian similar behavior of 40 kHz treatment presented in section 5.3.3. Ultrasonic treatment at lower frequency (20 kHz) showed higher acoustic energy than higher frequency ultrasound (40 kHz) (Sun, et al., 2024c). Combined with the stability result in this study, we can speculate that ultrasound with moderate acoustic energy may promote the system stability. Contrarily, stringent

shearing treatment induced by low frequency at 20 kHz, or 20 + 40 kHz may facilitate the formation of aggregates, which adversely affected the stability of the system.

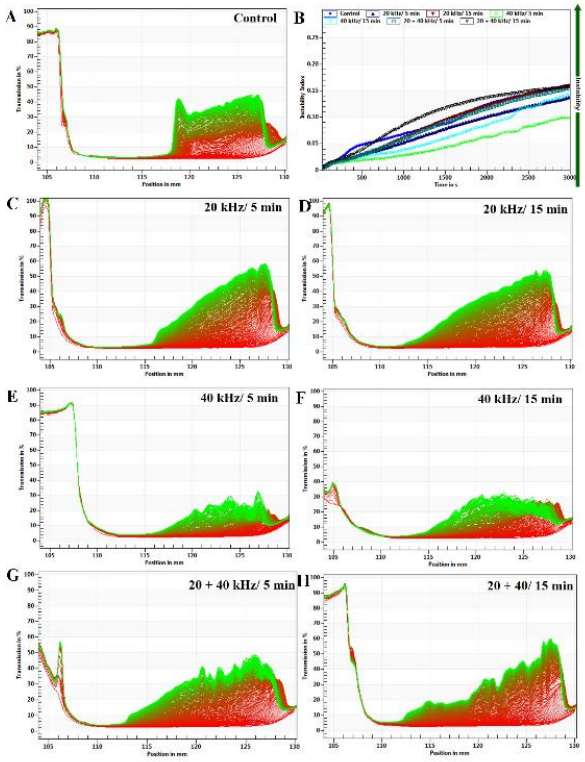



**Figure 5-5** Lumisizer phase separation near infrared (NIR) transmission profiles and instability index of MFGs/MFGM prepared from bovine raw milk treated by different ultrasonic intensities: A, control; B, instability index; C-D, 20 kHz treated for 5 min and 15 min; E-F, 40 kHz treated for 5 min and 15 min; G-H, Combined treatment using 20 kHz and 40 kHz for 5 min and 15 min.

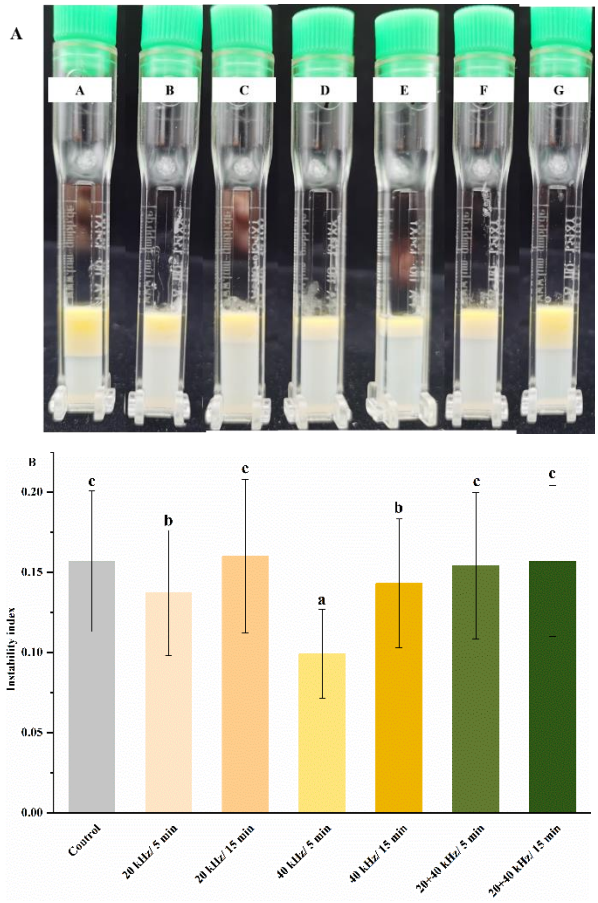



**Figure 5-6** (A) The visual cream layer of MFGs/MFGM after centrifugation by Lumisizer: A, control; B-C, 20 kHz treated for 5 min and 15 min; D-E, 40 kHz treated for 5min and 15 min; F-G Combined treatment using 20 kHz and 40 kHz for 5 min and 15 min. (B) Instability indexes of all the MFGs/MFGM at the end of centrifugation (3000 s).

From the start of analysis until 700 s, the control exhibited the highest instability index, suggesting the greatest degree of phase separation during this initial period. However, from 700 s onward to the end of the analysis period at 3000 s, concurrent treatment at 20 kHz and 40 kHz for 15 min displayed a consistently higher instability index than other treatments. Meanwhile, at the end of analyzing period (3000 s), the instability index for the control equalized to levels similar to those observed in the MFGs/MFGM subjected to dual-frequency treatment at 20 kHz and 40 kHz for 5 min (0.154), 15 min (0.157), and 20 kHz independently for 5 min (0.154) (Fig. 5-6 B). This data suggests that ultrasonic treatments, with the exception of 20 + 40 kHz/ 15 min treatment, generally enhanced the stability of MFGs/MFGM to varying extents

compared to control given their wider transmission profiles and higher instability indexes. This observation was in agreement with the FTIR results in section 5.3.1 which highlighted the poor repeatability of the sample distribution for the 20 + 40 kHz/ 15 min treatment. It can be inferred that phase separation may contribute to variations in sampling, thereby influencing the precision of the analyzed FTIR results.

### 5.3.5. Microstructure

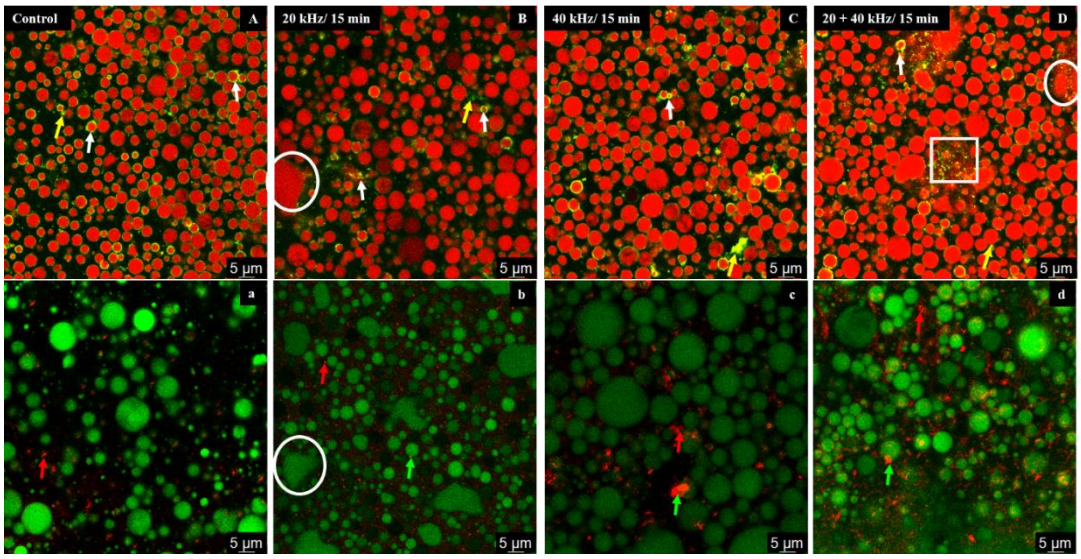



**Fig. 5-7.** Confocal laser scanning microscopy images of dual-stained MFGs/MFGM ingredients obtained from ultrasound-treated bovine raw milk at different ultrasonic intensities. A-D: control, 20 kHz/ 15 min, 40 kHz/ 15 min, and 20 + 40 kHz/ 15 min. Staining agents Nile Red and wheat germ agglutinin (WGA) were used to color neutral lipids (red) and membrane proteins (amber). White and yellow arrows highlight the membrane proteins present on the surface of MFGs/MFGM and within the whey phase. a-d: control, 20 kHz/ 15 min, 40 kHz/ 15 min, and 20 + 40 kHz/ 15 min. Staining of neutral lipids (green) and non-membrane proteins (red) was performed with Nile Red and fast green FCF. Green and red arrows indicate the non-membrane proteins on MFGs/MFGM surfaces and in the whey phase. The white circle highlights the flocculation of MFGs/MFGM fragments, and the white square marks the aggregated and unattached membrane proteins.

The ultrasound-induced structural changes in MFGs/MFGM are evident in Fig. 5-7. Most MFGs maintain an intact spherical shape after ultrasonic treatments at different intensities, as seen by the stained triglyceride in green (Fig. 5-7 A-D) or red (Fig. 5-7 a-d) in the core of MFGs. However, 20 kHz independently or combined with

40 kHz ultra-sonicated for 15 min caused the formation of irregular spheroids (Fig. 5-7 B, 5-7 D, and 5-7 b). This observation may be associated with the disintegration of fat globules induced by the acoustic stress, leading to the compromised MFGs integrity and release of triglycerides. More heterogeneous sizes of MFGs were observed in ultrasonic treated MFGs/MFGM than that of control, especially noticeable in MFGs/MFGM treated by combination of 20 kHz and 40 kHz for 15 min (Fig. 5-7 D and 5-7 d). This further confirms our previous study indicating a the multimodal distribution of particle sizes (Sun, Roos, & Miao, 2024c). Lee and Sherbon (2002) reported similar findings, noting increased surface area of MFGs and more pronounced non-uniformity in the MFGM structure in homogenized whole milk. MFG was wrapped by the tri-layer structure which consisted of phospholipids and membrane proteins. Prior to ultrasonic treatment, most of the membrane proteins are evenly distributed around the fat globules (Fig. 5-7A). However, these proteins were predominantly found in the whey phase after ultrasonic treatment, especially in samples processed at 20 kHz and 40 kHz for 15 min, with apparent flocculation of MFGM protein clusters evident in the while square. On the contrary, a significant amount of non-membrane proteins attached to the surface of ultrasonically treated fat globules, particularly in the MFGs/MFGM materials exposed to 20 kHz and 40 kHz concurrently ultra-sonicated for 15 min whereas most of them randomly distributed in the whey phase in control. This may be due to the increase of denatured non-membrane proteins, adhering to the surface of MFGs. The extent of protein-wrapped MFGs, estimated by the surface fraction model ($\Phi_m$) showed that MFGs/MFGM treated by 20 + 40 kHz/ 15 min exhibited a higher $\Phi_m$ value than other MFGs/MFGM (Sun, Roos, & Miao, 2024c). This observation may be linked to the increased $\zeta$ – potential due to the disruption of MFGs and subsequent membrane reorganization, exposing more negatively charged surface (Sun, Roos, & Miao, 2022).

### 5.3.6. Hierarchical cluster analysis

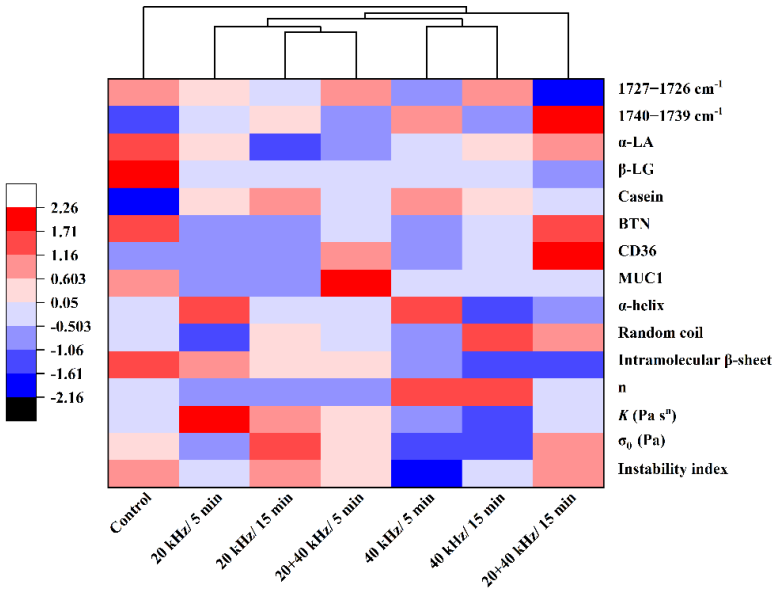



**Figure 5-8.** Hierarchical cluster analysis of MFGs/MFGM ingredients obtained from ultrasound-treated bovine raw milk. The color scale differentiates values as high (red) to low (blue).

The HCA results, illustrated in Fig. 5-8, reveal significant insights into the impact of ultrasonic treatments on the structural and compositional changes, rheological properties and instability indexes of MFGs/MFGM. The dendrogram generated by the HCA distinctly identified two main clusters: one encompassing the control sample and another grouping together the MFGs/MFGM under different ultrasonic intensities. Subsequently, 20 + 40 kHz/ 15 min treatment induced a notably differentiated impact on the analysed functionalities of MFGs/MFGM compared to other ultrasonic treatments. Additionally, the 40 kHz treatments formed a separated cluster, distinct from the 20 kHz and 20 + 40 kHz/ 5 min treatments. The latter group was further divided into two sub-clusters: one consisting solely of 20 kHz/ 5 min MFGs/MFGM, and another comprising MFGs/MFGM treated at both 20 kHz/ 15 min and 20 + 40 kHz/ 5 min.

The heat map associated with the HCA results clearly indicated that the ultrasonic treatments applied in this study significantly influenced the structure, composition, rheological properties, and emulsion stability of the MFGs/MFGM. Among all

treatments, the 20 + 40 kHz/15 min treatment stood out as having a more pronounced effect compared to the others.

## 5.4. Conclusion

Milk fat globules/membrane (MFGs/MFGM) materials derived from bovine raw milk treated by varying ultrasonic intensities, 20 kHz, 40 kHz, or a combination of 20 kHz and 40 kHz for duration of 5 min and 10 min, exhibited different physicochemical properties, rheological behaviour and emulsion stability compared to control MFGs/MFGM.

20 kHz and 40 kHz simultaneous processing for 15 min significantly influenced the ester groups of lipids and the interactions of hydrogen-bonded carbonyl groups in esters. The PCA result of Amide I grouped the 15 min with controls, and the 5 min ultra-sonicated MFGs/MFGM into another group. Nevertheless, qualitative analysis of the protein secondary structures within Amide I revealed inconsistent results; notably, the 15 min treatments induced more significant changes in the intramolecular β-sheet, random coil, and α-helix structure compared to 5 min treatment. This discrepancy underscore the need for the further research to elucidate the underlying causes of these contradictory outcomes.

Ultrasonic treatment promoted the transfer of membrane proteins into the rinsing phase and facilitated the adsorption of non-membrane proteins on the surfaces of fat globules. Moreover, all the MFGs/MFGM exhibited shear-thinning behaviour, except for the 40 kHz treated MFGs/MFGM, which displayed Newtonian behaviour at the higher shear rate, as indicated by flow behaviour indexes (n), of 1 or close to 1, regressed from the Herschel-Bulkley model. Physical stability of MFGs/MFGM emulsions was generally enhanced by ultrasonic treatment with the exception of 20 + 40 kHz/ 15 min treatment, which led to aggregated membrane proteins, as observed in CLSM images. This differentiation highlights the potential of specific ultrasonic treatment parameters to modify dairy product.

## CRediT authorship contribution statement

Yanjun Sun: Conceptualization, Data curation, Forma analysis, Investigation, Writing – original draft. Yrjö H. Roos: Writing – review & editing, Supervision. Song Miao: Funding acquisition, Project administration, Conceptualization, Supervision, Writing – review & editing.

## Declaration of competing interest

The authors declare that they have no known competing financial interests or personal relationships that could have appeared to influence the work reported in this paper.

## Acknowledgements

The project was supported by 'Teagasc-The Irish Agriculture and Food Development Authority (MDDT1392)' and 'The China Scholarship Council (No.202008410212)'.

## References

Ahn, N., Park, J. H., Chai, C., & Imm, J. Y. (2022). The interaction of milk sphingomyelin and proteins on stability and microstructure of dairy emulsions. *Journal of Dairy Science, 105*(5), 3832-3845.

Ayyash, M., Abdalla, A., Abu-Jdayil, B., Huppertz, T., Bhaskaracharya, R., Al-Mardeai, S., et al. (2022). Rheological properties of fermented milk from heated and high pressure-treated camel milk and bovine milk. *Lwt, 156*.

Banghart, L. R., Chamberlain, C. W., Velarde, J., Korobko, I. V., Ogg, S. L., Jack, L. J., et al. (1998). Butyrophilin is expressed in mammary epithelial cells from a single-sized messenger RNA as a type I membrane glycoprotein. *Journal of Biological Chemistry, 273*(7), 4171-4179.

Berton-Carabin, C. C., Sagis, L., & Schroën, K. (2018). Formation, structure, and functionality of interfacial layers in food emulsions. *Annual review of food science and technology, 9*, 551-587.

Bienvenue, A., Jiménez-Flores, R., & Singh, H. (2003). Rheological Properties of Concentrated Skim Milk: Importance of Soluble Minerals in the Changes in Viscosity During Storage. *Journal of Dairy Science, 86*(12), 3813-3821.

Dammak, I., & Sobral, P. J. d. A. (2018). Effect of different biopolymers on the stability of hesperidin-encapsulating O/W emulsions. *Journal of Food Engineering, 237*, 33-43.

Develi Isikli, N., Donmez, M. N., Kozan, N., & Karababa, E. (2015). Rheological properties of salep powder-milk mixture. *Journal of Food Science and Technology, 52*(10), 6556-6564.

Dufour, E., & Riaublanc, A. (1997). Potentiality of spectroscopic methods for the characterisation of dairy products. I. Front-face fluorescence study of raw, heated and homogenised milks. *Le Lait, 77*(6), 657-670.

Garczewska-Murzyn, A., Kiełczewska, K., & Smoczyński, M. (2022). The influence of buttermilk powder on the stability of emulsion and colloidal phases of homogenized milk. *European Food Research and Technology, 248*(10), 2629-2636.

Gebhardt, R., Takeda, N., Kulozik, U., & Doster, W. (2011). Structure and stabilizing interactions of casein micelles probed by high-pressure light scattering and FTIR. *Journal of Physical Chemistry B, 115*(10), 2349-2359.

Grelet, C., Fernandez Pierna, J. A., Dardenne, P., Baeten, V., & Dehareng, F. (2015). Standardization of milk mid-infrared spectra from a European dairy network. *Journal of Dairy Science, 98*(4), 2150-2160.

Grewal, M. K., Chandrapala, J., Donkor, O., Apostolopoulos, V., Stojanovska, L., & Vasiljevic, T. (2017). Fourier transform infrared spectroscopy analysis of physicochemical changes in UHT milk during accelerated storage. *International Dairy Journal, 66*, 99-107.

Hansen, S. F., Nielsen, S. D., Rasmusen, J. T., Larsen, L. B., & Wiking, L. (2020). Disulfide bond formation is not crucial for the heat-induced interaction between beta-lactoglobulin and milk fat globule membrane proteins. *Journal of Dairy Science, 103*(7), 5874-5881.

Jiang, B., Xia, Y., Zhou, L., Liang, X., Chen, X., Chen, M., et al. (2022). Safety and Tolerance Assessment of Milk Fat Globule Membrane- enriched Infant Formulas in Healthy Term Chinese Infants: A Randomised Multicenter Controlled Trial. *BMC pediatrics, 22*(1), 465.

Jukkola, A., Partanen, R., Rojas, O. J., & Heino, A. (2018). Effect of heat treatment and pH on the efficiency of micro-diafiltration for the separation of native fat globules from cream in butter production. *Journal of Membrane Science, 548*, 99-107.

Kher, A., Udabage, P., McKinnon, I., McNaughton, D., & Augustin, M. A. (2007). FTIR investigation of spray-dried milk protein concentrate powders. *Vibrational Spectroscopy, 44*(2), 375-381.

Kieferle, I., Hiller, K., Kulozik, U., & Germann, N. (2019). Rheological properties of fresh and reconstituted milk protein concentrates under standard and processing conditions. *Journal of Colloid and Interface Science, 537*, 458-464.

Kristensen, D., Jensen, P. Y., Madsen, F., & Birdi, K. S. (1997). Rheology and Surface Tension of Selected Processed Dairy Fluids: Influence of Temperature. *Journal of Dairy Science, 80*(10), 2282-2290.

Lee, S. J., & Sherbon, J. W. (2002). Chemical changes in bovine milk fat globule membrane caused by heat treatment and homogenization of whole milk. *Journal of Dairy Research, 69*(4), 555-567.

Lin, Y., Du, H., Roos, Y., & Miao, S. (2023). Transglutaminase crosslinked fish gelatins for emulsion stabilization: From conventional to Pickering emulsions. *Food Hydrocolloids, 144*.

Liu, Y., Boeren, S., Zhang, L., Zhou, P., & Hettinga, K. (2021). Ultrasonication retains more milk fat globule membrane proteins compared to equivalent shear-homogenization. *Innovative Food Science & Emerging Technologies, 70*, 102703.

Lu, N., Wang, J., Chen, Z., Zhang, X., Chen, C., & Wang, S. (2021). The effect of adding phospholipids before homogenization on the properties of milk fat globules. *Lwt, 146*, 111659.

Mohamed, H. J. J., Lee, E. K. H., Woo, K. C. K., Sarvananthan, R., Lee, Y. Y., & Mohd Hussin, Z. A. (2022). Brain-immune-gut benefits with early life supplementation of milk fat globule membrane. *JGH Open, 6*(7), 454-461.

Pan, Y., Liu, L., Tian, S., Li, X., Hussain, M., Li, C., et al. (2022). Comparative analysis of interfacial composition and structure of fat globules in human milk and infant formulas. *Food Hydrocolloids, 124*, 107290.

Patist, A., & Bates, D. (2008). Ultrasonic innovations in the food industry: From the laboratory to commercial production. *Innovative Food Science & Emerging Technologies, 9*(2), 147-154.

Peterson, J. A., Scallan, C. D., Ceriani, R. L., & Hamosh, M. (2001). Structural and functional aspects of three major glycoproteins of the human milk fat globule membrane. *Bioactive components of human milk*, 179-187.

Randhahn, H. (1973). Flow properties of milk and milk concentrates. *Milchwissenschaft, 28*(10), 620–628.

Ren, Q., Guo, F., Teng, F., & Ma, Y. (2021). A novel approach for the reconstitution of bovine milk fat globules with different-melting-temperature triacylglycerol cores. *Food Chemistry, 345*, 128563.

Spitsberg, V. L., Matitashvili, E., & Gorewit, R. C. (1995). Association and coexpression of fatty-acid-binding protein and glycoprotein CD36 in the bovine mammary gland. *European journal of biochemistry, 230*(3), 872-878.

Sun, Y., Roos, Y. H., & Miao, S. (2022b). Changes in Milk Fat Globules and Membrane Proteins Prepared from pH-Adjusted Bovine Raw Milk. *Foods, 11*(24), 4107.

Sun, Y., Roos, Y. H., & Miao, S. (2024c). Comparative study of interfacial properties and thermal behaviour of milk fat globules and membrane prepared from ultrasonicated bovine milk. *Ultrasonics Sonochemistry, 102*, 106755.

Sun, Y., Yu, X., Hussain, M., Li, X., Liu, L., Liu, Y., et al. (2022a). Influence of milk fat globule membrane and milk protein concentrate treated by ultrasound on the structural and emulsifying stability of mimicking human fat emulsions. *Ultrasonics Sonochemistry, 82*, 105881.

Velez-Ruiz, J., & Barbosa-Canovas, G. (1997). Effects of concentration and temperature on the rheology of concentrated milk. *Transactions of the ASAE, 40*(4), 1113-1118.

Vongsvivut, J., Heraud, P., Zhang, W., Kralovec, J. A., McNaughton, D., & Barrow, C. J. (2012). Quantitative determination of fatty acid compositions in micro-encapsulated fish-oil supplements using Fourier transform infrared (FTIR) spectroscopy. *Food Chemistry, 135*(2), 603-609.

Wang, X., Wei, W., Wu, R., Zhu, X., Ren, F., Liu, L., et al. (2022). Scientific Consensus on Milk Fat Globule Membrane and Its Ingredients. *Journal of Chinese Institute of Food Science and Technology*, 1-6.

Wiking, L., Gregersen, S. B., Hansen, S. F., & Hammershøj, M. (2022). Heat-induced changes in milk fat and milk fat globules and its derived effects on acid dairy gelation – A review. *International Dairy Journal, 127*, 105213.

Yerramilli, M., & Ghosh, S. (2017). Long-term stability of sodium caseinate-stabilized nanoemulsions. *Journal of Food Science and Technology, 54*(1), 82-92.

Zhao, L., Du, M., & Mao, X. (2019). Change in interfacial properties of milk fat globules by homogenization and thermal processing plays a key role in their in vitro gastrointestinal digestion. *Food Hydrocolloids, 96*, 331-342.

Zhou, Q., Sun, S.-Q., Yu, L., Xu, C.-H., Noda, I., & Zhang, X.-R. (2006a). Sequential changes of main components in different kinds of milk powders using two-dimensional infrared correlation analysis. *Journal of Molecular Structure, 799*(1-3), 77-84.

Zhou, Q., Sun, S. Q., Yu, L., Xu, C.-H., Noda, I., & Zhang, X.-R. (2006b). Sequential changes of main components in different kinds of milk powders using two-dimensional infrared correlation analysis. *Journal of Molecular Structure, 799*(1), 77-84.

## Supplementary materials

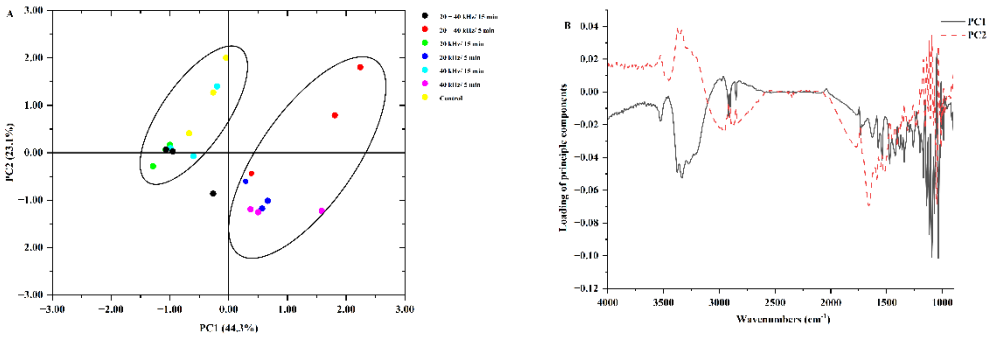
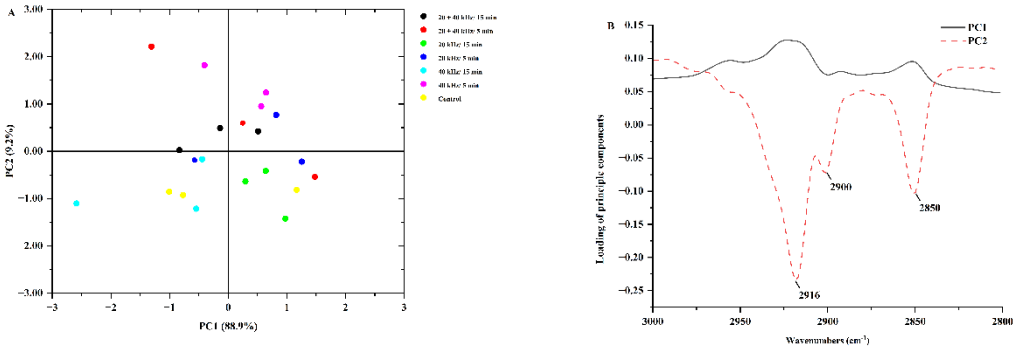



**Fig. S1.** PCA scores (A) and loading plots (B) of FTIR spectra in the region of 4000–900 $cm^{-1}$ of MFGs/MFGM prepared from bovine raw milk treated by different ultrasonic intensities.




**ig. S2.** PCA scores (A) and loading plots (B) of FTIR spectra in the region of 3000–2800 $cm^{-1}$ of MFGs/MFGM prepared from bovine raw milk treated by different ultrasonic intensities.

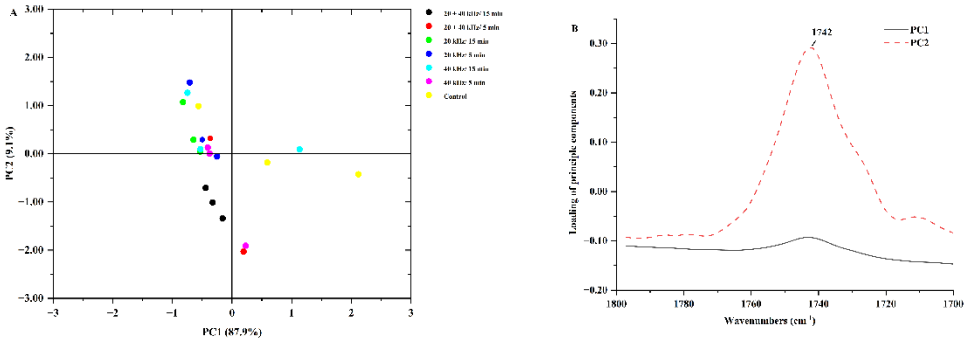
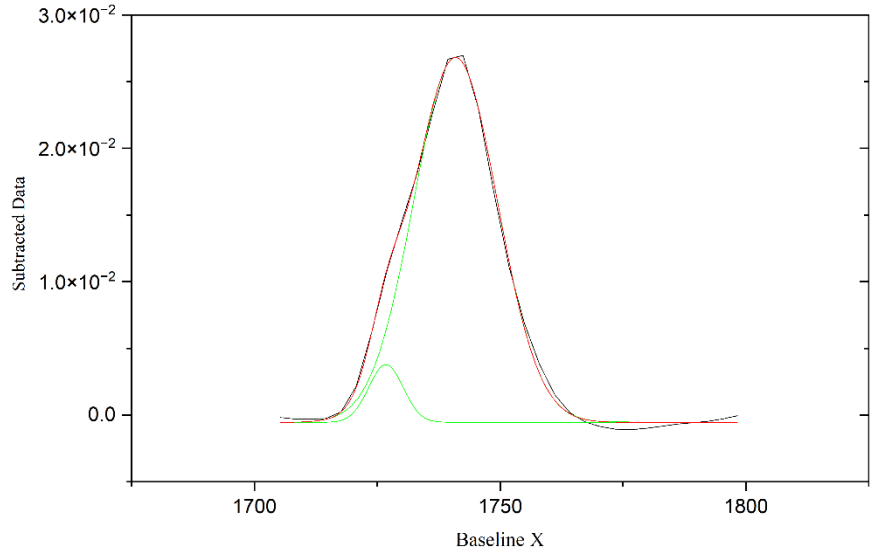



**Fig. S3.** PCA scores (A) and loading plots (B) of FTIR spectra in the region of 1800–1700 $cm^{-1}$ of MFGs/MFGM prepared from bovine raw milk treated by different ultrasonic intensities.

**A** **Peak Analysis (Control)**

Data Set:[Book3]Sheet1!B Date:14/05/2024
BaseLine:Line
Chi^2=1.58644E-07 Adj. R-Square=9.98153E-01 # of Data Points=31
SS=3.80746E-06 Degrees of Freedom=24




Fitting Results

| Peak Index | Peak Type | Area Intg | FWHM | Max Height | Center Grvty | Area IntgP |
|---|---|---|---|---|---|---|
| 1 | Gaussian | 0.03812 | 8.25791 | 0.00434 | 1726.77883 | 6.12741 |
| 2 | Gaussian | 0.58397 | 20.04946 | 0.02736 | 1740.9254 | 93.87259 |

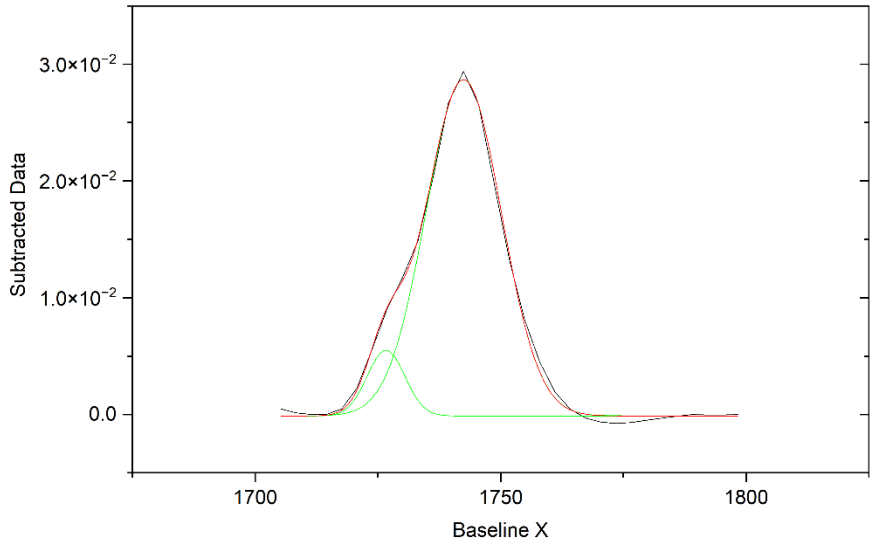
**B** **Peak Analysis (20 kHz/ 5 min)**

Data Set:[Book2]Sheet1!B Date:14/05/2024

BaseLine:Line

Chi^2=2.05711E-07 Adj. R-Square=9.97663E-01 # of Data Points=31

SS=4.93705E-06 Degrees of Freedom=24

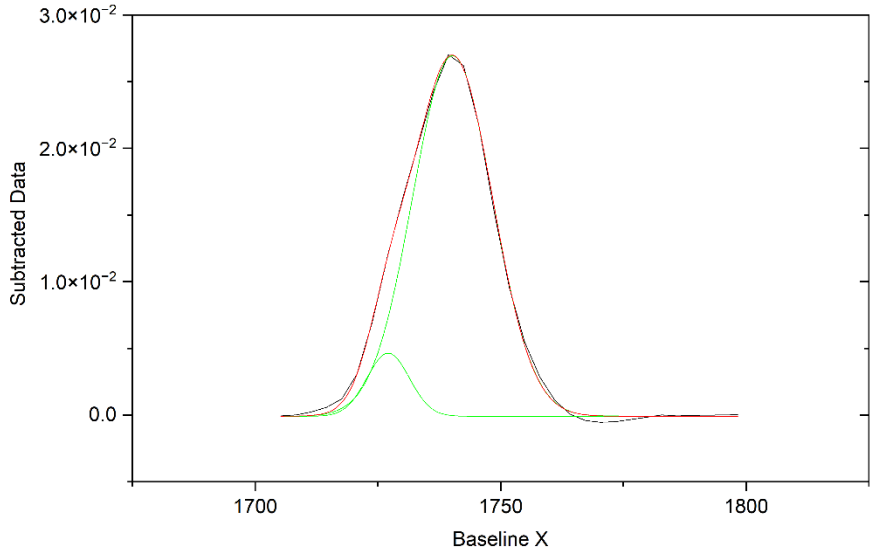



Fitting Results

| Peak Index | Peak Type | Area Intg | FWHM | Max Height | Center Grvty | Area IntgP |
|---|---|---|---|---|---|---|
| 1 | Gaussian | 0.05407 | 9.02848 | 0.00563 | 1726.67973 | 8.88 |
| 2 | Gaussian | 0.55481 | 18.08821 | 0.02881 | 1742.4747 | 91.12 |

**C** **Peak Analysis (20 kHz/ 15 min)**

Data Set:[Book5]Sheet1!B Date:14/05/2024
BaseLine:Line
Chi^2=7.14137E-08 Adj. R-Square=9.99152E-01 # of Data Points=31
SS=1.71393E-06 Degrees of Freedom=24

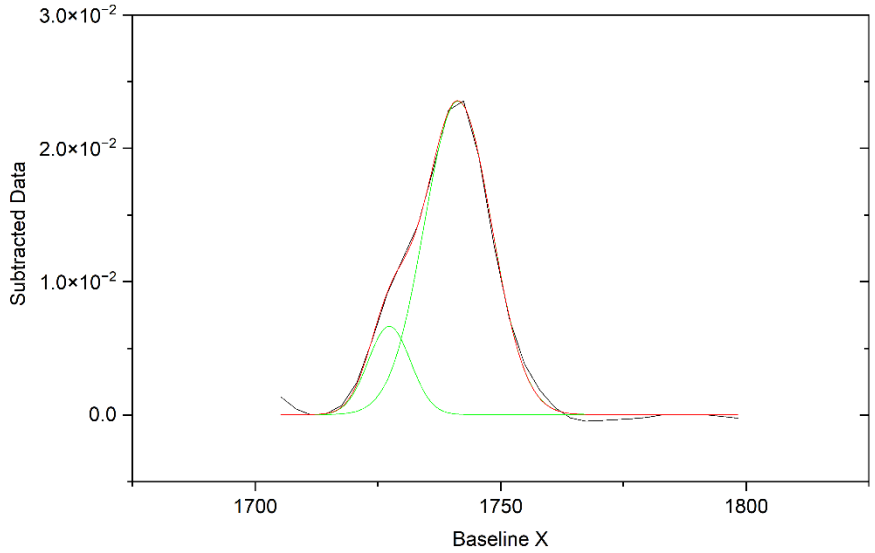



Fitting Results

| Peak Index | Peak Type | Area Intg | FWHM | Max Height | Center Grvty | Area IntgP |
|---|---|---|---|---|---|---|
| 1 | Gaussian | 0.55223 | 19.19323 | 0.02703 | 1740.2088 | 91.50617 |
| 2 | Gaussian | 0.05126 | 10.1868 | 0.00473 | 1727.10272 | 8.49383 |

**D** **Peak Analysis (40 kHz/ 5 min)**

Data Set:[Book6]Sheet1!B Date:14/05/2024
BaseLine:Line
Chi^2=1.72303E-07 Adj. R-Square=9.97002E-01 # of Data Points=31
SS=4.13528E-06 Degrees of Freedom=24

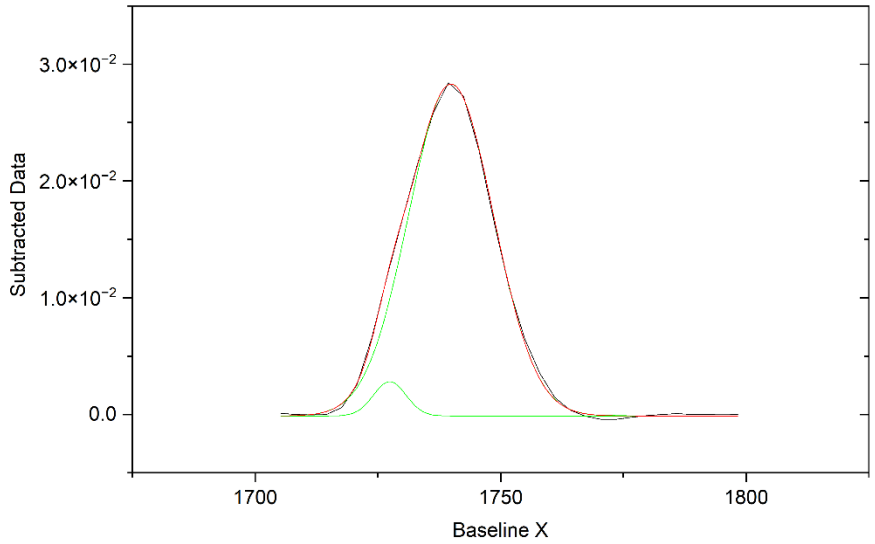



Fitting Results

| Peak Index | Peak Type | Area Intg | FWHM | Max Height | Center Grvty | Area IntgP |
|---|---|---|---|---|---|---|
| 1 | Gaussian | 0.07145 | 10.14304 | 0.00662 | 1727.3415 | 15.04425 |
| 2 | Gaussian | 0.40351 | 16.12391 | 0.02351 | 1741.31606 | 84.95575 |

**E** **Peak Analysis (40 kHz/ 15 min)**

Data Set:[Book7]Sheet1!B Date:14/05/2024
BaseLine:Line
Chi^2=5.28583E-08 Adj. R-Square=9.99434E-01 # of Data Points=31
SS=1.26860E-06 Degrees of Freedom=24

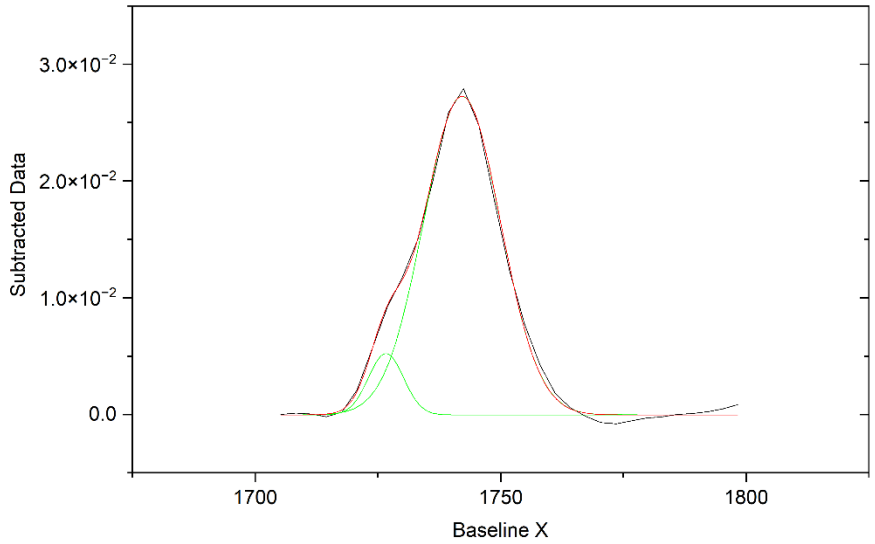



Fitting Results

| Peak Index | Peak Type | Area Intg | FWHM | Max Height | Center Grvty | Area IntgP |
|---|---|---|---|---|---|---|
| 1 | Gaussian | 0.02445 | 7.819 | 0.00294 | 1727.43453 | 3.82327 |
| 2 | Gaussian | 0.61495 | 20.31712 | 0.02844 | 1739.91138 | 96.17673 |

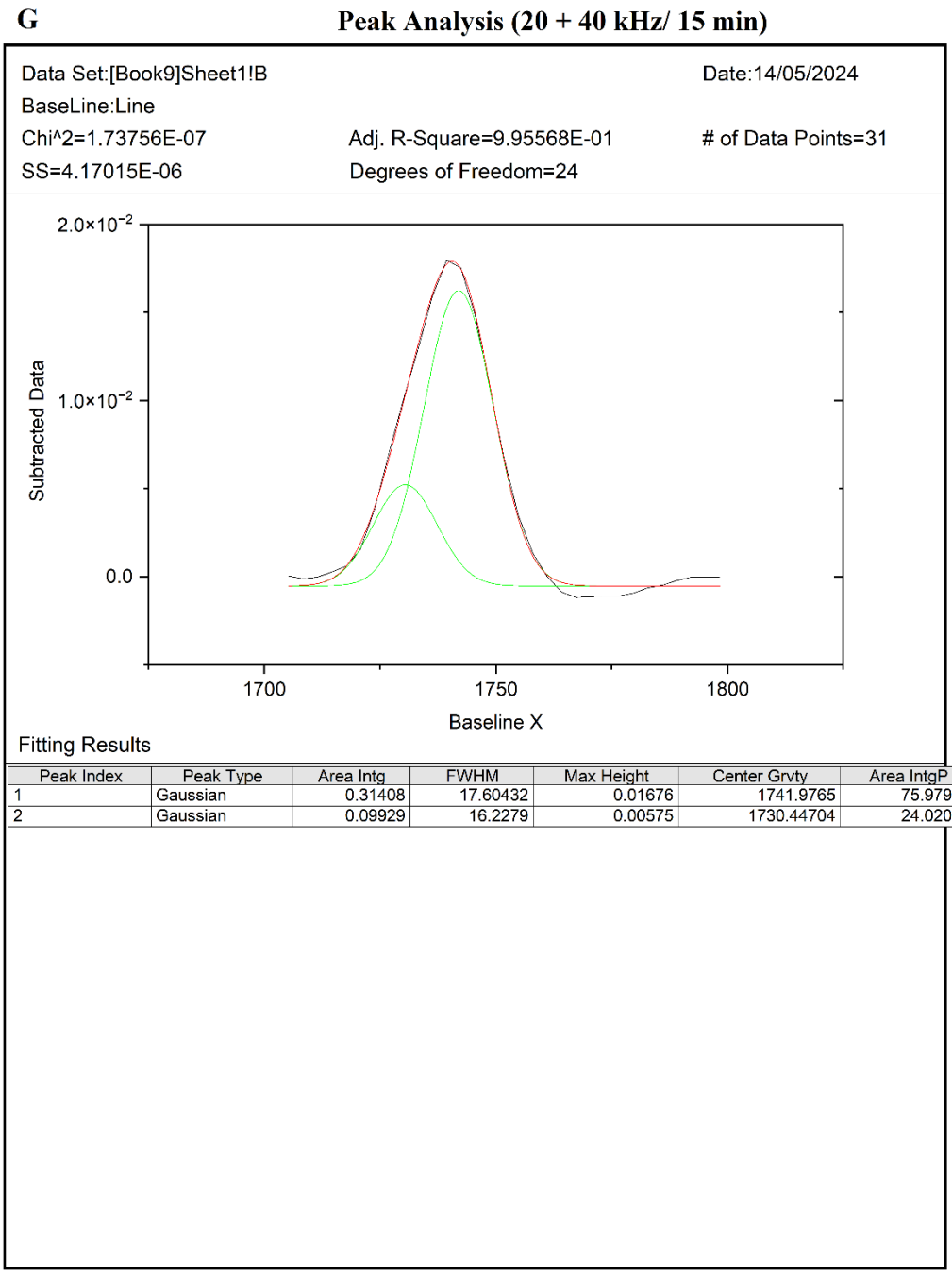
**F** **Peak Analysis (20 + 40 kHz/ 5 min)**

Data Set:[Book8]Sheet1!B Date:14/05/2024
BaseLine:Line
Chi^2=2.25353E-07 Adj. R-Square=9.97191E-01 # of Data Points=31
SS=5.40847E-06 Degrees of Freedom=24




Fitting Results

| Peak Index | Peak Type | Area Intg | FWHM | Max Height | Center Grvty | Area IntgP |
|---|---|---|---|---|---|---|
| 1 | Gaussian | 0.04709 | 8.42752 | 0.00525 | 1726.66858 | 8.07488 |
| 2 | Gaussian | 0.53608 | 18.45219 | 0.02729 | 1742.1529 | 91.92512 |




| Peak Index | Peak Type | Area Intg | FWHM | Max Height | Center Grvty | Area IntgP |
|---|---|---|---|---|---|---|
| 1 | Gaussian | 0.31408 | 17.60432 | 0.01676 | 1741.9765 | 75.97945 |
| 2 | Gaussian | 0.09929 | 16.2279 | 0.00575 | 1730.44704 | 24.02055 |

**Fig. S4.** Peak fitting of FTIR spectrum (Gaussian function) in the region of 1800–1700 $cm^{-1}$ of MFGs/MFGM prepared from bovine raw milk treated by different ultrasonic intensities. A, control; B, 20 kHz/ 5 min; C, 20 kHz/ 15 min; D, 40 kHz/ 5 min; E, 40 kHz/ 15 min; F, 20 + 40 kHz/ 5 min; G, 20 + 40 kHz/ 15 min

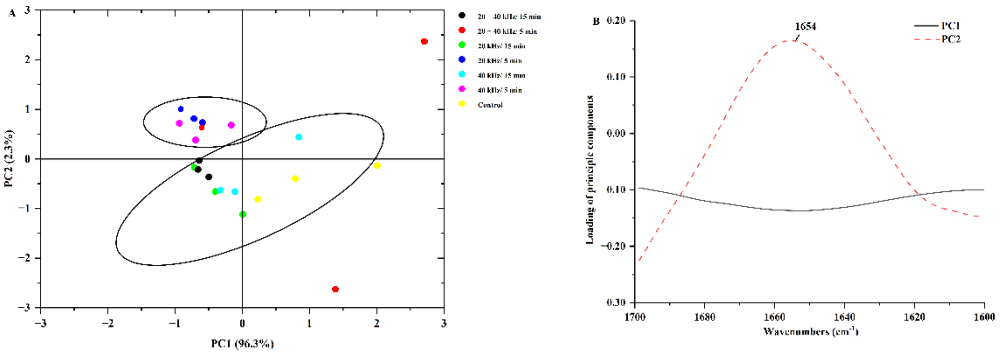



**Fig. S5.** PCA scores (A) and loading plots (B) of FTIR spectra in the region of 1700–1600 $cm^{-1}$ of MFGs/MFGM prepared from bovine raw milk treated by different ultrasonic intensities.

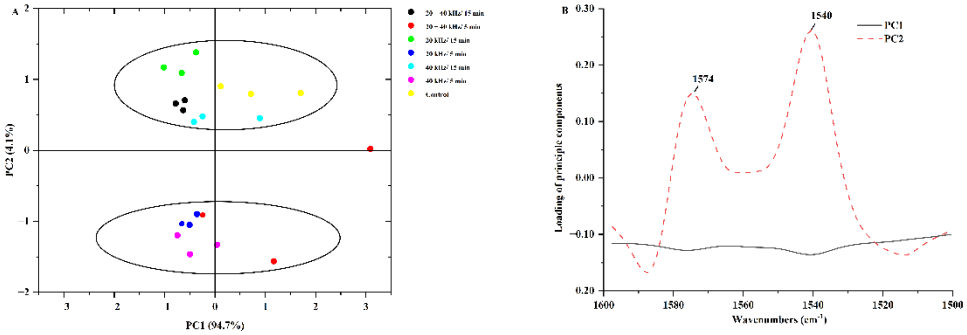
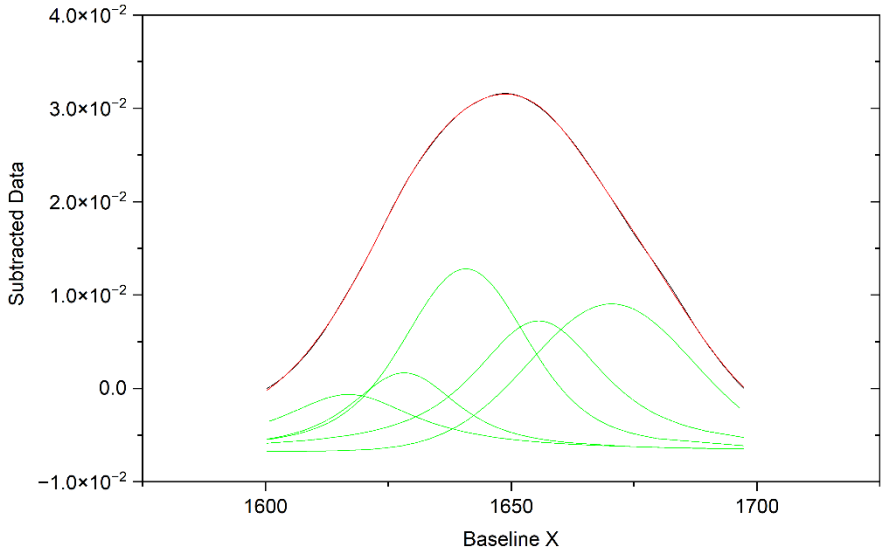



**Fig. S6.** PCA scores (A) and loading plots (B) of FTIR spectra in the region of 1600–1500 $cm^{-1}$ of MFGs/MFGM prepared from bovine raw milk treated by different ultrasonic intensities.

**A** **Peak Analysis (Control)**

Data Set:[originaldat1]Control!N"Subtracted_Data Y1" Date:14/05/2024
BaseLine:Line
Chi^2=1.02074E-08 Adj. R-Square=9.99911E-01 # of Data Points=69
SS=4.89954E-07 Degrees of Freedom=48

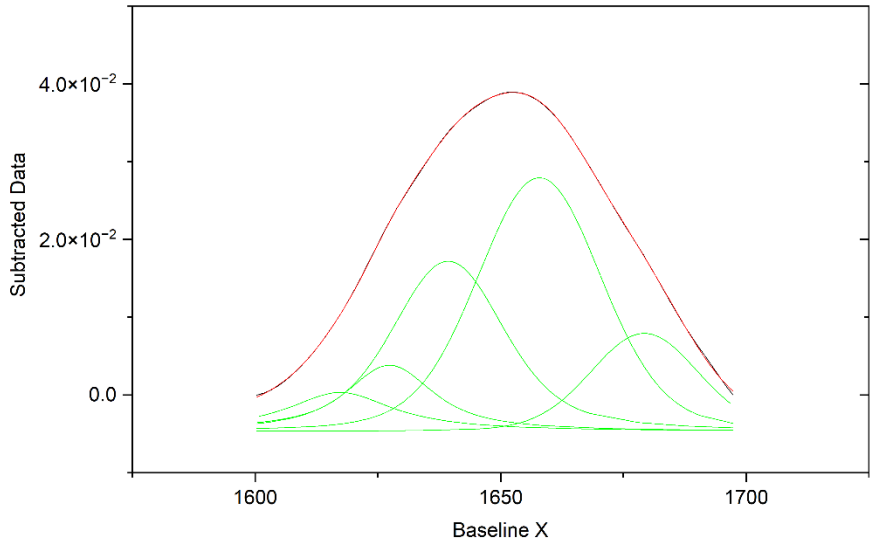



Fitting Results

| Peak Index | Peak Type | Area Intg | FWHM | Max Height | Center Grvty | Area IntgP |
|---|---|---|---|---|---|---|
| 1 | Voigt | 0.22101 | 34.03537 | 0.00608 | 1616.94317 | 9.44646 |
| 2 | Voigt | 0.26826 | 26.08863 | 0.00839 | 1628.26357 | 11.46635 |
| 3 | Voigt | 0.6868 | 30.2828 | 0.01953 | 1640.80731 | 29.35583 |
| 4 | Voigt | 0.53957 | 31.61498 | 0.01396 | 1655.61787 | 23.0629 |
| 5 | Voigt | 0.62392 | 39.22346 | 0.01578 | 1670.43421 | 26.66847 |

**B** **Peak Analysis (20 kHz/ 5 min)**

Data Set:[originaldat3]"20 kHz/5min"!R"Subtracted_Data Y2" Date:14/05/2024
BaseLine:Line
Chi^2=1.39765E-08 Adj. R-Square=9.99922E-01 # of Data Points=69
SS=6.70874E-07 Degrees of Freedom=48

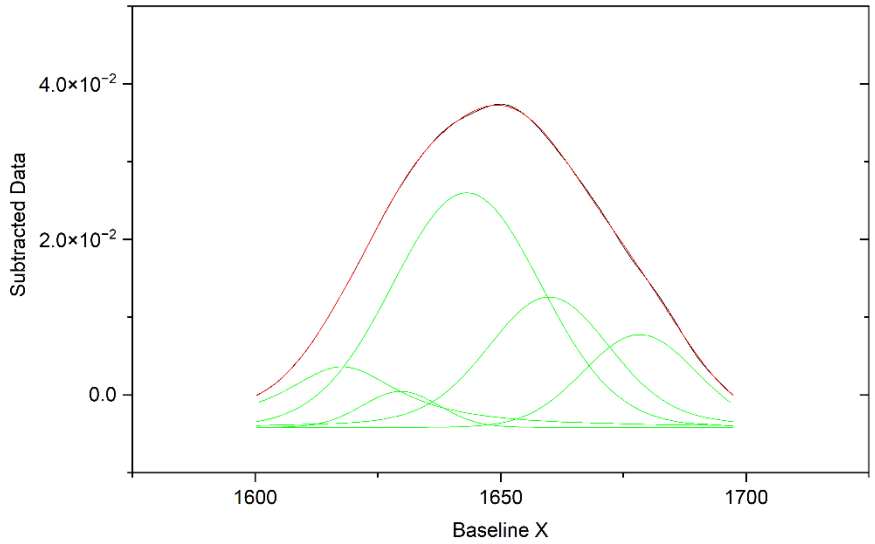



Fitting Results

| Peak Index | Peak Type | Area Intg | FWHM | Max Height | Center Grvty | Area IntgP |
|---|---|---|---|---|---|---|
| 1 | Voigt | 0.23056 | 21.24611 | 0.0085 | 1627.37872 | 9.29267 |
| 2 | Voigt | 0.68908 | 26.90331 | 0.02187 | 1639.34747 | 27.77304 |
| 3 | Voigt | 1.07193 | 29.79132 | 0.0326 | 1657.90507 | 43.2037 |
| 4 | Voigt | 0.33675 | 25.84974 | 0.0126 | 1679.26926 | 13.5726 |
| 5 | Voigt | 0.15279 | 26.25901 | 0.00501 | 1617.35359 | 6.15799 |

**C** **Peak Analysis (20 kHz/ 15 min)**

Data Set:[originaldat2]"20 kHz/15min"!N"Subtracted_Data Y1" Date:14/05/2024
BaseLine:Line
Chi^2=1.95366E-08 Adj. R-Square=9.99879E-01 # of Data Points=69
SS=9.37755E-07 Degrees of Freedom=48

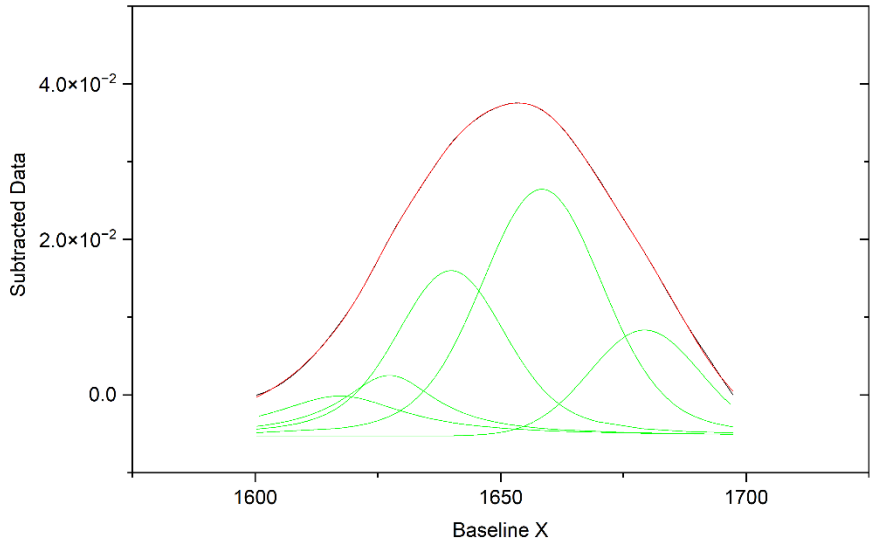



Fitting Results

| Peak Index | Peak Type | Area Intg | FWHM | Max Height | Center Grvty | Area IntgP |
|---|---|---|---|---|---|---|
| 1 | Voigt | 0.25195 | 28.54596 | 0.00778 | 1617.70191 | 10.6283 |
| 2 | Voigt | 0.09037 | 18.41672 | 0.00461 | 1629.66056 | 3.81227 |
| 3 | Voigt | 1.14995 | 35.72119 | 0.03014 | 1643.10984 | 48.50971 |
| 4 | Voigt | 0.55421 | 29.76161 | 0.01674 | 1659.8471 | 23.37882 |
| 5 | Voigt | 0.32408 | 26.85363 | 0.01191 | 1678.3242 | 13.6709 |

**D** **Peak Analysis (40 kHz/ 5 min)**

Data Set:[originaldat4]"40 kHz/5min"!N"Subtracted_Data Y1" Date:14/05/2024
BaseLine:Line
Chi^2=1.35106E-08 Adj. R-Square=9.99919E-01 # of Data Points=69
SS=6.48511E-07 Degrees of Freedom=48

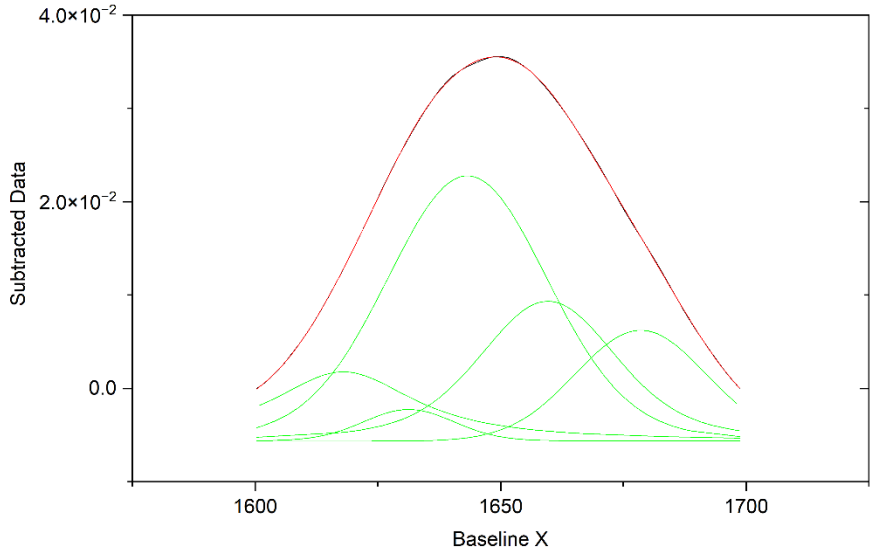



Fitting Results

| Peak Index | Peak Type | Area Intg | FWHM | Max Height | Center Grvty | Area IntgP |
|---|---|---|---|---|---|---|
| 1 | Voigt | 0.23466 | 23.57242 | 0.00777 | 1627.36011 | 9.498 |
| 2 | Voigt | 0.65392 | 26.63235 | 0.02124 | 1639.93921 | 26.46745 |
| 3 | Voigt | 1.03856 | 29.46077 | 0.0317 | 1658.41883 | 42.03563 |
| 4 | Voigt | 0.36219 | 26.46827 | 0.0136 | 1679.35358 | 14.65972 |
| 5 | Voigt | 0.18133 | 32.6299 | 0.00512 | 1617.19787 | 7.3392 |

**E** **Peak Analysis (40 kHz/ 15 min)**

Data Set:[originaldat5]"40 kHz/15min"!N"Subtracted_Data Y1" Date:14/05/2024
BaseLine:Line
Chi^2=5.55944E-09 Adj. R-Square=9.99962E-01 # of Data Points=70
SS=2.72412E-07 Degrees of Freedom=49

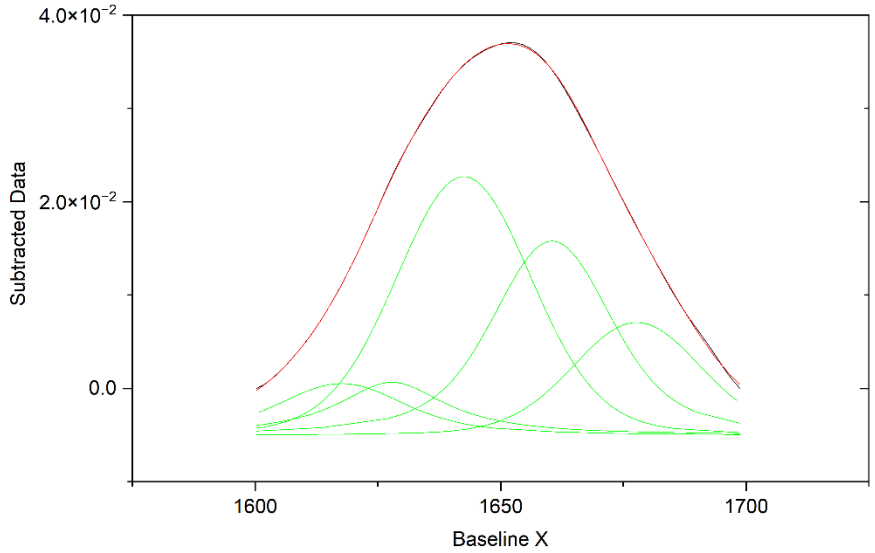



Fitting Results

| Peak Index | Peak Type | Area Intg | FWHM | Max Height | Center Grvty | Area IntgP |
|---|---|---|---|---|---|---|
| 1 | Voigt | 0.27853 | 35.19907 | 0.00742 | 1617.98827 | 11.26045 |
| 2 | Voigt | 0.08035 | 21.82122 | 0.00339 | 1631.32023 | 3.24861 |
| 3 | Voigt | 1.18325 | 38.68972 | 0.02842 | 1643.24085 | 47.83691 |
| 4 | Voigt | 0.56067 | 33.04972 | 0.01498 | 1659.64469 | 22.66725 |
| 5 | Voigt | 0.3707 | 31.34844 | 0.01187 | 1678.52746 | 14.98679 |

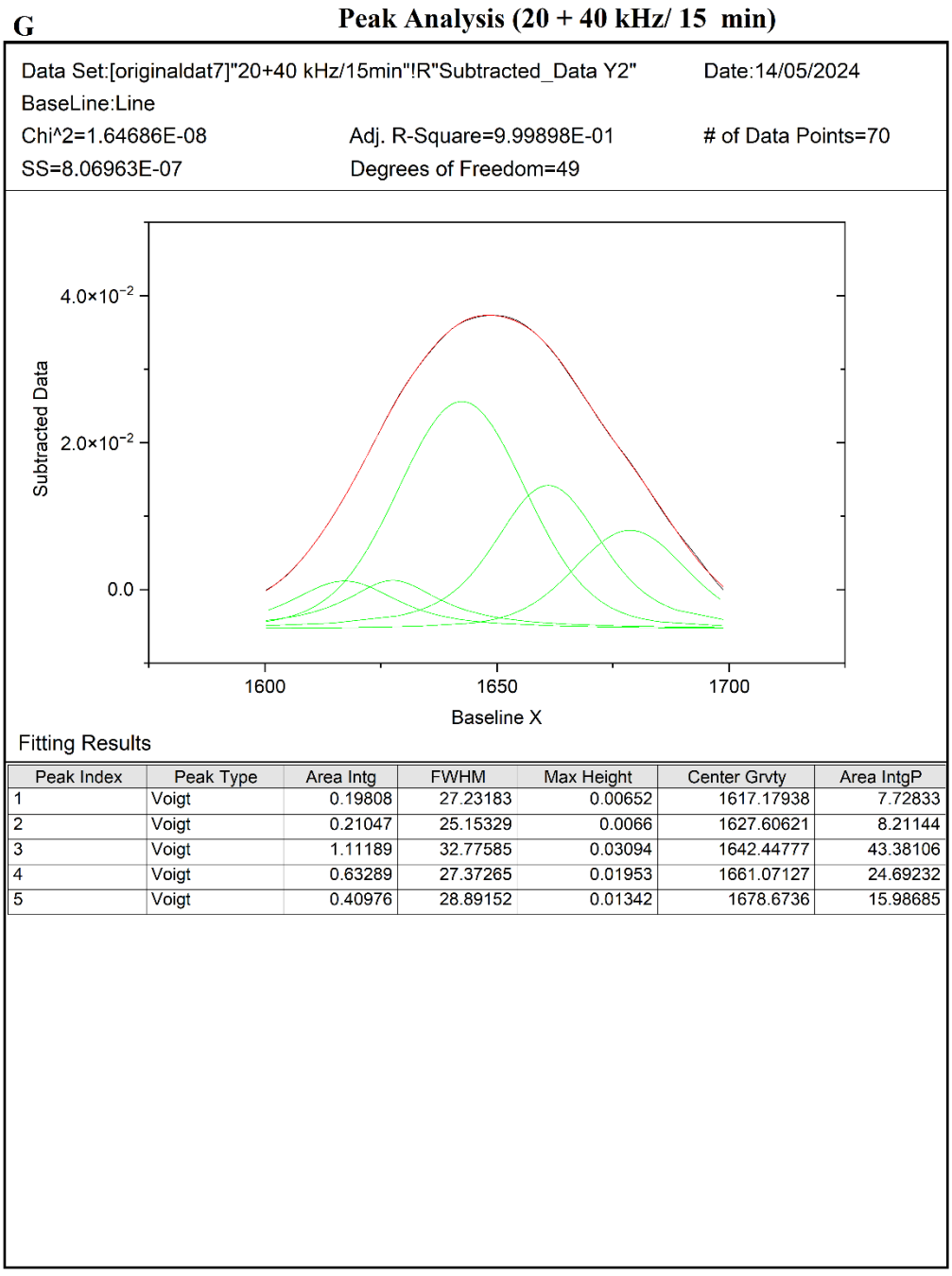
**F** **Peak Analysis (20 + 40 kHz/ 5 min)**

Data Set:[originaldat6]"20+40 kHz/5min"!N"Subtracted_Data Y1" Date:14/05/2024
BaseLine:Line
Chi^2=1.81964E-08 Adj. R-Square=9.99887E-01 # of Data Points=70
SS=8.91622E-07 Degrees of Freedom=49




Fitting Results

| Peak Index | Peak Type | Area Intg | FWHM | Max Height | Center Grvty | Area IntgP |
|---|---|---|---|---|---|---|
| 1 | Voigt | 0.18151 | 30.92847 | 0.00556 | 1617.6118 | 7.43057 |
| 2 | Voigt | 0.19197 | 26.95212 | 0.0057 | 1627.87777 | 7.85897 |
| 3 | Voigt | 0.98488 | 32.5412 | 0.02772 | 1642.50707 | 40.31923 |
| 4 | Voigt | 0.69655 | 28.71434 | 0.02082 | 1660.47678 | 28.51577 |
| 5 | Voigt | 0.38779 | 31.00838 | 0.0121 | 1677.71492 | 15.87545 |




Fitting Results

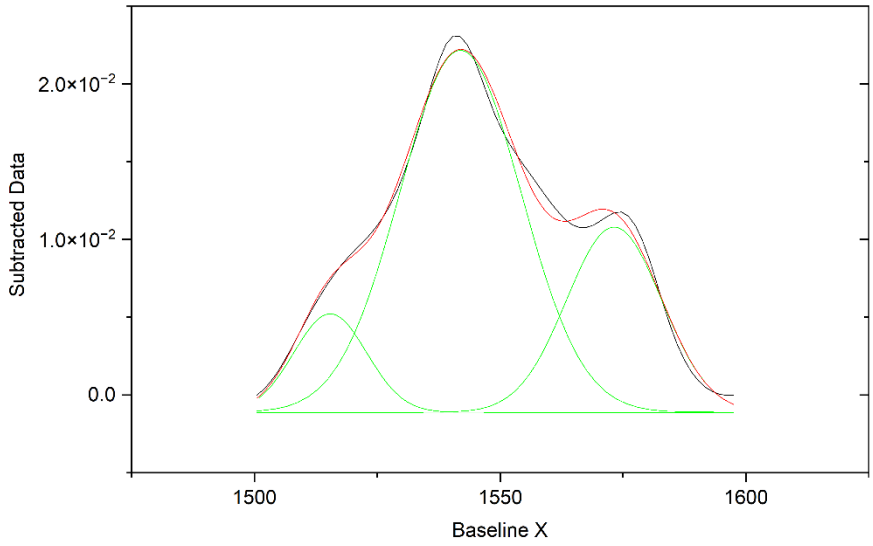
| Peak Index | Peak Type | Area Intg | FWHM | Max Height | Center Grvty | Area IntgP |
|---|---|---|---|---|---|---|
| 1 | Voigt | 0.19808 | 27.23183 | 0.00652 | 1617.17938 | 7.72833 |
| 2 | Voigt | 0.21047 | 25.15329 | 0.0066 | 1627.60621 | 8.21144 |
| 3 | Voigt | 1.11189 | 32.77585 | 0.03094 | 1642.44777 | 43.38106 |
| 4 | Voigt | 0.63289 | 27.37265 | 0.01953 | 1661.07127 | 24.69232 |
| 5 | Voigt | 0.40976 | 28.89152 | 0.01342 | 1678.6736 | 15.98685 |

**Fig. S7.** Peak fitting of FTIR spectrum (Voigt function) in the region of Amide I (1700–1600 $cm^{-1}$) of MFGs/MFGM prepared from bovine raw milk treated by different ultrasonic intensities. A, control; B, 20 kHz/ 5 min; C, 20 kHz/ 15 min; D, 40 kHz/ 5 min; E, 40 kHz/ 15 min; F, 20 + 40 kHz/ 5 min; G, 20 + 40 kHz/ 15 min.

**A**

## Peak Analysis (Control)

Data Set:[Book2]Sheet1!D  Date:14/05/2024
BaseLine:Line
Chi^2=3.50922E-07  Adj. R-Square=9.92154E-01  # of Data Points=69
SS=2.07044E-05  Degrees of Freedom=59




Fitting Results

| Peak Index | Peak Type | Area Intg | FWHM | Max Height | Center Grvty | Area IntgP |
|---|---|---|---|---|---|---|
| 1 | Gaussian | 0.11494 | 17.44518 | 0.00633 | 1515.44697 | 10.23968 |
| 2 | Gaussian | 0.72017 | 29.09368 | 0.02326 | 1541.9264 | 64.15559 |
| 3 | Gaussian | 0.28742 | 22.82697 | 0.0119 | 1573.19401 | 25.60473 |

**B**

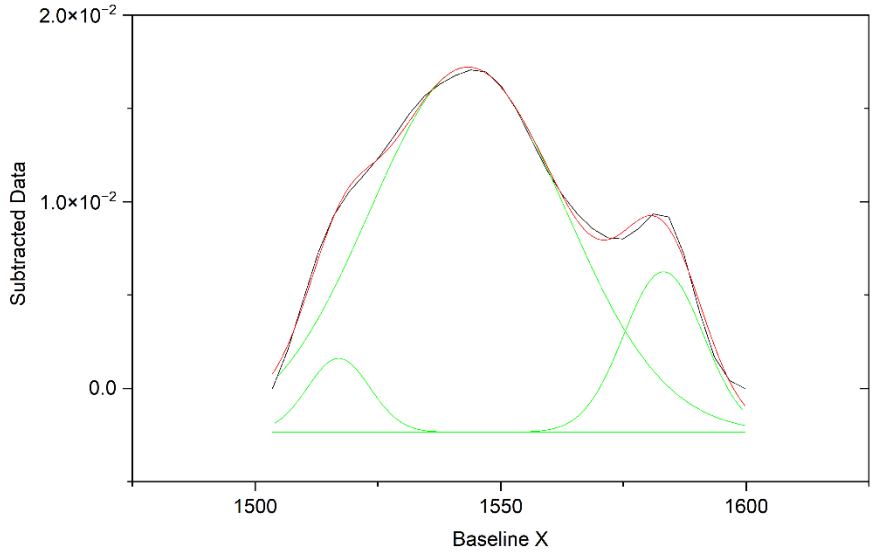
**Peak Analysis (20 kHz/ 5 min)**

Data Set:[Book3]Sheet1!B Date:14/05/2024

BaseLine:Line

Chi^2=1.81277E-07 Adj. R-Square=9.93371E-01 # of Data Points=32

SS=3.98809E-06 Degrees of Freedom=22

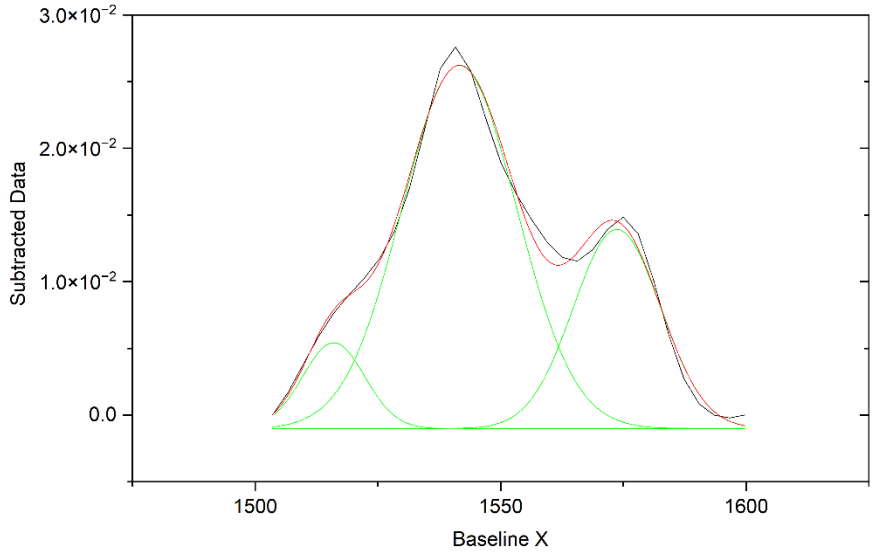



Fitting Results

| Peak Index | Peak Type | Area Intg | FWHM | Max Height | Center Grvty | Area IntgP |
|---|---|---|---|---|---|---|
| 1 | Gaussian | 0.06178 | 14.95006 | 0.00395 | 1517.03352 | 5.20568 |
| 2 | Gaussian | 0.95398 | 47.0372 | 0.01955 | 1543.35469 | 80.3783 |
| 3 | Gaussian | 0.1711 | 19.09718 | 0.00859 | 1583.17577 | 14.41601 |

**C** **Peak Analysis (20 kHz/ 15 min)**

Data Set:[Book4]Sheet1!B Date:14/05/2024
BaseLine:Line
Chi^2=8.73030E-07 Adj. R-Square=9.86509E-01 # of Data Points=32
SS=1.92067E-05 Degrees of Freedom=22

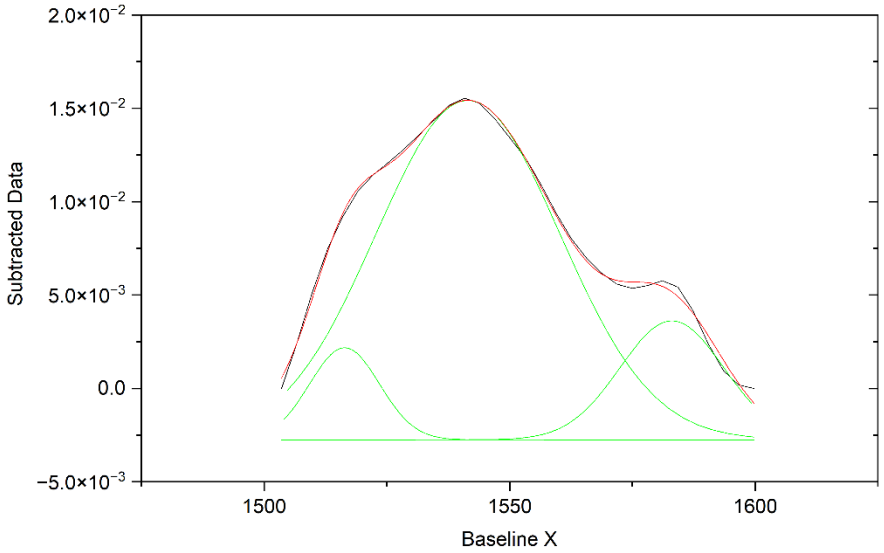



Fitting Results

| Peak Index | Peak Type | Area Intg | FWHM | Max Height | Center Grvty | Area IntgP |
|---|---|---|---|---|---|---|
| 1 | Gaussian | 0.0995 | 14.90732 | 0.00643 | 1516.01094 | 8.09362 |
| 2 | Gaussian | 0.79701 | 27.51997 | 0.02722 | 1541.60357 | 64.8331 |
| 3 | Gaussian | 0.33282 | 20.98536 | 0.01492 | 1573.6961 | 27.07328 |

**D** **Peak Analysis (40 kHz/ 5 min)**

Data Set:[Book5]Sheet1!B Date:14/05/2024
BaseLine:Line
Chi^2=1.12076E-07 Adj. R-Square=9.95371E-01 # of Data Points=32
SS=2.46567E-06 Degrees of Freedom=22

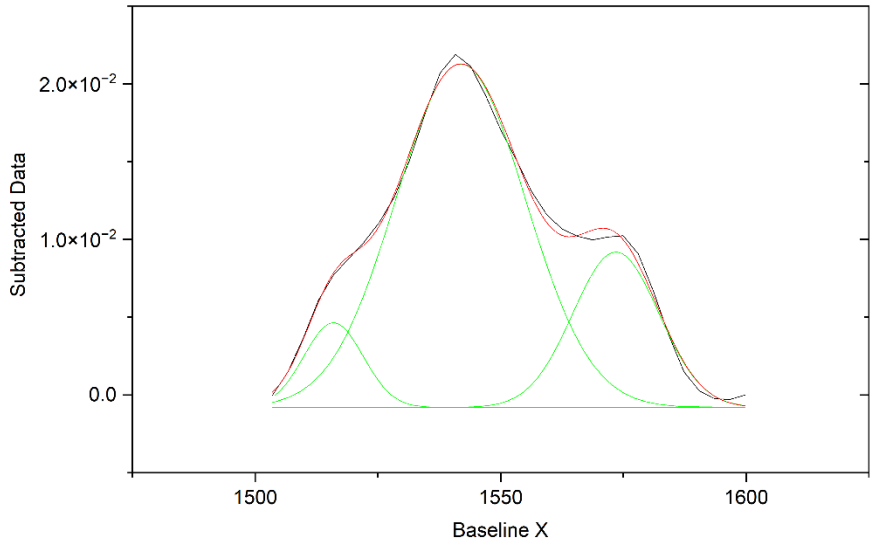



Fitting Results

| Peak Index | Peak Type | Area Intg | FWHM | Max Height | Center Grvty | Area IntgP |
|---|---|---|---|---|---|---|
| 1 | Gaussian | 0.0848 | 16.76945 | 0.00493 | 1516.39417 | 7.86458 |
| 2 | Gaussian | 0.83441 | 44.11965 | 0.01817 | 1541.5282 | 77.38487 |
| 3 | Gaussian | 0.15905 | 24.86771 | 0.00637 | 1583.04469 | 14.75055 |

**E** **Peak Analysis (40 kHz/ 15 minl)**

Data Set:[Book6]Sheet1!B Date:14/05/2024
BaseLine:Line
Chi^2=2.27055E-07 Adj. R-Square=9.95000E-01 # of Data Points=32
SS=4.99520E-06 Degrees of Freedom=22

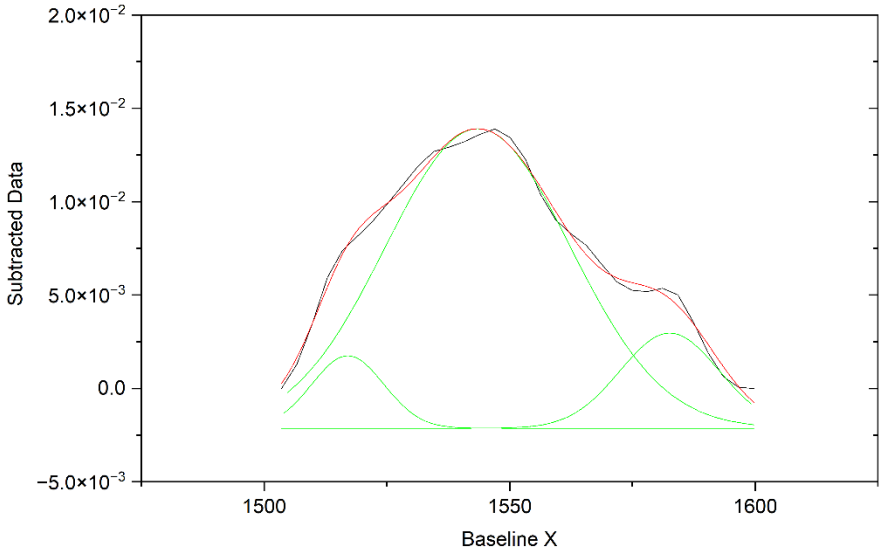



Fitting Results

| Peak Index | Peak Type | Area Intg | FWHM | Max Height | Center Grvty | Area IntgP |
|---|---|---|---|---|---|---|
| 1 | Gaussian | 0.08062 | 14.2133 | 0.00544 | 1515.98346 | 7.84251 |
| 2 | Gaussian | 0.72852 | 31.06138 | 0.02207 | 1541.88438 | 70.86745 |
| 3 | Gaussian | 0.21886 | 20.62707 | 0.00998 | 1573.48081 | 21.29004 |

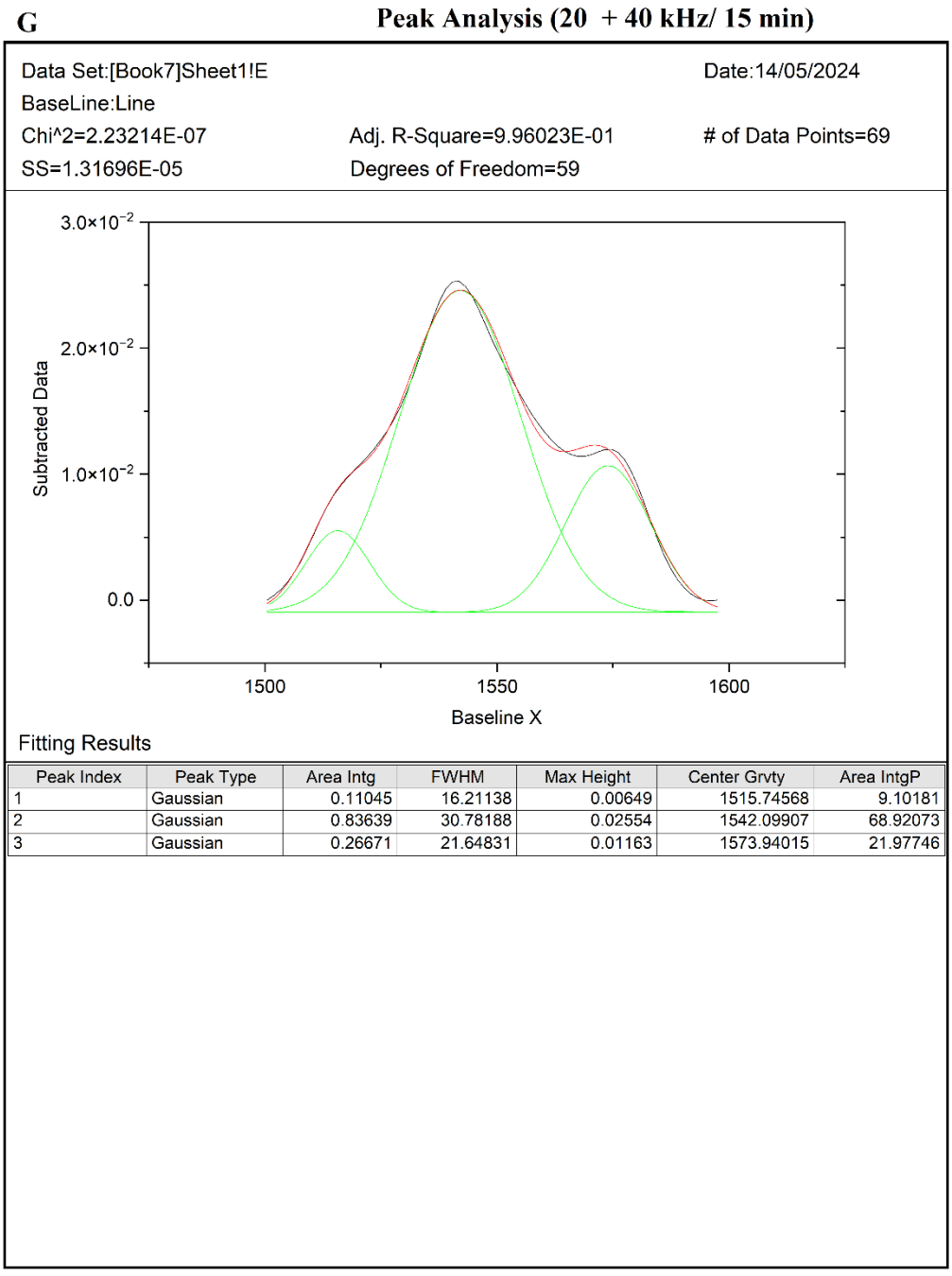
**F** **Peak Analysis (20 + 40 kHz / 5 min)**

Data Set:[Book1]Sheet1!B Date:14/05/2024
BaseLine:Line
Chi^2=1.97020E-07 Adj. R-Square=9.90146E-01 # of Data Points=32
SS=4.33443E-06 Degrees of Freedom=22




Fitting Results

| Peak Index | Peak Type | Area Intg | FWHM | Max Height | Center Grvty | Area IntgP |
|---|---|---|---|---|---|---|
| 1 | Gaussian | 0.0691 | 17.31015 | 0.00388 | 1517.06023 | 7.39427 |
| 2 | Gaussian | 0.74251 | 44.30293 | 0.01604 | 1543.54483 | 79.45471 |
| 3 | Gaussian | 0.1229 | 23.71573 | 0.00509 | 1582.59985 | 13.15102 |




| Peak Index | Peak Type | Area Intg | FWHM | Max Height | Center Grvty | Area IntgP |
|---|---|---|---|---|---|---|
| 1 | Gaussian | 0.11045 | 16.21138 | 0.00649 | 1515.74568 | 9.10181 |
| 2 | Gaussian | 0.83639 | 30.78188 | 0.02554 | 1542.09907 | 68.92073 |
| 3 | Gaussian | 0.26671 | 21.64831 | 0.01163 | 1573.94015 | 21.97746 |

**Fig. S8.** Peak fitting of FTIR spectrum (Gaussian function) in the region of Amide II (1600–1500 $cm^{-1}$) of MFGs/MFGM prepared from bovine raw milk treated by different ultrasonic intensities. A, control; B, 20 kHz/ 5 min; C, 20 kHz/ 15 min; D, 40 kHz/ 5 min; E, 40 kHz/ 15 min; F, 20 + 40 kHz/ 5 min; G, 20 + 40 kHz/ 15 min.

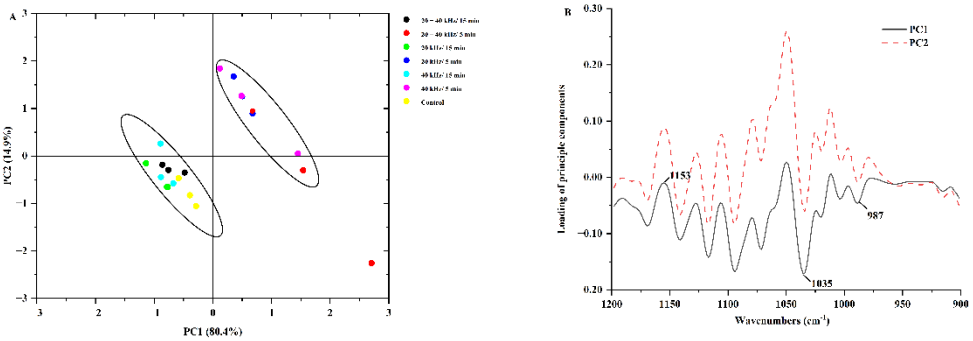
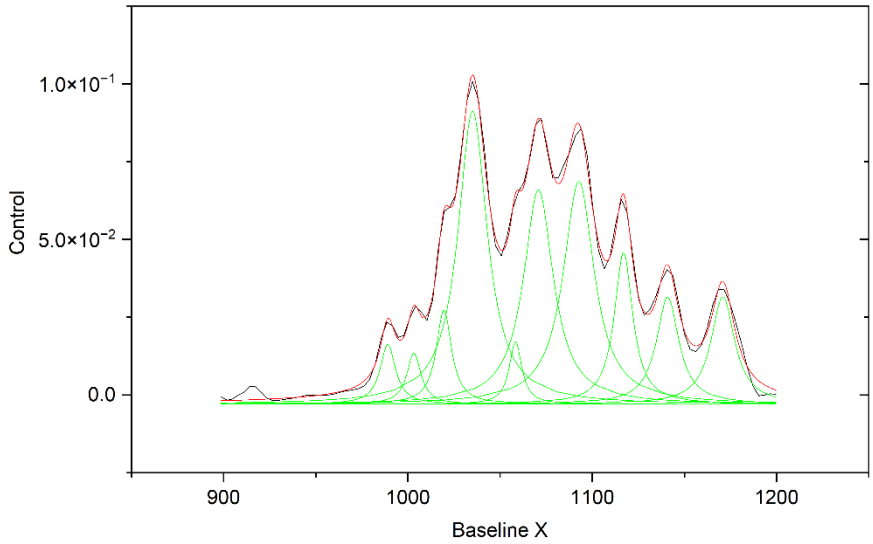



**Fig. S9.** PCA scores (A) and loading plots (B) of FTIR spectra in the region of 1200–900 $cm^{-1}$ of MFGs/MFGM prepared from bovine raw milk treated by different ultrasonic intensities.

**A** **Peak Analysis (control)**

Data Set:[Book7]Sheet1!B Date:14/05/2024
BaseLine:Line
Chi^2=4.16237E-06 Adj. R-Square=9.95435E-01 # of Data Points=98
SS=2.78879E-04 Degrees of Freedom=67




Fitting Results

| Peak Index | Peak Type | Area Intg | FWHM | Max Height | Center Grvty | Area IntgP |
|---|---|---|---|---|---|---|
| 1 | Lorentz | 0.29892 | 10.15197 | 0.01924 | 989.09164 | 2.81065 |
| 2 | Lorentz | 0.23665 | 9.39615 | 0.01639 | 1003.23568 | 2.22508 |
| 3 | Lorentz | 0.46662 | 10.04332 | 0.03025 | 1019.52472 | 4.38743 |
| 4 | Lorentz | 2.72683 | 19.21824 | 0.09419 | 1035.10164 | 25.63908 |
| 5 | Lorentz | 0.25448 | 8.19331 | 0.02012 | 1058.36521 | 2.39273 |
| 6 | Lorentz | 2.03228 | 19.62245 | 0.06885 | 1070.7965 | 19.10858 |
| 7 | Lorentz | 2.18813 | 20.42382 | 0.07157 | 1092.71599 | 20.57395 |
| 8 | Lorentz | 0.90208 | 12.20914 | 0.04861 | 1116.96225 | 8.48183 |
| 9 | Lorentz | 0.76253 | 14.86085 | 0.03438 | 1140.88523 | 7.16966 |
| 10 | Lorentz | 0.76693 | 15.6074 | 0.03451 | 1170.83202 | 7.21102 |

**B**

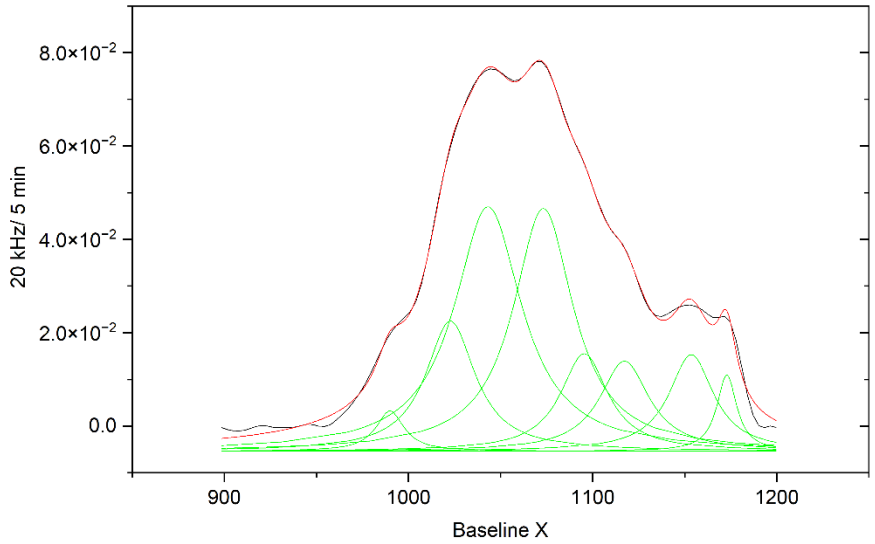
**Peak Analysis (20 kHz/ 5 min)**

Data Set:[Book2]Sheet1!B Date:14/05/2024

BaseLine:Line

Chi^2=1.46747E-06 Adj. R-Square=9.98083E-01 # of Data Points=98

SS=1.07125E-04 Degrees of Freedom=73




Fitting Results

| Peak Index | Peak Type | Area Intg | FWHM | Max Height | Center Grvty | Area IntgP |
|---|---|---|---|---|---|---|
| 1 | Lorentz | 0.23909 | 18.4964 | 0.00863 | 989.94329 | 2.20093 |
| 2 | Lorentz | 1.3285 | 32.65129 | 0.02788 | 1022.77189 | 12.22955 |
| 3 | Lorentz | 3.32336 | 44.6067 | 0.05234 | 1043.19052 | 30.59338 |
| 4 | Lorentz | 2.95868 | 39.61759 | 0.05199 | 1073.21294 | 27.23632 |
| 5 | Lorentz | 0.95187 | 31.27502 | 0.02089 | 1095.42929 | 8.76247 |
| 6 | Lorentz | 0.90659 | 32.74481 | 0.01929 | 1117.28732 | 8.34565 |
| 7 | Lorentz | 0.846 | 29.50074 | 0.02068 | 1153.51917 | 7.78793 |
| 8 | Lorentz | 0.30892 | 13.17645 | 0.01631 | 1172.83571 | 2.84377 |

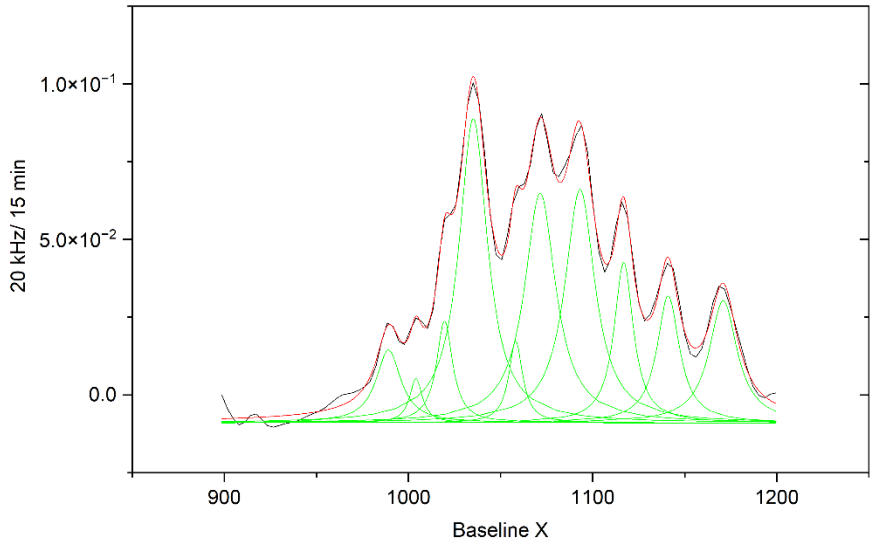
**C** **Peak Analysis (20 kHz/ 15 min)**

Date:14/05/2024

BaseLine:Line

Chi^2=5.27850E-06 Adj. R-Square=9.94776E-01 # of Data Points=98

SS=3.53659E-04 Degrees of Freedom=67




Fitting Results

| Peak Index | Peak Type | Area Intg | FWHM | Max Height | Center Grvty | Area IntgP |
|---|---|---|---|---|---|---|
| 1 | Lorentz | 0.57542 | 16.30179 | 0.02343 | 989.12892 | 4.85655 |
| 2 | Lorentz | 0.18341 | 8.36526 | 0.01423 | 1004.04171 | 1.54798 |
| 3 | Lorentz | 0.5318 | 10.62523 | 0.03263 | 1019.57176 | 4.48834 |
| 4 | Lorentz | 2.75766 | 18.71212 | 0.09772 | 1035.18305 | 23.27454 |
| 5 | Lorentz | 0.36663 | 9.06927 | 0.02624 | 1058.20913 | 3.09431 |
| 6 | Lorentz | 2.2753 | 20.53027 | 0.07383 | 1071.49718 | 19.20344 |
| 7 | Lorentz | 2.24103 | 19.94438 | 0.07499 | 1093.13544 | 18.91421 |
| 8 | Lorentz | 0.99469 | 12.73177 | 0.05147 | 1116.88231 | 8.3951 |
| 9 | Lorentz | 0.90725 | 14.91026 | 0.04078 | 1141.01148 | 7.65718 |
| 10 | Lorentz | 1.01521 | 18.51233 | 0.03924 | 1170.8669 | 8.56835 |

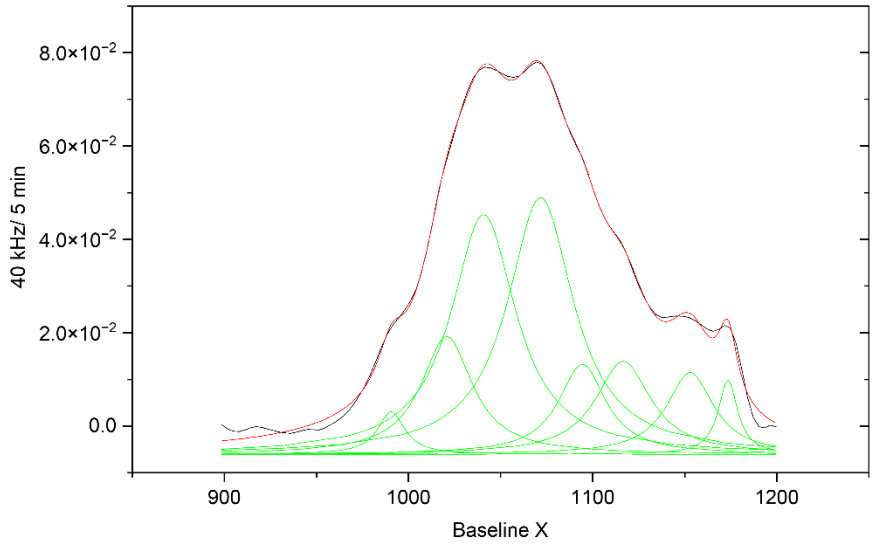
**D** **Peak Analysis (40 kHz/ 5 min)**

Data Set:[A40kHz5minPD]Sheet1!B Date:14/05/2024

BaseLine:Line

Chi^2=1.60298E-06 Adj. R-Square=9.97956E-01 # of Data Points=98

SS=1.17018E-04 Degrees of Freedom=73




Fitting Results

| Peak Index | Peak Type | Area Intg | FWHM | Max Height | Center Grvty | Area IntgP |
|---|---|---|---|---|---|---|
| 1 | Lorentz | 0.24666 | 17.99806 | 0.00913 | 990.61556 | 2.23965 |
| 2 | Lorentz | 1.24814 | 34.06224 | 0.0252 | 1020.79303 | 11.33305 |
| 3 | Lorentz | 3.13989 | 42.80003 | 0.05133 | 1040.75391 | 28.51019 |
| 4 | Lorentz | 3.41471 | 43.61689 | 0.05499 | 1071.69409 | 31.00555 |
| 5 | Lorentz | 0.88005 | 31.30333 | 0.0193 | 1094.35168 | 7.99087 |
| 6 | Lorentz | 1.03572 | 36.53521 | 0.01996 | 1116.62213 | 9.40433 |
| 7 | Lorentz | 0.75255 | 31.13731 | 0.01753 | 1152.93141 | 6.8331 |
| 8 | Lorentz | 0.29551 | 12.99658 | 0.01582 | 1173.43327 | 2.68326 |

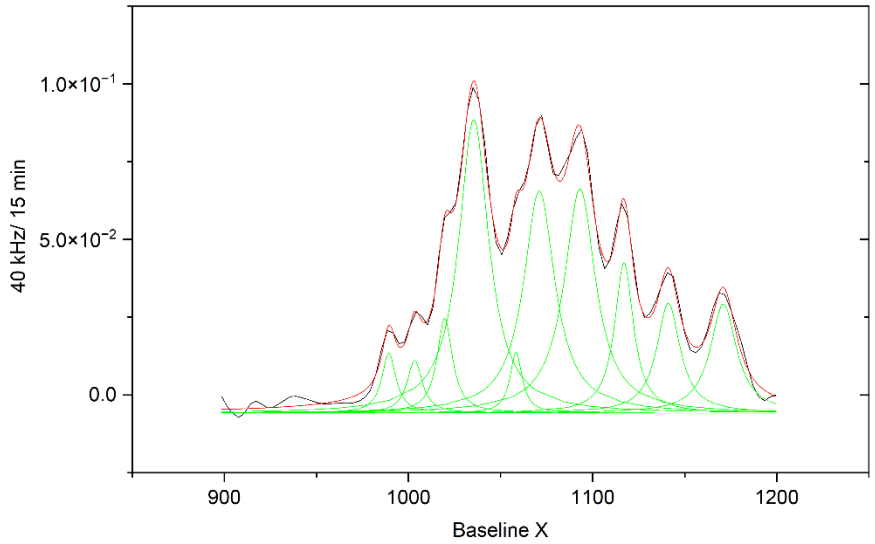
**E** **Peak Analysis (40 kHz/ 15 min)**

Date:14/05/2024

BaseLine:Line

Chi^2=4.25716E-06 Adj. R-Square=9.95580E-01 # of Data Points=97

SS=2.80972E-04 Degrees of Freedom=66




Fitting Results

| Peak Index | Peak Type | Area Intg | FWHM | Max Height | Center Grvty | Area IntgP |
|---|---|---|---|---|---|---|
| 1 | Lorentz | 0.27659 | 9.36098 | 0.01926 | 989.34153 | 2.49431 |
| 2 | Lorentz | 0.25849 | 9.95425 | 0.01692 | 1003.35797 | 2.33113 |
| 3 | Lorentz | 0.47328 | 10.13857 | 0.0304 | 1019.66296 | 4.26816 |
| 4 | Lorentz | 2.80436 | 19.75145 | 0.09436 | 1035.45835 | 25.29033 |
| 5 | Lorentz | 0.24228 | 8.06232 | 0.01946 | 1058.42583 | 2.18495 |
| 6 | Lorentz | 2.2154 | 20.67941 | 0.07139 | 1071.01892 | 19.97891 |
| 7 | Lorentz | 2.23514 | 20.75415 | 0.07201 | 1093.09506 | 20.1569 |
| 8 | Lorentz | 0.91198 | 12.43379 | 0.04829 | 1117.02898 | 8.22443 |
| 9 | Lorentz | 0.81423 | 15.49777 | 0.03529 | 1141.13037 | 7.34292 |
| 10 | Lorentz | 0.85693 | 17.37687 | 0.03505 | 1171.00691 | 7.72795 |

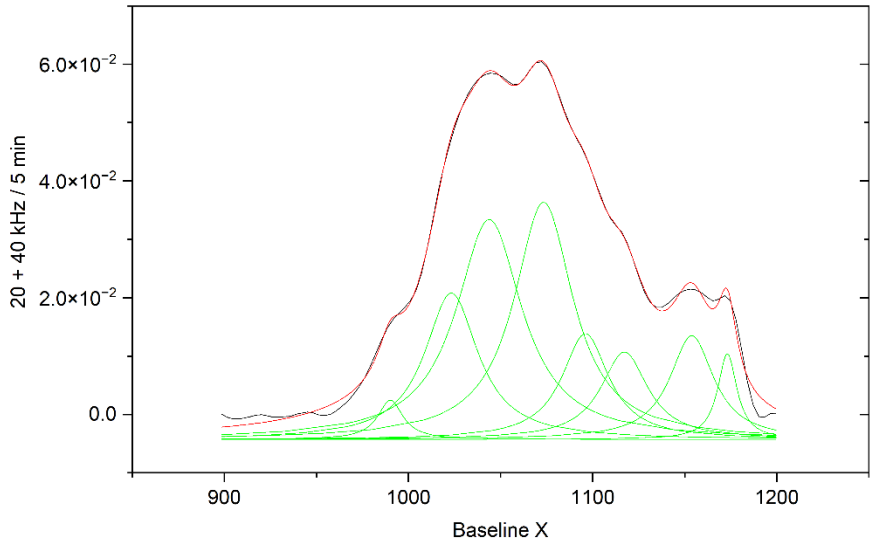
**F** **Peak Analysis (20 + 40 kHz/ 5 min)**

Date:14/05/2024

BaseLine:Line

Chi^2=1.14017E-06 Adj. R-Square=9.97520E-01 # of Data Points=98

SS=8.32325E-05 Degrees of Freedom=73

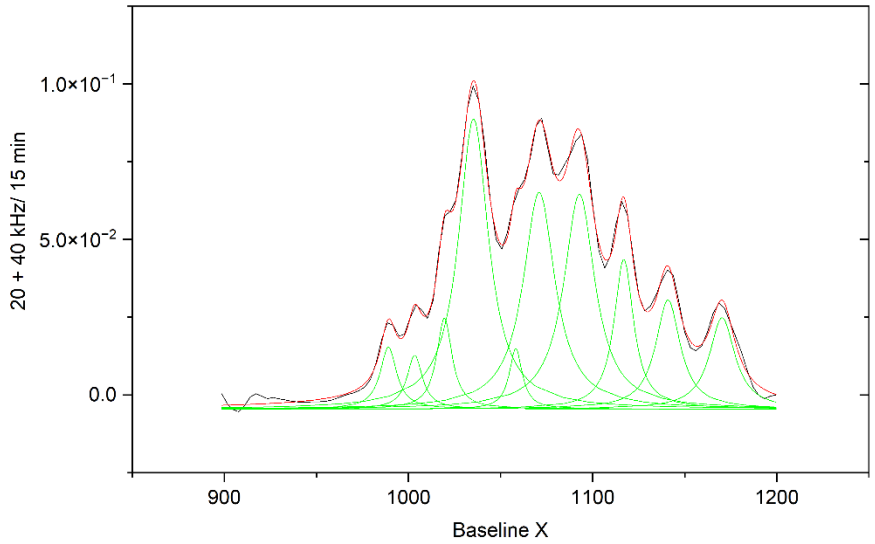



Fitting Results

| Peak Index | Peak Type | Area Intg | FWHM | Max Height | Center Grvty | Area IntgP |
|---|---|---|---|---|---|---|
| 1 | Lorentz | 0.16921 | 16.66376 | 0.00674 | 990.14983 | 1.98137 |
| 2 | Lorentz | 1.28009 | 35.16265 | 0.02509 | 1023.26395 | 14.98903 |
| 3 | Lorentz | 2.33602 | 43.44788 | 0.03767 | 1043.8197 | 27.35341 |
| 4 | Lorentz | 2.27916 | 38.99746 | 0.04063 | 1073.36854 | 26.68759 |
| 5 | Lorentz | 0.81797 | 30.94287 | 0.01814 | 1096.03906 | 9.57797 |
| 6 | Lorentz | 0.67112 | 31.06012 | 0.01498 | 1117.20519 | 7.85843 |
| 7 | Lorentz | 0.71726 | 29.06242 | 0.01778 | 1153.83056 | 8.39865 |
| 8 | Lorentz | 0.26932 | 12.73272 | 0.01468 | 1173.13113 | 3.15355 |

**G** **Peak Analysis (20 + 40 kHz/ 15 min)**

Data Set:[A2040kHz15min]Sheet1!B Date:14/05/2024
BaseLine:Line
Chi^2=3.21736E-06 Adj. R-Square=9.96558E-01 # of Data Points=98
SS=2.15563E-04 Degrees of Freedom=67




Fitting Results

| Peak Index | Peak Type | Area Intg | FWHM | Max Height | Center Grvty | Area IntgP |
|---|---|---|---|---|---|---|
| 1 | Lorentz | 0.33005 | 10.85413 | 0.0199 | 989.09036 | 3.02993 |
| 2 | Lorentz | 0.27059 | 10.22251 | 0.01726 | 1003.3669 | 2.48411 |
| 3 | Lorentz | 0.45575 | 10.17808 | 0.02916 | 1019.4766 | 4.18391 |
| 4 | Lorentz | 2.77766 | 19.81869 | 0.09316 | 1035.31869 | 25.4997 |
| 5 | Lorentz | 0.2567 | 8.55885 | 0.01945 | 1058.24722 | 2.35655 |
| 6 | Lorentz | 2.19703 | 21.03931 | 0.06964 | 1070.94199 | 20.16936 |
| 7 | Lorentz | 2.12576 | 20.59452 | 0.06899 | 1092.81694 | 19.51504 |
| 8 | Lorentz | 0.9353 | 12.81666 | 0.04809 | 1116.91077 | 8.58634 |
| 9 | Lorentz | 0.8427 | 16.17812 | 0.03506 | 1140.88988 | 7.73624 |
| 10 | Lorentz | 0.70138 | 16.90415 | 0.02933 | 1170.31659 | 6.43883 |

**Fig. S10.** Peak fitting of FTIR spectrum (Lorentz function) in the fingerprint region of 1200–900 $cm^{-1}$ of MFGs/MFGM prepared from bovine raw milk treated by different ultrasonic intensities. A, control; B, 20 kHz/ 5 min; C, 20 kHz/ 15 min; D, 40 kHz/ 5 min; E, 40 kHz/ 15 min; F, 20 + 40 kHz/ 5 min; G, 20 + 40 kHz/ 15 min.

# CHAPTER SIX

## Effects of high-methoxyl pectin on structure, composition, rheological properties of milk fat globules

**Abstract**

The study investigated the interactions between high-methoxyl pectin (HMP) and milk fat globules or membrane (MFGs/MFGM) ingredients. Mixtures of raw milk and HMP at concentration of 0.20 %, 0.30 %, and 0.40 % (w/w) (designated as 0.20 pectin (Pec), 0.30 Pec, and 0.40 Pec, respectively) underwent cream separation and ultra-centrifugation to enrich the MFGs/MFGM materials, with raw milk without HMP serving as a control. The control and 0.20 Pec exhibited multimodal particle sizes distributions with the additional peaks within the range 0.01 − 0.1 μm. HMP at 0.20 % level enhanced system stability of MFGs/MFGM, indicated by a higher ζ−potential and a lower instability index compared to 0.30 % and 0.40 % levels. Fourier transform infrared spectroscopy (FTIR) showed HMP increased the random coil (%), accompanied by a reduction of α-helix structure (%) in MFGs/MFGM ingredients. SDS-PAGE analysis reveal lower band intensities of MFGM proteins, such as periodic acid Shciff III (PAS III), cluster of differentiation 36 (CD36), and butyrophilin (BTN) in the upper layers of 0.40 Pec compared to 0.30 Pec and 0.20 Pec materials. Rheograms demonstrated decreased viscosity in all materials with HMP, indicating shear-thinning behaviour confirmed by flow behavior indexes (n) ($0 < n < 1$) using the Herschel-Bulkley model. Hierarchical cluster analysis (HCA) of the structural, compositional, physical stability, and rheological properties of MFGs/MFGM materials demonstrated that the 0.30 % and 0.40 % HMP levels gave the most pronounced effect.

**Keywords:** Milk fat globules; High-methoxyl pectin; Structural change; Compositional change; Physical instability; Rheological property

## 6.1. Introduction

Milk fat globule membrane (MFGM) is a tri-layer phospholipid structure enveloping triglycerides at its core with embedded proteins or trace physiological components. MFGM structure is crucial in preventing coalescence of fat globules, thereby forming a stable emulsion. Additionally, MFGM fragments have been demonstrated as a substitute for lecithin due to their surfactant and emulsifying abilities arising from their amphipathic membrane compositions (Jukkola, Partanen, Xiang, Heino, & Rojas, 2019). Sun, et al. (2022) reported that MFGM ingredients modified by ultrasonic treatment (20 kHz, 43 ± 3.4 W/cm$^2$) exhibited superior emulsifying stability and encapsulation compared to milk protein concentrate. Garczewska-Murzyn, Kiełczewska, and Smoczyński (2022) investigated the utility of buttermilk in stabilizing the emulsion and colloidal phases of homogenized milk, resulting in the homogenized fat globules with similar surface properties to those of unprocessed MFGs. This may be due to the transfer of native MFGM fragments into the buttermilk during churning. The oil-in-water emulsion system formed by milk sphingomyelin (SM) and micellar casein produced a uniform surface coating without causing protein displacement at the interfaces (Ahn, Park, Chai, & Imm, 2022).

MFGM proteins constitute approximately 25 to 70% of the mass of MFMG materials and about 1% of the overall protein content in milk (Holzmüller & Kulozik, 2016). As MFGM ingredients have only been commercially developed for several years, initial product development has emphasized the benefits of phospholipids for early infant nutritional development. Raza, Herzig, and Leppaluoto (2021) have extensively reviewed the physiological properties of MFGM across the lifespan, referring to MFGM as a potential panacea. In particular, the health benefits of MFGM proteins have gained significant interest. For instance, the multiple physiological tasks of xanthine oxidoreductase (XO) has been noted, such as producing reactive oxygen species and generating nitric oxide, regulating the blood pressure (Bortolotti, Polito, Battelli, & Bolognesi, 2021). Besides health benefits, the physicochemical and techno-functional properties of MFGM proteins are also worthy for further research, as they

can influence physiological properties to some extent. Industrially, sweet buttermilk or cheese whey are the primary raw materials for MFGM components preparation. MFGM proteins exist in combination with other milk components in commercial MFGM ingredients. From an industrial application perspective, research on the mixture of MFGM components with other ingredients, and their effects on processing properties is essential. However, research on this subject still remains limited.

In the dairy industry, pectin has been used as thickeners or gelling agents in yogurts to improve texture and prevent whey separation. Low-methoxyl pectin (LMP) is typically added prior to the fermentation, while high-methoxyl pectin (HMP) is introduced post-acidification. This is due to the HMP's ability to inhibit gelation, which otherwise results in the formation of liquid yogurt (Zhang, Goff, Liu, Luo, & Hu, 2024). HMP is more commonly used to prevent milk protein flocculation in acidified milk drinks. Additionally, pectin has been used to form coacervates with caseins or whey protein, enhancing their techno-functionalities. Hou, Fu, Chen, and Niu (2024) reported emulsification properties of whey protein improved through glycosylation modified by pectin. In fat-reduced products, whey protein-pectin complexes produced by thermomechanical treatment serve as fat replacers, enhancing the creaminess of the products (Filla & Hinrichs, 2023). The interactions between casein micelles and pectin are complicated and have been extensively investigated (Wusigale, Liang, & Luo, 2020). Maroziene and De Kruif (2000) reported that the adsorption of pectin onto casein micelles is pH-dependent. Their research showed that at pH 6.70, depletion interactions occurred in the system because of the non-adsorption between pectin and caseins, which, however, took place after lowering the pH to 5.30. Previous research has primarily focused on caseins and whey proteins. The interactions between pectin and MFGM proteins, which may also influence the stabilization of food systems, have not yet been investigated. Pan, et al., (2024) investigated how the addition order of MFGM and milk proteins during homogenization affects regulation of the lipid droplet interface in model infant formula emulsions. They concluded that the changes in the interfacial compositions of lipid

droplets affected lipid digestion by mitigating the aggregates and coalescence of protein and lipid droplets. Given the potential use of MFGs/MFGM ingredients in acidified dairy products, which typically contain HMP, it is essential to study how introducing HMP affects the interfacial composition MFGs droplets.

The present research studied the effect of HMP in raw milk on the structural and compositional modifications of MFGs or MFGM during the separation of cream. Additionally, the techno-functionalities, including physical stability and rheological property, were investigated to provide support and theoretical basis for industrial applications. Furthermore, all results were analyzed using hierarchical cluster analysis (HCA) to understand the HMP-dependent techno-functional property changes in MFGs or MFGM materials.6.2. Materials and methods

### 6.2.1. Materials and reagents

Fresh bovine milk (fat 4.22 ± 0.01%, protein 3.40 ± 0.01%, dry matter 13.30 ± 0.03%, pH 6.67 ± 0.03) was supplied by Teagasc animal & grassland research and innovation centre (Moorepark, Fermoy, Co. Cork, Ireland). HMP (YM-115H, citrus, total galacturonic acid ≥ 65 %) was kindly provided by CPKelco (Atlanta, USA) and used without further treatment. Phosphate buffered saline (PBS) (pH 7.20, 25℃) was made by mixing 1 tablet (Sigma-Aldrich®, Merck Life Science Ltd., Cork, Ireland) with 200 mL MiliQ water according to the instructions.

### 6.2.2 Sample preparation

A centrifugal separator (FT 15 Disc Bowl Centrifuge, Armfield co., Ringwood, UK) equipped with disk bowl was employed to separate the raw milk into cream and skim milk. Prior to the separation, four batches of raw milk were preheated to 40 − 45 ℃. Subsequently, HMP powder was slowly added to the raw milk at the concentration of 0.20 %, 0.30 %, and 0.40 % (w/w), respectively. During mixing, the mixtures of pectin and raw milk were stirred at a speed of 600 rpm for 30 min to prevent pectin clumping. At the end of the dispersion, the pH of raw milk with the

concentration of 0.20 %, 0.30 %, and 0.40 % (w/w) HMP was 6.63 ± 0.01, 6.60 ± 0.04, and 6.57 ± 0.02 (25 ℃), respectively. The separated skim milk, during separation, was re-added to the sample bowl twice to reach a fat content less than 0.5% (w/w). All the collected cream samples were subjected to the ultra-centrifugation for 15 min at 10000 × g (4 ℃) (Kendro Laboratory Products, Asheville, NC) to further enrich the MFGs ingredients. The upper layers were collected and rinsed with PBS buffer (Sun, Roos, & Miao, 2022). This rinsing step was performed two more times, and the top layers obtained from the last rinse were freeze-dried (Freezone, Labconco Corporation, Kansas, USA) for further analysis. Each treatment was conducted three times. Before some analysis, freeze-dried MFGs/MFGM materials were pre-heated at 30−35℃ to obtain the liquid state. Before some analysis, freeze-dried MFGs/MFGM materials were pre-heated at 30−35℃ to obtain the liquid state.

### 6.2.3 Particle size

Using the Mastersizer 3000 (Malvern Instruments, Malvern, UK) with laser light scattering, the particle size of milk and pectin mixtures was measured. The volume density (%) across various particle size distributions and volume distribution (D× (10), D× (50), and D× (90)) were recorded. The setting parameters were based on our previous research with modifications (Sun, et al., 2024c). Each sample was analyzed in triplicate. D× (10) and D× (90) indicate the particle sizes below which 10% and 90% of the sample fall, respectively, while D× (50) represents the median of the volume distribution. Additionally, the surface weighted mean D [3, 2] was recorded to calculate the specific surface area (SSA) following Equation (6-1), and the surface fraction ($\Phi_m$) model was used to estimate the change of surface protein in fat globules induced by the HMP addition according to Eq. (6-2):

$$SSA= 6/\rho D[3,2] \quad (6\text{-}1)$$

Where ρ indicates the particle density.

$$\Phi_m=(S_t - S_o)/S_o \quad (6\text{-}2)$$

Where $S_o$ is the original surface area of fat globules in control raw milk, and $S_t$ is the surface area of MFGs with HMP.

### 6.2.4. Zeta (ζ) potential

The effect of HMP addition on the surface charges of fat globules was investigated by the dynamic light scattering instrument (Nano–ZS, Malvern Instruments Ltd., Worcestershire, UK). Prior to analysis, the dilution of pre-melted (30 – 35 ℃) samples was conducted with PBS buffer following the previous report (Sun, Roos, & Miao, 2024a). The ζ–potential was recorded, and the fraction of fat globules' surface change was estimated according to the model in Eq. (6-3):

$$\Phi_e=1-\exp\left(-1.802\times10^{-3}\zeta_R^2\right) \quad (6\text{-}3)$$

Where $\zeta_R$ is the relative change of ζ–potential of fat globules induced by HMP addition compared to control ($\Phi_e$=0).

### 6.2.5. Fourier transform infrared spectroscopy (FTIR)

A Bruker Tensor 27 (Bruker Optik GmbH, Ettlingen, Germany) was employed to acquire the FTIR spectra of all samples, and Optics Platinum Attenuated Total Reflectance (ATR) cell (Pike Technology Inc., Madison, WI, USA) was used for the analysis. Before the analysis, approximately 20 mg of each ground freeze-dried sample was placed on the zinc ATR crystal aperture. The spectra were recorded by scanning from 4000 to 900 $cm^{-1}$ and processed in OPUS 7.5 software (Bruker Optik GmbH, Ettlingen, Germany) to eliminate the atmospheric vapour and carbon dioxide interference by subtracting the background signals. Additionally, spectra were subjected to data processing in OriginPro 2023 (OriginLab, Northampton, MA, USA), including noise reduction, baseline subtraction, second derivation, and peaks fitting and deconvolution (Sun et al., 2024a).

### 6.2.6. Sodium dodecyl sulphate polyacrylamide gel electrophoresis (SDS-PAGE)

The protein profiles of control and MFGs/MFGM isolates with HMP were characterized by SDS-PAGE, following a modified method described by Sun et al. (2022a). To investigate the binding of HMP to different types of milk proteins, samples from the upper, middle and lower layers of the final rinsing step (described Section in 2.2) were collected for non-reducing SDS-PAGE analysis, running for 45 min at 120 V. Caseins, whey proteins, and specific MFGM proteins, including mucin 1 (MUC1), the redox enzyme xanthin oxidase (XO), periodic acid Shciff III (PAS III), and butyrophilin (BTN), were marked on the SDS-PAGE bands. The densities of all these protein bands were quantitatively analysed by ImageJ software 1.36 b (Wayne Rasband, National Institutes of Health, Bethesda, MD, USA), and the results were normalized to a total of 100%.

### 6.2.7. Physical stability

The physical stability of MFGs/MFGM materials affected by HMP addition was tested using a Lumisizer (LUM GmbH, Berlin, Germany) which operated at 3000pm for 3000 s at 37 ± 2°C to accelerate the creaming of emulsions (Wu, Fitzpatrick, Cronin, & Miao, 2020). Specifically, 400 μL pre-heated MFGs/MFGM in the liquid state was injected into the test cuvettes and subjected to centrifugation. The space- and time-dependent transmission profiles (%) of droplets in all samples were scanned at 870 nm every 10 s, resulting in a total of 1,000 profiles being recorded. Data recording and instability calculations were conducted using the SEP View software (SepView 4.1, LUM GmbH).

### 6.2.8. Rheological properties

The viscosity of raw milk and its mixtures with HMP was investigated before MFGs/MFGM ingredients enrichment via centrifugation. During our preliminary experiments, severe phase separation was observed during rheological analysis when

samples were subjected to shear rate ranging from 0.1 $s^{-1}$ to 1000 $s^{-1}$. This phase separation resulted in poor reproducibility of the collected data, masking the impact induced by HMP addition on the rheological properties of MFGs/MFGM ingredients. Therefore, the analysis of rheological properties was conducted on the samples before the MFGs/MFGM isolation. 1 mL of each sample, as outlined in Section 2.2, was placed on the sample platform of the ARG 2 Rheometer (TA Instruments, Crawley, UK). A 60 mm diameter aluminum parallel plate was applied to shear the samples, and the gap size between the sample platform and the shearing plate was maintained at 300 μm through the analysis. Both viscosity (Pa.s) and shear stress (Pa) were recorded as functions of the shear rate ($s^{-1}$).

Additionally, the fluid properties of each pre-melted sample were estimated by conducting the non-liner fitting of shear rate against shear stress using the Power law model and Herschel-Bulkley (Randhahn, 1973).

Power law,

$$\sigma = K\dot{\Upsilon}^n \qquad (6\text{-}4)$$

and Herschel-Bulkley,

$$\sigma = \sigma_0 + K\dot{\Upsilon}^n \qquad (6\text{-}5)$$

where σ is the shear stress (Pa) and $\dot{\Upsilon}$ denotes the shear rate ($s^{-1}$). The parameter K (Pa $s^n$) indicates the consistency index, n is the flow behavior index, and the $\sigma_0$ in Eq. (5) refers to the yield stress (Pa). The flow behavior index (n) characterizes the rheological behaviour of fluids, specifically, shear-thinning for $0 < n < 1$, Newtonian for $n = 1$, and shear-thickening for $n > 1$.

### 6.2.9. Statistical analysis

All analyses were measured in triplicate unless otherwise indicated. The results were expressed as mean values ± standard deviation (SD). Variance analysis was

performed using Analysis of Variance (ANOVA), and the significance of mean differences was assessed using Fisher's test ($p < 0.05$). Additionally, Multivariate Statistical Analysis was conducted in OriginPro, with results visually represented through a heat map derived from Hierarchical Cluster Analysis (HCA). All statistical evaluations were carried out using the OriginPro 2023 software (OriginPro 2023, OriginLab Corporation, Northampton, USA).

## 6.3. Results and discussion

### 6.3.1. Particle size of MFGs/MFGM

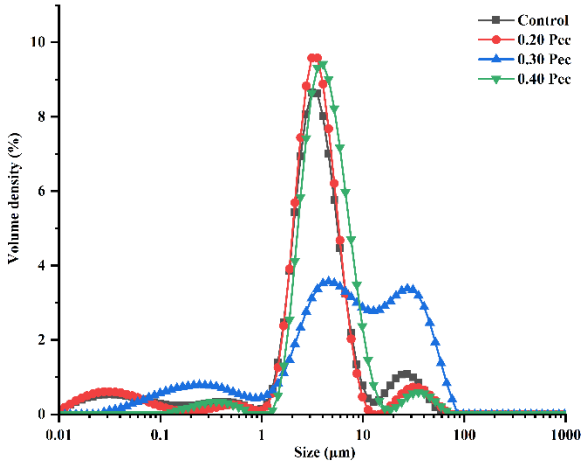



**Figure 6-1.** Dynamic light scattering measurements (Volume density, %) of fat globules in MFGs/ MFGM sourced from mixtures of raw milk and HMP. 0.20 Pec indicates the 0.20 % HMP addition (w/w), 0.30 Pec= 0.30 % (w/w); 0.40 Pec = 0.40 % (w/w).

Droplet size serves as an intuitive measure to investigate the degree of association between pectin and components of MFGs. Fig.6-1 illustrates the volume density (%) of control bovine milk and its mixtures with varying amounts of HMP (0.20 Pec, 0.30 Pec, and 0.40 Pec). All MFGs/MFGM exhibited droplet sizes from 0.01 to 100 μm, with the highest volume density (%) observed in the 1 to 10 μm range except for the 0.30 Pec MFGs/MFGM, followed by the 10 − 100 μm range. For the 0.4 Pec MFGs/MFGM, the volume density (%) of particles with the size range of 0.01 − 0.1

μm was negligible, while a lower volume density (%) was observed in the larger 10 to 100 μm range. The control and 0.20 Pec MFGs/MFGM displayed multimodal distributions, which exhibited additional peaks at particle sizes ranging from 0.01 to 0.1 μm, attributing to the formation of milk proteins aggregates induced by inter-protein reactions ( Filla, Nodin, & Hinrichs, 2023). This finding is in agreement with Graf, Protte, Weiss, and Hinrichs (2020), who demonstrated that whey protein aggregates within the 0.1 to 1 μm size range are not involved in complex formation. The bridging or the depletion mechanisms have been reported to be related to the flocculation of protein particles depending on the conditions (Dickinson, 2018). The volume density (%) within the 10 to 100 μm range in the 0.30 Pec MFGs/MFGM was significantly higher than in the control, 0.02 Pec and 0.04 Pec, whereas the volume density in the range of 1−10 μm was lower than in the other MFGs/MFGM. It is speculated that the 0.30 % HMP facilitated the formation of the bigger sizes of coacervates between HMP and milk proteins, which may result in a polydisperse and unstable system. According to the section 6.2.3, after the dispersion of HMP in the raw milk, pH of each batch decreased to 6.63 ± 0.01, 6.60 ± 0.04, and 6.57 ± 0.02 (25 ℃) with the addition of 0.20 %, 0.30 %, and 0.40 % (w/w) HMP. It has been reported that at neutral pH, pectin did not adsorb onto the NaCas-coated droplet surface because of electrostatic repulsion (Dickinson, 1998). However, above a critical concentration, nonadsorbing pectin can induce the destabilization emulsion by depletion flocculation (Wusigale, et al., 2020). This result was further substantiated by the volume distribution values in Table 6-1, where both D× (50) and D× (90) for the 0.30 Pec MFGs/MFGM were significantly higher than for the other treatments.

There was a steady decrease in the D× (10) values among all MFGs/MFGM as a function of HMP concentration deceased, as shown in Table 6-1. The D× (10) values for the 0.40 Pec MFGs/MFGM were 11.00 ± 0.58 μm, indicating that 10 % of the particles were smaller than this value. Surface fraction ($\Phi_m$) was used to characterise the surface change of fat globules after the HMP adding (Sharma, Oey, & Everett, 2015). Table 6-1 shows that increasing the amount of HMP resulted in more significant

changes in the surface of fat globules. The surface fraction ($\Phi_m$) for the sample with 0.4% HMP exhibited the highest value of 0.88, followed by MFGs/MFGM containing 0.30% and 0.20% HMP. Previous research indicated that MFGs/MFGM with more particles lying within higher volume density (%) showed more significant alterations on the fat globule surface, corresponding to higher $\Phi_m$ values (Sun, et al., 2024b). However, the results of this study are inconsistent with this trend. Specifically, the MFGs/MFGM with 0.30% HMP demonstrated a more pronounced change in volume density than the MFGs/MFGM with 0.40% HMP (Fig. 6-1).

In addition, the effect of mechanical shearing on the particle sizes of whey protein-pectin complexes was demonstrated by Protte, et al. (2017), who showed that higher shear rates induced a greater number of accessible and reactive groups to form large aggregates, even though shear forces tended to cause defragmentation. In the current study, the mechanical treatment from cream separation and centrifugation for the enrichment of MFGs or MFGM materials is inevitable, which may induce collisions in the system, resulting in varying particle sizes.

**Table 6-1** D× (10), D× (50), and D× (90) of the MFGs/MFGM materials isolated from bovine raw milk with the addition of HMP

| | D× (10) (μm) | D× (50) (μm) | D× (90) (μm) | Surface fraction ($\Phi_m$) |
|---|---|---|---|---|
| Control | $2.00\pm0.58^{d}$ | $3.57\pm0.02^{c}$ | $9.24\pm0.09^{b}$ | – |
| 0.20 Pec | $5.00\pm0.58^{c}$ | $3.51\pm0.01^{d}$ | $7.31\pm0.03^{c}$ | $0.12\pm0.03^{c}$ |
| 0.30 Pec | $8.00\pm0.58^{b}$ | $7.52\pm0.03^{a}$ | $40.00\pm0.10^{a}$ | $0.62\pm0.01^{b}$ |
| 0.40 Pec | $11.00\pm0.58^{a}$ | $4.43\pm0.03^{b}$ | $9.37\pm0.27^{b}$ | $0.88\pm0.00^{a}$ |

Superscript letters that differ in the same column denote significant differences between samples ($p < 0.05$). 'ns' stands for no significant difference ($p > 0.05$).

### 6.3.2. ζ-potential

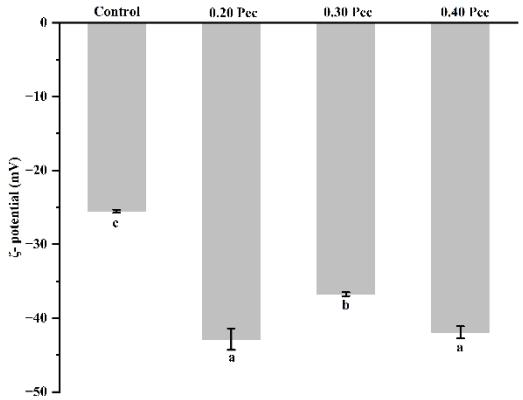



**Figure 6-2.** ζ−potential of MFGs/MFGM prepared from control and raw milk with HMP. Different superscript letters mean the significant difference between samples ($p < 0.05$).

The surface ζ−potential reflected the electrostatic repulsion between the droplets. Increased electrostatic repulsion reduces the possibility of collision, thereby enhancing the stability of the emulsion (Hou, et al., 2024). Fig. 6-2A shows the ζ−potential of MFGs/MFGM isolated from control and raw milk with added HMP. Compared to the control MFGs/MFGM (−25.53 mV), the addition of HMP affected ζ−potential significantly, shifting it towards more negative values to varying degrees. This may be attributed to the association of anionic HMP molecules with positively charged proteins (Tholstrup Sejersen, et al., 2007). Theoretically, HMP improved the stability of the emulsion systems as emulsions with an absolute ζ−potential value higher than 30 mV displays better stability (Honary & Zahir, 2013). Specifically, both the 0.20% (−42.87 mV) and 0.40 % (−41.93 mV) HMP addition facilitated the formation of stable system, followed by the 0.30 Pec with ζ−potential value of −36.77 mV. This observation was in line with the previous results on the volume density (%) in Fig. 6-1, which showed higher volume density (%) of HMP-milk protein coacervates in the larger size range of 10 −100 μm in the 0.30 Pec compared to other treatments. This effect may be attributed to the reduced the exposure of charged groups by the

formation of coacervates, resulting in a lower ζ−potential value. These findings are consistent with the previous research, where more negative magnitudes for ζ−potential were observed in the milk with the addition of negatively charged sodium hexametaphosphate (SHMP) and pectin (with esterification degree of 75.20) (Mocanu, Rolin, Mohammadifar, Mohammadi, & Bahrami, 2021).

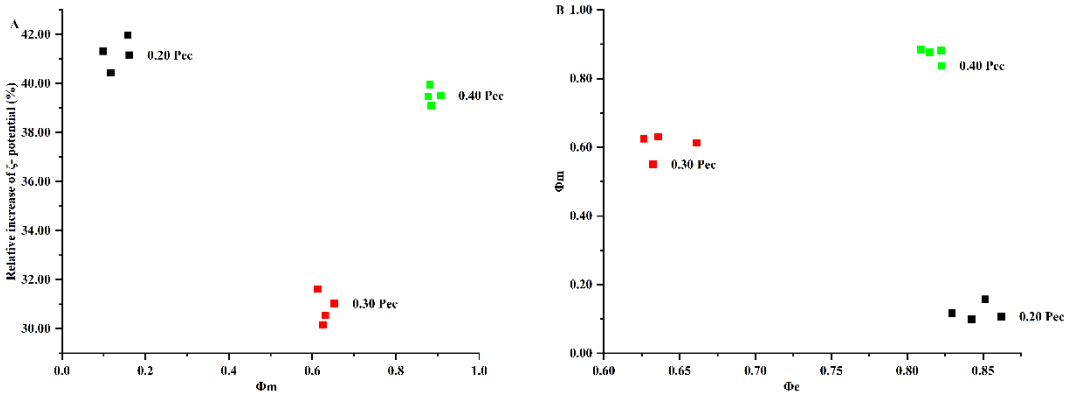



**Figure 6-3.** (A): The relative change in ζ−potential as the increase of surface fractions ($\Phi_m$) in MFGs prepared from control and raw milk with HMP added. (B): Scatters of Φ values obtained from Mastersizer measurements ($\Phi_m$) and estimated by the predictive model ($\Phi_e$).

Fig. 6-3A displays a randomly scattered distribution of $\zeta_R$ across all the HMP and milk mixtures as the magnitude of $\Phi_m$ increased. Notably, the 0.20 Pec MFGs/MFGM exhibited the highest $\zeta_R$, followed by the 0.40 Pec and 0.30 Pec. These findings agree with the ζ−potential results presented in Fig.6-2. Additionally, $\Phi_m$ was plotted against of the estimated change in the surface fraction ($\Phi_e$) of MFGs (Fig. 6-3B). Similar to the fitting between $\zeta_R$ and $\Phi_m$, none regression model could adequately fit the relationship between $\Phi_m$ and $\Phi_e$, indicating that the magnitude of $\zeta_R$ could not reliably predict the changes in surface coverage of fat globules induced by HMP addition (Sharma, et al., 2015). Furthermore, contradictory magnitudes of $\Phi_m$ and $\Phi_e$ were observed between the 0.20 Pec and 0.30 Pec MFGs/MFGM. Specifically, the value of $\Phi_m$ in the 0.30 Pec was higher than that in the 0.20 Pec, while the latter exhibited a lower value of $\Phi_e$.

### 6.3.3. FTIR

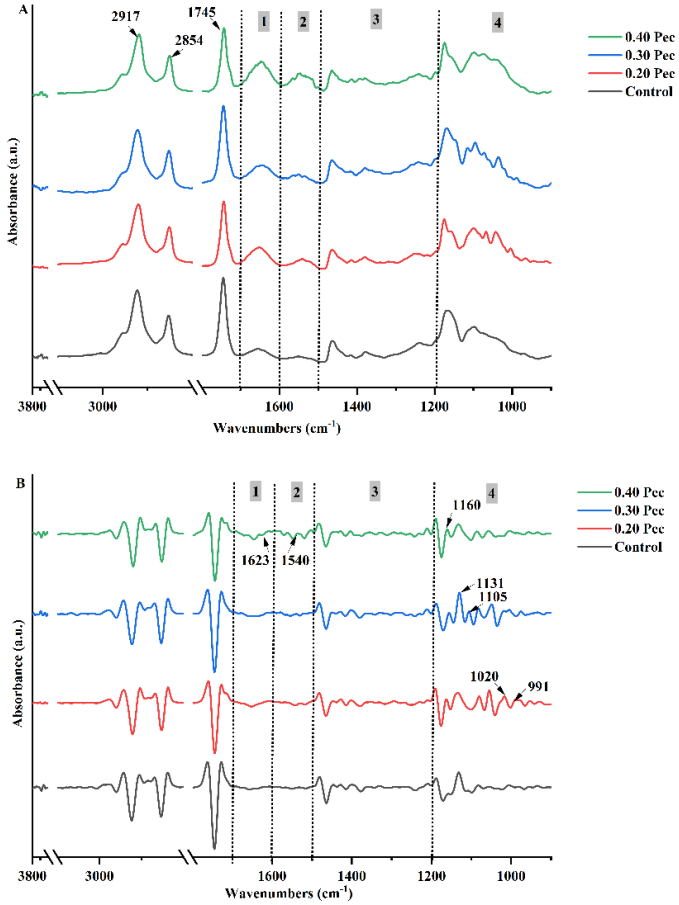



**Figure 6-4.** Original (A) and representative second derivation (B) FTIR spectra of MFGs/MFGM prepared from control and raw milk with HMP. (The spectra in the ranges of 3700−3100 $cm^{-1}$ and 2800−1800 $cm^{-1}$ are not displayed because no peak were detected for any samples, and all the spectra exhibited similarly flat plots. 0.20 Pec, 0.30 Pec, and 0.40 Pec indicate the HMP addition are 0.20 %, 0.30%, and 0.40 % (w/w), respectively.

Fig. 6-4 presents the FTIR spectra of MFGs/MFGM prepared from the bovine raw milk, with and without HMP enrichment. The milk proteins and phospholipids dominated the spectrum among all MFGs/MFGM, as the minor HMP addition ratio ranged between 0.20 % and 0.40 %. All MFGs/MFGM exhibited strong −CH stretching in the wavenumber range of 3000 − 2800 $cm^{-1}$, and symmetric stretching

modes of $-CH_2$ groups at 2917 $cm^{-1}$ and 2854 $cm^{-1}$ , which are associated with the acyl chains of triglycerides or phospholipids (Grewal, et al., 2017). There were no significant differences in the absorbance intensity or band area for these functional groups among all the MFGs/MFGM. This differed to work of Lan, Ohm, Chen, and Rao (2020) who reported a significant increase of hydrogen bonding in complexes with HMP which may be attributed to the higher HMP concentration varying from 0.05 to 1.00 % (w/w).

Moreover, significant C=O stretching vibrations of ester, aldehydes and ketones (1800 − 1700 $cm^{-1}$), Amide I (1700 − 1600 $cm^{-1}$), Amide II (1600 − 1500 $cm^{-1}$), Amide III (1500 − 1200 $cm^{-1}$), and the fingerprint region (1200 − 900 $cm^{-1}$), appeared in both the control and HMP-enriched MFGs/MFGM. The ester functional group of lipids and their interactions with proteins, indicated by C=O stretching vibrations, were observed at 1745 $cm^{-1}$. Both the original and 2nd derivative spectra revealed that HMP addition did not affect the absorbance and position of this band (Fig.6- 4A and 4B). The addition of 0.40 % HMP strengthened the Amide I and Amide II bands compared to other treatments, suggesting chemical reactions between the amino groups of milk proteins and the reduced carbonyl groups of HMP. Additional minor peaks in Amide I and Amide II were noted in the 0.40 Pec MFGs/MFGM (Fig.6-4B), particularly absorbance signals at 1623 $cm^{-1}$ and 1540 $cm^{-1}$, which are associated with the presence of melanoidins and the stretching and deformation of the double bond of carbonyl C=O, C=C, or C=N groups (Mohsin, et al., 2020). Peak fitting results (Fig.6S1-S4) within Amide I (1700 − 1600 $cm^{-1}$) (Table 6-2) supported this observation, indicating that intermolecular/aggregated β-sheet and side chain appeared in the 0.30 Pec and 0.20 Pec MFGs/MFGM, respectively. Meanwhile, both of these secondary structures were observed in the 0.40 Pec MFGs/MFGM, but not in the control. Additionally, HMP addition resulted in the increase in the random coil structures accompanied by a reduction of α-helix structure (%) than that in control MFGs/MFGM. This finding supported higher ζ−potential of all the mixtures of HMP and milk than of control which contains less extensional random coil structures.

**Table 6-2** Quantitative estimation of the secondary structure in MFGs/MFGM components derived from raw milk and its mixtures with HMP in region of Amide I (1700−1600 $cm^{-1}$)

| | Intermolecular/ aggregated β-sheet (%) | β-turn (%) | α-helix (%) | Random coil (%) | Intramolecular β-sheet (%) | Side chain (%) |
|---|---|---|---|---|---|---|
| Control | - | 6.11±0.00$^{c}$ | 67.91±0.00$^{a}$ | 5.17±0.03$^{d}$ | 20.82±0.00$^{b}$ | - |
| 0.20 Pec | - | 41.96±0.24$^{a}$ | 2.85±0.02$^{d}$ | 54.54±0.25$^{a}$ | - | 0.66±0.01$^{a}$ |
| 0.30 Pec | 2.87±0.22$^{a}$ | 3.46±0.00$^{d}$ | 42.93±0.01$^{b}$ | 13.38±0.02$^{c}$ | 37.36±0.01$^{a}$ | - |
| 0.40 Pec | 1.41±0.01$^{b}$ | 18.25±0.68$^{b}$ | 32.86±1.19$^{c}$ | 28.13±0.69$^{b}$ | 18.71±0.18$^{c}$ | 0.65±0.01$^{b}$ |

Superscript letters that differ in the same column denote significant differences between samples ($p < 0.05$).

The fingerprint region (1200 − 900 $cm^{-1}$) showed some different peaks from each individual sample. For instance, all milk-HMP mixtures presented new peaks around 1055 − 1048 $cm^{-1}$ not showing in control MFGs/MFGM, which could be the superposition of milk protein-lipids associations and HMP spectra. Compared to control MFGs/MFGM, more significant peak absorbance at 1160 $cm^{-1}$ was detected which migrated to 1155 $cm^{-1}$ with the 0.30 Pec addition. Additionally, 0.30 % Pec MFGs/MFGM have the strongest absorbance peaks at the bands of 1160 $cm^{-1}$ and 1105 $cm^{-1}$ among all MFGs/MFGM. The pure HMP powder was reported to present the peak at 1023 $cm^{-1}$ ascribed to the carboxyl group (Ghasemi, Jafari, Assadpour, & Khomeiri, 2017), which only presented in the both 0.20 Pec and 0.30 Pec, but not in the control and 0.40 Pec MFGs/MFGM. For 0.40 Pec MFGs/MFGM, this may be due to coacervates formed by proteins and HMP were removed during the centrifugation stage, resulting the undetectable residual HMP. A small peak only showing in the 0.20 Pec MFGs/MFGM at the bands of 991 $cm^{-1}$ attributing to the C=O stretching, indicating the formation of pectin and whey protein complex. This further verified more HMP retaining in the 0.20 Pec MFGs/MFGM than other treatments.

### 6.3.4. SDS-PAGE

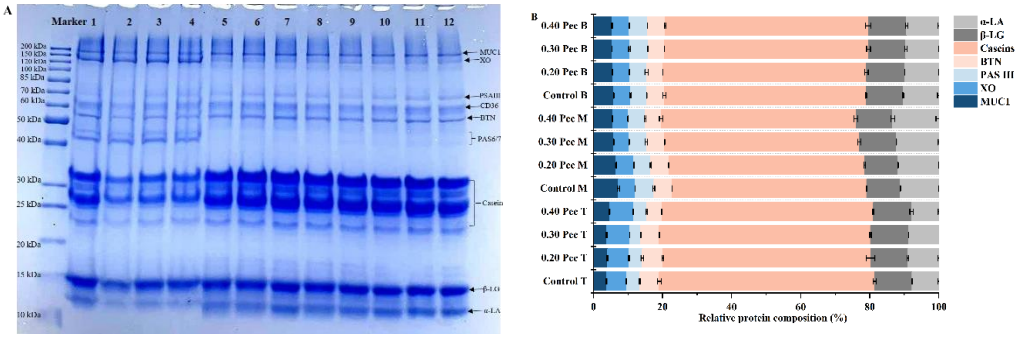



**Figure 6-5.** SDS-PAGE patterns obtained under non-reducing conditions for MFGs/MFGM material prepared from control and raw milk with HMP addition. (A) Lane 1-4, upper layer: control, 0.20 Pec, 0.30 Pec, and 0.40 Pec; Lane 5-8, middle layer: control, 0.20 Pec, 0.30 Pec, and 0.40 Pec; Lane 9-12, bottom layer: control, 0.20 Pec, 0.30 Pec, and 0.40 Pec. (B) The relative protein composition of MFGs/MFGM materials derived from densitometry measurements of bands in representative SDS-PAGE gels. The labels 0.20 Pec, 0.30 Pec, and 0.40 Pec indicate HMP addition of 0.20 %, 0.30%, and 0.40 % (w/w); T, M, and B represent upper, middle, and bottom layers.

The results of SDS-PAGE for the change in proteins in MFGs/MFGM after HMP addition during centrifugation are displayed in Fig. 6-5. Caseins are the primary protein type in all the MFGs/MFGM exhibiting the most intense bands in Fig. 6-5 A and the highest relative content, ranging from 52.88 % to 61.92% as shown by the quantitative results in Fig. 6-5 B, followed by β-LG and α-LA. For the MFGM proteins, as the PAS 6/7 only visible in the upper layers and no significant density different for the CD 36 bands of all MFGs/MFGM, thereby these two types of proteins were not subjected to calculate their relative content.

Caseins, whey proteins, and MFGM proteins, primarily including MUC1, XO, PAS III, and BTN, were observed in the upper layers of all MFGs/MFGM. This differs to the work of Maroziene, et al. (2000), who reported that 0.20 % of the HMP in skim milk induced the aggregation of proteins. Consequently, aggregations might precipitate and be removed during the rinsing step, potentially reducing the intensity of casein bands. In contrast, this reduction was not noted in the present study with the

same addition of 0.20% HMP comparing to control samples. This may be due to the different emulsion system (oil-protein-polysaccharides) in this study from the skim milk and polysaccharide system. Compared to the MFGM proteins in the middle and bottom layers among all MFGs/MFGM, the intensity of XO was stronger in the upper layers. However, larger amounts of the PAS III, CD 36, and BTN were detected in the middle and bottom layers, as verified by their pronounced bands in Fig. 6-5A and quantitative results in Fig. 6-5B. The differentiated distribution of MFGM proteins in different phases from centrifugation may be due to their different locations and binding degrees in the membrane. It has been documented that BTN and a portion of XO exhibit strong adhesion to MFGM following extraction pre-treatments, and PAS 6/7 is categorized as a peripheral protein (Holzmüller, Müller, Himbert, & Kulozik, 2016; Yamauchi, Shimizu, & Kanno, 1978). In contradiction to this theory, PAS 6/7 persisted on the surface of fat globules and was not removed during the rinsing step, as evidenced by the pronounced bands in the upper layers. In addition, this contradicted observation may not be induced by the HMP adding, as there were no significant differences in the PAS 6/7 content between the upper layers of control and HMP-added MFGs/MFGM.

In comparison with bands at the top of the well, with the molecular size >200 kDa, there was no significant difference between the control and HMP-added MFGs/MFGM, indicating that coacervates formed by the milk proteins and HMP were not observed. However, 0.30 % HMP addition increased the intensity of caseins, α-LA, and β-LG compared to the control. In contrast, the addition of 0.40 % HMP tended to reduce the intensity of both casein and whey proteins, likely transferring them to the rinsing phase during the centrifugation processing. Additionally, the bands for MFGM proteins in the 0.40 Pec MFGs/MFGM, including PAS III, CD 36, and BTN, presented lower intensity compared to the 0.30 Pec and 0.20 Pec MFGs/MFGM. No significant difference was observed in the BTN content between control and 0.20 Pec and 0.30 Pec MFGs/MFGM. However, the intensity of PAS III decreased with the increase of HMP content, particularly in the 0.40 Pec MFGs/MFGM. PAS III almost disappeared

in the upper layer, demonstrating that HMP addition caused the loss of PAS III, even though it is classified as an integral MFGM protein (Sun, Roos, & Miao, 2024c). In comparison with the bands in the middle and bottom layers among all MFGs/MFGM, pectin addition presented no significant effect on the MFGM proteins compositions, as indicated by the quantitative analysis in Fig. 6-5B.

Beyond the MFGM proteins, HMP addition also influence the caseins and whey proteins in the upper layers of all MFGs/MFGM. More caseins and whey proteins were retained in the upper layers after rinsing and centrifugation with the 0.30 % addition compared to the control. Conversely, HMP addition at 0.20% and 0.4 % facilitated the elimination of caseins and whey proteins during the rinsing step. This supports the findings in current study regarding the lower ζ – potential and more absorbance peaks observed in the FTIR spectra of the 0.30 Pec MFGs/MFGM.

### 6.3.5. Effect of HMP on the physical stability MFGs/MFGM materials

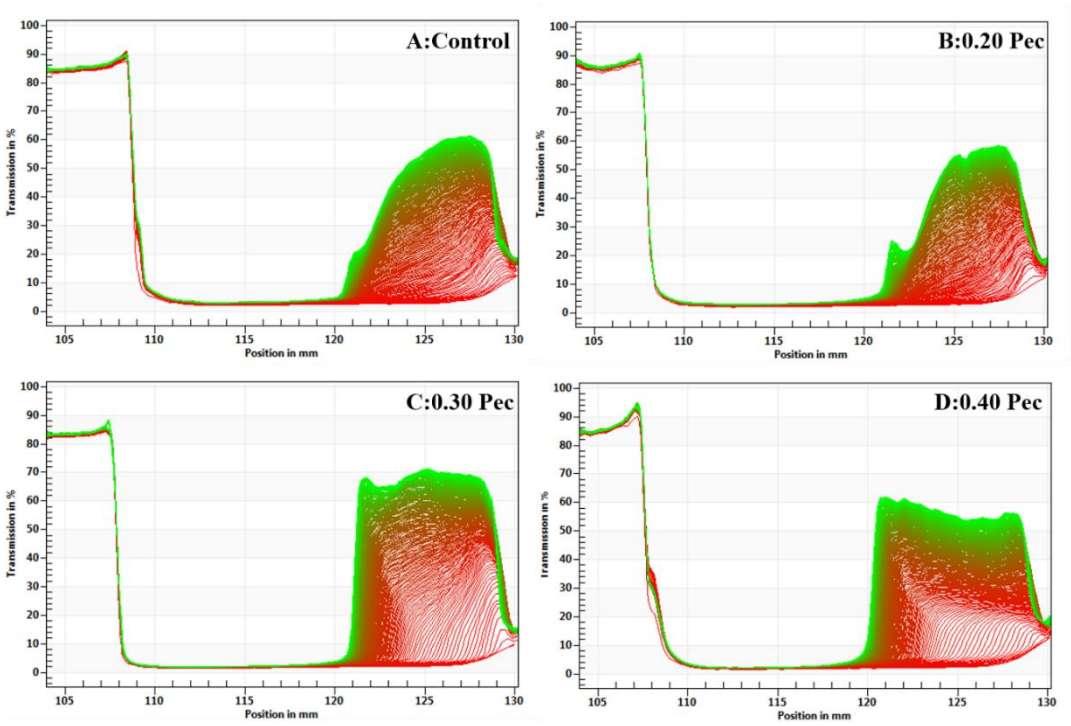



**Figure 6-6** Lumisizer phase separation near infrared (NIR) transmission profiles of MFGs/MFGM isolated from control and mixtures of bovine raw milk with HMP. A,

control; B, 0.20 Pec, 0.20% (w/w) HMP addition; C, 0.30 Pec, 0.30% (w/w) HMP addition; D, 0.40 Pec, 0.40% (w/w) HMP addition.

Lumisizer was employed to quantitatively analyse the physical stability of Lumisizer was employed to quantitatively analyse the physical stability of emulsions under accelerated centrifugal treatments. Fig. 6-6 displays the effect of HMP addition on the evolution of NIR transmission profiles of MFGs/MFGM isolation during centrifugation. The light intensity increased as scanning progressed from the bottom of the cuvettes positioned at 130 mm to the position of 120 mm, suggesting a reduction in the density of fat phase, which moved to the upper layer during centrifugation and scanning (Mao, Roos, & Miao, 2015). As shown in Fig. 6-6, the initial profiles displayed at the bottom (red transmission profiles), while the final profiles were located at the top (green transmission profiles). Compared to control, MFGs/MFGM with a 0.20 % HMP addition exhibited similar profiles presenting a faster increase in transmission rate than that the 0.30 Pec and 0.40 Pec MFGs/MFGM. Additionally, a polydisperse distribution (no sharp front) appeared at the top of transmission profiles in the 0.30 Pec and 0.40 Pec MFGs/MFGM, indicating the emulsion destabilization. Despite this, all MFGs/MFGM exhibited incomplete phase separation, as the final transmission file was not horizontal (Dammak & Sobral, 2018). The stability of the system may be due to the steric stabilization and electrostatic repulsion between the protein/pectin coacervates in the MFGs/MFGM with different concentration of HMP (pH from 6.57 to 6.63), with pectin loops and dangling tails repelling each other and keeping the particles dispersed, thereby preventing the aggregation of casein/pectin coacervates (Mocanu, et al., 2021). 0.3 % HMP facilitates the coacervates formation evidenced by the polydisperse distribution (no sharp front) appeared at the top of transmission profiles. These observations were substantiated by the results of instability index ranging from 0.062 to 0.229 among all MFGs/MFGM (Fig. 6-7A). The instability index was calculated based on the change in emulsion clarity during the phase separation, and an index with a magnitude of 0 indicated no alteration in

NIR transmission, while a magnitude of 1 denoted complete phase separation (Yerramilli & Ghosh, 2017).

As shown in Fig. 6-7A, the MFGs/MFGM isolations with a 0.30 % HMP addition exhibited the highest instability index throughout the test process, followed by the 0.40 Pec MFGs/MFGM. From the beginning of test to 1400 s, the control MFGs/MFGM were more stable, with smaller values of instability indices than the 0.20 Pec MFGs/MFGM. However, this trend reversed after 1400 s and continued until the end of the test (3000 s). These findings were in consistency with the results regarding the higher volume density (%) of 0.30 Pec MFGs/MFGM appearing in the larger particle range of 10 − 100 μm (Fig. 6-1). According to the ANOVA test with the significant level at 0.05, the instability index for the 0.30 Pec was significantly higher than for other MFGs/MFGM at the end of the test ($p < 0.05$). However, there was no significant difference between the control, 0.20 Pec and 0.40 Pec MFGs/MFGM ($p > 0.05$), indicating that the maximum degree of phase migration has completed.

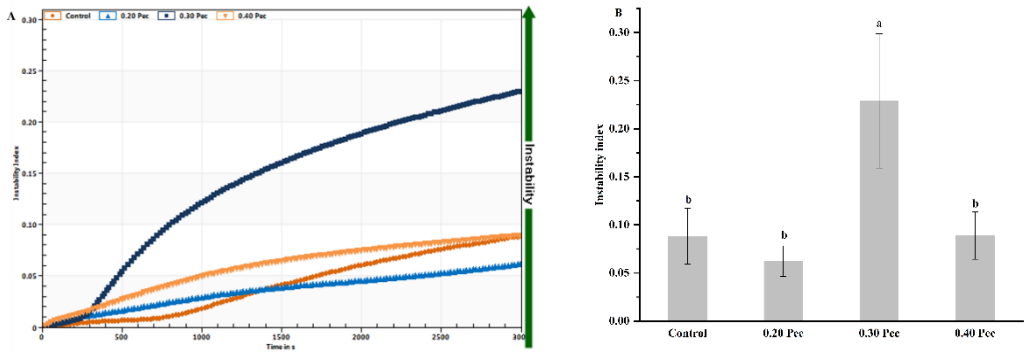



**Fig. 6-7** The change of the stability index over time during scanning (A) and the values of the scanning end point (B). 0.20 Pec, 0.20% (w/w) HMP addition; 0.30 Pec, 0.30% (w/w) HMP addition; 0.40 Pec, 0.40% (w/w) HMP addition. The presence of different superscript letters denotes a significant difference between MFGs/MFGM ($p < 0.05$).

### 6.3.6. Rheological properties

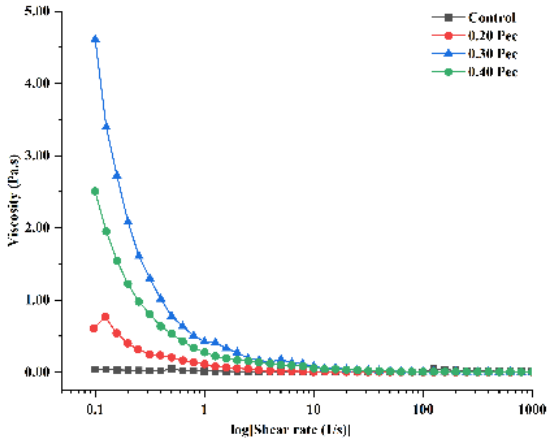



**Figure 6-8** Apparent viscosity of raw milk with different HMP levels (%), raw milk without HMP used as control. 0.20 Pec, 0.30 Pec, and 0.40 Pec indicate the HMP concentrations are 0.20 %, 0.30%, and 0.40 % (w/w).

The main compositions of all the MFGs/MFGM materials include milk proteins, milk lipids, and the coacervation formed by milk proteins and HMP. According to the Wusigale, et al. (2020), MFGs/MFGM system in this study could be categorized as non-complexing, in compatible & two-phase system. Fig.6-8 displays the shear flow plot of raw milk and its mixtures with HMP, showing that HMP increased the viscosity of raw milk to varying degree. By comparison, raw milk with a 0.30 % (w/w) HMP addition exhibited the highest viscosity throughout the analysis, followed by 0.40 Pec and 0.20 Pec. This indicates that the amount of HMP does not show a positive correlation with the viscosity in the milk system. These findings may be attributed to the formation of coacervates in the 0.30 Pec MFGs/MFGM, which showed a higher volume density (%) within the larger particle sizes range (10−100 μm). For all MFGs/MFGM, except the control, viscosity decreased as the shear rate ($s^{-1}$) increased, indicating shear-thinning behaviour. There is a negligible change for the control MFGs/MFGM throughout the measurement. Whole milk has been reported to behave as a Newtonian liquid when moderate shear rates were applied (Randhahn, 1974).

The regressed parameters of nonliner curve fitted by the Power law and Herschel-Bulkley models are presented in Table 6-3. Apart from 0.30 Pec (R2 = 0.835), all rheograms of MFGs/MFGM were fitted successfully by the Power law model with correlation coefficients $R^2$ > 0.930. For Power law fitting, control and 0.20 Pec MFGs/MFGM showed significantly higher flow behavior indexes (n) which was lowest for 0.30 Pec. This not only reflects the shear-thinning behaviour among all the MFGs/MFGM but also indicates the rate of viscosity declined. Accordingly, the lowest consistency coefficient (K, Pa sn) were observed for the control and 0.20 Pec MFGs/MFGM. An increase in K value in 0.30 Pec and 0.40 Pec has been reported to be related to an increase in the pectin concentration by improving the water absorption capacity. Moreover, the coacervation formed by HMP and milk protein may also affect the viscosity, especially MFGs/MFGM materials with 0.30 % and 0.40 % HMP additions. Although the HMP did not significanlty affect the protein or solid content of milk MFGs/MFGM, these components may change when subjected to shear treatment during analysis. It is speculated that shearing damage to the fat globule structure was reduced by using the raw milk instead of MFGs/MFGM-enriched ingredients for rheological analysis, but this damage was still unavoidable. As the shearing rate increased, MFGs structure may have been damaged, leading to the leakage of triglycerides and the proteins precipitation on the surface of the sample plate, particularly for the 0.30 Pec MFGs/MFGM.

The fitted flow behavior indexes (n) through Herschel-Bulkley model (Table 6-3) contradicted the trend of viscosity change shown in Fig. 6-8, as all MFGs/MFGM with HMP presented a shear-thickening property with flow behavior indexes ranging from 1.039 to 1.173 (n > 1). However, Fig. 6-8 displayed the shear-thinning flow plot of raw milk and its mixtures with HMP. Therefore, we infer that the Power law model is more suitable than the Herschel-Bulkley model for correctly reflecting the change in viscosity during shearing, despite better correlation coefficients $R^2$ ranging from 0.985 to 0.999 being obtained from Herchel-Bulkley model.

**Table 6-3** Regressed parameters of the Power law and Herschel-Bulkley models used to describe the flow curve of MFGs/MFGM prepared from bovine raw milk and its mixtures with HMP

| Samples | Power law | | | Herschel-Bulkley | | | |
|---|---|---|---|---|---|---|---|
| | *K* (Pa $s^n$) | n | $R^2$ | $\sigma_0$ (Pa) | *K*(Pa $s^n$) | n | $R^2$ |
| Control | $0.003\pm0.000^{c}$ | $0.921\pm0.011^{a}$ | 0.978 | $0.013\pm0.003^{d}$ | $0.002\pm0.000^{b}$ | $0.950\pm0.011^{c}$ | 0.990 |
| 0.20 Pec | $0.004\pm0.000^{bc}$ | $0.944\pm0.028^{a}$ | 0.988 | $0.087\pm0.004^{c}$ | $0.002\pm0.000^{b}$ | $1.061\pm0.011^{b}$ | 0.999 |
| 0.30 Pec | $0.074\pm0.026^{a}$ | $0.594\pm0.056^{c}$ | 0.835 | $0.566\pm0.030^{a}$ | $0.001\pm0.000^{b}$ | $1.173\pm0.058^{a}$ | 0.978 |
| 0.40 Pec | $0.030\pm0.009^{b}$ | $0.745\pm0.048^{b}$ | 0.933 | $0.377\pm0.029^{b}$ | $0.004\pm0.001^{a}$ | $1.039\pm0.042^{b}$ | 0.985 |

Superscript letters that differ in the same column denote significant differences between samples ($p < 0.05$).

### 6.3.7. Hierarchical cluster analysis (HCA)

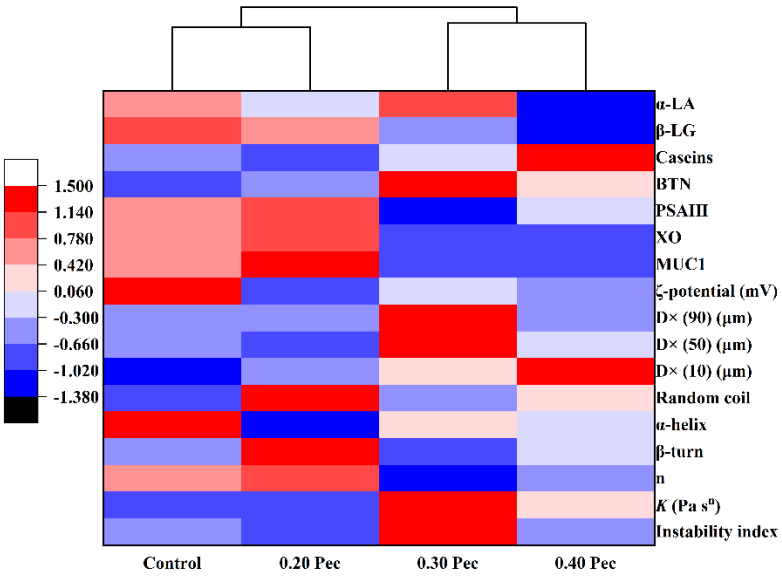



**Figure 6-9.** Hierarchical cluster analysis (HCA) of structural, compositional, physical instability, and rheological property changes in the MFG as a function of HMP additions. 0.20 Pec, 0.30 Pec, and 0.40 Pec indicate the HMP addition are 0.20 %, 0.30%, and 0.40 % (w/w), respectively.

A two-dimensional HCA was conducted to distinguish the effect of HMP additions on the structural, compositional, and rheological properties of MFGs or MFGM materials. In particular, the anlaysis included particle characteristics (volume distributions: D× (10), D× (50), and D× (90)), ζ−potential, relative protein contents

MFGM proteins, caseins, and whey proteins, as well as the flow behavior indexes (n) and consistency coefficient (*K*, Pa $s^n$) derived from the rheogram regression using the Power law model, and instablity indexes. As illustrated in Fig. 6-9, the control and 0.20 Pec were catagoried into one group, while 0.30 Pec and 0.40 Pec formed another group. Each treatment then formed its own distinct subgroup. These results indicate that HMP with the additions of 0.20 %, 0.30%, and 0.40 % (w/w) affected the structural, compositional, and characterision of rheology to vary degrees. Among all treatments, MFGs/MFMG materials with 0.30 % and 0.40 % HMP affected the techno-functionalities MFGs/MFGM more profoundly accroding to the grouping results.

## 6.4. Conclusion

The present study showed that high-methoxyl pectin (HMP) at concentration of 0.20 %, 0.30 %, and 0.40 % (w/w) significantly altered the structural, compositional, physical stability, and rheological property of milk fat globules or membrane (MFGs/MFGM) materials to varying extents. HCA confirmed that each treatment formed a distinct subgroup, underscoring the differential impact of each HMP concentration.

In particular, the HMP at 0.30 % facilitated the formation of coacervates between HMP and milk proteins, characterized by larger particle sizes ranging from 10 to 100 μm. This treatment also resulted in a lower ζ-potential, indicative of a higher number of positively charged casein micelles adsorbed onto the fat globules. Furthermore, HMP incorporation enhanced the absorbance at Amide I and Amide II bands, and altered the fingerprint regions, with new peaks emerging at 1055 − 1048 cm−1. The formation of coacervates between HMP and milk proteins were also evidenced by the reduced density of periodic acid Shciff III (PAS III), cluster of differentiation 36 (CD36), and butyrophilin (BTN), in the upper layers of MFGs/MFGM with 0.40% HMP. Changes in structure and composition induced by HMP correspondingly affected the physical stability and rheological properties of MFGs/MFGM. Notably,

milk with 0.30% HMP exhibited the poorest stability and a markedly increase in the apparent viscosity, as well as shear-thinning behaviour throughout the analysis.

Further research is suggested to investigate the mechanisms underlying the formation of coacervates between MFGM components and pectin, aiming to better explain some of the contradictory results in this study and understand how these coacervates affect the techno-functionalities of MFGM components. Additionally, the impact of pH reduction caused by the HMP introduction on the analysis results and the resulted phase instability affecting the accuracy of sampling should be considered in future studies.

**Declaration of competing interest**

All authors declare no conflict of interest.

**Author Statements**

Yanjun Sun: Conceptualization, Methodology, Writing-original draft, Data curation, Investigation, Funding acquisition. Yrjö H. Roos: Supervision, Writing review & editing. Song Miao: Supervision, Conceptualization, Writing-review & editing, Funding acquisition, Project administration, Investigation.

**Data availability**

Data will be made available on request.

**Acknowledgements**

The project was founded by 'The Open Project Program of State Key Laboratory of Dairy Biotechnology (No. SKLDB2022–007)', Teagasc-The Irish Agriculture and Food Development Authority (MDDT1392), and 'The China Scholarship Council (No.202008410212)'.

## Reference


Ahn, N., Park, J. H., Chai, C., & Imm, J. Y. (2022). The interaction of milk sphingomyelin and proteins on stability and microstructure of dairy emulsions. *Journal of Dairy Science*, *105*(5), 3832-3845.

Bortolotti, M., Polito, L., Battelli, M. G., & Bolognesi, A. (2021). Xanthine oxidoreductase: One enzyme for multiple physiological tasks. *Redox Biology*, *41*, 101882.

Dammak, I., & Sobral, P. J. d. A. (2018). Effect of different biopolymers on the stability of hesperidin-encapsulating O/W emulsions. *Journal of Food Engineering*, *237*, 33-43.

Dickinson, E. (1998). Stability and rheological implications of electrostatic milk protein–polysaccharide interactions. *Trends in Food Science & Technology*, *9*(10), 347-354.

Dickinson, E. (2018). Hydrocolloids acting as emulsifying agents – How do they do it? *Food Hydrocolloids*, *78*, 2-14.

Filla, J., Nodin, A., & Hinrichs, J. (2023). Influence of pH on particle size of thermomechanical stabilized whey protein-pectin complexes for technical scale production. *Food Hydrocolloids*, *144*, 108923.

Filla, J. M., & Hinrichs, J. (2023). Processing of whey protein-pectin complexes: Upscaling from batch lab scale experiments to a continuous technical scale process. *Journal of Food Engineering*, *347*, 111437.

Garczewska-Murzyn, A., Kiełczewska, K., & Smoczyński, M. (2022). The influence of buttermilk powder on the stability of emulsion and colloidal phases of homogenized milk. *European Food Research and Technology*, *248*(10), 2629-2636.

Ghasemi, S., Jafari, S. M., Assadpour, E., & Khomeiri, M. (2017). Production of pectin-whey protein nano-complexes as carriers of orange peel oil. *Carbohydrate Polymers*, *177*, 369-377.

Graf, B., Protte, K., Weiss, J., & Hinrichs, J. (2020). Concentrated whey as protein source for thermally stabilized whey protein-pectin complexes. *Journal of Food Engineering*, *269*, 109760.

Grewal, M. K., Chandrapala, J., Donkor, O., Apostolopoulos, V., Stojanovska, L., & Vasiljevic, T. (2017). Fourier transform infrared spectroscopy analysis of physicochemical changes in UHT milk during accelerated storage. *International Dairy Journal*, *66*, 99-107.

Holzmüller, W., & Kulozik, U. (2016). Technical difficulties and future challenges in isolating membrane material from milk fat globules in industrial settings – A critical review. *International Dairy Journal*, *61*, 51-66.

Holzmüller, W., Müller, M., Himbert, D., & Kulozik, U. (2016). Impact of cream washing on fat globules and milk fat globule membrane proteins *International Dairy Journal*, *59*, 52-61.

Honary, S., & Zahir, F. (2013). Effect of zeta potential on the properties of nano-drug delivery systems-a review (Part 2). *Tropical journal of pharmaceutical research*, *12*(2), 265-273.

Hou, K., Fu, X., Chen, H., & Niu, H. (2024). Characterization and emulsifying ability evaluation of whey protein-pectin conjugates formed by glycosylation. *Carbohydrate Polymers*, *329*, 121790.

Jukkola, A., Partanen, R., Xiang, W., Heino, A., & Rojas, O. J. (2019). Food emulsifiers based on milk fat globule membranes and their interactions with calcium and casein phosphoproteins. *Food Hydrocolloids, 94*, 30-37.

Lan, Y., Ohm, J.-B., Chen, B., & Rao, J. (2020). Phase behavior, thermodynamic and microstructure of concentrated pea protein isolate-pectin mixture: Effect of pH, biopolymer ratio and pectin charge density. *Food Hydrocolloids, 101*, 105556.

Mao, L., Roos, Y. H., & Miao, S. (2015). Effect of maltodextrins on the stability and release of volatile compounds of oil-in-water emulsions subjected to freeze–thaw treatment. *Food Hydrocolloids, 50*, 219-227.

Maroziene, A., & De Kruif, C. (2000). Interaction of pectin and casein micelles. *Food Hydrocolloids, 14*(4), 391-394.

Mocanu, M., Rolin, C., Mohammadifar, M. A., Mohammadi, R., & Bahrami, R. (2021). The effect of sodium hexametaphosphate on the efficiency of pectin in stabilizing acidified milk drinks. *Food Hydrocolloids, 118*, 106767.

Mohsin, G. F., Schmitt, F.-J., Kanzler, C., Epping, J. D., Buhrke, D., & Hornemann, A. (2020). Melanoidin formed from fructosylalanine contains more alanine than melanoidin formed from d-glucose with L-alanine. *Food Chemistry, 305*, 125459.

Protte, K., Ruf, T., Atamer, Z., Sonne, A., Weiss, J., & Hinrichs, J. (2017). Influence of shear stress, pectin type and calcium chloride on the process stability of thermally stabilised whey protein–pectin complexes. *Food Structure, 14*, 76-84.

Randhahn, H. (1973). Flow properties of milk and milk concentrates. *Milchwissenschaft, 28*(10), 620–628.

Randhahn, H. (1974). Contribution to the rheology of milk. *XIX International Dairy Congress, 1E*, 202.

Raza, G. S., Herzig, K. H., & Leppaluoto, J. (2021). Invited review: Milk fat globule membrane-A possible panacea for neurodevelopment, infections, cardiometabolic diseases, and frailty. *Jounal of Dairy Science, 104*, 19649.

Sharma, P., Oey, I., & Everett, D. W. (2015). Interfacial properties and transmission electron microscopy revealing damage to the milk fat globule system after pulsed electric field treatment. *Food Hydrocolloids, 47*, 99-107.

Sun, Y., Roos, Y. H., & Miao, S. (2022). Changes in Milk Fat Globules and Membrane Proteins Prepared from pH-Adjusted Bovine Raw Milk. *Foods, 11*(24), 4107.

Sun, Y., Roos, Y. H., & Miao, S. (2024a). Characterization of the microstructure, interfacial properties and crystallisation behaviours of milk fat globule and membrane isolated from acidified bovine milk and sweet whey. *Food Hydrocolloids*, 110246.

Sun, Y., Roos, Y. H., & Miao, S. (2024b). Comparative study of interfacial properties and thermal behaviour of milk fat globules and membrane prepared from ultrasonicated bovine milk. *Ultrasonics Sonochemistry, 102*, 106755.

Sun, Y., Roos, Y. H., & Miao, S. (2024c). A review of factors affecting the structure, compositions, and the techno-functionalities of bovine milk fat globule and membrane. *Trends in Food Science & Technology*, 104570.

Sun, Y., Yu, X., Hussain, M., Li, X., Liu, L., Liu, Y., Ma, S., Kouame, K. J. E., Li, C., Leng, Y., & Jiang, S. (2022). Influence of milk fat globule membrane and milk protein

concentrate treated by ultrasound on the structural and emulsifying stability of mimicking human fat emulsions. *Ultrasonics Sonochemistry, 82*, 105881.

Tholstrup Sejersen, M., Salomonsen, T., Ipsen, R., Clark, R., Rolin, C., & Balling Engelsen, S. (2007). Zeta potential of pectin-stabilised casein aggregates in acidified milk drinks. *International Dairy Journal, 17*(4), 302-307.

Wu, S., Fitzpatrick, J., Cronin, K., & Miao, S. (2020). Effect of sodium carbonate on the rehydration of milk protein isolate powder. *Food Hydrocolloids, 99*, 105305.

Wusigale, Liang, L., & Luo, Y. (2020). Casein and pectin: Structures, interactions, and applications. *Trends in Food Science & Technology, 97*, 391-403.

Yamauchi, K., Shimizu, M., & Kanno, C. (1978). Effect of Preparation on Properties of a Soluble Glycoprotein Fraction of Milk Fat Globule Membrane. *Journal of Dairy Science, 61*(6), 688-696.

Yerramilli, M., & Ghosh, S. (2017). Long-term stability of sodium caseinate-stabilized nanoemulsions. *Journal of Food Science and Technology, 54*(1), 82-92.

Zhang, H., Goff, H. D., Liu, C., Luo, S., & Hu, X. (2024). Preparation of liquid yogurt in the presence of pectin and its formation mechanism. *Food Chemistry, 452*, 139473.

## Supplementary materials

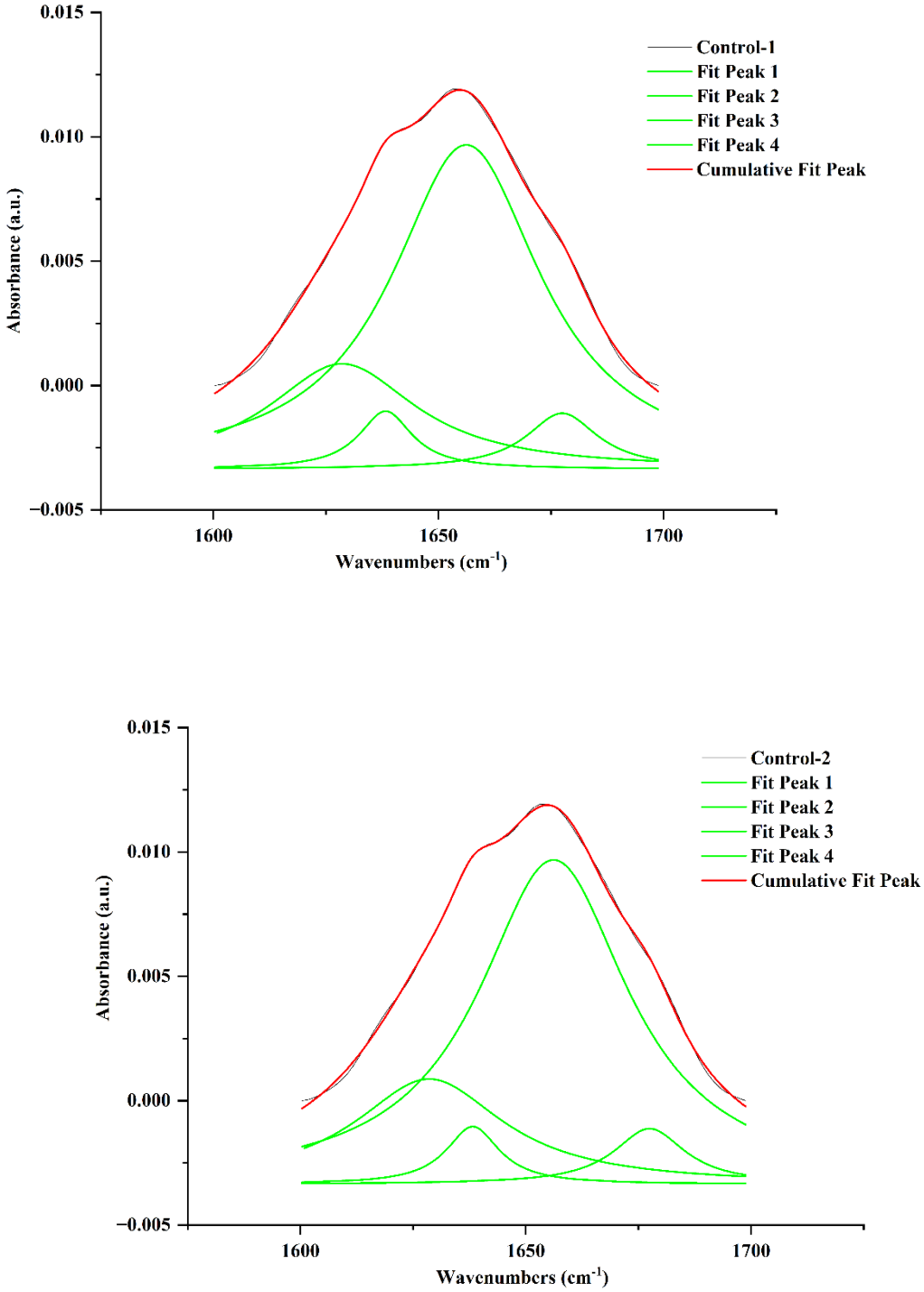



**Fig. S1-1 and S1-2.** Peak fitting of FTIR spectrum (Lorentz function) in the region of Amide I (1700–1600 $cm^{-1}$) of control MFGs/MFGM

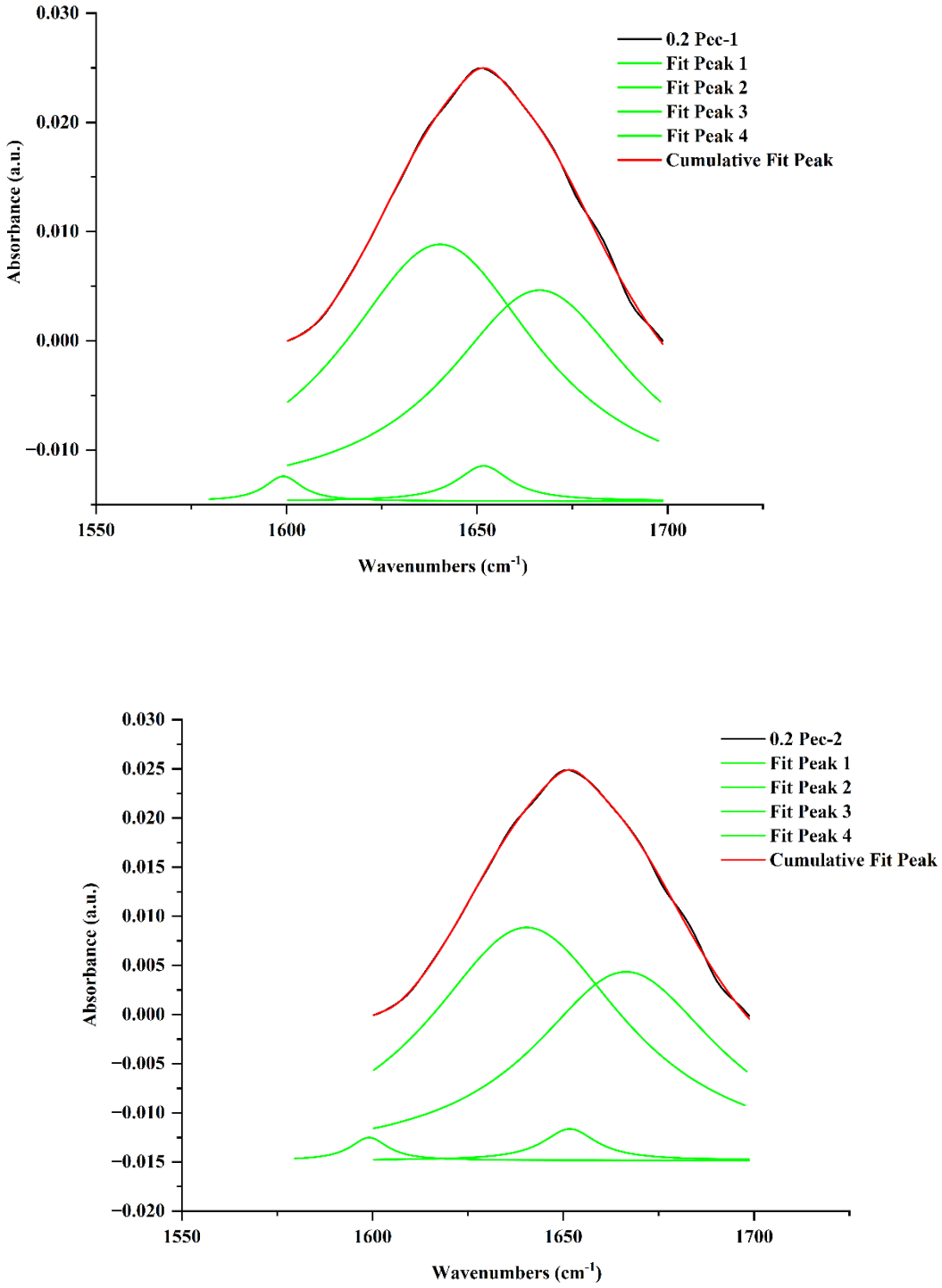



**Fig. S2-1 and S2-2.** Peak fitting of FTIR spectrum (Lorentz function) in the region of Amide I (1700–1600 $cm^{-1}$) of mixture of 0.2 % HMP (w/w) and MFGs/MFGM

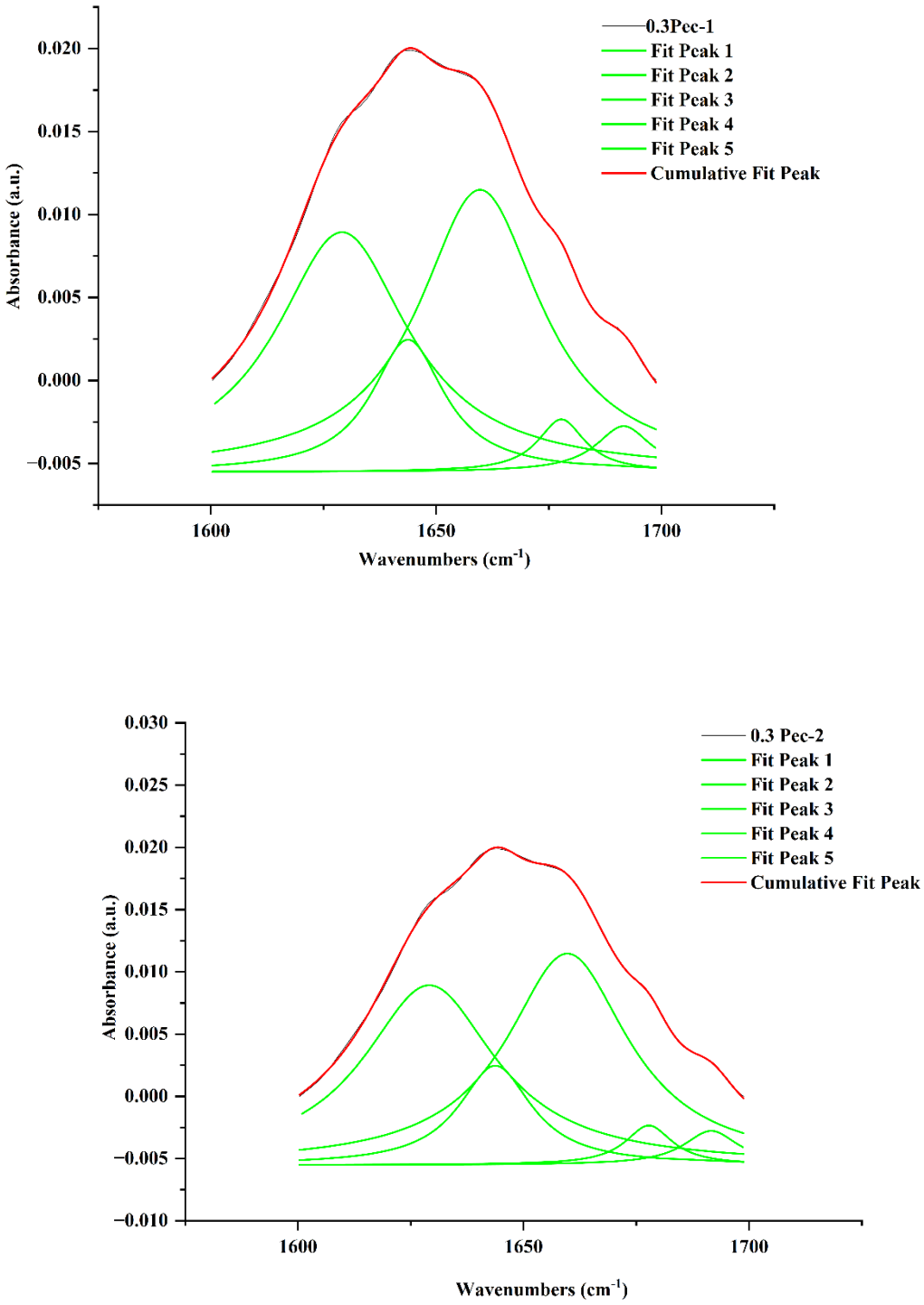



**Fig. S3-1 and S3-2.** Peak fitting of FTIR spectrum (Lorentz function) in the region of Amide I (1700–1600 $cm^{-1}$) of mixture of 0.3 % HMP (w/w) and MFGs/MFGM

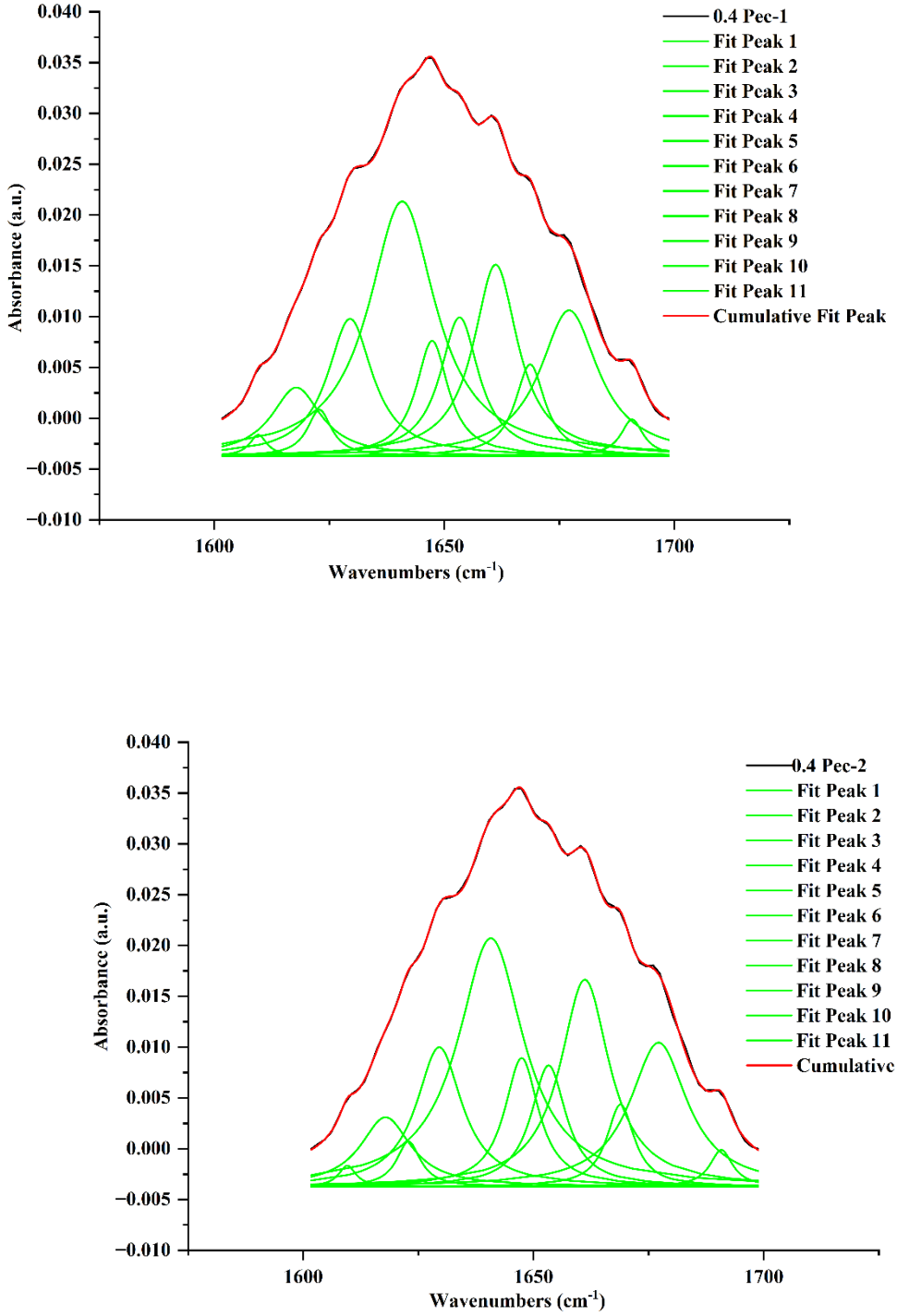



**Fig. S4-1 and S4-2.** Peak fitting of FTIR spectrum (Lorentz function) in the region of Amide I (1700–1600 $cm^{-1}$) of mixture of 0.4 % HMP (w/w) and MFGs/MFGM

# CHAPTER SEVEN

## General discussion

This thesis systematically investigated the changes in structure, composition, and techno-functionalities of MFGs and MFMG during the conventional dairy processing units, research on which remains scarce. Additionally, emerging non-thermal technique, ultrasound treatment, has been employed to modify the abovementioned properties of MFGs/MFGM. Specifically, **Chapter two** investigated the changes of MFGs structure and interfacial proteins prepared from pH-adjusted bovine raw milk during the cream separation, meanwhile, the skim milk phases were analysed. The pH-dependent interfacial properties and crystallisation behaviours of MFGs/MFGM materials related to the structural and compositional changes were studied accordingly in **Chapter three**. Moreover, MFGs/MFGM sourced from sweet whey was prepared to mimic the industrial MFGs/MFGM ingredients production. A comparative study was conducted to investigate the techno-functionalities of MFGs/MFGM materials isolated from ultrasonicated bovine milk. Specifically, the physical stability, interfacial properties, and thermal behaviours were characterized in **Chapter four and five**. **Chapter six** took a preliminary research on how the interactions between the HMP and MFGM proteins affect the stability and rheological properties of MFGs/MFGM emulsion.

## 7.1 Effect of acidification on the structure, composition, and techno-functionalities of MFGs/MFGM

### 7.1.1 Changes in the MFGs structure and MFGM proteins prepared from pH-adjusted bovine raw milk

Acidification-induced coagulation of milk protein has been extensively used in the dairy industry. In order to reduce the loss of MFGM proteins into the casein curd, Holzmüller, et al. (2016a) optimized the parameters for the preparation of MFGM materials from the buttermilk, particularly reducing the loss of the MFGM proteins into the casein curd. Additionally, pH-dependent functionalities of MFGM, including microstructure, rheological property, and the stability of lipid droplets, were investigated in previous research (Lopez, et al., 2017b). In those research, raw

materials for the MFGs or MFGM proteins preparation are by-products like buttermilk in which most MFGs are fragments rather than intact natural structure. To address this issue, untreated bovine milk was used as the raw material to prepare MFGs/MFGM via cream separation. Meanwhile, the commonly used pH conditions in dairy industries, pH 5.30 and 6.30, were used to pre-treat the raw milk with the citric acid solution prior to the separation. Compared to the size of fat globules in raw milk, cream samples presented the larger particles with the higher volume distribution values, including Dv (10), Dv (50), and Dv (90). Additionally, the magnitudes of Dv in pH 5.30 samples were significantly lower than control and samples with pH 6.30 ($p<0.05$). These findings indicated the mechanical force from centrifugation may damage the natural MFGM structure and aggregate to form the bigger globules with new membrane, thereby affected the size distribution of fat globules. Moreover, ζ- potential of cream samples decreased at pH 5.30 attributing to the increase in the exposure of negatively charged and/or hydrophobic areas (Sejersen, et al., 2007).

### 7.2.2 Characterization of the pH-dependent interfacial property and crystallisation behaviours of MFGs/MFGM materials

Dairy ingredients rich in MFGs/MFGM sourced from buttermilk or whey cream have been applied in IF products to mimic breast milk nutrition (Mohan, et al., 2020). The interfacial behaviour and thermodynamic properties of MFGs/MFGM ingredients play crucial roles in the powder product functionalities and shelf life. The change of structure and compositions of MFGs/MFGM induced by acidification may further affect these techno-functionalities. After the cream separation, centrifugation was employed to enrich the MFGs/MFGM from acidified bovine raw milk (pH 5.30 and pH 6.30). Meanwhile, MFGs/MFGM materials prepared from the sweet whey were prepared to mimic the industrial production and make the comparative analysis. According to the CLSM, rare intact globules were observed in the MFGM-C samples due to the mechanical treatments in the cheese process. Additionally, MFGM-C presented the higher absorbance in the ranges of 1700–1600 $cm^{-1}$ (Amide I protein)

and 1600–1500 $cm^{-1}$ (Amide II protein) identified by FTIR which was consistent with the higher proteins content of MFGM-C than MFGs/MFGM sourced from bovine milk. X-ray Diffraction Spectra (XRD) showed that fewer α and β' crystals appeared at pH 6.30 compared to control and pH 5.30 samples, and there were no detectable crystalline structures in MFGM-C. Additionally, the smallest heat enthalpy of crystallization ($\Delta H_C$) and melting ($\Delta H_M$) was observed in MFGM-C, followed by those at pH 6.30. By comparison, pH 6.30 induced more pronounced effects on the interfacial properties and thermal behaviours of MFGs/MFGM than pH 5.30 treatment.

## 7.2 Effect of ultrasonic treatment on the structure, composition, and techno-functionalities of MFGs/MFGM

### 7.2.1 Comparative study of interfacial properties and thermal behaviour of milk fat globules and membrane prepared from ultrasonicated bovine milk

The food industry has increasingly adopted non-thermal technologies, driven by consumer demand for products that are perceived as natural and minimally processed. Ultrasonic treatment is one of the most potent techniques that could be used in dairy processing. Low-frequency ultrasounds induce strong cavitation effects by forming and violent collapsing of bubbles in the solution, which is usually used to produce smaller particles, facilitate fat separation, improve the emulsion properties and adjust the crystallization behaviour of anhydrous milk fat (AMF) (Martini, et al., 2008; Juliano, et al., 2011; Leong, et al., 2014a; Leong, et al., 2014b; Krasulya, et al., 2016). In spite of the positive effects induced by the ultrasonic treatment, we are still unaware of any studies on the impact of high-intensity/low-frequency ultrasound on the interfacial properties, crystal transformation, crystallization and melting characteristics of the MFGs/MFGM materials.

We prepared the MFGs/MFGM samples from ultrasonicated bovine milk treated by low-frequency sonication. Specifically, 20 kHz and 40 kHz, was applied independently or synchronously on the bovine milk before the MFGs/MFGM

separation. Subsequently, interfacial properties were analysed indicated by the particle characterization, interfacial tension, surface charges and the surface hydrophobicity ($H_0$) of MFGs/MFGM. In addition, crystal forms, crystallization and melting of MFGs/ MFGM samples were investigated using the XRD and DSC. A significant increase in the volume density (%) of smaller particles (1-10 μm) was observed in the MFGs/MFGM materials prepared from ultrasonic treatments at 20 kHz/ 5 min and 20 + 40 kHz/ 5 min, accompanied by the significantly decreased the surface hydrophobicity ($H_0$) ($p<0.05$). 40 kHz/5 min MFGs/MFGM showed significantly higher ζ- potential compared to the other MFGs/MFGM ($p<0.05$) due to the more detectable negative charges. Additionally, ultrasonic treatments decreased the interfacial tension ($\pi$) between the air and MFGs/MFGM liquid phase. As the ultrasonic duration prolonged from 5 min to 15 min, 20 kHz ultra-sonicated treatments decreased the diffusion rate ($k_{diff}$) of MFGs/MFGM interfacial compositions significantly ($p<0.05$) but did not affect the adsorption or penetration rate ($k_a$) ($p>0.05$). Three typical crystal forms, α-crystal, β-form and β'-form, were observed in control and ultrasonicated 5 min MFGs/MFGM, but α-crystal disappeared in all the 15 min treated MFGs/MFGM. Ultrasonic duration has a more profound effect on the increase of β'- crystal than the intensity. Ultrasonic treatments promoted the crystallisation of MFGs/MFGM fat at higher temperature but increased the melting temperature of MFGs/MFGM.

### 7.2.2 Modifying physicochemical properties, rheology and creaming stability of milk fat globule and membrane through ultrasound treatment

MFGM ingredients are employed as a natural emulsifier in dairy industry, capitalizing on the amphipathic nature of polar lipids and glycoproteins. Moreover, the rheological properties of milk system are critical for processing efficiency in the dairy industry. An in-depth understanding of the rheological behaviours of milk liquids is essential for the design and evaluation of process units and operational equipment, such as the heat exchangers, heating and cooling rates, and the pressure losses in

pipelines (Velez-Ruiz, et al., 1997). A follow-up research on the physicochemical and rheological properties, as well as the emulsions stability of MFGs/MFGM was conducted to further understand the techno-functionalities induced by the ultrasonic treatment.

More pronounced changes in the regions of Amide II (1600−1500 $cm^{-1}$), Amide III (1500−1200 $cm^{-1}$), and fingerprint region (1200−1900 $cm^{-1}$) in MFGs/MFGM were observed in the 5 min ultrasonic duration compared to 15 min treatment. The PCA results for Amide I showed that the 15-min treatments grouped with the controls, while the control MFGs/MFGM formed a separate group. However, a qualitative analysis of the protein secondary structures within Amide I produced inconsistent results. Specifically, the 15 min treatments caused more pronounced changes in the intramolecular β-sheet, random coil, and α-helix structures compared to the 5-min treatments. This discrepancy highlights the necessity for further research to clarify the underlying causes of these contradictory findings. All the MFGs/MFGM exhibited shear-thinning behaviour, except for the 40 kHz treated MFGs/MFGM, which displayed non-Newtonian behaviour at the lower shear rate, as indicated by flow behaviour indexes (n), of 1 or close to 1, regressed from the Herschel-Bulkley model. 20 + 40 kHz/ 15 min treatment led to the aggregation of membrane proteins indicated by the CLSM images, suggesting the decline in the physical stability. This differentiation underscores the potential of specific ultrasonic treatment parameters to precisely modify dairy product characteristics, which could be pivotal for optimizing processing strategies in the dairy industry.

## 7.3 Effect of HMP addition on the structure, composition, and techno-functionalities of MFGs/MFGM

In the dairy industry, pectin is commonly used as a thickener or gelling agent in yogurts to improve texture and prevent whey separation. High-methoxyl pectin (HMP) is particularly used to prevent milk protein flocculation in acidified milk drinks. Additionally, pectin can form coacervates with caseins or whey proteins, thereby

enhancing their techno-functional properties. In fat-reduced products, whey protein-pectin complexes created through thermomechanical treatment act as fat replacers, improving the creaminess of the products (Filla, et al., 2023b). The interactions between casein micelles and pectin are complex and have been extensively studied (Wusigale, et al., 2020). The interactions between pectin and MFGM proteins, which may also influence the stabilization of food systems, have not yet been investigated. Our study examined the effect of adding HMP to raw milk on the structural and compositional changes of milk fat globules (MFGs) or MFGM during the cream separation process. Additionally, we investigated the techno-functional properties, such as physical stability and rheological characteristics, to provide a theoretical basis and support for industrial applications.

The results indicated that adding 0.30% HMP facilitated the formation of conjugates between HMP and milk proteins, resulting in larger particle sizes ranging from 10 to 100 μm. This treatment also led to a lower ζ-potential, suggesting an increased number of positively charged casein micelles adsorbed onto the fat globules. Additionally, the incorporation of HMP enhanced absorbance at the Amide I and Amide II bands and altered the fingerprint regions, with new peaks emerging at 1055–1048 $cm^{-1}$. The formation of coacervates between HMP and milk proteins was also evidenced by the reduced density of PAS III, CD 36, and BTN in the upper layers of MFGs/MFGM with 0.40% HMP. These structural and compositional changes induced by HMP affected the physical stability and rheological properties of MFGs/MFGM. Notably, MFGs/MFGM with 0.30% HMP exhibited the poorest stability, a significant increase in apparent viscosity, and shear-thinning behavior throughout the analysis.

### 7.4 Overall conclusions

The context of this thesis systematically investigated the structural, compositional, and techno-functionalities change of MFGs/MFGM prepared from bovine raw milk treated with acidification, ultrasonic treatment, and HMP addition using cream separator and ultra-centrifugation. Specifically, particle size and CLSM were

employed to analysis the structural changes of MFGs or MFGM visually; the results of ζ-potential, interfacial tension (π), surface hydrophobicity ($H_0$) indicated the surface change on the surface of the fat globules; the thermal behaviours and fat crystallization were evaluated by the XRD and DSC techniques. Based on all the results and discussion, the main conclusions of this research are listed as follows:

- pH 5.30 significantly decreased the particle size of MFGs/ MFMG more than 6.30 due to the damage of the natural MFGM structure and formation of larger fat globules with new membrane during cream separation **(Chapter 2)**.
- At pH 6.30, MFGs/MFGM materials presented more peaks in the fingerprint regions belonging to the protein-lipids associations with lower interfacial tension than at pH 6.70 and 5.30. X-ray Diffraction Spectra (XRD) showed fewer α and β' crystals at pH 6.30 with the smallest heat enthalpy of crystallization ($\Delta H_C$) and melting ($\Delta H_M$) **(Chapter 3)**.
- MFGM-C from cheddar whey had different structures and techno-functionalities, with no detectable crystalline structures, rare intact globules , and higher absorbance in the ranges of 1700−1600 $cm^{-1}$ (Amide I protein) and 1600−1500 $cm^{-1}$ (Amide II protein) identified by FTIR **(Chapter 3)**.
- Ultrasonic treatment at 20 kHz/ 5 min and 20 + 40 kHz/ 5 min increased the volume density (%) of smaller particles (1-10 μm) and significantly decreased the surface hydrophobicity ($H_0$) ($p<0.05$). 40 kHz/5 min MFGs/MFGM showed significantly higher ζ- potential compared to the other MFGs/MFGM ($p<0.05$) due to the more negative charges. Ultrasonic treatments also reduced interfacial tension (π) between the air and MFGs/MFGM liquid phase. With the duration of ultra-sonicated for 15 min, 20 kHz ultra-sonicated treatments decreased the diffusion rate ($k_{diff}$) of MFGs/MFGM interfacial compositions significantly ($p<0.05$) but did not affect the adsorption or penetration rate ($k_a$) ($p>0.05$) **(Chapter 4)**..
- Three typical crystal forms—α-crystal, β-form, and β'-form—were observed in all MFGs/MFGM, but α-crystal disappeared after 15 min of ultrasonic treatment.

Ultrasonic treatments promoted fat crystallization at higher temperatures and increased melting temperature **(Chapter 4)**.

- More pronounced changes in Amide II (1600−1500 $cm^{-1}$), Amide III (1500−1200 $cm^{-1}$), and fingerprint region (1200−1900 $cm^{-1}$) in MFGs/MFGM were observed after 5 min ultrasonic treatment, while 15 min treatments affected the intramolecular β-sheet, random coil, and α-helix structures more. 20 + 40 kHz/ 15 min treatment led to aggregated membrane proteins, indicating by the CLSM images and the decline in the physical stability. Most MFGs/MFGM exhibited shear-thinning behaviour, except the 40 kHz treated MFGs/MFGM, which showed non-Newtonian behaviour at the lower shear rate **(Chapter 5)**.
- HMP addition enhanced absorbance at the Amide I and Amide II bands and altered the fingerprint regions, with new peaks emerging at 1055–1048 $cm^{-1}$. Larger particle sizes ranging from 10 to 100 μm presented in the 0.30% HMP MFGs/MFGM, suggesting the formation of conjugates between HMP and milk proteins. This finding was also evidenced by the reduced density of PAS III, CD 36, and BTN in the upper layers of MFGs/MFGM with 0.40% HMP. These structural and compositional changes induced by HMP affected the physical stability and rheological properties of MFGs/MFGM. Notably, MFGs/MFGM with 0.30% HMP exhibited the poorest stability, a significant increase in apparent viscosity, and shear-thinning behavior throughout the analysis **(Chapter 6)**.

## 7.5 Industrial application prospect and future work

- Lab-scale centrifugation or ultracentrifugation used to isolate MFGs/MFGM materials may not accurately represent industrial processes. Research methods that better simulate industrial production are needed. Maintaining the natural membrane state of MFGs during isolation and processing is essential due to its crucial role in physiological properties. Factors affecting the structure, composition, and techno-functionalities of MFGs/MFGM require deeper exploration, especially from an

industrial application perspective, to fully harness their potential in food science and nutrition.

- Considering that some analysis methods may alter the structure or composition of MFGs, it is necessary to develop more non-invasive methods for real in situ observation. Further studies should systematically track the effects of industrial processing units on the physicochemical properties and functionalities of MFGs/MFGM products.
- Specific ultrasonic treatment parameters need to be identified to modify dairy product characteristics in targeted ways, which is crucial for optimizing processing strategies in the dairy industry
- The mechanisms underlying the formation of coacervates between MFGM components and pectin need to be investigated, aiming to better understand how these coacervates affect the techno-functional properties of MFGM components.

**Reference**

Filla, J. M., & Hinrichs, J. (2023). Processing of whey protein-pectin complexes: Upscaling from batch lab scale experiments to a continuous technical scale process. *Journal of Food Engineering, 347*, 111437.

Holzmüller, W., Gmach, O., Griebel, A., & Kulozik, U. (2016). Casein precipitation by acid and rennet coagulation of buttermilk: Impact of pH and temperature on the isolation of milk fat globule membrane proteins. *International Dairy Journal, 63*, 115-123.

Juliano, P., Kutter, A., Cheng, L. J., Swiergon, P., Mawson, R., & Augustin, M. A. (2011). Enhanced creaming of milk fat globules in milk emulsions by the application of ultrasound and detection by means of optical methods. *Ultrasonic Sonochemistry, 18*(5), 963-973.

Krasulya, O., Bogush, V., Trishina, V., Potoroko, I., Khmelev, S., Sivashanmugam, P., et al. (2016). Impact of acoustic cavitation on food emulsions. *Ultrasonic Sonochemistry, 30*, 98-102.

Leong, T., Johansson, L., Juliano, P., Mawson, R., McArthur, S., & Manasseh, R. (2014a). Design parameters for the separation of fat from natural whole milk in an ultrasonic litre-scale vessel. *Ultrasonic Sonochemistry, 21*(4), 1289-1298.

Leong, T., Juliano, P., Johansson, L., Mawson, R., McArthur, S. L., & Manasseh, R. (2014b). Temperature effects on the ultrasonic separation of fat from natural whole milk. *Ultrasonic Sonochemistry, 21*(6), 2092-2098.

Lopez, C., Cauty, C., Rousseau, F., Blot, M., Margolis, A., & Famelart, M. H. (2017). Lipid droplets coated with milk fat globule membrane fragments: Microstructure and functional properties as a function of pH. *Food Research International, 91*, 26-37.

Martini, S., Suzuki, A. H., & Hartel, R. W. (2008). Effect of High Intensity Ultrasound on Crystallization Behavior of Anhydrous Milk Fat. *Journal of the American Oil Chemists' Society, 85*(7), 621-628.

Mohan, M. S., O'Callaghan, T. F., Kelly, P., & Hogan, S. A. (2020). Milk fat: opportunities, challenges and innovation. *Critical Reviews in Food Science and Nutrition*, 1-33.

Sejersen, M. T., Salomonsen, T., Ipsen, R., Clark, R., Rolin, C., & Engelsen, S. B. (2007). Zeta-potential of pectin-stabilised casein aggregates in acidified milk drinks. *International Dairy Journal, 17*(4), 302-307.

Velez-Ruiz, J., & Barbosa-Canovas, G. (1997). Effects of concentration and temperature on the rheology of concentrated milk. *Transactions of the ASAE, 40*(4), 1113-1118.

Wusigale, Liang, L., & Luo, Y. (2020). Casein and pectin: Structures, interactions, and applications. *Trends in Food Science & Technology, 97*, 391-403.

**APPENDIX**

**Publications**

Trends in Food Science & Technology 150 (2024) 104570

Contents lists available at ScienceDirect

Trends in Food Science & Technology

journal homepage: www.elsevier.com/locate/tifs

# A review of factors affecting the structure, compositions, and the techno-functionalities of bovine milk fat globule and membrane

Yanjun Sun [a,b], Yrjö H. Roos [b], Song Miao [a,c,*]

[a] Teagasc Food Research Centre, Moorepark, Fermoy, Co. Cork, Ireland
[b] School of Food and Nutritional Sciences, University College Cork, Cork, Ireland
[c] China-Ireland International Cooperation Centre for Food Material Sciences and Structure Design, Fujian Agriculture and Forestry University, China

ARTICLE INFO

Handling Editor: Dr I Oey

*Keywords:*
Milk fat globule
Milk fat globule membrane structure
Membrane compositions
Heating treatment
Homogenization
Non-thermal processing

ABSTRACT

*Background:* Dairy powders enriched with milk fat globules (MFGs) and milk fat globule membrane (MFGM) materials are gaining interest in food industry due to their bioactive benefits, including the promotion of brain development and cognitive functions, as well as improvements in gut health and immunity. MFGs/MFGM ingredients have been incorporated into infant formula (IF) to bridge the nutritional gap between formula and breast milk. The structure and composition of MFGs/MFGM ingredients significantly influence their functionalities and physiological properties.

*Scope and approach:* This review provides an update on recent research concerning the factors influencing the structure, composition, and functionalities of MFGs/MFGM ingredients, including the species, lactation stage and feeding methods. Additionally, conventional separation methods are discussed versus novel membrane filtration techniques. The main part of this review covers the recent progress and trends arising from the influence of the industrial dairy produce units, including thermal treatment and low temperature storage, homogenization, and non-thermal processes.

*Key findings and conclusions:* Variability in reports on the structure and composition of MFGs/MFGM across studies poses challenges in discerning whether these differences arise from varied processing techniques or analytical methods. Establishing standard analytical methods remains an ongoing research topic. By-products such as cheese whey or buttermilk continue to serve as primary raw materials for the preparation of MFGs/MFGM ingredients in the industry. Studies on the preparation of MFGs/MFGM materials while maintaining their natural state are relatively limited. Further research into the structural and compositional changes of MFGs/MFGM during food processes is essential, as it has the potential to provide the key information on their physiological properties and tech-functionalities.

## 1. Introduction

Raw milk is a complex oil-in-water emulsion where milk fat is dispersed as globules, termed milk fat globules (MFGs). The diameter of MFGs in untreated raw milk ranges from 0.2 to 15 μm, with an average of 3–4 μm. MFGs are biosynthesised by encapsulating triacylglycerol (TAG) within lipid droplets, which are surrounded by a tri-layered membrane known as the milk fat globule membrane (MFGM) (Heid & Keenan, 2005).

Recent studies have proposed MFGs/MFGM ingredients as potential nutraceuticals in infant formula (IF), particularly due to their enrichment with phospholipid, ganglioside, and glycoprotein. Extensive research has demonstrated their health benefits in the food and pharmaceutical industries. Raza, Herzig, and Leppaluoto (2021) provided a comprehensive review of the clinical and physiological impacts of MFGM components throughout the lifespan, highlighting their roles in neurodevelopment, cardio-metabolic health, and frailty in older adults. The technological functionalities of MFGM, such as emulsification and probiotics encapsulation, are also gaining research interest (Fontecha et al., 2020). For instance, MFGM glycoproteins have been used in the encapsulation of *Lactobacillus*, with the size of the bacteria being a critical consideration in liposome designing to ensure complete encapsulation (Guerin, Burgain, Gomand, Scher, & Gaiani, 2019). Additionally, the glycoconjugates in milk are the primary macromolecules that

* Corresponding author. Teagasc Food Research Centre, Moorepark, Fermoy, Co. Cork, Ireland.
*E-mail address:* Song.Miao@teagasc.ie (S. Miao).

https://doi.org/10.1016/j.tifs.2024.104570
Received 8 April 2024; Received in revised form 23 May 2024; Accepted 3 June 2024
Available online 3 June 2024
0924-2244/© 2024 Elsevier Ltd. All rights are reserved, including those for text and data mining, AI training, and similar technologies.

prevent the adhesion of enteropathogens, known as the anti-adhesive ability. Conventional milk processing techniques, including heating and homogenization, can modify the adhesive properties of MFGM by regulating the release and conformation of its glycoconjugates (Douellou, Montel, & Thevenot Sergentet, 2017).

Bridging the nutritional gap between IF and breast milk remains a priority for dairy enterprises. Fat is a crucial nutritional component in IF, contributing approximately 50% of the energy required for the infants' growth and development. Human milk contains around 200 types of fatty acids, ranging from C4:0 to C26:0 (Mansson, 2008). Industrially, whole fat milk, anhydrous milk fat, or cream serves as excellent fat sources for IF nutritional fortification. The polar lipid profile of bovine milk has been reported to be more similar to human milk than that in soybean and sunflower kernels (van Nieuwenhuyzen & Tomás, 2008), eggs (Blesso, 2015) (Fig. 1). However, compared with human milk, bovine milk contains higher levels of saturated fatty acid (De Bhowmick, Guieysse, Everett, Reis, & Thum, 2023). To compensate for the nutritional shortcomings of milk fat with low levels of unsaturated fatty acids, vegetable oil with various chains of fatty acids are supplemented in IF products. According to the labels of IFs sold in the markets, these commonly include coconut oil, corn oil, soybean oil, canola oil, palm olein oil, and high oleic sunflower oil. In addition, *Moretierella* alpine oil and *Schizochytrium* sp. Oil are also noted in a few IF products, which are sources for arachidonic acid (ARA) and docosahexaenoic acid (DHA), respectively. Efforts to develop IF that is nutritionally close to breast milk have led to significant improvements, although some challenges remain, such as the deficiency in biogenically important compositions like MFGM-phospholipids or glycoproteins.

To date, several dairy giants like Fonterra, Arla, Hilmar, and FrieslandCampina, have introduced whey protein concentrate (WPC) enriched with MFGM components, emphasizing mainly the bioactive phospholipids. The typical components of commercial WPC ingredients produced by Arla (MFGM-10) and Friesland (Vivinal) are shown in Table 1. Total phospholipids in both products are approximately 6–10 %, and most of the compositions, about 65–76 %, are proteins. These WPC products, derived from cheese whey or butter milk (Fig. 2), are extensively applied in IF and yogurts targeted at the children's market. In China, a leading consumer of IF products, ongoing research efforts aim to address the imperfect quality standards for MFGM ingredients manufacturers and resolve the discrepancies in composition resulting from different processing methods, as noted in the 'Scientific consensus on milk fat globule membrane and its ingredients' (Wang et al., 2022). The consensus also points out the unsound analytical method for glycoproteins analysis. As outlined in the consensus, current research predominately explores the physiological properties of MFGs/MFGM. However, the specific functional components linked to health benefits are still unclear. Bioactive proteins or lipids in MFGs/MFGM are crucial not only for their health benefits but also for their techno-functional properties. A comparative analysis of their physiological and processing characteristics is essential to better understand their composition and structure. Nevertheless, the variability in the research results on MFGs/MFGM structure and compositions complicates the comparison between studies. Holzmüller and Kulozik (2016) suggest that the inconsistent reports on the MFGs/MFGM might be due to varied separation techniques. Moreover, natural variables such as cow's age, diet, breeds, health condition, as well as lactation stage, significantly affect the characterisation of MFGs/MFGM (Li, Delger, Dave, Singh, & Ye, 2022), as do the methods used in sample preparation and analysis (Wang, Qiao, Gao, Jiang, & Mu, 2021).

In summary, this review underscores the diverse research results on structure and compositions of MFGs/MFGM. There is a growing focus on their nutritional and techno-functional properties, particularly in infant and children products. Consequently, it is necessary to critically review both past and recent studies on the factors influencing MFGs/MFGM. In particular, the most frequently used industrial dairy processing units were compiled, including thermal treatment, homogenization, centrifugation, membrane filtration, and emerging non-thermal treatments. Additionally, this review provides an updated overview of other

**Table 1**
Typical compositions of commercial whey protein concentrate (WPC) enriched with phospholipids.

| Indicative values | MFGM-10 (Arla) | Vivinal (Friesland) |
|---|---|---|
| Protein (N*6.38) % | 69–76 | 65–72 |
| Fat % | 16–22 | 15–21 |
| Phospholipids % | 6–10 | 6–10 |
| Phosphatidyl ehtanolamine (PE)% | 1.9 | 2.4 |
| Phosphatidyl choline (PC)% | 1.8 | 2.2 |
| Phosphatidyl inositol (PI)% | 0.5 | 0.5 |
| Phosphatidyl serine (PS)% | 0.8 | 0.8 |
| Sphingomyelin ( SM ) % | 1.9 | 2.1 |

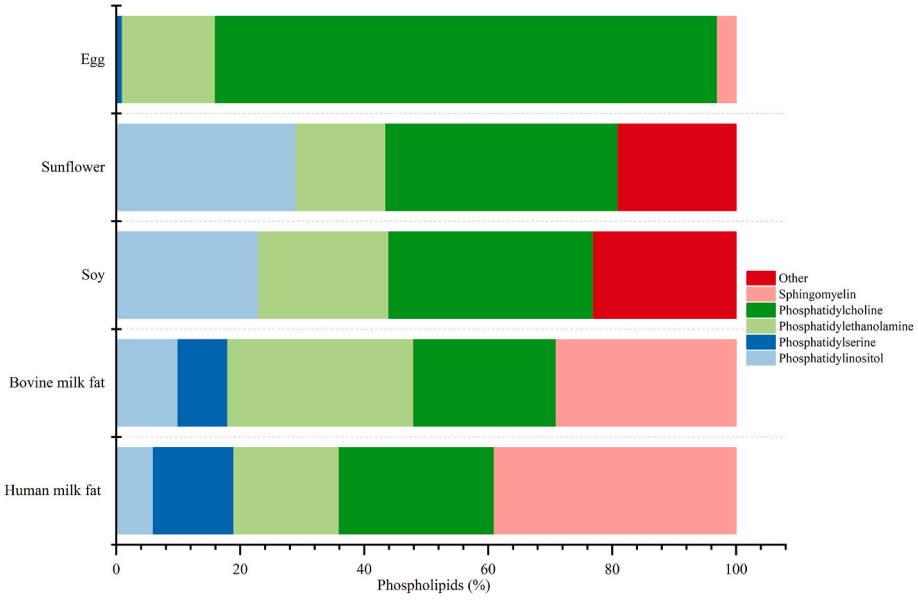



**Fig. 1.** Relative proportion of polar lipids (% of polar lipids) from human and bovine milk (Baars et al., 2016; Cilla, Diego Quintaes, Barberá, & Alegría, 2016), soybean and sunflower kernels (van Nieuwenhuyzen & Tomás, 2008), eggs (Blesso, 2015).

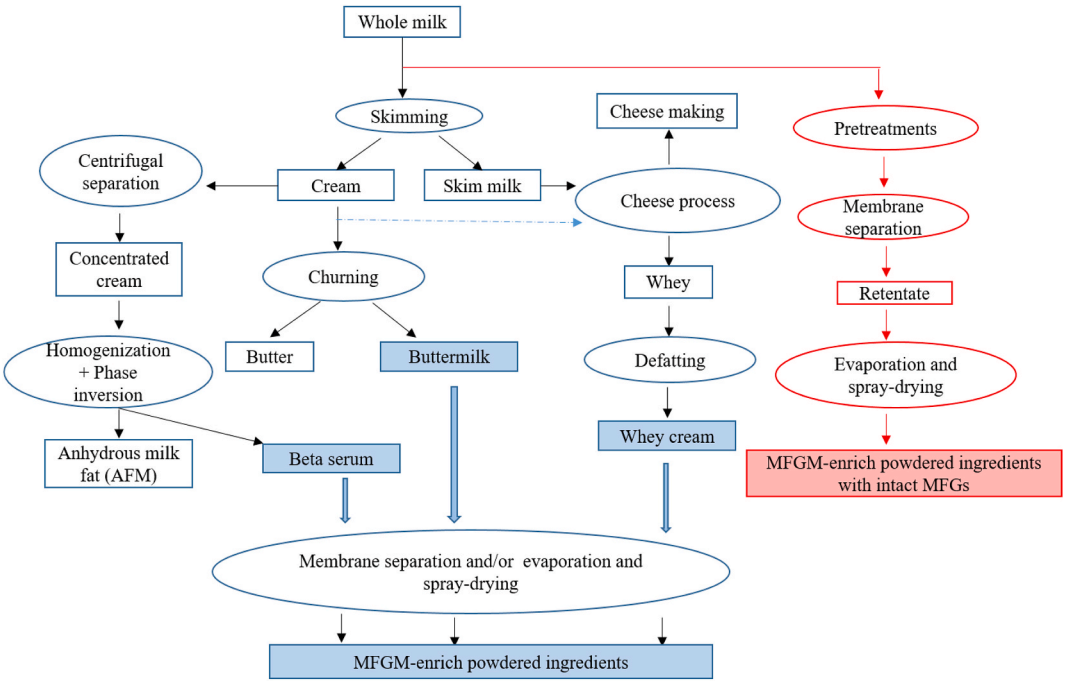



**Fig. 2.** Schematic processing of MFGM-enrich powdered ingredients from whole milk, beta serum, buttermilk and whey cream.

influential factors, such as animal species, feeding systems, and the lactation stage. Before the aforementioned discussion, this review begins with a short update on the identification of the structure and compositions of MFGs/MFGM.

## 2. Update on the structure and compositions of MFGs/MFGM

In this review, the discussion of the structure of MFGs is primarily focused on the membrane, as the core of MFGs mainly consists of triglycerides containing different fatty acids. The typical structure of MFGs and MFGM is shown in the schematic diagram Fig. 3. Each MFG contains about 96 % triglycerides, enveloped by a three-layered membrane with outer double layers and an inner monolayer. Approximately 2–6% mass of MFG is the membrane, in which 90% of the dry weight is proteins and polar lipids (Singh, 2006).

### 2.1. Polar lipids

Recent studies have highlighted that MFGM is a dynamic system containing complex types of polar lipids (40.6 % of each MFG). These heterogeneous polar lipids are distributed asymmetrically across the surface of the membrane (Lee et al., 2018). Although they represent only 0.2–1% of total milk lipids, they accounts for 26–40% of the lipids in MFGM (Fong, Norris, & MacGibbon, 2007). Polar lipids are categorized into three main types based on the structure of their fatty acid: glycerophospholipids, sphingomyelin, and glycosphingolipids. In glycerophospholipids, two fatty acids bond with glycerol at C-1 and C-2, while the C-3 position is linked to a phosphate group that may be bound to choline, inositol, serine, or ethanolamine group, forming phosphatidylcholine (PC), phosphatidylinositol (PI), phosphatidylserine (PS), and phosphatidylethanolamine (PE), respectively. Sphingomyelin (SM) is similar in structure to PC, replacing glycerol with a sphingosine group.

Both SM and PC are zwitterionic, contributing to their localization

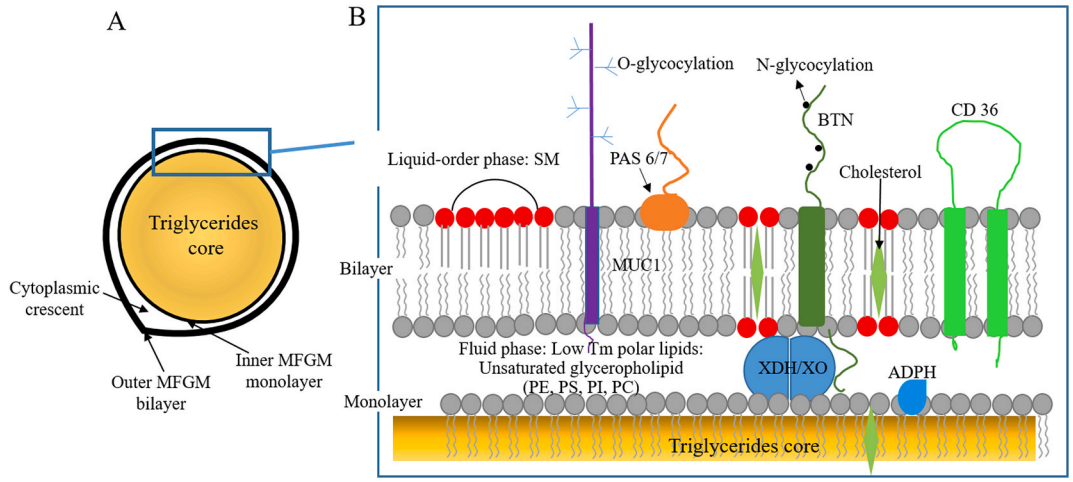



**Fig. 3.** Three-dimensional structure of milk fat globule (A) (Chai, Oh, & Imm, 2022); Schematic diagram of fat globule with arrangement of lipids and membrane proteins (B) (Dewettinck et al., 2008; Holzmüller & Kulozik, 2016; Lopez, Cauty, & Guyomarc'h, 2015).

primarily in the outer layer of the membrane, whereas PI, PE, and PS, which are anionic, are predominantly found on the inner membrane surface (Deeth, 1997). Cholesterol is interspersed within both the triacylglycerol phase and the bilayer membrane. Additionally, glycolipids and glycoproteins are randomly distributed on the outer membrane surface, rather than being confined to lipid crafts (Lopez, Madec, & Jimenez-Flores, 2010) (Fig. 3). The membrane encompasses two coexisting lipids phrases: a fluid matrix in a liquid disorder phrase and a liquid-order phrase. SM and saturated glycerol-phospholipids are the main components in the liquid order phrase, contributing to its higher phase transition temperature ($T_m$). Conversely, the liquid- disorder phase comprises glycerol phospholipids, which required less energy to undergo conformational changes due to their lower $T_m$ and less breakthrough force is needed to change conformation (Lopez, 2011).

The distribution of fatty acids within the MFGs varies, with palmitic acids (C16:0) and stearic acids (C18:0) found predominantly in the monolayer structure of MFGM. Major fatty acids associated with glycerol phospholipids include C16:0, C18:0, C18:1, and C18:2. Additionally, a significant amount of long-chain fatty acids (C20:0, C22:0, C23:0, C24:0, and C24:1) are present in SM, explaining its higher melting point and interaction with the cholesterol rigid domains in the bilayer membrane (Fong et al., 2007).

### 2.2. Membrane proteins

Membrane proteins account for approximately 25–70% of the mass of MFMG materials and about 1% of the total protein mass in milk (Holzmüller & Kulozik, 2016). In the early 1980s, the Milk Protein Nomenclature Committee published a proposal on the MFGM proteins classification scheme based on the molecular weight, staining characteristics, and protein mobility observed in sodium dodecyl sulphate polyacrylamide gel electrophoresis (SDS-PAGE) bands (Basch, Greenberg, & Farrell, 1985). Mather (2000) summarized the identities, characteristics, and sequences of the major MFGM-associated proteins. Currently, eight major proteins are commonly used to characterise the MFGM proteins, including mucin 1 (MUC1), periodic acid Shciff 3 (PAS3), cluster of differentiation 36 (CD36), butyrophilin (BTN), lactadherin or periodic acid Schiff 6/7 (PAS6/7), the redox enzyme xanthin oxidase/dehydrogenase (XO/XDH), adipophilin (ADPH) and fatty acid binding protein (FABP).

Utilizting a 1-dimensional SDS-PAGE combined with micro-capillary high-performance liquid chromatography equipped with a nanospray-tandem mass spectrometer, Reinhardt and Lippolis (2006) identified up to 120 membrane proteins. More recently, proteomic techniques have enabled the identification of as many as 616 types of membrane protein in bovine MFG (Wang, Cao, et al., 2021). These membrane proteins are highly glycosylated and are distributed at specific locations within the MFGM through various group bindings. BTN and CD 36 are integral or transmembrane proteins that span the bilayers. whereas PAS 6/7 is a periphery protein loosely attached to the outer surface of the bilayers; ADPH is located on the monolayer surface, and XDH/XO is positioned between the bilayers and monolayer (Evers, 2004; Mather, 2000) (Fig. 3).

More non-invasive analytical techniques have been applied to describe the lipid and protein domains of MFGM, such as confocal laser scanning microscopy (CLSM), Fourier transform infrared spectroscopy (Sun, Roos, & Miao, 2022), and atomic force microscopy (AFM) (Obeid et al., 2019). These techniques, alongside proteomics and lipidomics, facilitate qualitative and quantitative analyses of MFGM compositions. Despite the technical advancements, variations in analysis techniques and sample preparation methods continue to introduce uncertainties in the structural and conformational analysis of MFGs/MFGM.

### 2.3. Other compositions

Various saccharides such as protein-bound N-acetylglucosamin, manose, and fucose form glycosylation complexes by bonding with membrane proteins and lipids. These saccharides constitute critical bioactive components in MFGM and significantly contribute to its physiological effects. Oligosaccharides such as galactose, glucose, and sialic acid have been identified in glycolipids (Smoczyński, Staniewski, & Kiełczewska, 2014). Additionally, trace amounts of lipid-soluble vitamins and β-carotene are present in the triglyceride phase. Furthermore, several bioactive compounds found in milk, such as phosphodiesterase, 5′-nucelotidase, immunoglobulins, casein, or whey protein, have also been detected in MFGM. However, their presence may be attributed to the contamination during the separation and preparation process (Mather, 2000).

## 3. Factors affecting the structure, compositions, and techno-functionalities of MFGs/MFGM

### 3.1. Biosynthesis, species, lactation stage, and feeding system

- *Biosynthesis*

The biosynthesis of MFGM is primarily initiated on the plasma membrane (PM) because of its remarkably similar compositions to PM (Keenan, Morré, Olson, Yunghans, & Patton, 1970). However, subsequent studies in the 1980s, such as those by Kanno, Hattori, and Yamauchi (1987), identified membrane proteins and polypeptides in MFGM that were absent in PM, suggesting that PM is not the solely origin source.

The structure of MFGs/MFGM begins to alter during the secretion process (Holzmüller & Kulozik, 2016). Following the biosynthesis on PM, most MFGM proteins undergo posttranslational modifications (PTMs), which refers to the amino acid side chain modifications. PTMs are critical for regulating diverse cellular activities due to their regulatory impact at the molecular level. In addition, phosphorylation plays a vital role in regulating enzyme activities, membrane channels, and various proteins (Ramazi & Zahiri, 2021). Phosphorylation involves the transfers of a phosphate group from adenosine triphosphate to receptor residues, a reaction catalysed by kinase enzymes.

- *Species and lactation stage*

MFGs/MFGM exhibit significant variations across different mammalian species and lactation stages. Thum, Roy, Everett, and McNabb (2021) provided a detailed comparison of milk compositions from humans, bovines, caprine, and ovine, noting that bioactive compositions correlate with MFG sizes. Selecting herds based on specific MFG sizes could be an effect way to enrich bioactive proteins and lipids. Lactation and metabolic stages have a more significant influence on MFGs size than genetic or diet factors. The MFGM proteins in Murrah, Nili-Ravi and Mediterranean buffaloes have been identified using the tandem mass tag proteomic method by Li et al. (2021). A total of 1250 types of MFGM proteins were detected, with 103 being differentially expressed across various breeds. Moreover, Nili-Ravi milk contained more endoplasmic reticulum resident protein 29, and Murrah milk was characterized by an abundance of uromodulin. The immunological implications of species-specific MFGM compositions were explored by Felice, Owens, Kennedy, Hogan, and Lane (2021), who studied the impact of MFGM protein sources from cow, goat, sheep and buffalo (*Bubalus bubalis*) on immune system functionalities including antigen processing and presentation, immune response activity and molecular mediator of immune response productivity.

Additionally, the proteins and lipids in MFGs of different species were analysed by proteomic and lipidomic techniques. The number of proteins involved in the antigen processing differed among various species with cow, buffalo, goat and sheep containing 21, 23, 19 and 23, respectively. Goat milk fat was found to contain the highest proportion of phospholipids at 0.42%, followed by cow (0.35%), sheep (0.34%),

and buffalo (0.27%), according to 31P NMR spectroscopy results. It is important to note that variations in phospholipid content could also be partly attributed to differences in extraction methods.

Yang et al. (2020) quantitatively and qualitatively compared the MFGM phosphoproteomics between colostrum and mature breast milk using label-free quantitative technique. Their findings indicated that colostrum contained more phosphorylation sites. Additionally, the investigation of the metabolism of fatty acid in the core MFGs revealed distinct variations in fatty acid profiles among cows with different MFGs sizes. Notably, a higher concentration of unsaturated fatty acid was detected in the milk of cow with smaller MFG phenotype, despite all the cows being subjected to the same standardized diet (Walter, Shrestha, Fry, Leury, & Logan, 2020).

- *Feeding system*

The milk fat profile is the highly variable and is markedly affected by diets and feeding systems. Diet-induced milk fat depression (MFD) syndrome represents a challenge in the milk fat content and yield, as well as the changes in milk fatty acids. This syndrome was initially reported by Baumgard, Corl, Dwyer, Sæbø, and Bauman (2000) in dairy cows consuming diets rich in fermentable or plant oils, primarily driven by the rumen metabolite *trans*-10, *cis*-12 conjugated linoleic acid (CLA). CLA gains interest because of its anti-carcinogenic properties, and the most common natural form of CLA identified in milk is the *cis*-9, *trans*-11 isomer (Bauman & Griinari, 2001). A negative correlation between the fat concentration and the *trans*-10, *cis*-12 CLA in dairy ewes has been reported by Toral, Gervais, Hervás, Létourneau-Montminy, and Frutos (2020). Different forms of CLA have different effects on milk yield. Perfield et al. (2007) found that *trans*-9, *cis*-11 CLA had no effect on the milk fat yield whereas *trans*-10, *cis*-12 was responsible for the reduction in the milk fat synthesis. Additionally, *trans*-10, *cis*-12 and *cis*-9, *trans*-11 CLA supplementation in the feed did not affect milk yield compared to control samples but reduced both protein and fat content, especially the relative content of PC and PE. Moreover, CLA supplementation was found to decrease the particle size of MFGs, resulting in a higher specific surface area (Zhang, Xing, Huang, & Han, 2021). A study by Argov-Argaman et al. (2021) revealed that the phospholipid content in goat milk was lower when the goats were fed hey and confined, compared to those grazing brushland.

### 3.2. Effect of separation methods on the MFGs/MFGM materials

#### 3.2.1. Centrifugation and cream separator

MFGs/MFGM can be separated from milk using the cream separation/washing or centrifugation, mainly due to the density difference between the fat and skim milk phases. Holzmüller and Kulozik (2016) comprehensively reviewed the effect of centrifugation and washing conditions on the MFGs/MFGM. The efficiency of MFGs/MFGM isolation using lab-scale centrifugation and cream separation was compared. Specifically, the effects of each centrifugation step have been summarized, including the washing steps, washing solvents, temperature, dilution proportion, and centrifugation force (g). During the butter production, churning causes the breakage of MFGs, releasing MFGM fragments into buttermilk phrase. A label-free proteomic approach was employed to investigate the impact of varying cream churning duration (2, 4, 6, and 8 min) on the MFGM compositions. It was found that churning for 6 min resulted in the detection of 60 unique proteins, significantly more than those identified in the 2, 4, and 8 min churning groups (Zheng et al., 2020). Sun, Roos, and Miao (2022) demonstrated the effect of cream separation on the MFGs structure and MFGM proteins prepared from acidified bovine milk (pH 5.30 and 6.30). A profound reduction in BTN and PAS 6/7 has been reported at pH 5.30 following cream separation. Meanwhile, pH 5.30 induced a smaller particle size and lower zeta potential of MFGs compared to the control and samples at pH 6.30 during cream preparation. The particle size of MFGs can be effectively regulated by modifying the separation techniques employed, significantly impacting fat-related functionalities within food products. On an industrial scale, a two-stage centrifugal method was used by Dhungana, Truong, Bansal, and Bhandari (2021) to increase the size distribution of MFGs in milk. Critical parameters such as the size of top separating cone, feed rate and rotating rate of the bowls were optimized to maximally preserve the MFGs/MFGM in their natural state. This research provides valuable insights for scaling up the production of cream fractions with specific size distributions. Further, MFGs fractions ranging in size from millimetres to micrometers were layered and incorporated into an acid gel (induced by Glucono-δ-lactone), which exhibited superior oral tribological properties compared to control samples containing naturally-sized MFGs (Cheng et al., 2021). This pivotal discovery provides key information for regulating MFGs size in gel emulsion systems such as yogurt and cheese. Modulating the structure and distribution of MFGs within food system is of paramount interest to food industry, as it can influence the sensory properties and functionalities of the final products.

#### 3.2.2. Membrane separation

Membrane processing is a gentle processing method with a sustainable production system that has promising market prospects in the food and beverage industry. Membrane technology is extensively used in the dairy industry for various purposes such as spore removal, purification of active ingredients, optimization of milk proteins components, and processing of by-products. Cross-flow membrane filtration has replaced the traditional dead-end filtration in industry due to its higher efficiency and suitability for continuous production. Membranes are categorized bases on the minimum molecular weight threshold that cannot pass through, including reverse osmosis (RO), nanofiltration (NF), ultrafiltration (UF) and microfiltration (MF).

Membrane filtration has been used for the fractionation of MFGs/MFGM materials. Membrane fouling and the similar particle sizes of casein and MFGs are two major challenges in membrane separation. Efforts to address these issues have included strategies like removing or dissociating casein prior to membrane filtration. For instance, Wang, Cao, et al. (2021) utilized membranes with varying pore sizes (30, 50 and 100 kDa) to enrich MFGM proteins from butter serum. To enhance separation efficiency, the casein micelles in the buttermilk were precipitated through acidification before undergoing membrane filtration. This process allowed for the identification of approximately 395–399 MFGM proteins in the retentates using label-free proteomic analysis. Notably, fewer MFGM proteins were detected in the 100 kDa permeate, indicating that a 100 kDa cutoff was more effective for MFGM proteins enrichment compared to 30 kDa and 50 kDa membranes (Wang, Cao, et al., 2021). In addition to acidification, the application of chelating salts such as sodium citrate, sodium phosphate and sodium pyrophosphate has proven effective in removing casein by dissociating casein micelles into smaller fragments, thereby facilitating the isolation of MFGs/MFGM from buttermilk (Sun et al., 2017). Conversely, Holzmüller, Gmach, Griebel, and Kulozik (2016) explored an alternative method by inducing gel formation from casein in buttermilk through acidification or rennet addition, rather than fragmenting the casein. Zinc acetate and calcium acetate have been used to precipitate total lipid from the β-stream efficiently. Price, Fei, Clark, and Wang (2020) optimized the temperature and pH conditions, finding that calcium acetate precipitation at either 30 °C or 60 °C was most effective for recovering SM and PS. Although calcium acetate precipitation shows great potential for phospholipids recovery from the β-stream, it is less effective for MFGM proteins, as they were found predominantly in the supernatants after calcium acetate treatment (Price et al., 2020). In dairy research, the primary focus has shifted towards maintaining the integrity of MFGs/MFGM during isolation processes. In the studies mentioned above, by-products like cheese whey and buttermilk, in which MFGs/MFGM is often in a fragmented state, have served as the main source for isolation. Fresh raw milk, however, presents a more ideal

starting materials for preserving the natural state of MFGs or MFGM.

Hansen et al. (2018) explored the impact of the sequence of pasteurization relative to MF on the enrichment of the MFGM proteins from raw milk. Their findings indicated that conducting pasteurization after microfiltration did not significantly alter MFGM proteins. However, pasteurizing before filtration led to a reduction in PAS 6/7. Subsequent research by Hansen, Hogan, et al. (2020) focused on optimizing membrane pore size and filtration parameters to enhance the purity of MFGs/MFGM. They also adopted a milder pasteurization temperature of 72 °C for 15 s to minimize the protein denaturation instead of 80–85 °C/15 s in their previous research.

While many studies have endeavoured to isolate MFGs/MFGM from fresh milk, industrially, by-products remain the primary raw materials. Jukkola, Partanen, Rojas, and Heino (2018) introduced an 'ideal butter' process, where cream samples undergo MF/diafiltration (DF) before being churned into butter. This method effectively reduces serum protein drainage into buttermilk during churning, without compromising butter quality. However, the presence of small lipid droplets and MFGM fragments in the wash fluid during MF/DF stages raises questions about the ease of separating MFGs/MFGM from buttermilk. Another study by Hokkanen, Partanen, Jukkola, Frey, and Rojas (2021) profiled the proteins, lipids, fatty acids and thermal behaviours of MFGM in the buttermilk or butter serum derived from microfiltrated cream. Their results revealed a lower detection of phospholipids in buttermilk during the microfiltration process, alongside variations in the phospholipids-fat ratio and melting behaviour between buttermilk and butter serum.

Comparative analyses of centrifugation and membrane filtration for isolating MFGs/MFGM have been conducted by Holzmüller et al. (2016) and Jukkola et al. (2019). The diafiltration of sweet buttermilk whey or buttermilk from whey cream offers a preferable method with fewer losses of MFGs/MFGM compositions. Although both centrifugation and MF tend to fragment MFGs, MF causes less damage, leading to higher MFGM yields and improved separation efficiency (Jukkola et al., 2019).

### 3.3. The effects of dairy processes on the MFGs/MFGM materials

#### 3.3.1. Heat treatments and storage temperature

Heat treatment and refrigeration are commonly used in the dairy industry to inhibit microbial growth and ensure food safety throughout the products' shelf life. Heating or cooling treatments significantly affect the crystalline state of lipids, particularly the triglycerides in the core of MFGs, and can induce the agglutination or coalescence of MFGs as well as the attenuation and rupture of MFGM. Understanding the effect of temperature on the compositions and structure of MFGs/MFGM is of significant guidance for its practical industrial application.

- *Size and lipid profile of MFGs/MFGM*

Heating treatment has been reported to cause the loss of phospholipids in MFGs/MFGM by Wei et al. (2023). Their study noted that heat treatment of 90 °C for 20 min significanlty accelerated the loss of SM and cholesterol in MFGM more than at treatmetn at 60 °C for 20 min. Moreover, both 90 °C and 60 °C treatments induced an increase in the size of MFGs and a decrease in their zeta potential, likely due to the coalescence of MFGs and the rupture of MFGM (Wei et al., 2023). Additionally, pasteurization and fermentation have been reported to decrease the PS levels to 1.5- and 2-fold compared to those in the untreated goat milk from confinement or gazing fed system, respectively (Argov-Argaman et al., 2021).

- *Interaction with serum protein*

Heating induces the denaturation and conformational change of whey proteins, mainly α-LA, β-LG and BSA. The denatured and unfold structure of β-LG has been reported to more readily bind to the MFGM layer (Wiking, Gregersen, Hansen, & Hammershøj, 2022). The interaction is largely attributed to $Cys^{121}$, which facilitates the formation of β-LG self-aggregates or complexes with other milk components through thiol-disulfide interchange. Hansen, Nielsen, Rasmusen, Larsen, and Wiking (2020) further verified that noncovalent bindings, including hydrophobic interaction and hydrogen bonding, were paramount to the association between β-LG and MFGM, beyond the simple thiol-disulfide interaction model. Even with the use of thiol-blocking agents to inhibit the $Cys^{12}$ forming disulfide bonds with MFGM proteins, conjugates between MFGM and β-LG were still observed in the SDS-PAGE results. However, the exact type of MFGM proteins that β-LG specially formed non-covalent bonds with were not identified in their study.

Caprine or goat milk is a popular alternative to bovine milk in IF products due to its easier digestion and low allergic protein content ($\alpha_{S1}$-casein) and absence of A1 β-casein. Daomin et al. (2022) investigated various heat treatments on MFGM proteins using label-free proteomics technique, including ultra-pasteurization (85 °C/30 min, UP), ultra-high temperature sterilization (135 °C/5 s, UHT) and spray drying (inlet 160 °C and outlet 80 °C, SP). The results showed that UP and UHT treatment reduced MFGM protein levels, whereas SP had a less signficant effect on the number and abundance of MFGM proteins. Proteomic analysis and non-reduced SDS-PAGE revealed that β-LG and α-LA were likely to bind with XDH/XO and BTN. Recombined milk, prepared by mixing skim milk and milk fat to simulate whole milk, serves as an alternative in regions where fresh milk is scarce. The process of recombined milk impacts MFGM composition containing native MFGM constituents which are replaced by casein and whey on the surface of MFGs (Ji, Lee, & Anema, 2011). The preparation methods of recombined milk affected surface compositions of MFGM and thus its gelation property. Anantawat, Loveday, Singh, and Anema (2022) investigated how the sequence of heating and homogenization affects the composition of MFGM and its gelation properties. The results showed that homogenising milk fat with heat-treated skim milk (HEHO) resulted in lower proportion of κ-casein and denatured whey proteins on the fat globules. Nevertheless, higher amount of $\alpha_s$-casein and β-casein were present in HEHO than samples prepared by heating the blends of homogenising milk fat and skim milk (HOHE).

- *Elasticity of MFGM*

Quantitatively analyzing the interfacial components of MFGM presents significant challenges when using traditional analysis methods, such as solvent extraction and chromatography (Lopez, 2011). Non-destructive analytical methods have been developed to characterise the MFGs/MFGM. Atomic force microscopy (AFM) technique has emerged as a powerful tool for this purpose. Huang et al. (2023) employed AFM, combined with Young's modulus, to quantitatively analyze the elasticity of MFGM and its binding with serum proteins after being treated by different dairy units. Young's modulus can be used to reflect the rigidity of milk samples. Young's modulus E is calculated by fitting the force curve by Hertz model:

$$F = \frac{4}{3}\frac{E\delta^{\frac{3}{2}}\sqrt{R_{tip}}}{(1-\nu^2)}$$

where F: force, $R_{tip}$: tip radius (20 nm), δ: the indentation distance and $\nu$ the Poisson ratio, taken as 0.5 (Marsh, 2006).

Homogenization increased the Young's modulus (kPa) of raw milk more significantly compared to that in control raw milk, cream, UF retentate and standardized milk (Fig. 4A), indicating the increase of MFGM stiffness after homogenization (Balasuriya, Ong, Gras, & Dagastine, 2012). Moreover, AFM images have shown that the MFGM in ultra-pasteurized milk (121 °C/15 s) exhibits a smoother surface compared to both control and those treated at lower temperatures (63 °C and 84 °C) (Fig. 4B), indicating ultra-pasteurized milk damaged MFGM more than pasteurization (Huang et al., 2023). Additionally, AFM has been performed to quantitatively analyze the effect of acidification (pH

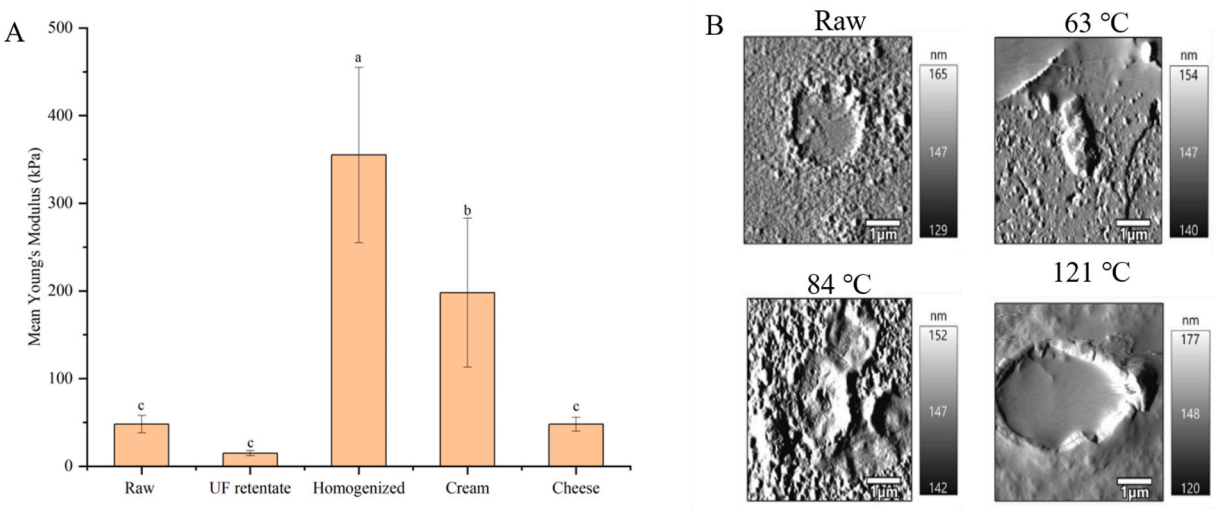



**Fig. 4.** (A) Value of the mean Young's modulus of the milk fat globule membrane of different milk samples. Different letters above the bars indicated statistically different ($p < 0.05$) (Balasuriya et al., 2012). (B) Atomic force microscopy (AFM) images of milk fat globules in raw and heating treated milk (Huang et al., 2023).

4.50) and UHT treatment on the binding of MFGs with milk proteins. The results indicate an increase in the interaction force from 176 pN to 296 pN following UHT treatment, suggesting the adsorption of denatured whey protein on the surface of MFGs or casein. This treatment results in more compact and stiffer milk acid gels in UHT-treated milk compared to those formed by untreated milk samples (Obeid et al., 2020).

- *Low temperature*

Low temperature is a standard practice for preserving milk products, but it also affect the structural and compositional aspects of MFGs/MFGM since milk fat fractions start to solidify at temperatures lower than 37 °C (Sherbon, 1974). A study conducted by Wei et al. (2021) demonstrated the impact of cold storage temperature and shelf life (4 °C, −20 °C and −80 °C for 30, 60, 90 and 120 days) on the phospholipid composition and fat globule structure in human milk. Quantitative analysis using $^{31}$P NMR showed a decrease in the total phospholipid of all samples after 120 days of storage. The degradation of phospholipid led to the release of inner triglyceride and subsequent flocculation of MFGs.

In brief, we conclude that different heating intensities affect the MFGs/MFMG structure, lead to the loss of interfacial compositions, influence the elasticity of MFGM, and promote the binding of MFGM with serum proteins. Nevertheless, it is worth noting that heating methods and conditions differ across the referenced studies, including variations in heating facilities, temperature and duration. In addition, the raw materials used for the MFGs/MFGM preparation and investigation also vary, such as goat or bovine milk, raw milk, cream or buttermilk, and human milk. It is evident that heating is not the sole process used in dairy production. Previous researches on the combination of thermal treatments with other dairy processes like homogenization, acidification, and membrane separation have already been reported but are not included in this review (Hansen et al., 2018; Jash & Rizvi, 2022; Ren, Li, Liu, & Ma, 2020). Consequently, a comprehensive review focusing on the combined effects of these dairy processing units on MFGs/MFGM would be both necessary and beneficial.

### 3.3.2. *Homogenization*

Homogenization, first developed in 1899, has become a fundamental process in the dairy industry. This technique reduces the MFGs size by forcing milk through a narrow gap at high velocity, enhancing the stability of milk emulsion. Typically, the temperature and pressure for homogenization are set at 50−70 °C and 10−25 MPa (100−250 bar) to optimize the efficiency and effectiveness of the process (Gösta Bylund, 1995). Apart from reducing the size of MFGs, homogenization also influences various chemical reactions on the newly formed MFGs, such as enzymatic hydrolysis, increased susceptibility to Cu ion-induced oxidation, light-induced flavour deterioration, and changes in colour.

In this review, we discuss two main types of homogenization treatments: conventional homogenization (0–100 MPa) and novel high-pressure homogenization (HPH) (>100 MPa). It should be noted that HPH differs from high hydrostatic pressure (HHP). While HHP processes samples in batches and is perceived as a non-thermal processing. HPH is a continuous processing operation. Details on HHP and its applications are further explored in part 3.3.3.3 of this review.

#### 3.3.2.1. *Conventional homogenization.*

- *MFGM protein and fatty acid*

Previous researches have explored the effect of homogenization pressure and temperature on the MFGM proteins and fatty acid of milk (Reis et al., 2020; Wang et al., 2019). Research conducted by Reis et al. (2020) highlights that increasing homogenization pressure (20−45 MPa) and preheating temperature (50−70 °C) before homogenization result in a reduction of MFGM proteins, especially CD36, FABP and PAS 6/7. Furthermore, more significant β-LG was observed on the surface of MFGs when subjected to homogenization at higher pressure, while preheating facilitated the interaction between α-LA and MFGM (Wang et al., 2019). Heterogeneous fatty acids serve as primary sources of volatile compounds in milk. Homogenization has been reported to induce the degradation of milk composition, particularly lipids, adversely affecting milk flavour. As the homogenization pressure escalates from 0 bar to 350 bar (at 45 or 65 °C), there is a significant increase in the concentration of methyl butanoate, dimethyl sulphide, dimethyl disulphide and carbon disulphide in milk samples. In comparison, an increase in homogenization pressure at 80 °C leads to greater formation of methyl ketones (Reis et al., 2020). In addition, Cohen, Shamay, and Argov-Argaman (2015) have identified a correlation between the sizes of MFGs and the fatty acids/phospholipids contents within them.

- *Crystallization*

Apart from the change of structure and compositions, particle size, thermal behaviour, and emulsifying ability of MFGs/MFGM are critical

in food application. Studies by Ren et al. (2020) indicate that homogenization at pressure of 20, 30, and 40 MPa promotes the crystallization of MFGs at elevated temperature (20.6 °C), attributed to the increased presence of saturated lipids in newly formed MFGs. Compared to control samples, homogenization inhibits the polymorphic transformation and reduces the β crystals proportion in the MFGs/MFGM (Ren et al., 2020).

- *Creaming*

While homogenization enhances the stability of milk and prevents the formation of a top cream layer, the addition of food additives is essential for long shelf life products in markets. Research by Lu et al. (2021) demonstrated that, in comparison to homogenized milk (20 MPa at 53 °C) without any additives, the incorporation of soybean lecithin efficiently enhanced the storage stability of milk before homogenization. In milk enriched with soybean lecithin, the surface area of MFGs closely resembles that of control raw milk, with fewer serum protein adhering to the MFGM, thereby preserving more native MFGM proteins (Lu et al., 2021).

*3.3.2.2. High-pressure homogenization (HPH).* HPH is an innovative technology employed in liquid food processing that uses high pressure to eliminate pathogenic microorganisms, enhance emulsify stability, and prolong the shelf life of food products (Zamora & Guamis, 2014). Kiełczewska, Ambroziak, Krzykowska, and Aljewicz (2021) compared the effects of HPH (100 MPa, 4–60 °C) and conventional homogenization (20 MPa, 60 °C) on the particle size of MFGs, MFGM proteins, and phospholipids in untreated raw milk, buttermilk and their mixtures (1:1). The finding indicated a significant increase in SM and a decrease of PS in samples treated with HPH. Correspondingly, more adsorption of serum proteins was found on the surface of MFGs after HPH treatments. Buttermilk powder has been highlighted as a natural emulsifier for enriching food products with MFGM fragments and serum in the food industry. Further research by Garczewska-Murzyn, Kiełczewska, and Smoczyński (2022) compared the effects of HPH (100 MPa at 4, 20, 40, and 60 °C) and conventional homogenization (20 MPa at 60 °C) on emulsions formed by mixing raw milk with varying concentrations of buttermilk powder (0.3−1.5%, w/v). The study demonstrated that a stable emulsion and colloidal phase were achieved after treatment at 100 MPa/20 °C, which is attributed to the reduction of volume weighted mean diameter D [4, 3].

*3.3.3. Non-thermal treatments*

The nutrient degradation and sensory decline associated with thermal treatment are well-documented challenges in contemporary dairy processing. These thermal methods often result in the loss of heat-sensitive nutrients, as well as undesirable changes in taste and texture. In response, the food industry has increasingly adopted non-thermal technologies, driven by consumer demand for products that are perceived as natural and minimally processed. Innovative non-thermal techniques include sonication, high hydrostatic pressure (HHP), pulsed electric field (PEF), dielectric barrier discharge plasma (DBD) and ultraviolet radiation. These methods strive to preserve the natural and nutritional qualities of food while ensuring food safety, and can also modify the techno-functionalities of food materials (Sun et al., 2014). Further research into the effect of non-thermal treatments on the MFGs/MFGM is helpful for preserving heat-sensitive components like phospholipids and glycoproteins.

*3.3.3.1. Ultrasound treatment.* Ultrasounds are acoustic waves in the range of 20 kHz and 1 GHz, which are classified into high-intensity (<1 W/cm$^2$) and low-intensity (10−1000 W/cm$^2$) based on their intensities (Mason, 1998). Research has shown that ultrasound treatments can reduce the size of MFGs and serve as an alternative method to traditional homogenization (Chambers, 1937). For instance, MFGs in raw milk samples treated by ultrasound at 35 kJ/L and shear-homogenization at 20 MPa presented similar size distributions. Moreover, more MFGM proteins were retained in ultrasound treated samples compared to shear-homogenization (Liu, Boeren, Zhang, Zhou, & Hettinga, 2021).

Ultrasound treatment (20 kHz, 10−50W) facilitates the formation of MFGs-protein complexes, which promotes acid-gel formation. Moreover, a strong gel was formed due to the denaturation of whey protein and the generation of casein-MFGs complexes (Gregersen, Wiking, & Hammershøj, 2019). In addition, ultrasound processing not only reduced the average particle size of MFGM fragments but also induced the compositional reorganisation on the surface of MFGs. Emulsions stabilised by ultrasound modified MFGM exhibited higher surface tension, enhancing the emulsifying capacity of MFGM (Chen, Sagis, & Sun, 2020).

Model emulsions enriched with MFGM materials have been designed to mimic breast milk, providing critical insights for IF production. For milk powder enriched with MFGs/MFGM ingredients, it is essential that milk or soy proteins envelop the MFGs to ensure a stable emulsion upon rehydration. Ultrasonic treatment has been shown to improve the solubility and emulsifying capacity of these ingredients. For instance, the solubility of MFGM rich in phospholipids (MPL, purchased from Hilmar USA) increased from 36% to 85.88% following ultrasonic treatment (20 kHz, 43 ± 3.4 W/cm$^2$), and the emulsifying stability of mimicking human fat emulsions fortified with ultrasonic treated MPL was significantly improved (Sun, Yu, et al., 2022). Furthermore, ultrasound treatment can influence the thermal behaviour and interfacial properties of MFGs/MFGM ingredients. Research by Sergeev et al. (2021) on the changes of thermal properties of goat lipids treated by 45 kHz ultrasound for 30 min revealed that butter made from ultrasound-treated goat milk exhibited lower crystallization temperature and higher melting enthalpies, due to the formation of β′-form crystals. This is supported by Sun, Roos, and Miao (2024) who found that raw milk treated independently or synchronously with ultrasound at 20 kHz and 40 kHz for 15 min induced the disappearance of α-crystals in MFGs/MFGM, with only β-form and β′-form detected. In addition, a significant decrease in the interfacial tension (π) between the air and MFGs/MFGM liquid phase was noted after 20 kHz treatment for 15 min.

*3.3.3.2. Supercritical-$CO_2$ (SC–$CO_2$).* SC-$CO_2$ processing has gained prominence in recent years due to its high efficiency and environmental sustainability. This technique involves exposing a substrate to specific pressure-temperature conditions, transforming it into a supercritical solvent capable of selectively dissolving target compounds from the substrates (Sahena et al., 2009).

Research into the application of SC-$CO_2$ for purifying lipids/fatty acid was conducted by Friedrich and Pryde (1984) in the early 1980s, focusing on optimizing the temperature and pressure of SC-$CO_2$ to increase the solubility of soybean oil triglycerides. Buttermilk powder with a good creamy flavor is rich in phospholipids, and is widely used in desserts, ice cream and yogurt processing. The combination of membrane filtration technology and SC-$CO_2$ has been reported to effectively extract phospholipids from buttermilk powder, resulting in a 5-time increase in the phospholipids than the original samples (Spence, Jimenez-Flores, Qian, & Goddik, 2009). This process involved hydrolyzing the buttermilk powder and then being ultrafiltered by 50 kDa membrane, followed by SC-$CO_2$ extraction that enriched the phospholipid content to 56.24 % on a dry matter basis (Barry, Dinan, & Kelly, 2017). Phospholipids are excellent materials for liposome synthesis. A novel approach combing SC-$CO_2$ and ethanol-modified method has facilitated the extraction of phospholipids with a concentration up to 75%. The phospholipids were subsequently used in a venture-based system (Vent-RESS) for the synthesis of liposomes. This system proved effective in encapsulating Vitamins E and C within the MFGM-derived liposomes, serving as models to assess the heating stability and encapsulation efficiency (Apratim Jash and Rizvi, 2020). Despite these

advancements, there remains a gap in research concerning the effects of SC-$CO_2$ on the structural change and specific types of phospholipids.

*3.3.3.3. High hydrostatic pressure (HHP).* HHP involves generating pressure ranging from 100 to 900 MPa by reducing the volume of treatment chamber or pumping a pressurizing medium into the chamber. HHP applies pressure uniformly and statically to samples without altering their shape (San Martin, Barbosa-Canovas, & Swanson, 2002). This technique has been extensively studied for its effects on the structure and functionalities of MFGs/MFGM.

HHP treatment has been verified to affect the MFGs size, free fatty acid content, the interaction between MFGM and milk proteins, and the creaming ability of MFGs/MFGM in the emulsion. The impact of high pressure (200−500 MPa) and storage (4 °C) on the particle size, protein distribution, colour, and fatty acid profile of caprine milk was analysed by Kiełczewska, Jankowska, Dąbrowska, Wachowska, and Ziajka (2020). The results showed that high pressure facilitated the agglomeration of MFGs, leading to an increase in particle size of MFGs. Notably, while the fatty acid profile remained stable under pressure, there were observable changes in the colour parameters of the milk.

Furthermore, the polymorphic behaviour of triglycerides, influenced by the types of fatty acid was examined under high-pressure conditions. This behavior significantly affects the melting and crystallization properties of lipids. Vella et al. (2021) investigated the effects of high pressure on triglyceride polymorphism in milk fat. Small-angel X-ray scattering with pressure up to1430 and 1480 MPa was used to treat and observe the samples. Their results showed that tilted β' 2L1 and α 3L1 structures were more susceptible to compression under high pressure. In anhydrous milk fat samples, triglyceride remained in a liquid state and predominantly formed α 3L structures after HHP treatment.

*3.3.3.4. Pulsed electric field (PEF).* PEF is a promising non-thermal treatment increasingly applied in the processing of liquid foodstuffs. The core component of PEF is the high-voltage pulse generator, which produces electric pulses from the rapid discharge of electric energy within a short period of time (Blahovec, Vorobiev, & Lebovka, 2017).

In a comprehensive review, Sharma, Oey, and Everett (2014) summarised studies on the effects of PEF treatment on MFGs/MFGM between 2000 and 2014. This review highlighted significant findings related to changes in MFGs size and interfacial zeta potential induced by PEF while noting a scarcity of reports on the compositional and structural changes. Transmission electron microscopy (TEM) has been employed to observe the effect of PEF treatment on the surface coverage of MFGM with plasma protein. Notably, PEF-treated milk (20 kV/cm for 34 μs) exhibited increased adsorption of casein micelles on the interface of MFGs compared to untreated raw milk. The increase in surface hydrophobicity of MFGs/MFGM after PEF treatment was further confirmed in subsequent studies (Sharma, Oey, & Everett, 2016). Comparative studies by the same researchers in 2015 found that pre-heating at 55 °C for 24 s more significantly altered the plasma proteins on the surface of MFGs than PEF treatment, indicating that thermal treatment causes more serious surface damage to native MFGs (Sharma, Oey, & Everett, 2015). Interestingly, xanthine oxidase denaturation was approximately 13% lower in PEF-treated samples compared to those subjected to thermal treatment. Furthermore, Yang, Suwal, Andersen, Otte, and Ahrné (2021) investigated the relationship between the particle size of MFGs and changes in MFGM proteins induced by PEF treatment. It turned out that a more pronounced effect on MFGM proteins was observed in small MFGs after PEF treatment due to significant protein adsorption. Moreover, the phospholipids in MFGs remained unchanged in cream samples treated with PEF (37 kV/cm field strength, 65 °C). Additionally, increased interactions between β-lactoglobulin and MFGM proteins were evidenced by SDS-PAGE results. Another significant advantage of PEF is its ability to maintain the original biological activities of food components. For instance, PEF-treated cream exhibited similar antiproliferative activity to untreated samples, while pasteurization induced the loss of antiproliferative activity in cream samples. Further investigation is required to elucidate the specific components responsible for the antiproliferative activity observed in these samples (Xu, Walkling-Ribeiro, Griffiths, & Corredig, 2015).

Additionally, Mohamad, Shah, Sulaiman, Mohd Adzahan, and Aadil (2020) reported that PEF treatment led to a reduction in total saturated fatty acids and polyunsaturated fatty acids in goat milk (1 kHz, 8 μs, electrode gap distance 4.7 mm, chamber diameter 3.5 mm, and flow rate 2.5 L/h), while total monounsaturated fatty acids increased (Mohamad et al., 2020). Moreover, moderate PEF at intensities (9 and 16 kV $cm^{-1}$, 30 μs) modified the MFGs structure accompanied by changes in lipase activity and fatty acid (FA) profile (Yang et al., 2021).

*3.3.3.5. Dielectric barrier discharge (DBD) plasma reactor.* Cold plasma is particularly suitable for treating heat-sensitive food, as it maintains the samplesat a relatively low temperature (30–60 °C) throughout the treatment process (Coutinho et al., 2018). However, there are scarce studies focused on the effect of DBD treatment on the compositions, structure and functionalities of food. One such study by Kim et al. (2015) showed that indirect plasma treatment, where plasma is generated near but not in direct contact with the sample, did not alter the concentration of the various fatty acids, except for butyric acid and caprylic acid. Further research by Sarangapani, Ryan Keogh, Dunne, Bourke, and Cullen (2017) found that DBD (60−80 V for 30 min) induced lipid oxidation, leading to the formation of oxidation byproducts, such as ozonides, aldehydes, and carboxylic acids, as identified by Fourier transform infrared spectroscopy (FTIR). Meanwhile, hydroperoxides of oleic acid and linoleic acid were detected for the first time by $^{1}$H NMR, suggesting a fatty acid transformation following the Criegee mechanism after DBD treatment (Sarangapani et al., 2017).

Ali (2021) investigated the effects of DBD treatment (at 100 V and 1.5 A for duration of 10, 20, 30 and 40 min) on the MFGM, using pasteurization samples (68 °C for 30 min) as a control. The finding indicated an increase in saturated fatty acids in DBD-treated MFGM samples. Moreover, an interaction between non-membrane proteins and MFGM was evident in DBD-treated samples, as demonstrated by the weak bonding between casein and whey protein. The particle size of MFGs increased with prolonged plasma treatment time, likely due to the accumulation of smaller MFGs on the surface of larger MFGs, forming large aggregates.

## 4. Conclusions and future perspectives

The structural, compositional, and tech-functional characteristics of MFGs/MFGM reported in various studies exhibit significant variation, attributable to a complex array of factors. Dairy processing techniques that involve shearing, for instance, have been shown to alter MFGs size and form new membranes, while more intensive treatments can disintegrate the globules into membrane fragments. Conversely, milder techniques such as membrane filtration and various non-thermal treatments may partly preserve the natural state of MFGs/MFGM after processing. The effects of thermal treatments and homogenization on the MFGs/MFGM under diverse conditions have been extensively investigated. This review, however, only broadly addresses the effect of various factors on the lipids, MFGM proteins, thermal properties, and interactions between MFGs/MFGM and serum proteins. There remains a significant need to compile and update knowledge on other functionalities, including emulsification and encapsulation within delivery systems. WPC enriched with MFGs/MFGM has already been utilized in infant formula design. The establishment of standardized analytical methods for assessing the compositions of MFGs/MFGM is urgently required, particularly non-invasive techniques that minimize discrepancies caused by sample preparations.

Some researchers have been working on the bioactivities of MFGs/

MFGM and attempting to pinpoint the specific compositions responsible for certain bioactivities, the results have yet to fully determine these relationships. Lab-scale centrifugation or ultracentrifugation, commonly employed in the isolation of MFGs/MFGM materials, may not adequately reflect industrial processes, suggesting a need for research methods that better simulate industrial production. Given the crucial role of tri-layer structure of MFGM in physiological properties, maintaining the natural membrane state during isolation and processing is vital. In summary, the factors affecting the structure, compositions, and techno-functionalities of MFGs/MFGM requires deeper exploration, particularly from an industrial application standpoint, to harness their full potential in food science and nutrition.

## Author contributions

Yanjun Sun: Conceptualization, Methodology, Writing-original draft, Visualization. Yrjö H. Roos: Supervision, Writing review & editing. Song Miao: Supervision, Conceptualization, Writing-review & editing, Funding acquisition, Project administration.

## Declaration of competing interest

All authors declare no conflict of interest.

## Data availability

Data will be made available on request.

## Acknowledgements

The project was founded by 'The China Scholarship Council (No.202008410212)' and Teagasc-The Irish Agriculture and Food Development Authority (MDDT1392).

## References

Ali, F. (2021). Nonthermal and thermal treatments impact the structure and microstructure of milk fat globule membrane. *International Journal of Dairy Technology, 0*, 1–10.
Anantawat, V., Loveday, S. M., Singh, H., & Anema, S. G. (2022). Acid gelation of heat-treated recombined milk: Fat globule membrane composition and gelation functionality. *International Dairy Journal, 125*, Article 105243.
Apratim Jash, A. U., & Rizvi, S. S. H. (2020). Synthesis of multivitamin-loaded heat stable liposomes from milk fat globule membrane phospholipids by using a supercritical-CO2 based system. *Green Chemistry, 22*(16), 5345–5356.
Argov-Argaman, N., Glasser, T., Muklada, H., Hadaya, O., Mesilati-Stahy, R., Raz, C., et al. (2021). Lipidome changes, with a focus on phospholipids, due to feeding systems and processing in goat milk. *Food Chemistry, 340*, Article 127938.
Baars, A., Oosting, A., Engels, E., Kegler, D., Kodde, A., Schipper, L., et al. (2016). Milk fat globule membrane coating of large lipid droplets in the diet of young mice prevents body fat accumulation in adulthood. *British Journal of Nutrition, 115*, 1930–1937.
Balasuriya, T. S., Ong, L., Gras, S. L., & Dagastine, R. R. (2012). Changes in morphological and nano-mechanical properties of the milk fat globule membrane during processing. *RSC Advances, 2*, 2384–2394.
Barry, K. M., Dinan, T. G., & Kelly, P. M. (2017). Pilot scale production of a phospholipid-enriched dairy ingredient by means of an optimised integrated process employing enzymatic hydrolysis, ultrafiltration and super-critical fluid extraction. *Innovative Food Science & Emerging Technologies, 41*, 301–306.
Basch, J. J., Greenberg, R., & Farrell, H. M., Jr. (1985). Identification of the milk fat globule membrane proteins. II. Isolation of major proteins from electrophoretic gels and comparison of their amino acid compositions. *Biochimica et Biophysica Acta, 830*, 127–135.
Bauman, D. E., & Griinari, J. M. (2001). Regulation and nutritional manipulation of milk fat: Low-fat milk syndrome. *Livestock Production Science, 70*, 15–29.
Baumgard, L. H., Corl, B. A., Dwyer, D. A., Sæbø, A., & Bauman, D. E. (2000). Identification of the conjugated linoleic acid isomer that inhibits milk fat synthesis. *American Journal of Physiology - Regulatory, Integrative and Comparative Physiology, 278*, R179–R184.
Blahovec, J., Vorobiev, E., & Lebovka, N. (2017). Pulsed electric fields pretreatments for the cooking of foods. *Food Engineering Reviews, 9*, 71–81.
Blesso, C. N. (2015). Egg phospholipids and cardiovascular health. *Nutrients, 7*, 2731–2747.
Chai, C., Oh, S., & Imm, J. Y. (2022). Roles of milk fat globule membrane on fat digestion and infant nutrition. *Food Science of Animal Resources, 42*, 351–371.
Chambers, L. (1937). Sonic homogenization of milk and ice cream mix. *Jounal of Dairy Science, 20*, 450–451.
Chen, M., Sagis, L. M. C., & Sun, Q. (2020). Emulsification and dilatational surface rheology of ultrasonicated milk fat globule membrane (MFGM) materials. *LWT - Food Science and Technology, 133*, Article 110094.
Cheng, W., Liu, H., Shen, Q., Liu, C., Zhou, H., & Luo, J. (2021). A novel approach for modulating the spatial distribution of fat globules in acid milk gel and its effect on the perception of fat-related attributes. *Food Research International, 140*, Article 109990.
Cilla, A., Diego Quintaes, K., Barberá, R., & Alegría, A. (2016). Phospholipids in human milk and infant formulas: Benefits and needs for correct infant nutrition. *Critical Reviews in Food Science and Nutrition, 56*, 1880–1892.
Cohen, B. C., Shamay, A., & Argov-Argaman, N. (2015). Regulation of lipid droplet size in mammary epithelial cells by remodeling of membrane lipid composition—a potential mechanism. *PLoS One, 10*, Article 0121645.
Coutinho, N. M., Silveira, M. R., Rocha, R. S., Moraes, J., Ferreira, M. V. S., Pimentel, T. C., et al. (2018). Cold plasma processing of milk and dairy products. *Trends in Food Science & Technology, 74*, 56–68.
Daomin, Y., Lina, Z., Yixuan, Z., Mengyu, H., Yancong, W., Jun, T., et al. (2022). Changes in caprine milk fat globule membrane proteins after heat treatment using a label-free proteomics technique. *Foods, 11*, 2705.
De Bhowmick, G., Guieysse, B., Everett, D. W., Reis, M. G., & Thum, C. (2023). Novel source of microalgal lipids for infant formula. *Trends in Food Science & Technology, 135*, 1–13.
Deeth, H. C. (1997). The role of phospholipids in the stability of milk fat globules. *Australian Journal of Dairy Technology, 52*, 44–46.
Dewettinck, K., Rombaut, R., Thienpont, N., Le, T. T., Messens, K., & Van Camp, J. (2008). Nutritional and technological aspects of milk fat globule membrane material. *International Dairy Journal, 18*, 436–457.
Dhungana, P., Truong, T., Bansal, N., & Bhandari, B. (2021). A novel continuous method for size-based fractionation of natural milk fat globules by modifying the cream separator. *International Dairy Journal, 125*, Article 105209.
Douellou, T., Montel, M. C., & Thevenot Sergentet, D. (2017). Invited review: Anti-adhesive properties of bovine oligosaccharides and bovine milk fat globule membrane-associated glycoconjugates against bacterial food enteropathogens. *Journal of Dairy Science, 100*, 3348–3359.
Evers, J. M. (2004). The milkfat globule membrane—methodologies for measuring milkfat globule (membrane) damage. *International Dairy Journal, 14*, 747–760.
Felice, V. D., Owens, R. A., Kennedy, D., Hogan, S. A., & Lane, J. A. (2021). Comparative structural and compositional analyses of cow, Buffalo, goat and sheep cream. *Foods, 10*, 2643.
Fong, B. Y., Norris, C. S., & MacGibbon, A. K. H. (2007). Protein and lipid composition of bovine milk-fat-globule membrane. *International Dairy Journal, 17*, 275–288.
Fontecha, J., Brink, L., Wu, S., Pouliot, Y., Visioli, F., & Jimenez-Flores, R. (2020). Sources, production, and clinical treatments of milk fat globule membrane for infant nutrition and well-being. *Nutrients, 12*, 1607.
Friedrich, J. P., & Pryde, E. H. (1984). Supercritical CO2 extraction of lipid-bearing materials and characterization of the products. *Journal of the American Oil Chemists Society, 61*, 223–228.
Garczewska-Murzyn, A., Kiełczewska, K., & Smoczyński, M. (2022). The influence of buttermilk powder on the stability of emulsion and colloidal phases of homogenized milk. *European Food Research and Technology, 248*, 2629–2636.
Gösta Bylund, M. S. (1995). *Dairy processing handbook*. Lund, Sweden: Tetra Pak Processing Systems AB.
Gregersen, S. B., Wiking, L., & Hammershøj, M. (2019). Acceleration of acid gel formation by high intensity ultrasound is linked to whey protein denaturation and formation of functional milk fat globule-protein complexes. *Journal of Food Engineering, 254*, 17–24.
Guerin, J., Burgain, J., Gomand, F., Scher, J., & Gaiani, C. (2019). Milk fat globule membrane glycoproteins: Valuable ingredients for lactic acid bacteria encapsulation? *Critical Reviews in Food Science and Nutrition, 59*, 639–651.
Hansen, S. F., Hogan, S. A., Tobin, J., Rasmussen, J. T., Larsen, L. B., & Wiking, L. (2020a). Microfiltration of raw milk for production of high-purity milk fat globule membrane material. *Journal of Food Engineering, 276*, Article 109887.
Hansen, S. F., Nielsen, S. D., Rasmusen, J. T., Larsen, L. B., & Wiking, L. (2020b). Disulfide bond formation is not crucial for the heat-induced interaction between beta-lactoglobulin and milk fat globule membrane proteins. *Jounal of Dairy Science, 103*, 5874–5881.
Hansen, S. F., Petrat-Melin, B., Rasmussen, J. T., Larsen, L. B., Ostenfeld, M. S., & Wiking, L. (2018). Placing pasteurisation before or after microfiltration impacts the protein composition of milk fat globule membrane material. *International Dairy Journal, 81*, 35–41.
Heid, H. W., & Keenan, T. W. (2005). Intracellular origin and secretion of milk fat globules. *European Journal of Cell Biology, 84*, 245–258.
Hokkanen, S. P., Partanen, R., Jukkola, A., Frey, A. D., & Rojas, O. J. (2021). Partitioning of the milk fat globule membrane between buttermilk and butter serum is determined by the thermal behaviour of the fat globules. *International Dairy Journal, 112*, Article 104863.
Holzmüller, W., Gmach, O., Griebel, A., & Kulozik, U. (2016). Casein precipitation by acid and rennet coagulation of buttermilk: Impact of pH and temperature on the isolation of milk fat globule membrane proteins. *International Dairy Journal, 63*, 115–123.
Holzmüller, W., & Kulozik, U. (2016). Technical difficulties and future challenges in isolating membrane material from milk fat globules in industrial settings – a critical review. *International Dairy Journal, 61*, 51–66.

Huang, Y., Wei, T., Chen, F., Tan, C., Gong, Z., Wang, F., et al. (2023). Effects of various thermal treatments on interfacial composition and physical properties of bovine milk fat globules. *Food Research International, 167*, Article 112580.
Jash, A., & Rizvi, S. S. H. (2022). Heat-stable liposomes from milk fat globule membrane phospholipids for pH-triggered delivery of hydrophilic and lipophilic bioactives. *Innovative Food Science & Emerging Technologies, 79*.
Ji, Y. D., Lee, S. K., & Anema, S. G. (2011). Effect of heat treatments and homogenisation pressure on the acid gelation properties of recombined whole milk. *Food Chemistry, 129*, 463–471.
Jukkola, A., Hokkanen, S., Kämäräinen, T., Partanen, R., Heino, A., & Rojas, O. J. (2019). Changes in milk fat globules and membrane lipids under the shear fields of microfiltration and centrifugation. *Journal of Membrane Science, 573*, 218–225.
Jukkola, A., Partanen, R., Rojas, O. J., & Heino, A. (2018). Effect of heat treatment and pH on the efficiency of micro-diafiltration for the separation of native fat globules from cream in butter production. *Journal of Membrane Science, 548*, 99–107.
Kanno, C., Hattori, H., & Yamauchi, K. (1987). Lipid composition of plasma membranes isolated from lactating bovine Mammary Glan. *Agricultural and Biological Chemistry, 51*(ll), 2995–3001.
Keenan, T., Morré, D. J., Olson, D. E., Yunghans, W., & Patton, S. (1970). Biochemical and morphological comparison of plasma membrane and milk fat globule membrane from bovine mammary gland. *The Journal of Cell Biology, 44*, 80–93.
Kiełczewska, K., Ambroziak, K., Krzykowska, D., & Aljewicz, M. (2021). The effect of high-pressure homogenisation on the size of milk fat globules and MFGM composition in sweet buttermilk and milk. *International Dairy Journal, 113*, Article 104898.
Kiełczewska, K., Jankowska, A., Dąbrowska, A., Wachowska, M., & Ziajka, J. (2020). The effect of high pressure treatment on the dispersion of fat globules and the fatty acid profile of caprine milk. *International Dairy Journal, 102*, Article 104607.
Kim, H.-J., Yong, H. I., Park, S., Kim, K., Choe, W., & Jo, C. (2015). Microbial safety and quality attributes of milk following treatment with atmospheric pressure encapsulated dielectric barrier discharge plasma. *Food Control, 47*, 451–456.
Lee, H., Padhi, E., Hasegawa, Y., Larke, J., Parenti, M., Wang, A., et al. (2018). Compositional dynamics of the milk fat globule and its role in infant development. *Frontiers in Pediatrics, 6*, 313.
Li, S., Delger, M., Dave, A., Singh, H., & Ye, A. (2022). Seasonal variations in the composition and physicochemical characteristics of sheep and goat milks. *Foods, 11*.
Li, S., Yang, Y., Chen, C., Li, L., Valencak, T. G., & Ren, D. (2021). Differences in milk fat globule membrane proteins among Murrah, Nili-Ravi and Mediterranean buffaloes revealed by a TMT proteomic approach. *Food Research International, 139*, Article 109847.
Liu, Y., Boeren, S., Zhang, L., Zhou, P., & Hettinga, K. (2021). Ultrasonication retains more milk fat globule membrane proteins compared to equivalent shear-homogenization. *Innovative Food Science & Emerging Technologies, 70*, Article 102703.
Lopez, C. (2011). Milk fat globules enveloped by their biological membrane: Unique colloidal assemblies with a specific composition and structure. *Current Opinion in Colloid & Interface Science, 16*, 391–404.
Lopez, C., Cauty, C., & Guyomarc'h, F. (2015). Organization of lipids in milks, infant milk formulas and various dairy products: Role of technological processes and potential impacts. *Dairy Science & Technology, 95*, 863–893.
Lopez, C., Madec, M.-N., & Jimenez-Flores, R. (2010). Lipid rafts in the bovine milk fat globule membrane revealed by the lateral segregation of phospholipids and heterogeneous distribution of glycoproteins. *Food Chemistry, 120*, 22–33.
Lu, N., Wang, J., Chen, Z., Zhang, X., Chen, C., & Wang, S. (2021). The effect of adding phospholipids before homogenization on the properties of milk fat globules. *LWT - Food Science and Technology, 146*, Article 111659.
Mansson, H. L. (2008). Fatty acids in bovine milk fat. *Food & Nutrition Research, 52*, 1821.
Marsh, D. (2006). Elastic curvature constants of lipid monolayers and bilayers. *Chemistry and Physics of Lipids, 144*, 146–159.
Mason, T. (1998). Power ultrasound in food processing–the way forward. *Ultrasound in food processing*, 105–126.
Mather, I. H. (2000). A review and proposed nomenclature for major proteins of the milk-fat globule membrane. *Jounal of Dairy Science, 83*, 203–247.
Mohamad, A., Shah, N. N. A. K., Sulaiman, A., Mohd Adzahan, N., & Aadil, R. M. (2020). Impact of the pulsed electric field on physicochemical properties, fatty acid profiling, and metal migration of goat milk. *Journal of Food Processing and Preservation, 44*, Article 14940.
Obeid, S., Guyomarc'h, F., David-Briand, E., Gaucheron, F., Riaublanc, A., & Lopez, C. (2019). The phase and charge of milk polar lipid membrane bilayers govern their selective interactions with proteins as demonstrated with casein micelles. *Journal of Colloid and Interface Science, 534*, 279–290.
Obeid, S., Guyomarc'h, F., Tanguy, G., Leconte, N., Rousseau, F., Dolivet, A., et al. (2020). The adhesion of homogenized fat globules to proteins is increased by milk heat treatment and acidic pH: Quantitative insights provided by AFM force spectroscopy. *Food Research International, 129*, Article 108847.
Perfield, J. W., Lock, A. L., Griinari, J. M., Saebo, A., Delmonte, P., Dwyer, D. A., et al. (2007). Trans-9, cis-11 conjugated linoleic acid reduces milk fat synthesis in lactating dairy cows. *Journal of Dairy Science, 90*, 2211–2218.
Price, N., Fei, T., Clark, S., & Wang, T. (2020). Application of zinc and calcium acetate to precipitate milk fat globule membrane components from a dairy by-product. *Jounal of Dairy Science, 103*, 1303–1314.
Ramazi, S., & Zahiri, J. (2021). Posttranslational modifications in proteins: Resources, tools and prediction methods. *Database, 2021*.
Raza, G. S., Herzig, K. H., & Leppaluoto, J. (2021). Invited review: Milk fat globule membrane-A possible panacea for neurodevelopment, infections, cardiometabolic diseases, and frailty. *Jounal of Dairy Science, 104*, Article 19649.
Reinhardt, T. A., & Lippolis, J. D. (2006). Bovine milk fat globule membrane proteome. *Journal of Dairy Research, 73*, 406–416.
Reis, M. G., Harris, P., Berry, C., Nguyen, H., Maclean, P., & Weeks, M. (2020). Tracking changes in volatile components and lipids after homogenisation and thermal processing of milk. *International Dairy Journal, 103*, Article 104624.
Ren, Q., Li, Q., Liu, H., & Ma, Y. (2020). Thermal and storage properties of milk fat globules treated with different homogenisation pressures. *International Dairy Journal, 110*, Article 104725.
Sahena, F., Zaidul, I. S. M., Jinap, S., Karim, A. A., Abbas, K. A., Norulaini, N. A. N., et al. (2009). Application of supercritical CO2 in lipid extraction – a review. *Journal of Food Engineering, 95*, 240–253.
San Martin, M. F., Barbosa-Canovas, G. V., & Swanson, B. G. (2002). Food processing by high hydrostatic pressure. *Critical Reviews in Food Science and Nutrition, 42*, 627–645.
Sarangapani, C., Ryan Keogh, D., Dunne, J., Bourke, P., & Cullen, P. J. (2017). Characterisation of cold plasma treated beef and dairy lipids using spectroscopic and chromatographic methods. *Food Chemistry, 235*, 324–333.
Sergeev, A., Shilkina, N., Motyakin, M., Barashkova, I., Zaborova, V., Kanina, K., et al. (2021). Anhydrous fat crystallization of ultrasonic treated goat milk: DSC and NMR relaxation studies. *Ultrasonics Sonochemistry, 78*, Article 105751.
Sharma, P., Oey, I., & Everett, D. W. (2014). Effect of pulsed electric field processing on the functional properties of bovine milk. *Trends in Food Science & Technology, 35*, 87–101.
Sharma, P., Oey, I., & Everett, D. W. (2015). Interfacial properties and transmission electron microscopy revealing damage to the milk fat globule system after pulsed electric field treatment. *Food Hydrocolloids, 47*, 99–107.
Sharma, P., Oey, I., & Everett, D. W. (2016). Thermal properties of milk fat, xanthine oxidase, caseins and whey proteins in pulsed electric field-treated bovine whole milk. *Food Chemistry, 207*, 34–42.
Sherbon, J. W. (1974). Crystallization and fractionation of milk fat. In J.o. t. A. O. C. Society (Ed.), *Symposium "milk lipids," AOCS fall meeting* (Vol. 51, pp. 22–25). Ottawa, Ontario, Canad.
Singh, H. (2006). The milk fat globule membrane—a biophysical system for food applications. *Current Opinion in Colloid & Interface Science, 11*, 154–163.
Smoczyński, M., Staniewski, B., & Kiełczewska, K. (2014). Composition and structure of the bovine milk fat globule membrane—some nutritional and technological implications. *Food Reviews International, 28*, 188–202.
Spence, A. J., Jimenez-Flores, R., Qian, M., & Goddik, L. (2009). Phospholipid enrichment in sweet and whey cream buttermilk powders using supercritical fluid extraction. *Jounal of Dairy Science, 92*, 2373–2381.
Sun, Y., Chen, J., Zhang, S., Li, H., Lu, J., Liu, L., et al. (2014). Effect of power ultrasound pre-treatment on the physical and functional properties of reconstituted milk protein concentrate. *Journal of Food Engineering, 124*, 11–18.
Sun, Y., Liu, Z., Li, H., Li, S., Mo, B., & Lv, J. (2017). Functionality of milk protein concentrate 80 with emulsifying salts and its applications in analogue cheeses. *International Journal of Food Properties, 20*, 2594–2607.
Sun, Y., Roos, Y. H., & Miao, S. (2022). Changes in milk fat globules and membrane proteins prepared from pH-adjusted bovine raw milk. *Foods, 11*, 4107.
Sun, Y., Roos, Y. H., & Miao, S. (2024). Comparative study of interfacial properties and thermal behaviour of milk fat globules and membrane prepared from ultrasonicated bovine milk. *Ultrasonics Sonochemistry, 102*.
Sun, Y., Yu, X., Hussain, M., Li, X., Liu, L., Liu, Y., et al. (2022). Influence of milk fat globule membrane and milk protein concentrate treated by ultrasound on the structural and emulsifying stability of mimicking human fat emulsions. *Ultrasonics Sonochemistry, 82*, Article 105881.
Thum, C., Roy, N. C., Everett, D. W., & McNabb, W. C. (2021). Variation in milk fat globule size and composition: A source of bioactives for human health. *Critical Reviews in Food Science and Nutrition*, 1–27.
Toral, P. G., Gervais, R., Hervás, G., Létourneau-Montminy, M. P., & Frutos, P. (2020). Relationships between trans-10 shift indicators and milk fat traits in dairy ewes: Insights into milk fat depression. *Animal Feed Science and Technology, 261*, Article 114389.
van Nieuwenhuyzen, W., & Tomás, M. C. (2008). Update on vegetable lecithin and phospholipid technologies. *European Journal of Lipid Science and Technology, 110*, 472–486.
Vella, J., Hemar, Y., Gu, Q., Wu, Z. R., Li, N., & Söhnel, T. (2021). In-situ SAXS investigation of high-pressure triglyceride polymorphism in milk cream and anhydrous milk fat. *LWT - Food Science and Technology, 135*, Article 110174.
Walter, L., Shrestha, P., Fry, R., Leury, B. J., & Logan, A. (2020). Lipid metabolic differences in cows producing small or large milk fat globules: Fatty acid origin and degree of saturation. *Jounal of Dairy Science, 103*, 1920–1930.
Wang, M., Cao, C., Wang, Y., Li, H., Li, H., & Yu, J. (2021). Comparison of bovine milk fat globule membrane protein retention by different ultrafiltration membranes using a label-free proteomic approach. *LWT - Food Science and Technology, 144*, Article 111219.
Wang, Y., Liu, M., Qu, X., Wang, S., Ma, Z., Zhang, R., et al. (2019). Changes in the fat globule membrane protein components of pasteurized milk caused by different homogenization conditions determined using a label-free proteomic approach. *LWT - Food Science and Technology, 115*, Article 108430.
Wang, C., Qiao, X., Gao, Z., Jiang, L., & Mu, Z. (2021). Advancement on milk fat globule membrane: Separation, identification, and functional properties. *Frontiers in Nutrition, 8*, Article 807284.
Wang, X., Wei, W., Wu, R., Zhu, X., Ren, F., Liu, L., et al. (2022). Scientific consensus on milk fat globule membrane and its ingredients. *Journal of Chinese Institute of Food Science and Technology*, 1–6.

Wei, W., Cheng, J., Yang, J., Chen, C., Jin, Q., Song, J., et al. (2021). Phospholipid composition and fat globule structure change during low temperature storage of human milk. *LWT - Food Science and Technology, 150*, 1–7.

Wei, T., Huang, Y., Weng, C., Chen, F., Tan, C., Liu, W., et al. (2023). Lipid rafts may affect the coalescence of milk fat globules through phase transition after thermal treatment. *Food Chemistry, 399*, Article 133867.

Wiking, L., Gregersen, S. B., Hansen, S. F., & Hammershøj, M. (2022). Heat-induced changes in milk fat and milk fat globules and its derived effects on acid dairy gelation – a review. *International Dairy Journal, 127*, Article 105213.

Xu, S., Walkling-Ribeiro, M., Griffiths, M. W., & Corredig, M. (2015). Pulsed electric field processing preserves the antiproliferative activity of the milk fat globule membrane on colon carcinoma cells. *Jounal of Dairy Science, 98*, 2867–2874.

Yang, M., Deng, W., Cao, X., Wang, L., Yu, N., Zheng, Y., et al. (2020). Quantitative phosphoproteomics of milk fat globule membrane in human colostrum and mature milk: New insights into changes in protein phosphorylation during lactation. *Journal of Agricultural and Food Chemistry, 68*, 4546–4556.

Yang, S., Suwal, S., Andersen, U., Otte, J., & Ahrné, L. (2021). Effects of pulsed electric field on fat globule structure, lipase activity, and fatty acid composition in raw milk and milk with different fat globule sizes. *Innovative Food Science & Emerging Technologies, 67*, Article 102548.

Zamora, A., & Guamis, B. (2014). Opportunities for ultra-high-pressure homogenisation (UHPH) for the food industry. *Food Engineering Reviews, 7*, 130–142.

Zhang, M., Xing, Z., Huang, Q., & Han, L. (2021). Effect of conjugated linoleic acid supplementation on fat globule size in raw milk. *International Dairy Journal, 115*, 1–7.

Zheng, S., Wang, M., Yang, F., Li, H., Li, H., & Yu, J. (2020). Changes in bovine milk fat globule membrane protein components of cream caused by different extent of churning using a label-free proteomic approach. *LWT - Food Science and Technology, 134*, Article 110058.

foods

MDPI

*Article*

# Changes in Milk Fat Globules and Membrane Proteins Prepared from pH-Adjusted Bovine Raw Milk

**Yanjun Sun [1,2,3], Yrjö H. Roos [3] and Song Miao [2,3,4,*]**

[1] State Key Laboratory of Dairy Biotechnology, Shanghai Engineering Research Center of Dairy Biotechnology, Dairy Research Institute, Bright Dairy & Food Co., Ltd., Shanghai 200436, China
[2] Teagasc Food Research Centre, P61C996 Cork, Ireland
[3] School of Food and Nutritional Sciences, University College Cork, T12R229 Cork, Ireland
[4] China-Ireland International Cooperation Centre for Food Material Sciences and Structure Design, Fujian Agriculture and Forestry University, Fuzhou 350002, China
* Correspondence: song.miao@teagasc.ie; Tel.: +353-(25)42468

**Abstract:** Milk fat globules (MFGs) have tri-layer biological membrane structures, and their compositions are gaining more interest for their physiological benefits. In this study, the changes in MFGs and milk fat globule membrane (MFGM) proteins after cream separation from different pH bovine raw milk were investigated. Raw milk samples were adjusted to pH 5.30 and 6.30 using citric acid at 25 °C. The effect of pH and centrifugation on the structure of MFGs was evaluated by means of particle size, zeta potential and confocal laser scanning microscopy (CLSM). Sodium dodecyl sulfate-polyacrylamide gel electrophoresis (SDS-PAGE) was used to analyze the proteins in the obtained fractions. It was found that both pH and centrifugation could affect the particle size of all samples. As the volume distribution (Dv; Dv (10), Dv(50)and Dv (90)) decreased, the corresponding specific surface area (SSA) increased, and span and uniformity values showed the same trend. The decrease in the zeta potential of MFG correlated with the Dv(50), which was further confirmed by CLSM observation. More butyrophilin (BTN) and periodic acid Schiff 6/7 (PAS 6/7) were lost in cream samples at pH 5.30. The findings could provide valuable knowledge for the application of MFGs ingredient in the food industry since their structures and compositions could affect their potential functional and physiological properties.

**Keywords:** milk fat globules; membrane proteins; compositions; structure

check for updates

**Citation:** Sun, Y.; Roos, Y.H.; Miao, S. Changes in Milk Fat Globules and Membrane Proteins Prepared from pH-Adjusted Bovine Raw Milk. *Foods* **2022**, *11*, 4107. https://doi.org/10.3390/foods11244107

Academic Editor: Piero Franceschi

Received: 26 October 2022
Accepted: 13 December 2022
Published: 19 December 2022

**Publisher's Note:** MDPI stays neutral with regard to jurisdictional claims in published maps and institutional affiliations.

**Copyright:** © 2022 by the authors. Licensee MDPI, Basel, Switzerland. This article is an open access article distributed under the terms and conditions of the Creative Commons Attribution (CC BY) license (https://creativecommons.org/licenses/by/4.0/).

## 1. Introduction

Bovine milk is an O/W emulsion at 37 °C or above in which lipids are present in the state of microscopic globules called milk fat globules (MFGs). Approximately 95% of MFGs are comprised of heterogeneous triglycerides, which locate in the inner core of MFGs. Milk fat globule membranes (MFGMs) enclose MFGs in a three-layer biological membrane [1]. MFGMs have gained much interest due to their multilayer structure and variety amounts of polar lipids and membrane proteins. MFGM acts as a natural emulsifying agent, preventing the flocculation and coalescence of the MFGs in milk [2]. Besides, it could protect the fat against enzymatic action.

The MFGM proteins account for approximately 1–4% of the total protein fraction in milk [1] but 25–70% of the MFGM compositions. Up-to-date proteomic techniques, including two-dimensional gel electrophoresis and mass spectrometry, revealed over 100 MFG-associated proteins [3]. Many of these proteins present at the interface of MFGM and the aqueous phase are heavily glycosylated. Most studies have focused on eight major proteins: periodic acid Schiff III (PAS III), butyrophilin (BTN), cluster of differentiation 36 (CD 36), mucin 1 (MUC 1), the redox enzyme xanthine oxidase/dehydrogenase (XO/XDH), lactadherin or periodic acid Schiff 6/7 (PAS 6/7), adipophilin (ADPH) and fatty acid binding

protein (FABP) [1,4,5]. About 40% of the MFGM proteins are glycoproteins, and XO/XDH constitutes 12–13% of the total. Each of the other proteins in MFGM is at or below 5% [6,7].

MFGM proteins have been reviewed for their bioactivity and positive effects on defense mechanisms for breastfed infants. Research has demonstrated that some MFGM glycoproteins have been shown to protect immature infants against gut-derived pathogens [8,9]. BTN, lactadherin and MUC1 in both the human and the bovine present antimicrobial effects [10]. Defatted bovine MFGM fractions, including proteins and glycoproteins, were reported to inhibit *E. coli* O157:H7 strains adhering to HT-29 cells. Their result also showed that in vitro, breast cancer cell lines could be inhibited by FABP at extremely low concentrations [11]. MUC1 may play immune-protective roles in the suckling neonate by binding to and sequestering pathogenic microorganisms within the gut lumen. Mana et al. treated C57BL/6 mice with BTN either before or after immunization with oligodendrocyte glycoprotein. Their results showed that experimental autoimmune encephalomyelitis associated with multiple sclerosis can be prevented or suppressed by BTN [7,12].

It is assumed that the compositions and structure of MFGs change during secretion, storage, isolation and application. The MFG structure was affected by different isolation methods and conditions. Holzmüller et al. [13] reviewed the most advancing front in the MFGs composition separation and respective results. Research on the compositional and structural variation between MFGs was evaluated and consolidated. In the end, they suggested a new definition of MFGM proteins regarding the isolation method. Effect of different unit operations used in the processing on the MFGs (e.g., agitation, homogenization, heating treatment, concentration, drying and freezing.) have been investigated [2,14,15].

Acidification-induced coagulation of milk protein has been extensively used in the dairy industry. In order to reduce the loss of MFGM proteins into the casein curd, Holzmüller et al. investigated the effects of buttermilk's pH, temperature and preheating on the rennet- and acid-induced coagulation of buttermilk [16]. According to Lopez et al., the microstructure and rheology of emulsions, as well as the stability of lipid droplets coated by MFGM, were shown to be pH-dependent [9]. MFGM-rich emulsions were prepared from butter serum using a process described in Gassi et al.'s study [17]. Under pH 5.5, lipid droplets aggregated and gels formed in the emulsions, which could affect the droplets' microstructures [9].

Commercial MFGM products are usually made from dairy by-products, including whey and buttermilk. Membrane separation and cream washing are the two most typical operations in MFG compositions preparation. Membrane filtration systems are being exploited by the dairy industry for the fractionation of milk proteins. Because milk-fat-rich dairy fluid contributes to membrane fouling, skim milk is frequently utilized for membrane filtration. Higher cross-flow velocities, which produce a higher shear and transmembrane pressure (TMP) and permeate flux, could minimize fouling and prevent particle deposition. In addition, interactions between MFGM components and the size similarity with casein micelles remain problems on which some researchers are still working. Cream separator is the easiest way to separate milk into cream and skimmed milk. Before the membrane treatment, cream separation is a commonly used method to concentrate the MFGs compositions from either whey or buttermilk.

Dairy companies have been working on preparing natural MFGs and their compositions with more intact structures. Raw milk is now considering the original material to isolate MFGs because most MFGs in whey or buttermilk are fragments. The most stable and best-working pH for rennet is 5.30–6.30. Casein is a group name for the mixture of β, α and κ-casein (CN) which starts to precipitate at pH 5.30 [18]. However, just several studies are available on the effect of pH on MFGs and their membranes compositions before and after cream separation [2,19,20]. Two of the commonly used pH conditions in dairy processing, with pH values of 6.30 and 5.30, were investigated in this research. Furthermore, it is still unclear how to differentiate MFGs from MFGM damage, as well as how proteins are released during MFGM fragment disruptions.

Therefore, this study examines the changes in MFGs and MFGM proteins during cream separation from bovine milk at different pH conditions. The physicochemical properties and the microstructure of MFGs and MFGM proteins before and after cream separation are investigated. Meanwhile, the results are discussed in comparison with untreated raw milk. This study could provide technical information for a better understanding of the effect of dairy operation units on the structure and composition changes of MFGs and MFGMs. This is crucial for future studies on the physiological properties of MFGs and related compositions.

## 2. Materials and Methods

### 2.1. Materials

Raw bovine milk (fat 4.08 ± 0.02%, protein 3.57 ± 0.01%, dry matter 13.03 ± 0.02%, pH 6.74 ± 0.04) was collected from the Teagasc dairy herd (Moorepark, Fermoy, Co. Cork, Ireland). The raw bovine milk was untreated by any other unit operation except for the rapid chilling from 37 to 4 °C with a plate heat exchanger (UK Exchangers Ltd., Buckinghamshire, UK).

Chemicals for gel electrophoresis were bought from Thermo Scientific Inc. (Thermo Fisher Scientific Inc., Cork, Ireland). All solutions were prepared using MilliQ water except as otherwise noted.

### 2.2. Preparation of Samples

Centrifugal separation was performed using a disk bowl centrifugal separator (FT 15 Disc Bowl Centrifuge, Armfield co., Ringwood, UK) equipped with 19 disks. Firstly, 3 batches of raw milk collected from a 4 °C refrigerator, each of 5 kg, were preheated to 25–30 °C in a water bath (GFL 1012, Gesellschaft fuer Labortec, Burgwedel, Germany). Before the raw milk was separated into cream and skim fractions by a centrifugal separator, 2 batches of 5 kg raw milk were adjusted to pH 5.30 and 6.30, respectively. Batches of pH 6.74 ± 0.04 were taken as the control reference. Secondly, we continued to heat all batches of raw milk to 50–55 °C and incubated them during the whole separation process. The skim milk phase was added back into the separator one more time to maximally defat the skim milk. The cream and skim milk phases of each batch were collected separately and kept at 4 °C before analysis. The collected samples were named 6.74 R (raw milk pH 6.74), 6.30 R (raw milk pH 6.30), 5.30 R (raw milk pH 5.30), 6.74 C (cream pH 6.74), 6.30 C (cream pH 6.30), 5.30 C (cream pH 5.30), 6.74 S (skim milk pH 6.74), 6.30 S (skim milk pH 6.30) and 5.30 S (skim milk pH 5.30). Throughout the heating and pH adjustment process, all batches of samples were stirred gently to avoid part denaturation of the proteins induced by uneven temperature and excessive acidification, and 0.02% ($g/g$) azide sodium was added to prevent microbiological growth.

### 2.3. Compositions Analysis

Fat, protein and non-fat solids (SNFs) were analyzed with DairySpec FT-15 (Bentley Instruments Inc., Chaska, MN, USA). 30 mL of liquid sample was mixed thoroughly before analysis to avoid uneven sampling. All samples from the 4 °C storage were preheated to 25 °C in a water bath. For fat content analysis, cream samples needed to be diluted 10 times with MilliQ water. After the dilution of cream samples, the protein content is close to the detection limit (0-50%)of DairySpec FT-15, so that Kjeldahl method [21] was used to quantitatively analyze the protein content of cream samples (N × 6.38).

### 2.4. Particle Size Analysis

Particle size distributions of different pH samples were measured using a Mastersizer 3000 (Malvern Instruments, Malvern, UK) equipped with a laser light scattering. The refractive index for milk fat and water was set to 1.456 and 1.333, respectively. Particle sizes were recorded after at least 30 s of stabilization after adding samples to the measurement

device. The amount of samples depends on if the obscuration could reach the range of 3–20% [4,22]. The data were calculated according to Mie theory.

Samples were analyzed 3 times, and the data are expressed as volume distributions. Dv (10) and Dv (90) stand for the size of particles below which 10%/90% of the sample lies. Dv (50) means the size in microns at which 50% of the sample is smaller and 50% is larger, also known as the median of the volume distribution. Span is the measurement of the width of the distribution. The narrower the distribution, the smaller the span becomes. Uniformity is a measure of the absolute deviation from the median. Uniformity could demonstrate the degree of particle size distribution and the gradient of the distribution curve [23]. The value of the specific surface area (SSA) of all samples was calculated as the surface area of the particles per unit weight. The equation is as follows:

$$\mathrm{SSA} = 6/\mathrm{pD}\,[3,2] \quad (1)$$

where p is the particle density, and D [3,2] is the surface-weighted mean.

### 2.5. Zeta Potential

The zeta potential, as an indicator for the change of the milk fat globule surface, was analyzed by a dynamic light scattering instrument (Nano-ZS, Malvern Instruments Ltd., Worcestershire, UK) [22]. The Zetasizer software version 7.12 (Malvern Instruments Ltd.) was used to collect and analyze data. Zeta potential is evaluated by measuring the electrophoresis mobility and then calculated by the Henry equation. The Henry equation is:

$$U_E = 2\varepsilon z f(\mathrm{Ka})/3\eta \quad (2)$$

where:

z: Zeta potential

$U_E$: Electrophoretic mobility

$\varepsilon$: Dielectric constant

$\eta$: Viscosity

$f$(Ka): Henry's function, in this case, is 1.5 and is referred to as the Smoluchowski approximation since the double layer κ-1 of MFGs (around 1.1 nm) is smaller than their radius [24].

The electrophoretic mobility is obtained by performing an electrophoresis experiment on the sample and measuring the velocity of the particles using laser Doppler velocimetry. Samples were diluted by MilliQ water and analyzed in a Malvern Dip Cell at 25 °C. The requirement that zeta potential tests should be performed on diluted dispersion, which modifies the samples' structural characteristics, is a drawback. Additionally, dilution times and diluent types have a significant impact on the outcomes. In order to reduce the diluent-type effect, MilliQ water was used as the diluent. In preliminary experiments, the effect of MilliQ water dilution times (50, 100 and 1000 times) on the zeta potential was tested, and there was no significant difference between 100 and 1000 times. Thus, all samples were diluted 100 times in this research, and a 2-min equilibrium time was allowed before each measurement. Three readings were collected from each sample.

### 2.6. Sodium Dodecyl Sulphate Polyacrylamide Gel Electrophoresis (SDS–PAGE)

SDS-PAGE was conducted according to the method described by Ye, A. et al. with revised [25].

A Mini-PROTEIN Tetra cell was used for the protein analysis (Bio-Rad, Laboratories, inc. USA). Proteins in the raw milk, skim milk and cream were analyzed by reducing SDS–PAGE. Under reducing conditions, both non-covalently-linked and disulfide-linked complexes were dispersed and migrated into the resolving gel. The NuPAGE MOPS SDS Running Buffer (20×; 50 mM MOPS, 50 mM Tris Base, 0.1% SDS, 1 mM EDTA, pH 7.7) was purchased from Thermo Fisher Scientific Inc., which is used with NuPAGE Novex Bis-Tris Gels (Thermo Fisher Scientific Inc., Cork, Ireland) to resolve mid-size proteins.

For electrophoresis, dilute this buffer to 1× with MilliQ water. The NuPAGE Antioxidant (Thermo Fisher Scientific Inc., Cork Ireland) was used to avoid reoxidization.

MilliQ water was used to dilute the samples to a protein concentration of 40 µg/mL, then mixed with 4× NuPAGE LDS sample buffer (106 mM Tris–HCl, 141 mM Tris Base, 2% LDS, 10% glycerol, 0.51 mM EDTA, 0.22 mM SERVA coomassie blue G250, 0.175 mM phenol red, pH 8.5). The NuPAGE Reducing Agent (10×; Thermo Fisher Scientific Inc., Cork, Ireland) contained 500 mM dithiothreitol (DTT) and was added to the samples at least one hour before loading the samples to prevent reoxidation during storage and producing inconsistent results.

A criterion 12% NuPAGE Novex Bis-Tris Gels (Thermo Fisher Scientific Inc., Cork, Ireland) was used to separate proteins. All samples were heated to 70 °C and inoculated for 5 min to denature the proteins. Before being loaded into the gels, denatured samples needed to cool down to room temperature and centrifuged. A marker with a molecular weight between 10–200 kDa (Thermo Fisher Scientific Inc., Ireland) was used.

Gels were run at 120 V for 45 min and then dyed the proteins with Coomassie blue for more than 60 min with gentle shaking. A solution containing 45% ethanol and 5% acetic acid was used to destain the gels. After being destained for 50 min, the solution was changed to remove the stain overnight. Typical MFGM proteins (PAS 6/7, BTN and XO) and milk serum proteins (α-LA, β-LG and caseins) were selected to relatively quantify the analysis. The relative density of representative proteins was analyzed using ImageJ software 1.36 b (Wayne Rasband, National Institutes of Health, Bethesda, MD, USA) and normalized to 100%.

### 2.7. Confocal Laser Scanning Microscopy (CLSM)

CLSM could be used to qualitatively analyze different types of proteins adsorbed on the surface of MFGs, which demonstrates the effect of treatment on the reconstruction of protein and fat globules. Non-polar lipids, which were mostly triglyceride, were labeled with Nile Red (9- (diethylamino)-5 H-benzo[*a*]phenoxazin-5-one, Sigma–Aldrich®, Merck Life Science Ltd., Cork, Ireland), and serum protein and glycoproteins with fluorescent Fast Green (FCF; N-ethyl-N-[4-[[4-[ethyl[(3-sulfophenyl)methyl]amino]phenyl](4-hydroxy-2-sulfophenyl)methylene]-2,5-cyclohexadien-1-ylidene]-3-sulfo-benzenemethanaminium, disodium salt, Cayman Chemical, Ann Arbor, MI, USA) and wheat germ agglutinin (WGA; Alexa Fluro® 488 conjugate, Invitrogen, Ltd., Renfrew, UK), respectively [26,27]. Considering the low fat content of the skim milk, only the raw milk and cream samples (80 µL) were dual-stained with a 10 µL mixture of Nile red (0.1%, *w*/*v*, in polyethylene glycol-200) and FCF (0.1%, w/v, in distilled water; FCF: Nile red = 3:1 *v*/*v*). In addition, WGA (50 µL, 1 mg/mL in PBS) was mixed with Nile red in a proportion of 1:1 (*v*/*v*). All dyed samples were kept in the dark for 30 min at room temperature to ensure complete staining. The proportion between the sample and stain was optimized in the pre-experiment to take account of the variation of pH and incomplete dyeing.

Leica TCS SP5 microscope (Leica Microsystems GmbH, Wetzlar, Germany) was used to detect at room temperature (25 ± 2 °C). Nile red, FCF and WGA were excited using a He-Ne laser, and emission wavelengths were detected between 565–625 nm, 632–719 nm and 493–550 nm, respectively. A 63×oil-immersion lens was used to observe the samples. Two channels—FCF or WGA channel 1 and Nile red channel 2—were used for CLSM observation. Dual-stain imageswere obtained by merging images produced in 2 different channels. No less than 10 images were recorded for each sample. Of all the images, the representative 1 for each experiment was chosen. Leica application suite X (3.7.5.24914; Leica Microsystem CMS GmbH, Wetzlar, Germany) was used for image processing and analysis. Two-dimensional images presented a resolution of 512 × 512 pixels, and a scaling factor was used to convert the pixel scale values into micrometers.

### 2.8. Statistical Analysis

There was triplication of each experiment. Each value represents the mean of at least 3 measurements, and values are expressed as means ± standard deviations. A 1-way ANOVA was used to calculate significant differences (95.0% confidence level) between the samples using Minitab 17 Statistical Software (Minitab Inc. State College, PA, USA).

## 3. Results

### 3.1. Composition Analysis

The fat, protein and SNF contents of all samples are shown in Table 1. The amount of protein included serum proteins and MFGM proteins. After cream separation, the fat in all cream samples was between 39.90–40.5% ignoring the pH variation, but the protein content significantly varied with different pH values. 6.30 C had the most proteins (2.01 ± 0.02%), followed by 5.30 C and 6.74 C (1.76 ± 0.03% and 1.50 ± 0.01%). There was no significant difference in the amount of fat, proteins and SNF in raw milk samples ($p > 0.05$) as a function of pH decrease. For skim milk samples, 6.74 S and 6.30 S presented a similar protein amount, while 5.30 S had a higher content of fat and protein. From the data analysis above, we could speculate that the pH 5.30 condition was the main reason for the difference. The pH 5.3 condition is close to the pI of some proteins. Partial aggregates of proteins in raw milk are easy to get into the skim milk phase during the cream separation process.

**Table 1.** Composition analysis of raw milk, skim milk and cream samples at different pH.

| Samples | Fat (g/100 g) | Protein (g/100 g) | SNF (Solid Non-Fat; g/100 g) |
|---|---|---|---|
| 6.74 R | 4.85 ± 0.04 $^{a}$ | 3.55 ± 0.00 $^{a}$ | 12.36 ± 0.10 $^{a}$ |
| 6.30 R | 4.83 ± 0.02 $^{a}$ | 3.66 ± 0.04 $^{a}$ | 12.33 ± 0.12 $^{a}$ |
| 5.30 R | 4.90 ± 0.01 $^{a}$ | 3.63 ± 0.00 $^{a}$ | 12.23 ± 0.01 $^{a}$ |
| 6.74 S | 0.14 ± 0.00 $^{b}$ | 3.74 ± 0.03 $^{b}$ | 12.79 ± 0.06 $^{a}$ |
| 6.30 S | 0.23 ± 0.02 $^{a}$ | 3.76 ± 0.05 $^{b}$ | 12.84 ± 0.07 $^{a}$ |
| 5.30 S | 0.27 ± 0.01 $^{a}$ | 3.82 ± 0.01 $^{a}$ | 12.76 ± 0.02 $^{a}$ |
| 6.74 C | 40.50 ± 0.80 $^{a}$ | 1.50 ± 0.01 $^{c}$ | 0.40 ± 0.01 $^{a}$ |
| 6.30 C | 40.40 ± 1.02 $^{b}$ | 2.01 ± 0.02 $^{a}$ | 0.49 ± 0.02 $^{a}$ |
| 5.30 C | 39.90 ± 1.01 $^{b}$ | 1.76 ± 0.03 $^{b}$ | 0.43 ± 0.01 $^{a}$ |

Data in the table represent the mean ± SD of three replicates; Different superscript letters among the same types of samples (raw milk, skim milk and cream) in the same column refer to statistically significant differences ($p < 0.05$); 6.74 R (raw milk pH 6.74), 6.30 R (raw milk pH 6.30), 5.30 R (raw milk pH 5.30), 6.74 C (cream pH 6.74), 6.30 C (cream pH 6.30), 5.30 C (cream pH 5.30), 6.74 S (skim milk pH 6.74), 6.30 S (skim milk pH 6.30) and 5.30 S (skim milk pH 5.30).

### 3.2. Particle Size

The Dv(10), Dv(50) and Dv(90) of cream samples are significantly higher than those of raw milk and skim milk samples ($p < 0.05$) except for skim milk under the pH 5.3 condition (Table 2). This result could be explained by the fact that the fat globules present bigger particle sizes than milk proteins. According to the results of composition analysis in Section 3.1, fat content in cream samples was significantly higher than that in raw milk and skim milk samples. It was reported that the size of milk fat globules in untreated milk varied from 0.2–15 μm, with a mean diameter of 3–4 μm [28]. Native casein micelles which exist as the particles in milk, consist of casein proteins and calcium phosphate [18].

**Table 2.** Fat globule size, SSA, span and uniformity of raw milk, cream and skim milk samples with different pH.

| Samples | Dv(10) (μm) | Dv(50) (μm) | Dv(90) (μm) | Specific Surface Area ($cm^2/g$) | Span | Uniformity |
|---|---|---|---|---|---|---|
| 6.74 R | 0.03 ± 0.00 $^{e}$ | 0.65 ± 0.21 $^{f}$ | 7.65 ± 0.06 $^{e}$ | 65.41 ± 1.06 $^{c}$ | 5.51 ± 0.81 $^{d}$ | 2.14 ± 0.23 $^{b}$ |
| 6.30 R | 0.04 ± 0.00 $^{e}$ | 2.52 ± 0.19 $^{e}$ | 12.37 ± 2.13 $^{d}$ | 56.96 ± 2.03 $^{d}$ | 6.41 ± 0.55 $^{c}$ | 2.49 ± 0.11 $^{b}$ |
| 5.30 R | 0.04 ± 0.00 $^{e}$ | 2.96 ± 0.20 $^{e}$ | 10.53 ± 0.07 $^{c}$ | 47.68 ± 4.11 $^{e}$ | 8.05 ± 0.29 $^{b}$ | 4.41 ± 0.30 $^{a}$ |
| 6.74 C | 2.16 ± 0.00 $^{a}$ | 8.93 ± 0.11 $^{a}$ | 51.42 ± 0.73 $^{a}$ | 1.69 ± 0.13 $^{h}$ | 3.62 ± 0.31 $^{d}$ | 1.67 ± 0.01 $^{d}$ |
| 6.30 C | 1.57 ± 0.02 $^{b}$ | 7.28 ± 0.10 $^{b}$ | 48.21 ± 2.10 $^{b}$ | 2.04 ± 0.05 $^{g}$ | 4.88 ± 0.20 $^{e}$ | 1.78 ± 0.09 $^{d}$ |
| 5.30 C | 0.97 ± 0.04 $^{c}$ | 5.86 ± 0.26 $^{c}$ | 48.14 ± 8.50 $^{b}$ | 2.28 ± 0.02 $^{g}$ | 12.65 ± 0.41 $^{a}$ | 2.43 ± 0.25 $^{b}$ |
| 6.74 S | 0.02 ± 0.00 $^{e}$ | 0.07 ± 0.01 $^{g}$ | 0.25 ± 0.01 $^{f}$ | 110.10 ± 2.35 $^{a}$ | 3.06 ± 0.06 $^{f}$ | 1.97 ± 0.24 $^{c}$ |
| 6.30 S | 0.02 ± 0.00 $^{e}$ | 0.08 ± 0.02 $^{g}$ | 0.28 ± 0.00 $^{f}$ | 103.62 ± 10.24 $^{b}$ | 3.15 ± 0.13 $^{f}$ | 2.57 ± 0.07 $^{b}$ |
| 5.30 S | 0.81 ± 0.02 $^{d}$ | 5.29 ± 0.52 $^{d}$ | 9.18 ± 0.24 $^{c}$ | 8.32 ± 0.21 $^{f}$ | 1.59 ± 0.08 $^{g}$ | 0.43 ± 0.00 $^{e}$ |

Data in the table represent the mean ± SD of three replicates; Different superscript letters in the same column refer to statistically significant differences ($p < 0.05$); 6.74 R (raw milk pH 6.74), 6.30 R (raw milk pH 6.30), 5.30 R (raw milk pH 5.30), 6.74 C (cream pH 6.74), 6.30 C (cream pH 6.30), 5.30 C (cream pH 5.30), 6.74 S (skim milk pH 6.74), 6.30 S (skim milk pH 6.30) and 5.30 S (skim milk pH 5.30).

Native bovine milk is a semi-stable emulsion at 37 °C or above in which casein micelles at pH 6.70 are generally assumed to remain in suspension due to the hairy layer of κ-casein providing steric and electrostatic repulsion [29]. Hydrophobic and hydrophilic radicals on the surface of MFGs, acting as natural emulsifying agents, play an important role in preventing the flocculation and coalescence of the globules and keeping the charge balance between milk protein and fat globules. Acid induced an increased attachment of milk protein to the surface of MFGs due to the charge change of MFGs and serum protein. This could be the reason for the slight increase of Dv(10), Dv(50) and Dv(90) in raw milk samples with the pH decrease. Cream samples presented the opposite trend to raw milk with the smallest Dv(10), Dv(50) and Dv(90) at pH 5.30, which were between 0.97 ± 0.04 and 48.14 ± 8.50 μm. This is inconsistent with Holzmüller et al. [16], who reported larger particles with decreasing pH. The shear force in the disc stack of the cream separator resulted in MFGs disruption, which led to the coalescence of the fat globules and then contributed to the increase of particle size [30].

No effect of pH on Dv(10), Dv(50) and Dv(90) of skim milk samples was detected between 6.74 and 6.30, but there was a sharp increase as the pH continually decreased to 5.30. Casein, with an isoelectric point at pH 4.6, tended to coalesce and precipitate from milk with lower pH, at which condition particle size values moved towards large ones (Table 2 and Figure 1C).

Data in Table 2 showed that as the Dv(10), Dv(50) and Dv(90) decreased, the corresponding SSA increased. This accords with P. Sharma et al.'s report, which showed that the D [3,2] of untreated whole milk decreased with the intensity of pulsed electric field treatment [19], while the corresponding SSA increased. The trends for span and uniformity were comparable. It was shown that more homogenous particle sizes in samples presented smaller uniformity [23]. Cream samples presented higher span and uniformity values than raw milk and skim milk samples. Accordingly, particle size in cream samples was wider and more multitudinous (Figure 1B). Generally, the main particle size of raw milk samples was between 0.01 and 174 μm (Figure 1A), while skim milk samples with pH 6.74 and 6.30 present the narrowest size distribution, between 0.01 and 9.98 μm (Figure 1C).

According to these results, we speculated that under the same pH condition, the change in particle size of fat globules could be attributed to the shear force produced by the separator. It could be due to the coalescence or damage of MFGs and the loss of MFGM materials [31]. Besides, most of the presumed stabilizing materials (caseins and whey proteins) are lost during the cream separation. However, in this and Holzmüller et al.'s [4] previous research, the shear force of the cream separator was not quantitatively analyzed, and the relation between the extent of shear force and fat globules damage was not confirmed. Thus, the effect of shear force on the integrity of MFGs still needs to be further investigated. In addition, we could conclude that the pH variation could be an

important factor in changing the particle size of all samples. Either because the change of proteins on the surface of MFGs, or the attachment of casein or whey proteins on MFGMs.

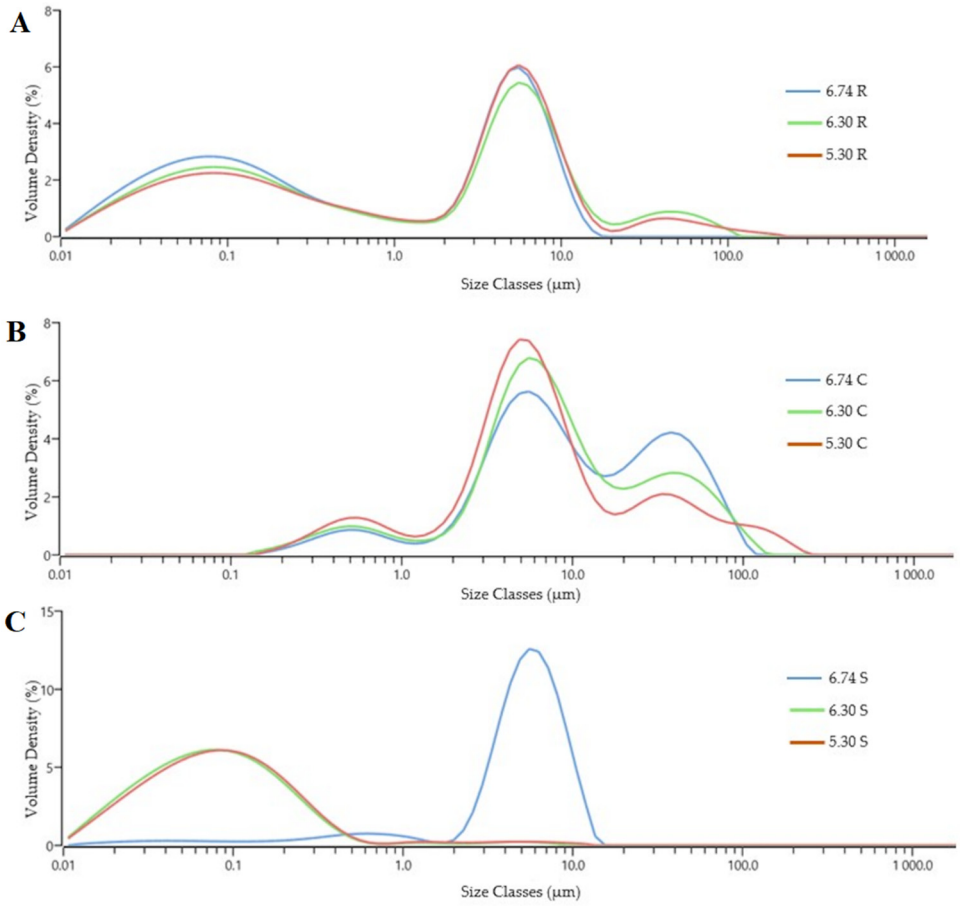



**Figure 1.** Volume density (%) of raw milk (**A**), cream samples (**B**) and skim milk (**C**) at different pH. 6.74 R (raw milk pH 6.74), 6.30 R (raw milk pH 6.30), 5.30 R (raw milk pH 5.30), 6.74 C (cream pH 6.74), 6.30 C (cream pH 6.30), 5.30 C (cream pH 5.30), 6.74 S (skim milk pH 6.74), 6.30 S (skim milk pH 6.30) and 5.30 S (skim milk pH 5.30).

### *3.3. Zeta Potential*

The stability of casein micelles and milk fat has been associated with zeta potential value. The measured zeta potentials of all samples are illustrated in Figure 2. All of the samples showed a negative zeta potential. According to Michalski et al. [32], casein micelles and MFGs both have negative charges between pH 6.60–6.70 at 25 °C, and their apparent zeta potential is negative. Thus, it should be noted that the description of the increase or decrease of zeta potential in this study is not used algebraically but refer to their absolute values. Hence, it should be understood that algebra is not used in this research to describe how the zeta potential increases or decreases; rather, it refers to the absolute magnitude of the zeta potential.

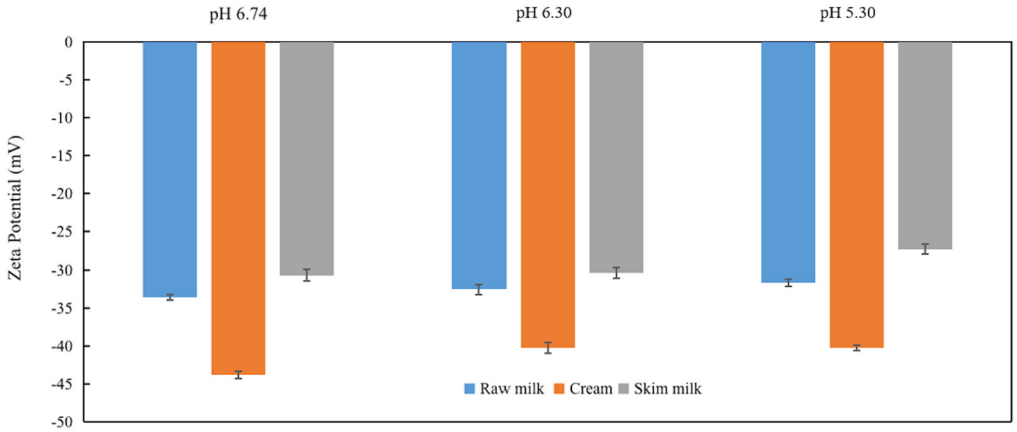



**Figure 2.** Zeta potential of raw milk, cream and skim milk as a function of pH.

The zeta potential of raw milk with pH 6.74, when measured at 25 °C, was −33.60 mV (Figure 2), which was much higher than the previously published reports. P. Sharma et al. [19] and Michalski et al. [33] showed that the zeta potential value of whole milk at physiological pH (6.60–7.0) was −13.7 ± 0.1 mV. Some other researchers published −22 mV for whole milk at pH 6.67 [34,35]. Jukkola et al. investigated the effect of diafiltration media on the separation of MFGs via microfiltration [20]. The zeta potential values for the feed milk were −30 mV, which is quite close to our results. Comparing zeta potential results of different research is challenging since many factors greatly influence the obtained value. Michalski, Michel et al. [33] found that different analysis techniques, including laser Doppler electrophoresis (particularly the scattered light angle) or electroacoustic methods, could affect the zeta potential [19]. Other experimental conditions (e.g., diluent and temperature) could also significantly affect the zeta potential value [36] and hence the zeta potential. There was no significant difference in the zeta potential of raw milk between pH 6.74 and 5.30 (25 °C; $p > 0.05$)

The zeta potential of skim samples of different pH varied from −27.3 to −30.7 mV, which was relatively lower than that of cream and raw milk samples. At a pH of 6.7–6.8 (25 °C), reconstituted skim milk was found to have a zeta potential of −34.6 ± 3.6 mV [37]. The charge of casein switches from negative to positive as the pH decrease [38]. This could explain why the zeta potential of skim milk samples at pH 5.30 (−27.3 mV) was significantly ($p < 0.05$) lower than that of pH 6.74 (−30.7 mV). At lower pH, there was more adsorption of caseins and whey proteins on the MFGs surface in raw milk samples. However, after mechanical treatment in the centrifugation process, the amount of the adsorbing serum proteins decreased, thus decreasing the zeta potential in skim samples.

pH 5.30 condition further decreased the zeta potential of cream samples to −40.3 mV. This might be a result of a modification to the MFGM protein, which leads to an increase in the exposure of negatively charged and/or hydrophobic areas [37]. The findings for zeta potential were consistent with those for particle size at pH 5.30, leading to the smaller particle size of cream samples. For conducting particles, the zeta potential value generally depends on their particle size [33,39].

### *3.4. SDS-PAGE*

The change in serum and MFGM protein with the pH variation was determined by SDS-PAGE under reducing condition (Figure 3). Meanwhile, relative protein content was quantified by combining densitometry with the total lane signal intensity (Figure 4). The electrophoresis mobility of proteins was used to define their molecular weight as well as numerous published literatures: caseins 19–34 kDa, β-LG 18 kDa, α-LA 14 kDa, XO 146–155 kDa, BTN 66–67 kDa and PAS 6/7 47–59 kDa [5,40–43].

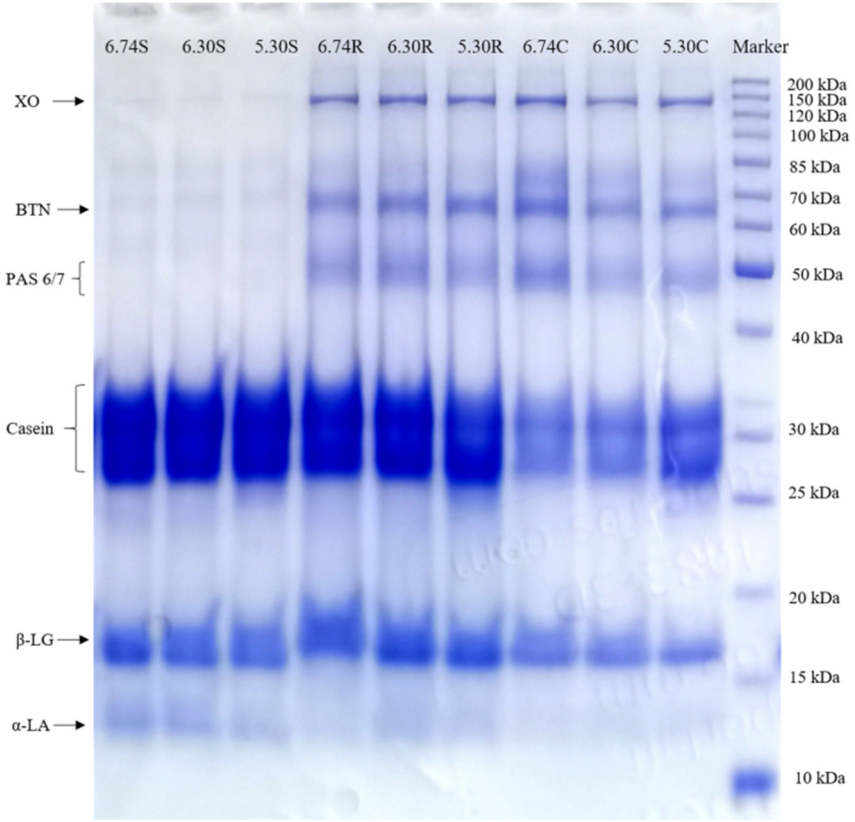



**Figure 3.** SDS-PAGE shows the predominant proteins presenting in raw milk, cream and skim milk with different pH.· 6.74 R (raw milk pH 6.74), 6.30 R (raw milk pH 6.30), 5.30 R (raw milk pH 5.30), 6.74 C (cream pH 6.74), 6.30 C (cream pH 6.30), 5.30 C (cream pH 5.30), 6.74 S (skim milk pH 6.74), 6.30 S (skim milk pH 6.30) and 5.30 S (skim milk pH 5.30). PAS 6/7, periodic acid Schiff 6 and 7; BTN, butyrophilin; XO, xanthine oxidase; α-LA, α-lactalbumin; β-LG, β-lactoglobulin.

Qualitative differences between the individual samples depend on the intensity of the protein bands. Higher relative intensities typically denote a higher protein content. A loss of XO, BTN and PAS 6/7 in skim milk samples was observed in Figure 3. The protein profile of cream samples differed from that of the skim milk, with more dominant MFGM proteins at the expense of casein, β-LG and α-LA.

It was more prominent in the incorporation of α-LA in cream samples at lower pH during centrifugal separation. The relative content of α -LA in cream samples at pH 5.30 increased by 19.18% than that in 6.74 C samples (Figure 4). However, at pH 5.30, the levels of α-LA in both the raw milk and the skim samples were reduced, which was predicted based on the influence of charge on the solubility of α-LA in casein micelles. The solubility of α-LA decreased by a higher calcium quantity in the aqueous phase caused by the release of calcium phosphate from micelles under acidic conditions [44].

β-LG was reported to interchangeably interact with MFGM proteins via sulfhydryl-disulfide, then bound to the casein micelles through κ-casein [25]. A lower pH condition apparently is not helpful for this interaction since either raw milk or cream samples showed less β-LG amounts at pH 5.30.

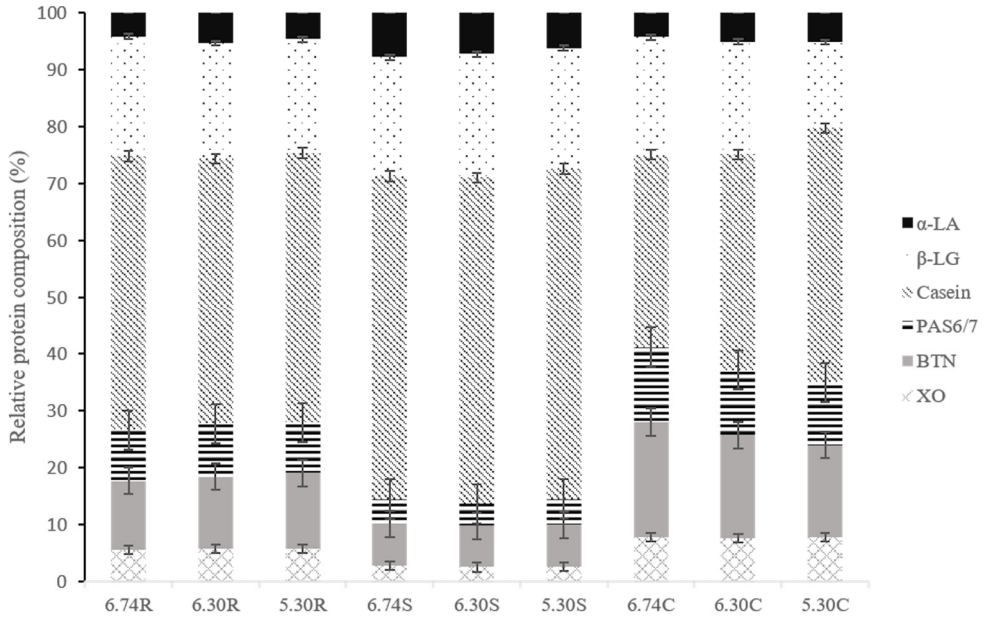



**Figure 4.** Relative protein compositions of raw milk, cream and skim milk samples derived from densitometry measurements of bands in a representative SDS-PAGE gel; 6.74 R (raw milk pH 6.74), 6.30 R (raw milk pH 6.30), 5.30 R (raw milk pH 5.30), 6.74 C (cream pH 6.74), 6.30 C (cream pH 6.30), 5.30 C (cream pH 5.30), 6.74 S (skim milk pH 6.74), 6.30 S (skim milk pH 6.30) and 5.30 S (skim milk pH 5.30).

Regarding BTN, PAS 6/7 and XO, both Figures 3 and 4 showed the lower pH led to a higher BTN and PAS 6/7 loss in cream samples. However, the relative content of XO in all samples had no significant variation as pH decreased ($p > 0.05$). The theoretical pI of BTN is 5.32. [16,40], this protein tends to precipitate at pH 5.30. This could explain the more intense BTN bands in raw milk samples at pH 5.30 since BTN was released from the MFGM and formed purer aggregates. BTN is typically referred to as an integral protein, whereas PAS 6/7 is classified as a periphery protein [4]. BTN and part of XO were reported to strongly attach to MFGM after the extracted pre-treatment with Triton X-100, sodium deoxycholate and guanidine hydrochloride [45]. The amount of PAS 6/7 in the 6.74 S samples was reduced by 51.90% more than that in the 6.74 R samples, with a relative intensity of only 7.34 and 4.29% for BTN and XO in 6.74 S, respectively (Figure 4). This outcome was inconsistent with the binding of MFGM proteins previously mentioned. It was positive to find that cream samples contained a more significant amount of MFGM proteins than skim and raw milk samples ($p < 0.05$), with a range of 7.59–88%, 16.09–20.12% and 10.98–13.14 %, respectively. This confirmed that not only loosely-bound membrane components but also integral proteins were lost during cream separation [46]. The results above are consistent with the particle size shift in Section 3.2, which shows that cream samples present higher Dv (10), Dv (50) and Dv (90) values than skim and raw milk.

Overall, shear force plus the pH decreasing during the cream separation process did change the protein compositions of MFGM. Probably due to fat globule damage, parts of MFGM materials are released from the fat globule and partitioned into the serum phase or associated with the serum proteins.

### *3.5. CLSM*

The CLSM technique was developed to detect the MFGs in their native or specific environments (i.e., certain pH conditions) in a non-destructive manner. In our research, the samples were dual-stained by combining Nile Red with FCF or WGA.

The microstructural comparison of raw milk and cream samples with different pH are shown in Figures 5 and 6. Just as the conclusions from amounts of previous research, milk

fat existed in the state of regular spheres [27,47,48]. Triglyceride was the main composition of MFGs and could be observed in the core of MFGs, which showed green (Figure 5) or red fluorescence (Figure 6). Serum proteins including casein and whey protein were stained using FCF and presented red color, as shown in Figure 5. MFGs were covered by MFGM that consisted of heterogeneous glycoproteins stained by fluorescent green color (Figure 6).

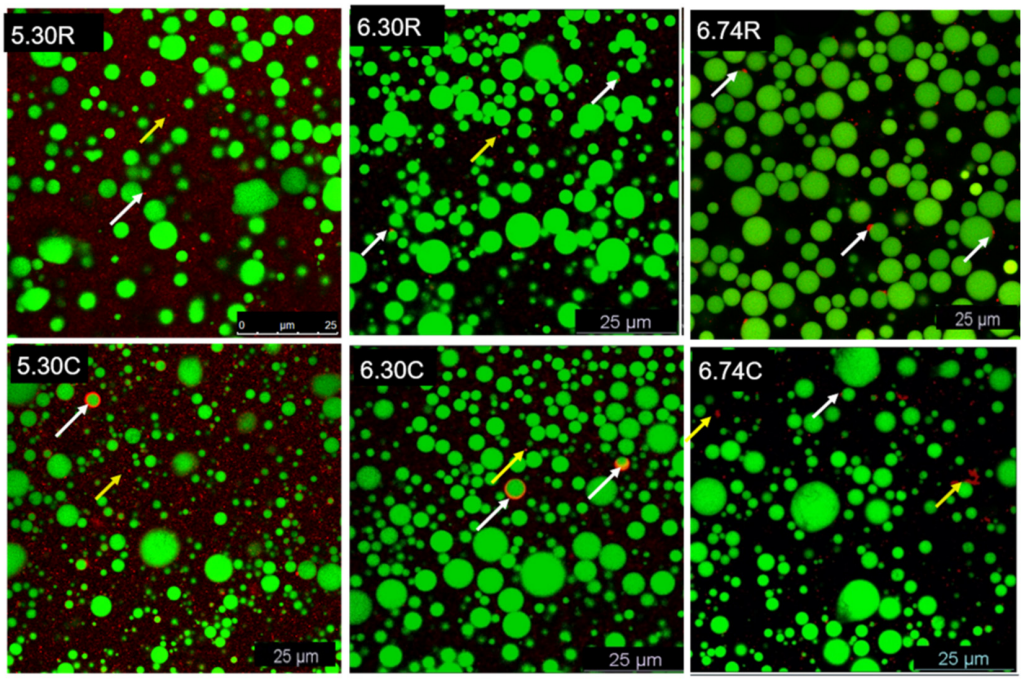



**Figure 5.** Confocal images of dual-stained milk fat globules in raw milk and cream at different pH. White and yellow arrows mark the serum proteins attaching on the surface of MFGs and drifting in the liquid phase, respectively. MFGs stained with Nile Red (green), and serum proteins stained with fluorescent Fast Green. 6.74 R (raw milk pH 6.74), 6.30 R (raw milk pH 6.30), 5.30 R (raw milk pH 5.30), 6.74 C (cream pH 6.74), 6.30 C (cream pH 6.30), 5.30 C (cream pH 5.30), 6.74 S (skim milk pH 6.74), 6.30 S (skim milk pH 6.30) and 5.30 S (skim milk pH 5.30).

Cream samples contained fewer serum proteins than raw milk samples, which was confirmed by the weaker fluorescent signal (red color). This could be identified by the results of the composition analysis in Section 3.1. Serum proteins, especially caseins, tended to form network structures at pH 5.30. In comparison with pH 6.30 and 6.74, either 5.30 R or 5.30 C samples showed the evident network structure formed by serum proteins (Figures 5 and 6. Cream samples showed bigger MFGs than raw milk samples, and this result is in accordance with the particle size analysis in Section 3.2.

CLSM images demonstrated that pH adjustment promoted serum protein adsorption on the outer layer of fat globules (Figure 5). Compared to cream samples, protein adsorption was more pronounced in raw milk samples, perhaps due to the lower protein content of cream samples or the desorption from the surface of MFGs during centrifugation. As for the glycoproteins, the fluorescent signals on the surface of cream samples were more discontinuous than that for the raw milk samples (Figure 6). Meanwhile, at pH 5.30, more flocculation and coalescence of MFGM proteins were observed on the surface or in the serum phase of raw milk and cream samples. This result is in contrast to the SDS-PAGE analysis that showed the more amounts of MFGM proteins in cream samples and lower pH value further exacerbated this phenomenon. We speculated that SDS-PAGE samples preparation in this research could not tell the exact location of MFGM proteins which were either on the surface of the MFGs or in the serum phase. Since the CLSM is only a qualitative analysis method, it is impossible to accurately calculate the total MFGM proteins

in the observing views. Thus, non-invasive and quantitative methods are expected to be developed in further research.

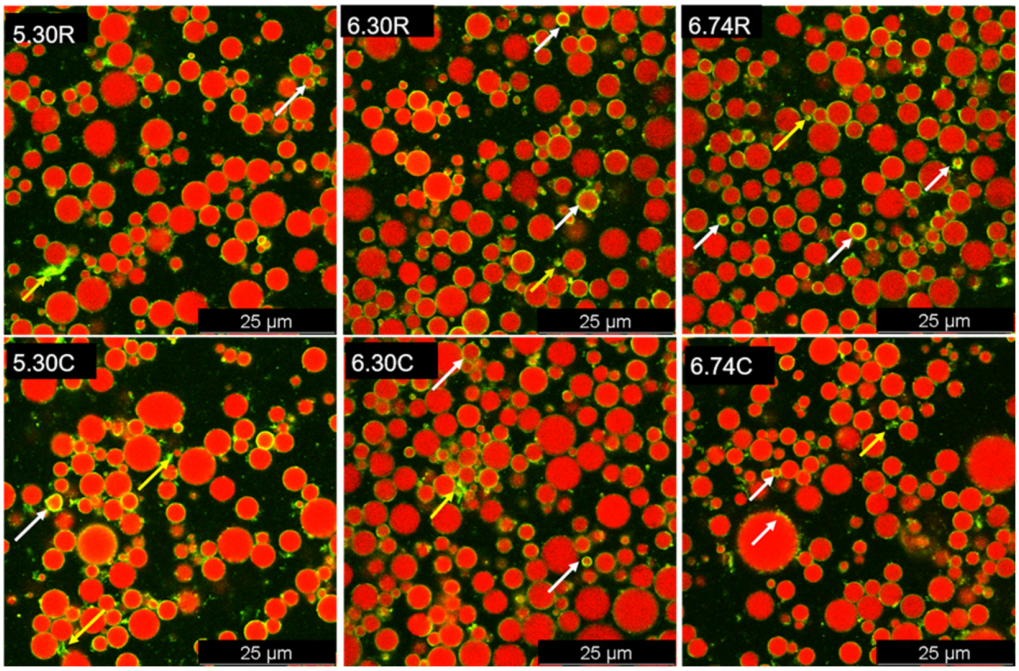



**Figure 6.** Confocal micrographs of double-stained milk fat globules in raw milk and cream at different pH. White arrows mark the glycoproteins attaching to the surface of MFGs, while yellow arrows mark the coalescent glycoproteins. MFGs were dyed with Nile Red (red), and glycoproteins were dyed with wheat germ agglutinin (WGA; yellow-green. 6.74 R (raw milk pH 6.74), 6.30 R (raw milk pH 6.30), 5.30 R (raw milk pH 5.30), 6.74 C (cream pH 6.74), 6.30 C (cream pH 6.30), 5.30 C (cream pH 5.30), 6.74 S (skim milk pH 6.74), 6.30 S (skim milk pH 6.30) and 5.30 S (skim milk pH 5.30).

## 4. Conclusions

In spite of the functionality and physiology of MFGs being widely researched in recent years, the effect of dairy processing on this is poorly understood. This research unprecedentedly demonstrated the implication of pH adjusting on the structure of MFGs and MFGM protein compositions during the cream separation. SDS-PAGE images and relative quantitative data showed that a loss of MFGM proteins after cream separation was inevitable, especially the BTN and PAS 6/7 at pH 5.30. Meanwhile, casein and whey protein tended to absorb on the surface of MFGs or form networks under the pH 5.30 condition, but mechanical force during centrifugation could desorb the attached serum proteins or the intrinsic glycoproteins. Thus, this led to the particle size change of MFGs and the rearrangement of MFGM compositions. Particle size (Dv (10), Dv(50) and Dv (90)) and zeta potential of cream samples decrease at lower pH 5.30.

Only two typical pH conditions (pH 5.30 and 6.30) were investigated in the present study, and how the pH variation and centrifugation affected the lipids of MFGMs and their physiological properties was not studied. Considering some analysis methods probably bringing about the structure or compositional changes of MFGs, more non-invasive methods need to be developed to conduct the real in situ observation.

**Author Contributions:** Conceptualization, Y.S. and S.M.; Data curation, Y.S.; Formal analysis, Y.S.; Funding acquisition, S.M.; Investigation, Y.S.; Methodology, Y.S.; Project administration, S.M.; Supervision, Y.H.R. and S.M.; Validation, Y.S.; Visualization, Y.S.; Writing—original draft, Y.S.; Writing—review & editing, Y.H.R. and S.M. All authors have read and agreed to the published version of the manuscript.

**Funding:** the Open Project Program of State Key Laboratory of Dairy Biotechnology (No. SKLDB2022-007) and the China Scholarship Council (No.202008410212).

**Data Availability Statement:** Data generated during the study are available from the corresponding author upon request.

**Conflicts of Interest:** Authors are also from Teagasc Food Centre. The objectivity and authenticity of the experimental results and discussion were not affected.

## References

1. Liao, Y.; Alvarado, R.; Phinney, B.; Lönnerdal, B. Proteomic Characterization of Human Milk Fat Globule Membrane Proteins during a 12 Month Lactation Period. *J. Proteome Res.* **2011**, *10*, 3530–3541. [CrossRef] [PubMed]
2. Singh, H.; Gallier, S. Nature's complex emulsion: The fat globules of milk. *Food Hydrocoll.* **2017**, *68*, 81–89. [CrossRef]
3. Vanderghem, C.; Bodson, P.; Danthine, S.; Paquot, M.; Deroanne, C.; Blecker, C. Milk fat globule membrane and buttermilks from composition to valorization. *Biotechnol. Agron. Soc. Environ.* **2010**, *14*, 485–500.
4. Holzmüller, W.; Müller, M.; Himbert, D.; Kulozik, U. Impact of cream washing on fat globules and milk fat globule membrane proteins. *Int. Dairy J.* **2016**, *59*, 52–61. [CrossRef]
5. Fong, B.Y.; Norris, C.S.; MacGibbon, A.K.H. Protein and lipid composition of bovine milk-fat-globule membrane. *Int. Dairy J.* **2007**, *17*, 275–288. [CrossRef]
6. Gorewit, V.L.S.a.R.C. Isolation, Purification and Characterization of Fatty-Acid-Binding Protein from Milk. *Pak. J. Nutr.* **2002**, *1*, 43–48.
7. Mana, P.; Goodyear, M.; Bernard, C.; Tomioka, R.; Freire-Garabal, M.; Linares, D. Tolerance induction by molecular mimicry: Prevention and suppression of experimental autoimmune encephalomyelitis with the milk protein butyrophilin. *Int. Immunol.* **2004**, *16*, 489–499. [CrossRef]
8. Timby, N.; Hernell, O.; Vaarala, O.; Melin, M.; Lonnerdal, B.; Domellof, M. Infections in infants fed formula supplemented with bovine milk fat globule membranes. *J. Pediatr. Gastroenterol. Nutr.* **2015**, *60*, 384–389. [CrossRef]
9. Lopez, C.; Cauty, C.; Rousseau, F.; Blot, M.; Margolis, A.; Famelart, M.H. Lipid droplets coated with milk fat globule membrane fragments: Microstructure and functional properties as a function of pH. *Food Res. Int.* **2017**, *91*, 26–37. [CrossRef]
10. Peterson, J.A.; Patton, S.; Hamosh, M. Glycoproteins of the human milk fat globule in the protection of the breast-fed infant against infections. *Neonatology* **1998**, *74*, 143–162. [CrossRef]
11. Ross, S. Targeting the Glycome of the Milk Fat Globule Membrane for Anti-Infective Properties. Doctoral Thesis, National University of Ireland, Galway, Ireland, October 2016.
12. Spitsberg, V.L. Invited Review: Bovine Milk Fat Globule Membrane as a Potential Nutraceutical. *J. Dairy Sci.* **2005**, *88*, 2289–2294. [CrossRef] [PubMed]
13. Holzmüller, W.; Kulozik, U. Technical difficulties and future challenges in isolating membrane material from milk fat globules in industrial settings—A critical review. *Int. Dairy J.* **2016**, *61*, 51–66. [CrossRef]
14. Murthy, A.V.R.; Guyomarc'h, F.; Lopez, C. The temperature-dependent physical state of polar lipids and their miscibility impact the topography and mechanical properties of bilayer models of the milk fat globule membrane. *Biochim. Biophys. Acta. Biomembr.* **2016**, *1858*, 2181–2190. [CrossRef] [PubMed]
15. Lopez, C.; Blot, M.; Briard-Bion, V.; Cirie, C.; Graulet, B. Butter serums and buttermilks as sources of bioactive lipids from the milk fat globule membrane: Differences in their lipid composition and potentialities of cow diet to increase n-3 PUFA. *Food Res. Int.* **2017**, *100*, 864–872. [CrossRef] [PubMed]
16. Holzmüller, W.; Gmach, O.; Griebel, A.; Kulozik, U. Casein precipitation by acid and rennet coagulation of buttermilk: Impact of pH and temperature on the isolation of milk fat globule membrane proteins. *Int. Dairy J.* **2016**, *63*, 115–123. [CrossRef]
17. Gassi, J.Y.; Blot, M.; Beaucher, E.; Robert, B.; Leconte, N.; Camier, B.; Rousseau, F.; Bourlieu, C.; Jardin, J.; Briard-Bion, V. Preparation and characterisation of a milk polar lipids enriched ingredient from fresh industrial liquid butter serum: Combination of physico-chemical modifications and technological treatments. *Int. Dairy J.* **2016**, *52*, 26–34. [CrossRef]
18. De Kruif, C. Casein micelle interactions. *Int. Dairy J.* **1999**, *9*, 183–188. [CrossRef]
19. Sharma, P.; Oey, I.; Everett, D.W. Interfacial properties and transmission electron microscopy revealing damage to the milk fat globule system after pulsed electric field treatment. *Food Hydrocoll.* **2015**, *47*, 99–107. [CrossRef]
20. Jukkola, A.; Partanen, R.; Rojas, O.J.; Heino, A. Separation of milk fat globules via microfiltration: Effect of diafiltration media and opportunities for stream valorization. *J. Dairy Sci.* **2016**, *99*, 8644–8654. [CrossRef]
21. *ISO 8968-1: 2001*; Milk–Determination of Nitrogen Content–Part 1: Kjeldahl Method. ISO: Geneva, Switzerland, 2001.
22. Michalski, M.-C.; Briard, V.; Michel, F. Optical parameters of milk fat globules for laser light scattering measurements. *Lait* **2001**, *81*, 787–796. [CrossRef]
23. Mercan, E.; Sert, D.; Akın, N. Effect of high-pressure homogenisation on viscosity, particle size and microbiological characteristics of skim and whole milk concentrates. *Int. Dairy J.* **2018**, *87*, 93–99. [CrossRef]
24. Van Oss, C.J. *Forces Interfaciales en Milieux Aqueux*; Masson: Issy Les Moulineaux, France, 1996.
25. Ye, A.; Singh, H.; Taylor, M.W.; Anema, S. Interactions of whey proteins with milk fat globule membrane proteins during heat treatment of whole milk. *Lait* **2004**, *84*, 269–283. [CrossRef]

26. Jukkola, A.; Partanen, R.; Rojas, O.J.; Heino, A. 4-2(CLSM)Effect of heat treatment and pH on the efficiency of micro-diafiltration for the separation of native fat globules from cream in butter production. *J. Membr. Sci.* **2018**, *548*, 99–107. [CrossRef]
27. Lopez, C.; Madec, M.-N.; Jimenez-Flores, R. Lipid rafts in the bovine milk fat globule membrane revealed by the lateral segregation of phospholipids and heterogeneous distribution of glycoproteins. *Food Chem.* **2010**, *120*, 22–33. [CrossRef]
28. Smoczyński, M. Role of phospholipid flux during milk secretion in the mammary gland. *J. Mammary Gland Biol. Neoplasia* **2017**, *22*, 117–129. [CrossRef]
29. Wong, D.W.; Camirand, W.M.; Pavlath, A.E.; Parris, N.; Friedman, M. Structures and functionalities of milk proteins. *Crit. Rev. Food Sci. Nutr.* **1996**, *36*, 807–844. [CrossRef]
30. Evers, J.M. The milkfat globule membrane—Compositional and structural changes post secretion by the mammary secretory cell. *Int. Dairy J.* **2004**, *14*, 661–674. [CrossRef]
31. Zheng, H.; Jimenez-Flores, R.; Everett, D.W. Bovine milk fat globule membrane proteins are affected by centrifugal washing processes. *J. Agric. Food Chem.* **2013**, *61*, 8403–8411. [CrossRef]
32. Michalski, M.-C.; Cariou, R.; Michel, F.; Garnier, C. Native vs. damaged milk fat globules: Membrane properties affect the viscoelasticity of milk gels. *J. Dairy Sci.* **2002**, *85*, 2451–2461. [CrossRef]
33. Michalski, M.-C.; Michel, F.; Sainmont, D.; Briard, V. Apparent ζ-potential as a tool to assess mechanical damages to the milk fat globule membrane. *Colloids Surf. B Biointerfaces* **2002**, *23*, 23–30. [CrossRef]
34. Gülseren, İ.; Alexander, M.; Corredig, M. Probing the colloidal properties of skim milk using acoustic and electroacoustic spectroscopy. Effect of concentration, heating and acidification. *J. Colloid Interface Sci.* **2010**, *351*, 493–500. [CrossRef] [PubMed]
35. Kühnl, W.; Piry, A.; Kaufmann, V.; Grein, T.; Ripperger, S.; Kulozik, U. Impact of colloidal interactions on the flux in cross-flow microfiltration of milk at different pH values: A surface energy approach. *J. Membr. Sci.* **2010**, *352*, 107–115. [CrossRef]
36. Anderson, M.; Cawston, T. The milk-fat globule membrane. *J. Dairy Res.* **1975**, *42*, 459–483. [CrossRef]
37. Sejersen, M.T.; Salomonsen, T.; Ipsen, R.; Clark, R.; Rolin, C.; Engelsen, S.B. Zeta potential of pectin-stabilised casein aggregates in acidified milk drinks. *Int. Dairy J.* **2007**, *17*, 302–307. [CrossRef]
38. Tuinier, R.; De Kruif, C. Stability of casein micelles in milk. *Chem. Phys.* **2002**, *117*, 1290–1295. [CrossRef]
39. Roy, M.T.; Gallardo, M.; Estelrich, J. Influence of size on electrokinetic behavior of phosphatidylserine and phosphatidylethanolamine lipid vesicles. *J. Colloid Interface Sci.* **1998**, *206*, 512–517. [CrossRef]
40. Dewettinck, K.; Rombaut, R.; Thienpont, N.; Le, T.T.; Messens, K.; Van Camp, J. Nutritional and technological aspects of milk fat globule membrane material. *Int. Dairy J.* **2008**, *18*, 436–457. [CrossRef]
41. Jiménez-Flores, R.; Brisson, G. The milk fat globule membrane as an ingredient: Why, how, when? *Dairy Sci. Technol.* **2008**, *88*, 5–18. [CrossRef]
42. Singh, H. The milk fat globule membrane—A biophysical system for food applications. *Curr. Opin. Colloid Interface Sci.* **2006**, *11*, 154–163. [CrossRef]
43. Smoczyński, M.; Staniewski, B.; Kiełczewska, K. Composition and Structure of the Bovine Milk Fat Globule Membrane—Some Nutritional and Technological Implications. *Food Reviews Int.* **2012**, *28*, 188–202. [CrossRef]
44. Dalgleish, D.G.; Corredig, M. The structure of the casein micelle of milk and its changes during processing. *Annu. Rev. Food Sci. Technol.* **2012**, *3*, 449–467. [CrossRef] [PubMed]
45. Yamauchi, K.; Shimizu, M.; Kanno, C. Effect of preparation on properties of a soluble glycoprotein fraction of milk fat globule membrane. *J. Dairy Sci.* **1978**, *61*, 688–696. [CrossRef]
46. Le, T.T.; Van Camp, J.; Rombaut, R.; van Leeckwyck, F.; Dewettinck, K. Effect of washing conditions on the recovery of milk fat globule membrane proteins during the isolation of milk fat globule membrane from milk. *J. Dairy Sci.* **2009**, *92*, 3592–3603. [CrossRef] [PubMed]
47. Waninge, R.; Nylander, T.; Paulsson, M.; Bergenståhl, B. Milk membrane lipid vesicle structures studied with Cryo-TEM. *Colloids Surf. B: Biointerfaces* **2003**, *31*, 257–264. [CrossRef]
48. Nguyen, H.T.H.; Ong, L.; Beaucher, E.; Madec, M.-N.; Kentish, S.E.; Gras, S.L.; Lopez, C. Buffalo milk fat globules and their biological membrane: In situ structural investigations. *Food Res. Int.* **2015**, *67*, 35–43. [CrossRef]

Food Hydrocolloids 156 (2024) 110246

Contents lists available at ScienceDirect

Food Hydrocolloids

journal homepage: www.elsevier.com/locate/foodhyd

# Characterization of the microstructure, interfacial properties and crystallization behaviours of milk fat globule and membrane isolated from acidified bovine milk and sweet whey

Yanjun Sun [a,b,c], Yrjö H. Roos [c], Song Miao [b,d,*]

[a] State Key Laboratory of Dairy Biotechnology, Shanghai Engineering Research Centre of Dairy Biotechnology, Dairy Research Institute, Bright Dairy & Food Co., Ltd., Shanghai, 200436, China
[b] Teagasc Food Research Centre, Moorepark, Fermoy, Co. Cork, Ireland
[c] School of Food and Nutritional Sciences, University College Cork, Cork, Ireland
[d] China-Ireland International Cooperation Centre for Food Material Sciences and Structure Design, Fujian Agriculture and Forestry University, China

ARTICLE INFO

*Keywords:*
Milk fat globules/milk fat globule membrane
Acidified bovine milk
Physicochemical properties
Interfacial tension
Different scanning calorimetry (DSC)
X-ray diffraction (XRD)

ABSTRACT

Milk fat globule and membrane (MFGs/MFGM) ingredients are the main source of the phospholipid supplementation in the dairy industry. Their physicochemical properties and functionalities play important roles in their application. This study investigated the effect of acidification (pH 6.30 and pH 5.30) on the microstructure, interfacial and thermal properties of MFGs/MFGM sourced from bovine milk (control pH 6.70). Meanwhile, sweet whey was prepared to mimic the raw material used in the industrial production of MFGs/MFGM (MFGM-C). The study revealed a broad particle size distribution of MFGs/MFGM at pH 5.30, while smaller particles were found in MFGM-C. This was confirmed by confocal scanning microscopy (CLSM) images, which showed that few intact MFGs existed in the MFGM-C. Fourier Transform Infrared Spectroscopy (FTIR) indicated more peaks belonging to protein-lipids associations presented at pH 6.30. Additionally, the interfacial tension of MFGs/MFGM at pH 6.30 was significantly lower than at pH 6.70 and 5.30. X-ray Diffraction Spectra (XRD) showed that the fat in MFGM-C exhibited no detectable crystalline structures, and fewer α and β′ crystals appeared at pH 6.30. All MFGs/MFGM from bovine milk or whey exhibited both exothermic and endothermal events. The smallest heat enthalpy of crystallization ($\Delta H_C$) and melting ($\Delta H_M$) was observed in MFGM-C, followed by those at pH 6.30. Compared to MFGs/MFGM at pH 6.70, pH 6.30 induced more profound effects on the interfacial and thermal properties of MFGs/MFGM than pH 5.30. Acidification and the use of different raw materials lead to differentiation in the physicochemical and techno-functionalities of MFGs/MFGM.

## 1. Introduction

In mammal milk, most lipids exist in milk fat globules (MFGs) wrapped by the unique tri-layer membrane-milk fat globule membrane (MFGM) (Huang, et al., 2023). Milk fat provides 50–60% of the energy required for the neonate's growth. The bioactive compositions of the MFGs/MFGM, such as phospholipids and glycoproteins, are gaining significant interest for their important role in promoting new-borns' brain and intelligence development (Mohamed, et al., 2022; Nieto-Ruiz, et al., 2022). Infant formula (IF) is an essential nutrient for neonates having no adequate source of breast milk. Dairy ingredients rich in MFGs/MFGM sourced from buttermilk or whey cream have been applied in IF products to mimic breast milk nutrition (Mohan, O'Callaghan, Kelly, & Hogan, 2020).

Structural and compositional changes of MFGs/MFGM during dairy processing have been investigated in many studies, including MFGs/MFGM separation methods, heating treatments or storage temperature, homogenisation, and non-thermal treatments (Huang, et al., 2023; Kiełczewska, Ambroziak, Krzykowska, & Aljewicz, 2021; Liu, Boeren, Zhang, Zhou, & Hettinga, 2021; Ren, Li, Liu, & Ma, 2020; Wei et al., 2021). However, research on the effect of these processes on the techno-functionalities of MFGs/MFGM is still lacking. Different sizes of native fat globules (NFG) separated from raw milk by a modified commercial cream separator affected the foamability of milk. The size of air bubbles in foam increased with the increase in NFG size, while the foamability was not affected by the NFG size (Ho, Dhungana, Bhandari,

* Corresponding author. Teagasc Food Research Centre, Moorepark, Fermoy, Co. Cork, Ireland.
*E-mail address:* Song.Miao@teagasc.ie (S. Miao).

https://doi.org/10.1016/j.foodhyd.2024.110246
Received 4 February 2024; Received in revised form 23 May 2024; Accepted 28 May 2024
Available online 29 May 2024
0268-005X/© 2024 Elsevier Ltd. All rights are reserved, including those for text and data mining, AI training, and similar technologies.

& Bansal, 2021). Reconstructing MFG (RMFG) with different-melting-temperature triacylglycerols (TAG) was prepared by Ren, Guo, Teng, and Ma (2021) to improve its techno-functionalities and nutritional properties. Additionally, Ren et al. (2020) demonstrated that pasteurisation and homogenisation treatments affected the thermodynamic properties and fat polymorphs of fat globules during seven days of storage at 4 °C. MFGs/MFGM ingredients play an important role in the emulsifying stability of IF products (Li & Van der Meeren, 2022). The interfacial layer of MFGs/MFGM is more likely to be involved with emulsion formation and destabilization.

Commercial MFGs/MFGM ingredients have been prepared from sweet whey or buttermilk. The processes for the MFGs/MFGM ingredients production involve acidification, heating, and coagulation (Fontecha, et al., 2020). Acidification is one of the most commonly used processing methods in dairy products, such as yogurts, cheeses, and lactic fermented beverages or acidic milk drinks. Specifically, pH conditions at 5.30 and 6.30 are involved in the processing of these products. According to previous research, different pH conditions have been proven to affect the isolating efficiency of MFGM proteins from buttermilk or native MFGs from cream (Holzmüller, Gmach, Griebel, & Kulozik, 2016; Jukkola, Partanen, Rojas, & Heino, 2018). We hypothesise that the acidification treatment may change the structure and compositions of MFGs/MFGM, which further affects the interfacial behaviour, thermodynamic properties, and fat polymorphs in MFGs/MFGM materials. To verify this hypothesis, we investigated the effect of pH conditions at 5.30 and 6.30 on the interfacial properties and fat crystallization behaviours of MFGs/MFGM.

Herein, MFGs/MFGM ingredients were isolated from acidified bovine raw milk (pH 5.30 and pH 6.30) by cream separator, followed by centrifugation to further enrich the samples. Meanwhile, MFGs/MFGM from the sweet whey were prepared to mimic the industrial MFGs/MFGM preparation and allow for comparative analysis. The compositions of collected MFGs/MFGM ingredients were profiled by Fourier transform infrared spectroscopy (FTIR), and the microstructure was observed by confocal laser scanning microscopy (CLSM). We investigated the effect of acidification on the surface charges and air/liquid interfacial properties of MFGs/MFGM by determining the zeta (ζ) potential and interface tension respectively. Using Different Scanning Calorimetry (DSC) combined with X-ray diffraction (XRD), the evolution of milk fat polymorphs and crystal types in MFGs/MFGM was investigated, and also the crystallization and melting behaviours. Through these analytical methods, we aimed at gaining more information on the pH-dependent properties of MFGs/MFGM. Meanwhile, the effect of different raw sources on the techno-functionalities of MFGs/MFGM was investigate by using whey and bovine milk as the raw materials for the MFGs/MFGM preparation. MFGs/MFGM ingredients are the main source of the phospholipids supplement in dairy products. The information acquired from this study may be beneficial for the industrial MFGs/MFGM preparation and their application in dairy products.

## 2. Materials and methods

### 2.1. Materials and reagents

Fresh bovine milk (fat 4.13 ± 0.03%, protein 3.37 ± 0.02%, dry matter 13.10 ± 0.02%, pH 6.70 ± 0.04) was collected from the Teagasc dairy herd (Moorepark, Fermoy, Co. Cork, Ireland) and stored in the 4 °C refrigerator instantly after milking.

Nile Red (9- (diethylamino)-5 H-benzo[a]phenoxazin-5-one), Fast Green FCF (disodium 2-[[4-[ethyl-[(3-sulfonatophenyl)methyl]amino] phenyl]-[4-[ethyl-[(3-sulfonatophenyl) methyl] azaniumylidene] cyclohexa-2,5-dien-1-ylidene]methyl]-5-hydroxybenzenesulfonate), Polyethylene glycol 200, azide sodium and PBS tablets were purchased from Sigma-Aldrich®, Merck Life Science Ltd., Cork, Ireland. Starters (DVS, EASY-SET 3000), and rennet (CHY-MAX Supreme) was obtained from Chr. Hansen Inc., Copenhagen, Demark. Food grade $CaCl_2$ was purchased from Occidental Chemical Corporation, Michigan, USA.

### 2.2. Samples preparation

#### 2.2.1. Separation of cream samples from acidified bovine milk

Pre-heated bovine raw milk (30–43 °C) was separated into cream and skim milk using a disk bowl centrifugal separator (FT 15 Disc Bowl Centrifuge, Armfield Co., Ringwood, UK) at a rated throughput of 125L/h. Centrifugation speed was kept at 8500 rpm by controlling the motor housing. Before cream separation, two batches of raw milk were adjusted to pH 6.30 and 5.30 respectively, while the third batch without pH adjustment (6.70 ± 0.03) was used as the control. Each pH adjustment was repeated with three bathes. During the cream separation, skim milk was added back into the separating bowl to be maximally defatted. The cream phase of all samples was collected and cooled down to 4 °C for further isolation.

#### 2.2.2. Preparation of sweet whey from the cheddar cheese drainage

Pilot-scale cheddar whey was produced and used as raw materials to isolate MFGs/MFGM. Cheddar was manufactured using the standard procedure described by Voigt, Donaghy, Patterson, Stephan, and Kelly (2010) with some modifications. Pasteurized (70–72 °C, 15–20 s) bovine milk 10 L was cooled down and kept at 30–35 °C, which is the most suitable condition for starter growth (DVS, EASY-SET 3000, Chr. Hansen Inc., Copenhagen, Demark) and rennet coagulation (CHY-MAX Supreme, Chr. Hansen Inc., Copenhagen, Demark). Starters were added to acidify the milk from pH 6.70 ± 0.03 to 6.30 ± 0.02. After that, pre-dispersed rennet (40 IMCU/L) and food grade $CaCl_2$ (Occidental Chemical Corporation, Michigan, USA) (0.01 %, w/w) were added into the pasteurized milk. The formed curd was cut into 1 $cm^3$ grains. Subsequently, the tank was continually heated and kept at 45 °C for 15 min to facilitate curd shrinkage and whey drainage. A sieve with a mesh number of 0.5 cm was used to filter the collected whey (pH 6.25 ± 0.03) until no visible curd grains were observed. The cheese-making process was repeated three times, and the three batches of whey were collected.

#### 2.2.3. Isolation of MFGs/MFGM materials

Ultra-centrifugation (10 000×*g*, 15 min at 4 °C) was applied to further enrich the MFGs/MFGM compositions from the cream or whey (Zamora, Ferragut, Guamis, & Trujillo, 2012). Specifically, the upper layer was collected and mixed with an equivalent volume of PBS buffer. The mixture was dispersed in a water bath (35−40 °C) for 10 min and vortexed thoroughly before the second centrifugation. The centrifugation and supernatant rinse were repeated three times. The collected upper layers from the third time were freeze-dried for 72 h for further analysis. 0.03% (g/g) azide sodium was added to the supernatant to prevent microbiological growth. The freeze-dried samples were named after pH conditions: pH 6.70, pH 6.30, and pH 5.30. The samples made from whey were named MFGM-C. The compositions of all samples were analysed by DairySpec FT-15 (Bentley Instruments Inc., Chaska, MN, USA) (Table 1).

**Table 1**
The composition of freeze-dried MFGs/MFGM isolated from acidified bovine milk and sweet whey.

| Samples | Protein (%, w/w) | Fat (%, w/w) | Lactose(%, w/w) |
|---|---|---|---|
| MFGM-C | 14.23 ± 0.05$^{a}$ | 23.44 ± 0.19 $^{b}$ | 0.23 ± 0.01$^{b}$ |
| pH 6.70 | 2.99 ± 0.02 $^{b}$ | 74.97 ± 0.25 $^{a}$ | 0.14 ± 0.00$^{c}$ |
| pH 6.30 | 1.10 ± 0.01 $^{c}$ | 75.29 ± 1.15 $^{a}$ | 0.29 ± 0.03 $^{a}$ |
| pH 5.30 | 0.72 ± 0.00 $^{d}$ | 74.62 ± 1.64 $^{a}$ | – |

Notes:Different superscript letters in the same column indicate the significant ($p < 0.05$) differences between the samples.
'–' means not detection.

### 2.3. Particle size distribution

Mastersizer 3000 (Malvern Instruments, Malvern, UK) equipped with a laser light scattering was performed to investigate the particle size distribution of MFGM-C and MFGs/MFGM with different pH. The measurement method was carried out according to the previous research with modifications (Sun, Roos, & Miao, 2022). Samples were heated in a water bath (30–35 °C) until they completely melted before being analysed. The statistics of the particle distribution were calculated using the Mastersizer–v 3.7.1 software.

### 2.4. Confocal laser scanning microscopy (CLSM)

The microstructure of lipid droplets and milk protein in MFGs/MFGM was measured by a Leica TCS SP5 microscope (Leica Microsystems GmbH, Wetzlar, Germany). Neutral lipids (mainly refers to triglycerides) and milk proteins were labelled by Nile Red and Fast Green FCF, respectively. Samples were dual-stained, and the preparation method referred to the previous research with slight modifications (Pan, et al., 2024). Specifically, 0.1% (w/v) Nile Red was made in polyethylene glycol-200 solvent, and distilled water was used to dissolve FCF to a concentration of 0.1% (w/v). 50 μL MFGs/MFGM samples, 30 μL Nile Red, and 10 μL FCF were added into the 1.5 mL Eppendorf and mixed thoroughly. Stained samples were kept in the dark for 30 min at room temperature. The equipment setting and operation for the Leica TCS SP5 microscope followed our previous report (Sun, Roos, & Miao, 2022)。

### 2.5. Fourier transform infrared spectroscopy (FTIR)

FTIR spectroscopy (Bruker Tensor 27, Bruker Optik GmbH, Ettlingen, Germany) equipped with an Optics Platinum Attenuated Total Reflectance (ATR) cell (Pike Technology Inc., Madison, WI, USA) was used to acquire the IR spectra of MFGs/MFGM samples. The freeze-dried sample was gently ground into a fine powder before evenly spreading down on the aperture. IR spectra were recorded at room temperature (20−25 °C) from 900 to 4000 $cm^{-1}$ with an average of 120 scans at a resolution of 4 $cm^{-1}$. Background measurement was performed with consistent instrumental settings with the sample spectra acquisition. Spectral data recording, atmosphere compensation (removing the presence of atmospheric vapour and carbon dioxide from the spectra), and vector normalization were conducted by OPUS 7.5 software (Bruker Optik GmbH, Ettlingen, Germany). Each experiment was repeated three times.

Peak fitting and deconvolution were applied with OriginPro 2023 (OriginLab Corporation, Northampton, US) to pull apart and sharpen the overlapping hidden peaks in the range of 1200–900 $cm^{-1}$. The second derivative (zero) method was used to find the baseline anchor points and detect the baseline. Peak finding was performed using the second derivation (searching hidden peaks), and only positive direction peaks were found. Savityzky–Golay function was used to perform the smooth derivative with the 10–20 points of window and polynomial order of 2. Peaking fitting was conducted using the Gaussian function, and all peak widths and centre, as well as baseline parameters, were fixed or released until the best fit was achieved ($R^2 > 0.996$, reduced chi-square $<1 \times 10^{-6}$).

### 2.6. Interfacial tension

Freeze-dried MFGs/MFGM were heated in a water bath (30–35 °C), and the melted liquid samples were deemed as a W/O emulsion used to perform the interfacial tension and zeta (ζ) potential measurements. An optical tensiometer (Oneattension Theta lite, Biolin Scientific, Espoo, Finland) was applied to comparatively assess the impact of acidification and different raw materials on the interfacial tension of MFGs/MFGM collections. The pendant drop method and 'Advanced (two phases frame per second (FPS))' mode were set during the analysis. The hooked needle was used, which, according to the manual, was described as the higher stability for the measurement due to the minor effect from the airflow and negligible losses of evaporation. Young-Laplace equation was used to calculate the interfacial tension. Around 5−7 μL liquid sample droplet was squeezed out of the needle until its volume kept steady. During the test, images were recorded at 0.1 % frame per second FPS, and the total duration was 20 s. The resulting data were collected and analysed by Oneattension software (Version 4.1.6, Biolin Scientific, Espoo, Finland).

### 2.7. Zeta (ζ) potential

The dynamic light scatting instrument (Nano–ZS, Malvern Instruments Ltd., Worcestershire, UK) was used to measure electrophoretic mobility which was used to calculate the ζ-potential by application of the Henry equation (Michalski, Michel, Sainmont, & Briard, 2002). The melted liquid samples were diluted 100 times with MiliQ water. Before each analysis, all diluted samples were left to equilibrate at room temperature for 2 min. The ζ-potential of each sample was read three times automatically. The fraction of MFGs/MFGM surface covered with non-membrane milk protein (Φ) was calculated from an estimative model based on the relative change in ζ-potential:

$$\Phi = 1 - \exp\left(-1.802 \times 10^{-3}\zeta_R^2\right) \quad (1)$$

where, $\zeta_R$ was the relative change of ζ–potential of samples compared to the unprocessed raw milk which was assumed that $\Phi = 0$.

### 2.8. X–ray diffraction (XRD)

XRD analysis of the freeze-dried MFGs/MFGM was performed on a powder diffractometer STOE STAID MP (STOE, Darmstadt, Germany) equipped with Cu radiation ($\lambda = 1.5406$ nm; current, 40 mA; voltage, 40 kV). The diffraction patterns were recorded in a diffraction range of 2θ from 5° to 30° with a scanning speed of 1°/min. Freeze-dried powder samples were placed on the metal plates with film on both sides to seal the samples in.

The collected raw data were smoothened using the adjacent-averaging method, and the points of the window were set to 20. Meanwhile, baseline subtraction (Asymmetric least squares mode with asymmetric factor 0.001, threshold 0.05, smoothing factor 4, and number of literation 10) was performed using Originpro 2023.

Bragg Equation was used to characterize the short space (d) of the milk fat crystal as a function of scattering angle (Pope, 1997):

$$d = n\lambda / 2\sin\theta \quad (2)$$

where d = interplanar spacing or d-spacing (Å); n = 1 (order of diffraction); λ = 1.5406 nm; θ = peak position (In radians).

The typical crystalline forms in milk fat, α, β and β′, were identified by the reported corresponding d-spacing: α = 4.15 Å (2θ = 21.41°), β′1 = 3.8 Å (2θ = 23.41°), β′2 = 4.2 Å (2θ = 21.15°), β = 4.6 Å (2θ = 19.30°) (D'Souza, deMan, & deMan, 1990; Han et al., 2014). In addition, the relative degree of crystallinity of α, β, and β′ was calculated by integrating the area under the curve using Originpro 2023 (OriginLab Corporation, US) according to the following equation:

$$\text{Crystallinity} = \text{Area of crystalline peaks} / (\text{Area of crystalline and amorphous peaks}) \times 100 \quad (3)$$

### 2.9. Different scanning calorimetry (DSC)

The thermal behaviour of MFGs/MFGM materials separated from cream and sweet whey samples was investigated using DSC (DSC Q2000, TA Instruments, Crawley, UK). 10 −15 mg of each freeze-dried powder sample was hermetically sealed in an aluminium pan while an empty sealed pan was used as reference. Nitrogen was used as the shielding gas and purged the system at 50 mL/min. The time-temperature program was: Cycle 1: Equilibrate at 4 °C; Cycle 2–3: Ramp 10 °C/min to 60 °C and isothermal for 15 min; Cycle 4–5: Ramp 10 °C/min to −60 °C and isothermal for 5 min; Cycle 6: Ramp 10 °C/min to 60 °C. The purpose of 1–3 cycles was to eliminate the crystal and melting history differentiation during the sample preparation. The thermal parameters of all the thermograms were exported through Universal Analysis 2000 (TA Instruments–Waters LLC, New Castle, US). The peaks for melting ($T_M$)/crystal ($T_C$), and the corresponding endothermic ($\Delta H_M$)/exothermic ($\Delta H_C$) enthalpy (J $g^{-1}$) were analysed in the OriginPro 2023 system.

### 2.10. Statistical analysis

All measurements were performed in triplicate unless otherwise indicated. Each value represented the mean of three measurements and was presented as mean ± standard deviation (SD). One-way ANOVA was conducted for all the analyses at the significance level of $p < 0.05$, except for interfacial tension, where more strict levels of $p < 0.01$ and $p < 0.001$ were used. The ANOVA was performed in the OriginPro 2023 software, which was also used to plot all the figures.

## 3. Results and discussion

### 3.1. Particle size and microstructure of MFGs/MFGM

Most of the particles in MFGs/MFGM at pH 5.30 distributed in the range of 10–1000 μm with, the highest volume density of 109.91 μm, followed by pH 6.30 (53.09 μm) and pH 6.70 samples (19.87 μm) (Fig. 1A). This observation may be due to more non-membrane milk proteins associated with the MFGs/MFGM fragments at pH 5.30, which may not be washed away during the MFGs/MFGM enrichment by centrifugation. Comparatively, MFGs/MFGM isolated from cheese whey presented a smaller size distribution than samples prepared from bovine raw milk. Particles in MFGM-C were mainly distributed over the range of 0.01–1 μm and 5−50 μm. The intact MFGs may break down into fragments because of the mechanical shearing treatment during the whey drainage process, which induced the increased distribution of smaller particle sizes (Zhou, et al., 2021).

CLSM images visually displayed particle size differentiation mentioned above (Fig. 1B). From Fig. 1B, more attached non-membrane milk proteins were observed on the MFGs surface at pH 5.30 than at pH 6.30 and 6.70. Furthermore, at pH 5.30, non-membrane milk proteins formed network structures with intact MFGs embedded in them. In comparison, rare intact MFGs were observed, and MFGs/MFGM fragments mainly existed in MFGM-C. In addition, more pronounced non-membrane milk proteins were observed adsorbing around the MFGs/MFGM fragments in MFGM-C than in MFGs/MFGM with different pH conditions. This may be attributed to coagulation in the MFGM-C preparation, which promoted the interaction of non-membrane proteins with MFGs/MFGM or fragments.

### 3.2. FTIR

Fig. 2A shows the FTIR spectra of MFGM-C and MFGs/MFGM at different pH conditions. The full wavenumbers (4000–900 $cm^{-1}$) were divided into six different regions according to the functional groups, and the corresponding milk components associated with each region were listed in Table 2. The second derivative (Fig. 2 B) and peaks deconvolution were further applied between 1200 and 900 $cm^{-1}$ (Fig. 3) to separate the overlapping peaks and provide a complete comparison of the spectra (Hong Bui, Cozzolino, Zisu, & Chandrapala, 2021).

Peaks at 2925 and 2852 $cm^{-1}$ in region 1 were observed in all samples, which may be assigned to asymmetric and symmetric stretching modes of $–CH_2$ groups of acyl chains in TGAs or phospholipids, respectively (Fig. 2A). Peak positioned at 2963 $cm^{-1}$ became more obvious in the 2nd derivation spectra (Fig. 2B), which was associated with the C–H bending of $–CH_3$ (Grewal, et al., 2017). An apparent peak with intense absorbance at 1945 $cm^{-1}$ in region 2 was detected, which may mainly relate to the C═O stretching vibrations in lipid-protein conjugates or ester bonds of lipids (Nicolaou et al., 2008) (Fig. 2A). Peaks over the range of 3000−2800 $cm^{-1}$ and 1800−1700 $cm^{-1}$ were observed in all spectra. Combined with Tables 2, it was concluded that all MFGs/MFGM presented a similar lipids fingerprint.

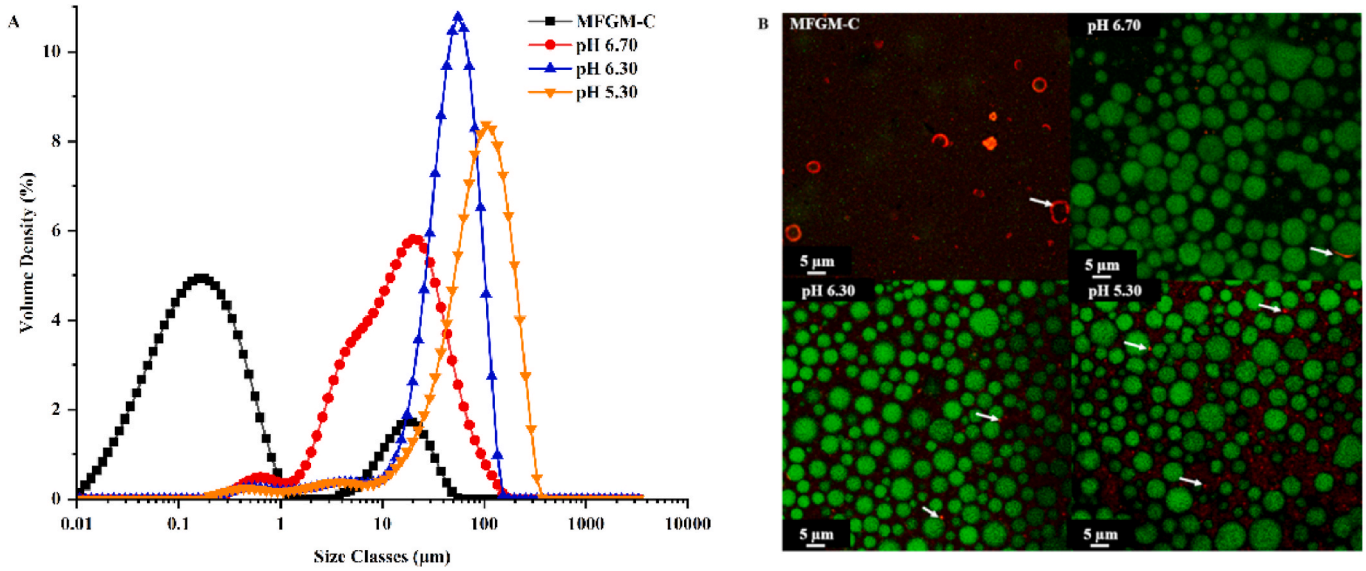



**Fig. 1.** Particle size distribution (A) and microstructure (B) of MFGs/MFGM isolated from acidified bovine raw milk and sweet whey (MFGM-C). Confocal laser scanning microscopy (CLSM) was used to observe and capture the images. Neutral lipids (mainly triglyceride) and non-membrane milk protein were stained with Nile red and fast green FCF (white arrows pointing at the adsorbed non-membrane milk proteins on the MFGs). Scale bar = 5 μm.

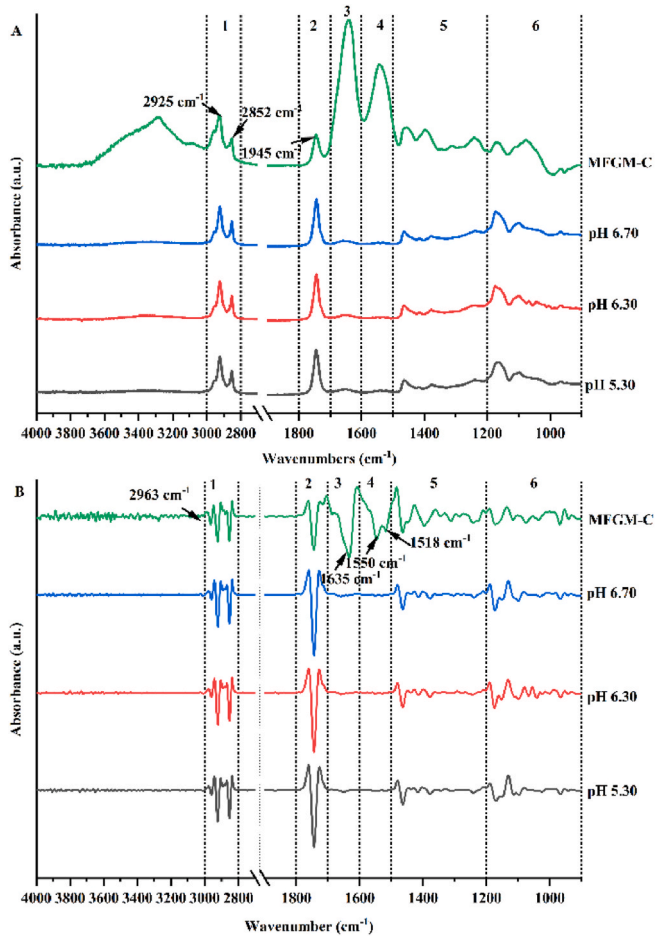



**Fig. 2.** Original (A) and representative second derivation (B) FTIR spectra of MFGs/MFGM from acidified bovine milk and sweet whey (MFGM-C) (Spectra between 2700 and 1900 $cm^{-1}$ did not be shown because there was no peak was detected for all samples, and all the spectra exhibited the similar flat plots).

**Table 2**
Six regions of different FTIR spectra correspond to specific milk components.

| Region No. | FTIR wavenumbers ($cm^{-1}$) | Milk components | Reference |
|---|---|---|---|
| 1 | 3000–2800 | Asymmetric and symmetric stretching modes of $CH_2$ groups of acyl chains of triglycerides or phospholipids | (Nicolaou & Goodacre, 2008; Grewal et al., 2017) |
| 2 | 1800–1700 | C═O stretching vibrations of ester, aldehydes and ketones | Vongsvivut, et al. (2012) |
| 3 | 1700–1600 | Amide I protein | Kher, Udabage, McKinnon, McNaughton, and Augustin (2007) |
| 4 | 1600–1500 | Amide II protein | |
| 5 | 1500–1200 | Amide III protein | Grewal, et al. (2017) |
| 6 | 1200–900 | Membrane lipids, protein–lipid associations, lactose | Zhou, et al. (2006) |

The wavenumbers from regions 3 to 5 were used to characterize protein groups, which were attributed to amide I (1700–1600 $cm^{-1}$), amide II (1600–1500 $cm^{-1}$), and amide III (1500–1200 $cm^{-1}$). None of the samples showed obvious absorbance peaks in the amide I and amide II regions except MFGM-C. This finding was due to a higher amount of protein in MFGM-C (Table 1). According to compositional analysis results in Table 1, the protein content in MFGM-C was 14.23 % (w/w), significantly higher than that in cream-sourced MFGs/MFGM (0.72−2.99 %, w/w). It can be inferred that high-speed centrifugation during the isolation of MFGs/MFGM from the acidified milk removed most of the non-membrane milk proteins in the cream. Casein structure was changed by chymosin during the cheese rennet stage, making its association with MFGs/MFGM fragments more difficult to remove by centrifugation. A typical β-sheet protein structure at 1635 $cm^{-1}$ was only detected in MFGM-C (Fig. 2 B). In addition, hidden peaks in MFGM-C at 1550 $cm^{-1}$ and 1518 $cm^{-1}$ corresponding to C–N or N–H stretching and tyrosine in free amino acid were presented in the second derivation spectra (De Meutter & Goormaghtigh, 2021; Sadat & Joye, 2020; Yang, Yang, Kong, Dong, & Yu, 2015).

A weak signal of protein secondary structure was detected in MFGs/MFGM within the amide III range (region 5, 1500–1200 $cm^{-1}$), which mainly may be due to the co-existence of MFGM proteins and conjugation of non-membrane milk proteins with MFGs/MFGM. The spectra between 1500 and 1200 $cm^{-1}$ showed no significant difference among the different pH conditions when comparing the original and second derivative spectra. It may be because of the weak absorbance and high noise signal in this range. In addition, it is difficult to distinguish MFGs/MFGM materials at different pH between 1200 and 900 $cm^{-1}$ because of the multimodal. Hence, peak deconvolution was applied to this region to search for the hidden peaks. Two separated peaks, 1175 $cm^{-1}$ and 1148 $cm^{-1}$, were observed between 1200 $cm^{-1}$ and 1135 $cm^{-1}$ at all pH conditions (Fig. 3 A, B, and C) except for MFGM-C (Fig. 3 D), in which only one central peak at 1166 $cm^{-1}$ was detected. Peaks detected at 1175 $cm^{-1}$ and 1148 $cm^{-1}$ were used to characterize the stretching vibration of C–O–C in the ester bond of TGAs or fatty acids. The stretching of C–O at 1166 $cm^{-1}$ was reported to relate to the ester group due to asymmetric vibrations of C–C(=O)–O (Mekonnen, 2023). More hidden peaks were brought out after curve fitting within 1135−900 $cm^{-1}$ at the lower pH than the control (pH 6.70), especially at pH 6.30, in which three more peaks were found. According to Table 2, different components, such as membrane lipids, protein–lipid associations, and lactose, had absorbance signals within spectra 1200−900 $cm^{-1}$. Since the preparation methods removed most lactose (Table 1), we speculated that the different spectra may be attributed to the different degrees of association between non-membrane milk protein and milk fat. The change of non-membrane milk protein conformation at different pH conditions may affect their bonding ability with the MFGs/MFGM fragments. This result was supported by the formation of partially folded intermediate casein structure induced by the pH variation (Chakraborty & Basak, 2007). It can be inferred that more types of conjugates were formed between non-membrane milk proteins and MFGs/MFGM at pH 6.30 condition, as verified by the more corresponding observable peaks.

### 3.3. Interfacial tension

The change in composition and structural rearrangement on the surface of MFGs/MFGM can be reflected by analysing the interfacial tension between air and liquid emulsion droplets. In our pre-experiment (data not shown), the recording time was set as 600 s, but the results showed relative stablility during the entire analysis. There was no significant difference from the initial recording to the final reading at 600 s. Therefore, the recording time in this study only lasted 20 s. It can be argued that the interfacial compositions of MFGs completed rearrangement during the preparation stage and interfacial tension remained constant during the entire analysis.

As shown in Fig. 4, the interfacial tension of MFGs/MFGM at pH 6.70 (41.00 ± 1.00 mN/m) was significantly higher than that of MFGs/MFGM at pH 6.30 and 5.30 ($p < 0.05$), while the lowest interfacial tension magnitude was observed in MFGM-C (24.67 ± 0.58 mN/m). The interfacial tension of MFGM-C was significantly lower than that of pH 6.70 and pH 5.30 at a significant level of 0.001 ($p < 0.001$), and also

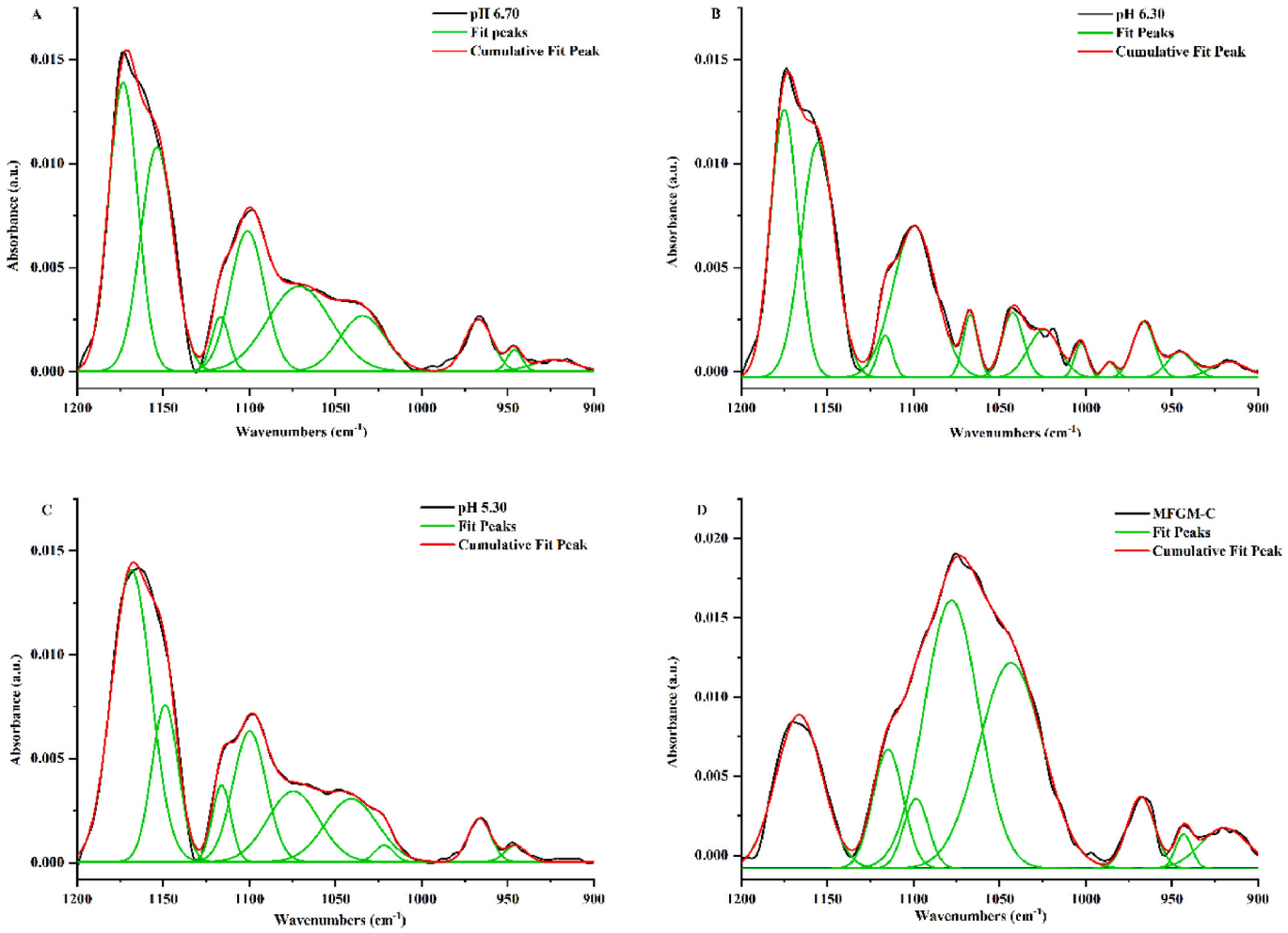



**Fig. 3.** Curve fitted regions (1200–900 $cm^{-1}$) in FITR spectra of MFGs/MFGM separated from pH 6.70 (A), pH 6.30 (B), pH 5.30 (C) bovine milk and MFGM-C (D).

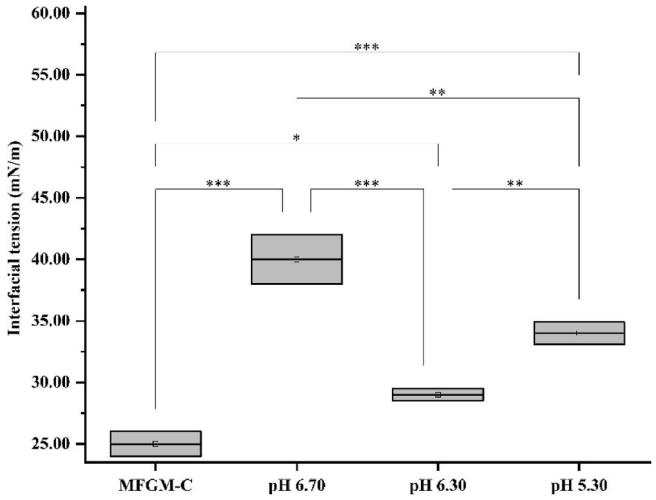



**Fig. 4.** Interfacial tension of MFGs/MFGM isolated from acidified bovine milk and sweet whey (MFGM-C). *, ** and *** represent $p < 0.05$, $p < 0.01$ and $p < 0.001$, respectively.

lower than MFGs/MFGM at pH 6.30 at a significant level of 0.05 ($p < 0.05$). The adsorption of non-membrane milk proteins on the surface of MFGs has been reported to be inversely proportional to the interfacial tension (Michalski, et al., 2002). This result was consistent with the images of CLSM in Fig. 1B, in which, visually, more non-membrane milk proteins were observed surrounding MFGs at pH 5.30 than at pH 6.70 and 6.30. In addition, interfacial tension has been reported to positively correlate with particle size (Ho, et al., 2021). This finding confirmed the particle size results of MFGM-C in Fig. 1A, showing that a smaller volume density (%) of bigger particles was detected in MFGM-C, which has the lowest interfacial tension. However, MFGs/MFGM at pH 6.70 presented the opposite trend, which shows the lower volume density (%) of bigger particle size (19.87 μm) but higher interfacial tension than MFGs/MFGM at pH 6.30 and 5.30. Most intact MFGs were crushed into fragments during the MFGM-C preparation, which was confirmed by the CLSM images (Fig. 1B). It can be speculated that particle size and the compositions on the surface of MFGs played an important role in the interfacial tension. Perhaps there were more exposed hydrophilic and hydrophobic groups in the MFGM-C, which easily adsorbed on the interface of oil and air, thus forming a more stable droplet structure with lower interfacial tension.

### 3.4. *ζ-potential*

Zeta potential indicates the change in MFGs structure and the interfacial composition. It indirectly predicts the potential emulsifying ability of MFGs/MFGM in the emulsion. As the MFGs and casein micelles carry a negative net charge, the MFGs/MFGM in this research exhibited negative ζ-potential. Herein, ζ-potential variation refers to the absolute value change.

The ζ-potential of MFGs/MFGM at pH 6.70 was −37.6 ± 0.11 mV

(Table 4), and pH decrease resulted in a significant increase in the ζ–potential to −39.4 ± 0.24 mV at pH 6.30 and −40.6 ± 0.18 mV at pH 5.30 samples ($p < 0.05$). This result may be explained by the preferential adsorption of non-membrane milk protein on the MFGs at lower pH conditions. The adsorption of casein micellar on the MFGs contributed to more detected negative charges at pH 5.30. The ζ-potential of MFGM-C (−28.30 ± 0.30 mV) was significantly lower than that of MFGs/MFGM sourced from acidified bovine milk, even though the pH of MFGM-C was close to pH 6.30. Combined with the unique MFGs/MFGM fragments structure in MFGM-C (Fig. 1B), it may be inferred that intact MFGs/MFGM structure facilitated the movement of negatively charged particles or molecules, and the velocity is positively proportional to ζ-potential.

It has been reported that surface weighted mean-D [3, 2] of MFGs/MFGM presented an opposite change tendency with the ζ-potential (Michalski, et al., 2002). On the contrary, the results of ζ-potential of MFGs/MFGM in this study presented a similar trend to the change in particle size. The opposite results may be due to the different mechanical shear intensities. Michalski et al. (2021) applied homogenisation, a more stringent treatment than the centrifugation used in this study. The ζ-potential of unprocessed raw milk was −32.10 ± 0.10 mV, which was used as the reference to calculate the MFGs surface fraction (Φ). There was a significant increase of Φ in MFGs/MFGM as a function of pH decrease. This finding confirmed the CLSM results in 3.1.1 which showed more attached non-membrane milk protein on the surface of MFGs at pH 5.30.

It is worth noting that the ζ-potential of unprocessed raw milk in this research is inconsistent with previous research in which the ζ-potential of untreated whole milk has been reported between −13.10 ± 0.50 mV and −13.70 ± 0.10 mV (Michalski, et al., 2002; Sharma, Oey, & Everett, 2015). However, it was in agreement with the results from Jukkola, Partanen, Rojas, and Heino (2016), who reported that the ζ-potential of MFGs separated via microfiltration was −30.10 ± 0.10 mV. Many variables, such as diet, lactation, and processing units, affect the composition and structure of raw milk. All these factors would alter the surface charge of MFGs/MFGM, and thus the ζ-potential. Therefore, this research mainly focused on the comparative analysis of ζ-potential between MFGs/MFGM at different pH levels and sourced from different materials. In addition, all the MFGs/MFGM in this study were isolated from the same batch of raw bovine milk and were analysed with the same method.

### 3.5. XRD

The polymorphic structure of MFGs/MFGM materials prepared from acidified bovine milk and sweet whey was acquired by wide angle X-ray scattering configuration (Fig. 5A). The typical polymorphs, β′ crystal form, were identified in all acidified MFGs/MFGM materials at 20.13°, 20.84° and 23.34°. In addition, apparent peaks at 18.95° and 21.65° were identified, which were related to α and β arrangement, respectively (Ren, et al., 2020). However, broad peaks instead of sharp crystal peaks were observed in MFGM-C. This may be attributed to the different existing state of triglyceride in MFGM-C compared to MFGs/MFGM isolated from acidified bovine raw milk (Fig. 1B).

According to Fig. 5B, the relative crystallinity of β′ crystal ($\beta'_1 + \beta'_2$) in all samples is significantly higher than α and β forms. This result is supported by Wright and Marangoni (2006a), who reported that the major polymorph in milk fat is β′ crystal, and milk fat is defined as β′ fat. Specifically, more than 50 % of crystal type in pH 6.70 and 5.30 cream were β′ crystal, while at pH 6.30, it was only 40.32 % due to the lower proportion of $\beta'_2$. The differences might be associated with the difference in MFGs interfacial curvature. It has been reported that the surface curvature of MFGs may change the crystalline characteristic because the formation of crystals starts between the lipid droplets and the inner monolayer membrane (Murthy, Guyomarc'h, Paboeuf, Vie, & Lopez, 2015).

Furthermore, MFGs size has been proven to play an important role in the formation of different crystalline types (Ren, et al., 2020). Smaller particle sizes of MFGs could inhibit the polymorphism transition, and it is easy to form small-sized polymorphs, such as α and β′ forms. The results of this study contradict this theory. pH 5.30 presented a higher volume density (8.37%) for bigger particles (105.83 μm) but contained higher amounts of α and β′ crystals than β crystals compared to MFGs/MFGM at pH 6.30 and 6.70.

The amount of β crystal (36.72%) in MFGs/MFGM at pH 6.30 was significantly higher than that in the control (6.79%) and at pH 5.30 (11.05%). β crystal has been reported to be the most stable crystal form in milk fat (Ren, et al., 2020). IAdditionally, β crystals melted at a higher temperature than α and β′ crystals because of their densest triclinic sub-cell packing (Wright et al., 2006a).

This study shows that decreased pH from 6.70 to 6.30 promoted a lower relative intensity of α crystals (22.96%) in MFGs/MFGM. Acidification and shearing treatment may cause changes in the types of fatty acids and TGA in MFGs/MFGM, which would affect the MFGs diffraction patterns. Tripalmitoyl glycerol (PPP) and trioleolyl glycerol (OOO) tend to form β crystals, while 1,3–dipalmitoyl–2–oleoyl–glycerol (POP) and

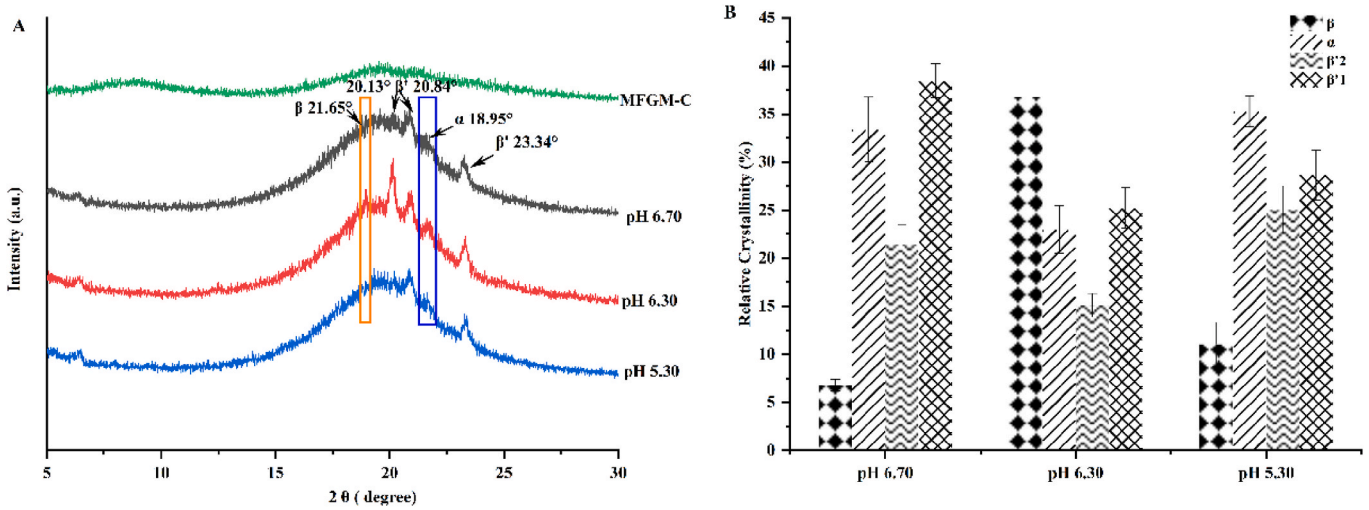



**Fig. 5.** XRD patterns (A) and the relative crystallinity (B) of β, α, β′2, and β′1 crystals in MFGs/MFGM isolated from different pH bovine milk or sweet whey. Relative crystallinity in MFGM-C was not shown because no crystal peaks were detected during the integration process.

1–palmitoyl–2–oleoyl–3–stearoyl–glycerol (POS) typically form α and β′ crystals (Zhang, et al., 2014). Based on this theory, we speculated that MFGs/MFGM at pH 6.70 and 5.30 may have more POP and POS than those at pH 6.30. Further investigation is needed to quantify and profile the fatty acid and TGA in MFGs/MFGM materials prepared from acidified raw milk or sweet whey.

### 3.6. DSC

DSC coupled with XRD has been used to elucidate the correlation between the polymorphism and thermal properties of milk fat (Lopez, Bourgaux, Lesieur, & Ollivon, 2007). Two main exothermic events were detected during the cooling stage in all cases (Fig. 6A), which was in good agreement with the previous research (Lambert, et al., 2018; Lopez, Lesieur, Bourgaux, Keller, & Ollivon, 2001). The exothermal curves were more complicated, with more peaks and curves than the endothermal thermograms. This finding indicated that sub-stable crystals melted firstly during the endothermic phase. Meanwhile, the un-melted crystals continually rearranged and formed more stable structures, which eventually melted at higher temperatures (Bootello, et al., 2013).

At pH 6.70, the first exothermic event started at 19.11 °C, with the maximum exothermic heat flow at 11.94 °C, followed by the second maximum at 6.83 °C (Fig. 6A). In comparison, the first crystallization peaks for MFGs/MFGM at pH 6.30 and 5.30 occurred at 12.74 °C and 12.49 °C, which were significantly higher than that at pH 6.70 (Table 3). Subsequently, the second exothermal event in MFGs/MFGM at pH 5.30 occurred at 7.14 °C, followed by 6.83 °C and 6.17 °C at pH 6.70 and 6.30, respectively. There is no correlation and consistency in the change of crystallization temperature of MFGs/MFGM as pH decreases. Regarding MFGM-C, the higher crystallization temperature peaks positioned around 12 °C did not appear, and only one exothermic peak with the maximum peak value at 5.48 °C was detected. According to previous XRD results on anhydrous milk fat, spectra at 12 °C were assigned to unstable α crystals and coexisted with relatively stable β′ crystals (Lambert, et al., 2018). This result confirmed the undetected crystal forms in the MFGM-C resulting from XRD.

It has been reported that the decrease in MFGs size is attributed to the delay of the crystallization because more time is needed to form the nucleus in smaller MFGs (Michalski, Ollivon, Briard, Leconte, & Lopez, 2004). This finding explained the lower crystallization temperature of MFGs/MFGM at pH 6.70, which have a higher volume density (%) of smaller particle size than at pH 6.30 and 5.30 according to the results in section 3.1.3.

Similarly, two major endothermic events were observed in the MFGs/MFGM at different pH levels and in MFGM-C during the heating stage. In all cases, the first significant heat absorption maximum peak was close to 15 °C, and the second was between 30 °C and 35 °C (Fig. 6 B). These two heat flows were attributed to the medium-melting-temperature fractions and high-melting-temperature fractions. respectively (Sert & Mercan, 2020). In addition, the endotherm at 15 °C and around 33.8 °C may be associated with the transferring from α to β′ form and the melting of β′ form, respectively (Timms, 1980). MFGs/MFGM at pH 6.30 melted at a higher temperature (14.77 °C–14.95 °C) than at pH 5.30 and the control. Compared with MFGs/MFGM at different pH levels, the first endothermic event for MFGM-C occurred at a higher temperature (16.84 °C). According to the particle size and

**Table 3**
The effect of acidification and different sources of MFGs/MFGM on the ζ-potential and surface coverage (Φ) of globules.

| | ζ–potential (mV) | $\zeta_R$ (%) | Φ |
|---|---|---|---|
| Unprocessed raw milk | −32.17 ± 0.12$^{e}$ | – | – |
| MFGM–C | −28.30 ± 0.30$^{d}$ | −11.84 ± 0.93$^{d}$ | 0.14 ± 0.02$^{d}$ |
| pH 6.70 | −37.60 ± 0.11$^{c}$ | 17.14 ± 0.31$^{c}$ | 0.27 ± 0.01$^{c}$ |
| pH 6.30 | −39.40 ± 0.24$^{b}$ | 22.74 ± 0.62$^{b}$ | 0.43 ± 0.02$^{b}$ |
| pH 5.30 | −40.60 ± 0.18$^{a}$ | 26.48 ± 1.56 $^{a}$ | 0.53 ± 0.04$^{a}$ |

Notes: Different superscript letters in the same column indicate significant ($p < 0.05$) differences among the samples.

**Table 4**
Enthalpy, crystallization and melting temperature of MFGs/MFGM isolated from bovine milk and sweet whey.

| | Crystallization | | | Melting | | |
|---|---|---|---|---|---|---|
| | $T_{C1}$ (°C) | $T_{C2}$ (°C) | $\Delta H_C$ (J $g^{-1}$) | $T_{M1}$(°C) | $T_{M2}$(°C) | $\Delta H_M$(J $g^{-1}$) |
| MFGM-C | – | 5.48 ± 0.01$^{d}$ | 0.73 ± 0.00$^{c}$ | 16.93 ± 0.13$^{a}$ | 32.37 ± 0.24$^{a}$ | 0.10 ± 0.01$^{c}$ |
| pH 6.70 | 11.94 ± 0.03$^{c}$ | 6.83 ± 0.04$^{b}$ | 8.18 ± 0.01$^{a}$ | 14.71 ± 0.08$^{c}$ | 30.23 ± 0.04$^{b}$ | 0.63 ± 0.04$^{a}$ |
| pH 6.30 | 12.74 ± 0.01$^{a}$ | 6.17 ± 0.03$^{c}$ | 6.56 ± 0.05$^{b}$ | 14.95 ± 0.02$^{b}$ | 30.71 ± 0.36$^{b}$ | 0.31 ± 0.00$^{b}$ |
| pH 5.30 | 12.49 ± 0.11$^{b}$ | 7.14 ± 0.06$^{a}$ | 8.33 ± 0.02$^{a}$ | 14.77 ± 0.03$^{bc}$ | 30.82 ± 0.22$^{b}$ | 0.27 ± 0.03$^{b}$ |

Notes:
1. Abbreviations are: $T_{C1}$ and $T_{C2}$, the points of crystallization for the first and second peaks, $\Delta H_C$, enthalpy of crystallization; $T_{M1}$ and $T_{M2}$, the temperature of melting for the first and second peaks, $\Delta H_M$, enthalpy of melting.
2. Different superscript letters in the same column indicate significant ($p < 0.05$) differences among the samples.

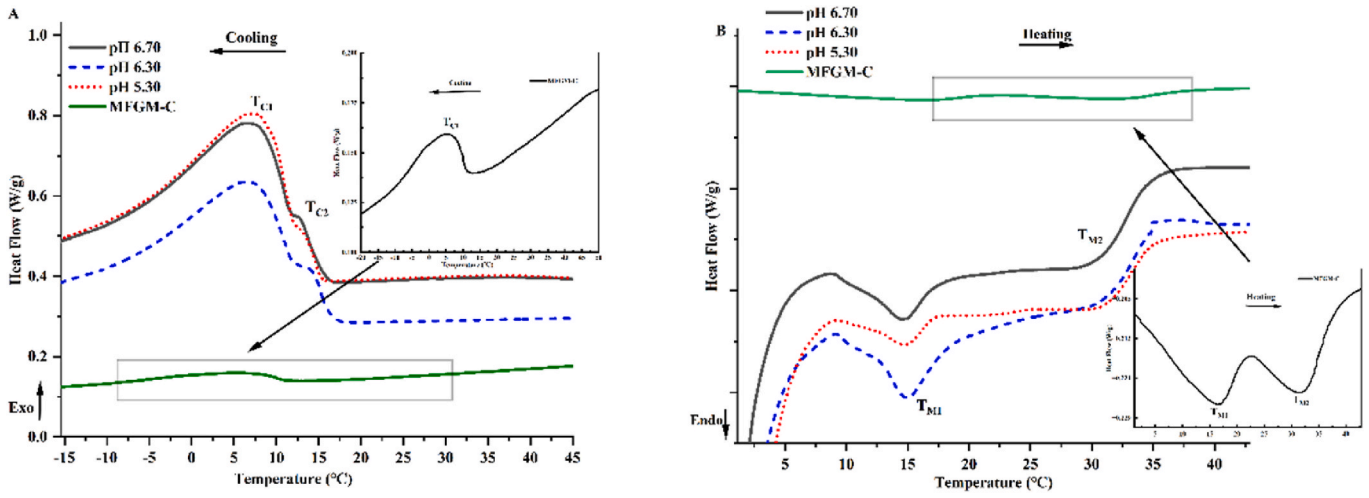



**Fig. 6.** Crystallization (A) and melting (B) thermograms of MFGs/MFGM prepared from different pH bovine milk and sweet whey.

microstructure results, MFGM-C presented a rare intact MFGs structure and smaller particle size than MFGs/MFGM at different pH conditions. In addition, the preparation of MFGM-C from whey involved more severe heating treatments, during which the crystals were re-formed and glycerol re-crystallized. These findings may have been attributed to the lower crystallization and higher melting temperature of MFGM-C (Wright & Marangoni, 2006b).

The enthalpy for crystal formation ($\Delta H_C$) and melting ($\Delta H_M$) in MFGM-C was significantly lower than in the control and acidified MFGs/MFGM ($p < 0.05$) (Table 3). There was no significant difference in the $\Delta H_C$ between MFGs/MFGM at pH 6.70 and 5.30 ($p > 0.05$), while MFGs/MFGM at pH 6.30 exhibited the lowest $\Delta H_C$. Moreover, less $\Delta H_M$ was detected in MFGs/MFGM at pH 6.30 than at 6.70 during the melting stage. This result contradicts to the XRD results, from which β crystals had the highest proportion in MFGs/MFGM at pH 6.30. As β crystal has a more stable structure than that of α and β′ crystals, more energy should be needed for the crystal formation and melting at pH 6.30. It may be inferred that, except for the crystal forms, the different associations between non-membrane milk protein and MFGs/MFGM demonstrated by the FTIR results (Fig. 3) may be attributed to the lower $\Delta H_C$ and $\Delta H_M$ of MFGs/MFGM at pH 6.30.

## 4. Conclusion

Our results demonstrated that MFGs/MFGM ingredients prepared from pH 6.30 and 5.30 bovine milk presented significantly different physicochemical properties, microstructure, surface charges, interfacial tension, crystal forms, and thermal properties compared to the control (pH 6.70). In contrast, MFGs/MFGM derived from sweet whey exhibited significantly different techno-functional properties compared to those sourced from bovine milk. MFGM-C prepared from sweet whey contained rare intact globule structures and exhibited more protein compositions, as identified by FTIR spectra in the ranges of 1700−1600 $cm^{-1}$ (Amide I protein) and 1600−1500 $cm^{-1}$ (Amide II protein). Additionally, MFGM-C presented lower interfacial tension and zeta potential than MFGs/MFGM from bovine raw milk. No apparent polymorphs were observed in MFGM-C, and lower exothermic or endothermic enthalpy was required during the heating and quenching procedures. Acidification, especially under pH 6.30 conditions, led to the adsorption of non-membrane milk proteins on the MFGs or MFGM fragments, forming more types of conjugate detected by FTIR. Consequently, this induced changes in the proportion of fat crystal form and thermal behaviour of MFGs/MFGM at pH 6.30.

In conclusion, this study provides critical information for developing MFGs/MFGM ingredients and their application in the food industry. However, this study is only a preliminary exploration of the influence of industrial MFGs/MFGM processing units on its properties. Further studies can be conducted to systematically track the effect of cheese processing on the physicochemical properties and functionalities of MFGs/MFGM, including heating, rennet, acidification, and whey drainage.

## CRediT authorship contribution statement

**Yanjun Sun:** Writing – original draft, Resources, Methodology, Investigation, Funding acquisition, Formal analysis, Data curation, Conceptualization. **Yrjö H. Roos:** Writing – review & editing, Supervision. **Song Miao:** Writing – review & editing, Supervision, Project administration, Funding acquisition, Conceptualization.

## Declaration of competing interest

The authors declare that they have no known competing financial interests or personal relationships that could have appeared to influence the work reported in this paper.

## Data availability

Data will be made available on request.

## Acknowledgements

The project was founded by 'The Open Project Program of State Key Laboratory of Dairy Biotechnology (No. SKLDB 2022–007)' and 'The China Scholarship Council (No.202008410212)'.

## References

Bootello, M. A., Hartel, R. W., Levin, M., Martinez-Blanes, J. M., Real, C., Garces, R., et al. (2013). Studies of isothermal crystallisation kinetics of sunflower hard stearin-based confectionery fats. *Food Chemistry, 139*(1–4), 184–195.

Chakraborty, A., & Basak, S. (2007). pH-induced structural transitions of caseins. *Journal of Photochemistry and Photobiology B: Biology, 87*(3), 191–199.

De Meutter, J., & Goormaghtigh, E. (2021). Amino acid side chain contribution to protein FTIR spectra: Impact on secondary structure evaluation. *European Biophysics Journal, 50*(3–4), 641–651.

Fontecha, J., Brink, L., Wu, S., Pouliot, Y., Visioli, F., & Jimenez-Flores, R. (2020). Sources, production, and clinical treatments of milk fat globule membrane for infant nutrition and well-being. *Nutrients, 12*(6), 1607.

Grewal, M. K., Chandrapala, J., Donkor, O., Apostolopoulos, V., Stojanovska, L., & Vasiljevic, T. (2017). Fourier transform infrared spectroscopy analysis of physicochemical changes in UHT milk during accelerated storage. *International Dairy Journal, 66*, 99–107.

Ho, T. M., Dhungana, P., Bhandari, B., & Bansal, N. (2021). Effect of the native fat globule size on foaming properties and foam structure of milk. *Journal of Food Engineering, 291*, Article 110227.

Holzmüller, W., Gmach, O., Griebel, A., & Kulozik, U. (2016). Casein precipitation by acid and rennet coagulation of buttermilk: Impact of pH and temperature on the isolation of milk fat globule membrane proteins. *International Dairy Journal, 63*, 115–123.

Hong Bui, A. T., Cozzolino, D., Zisu, B., & Chandrapala, J. (2021). Infrared analysis of ultrasound treated milk systems with different levels of caseins, whey proteins and fat. *International Dairy Journal, 117*, Article 104983.

Huang, Y., Wei, T., Chen, F., Tan, C., Gong, Z., Wang, F., et al. (2023). Effects of various thermal treatments on interfacial composition and physical properties of bovine milk fat globules. *Food Research International, 167*, Article 112580.

Jukkola, A., Partanen, R., Rojas, O. J., & Heino, A. (2016). Separation of milk fat globules via microfiltration: Effect of diafiltration media and opportunities for stream valorization. *Journal of Dairy Science, 99*(11), 8644–8654.

Jukkola, A., Partanen, R., Rojas, O. J., & Heino, A. (2018). Effect of heat treatment and pH on the efficiency of micro-diafiltration for the separation of native fat globules from cream in butter production. *Journal of Membrane Science, 548*, 99–107.

Kher, A., Udabage, P., McKinnon, I., McNaughton, D., & Augustin, M. A. (2007). FTIR investigation of spray-dried milk protein concentrate powders. *Vibrational Spectroscopy, 44*(2), 375–381.

Kiełczewska, K., Ambroziak, K., Krzykowska, D., & Aljewicz, M. (2021). The effect of high-pressure homogenisation on the size of milk fat globules and MFGM composition in sweet buttermilk and milk. *International Dairy Journal, 113*, Article 104898.

Lambert, A., Bougrioua, F., Abbas, O., Courty, M., El Marssi, M., Faivre, V., et al. (2018). Temperature dependent Raman and X-ray diffraction studies of anhydrous milk fat. *Food Chemistry, 267*, 187–195.

Li, H., & Van der Meeren, P. (2022). Sequential adsorption of whey proteins and low methoxy pectin at the oil-water interface: An interfacial rheology study. *Food Hydrocolloids, 128*, Article 107570.

Liu, Y., Boeren, S., Zhang, L., Zhou, P., & Hettinga, K. (2021). Ultrasonication retains more milk fat globule membrane proteins compared to equivalent shear-homogenization. *Innovative Food Science & Emerging Technologies, 70*, Article 102703.

Lopez, C., Bourgaux, C., Lesieur, P., & Ollivon, M. (2007). Coupling of time-resolved synchrotron X-ray diffraction and DSC to elucidate the crystallisation properties and polymorphism of triglycerides in milk fat globules. *Le Lait, 87*(4–5), 459–480.

Lopez, C., Lesieur, P., Bourgaux, C., Keller, G., & Ollivon, M. (2001). Thermal and structural behavior of milk fat. *Journal of Colloid and Interface Science, 240*(1), 150–161.

Mekonnen, K. D. (2023). Fourier transform infrared spectroscopy as a tool for identifying the unique characteristic bands of lipid in oilseed components: Confirmed via Ethiopian indigenous desert date fruit. *Heliyon, 9*(4), Article 14699.

Michalski, M. C., Michel, F., Sainmont, D., & Briard, V. (2002). Apparent ζ-potential as a tool to assess mechanical damages to the milk fat globule membrane. *Colloids and Surfaces B: Biointerfaces, 23*(1), 23–30.

Michalski, M. C., Ollivon, M., Briard, V., Leconte, N., & Lopez, C. (2004). Native fat globules of different sizes selected from raw milk: Thermal and structural behavior. *Chemistry and Physics of Lipids, 132*(2), 247–261.

Mohamed, H. J. J., Lee, E. K. H., Woo, K. C. K., Sarvananthan, R., Lee, Y. Y., & Mohd Hussin, Z. A. (2022). Brain-immune-gut benefits with early life supplementation of milk fat globule membrane. *JGH Open, 6*(7), 454–461.

Mohan, M. S., O'Callaghan, T. F., Kelly, P., & Hogan, S. A. (2020). Milk fat: Opportunities, challenges and innovation. *Critical Reviews in Food Science and Nutrition*, 1–33.

Murthy, A. V., Guyomarc'h, F., Paboeuf, G., Vie, V., & Lopez, C. (2015). Cholesterol strongly affects the organization of lipid monolayers studied as models of the milk fat globule membrane: Condensing effect and change in the lipid domain morphology. *Biochimica et Biophysica Acta, 1848*, 2308–2316.

Nicolaou, N., & Goodacre, R. (2008). Rapid and quantitative detection of the microbial spoilage in milk using Fourier transform infrared spectroscopy and chemometrics. *The Analyst, 133*(10), 1424–1431.

Nieto-Ruiz, A., Garcia-Santos, J. A., Verdejo-Roman, J., Dieguez, E., Sepulveda-Valbuena, N., Herrmann, F., et al. (2022). Infant formula supplemented with milk fat globule membrane, long-chain polyunsaturated fatty acids, and synbiotics is associated with neurocognitive function and brain structure of healthy children aged 6 Years: The COGNIS study. *Frontiers in Nutrition, 9*, Article 820224.

Pan, Y., Liu, S., Li, J., Hussain, M., Bora, A. F. M., Li, X., et al. (2024). Regulating the lipid droplet interface based on milk fat globule membrane and milk proteins to improve lipid digestion of model infant formula emulsion. *Food Hydrocolloids, 146*.

Pope, C. G. (1997). X-ray diffraction and the bragg equation. *Journal of Chemical Education, 74*(1), 129.

Ren, Q., Guo, F., Teng, F., & Ma, Y. (2021). A novel approach for the reconstitution of bovine milk fat globules with different-melting-temperature triacylglycerol cores. *Food Chemistry, 345*, Article 128563.

Ren, Q., Li, Q., Liu, H., & Ma, Y. (2020). Thermal and storage properties of milk fat globules treated with different homogenisation pressures. *International Dairy Journal, 110*, Article 104725.

Sadat, A., & Joye, I. J. (2020). Peak fitting applied to fourier transform infrared and Raman spectroscopic analysis of proteins. *Applied Sciences, 10*(17).

Sert, D., & Mercan, E. (2020). Characterisation of physicochemical, microbiological, thermal, oxidation properties and fatty acid composition of butter produced from thermosonicated cream. *International Dairy Journal, 109*, Article 104777.

Sharma, P., Oey, I., & Everett, D. W. (2015). Interfacial properties and transmission electron microscopy revealing damage to the milk fat globule system after pulsed electric field treatment. *Food Hydrocolloids, 47*, 99–107.

Sun, Y., Roos, Y. H., & Miao, S. (2022). Changes in milk fat globules and membrane proteins prepared from pH-adjusted bovine raw milk. *Foods, 11*(24), 4107.

Timms, R. (1980). The phase behaviour and polymorphism of milk fat, milk fat fractions and fully hardened milk fat. *Australian Journal of Dairy Technology, 35*(2), 47.

Voigt, D. D., Donaghy, J. A., Patterson, M. F., Stephan, S., & Kelly, A. L. (2010). Manufacture of Cheddar cheese from high-pressure-treated whole milk. *Innovative Food Science & Emerging Technologies, 11*(4), 574–579.

Vongsvivut, J., Heraud, P., Zhang, W., Kralovec, J. A., McNaughton, D., & Barrow, C. J. (2012). Quantitative determination of fatty acid compositions in micro-encapsulated fish-oil supplements using Fourier transform infrared (FTIR) spectroscopy. *Food Chemistry, 135*(2), 603–609.

Wei, W., Cheng, J., Yang, J., Chen, C., Jin, Q., Song, J., et al. (2021). Phospholipid composition and fat globule structure change during low temperature storage of human milk. *Lwt, 150*, 1–7.

Wright, A. J., & Marangoni, A. G. (2006a). Crystallization and rheological properties of milk fat. In P. L. H. M. E. A. d. c. p, & P. F. Fox (Eds.), *Advanced dairy chemistry, lipids* pp. 245–291). Boston: Springer.

Wright, A. J., & Marangoni, A. G. (2006b). Formation, structure, and rheological properties of ricinelaidic acid-vegetable oil organogels. *Journal of the American Oil Chemists' Society, 83*(6), 497–503.

Yang, H., Yang, S., Kong, J., Dong, A., & Yu, S. (2015). Obtaining information about protein secondary structures in aqueous solution using Fourier transform IR spectroscopy. *Nature Protocols, 10*(3), 382–396.

Zamora, A., Ferragut, V., Guamis, B., & Trujillo, A. J. (2012). Changes in the surface protein of the fat globules during ultra-high pressure homogenisation and conventional treatments of milk. *Food Hydrocolloids, 29*(1), 135–143.

Zhang, X., Li, L., Xie, H., Liang, Z., Su, J., Liu, G., et al. (2014). Effect of temperature on the crystalline form and fat crystal network of two model palm oil-based shortenings during storage. *Food and Bioprocess Technology, 7*, 887–900.

Zhou, X., Hadiatullah, H., Guo, T., Yao, Y., Li, C., & Wang, X. (2021). Dairy processing affects the gut digestion and microecology by changing the structure and composition of milk fat globules. *Journal of Agricultural and Food Chemistry, 69*(35), 10194–10205.

Zhou, Q., Sun, S. Q., Yu, L., Xu, C.-H., Noda, I., & Zhang, X.-R. (2006). Sequential changes of main components in different kinds of milk powders using two-dimensional infrared correlation analysis. *Journal of Molecular Structure, 799*(1), 77–84.

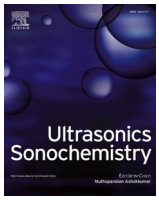
Ultrasonics Sonochemistry 102 (2024) 106755



Contents lists available at ScienceDirect

Ultrasonics Sonochemistry

journal homepage: www.elsevier.com/locate/ultson





# Comparative study of interfacial properties and thermal behaviour of milk fat globules and membrane prepared from ultrasonicated bovine milk

Yanjun Sun [a,b], Yrjö H. Roos [b], Song Miao [a,c,*]

[a] Teagasc Food Research Centre, Moorepark, Fermoy, Co. Cork, Ireland
[b] School of Food and Nutritional Sciences, University College Cork, Cork, Ireland
[c] China-Ireland International Cooperation Centre for Food Material Sciences and Structure Design, Fujian Agriculture and Forestry University, China

ARTICLE INFO

*Keywords:*
Milk fat globules
Ultrasonic treatment
Interfacial properties
X-ray diffraction
DSC

ABSTRACT

Milk fat globules or milk fat globule membranes (MFGs/MFGM) have been added to the infant formula to fortify the phospholipids and narrow the nutritional gap from breast milk. The main aim of this study was to profile the interfacial and thermal properties of MFGs/MFGM prepared from ultrasonicated bovine milk. Bovine milk was sonicated at ultrasonic intensities of 20 kHz and 40 kHz independently or synchronously with the duration time of 0 min (control), 5 min, 10 min, and 15 min (work/rest cycles = 5 s: 3 s). Ultrasonic treatments at 20 kHz/ 5 min and 20 + 40 kHz/ 5 min improved the volume density (%) of smaller particles (1–10 μm) while significantly decreasing the surface hydrophobicity ($H_0$) ($p < 0.05$). 40 kHz/5 min samples showed significantly higher ζ-potential than the other samples ($p < 0.05$), which might be because more negative charges were detected. In comparison with control samples, ultrasonic treatments decreased the interfacial tension (π) between the air and MFGs/MFGM liquid phase. 20 kHz ultra-sonicated treatments decreased the diffusion rate ($k_{diff}$) of MFGs/MFGM interfacial compositions significantly as the duration prolonged from 5 min to 15 min ($p < 0.05$) but did not affect the adsorption or penetration rate ($k_a$) ($p > 0.05$). X-ray diffraction (XRD) results showed that α-crystal peaks only existed in control and ultrasonicated 5 min samples but disappeared in all 15 min samples. According to the different scanning calorimetry (DSC), one or two new exothermic events (in the range of 17.29 – 18.81 ℃ and 22.14 – 25.21 ℃) appeared after ultrasonic treatments, which, however, were not found in control samples. Ultrasonic treatments resulted in the low-melting fractions (LMF) ($T_{M1}$) peaks undetectable in MFGs/MFGM samples in which only peaks of medium-melting fractions (MMF) ($T_{M2}$) and high-melting fractions (HMF) ($T_{M3}$) were detected. Compared with the control, both enthalpies of crystallisation ($\Delta H_C$) and melting ($\Delta H_M$) decreased in ultrasonicated samples. In conclusion, ultrasonic treatment affects the interfacial and thermal properties of MFGs/MFGM.

## 1. Introduction

Infant formulas are the essential food source for new-borns in the first half-year when breast milk is unavailable. Milk fat in infant formulas could supply infants with energy and vital lipophilic nutrients. Milk fat globules/membrane (MFGs/MFGM) ingredients have been clinically documented to be safe for infant formula enrichment and associated with benefits for the infant's neurocognitive development, brain structure, and body growth [1,2]. Commercially produced whey protein concentrate (WPC) enriched with MFGs/MFGM ingredients has been used in the infant formula to narrow the nutritional differences from breast milk. In addition to the health benefits, the effects of MFGs/MFGM ingredients supplement on the infant formula's physicochemical properties and functionality have been examined, but only in a few studies. MFGs/MFGM was proved to induce the interfacial composition and microstructure changes of fat globules in infant formula by reducing the thicknesses of the MFGM [3]. The combination of the homogenization process and buttermilk powder addition resulted in the decreased fat globule diameter of infant formula but the improved colloidal stability of milk proteins [4].

Industrially, MFGs/MFGM ingredients are added to infant formula by wetly mixing with other nutrients, followed by homogenizing, concentrating, and spray drying. The physicochemical properties of infant formula powders are affected not only by the processing units, such

* Corresponding author at: Teagasc Food Research Centre, Moorepark, Fermoy, Co. Cork, Ireland.
*E-mail address:* Song.Miao@teagasc.ie (S. Miao).

https://doi.org/10.1016/j.ultsonch.2024.106755
Received 17 December 2023; Received in revised form 2 January 2024; Accepted 4 January 2024
Available online 9 January 2024
1350-4177/© 2024 The Author(s). Published by Elsevier B.V. This is an open access article under the CC BY-NC-ND license (http://creativecommons.org/licenses/by-nc-nd/4.0/).

as concentration times and spray drying temperature but also by the functionality of each nutrient [5–7]. The glass transition temperature ($T_g$), interfacial compositions, and lactose crystallization are essential in minimizing deteriorative changes during infant formula storage. However, MFGs/MFGM, as a newly developed dairy ingredient, to date, the knowledge of its interfacial and thermal properties is limited. Homogenization was reported to affect the thermodynamics of fat crystals and the polymorphs during storage [8]. The effect of pasteurization on the crystallization, melting properties, and the crystal polymorphism of MFGs/ MFGM was characterized in previous research [9].

Ultrasonic treatment is one of the most potent techniques that could be used in dairy processing. According to the frequency ranges, ultrasonic frequencies can be classified into three categories: Low frequency (20 kHz − 100 kHz), medium frequency (100 kHz − 1 MHz) and high frequency (1 MHz − 10 MHz). Meanwhile, based on intensity, different frequency ultrasounds could also be divided into high- intensity (>1 W/ cm $^2$) and low-intensity ultrasound (below 1 W/ cm $^2$) [10]. Low-frequency ultrasounds induce strong cavitation effects by forming and violent collapsing of bubbles in the solution, which is usually used to produce smaller particles, facilitate fat separation, improve the emulsion properties, and adjust the crystallization behaviour of anhydrous milk fat (AMF) [11–15]. Specifically, the efficacy of specific ultrasonic density in separating fat from milk was optimized in the previous investigation [12]. Compared with shear-homogenization, more MFGM proteins were retained after being ultrasonicated at 20 kHz for 30 s − 180 s [16]. These researchers focused on the ultrasonication-induced functional change of MFGs/MFGM in other food systems, including cream, infant formula, or AFM, other than the 'native and pure' MFGs/ MFGM systems. Despite the positive effects induced by the ultrasonic treatment, we are still unaware of any studies on the impact of high-intensity/low-frequency ultrasound on the interfacial properties, crystal transformation, crystallization, and melting characteristics of the MFGs/MFGM materials.

We prepared the MFGs/MFGM samples from ultrasonicated bovine milk in this study. Low-frequency sonication, 20 kHz and 40 kHz was applied independently or synchronously on the bovine milk before the MFGs/MFGM separation. Subsequently, particle characterization, interfacial tension, surface charges, and the surface hydrophobicity of MFGs/MFGM were analysed to evaluate the interfacial properties. In addition, crystal forms, crystallization, and melting of MFGs/ MFGM samples were investigated using the XRD and DSC. Understanding the interfacial and thermal behaviours of the MFGs/MFGM separated from ultrasonicated bovine milk would be useful for the development of MFGs/MFGM enriched dairy ingredients and their application in infant formula or other food.

## 2. Materials and methods

### 2.1. Materials and reagents

Raw bovine milk (fat 4.08 ± 0.02 %, protein 3.57 ± 0.01 %, dry matter 13.03 ± 0.02 %, pH 6.67 ± 0.04) was collected from the Teagasc dairy herd (Moorepark, Fermoy, Co. Cork, Ireland). After milking, the raw bovine milk was not processed by any other unit operation except for the rapid chilling from 37 ℃ to 4 ℃ using a plate heat exchanger (UK Exchangers Ltd., Buckinghamshire, UK).

Azide sodium, 1-anilinonaphthalene-8 sulfonic acid (ANS) and Phosphate-buffered saline (PBS) tablets, Nile Red (9- (diethylamino)-5H-benzo[a]phenoxazin-5-one), Fast Green FCF (disodium 2-[[4-[ethyl-[(3-sulfonatophenyl)methyl]amino]phenyl]-[4-[ethyl-[(3-sulfonatophenyl) methyl] azaniumylidene] cyclohexa-2,5-dien-1-ylidene] methyl]-5-hydroxybenzenesulfonate) were purchased from Sigma–Aldrich®, Merck Life Science Ltd., Cork, Ireland. All solutions were prepared using MilliQ water except as otherwise noted.

### 2.2. Ultrasonic treatments

Ultrasonic treatments with different intensities were applied to the bovine milk following the methods described by Zhao et al. and Sun et al. with modifications [17,18]. Bovine milk at 4 ℃ was preheated to 30–35 ℃ in a water bath to ensure that the milk fat was in liquid. After that, the preheated milk was divided into 10 aliquots for testing, and each aliquot was 10 kg. One of the aliquots was used as control, and the other 9 aliquots were sonicated at different conditions by the ultrasonic facility fitted with a cooling jacket and the double frequency ultrasonic reactors (WKS1200/2J, Jiangsu Jiangda Wukesong Biotechnology Co., LT, Zhejiang, China). The independent working model at frequency 20 kHz or 40 kHz, and synchronous models (20 kHz and 40 kHz probes working together) were applied with different durations (5 min, 10 min, and 15 min in 5 s: 3 s work/rest cycles). The temperature of each sample was instantly recorded at the end of the ultrasonic treatment for any variation (as shown in Table S1). Ultrasound energy would be partly lost due to the heat and sound generated during the treatment. The equation (Eq. (1)) was applied to estimate the dissipated acoustic power ($P$) in the liquid, which was expressed as watts per unit volume of sonicated liquid (W cm$^{-3}$):

$$P = mCdT/dt \quad (1)$$

where $m$ stands for the mass of the sample for each treatment (in g), and $C$ is the heat capacity of the sample (in J/g ℃$^{-1}$). $dT/dt$ is the temperature change of samples as the ultrasound exposure (℃/s). The calculated results of ultrasound acoustic power ($P$) after all treatments are shown in Table 1.

### 2.3. Isolation of MFGs/MFGM samples

MFGs/MFGM samples were enriched from ultrasonicated bovine milk using ultracentrifugation (10000 × g, 15 min at 4 ℃) (Kendro Laboratory Products, Asheville, NC) following the methods in previous researches with modifications [19,20]. Specifically, 25 mL ultrasonicated milk was centrifuged, and the serum phase (lower layer) was carefully discarded. The collected top layer was mixed with a triple volume of PBS buffer (volume of sample: buffer = 1:3). The mixture of the sample with buffer was pre-heated in a 30–35 ℃ water bath until melted into a liquid state, then thoroughly mixed by the vortex. The centrifugation and rinse steps were repeated two more times. The supernatant from the third time was freeze-dried for 72 h for further analysis. The collected samples were named as the ultrasonic conditions: 20 kHz/5 min, 20 kHz/10 min, 20 kHz/15 min, 40 kHz/5 min, 40 kHz/ 10 min, 40 kHz/15 min, 20 + 40 kHz/5 min, 20 + 40 kHz/10 min and 20 + 40 kHz/15 min.

### 2.4. Chemical compositions of the MFGs/MFGM

The compositions of all collected freeze-dried MFGs/MFGM

**Table 1**
Acoustic power ($P$) generated by different ultrasonic intensities and durations in bovine milk.

| Samples | $P$ (W) |
|---|---|
| 20 kHz/ 5 min | 78.49 ± 1.76$^{c}$ |
| 20 kHz/ 10 min | 98.96 ± 7.66$^{b}$ |
| 20 kHz/ 15 min | 145.28 ± 3.52$^{a}$ |
| 40 kHz/ 5 min | 19.66 ± 0.74$^{f}$ |
| 40 kHz/ 10 min | 29.25 ± 0.49$^{ef}$ |
| 40 kHz/ 15 min | 29.25 ± 0.49$^{ef}$ |
| 20 + 40 kHz/ 5 min | 25.03 ± 2.03$^{f}$ |
| 20 + 40 kHz/ 10 min | 39.33 ± 1.49$^{e}$ |
| 20 + 40 kHz/ 15 min | 51.68 ± 7.28$^{d}$ |

*Notes*: Different superscript letters in the same column indicate significant ($p < 0.05$) differences between the samples.

materials were analysed by DairySpec FT–15 (Bentley Instruments Inc., Chaska, MN, USA). Before the analysis, the samples were diluted 5 times by MiliQ water and then heated at 30 – 35 ℃ to make the even solutions. The protein and fat content of all samples are given in Table 2.

### 2.5. The characterization of interfacial properties of MFGs/MFGM

#### 2.5.1. Particle size determination

The particle size of MFGs/MFGM samples was analysed using Mastersizer 3000 (Malvern Instruments, Malvern, UK) equipped with a laser light scattering, and Mie theory was used to calculate the results. The refractive index of milk fat and water were 1.456 and 1.333, respectively. Sample droplets were dropped into the sampling vessel containing deionised water until the obscuration reading reach 3 – 20 %. In addition, each sample was equilibrated 30 s before the recording, and the stirring speed was set to 2000 rpm throughout the analysis. Volume density (%) at different particle size distributions was recorded. Meanwhile, the span was reported, which was used to assess the width of the particle size distribution, and the narrower span reflected the more even distribution [21].

On the assumption that most particles in all samples were spherical and non-porous, specific surface area (SSA) was employed to calculate the surface area of the particles per unit weight according to the following Eq. (2):

$$SSA = 6/\rho D[3,2] \tag{2}$$

where ρ stands for the particle density [21]. Additionally, the extent of MFGs/MFGM wrapped by proteins was calculated by the surface fraction ($\Phi_m$) model according to Eq. (3)

$$\Phi_m = (S_t - S_o)/S_o \tag{3}$$

where $S_o$ is the original surface area of MFGs/MFGM in control raw milk, and $S_t$ is the surface area of MFGs/MFGM in ultrasonicated samples.

#### 2.5.2. Zeta (ζ) potential

The ζ − potential was analysed by the dynamic light scattering instrument (Nano–ZS, Malvern Instruments Ltd., Worcestershire, UK). It has been reported that the un-adsorbed compositions, such as casein micelles, showed no significant effect on the result of ζ − potential of fat globules [22]. The sample preparation method referred to our previous research with modifications [21]. Specifically, the pre-melted (30 – 35 ℃) samples were diluted 100 times with MiliQ water and then mixed thoroughly by the vortex. All samples were analysed at room temperature, and three runs were conducted automatically for each analysis. In addition, based on the relative change of ζ − potential ($\zeta_R$), an estimative model was applied to assess the fraction of MFGs/MFGM surface change:

**Table 2**
The compositions of freeze-dried MFGs/MFGM samples isolated from control and ultrasonicated bovine milk.

| Samples | Protein (%, w/w) | Fat (%, w/w) |
|---|---|---|
| Control | $3.05 \pm 0.05^{a}$ | $73.45 \pm 0.01^{ns}$ |
| 20 kHz/ 5 min | $1.96 \pm 0.03^{d}$ | $74.62 \pm 2.99$ |
| 20 kHz/ 10 min | $1.54 \pm 0.01^{e}$ | $75.29 \pm 0.25$ |
| 20 kHz/ 15 min | $1.25 \pm 0.02^{f}$ | $74.97 \pm 3.35$ |
| 40 kHz/ 5 min | $1.72 \pm 0.01^{e}$ | $74.32 \pm 2.55$ |
| 40 kHz/ 10 min | $2.99 \pm 0.00^{a}$ | $73.42 \pm 1.53$ |
| 40 kHz/ 15 min | $2.78 \pm 0.11^{b}$ | $76.49 \pm 4.76$ |
| 20 + 40 kHz/ 5 min | $2.1 \pm 0.07^{d}$ | $74.14 \pm 1.47$ |
| 20 + 40 kHz/ 10 min | $2.65 \pm 0.14^{b}$ | $75.24 \pm 2.96$ |
| 20 + 40 kHz/ 15 min | $2.44 \pm 0.04^{c}$ | $73.56 \pm 0.73$ |

*Notes*: Different superscript letters in the same column indicate significant ($p < 0.05$) differences between the samples. 'ns' means no significant difference ($p > 0.05$).

$$\Phi_e = 1 - \exp\left(-1.802 \times 10^{-3}\zeta_R^2\right) \tag{4}$$

where $\zeta_R$ was the relative change of ζ–potential of MFGs/MFGM samples after ultrasonic treatment in comparison with the control which was assumed that $\Phi_e = 0$.

#### 2.5.3. Surface hydrophobicity ($H_0$)

The $H_0$ determination referred to the method described by Sun et al. [18] in which ANS was used as a fluorescent probe. The control and ultrasonicated samples were preheated at 30 – 35 ℃ until milk fat was completely melted, and the melted samples were diluted with PBS buffer (0.1 M, pH 7.0) to a series of protein concentrations ranging from 0.01 % to 0.06 % mg $mL^{-1}$. Before the dilution, LECO FP 628 (LECO Corp., Benton Harbor, MI, USA) was used to quantify the protein content of each sample with a nitrogen conversion factor of 6.38.

40 μL of stock solution of 8 mM ANS (in PBS buffer 0.1 M, pH 7.0) was mixed with the above-diluted samples and incubated for 15 min in the dark at room temperature. The fluorescence intensity (FI) was analysed by a fluorescence spectrometer (Varian Cary Eclipse, New Jersey, USA) at 390 nm (excitation wavelength) and 470 nm (emission wavelength), with a slit width of 2.5 nm and scanning speed of 5 nm $s^{-1}$. The initial slope of the FI as a function of protein concentration was calculated and defined as the $H_0$.

#### 2.5.4. Interfacial tension (π)

Dynamic interfacial tension (π) between the air and liquid droplets of MFGs/MFGM samples was determined by an optical tensiometer (Oneattension Theta lite, Biolin Scientific, Espoo, Finland) equipped with a pendant drop apparatus. The π measurement was performed in a temperature-controlled room (25 ℃). A drop of the liquid sample with a volume between 6–8 μL was pushed out of a glass syringe. The profile of the droplet was captured by a built-in high-resolution camera. Young-Laplace equation was used to fit the drop shape and calculate the π in Oneattension software (Version 4.1.6, Biolin Scientific, Finland). In our preliminary experiment, the recording time was optimised and 15 s was chosen because π values fluctuated greatly after 15 s. Therefore, the analysis lasted 15 s with a recording rate of 0.1 % frame per second (FPS) in the current study. All the results were expressed in the unit of mN/ m.

Kinetic parameters were used to characterize MFGs/MFGM interfacial protein change. According to previous researches, the main processes for the adsorption of proteins within the different layers were: (i) diffusion or migration of proteins to the interface, (ii) adsorption (penetration), (iii) unfolding and rearrangement of proteins [23,24]. The diffusion or migration step (i) can be fitted by the Ward − Tordai equation to model the change of π as a function of time (t) (Eq. (5)).

$$\pi = 2C_0KT(Dt/3.14)^{0.5} \tag{5}$$

where $C_0$ is the protein concentration, $K$ is the Boltzmann constant and $T$ is the temperature, $D$ is the diffusion coefficient and $t$ is the adsorption time. The diffusion or migration process was reported to be mainly controlled by protein diffusion [24]. It was possible to obtain the diffusion rate ($k_{diff}$) of the protein by calculating the slope of π versus $t^{0.5}$ plot by the linear fitting.

The adsorption (penetration), unfolding or rearrangement rate of molecules between the interface of air and oil can be analysed by the first-order equation proposed by Graham and Philips [24] (Eq. (6)):

$$\ln[(\pi f - \pi t/(\pi f - \pi 0)] = -k_i t \tag{6}$$

where $\pi_f$ and $\pi_0$ are interfacial tension at the final and starting measurement points respectively, and $\pi_t$ is the initial point. $k_i$ is the first-order rate constant. Two linear regions were monitored yielding from the plot of ln [($\pi_f$ -$\pi_t$/ ($\pi_f$– $\pi_0$)] versus time (s). The first and second slopes were taken as the first-order constant of adsorption (penetration) ($k_a$) and rearrangement ($k_r$) of molecules between the air and oil interface

[25].

#### 2.5.5. Confocal laser scanning microscopy (CLSM)

A Leica TCS SP5 microscope (Leica Microsystems GmbH, Wetzlar, Germany) was used to observe the serum proteins and lipids in the MFGs/MFGM samples. All the samples were dual-stained by Nile Red and Fast Green FCF. A 0.1 % (w/v) Nile Red and FCF was used to dye neutral lipids and serum proteins respectively. 1.5 mL of the sample was mixed with 30 μL Nile Red and 10 μL FCF. The prepared sampleswere observed on the microscope referring to our previous report[21].

### 2.6. The characterization of thermal properties of MFGs/MFGM

#### 2.6.1. X–ray diffraction (XRD)

XRD can characterize the change of polymorphs in milk fat by monitoring the intensity and position of the spectra peaks. In this study, the polymorphic forms of ultrasonicated samples were determined by a powder diffractometer STOE STAID MP (STOE, Darmstadt, Germany) mounted with Cu radiation (λ = 1.5406 nm; current, 40 mA; voltage, 40 kV). All the freeze-dried samples were carefully ground into a fine powder using a cleaned mortar and pestle. The ground powder was sealed in a custom metal plate with films covered on both sides. XRD patterns were recorded with a scanning speed of 1°/ min in the range of $2\theta = 5^{\circ} - 30^{\circ}$.

The normalization, smoothness and calculation of full width at half-maximum (FWHM) of the crystal peaks were performed in Origin software (Originpro 2021, OriginLab Corporation, Northampton, US). Savitzky–Golay method was used to smooth the spectra with points of windows 5 and polynomial order 2. The peak analyser in Origin was used to calculate the relative crystallinity (%) by integrating the corresponding peak areas. The baseline mode was set as 'constant Y = Minimum value', and only positive peaks with threshold weight (%) higher than 20 were found using the 'Local Maximum' method.

Typical crystalline forms, α, β, and β', were identified by the conversion of each diffraction peak to the unique corresponding d-spacing. According to the previous reports, the short spacing positions used to fingerprint the crystals in milk fats are α = 4.14–4.16 Å ($2\theta = 21.32^{\circ} - 21.46^{\circ}$), $\beta'_1$ = 3.80–3.85 Å ($2\theta = 23.06^{\circ} - 23.70^{\circ}$) and 4.20–4.25 Å ($2\theta = 20.86–21.39^{\circ}$), $\beta'_2$ = 4.30–4.37 Å ($2\theta = 20.29–20.88^{\circ}$), β = 4.52–4.65 Å ($2\theta = 19.05–19.64^{\circ}$) [8,9,26–28].

The relative crystallinity of α, β and β' polymorphs was the percentage of each crystal peak area in the total peak area which was set as 100 % (Eq. (7).

$$\text{Crystallinity} = (\text{Area of crystalline peaks}) \times 100/\text{Area of all peaks}(\text{Crystalline} + \text{Amorphous}) \quad (7)$$

#### 2.6.2. Different scanning calorimetry (DSC)

The thermal behaviour of MFGs/MFGM samples was investigated on a DSC (DSC Q2000, TA Instruments, Crawley, UK). Sample preparation and analysis method referred to the reported researches on goat milk and MFGs with modifications [29,30]. Each 10–15 mg ground powder was hermetically sealed into an aluminium pan (tolerable temperature from − 180 to 600 ℃), and the powder should evenly cover the whole bottom of the pan. Meanwhile, a hermetically sealed aluminium pan without sample was used as a reference. Nitrogen was used to purge the system at 50 mL/min. All the DSC measurements were carried out with the same time–temperature program: Cycle 1: Equilibrate at 4℃; Cycle 2–3: Ramp 10℃/min to 60℃ and keep the isothermal temperature for 15 min; Cycle 4–5: Ramp 10℃/min to –60℃ and keep the isothermal temperature for 5 min; Cycle 6: Ramp 10℃/min to 60℃. The equilibration at 4℃ (Cycle1) and isothermal stabilization at 60 ℃ for 15 min (Cycle 2–3) were used to erase the crystal and melting history of all the samples. The crystallization and melting profiles were obtained during the cooling (Cycles 4–5) and heating (Cycle 6) procedures, respectively. All the thermograms were collected and exported by Universal Analysis 2000 (TA Instruments–Waters LLC, New Castle, US). The heat flow curves (W/g) as the function of temperature were plotted in the Origin software system (Originpro 2021, OriginLab Corporation, Northampton, US). The peak analyzer function in the Origin system was used to find the peak values. The endothermic ($\Delta H_M$) and exothermic ($\Delta H_C$) enthalpy (J/g) for each sample were calculated by integrating the area of the corresponding peaks.

### 2.7. Statistical analysis

All experiments and measurements were performed three times unless otherwise indicated. Data were expressed as the mean value ± standard deviation (SD). The resulting data were submitted to the OriginPro 2023 software system (OriginPro 2023, OriginLab Corporation, Northampton, USA) to evaluate the significant differences between samples. The variant analysis was performed (ANOVA) to test the differences between the groups at the significance level of $p < 0.05$, except for interfacial tension for which a more strict level of $p < 0.01$ and $p < 0.001$ were used.

## 3. Results and discussion

### 3.1. The effect of ultrasonic treatments on the interfacial properties of MFGs/MFGM

#### 3.1.1. Particle size distribution

Particle size distribution of MFGs/MFGM samples prepared from ultrasonicated bovine milk is shown in Fig. 1A. Similar to control samples, most MFGs/MFGM particles in ultrasonicated samples are distributed in the range of 1–10 μm and 10–400 μm. Small amounts of particles distributed between 0.01 μm and 0.1 μm were only identified in control and 20 kHz/ 5 min samples, while these tiny particles were not observed in other samples.

As the ultrasound duration time prolonged, there was an apparent movement of particle size distribution from 50 μm towards 400 μm for 20 kHz treated samples. The same trend was observed for samples treated at 20 + 40 kHz, which, meanwhile, presented multimodal distribution, especially for samples treated at 20 + 40 kHz/ 10 min. This may be due to the formation of aggregates by MFG fragments or the adsorption of plasma proteins on the surface of MFGs/MFGM (Fig. 1C). This result was inconsistent with the findings of previous researchers who reported that ultrasonic treatment would decrease the particle size of milk protein dispersion, milk phospholipid solution, or emulsions [16,31]. Ultrasonic treatment at a certain intensity had the same impact as shear homogenisation. The acoustic cavitation could be generated by ultrasound, with results corresponding to mechanical shearing by the continual forming and collapsing of bubbles [16]. Compared with control samples, 20 kHz independently or synchronously with 40 kHz ultrasonic treatment for 5 min exhibited a lower volume density (%) of 10–100 μm at the expense of higher 1–10 μm particles. Therefore, these two ultrasonic conditions presented corresponding effects ondecreasing of the particle size as homogenisation shearing.

Generally, as a function of acoustic power, the volume density (%) of particle size distribution increases firstly, followed by a decreasing trend. The increased volume density (%) of bigger particles under 40 kHz conditions may be because intact MFGs broke into fragments that aggregated into bigger particles. As the treatment duration was prolonged, or the increase in ultrasonic intensity, the formed big size aggregates dispersed into multimodal distribution, as shown for the 20 + 40 kHz treated samples. In addition, excessive shearing induced by a higher ultrasound intensity at 20 kHz conditions further dispersed the different sizes of particles and facilitated less multimodal particle distribution. That result may explain why samples treated at 20 kHz displayed more even particle distribution than the lower acoustic power treated samples.

According to Fig. 1B, the span of 20 + 40 kHz/ 10 min samples was

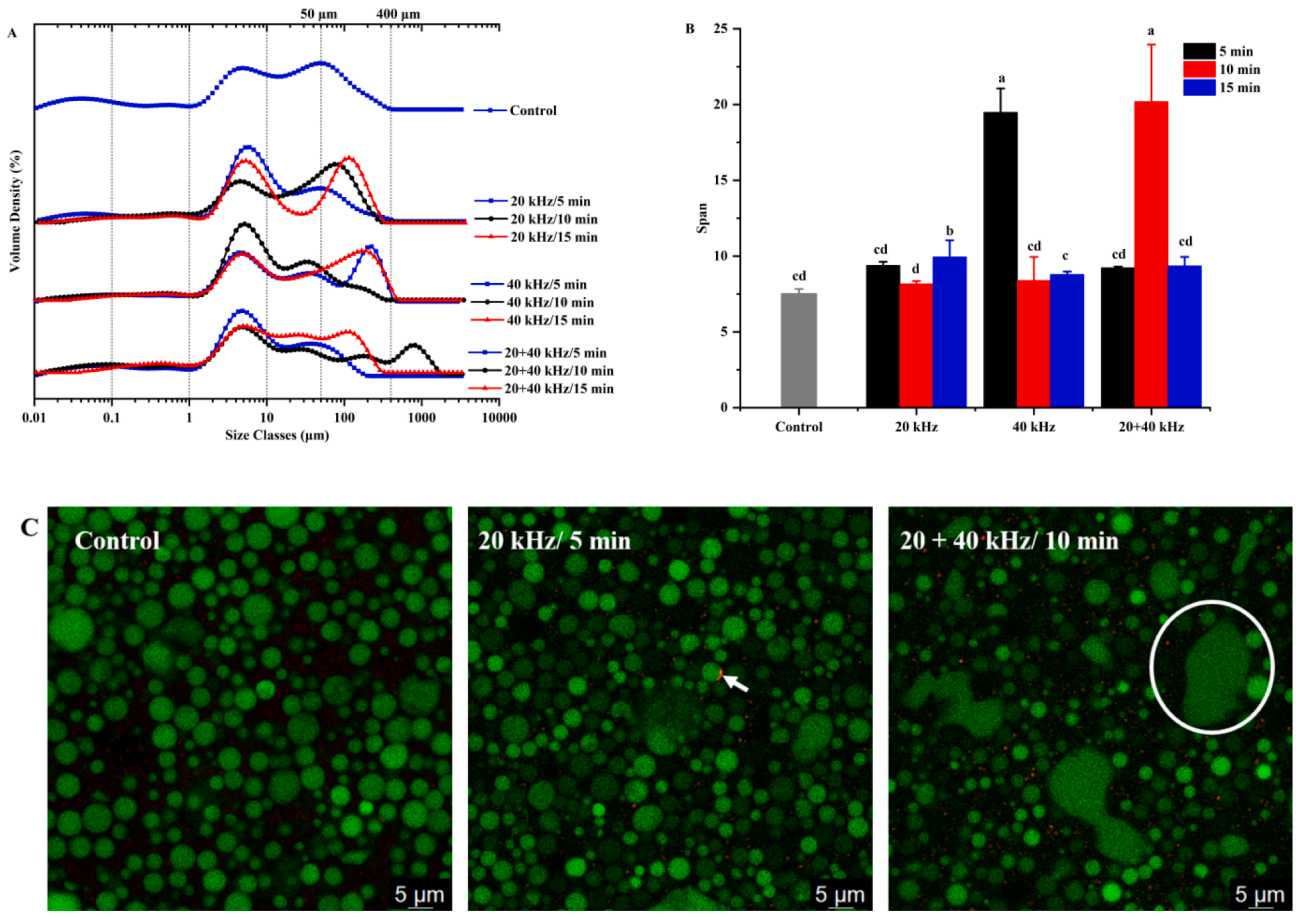



**Fig. 1.** Particle size distribution (A) and span (B) of MFGs/MFGM samples prepared from control and bovine milk treated by different ultrasound intensities. The different letters indicate that each sample has a significant difference ($p < 0.05$). Confocal laser scanning microscopy images of control and ultrasonic treated MFGs/MFGM samples (20 kHz/ 5 min and 20 + 40 kHz/10 min) (C). Neutral lipids and serum plasma protein were stained with Nile red and fast green FCF (white arrows pointing at the plasma proteins on the surface of MFGs/MFGM; aggregated MFGs/MFGM fragments in white circle). Scale bar = 5 μm. (For interpretation of the references to colour in this figure legend, the reader is referred to the web version of this article.)

significantly higher than other samples ($p < 0.05$), followed by 40 kHz/ 5 min and 20 kHz/15 min samples. The result was in accordance with the particle size distribution results in Fig. 1A. The surface change of MFGs/MFGM induced by the acoustic wave was characterised by the surface fraction ($\Phi_m$) model (Table.3). Table 3 showed that both 40 kHz and 20 + 40 kHz treated 15 min samples have higher $\Phi_m$ values which could be due to the increase of plasma proteins adsorption on the surface of MFGs/MFGM. This agreed with the size distribution results in Fig. 1A, which showed that more particles with a higher volume density (%) were detected in 40 kHz/ 15 min and 20 + 40 kHz/ 15 min samples.

**Table 3**
Effect of different ultrasonic intensities on surface change of MFGs/MFGM calculated by the surface fraction ($\Phi_m$) model.

| Samples | $\Phi_m$ |
|---|---|
| 20 kHz/ 5 min | $0.27 \pm 0.02^{d}$ |
| 20 kHz/ 10 min | $0.79 \pm 0.01^{a}$ |
| 20 kHz/ 15 min | $0.61 \pm 0.05^{b}$ |
| 40 kHz/ 5 min | $0.56 \pm 0.04^{b}$ |
| 40 kHz/ 10 min | $0.48 \pm 0.02^{c}$ |
| 40 kHz/ 15 min | $0.81 \pm 0.01^{a}$ |
| 20 + 40 kHz/ 5 min | $0.16 \pm 0.02^{e}$ |
| 20 + 40 kHz/ 10 min | $0.17 \pm 0.01^{e}$ |
| 20 + 40 kHz/ 15 min | $0.81 \pm 0.01^{a}$ |

*Notes*: Different superscript letters in the same column indicate significant ($p < 0.05$) differences between samples.

### 3.1.2. Zeta (ζ) potential

The effect of ultrasonic treatments on the ζ − potential of MFGs/MFGM is presented in Fig. 2. In agreement with the previous research, the ζ − potential of all samples exhibited negative values, which indicated that negative charges were present [32]. The change of ζ − potential in this study referred to the comparison of the absolute values. According to Fig. 2, ultrasound treatments at 20 kHz/ 15 min, 40 kHz/ 5 min, 40 kHz/10 min, and 20 + 40 kHz/ 10 min significantly increased the ζ − potential to varying degrees ($p < 0.05$). This finding was in contrast with the previous research, which reported that ζ − potential of the raw milk decreased after treatment by 475 W ultrasound with energy densities of 7 kJ /mL [33]. However, Scudino et al. (2020) reported an increase of ζ − potential in raw milk after 100 W ultrasonic treatment and presented a similar effect to our study [34]. In this study, 40 kHz treated samples with a duration of 5 min showed the highest ζ − potential which increased by 14.20 % compared to the control samples, followed by the 20 + 40 kHz/10 min samples with an increase of 10.80 %. It can be inferred that these ultrasonication conditions may cause the rupture of MFGs followed by the reconfiguration of the membrane with more negative charge exposure, consequently causing the increased ζ − potential.

The correlation between $\zeta_R$ and $\Phi_m$ was fitted by polynomial regression (Fig. 3). Fig. 3 A showed nonlinear relationships between the $\zeta_R$ and $\Phi_m$ for 20 kHz and 40 kHz treated samples with $R^2 = 0.990$ and $R^2 = 0.997$, respectively. This finding is in accordance with the results from Michalski et al. (2002) [35] and Sharma et al. (2015) [22]. In their

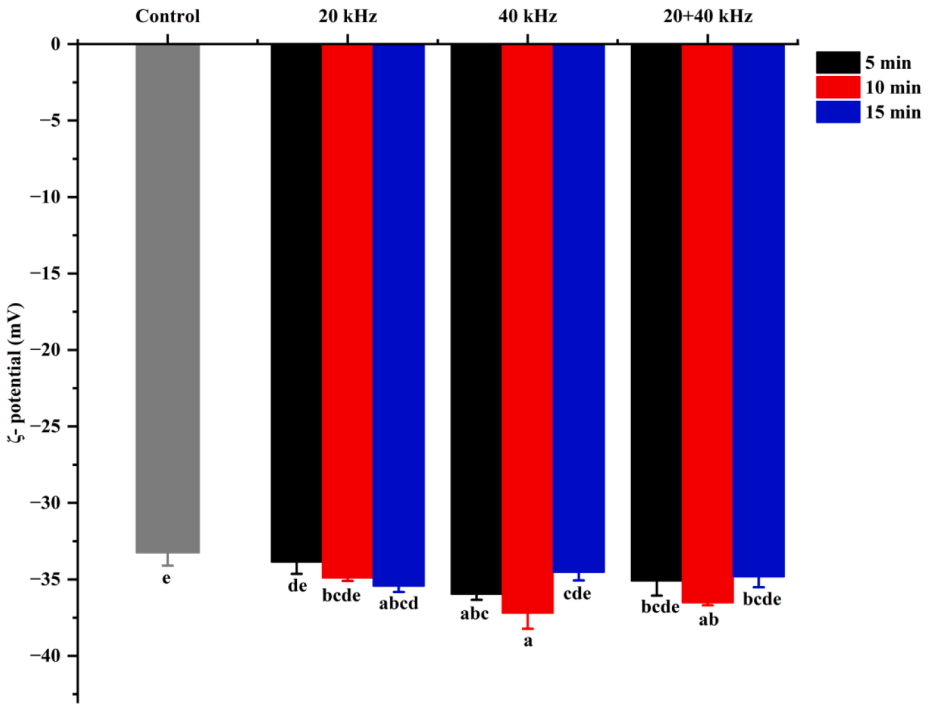



**Fig. 2.** ζ − potential of control and MFGs/MFGM prepared from ultrasonic-treated bovine milk. Different superscript letters mean the significant difference between samples ($p < 0.05$).

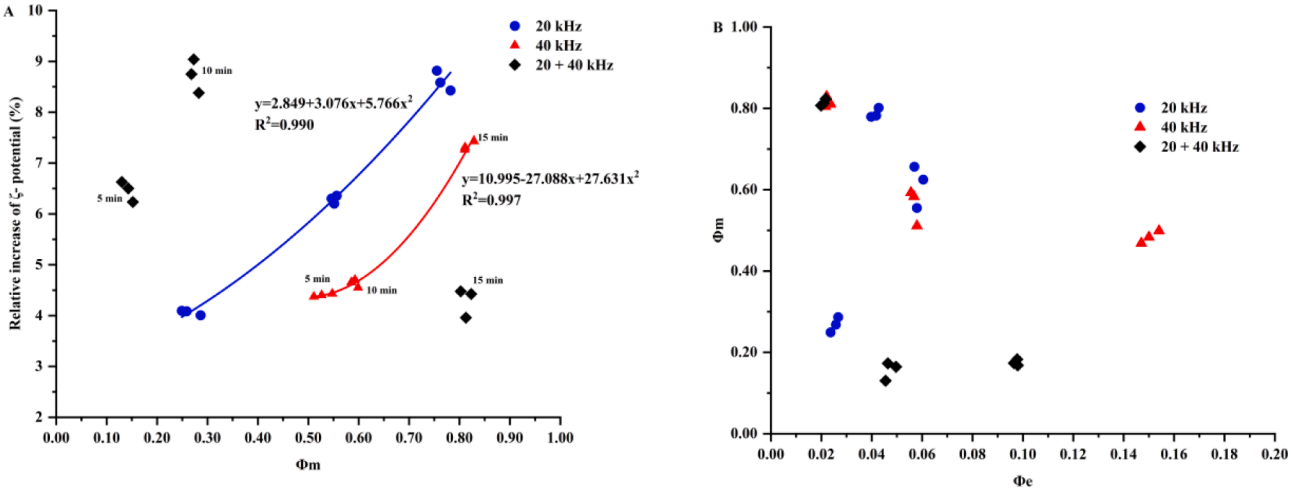



**Fig. 3.** The relative increase of ζ − potential ($\zeta_R$) for control and ultrasonic-treated samples as a function of measured surface fraction ($\Phi_m$) of MFGs/MFGM samples (A). Scatters of Φ values by Mastersizer measurement ($\Phi_m$) and the predictive model estimated ($\Phi_e$) (Eq. (4)) (B).

studies, $\zeta_R$ and $\Phi_m$ of MFGs followed a nonlinear trend after different mechanical treatments, including homogenisation, ultra-sonication, high-shear mixing [36], and pulsed electric field treatment [22]. According to the fitted curves, in 20 kHz and 40 Hz samples, $\zeta_R$ and $\Phi_m$ exhibited a positive correlation as the ultrasonic duration time was prolonged. However, it is worth noting that 20 + 40 kHz ultrasonicated samples with different duration times did not follow a nonlinear or linear correlation between the $\zeta_R$ and $\Phi_m$ (Fig. 3A). In 20 + 40 kHz treated samples, there was a significant increase in both $\zeta_R$ and $\Phi_m$ values for 10 min treated compared to 5 min duration samples ($p < 0.05$), whereas the 15 min samples displayed the lowest $\zeta_R$ and $\Phi_m$.

Previous researches proved a good correlation fitted by a quadratic regression model between the estimated $\Phi_e$ and the measured $\Phi_m$ with a co-efficient square ($R^2$) higher than 0.960 [22,36]. This finding indicates that $\zeta_R$ values can be used to predict the surface coverage fraction of MFGs/MFGM by plasma proteins. However, in our research, there was no statistical correlation for $\Phi_e$ versus measured $\Phi_m$ in terms of ultrasonic intensity and duration time (Fig. 3B). Factors attributed to the different results could be the acoustic power difference or the MFG sample preparation methods, which need to be verified in further investigation.

### 3.1.3. *Surface hydrophobicity ($H_0$)*

The change of the hydrophobic group has been used to reflect the protein structure change. ANS displayed high affinity to hydrophobic groups, which could be used to determine the exposed protein hydrophobic sites [37].

As shown in Fig. 4, different letters above each column mean the significant difference between samples resulting from ANOVA conducted on all the samples together. In comparison with control samples,

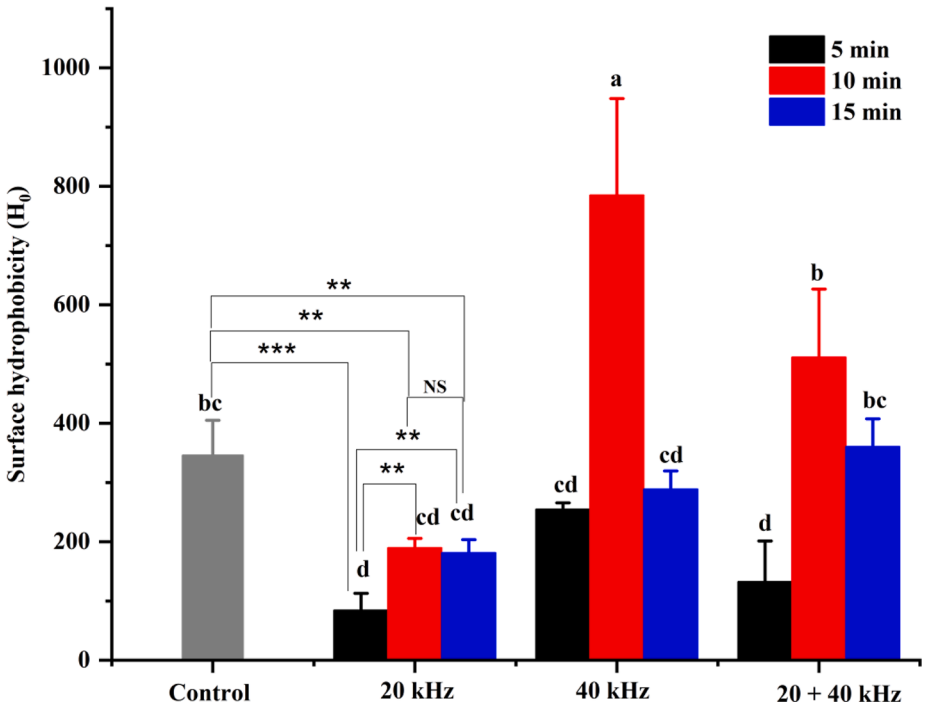



**Fig. 4.** Surface hydrophobicity ($H_0$) of control and MFGs/MFGM samples prepared from bovine milk treated by ultrasound at different intensities. Different superscript letters mean the significant difference between samples ($p < 0.05$). *, ** and *** represent $p < 0.05$, $p < 0.01$ and $p < 0.001$, respectively.

40 kHz with a duration of 10 min significantly increased $H_0$, while there was a significant decrease of $H_0$ for 20 kHz/ 5 min and 20 + 40 kHz/ 5 min samples ($p < 0.05$). Samples treated at other ultrasonic conditions showed insignificant differences from control samples ($p > 0.05$). Ultrasound may facilitate the exposure of hydrophobic protein domains or amino acid residues buried in the molecules and then induce the increase of $H_0$ in 40 kHz/ 10 min samples [37]. In addition, it was reported that the bigger size of particles improved the $H_0$, which was related to the higher contact area for the connection of hydrophobic domains with the ANS probe [38]. However, this theory was in contrast with the results in Fig. 1. A more extensive particle distribution ranging from 400 − 1000 μm was detected in the 20 + 40 kHz/ 10 min samples, which, however, displayed no significant difference of $H_0$ with control samples ($p > 0.05$).

To further compare the effect of ultrasonic frequency on the $H_0$, ANOVA was conducted between the 20 kHz and control groups and within the 20 kHz groups. Within the 20 kHz treated group, ultrasound with a duration of 10 min and 15 min resulted in a significantly higher $H_0$ than that of 5 min samples ($p < 0.01$). This result could be due to exposure of more hydrophobic regions as the treatment time was prolonged at 20 kHz. In addition, more hydrophobic groups were detected in control groups than in ultrasound at 20 kHz groups (Fig. 4). This may be because the higher ultrasonic acoustic power was produced at 20 kHz conditions (Table 1). The excessive mechanical shearing induced by the higher energy ultrasonic treatment may lead to the unfolding of protein molecules, which causes the extension of non-covalent bonds, masking the hydrophobic regions and preventing their reaction with the ANS probe [39]. Herein, compared with the control samples, $H_0$ did not change regularly with the ultrasonic intensities, duration time, or the acoustic powder.

### 3.1.4. *Interfacial tension (π)*

Interfacial tension (π) has been reported to indicate the dynamic information of molecule adsorption at the gas/ liquid and liquid/ liquid interfaces [23]. In this study, the effect of ultrasound treatments on the rearrangement of MFGs/MFGM interfacial compositions was investigated by comparatively analysing the π between the air and liquid droplets.

Fig. 5A showed that the π decreased as a function of time ($t^{0.5}$) irrespective of ultrasound intensity and durations, and there was a significant decrease in the decrease rate of π with time. This finding might be explained by the increase of electrostatic energy on the surface of MFGs/ MFGM droplets with the analysis time, which would prevent the further adsorption of protein [40]. In this study, the π values of all the samples ranged from 46.520 to 36.250 mN/ m, similar to the previous research on cream samples with different particle sizes [41].

In comparison with control samples, ultrasonic treatment significantly resulted in the decrease of π ($p < 0.05$). Meanwhile, as the ultrasonic duration was prolonged, a more profound decrease in π than control samples was observed with the same ultrasonic intensity. Comparatively, 40 kHz ultrasonic treatments decreased π less efficiently than the other frequencies, and at the end of the monitoring point (15 s), the π of 40 kHz/ 15 min treated samples was 38.890 mN/ m, which was 16.095 % lower than the control samples. By comparison, 20 kHz presented a more profound decrease in π, especially with 15 min treatment, which was 29.877 % lower than control. This result may be attributed to the higher energy intensity and output power of 20 kHz frequency than the other conditions (Table 1). It can be inferred that the intenser mechanical shearing facilitated the interfacial tension change of MFGs/ MFGM more efficiently.

The diffusion ($k_{diff}$), adsorption (penetration) ($k_a$), and rearrangement ($k_r$) rate of interfacial compositions in MFGs/MFGM were calculated by linear fitting of the curves plotted according to the Eq. (5) and Eq. (6), respectively (Table 4). The $k_{diff}$, $k_a$, and $k_r$ for control and 20 kHz/ 10 min samples were not included in Table 4 because π changed continuously during the whole analysis process, which made it impossible to do the linear fitting. The initial π value of control and 20 kHz/ 10 min in this research was 46.520 and 36.68 mN/ m. According to previous researches, $k_{diff}$ could not be appropriately detected by the pendant drop method if the $\pi > 10$ mN/ m because the diffusion step was too fast to be captured [23,42]. However, in this study, good linear fits for plots π versus $t^{0.5}$ were obtained for all the other samples except for control and 20 kHz/ 10 min samples. The π values of all samples at the beginning were between 32.990 and 45.505 mN/ m, which were well

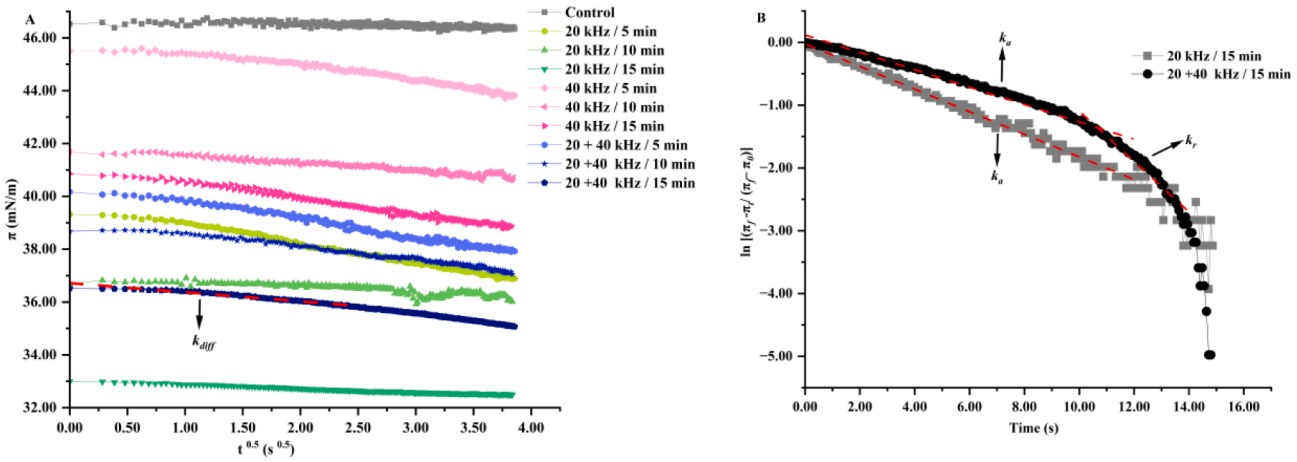



**Fig. 5.** (A) Interfacial tension (π) as a function of time ($t^{0.5}$) at the surface of sample droplets (control and samples treated at different ultrasonic intensities), $k_{diff}$ is the diffusion rate. (B) The profile rate of protein adsorption and rearrangement for 20 kHz/ 15 min and 20 + 40 kHz/ 15 min samples, $k_a$ and $k_r$ are the first-order rate of adsorption (penetration) and rearrangement, respectively.

**Table 4**
Diffusion ($k_{diff}$), adsorption ($k_a$) and rearrangement rate ($k_r$) of MFG/MFGM samples treated by ultrasound with different intensities.

| Samples | $k_{diff}$ | $R^2$ | $k_a$ | $R^2$ | $k_r$ | $R^2$ |
|---|---|---|---|---|---|---|
| Control | – | – | – | – | – | – |
| 20 kHz/ 5 min | −0.728 ± 0.004 $^{g}$ | 0.994 | −0.177 ± 0.002$^{b}$ | 0.982 | – | – |
| 20 kHz/ 10 min | – | – | – | – | – | – |
| 20 kHz/ 15 min | −0.139 ± 0.003$^{a}$ | 0.985 | −0.175 ± 0.002$^{b}$ | 0.989 | – | – |
| 40 kHz/ 5 min | −0.488 ± 0.008$^{d}$ | 0.960 | −0.121 ± 0.002$^{a}$ | 0.970 | – | – |
| 40 kHz/ 10 min | −0.562 ± 0.016$^{e}$ | 0.947 | −0.133 ± 0.003$^{a}$ | 0.937 | – | – |
| 40 kHz/ 15 min | −0.273 ± 0.006$^{b}$ | 0.950 | −0.191 ± 0.022$^{b}$ | 0.958 | – | – |
| 20 + 40 kHz/ 5 min | −0.679 ± 0.006$^{f}$ | 0.983 | −0.177 ± 0.003$^{b}$ | 0.968 | – | – |
| 20 + 40 kHz/ 10 min | −0.491 ± 0.005$^{d}$ | 0.981 | −0.131 ± 0.002$^{a}$ | 0.983 | – | – |
| 20 + 40 kHz/ 15 min | −0.443 ± 0.005$^{c}$ | 0.981 | −0.134 ± 0.001$^{a}$ | 0.979 | 0.551 ± 0.019 | 0.965 |

*Notes*: $k_{diff}$ is the initial diffusion rate calculated by liner fitting of the π versus $t^{0.5}$ plot.
$k_a$ and $k_r$ are the adsorption (penetration) and rearrangement rate, the slope obtained by linearly fitting the plot of ln $[(\pi_f - \pi_t/ (\pi_f - \pi_0)]$ versus time (s).
$R^2$ is the coefficient of determination (COD).
Different superscript letters in the same column indicate significant ($p < 0.05$) difference between samples.
'-' means not calculated.

above 10 mN/ m. The contradiction in these results could be due to the interfaces between different phases. The interfaces in current research refer to the contact surface of the air/water while the abovementioned reports investigated the interfaces between oil and water.

Regarding the effect of ultrasound frequency and duration on the $k_{diff}$, $k_a$, and $k_r$ of MFGs/MFGM, 40 kHz treated for 10 min promoted the protein diffusion more efficiently than 5 min at the same frequency. 20 kHz treatment with 5 min duration reduced the diffusion rate of MFGs/MFGM interfacial compositions more significantly compared with 20 kHz/ 15 min treatment ($p < 0.05$) but had no significant effect on the adsorption or penetration rate ($p > 0.05$). The increase in hydrophobicity has been reported to speed up the diffusion rate of whey protein at the oil–water interfaces [42]. This finding confirmed the hydrophobicity results in 3.3, which showed that 20 kHz/ 15 min displayed significantly higher $H_0$ than 20 kHz/ 5 min according to the ANOVA within the 20 Hz groups. Contrarily, $k_{diff}$ and $k_a$ results of samples synchronously treated by 20 kHz and 40 kHz treatment showed an opposite trend to the hydrophobicity results from 3.3. Apart from the hydrophobicity, protein conformation, molecular dimensions and electrostatic state could also affect the diffusion and adsorption rate of proteins at different interfaces [23,42].

Another interesting finding was that, during the adsorption or penetration step, only one linear region was fitted and $k_a$ was calculated for all samples. The $k_r$ of MFGs/MFGM interfacial compositions in all the samples could not be calculated by linear fitting the plot of ln $[(\pi_f - \pi_t/ (\pi_f - \pi_0)]$ versus time (s), except for 20 + 40 kHz/15 min samples (Fig. 5B). It may be because of the surface evaporation of sample droplets during the analysis. The mechanism behind this phenomenon is still unclear, and further research needs to be conducted to investigate.

### 3.2. The effect on ultrasonic treatments on the thermal behaviour of MFGs/MFGM

#### 3.2.1. XRD

XRD has been used to identify the polymorphic forms in milk fat by characterizing the crystal types measured by the d-spacing (Å) [43].

The spectra of XRD patterns for control and ultrasonicated samples with 5 min and 15 min durations were shown in Fig. 6A and 6B. No significant difference was detected between the 5 min and 10 min treated samples (data for 10 min treatment not shown) at the same ultrasonic intensity ($p > 0.05$). Fig. 6A showed that three typical crystals, α-crystal, β-form and β'-form, coexisted in the control and 20 kHz, 40 kHz and 20 + 40 kHz treated for 5 min samples. However, peaks for α-crystal disappeared as treatment time was prolonged to 15 min, while only β-form and β'-form were detected in all 15 min treated samples. In addition, ultrasound treatment did not shift the polymorphs position but only affected the intensity of the corresponding peaks (Fig. 6A and 6B). The identified polymorphs were relatively quantified by integrating the corresponding peak areas (Fig. 6C). In all cases, β' form was the major crystal, supported by previous researches which classified milk fat as β'-fat [8,44]. In comparison with control samples, 20 kHz or 20 kHz synchronized with 40 kHz treatment for 5 min significantly increased the α-crystal content and impeded the transition of metastable β'-crystals to stable β-form. Limited change was detected for the peak area of α-crystals in 40 kHz/ 5 min samples than in control samples, which may be related to an unobvious effect induced by the lower acoustic power (*P*) at 40 kHz/ 5 min condition.

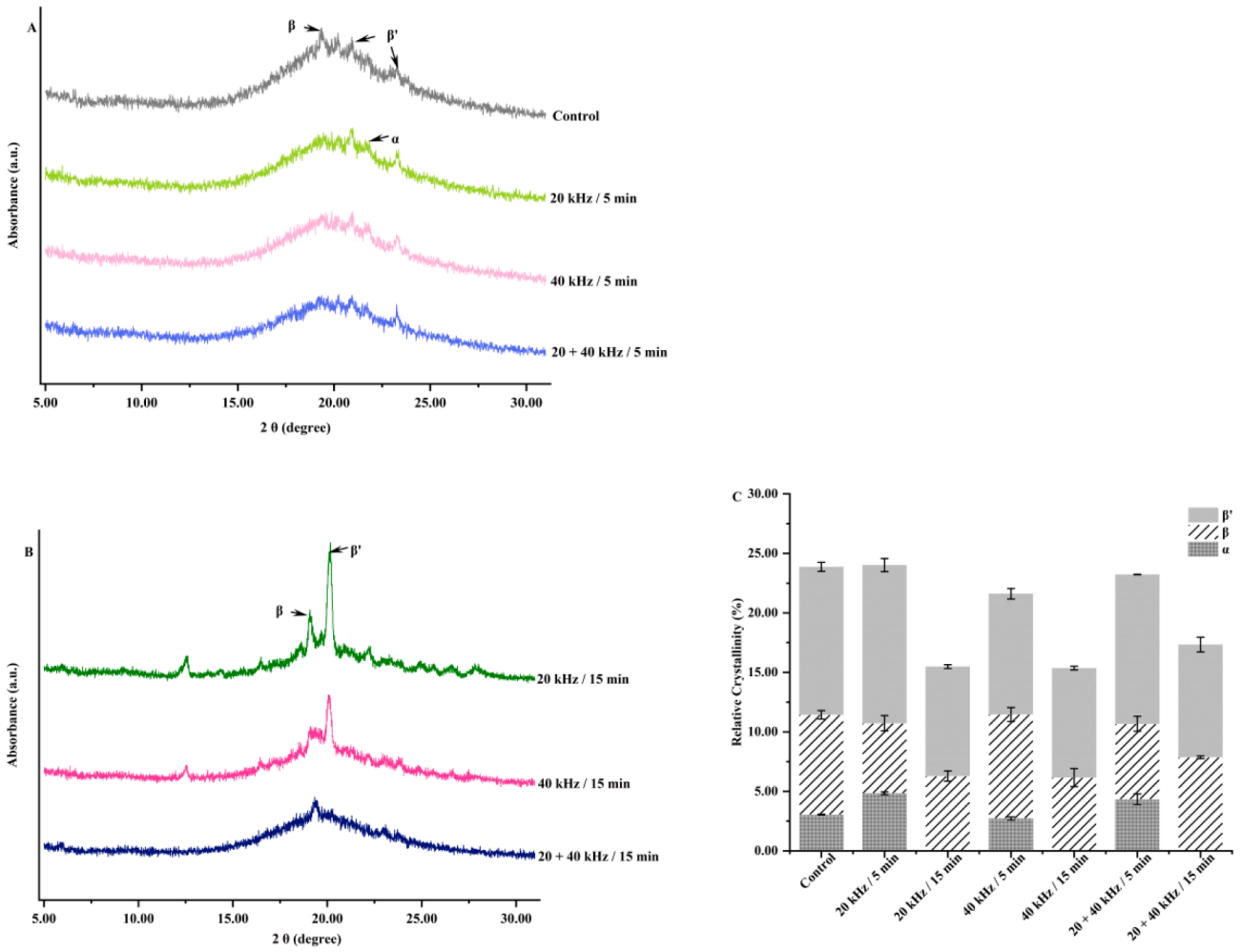



**Fig. 6.** X-ray spectra of control and ultrasonic-treated 5 min samples (A) and 15 min duration MFGs/MFGM samples (B); (C) relative crystallinity of α, β, and β' crystals in MFGs/MFGM samples.

It appears from Fig. 6C that prolonged ultrasonic time decreased the β'-forms more profoundly than the increase in ultrasonic intensity. Especially in the 40 kHz/ 15 min samples, only 9.21 % of β'-form was detected, which was 26.01 % less than that in control samples. However, treatment at 40 kHz for 5 min resulted in 18.41 % less β'-crystals than control samples. 15 min duration at all ultrasound intensity significantly promoted the transition of unstable α-forms into the metastable β'-crystals. Of these, treatments of 20 kHz/ 15 min and 40 kHz/ 15 min were the most efficient in facilitating the formation of stable β-form polymorphs in the MFGs/ MFGM; however, in which the major polymorph was still β'-form. This finding was supported by previous studies on MFG samples treated with different homogenised pressures [8]. 20 kHz/5 min samples contained the least amount of stable β-form polymorphs than the other samples; meanwhile, from the abovementioned results in 3.1, a higher percentage of MFGs/MFGM particles in 20 kHz/ 5 min presented in the lower particle size range (Fig. 1A). This finding is inconsistent with the research reporting that smaller MFGs constrained the formation of larger sized β-polymorphs on the surface of droplets [45].

The type of fat crystals plays an important role in the application of milk fat. In this research, 40 kHz treated MFGs/MFMG samples contained the most β crystals, while more β'-crystals were detected in 20 kHz/ 5 min treated samples. It was reported that β crystals with large sizes and higher melting temperatures are suitable for hard consistency texture application, while β'-crystals help improve the spreadability of fat by forming a fine crystal network [46].

### 3.2.2. DSC

The crystallization and melting thermograms of MFGs/MFGM samples prepared from the control and ultrasonic bovine milk are shown in Figs. 7 and 8, respectively.

According to Fig. 7 (A-D), two crystallization peaks were detected in all samples at approximate values of 10.50 ℃ ($T_{C1}$) and 14.00 ℃ ($T_{C2}$). There was no significant difference between the $T_{C1}$ and $T_{C2}$ of all samples ($p < 0.05$). Comparatively, except for the peaks at $T_{C1}$ and $T_{C2}$, one or two new exothermic events appeared in the range of 17.29 – 18.81 ℃ ($T_{C3}$) and 22.14 – 25.21 ℃ ($T_{C4}$) in ultrasonicated samples but not in control samples. In other words, the ultrasonic treatment improved the crystallisation of MFGs/MFGM at a higher temperature, supported by Martini, Suzuki, and Hartel [15]. This result may be because cavitation generated by the ultrasound facilitated the nucleation [47]. Only a slight difference was observed for the $T_{C3}$ and $T_{C4}$ in ultrasonicated MFGs/MFGM samples. The 20 + 40 kHz/ 15 min treatment promoted the crystallization more efficiently than other treatments because of the significantly higher $T_{C4}$ (Table 5).

Ultrasonic treatments induced the decrease of $\Delta H_C$ (J/g) in MFGs/ MFGM samples in different degrees compared with the control samples. There was a decrease in the $\Delta H_C$ (J/g) of MFGs/MFGM samples as the treating time was prolonged at the same ultrasonic intensity. 15 min ultrasonicated MFGs/MFGM samples at different intensities of 20 kHz, 40 kHz, or 20 + 40 kHz showed no significant difference in $\Delta H_C$ (J/g) (Table 5). This finding indicated that ultrasonic duration time presented a more profound effect on the decrease of $\Delta H_C$ (J/g) than the intensity.

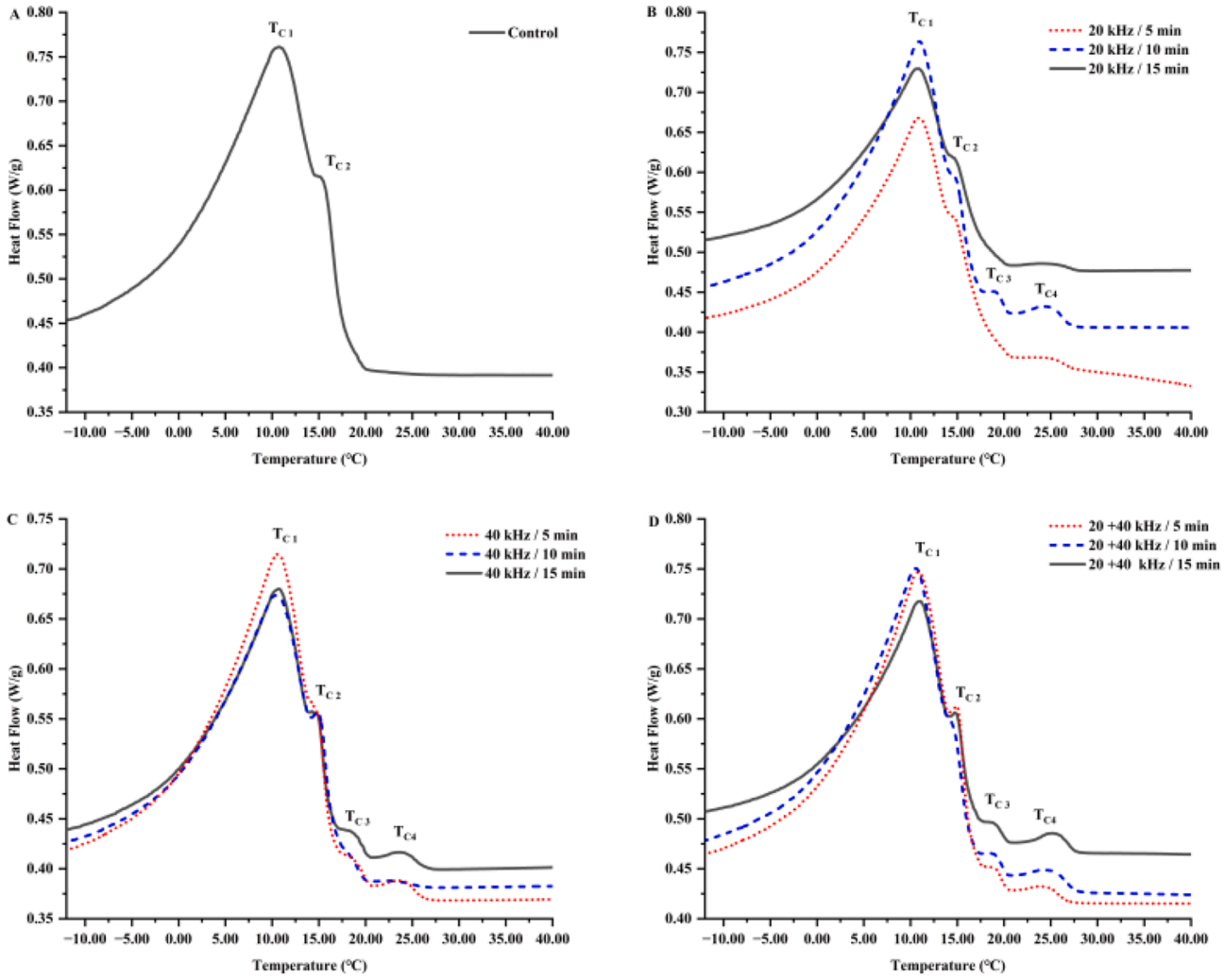



**Fig. 7.** DSC crystallization thermograms of MFGs/MFGM samples separated from the control and ultrasonic-treated bovine milk, $T_{C1}$-$T_{C4}$ are crystallization temperatures.

In agreement with the previous researches, three melting peaks were detected in control sample at 10.23 ± 0.19 ℃, 18.08 ± 0.07℃ and 34.10 ± 0.84℃, which indicated the existence of low-melting fraction (LMF) ($T_{M1}$), medium-melting fraction (MMF) ($T_{M2}$) and high-melting fraction (HMF) ($T_{M3}$) (Fig. 8 A) [29,47]. However, LMF peaks disappeared in all ultrasonicated samples, while only the MMF and HMF peaks were observed (Fig. 8 B-D). Table 5 showed no significant difference of $T_{M2}$ and $T_{M3}$ between control and ultrasonic samples. Furthermore, different ultrasonic intensities and duration times did not affect the melting temperature of all MFGs/MFGM samples. This result was supported by the previous finding on the butter produced from thermos-sonicated cream (20 kHz, 85 ℃ with the duration of 5, 10, and 15 min) [47]. However, Sergeev et al. (2021) reported that melting peaks in anhydrous fat prepared from goat milk presented unimodal distribution after the ultrasonic treatment with operating frequency at 45 kHz and output power of 12.30 ± 1.8 W for 120 s [29]. It can be inferred that the crystal formation and melting may have happened during the MFGs/MFGM samples preparation stage, which may not be observed during the DSC process.

Within the same ultrasonic frequency group, $\Delta H_M$ values of all the ultrasonicated 15 min samples decreased significantly compared to the 5 min and 10 min duration treatments except for 20 kHz groups ($p < 0.05$). This result was similar to the results on $\Delta H_C$. In other words, less enthalpy was needed to melt the fat crystals in 15 min ultrasonicated samples than for 5 min and 10 min samples. This finding confirmed the results on the XRD in which more unstable and metastable β' were detected in the 15 min ultrasonicated samples than the amount of stale β crystals. Less energy was needed for the deformation and melting of metastable β' than stable β crystal. However, this differed from the study on the butter, which displayed an increase of the energy required to melt after thermos-sonication (20 kHz, 85 ℃ for 10 min) [48].

## 4. Conclusion

In this study, different acoustic powers generated by the 20 kHz and 40 kHz, independently or synchronously working conditions have been shown to affect the interfacial properties and thermal behaviour of MFGs/MFGM samples.

20 kHz treatments led to a relatively even particle distribution in MFGs/MFGM than 40 kHz and 20 + 40 kHz treated samples. The relative ζ − potential ($\zeta_R$) could not be used to predict the surface change of MFGs/MFGM after ultrasonic treatments because there was no statistical correlation between the estimated ($\Phi_e$) and the measured surface fraction ($\Phi_m$). Ultrasound treatment significantly resulted in the decrease of π in all samples ($p < 0.05$). Three typical crystal forms, α-crystal, β-form, and β'-form, were observed in control and ultrasonicated 5 min samples, but α-crystal disappeared in all the 15 min treated samples. Ultrasonic duration has a more profound effect on the increase of β'- crystal than the intensity. Ultrasonic treatments promoted the crystallisation of MFGs/MFGM fat at higher temperature but

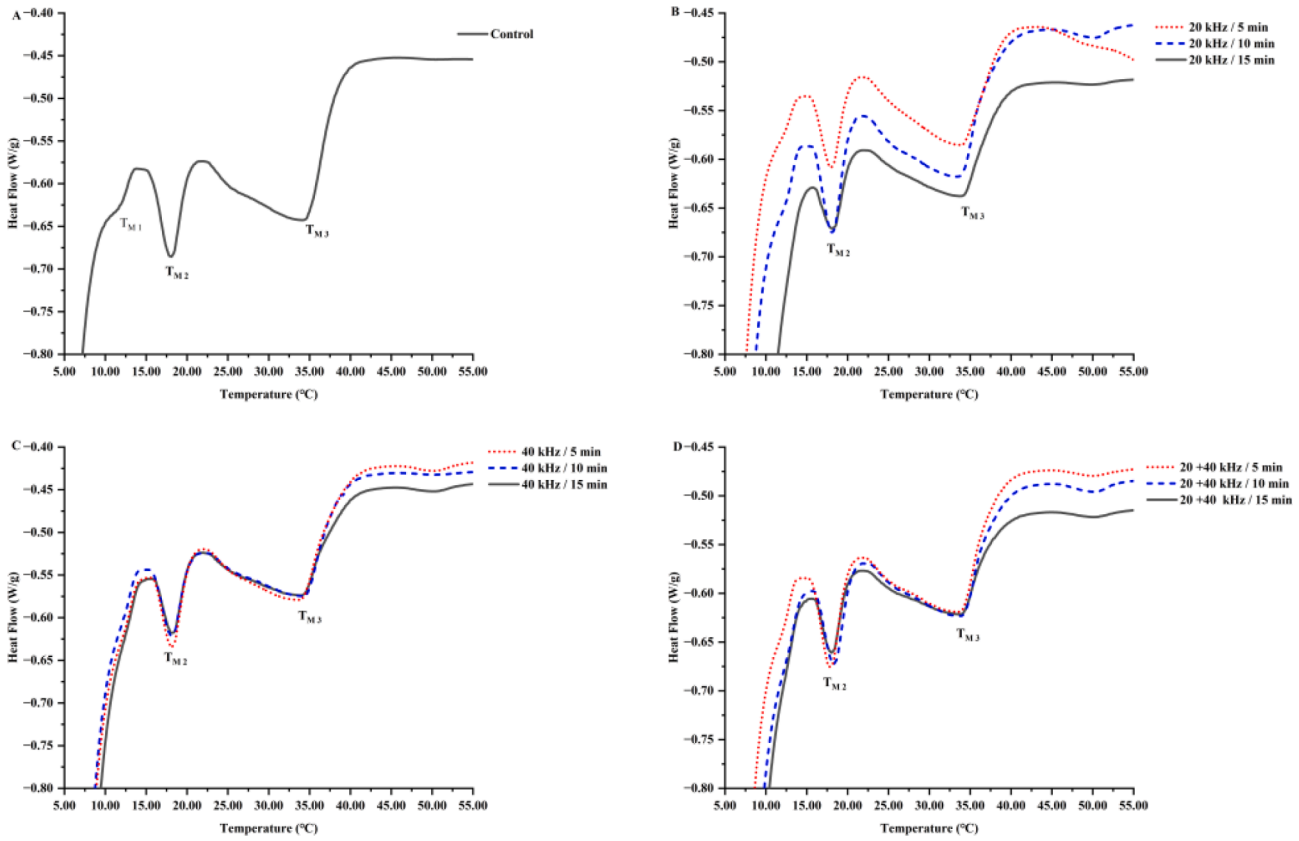



**Fig. 8.** DSC melting thermograms of MFGs/MFGM samples separated from the control and ultrasonic-treated bovine milk, $T_{M1}$-$T_{M3}$ are melting temperatures.

**Table 5**
Characteristic enthalpy, crystallization and melting temperature of MFGs/MFGM separated from bovine milk with and without ultrasonic treatment.

| | Crystallization | | | | | Melting | | | |
|---|---|---|---|---|---|---|---|---|---|
| | $T_{C1}$ (°C) | $T_{C2}$ (°C) | $T_{C3}$ (°C) | $T_{C4}$ (°C) | $\Delta H_C$ (J/g) | $T_{M1}$(°C) | $T_{M2}$(°C) | $T_{M3}$(°C) | $\Delta H_M$(J/g) |
| Control | $10.73 \pm 0.07^{ns}$ | $14.58 \pm 0.49^{ns}$ | – | – | $5.53 \pm 0.72^{ab}$ | $10.23 \pm 0.19$ | $18.08 \pm 0.07^{ns}$ | $34.10 \pm 0.84^{ns}$ | $3.34 \pm 0.02^{a}$ |
| 20 kHz/ 5 min | $10.86 \pm 0.84$ | $14.10 \pm 0.52$ | – | $23.37 \pm 0.44^{bc}$ | $5.63 \pm 0.97^{a}$ | – | $18.01 \pm 0.11$ | $33.82 \pm 0.38$ | $1.96 \pm 0.76^{b}$ |
| 20 kHz/ 10 min | $10.98 \pm 0.59$ | $13.94 \pm 008$ | $18.81 \pm 0.77^{a}$ | $24.26 \pm 0.25^{ab}$ | $4.79 \pm 0.66^{abc}$ | – | $18.09 \pm 0.46$ | $33.45 \pm 0.06$ | $2.41 \pm 0.35^{ab}$ |
| 20 kHz/ 15 min | $10.87 \pm 0.96$ | $14.18 \pm 0.35$ | – | $23.90 \pm 0.06^{ab}$ | $3.51 \pm 0.05^{c}$ | – | $18.08 \pm 0.07$ | $34.10 \pm 0.84$ | $1.94 \pm 0.44^{b}$ |
| 40 kHz/ 5 min | $10.52 \pm 0.05$ | $13.97 \pm 0.44$ | $17.28 \pm 0.52^{c}$ | $23.35 \pm 0.98^{bc}$ | $4.85 \pm 0.44^{abc}$ | – | $18.08 \pm 0.97$ | $33.55 \pm 0.81$ | $2.68 \pm 0.08^{ab}$ |
| 40 kHz/ 10 min | $10.44 \pm 0.19$ | $14.77 \pm 0.78$ | $17.29 \pm 0.51^{bc}$ | $22.14 \pm 0.28^{c}$ | $4.21 \pm 0.16^{abc}$ | – | $18.07 \pm 0.03$ | $34.13 \pm 0.22$ | $2.38 \pm 0.03^{ab}$ |
| 40 kHz/ 15 min | $10.68 \pm 0.29$ | $14.25 \pm 0.26$ | $17.29 \pm 0.25^{bc}$ | $23.53 \pm 0.36^{bc}$ | $3.88 \pm 0.99^{bc}$ | – | $18.09 \pm 0.19$ | $33.92 \pm 0.76$ | $2.29 \pm 0.44^{b}$ |
| 20 + 40 kHz/ 5 min | $10.79 \pm 0.34$ | $14.88 \pm 0.76$ | $17.62 \pm 0.38^{abc}$ | $23.71 \pm 0.84^{b}$ | $4.56 \pm 0.29^{abc}$ | – | $17.89 \pm 0.16$ | $33.52 \pm 0.15$ | $2.47 \pm 0.13^{ab}$ |
| 20 + 40 kHz/ 10 min | $10.54 \pm 0.97$ | $13.89 \pm 0.85$ | $18.57 \pm 0.06^{ab}$ | $24.22 \pm 0.04^{ab}$ | $4.58 \pm 0.52^{abc}$ | – | $18.31 \pm 0.91$ | $33.75 \pm 0.48$ | $2.47 \pm 0.24^{ab}$ |
| 20 + 40 kHz/ 15 min | $11.05 \pm 0.97$ | $14.72 \pm 0.65$ | $17.63 \pm 0.38^{abc}$ | $25.21 \pm 0.49^{a}$ | $3.48 \pm 0.34^{c}$ | – | $18.04 \pm 0.07$ | $33.71 \pm 0.52$ | $1.92 \pm 0.04^{b}$ |

*Notes*: Asbbreviations are: $T_{C1} - T_{C4}$, the temperature of crystallisation peaks, $\Delta H_C$, enthalpy of crystallisation; $T_{M1} - T_{M4}$, the temperature of melting peaks, $\Delta H_M$, enthalpy of melting.
Different superscript letters in the same column indicate significant ($p < 0.05$) differences between samples. 'ns' means no significant difference ($p > 0.05$).

increased the melting temperature of MFGs/MFGM.

In summary, interfacial properties and thermal behaviour of MFGs/MFGM samples were affected by ultrasonic treatments, which, however, did not display a consistent correlation with the ultrasonic acoustic energy. MFGs/MFGM is a complicated mixture. Therefore, specific ultrasonic conditions should be optimised according to the different functionalities and applications.

## CRediT authorship contribution statement

**Yanjun Sun:** Conceptualization, Data curation, Forma analysis, Investigation, Writing – original draft.. **Yrjö H. Roos:** Writing – review & editing, Supervision. **Song Miao:** Funding acquisition, Project administration, Conceptualization, Supervision, Writing – review & editing.

## Declaration of competing interest

The authors declare that they have no known competing financial interests or personal relationships that could have appeared to influence the work reported in this paper.

## Acknowledgements

The project was supported by 'The Open Project Program of State Key Laboratory of Dairy Biotechnology (No. SKLDB2022–007)', Teagasc-The Irish Agriculture and Food Development Authority (MDDT1392) and 'The China Scholarship Council (No.202008410212)'.

## Appendix A. Supplementary data

Supplementary data to this article can be found online at https://doi.org/10.1016/j.ultsonch.2024.106755.

## References

[1] A. Nieto-Ruiz, J.A. Garcia-Santos, J. Verdejo-Roman, E. Dieguez, N. Sepulveda-Valbuena, F. Herrmann, T. Cerdo, R. De-Castellar, J. Jimenez, M.G. Bermudez, M. Perez-Garcia, M.T. Miranda, M.C. Lopez-Sabater, A. Catena, C. Campoy, Infant Formula Supplemented With Milk Fat Globule Membrane, Long-Chain Polyunsaturated Fatty Acids, and Synbiotics Is Associated With Neurocognitive Function and Brain Structure of Healthy Children Aged 6 Years: The COGNIS Study, Front Nutr 9 (2022) 820224.
[2] B. Jiang, Y. Xia, L. Zhou, X. Liang, X. Chen, M. Chen, X. Li, S. Lin, N. Zhang, L. Zheng, M. Tao, P. Petocz, S. Gallier, A. Rowan, B. Wang, Safety and Tolerance Assessment of Milk Fat Globule Membrane- enriched Infant Formulas in Healthy Term Chinese Infants: A Randomised Multicenter Controlled Trial, BMC Pediatr. 22 (2022) 465.
[3] Y. Pan, L. Liu, S. Tian, X. Li, M. Hussain, C. Li, L. Zhang, Q. Zhang, Y. Leng, S. Jiang, S. Liang, Comparative analysis of interfacial composition and structure of fat globules in human milk and infant formulas, Food Hydrocoll. 124 (2022) 107290.
[4] A. Garczewska-Murzyn, K. Kielczewska, M. Smoczyński, The influence of buttermilk powder on the stability of emulsion and colloidal phases of homogenized milk, Eur. Food Res. Technol. 248 (2022) 2629–2636.
[5] J. Saxena, B. Adhikari, R. Brkljaca, T. Huppertz, J. Chandrapala, B. Zisu, Inter-relationship between lactose crystallization and surface free fat during storage of infant formula, Food Chem 322 (2020) 126636.
[6] R.S. Reddy, C.T. Ramachandra, S. Hiregoudar, U. Nidoni, J. Ram, M. Kammar, Influence of processing conditions on functional and reconstitution properties of milk powder made from Osmanabadi goat milk by spray drying, Small Rumin. Res. 119 (2014) 130–137.
[7] Y. Fang, S. Rogers, C. Selomulya, X.D. Chen, Functionality of milk protein concentrate: Effect of spray drying temperature, Biochem. Eng. J. 62 (2012) 101–105.
[8] Q. Ren, Q. Li, H. Liu, Y. Ma, Thermal and storage properties of milk fat globules treated with different homogenisation pressures, Int. Dairy J. 110 (2020) 104725.
[9] Q. Ren, L. Li, O.E. Dudu, Y. Ma, Thermal and structural changes of pasteurized milk fat globules during storage, Food, Bioscience 28 (2019) 27–35.
[10] R.K. Bhaskaracharya, S. Kentish, M. Ashokkumar, Selected Applications of Ultrasonics in Food Processing, Food Eng. Rev. 1 (2009) 31–49.
[11] O. Krasulya, V. Bogush, V. Trishina, I. Potoroko, S. Khmelev, P. Sivashanmugam, S. Anandan, Impact of acoustic cavitation on food emulsions, Ultrason Sonochem 30 (2016) 98–102.
[12] T. Leong, L. Johansson, P. Juliano, R. Mawson, S. McArthur, R. Manasseh, Design parameters for the separation of fat from natural whole milk in an ultrasonic litre-scale vessel, Ultrason Sonochem 21 (2014) 1289–1298.
[13] P. Juliano, A. Kutter, L.J. Cheng, P. Swiergon, R. Mawson, M.A. Augustin, Enhanced creaming of milk fat globules in milk emulsions by the application of ultrasound and detection by means of optical methods, Ultrason Sonochem 18 (2011) 963–973.
[14] T. Leong, P. Juliano, L. Johansson, R. Mawson, S.L. McArthur, R. Manasseh, Temperature effects on the ultrasonic separation of fat from natural whole milk, Ultrason Sonochem 21 (2014) 2092–2098.
[15] S. Martini, A.H. Suzuki, R.W. Hartel, Effect of High Intensity Ultrasound on Crystallization Behavior of Anhydrous Milk Fat, J. Am. Oil Chem. Soc. 85 (2008) 621–628.
[16] Y. Liu, S. Boeren, L. Zhang, P. Zhou, K. Hettinga, Ultrasonication retains more milk fat globule membrane proteins compared to equivalent shear-homogenization, Innov. Food Sci. Emerg. Technol. 70 (2021) 102703.
[17] X. Zhao, X. Fan, X. Shao, M. Cheng, C. Wang, H. Jiang, X. Zhang, C. Yuan, Modifying the physicochemical properties, solubility and foaming capacity of milk proteins by ultrasound-assisted alkaline pH-shifting treatment, Ultrason Sonochem 88 (2022) 106089.
[18] S. Yanjun, C. Jianhang, Z. Shuwen, L. Hongjuan, L. Jing, L. Lu, H. Uluko, S. Yanling, C. Wenming, G. Wupeng, L. Jiaping, Effect of power ultrasound pre-treatment on the physical and functional properties of reconstituted milk protein concentrate, J. Food Eng. 124 (2014) 11–18.
[19] A. Zamora, V. Ferragut, B. Guamis, A.J. Trujillo, Changes in the surface protein of the fat globules during ultra-high pressure homogenisation and conventional treatments of milk, Food Hydrocoll. 29 (2012) 135–143.
[20] Y. Huang, T. Wei, F. Chen, C. Tan, Z. Gong, F. Wang, Z. Deng, J. Li, Effects of various thermal treatments on interfacial composition and physical properties of bovine milk fat globules, Food Res. Int. 167 (2023) 112580.
[21] Y. Sun, Y.H. Roos, S. Miao, Changes in Milk Fat Globules and Membrane Proteins Prepared from pH-Adjusted Bovine Raw Milk, Foods 11 (2022) 4107.
[22] P. Sharma, I. Oey, D.W. Everett, Interfacial properties and transmission electron microscopy revealing damage to the milk fat globule system after pulsed electric field treatment, Food Hydrocoll. 47 (2015) 99–107.
[23] L. Seta, N. Baldino, D. Gabriele, F.R. Lupi, B. de Cindio, The effect of surfactant type on the rheology of ovalbumin layers at the air/water and oil/water interfaces, Food Hydrocoll. 29 (2012) 247–257.
[24] D.E. Graham, M.C. Phillips, Proteins at liquid interfaces: III. Molecular structures of adsorbed films, J. Colloid Interface Sci. 70 (1979) 427–439.
[25] N.A. Camino, O.E. Pérez, C.C. Sanchez, J.M. Rodriguez Patino, A.M.R. Pilosof, Hydroxypropylmethylcellulose surface activity at equilibrium and adsorption dynamics at the air–water and oil–water interfaces, Food Hydrocoll. 23 (2009) 2359–2368.
[26] A. Logan, C. Lopez, M. Xu, L. Day, S. Oiseth, M.A. Augustin, Tempering governs the milk fat crystallisation and viscoelastic behaviour of unprocessed and homogenised creams, Food Res Int 147 (2021) 110557.
[27] C. Lopez, K. Cheng, J. Perez, Thermotropic phase behavior of milk sphingomyelin and role of cholesterol in the formation of the liquid ordered phase examined using SR-XRD and DSC, Chem Phys Lipids 215 (2018) 46–55.
[28] A. Lambert, F. Bougrioua, O. Abbas, M. Courty, M. El Marssi, V. Faivre, S. Bresson, Temperature dependent Raman and X-ray diffraction studies of anhydrous milk fat, Food Chem 267 (2018) 187–195.
[29] A. Sergeev, N. Shilkina, M. Motyakin, I. Barashkova, V. Zaborova, K. Kanina, N. Dunchenko, O. Krasulya, N.S.M. Yusof, Anhydrous fat crystallization of ultrasonic treated goat milk: DSC and NMR relaxation studies, Ultrason. Sonochem. 78 (2021) 105751.
[30] Q. Ren, F. Guo, F. Teng, Y. Ma, A novel approach for the reconstitution of bovine milk fat globules with different-melting-temperature triacylglycerol cores, Food Chem 345 (2021) 128563.
[31] Y. Sun, X. Yu, M. Hussain, X. Li, L. Liu, Y. Liu, S. Ma, K.J.E. Kouame, C. Li, Y. Leng, S. Jiang, Influence of milk fat globule membrane and milk protein concentrate treated by ultrasound on the structural and emulsifying stability of mimicking human fat emulsions, Ultrason. Sonochem. 82 (2022) 105881.
[32] A. Jukkola, R. Partanen, O.J. Rojas, A. Heino, Separation of milk fat globules via microfiltration: Effect of diafiltration media and opportunities for stream valorization, J Dairy Sci 99 (2016) 8644–8654.
[33] G.G. Kurup, B. Adhikari, B. Zisu, Application of high-frequency ultrasound standing waves for the recovery of lipids from high-fat dairy effluent, Ultrason Sonochem 63 (2020) 104944.
[34] H. Scudino, E.K. Silva, A. Gomes, J.T. Guimaraes, R.L. Cunha, A.S. Sant'Ana, M.A. A. Meireles, A.G. Cruz, Ultrasound stabilization of raw milk: Microbial and enzymatic inactivation, physicochemical properties and kinetic stability, Ultrason Sonochem 67 (2020) 105185.
[35] Membrane Properties Affect the Viscoelasticity of Milk Gels, M.C. Michalski, R. Cariou, F. Michel, C. Garnier, Native vs. Damaged Milk Fat Globules, J. Dairy Sci. 85 (2002) 2451–2461.
[36] F.o.M. Marie-Caroline Michalski , Damien Sainmont,, V.r. Briard, Apparent -potential as a tool to assess mechanical damages to the milk fat globule membrane, Colloids and Surfaces B: Biointerfaces 23, 23 (2001) 23–30.
[37] Y. Meng, Z. Liang, C. Zhang, S. Hao, H. Han, P. Du, A. Li, H. Shao, C. Li, L. Liu, Ultrasonic modification of whey protein isolate: Implications for the structural and functional properties, Lwt 152 (2021).
[38] B. Song, P. Yao, Y. Zhang, X. Pang, S. Zhang, J. Lv, Ultrasound pretreatment prior to spray drying improve the flowability and water sorption properties of micellar casein concentrate, Ultrason Sonochem 87 (2022) 106049.
[39] A.B. Tomé Constantino, E.E. Garcia-Rojas, Modifications of physicochemical and functional properties of amaranth protein isolate (Amaranthus cruentus BRS Alegria) treated with high-intensity ultrasound, J. Cereal Sci. 95 (2020).
[40] H. Li, P. Van der Meeren, Sequential adsorption of whey proteins and low methoxy pectin at the oil-water interface: An interfacial rheology study, Food Hydrocoll. 128 (2022) 107570.
[41] T.M. Ho, P. Dhungana, B. Bhandari, N. Bansal, Effect of the native fat globule size on foaming properties and foam structure of milk, J. Food Eng. 291 (2021) 110227.
[42] B. Zhou, J.T. Tobin, S. Drusch, S.A. Hogan, Dynamic adsorption and interfacial rheology of whey protein isolate at oil-water interfaces: Effects of protein concentration, pH and heat treatment, Food Hydrocoll. 116 (2021).
[43] E. ten Grotenhuis, G.A. van Aken, K.F. van Malssen, H. Schenk, Polymorphism of milk fat studied by differential scanning calorimetry and real-time X-ray powder diffraction, Journal of the American Oil Chemists' Society 76 (1999) 1031–1039.
[44] A. Wright, A. Marangoni, in: Crystallization and Rheological Properties of Milk Fat, in: P.l.h.m.e.a.d.c.p, Advanced Dairy Chemistry Springer, Boston, 2006, pp. 245–291.
[45] C. Lopez, C. Bourgaux, P. Lesieur, S. Bernadou, G. Keller, M. Ollivon, Thermal and Structural Behavior of Milk Fat, J. Colloid Interface Sci. 254 (2002) 64–78.

[46] J.F. Toro-Vazquez, M. Briceño-Montelongo, E. Dibildox-Alvarado, M. Charó-Alonso, J. Reyes-Hernández, Crystallization kinetics of palm stearin in blends with sesame seed oil, J. Am. Oil Chem. Soc. 77 (2000) 297–310.

[47] D. Sert, E. Mercan, Characterisation of physicochemical, microbiological, thermal, oxidation properties and fatty acid composition of butter produced from thermosonicated cream, Int. Dairy J. 109 (2020) 104777.

[48] P. Buldo, J.J.K. Kirkensgaard, L. Wiking, Crystallization mechanisms in cream during ripening and initial butter churning, J Dairy Sci 96 (2013) 6782–6791.

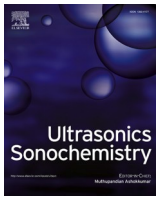
Ultrasonics Sonochemistry 111 (2024) 107058



Contents lists available at ScienceDirect

Ultrasonics Sonochemistry

journal homepage: www.elsevier.com/locate/ultson



# Modifying physicochemical properties, rheology, and creaming stability of milk fat globule and membrane through ultrasound treatment

Yanjun Sun [a,b], Yrjö H. Roos [b], Song Miao [a,c,*]

[a] Teagasc Food Research Centre, Moorepark, Fermoy, Co. Cork, Ireland
[b] School of Food and Nutritional Sciences, University College Cork, Cork, Ireland
[c] China-Ireland International Cooperation Centre for Food Material Sciences and Structure Design, Fujian Agriculture and Forestry University, China

ARTICLE INFO

*Keywords:*
Milk fat globules
Ultrasonic treatment
FTIR
Rheological property
Physical instability

ABSTRACT

The healthy benefits of milk fat globules and membrane (MFGs/MFGM) ingredients are increasingly recognized in the dairy industry. In this research, we examined the effects of ultrasonic treatment on the physicochemical and rheological properties, as well as the emulsions stability of MFGs/MFGM derived from bovine raw milk. Fresh milk was subjected to sonication at frequencies of 20 kHz and 40 kHz, either individually or simultaneously, for durations of 5 min or 15 min, using work/rest cycles of 5 s on and 3 s off. Bovine milk, without any treatment, served as the control. Regardless of the intensity difference, ultrasonic treatment for 5 min resulted in more pronounced changes in the regions of Amide II (1600–1500 $cm^{-1}$), Amide III (1500–1200 $cm^{-1}$), and fingerprint region (1200–1900 $cm^{-1}$) compared to both the 15 min treatments and control MFGs/MFGM. Principal component analysis (PCA) conducted on the entire spectra, as well as in the regions of Amide I, Amide II, and the fingerprint spectra, clustered the 5 min treatment distinctly from the control and MFGs/MFGM ultrasonically treated for 15 min. MFGs/MFGM samples following 20 kHz and 40 kHz synchronous treatment for 15 min exhibited lower absorbance bands at 1727–1726 $cm^{-1}$, whereas a higher content at 1740 $cm^{-1}$ was observed compared to control MFGs/MFGM. Additionally, a more significant reduction in the intramolecular β-sheet content in 20 + 40 kHz/ 15 min treatment was observed. According to the sodium dodecyl sulphate polyacrylamide gel electrophoresis (SDS-PAGE) patterns, a diminished intensity of Periodic Acid Schiff 6/7 (PAS 6/7) bands was observed across all the MFGs/MFGM. Ultrasonic treatment retained more caseins while reducing the β –LG levels compared to the controls, enhancing the stability of MFGs/MFGM, except in MFGs/ MFGM subjected to 20 and 40 kHz simultaneously treated for 15 min. The irregular sphericity of fat globules was noted particularly in MFGs/MFGM treated at 20 kHz independently or in combination with 40 kHz for 15 min. According to the confocal laser scanning microscopy (CLSM), ultrasonic treatment facilitated the binding of caseins or whey proteins to the MFGs surface and induced flocculation of membrane proteins. Hierarchical cluster analysis (HCA) heat map further underscored the impact of ultrasonic treatments on the structural and compositional changes, as well as rheology and emulsions stability, of MFGs/MFGM.

## 1. Introduction

Milk fat primarily exists in the form of globules (MFGs) characterized by a core of triacylglycerol enveloped by a tri-layer structure known as milk fat globule membrane (MFGM). The MFGM is rich in phospholipids and glycoproteins, which are crucial for the neurocognitive function and confer brain-immune-gut benefits [1,2]. Dairy producers, such as Fonterra, Arla, and FrieslandCampina, have developed whey protein concentrate (WPC) ingredients enriched with MFGM compositions derived from cheese whey or butter milk [3]. These commercial ingredients are used to fortify infant formula (IF) to mimic the natural nutritional profile of human milk, addressing the deficiency of functional lipids and membrane-bound proteins in existing IF products. Despite these advancements, the industry lacks standardized quality regulations to oversee the production of MFGM ingredients, and analytical methods for MFGM proteins remain undeveloped [4]. Consequently, the compositions of the MFGM ingredients vary significantly between different manufacturers, leading to heterogeneous outcomes. Whey proteins predominate in these formulations, with phospholipid content typically ranging from 6–10 %; however,

* Corresponding author.
*E-mail address:* Song.Miao@teagasc.ie (S. Miao).

https://doi.org/10.1016/j.ultsonch.2024.107058
Received 1 July 2024; Received in revised form 14 August 2024; Accepted 2 September 2024
Available online 4 September 2024
1350-4177/© 2024 Published by Elsevier B.V. This is an open access article under the CC BY-NC-ND license (http://creativecommons.org/licenses/by-nc-nd/4.0/).

membrane proteins are often not specified on product labels [3].

In addition to nutritional enhancement, the role of MFGM fragments in improving the technical functionalities of IFs and emulsions has been extensively studied. This includes investigations into the interfacial composition and structure of MFGs within IF products [5], as well as the stability of emulsion and colloidal phases in homogenized milk [6]. MFGM fragments have been shown to alter the composition and conformational structure at the oil–water interface, thereby influencing the stability of dairy emulsions [7]. MFGM ingredients are employed as a natural emulsifier in dairy industry due to the amphipathic nature of polar lipids and glycoproteins.

Moreover, the rheological properties of milk system are critical for processing efficiency in the dairy industry. An in-depth understanding of the rheological behaviours of milk liquids is essential for the design and evaluation of process units and operational equipment, such as the heat exchangers, heating and cooling rates, and the pressure losses in pipelines [8]. The rheological behaviour of milk products is complex and significantly affected by temperature and the concentration of dispersed phases [9]. For instance, the viscosity of the concentred skim milk must be strictly controlled to avoid detrimental effects on the properties of milk powder [10].

The structure, composition, and techno-functionalities of MFGs or MFGM have been documented in previous reviews [11]. However, there is a compelling need to explore the impact of various preparation steps on MFGM functionalities, including heating, membrane filtration, mechanical shearing, and non-thermal treatments like ultrasonic processing. Ultrasound induces physical and chemical effects in foods due to acoustic cavitation, characterized by the continuous formation and implosion of microbubbles [12]. Research has shown that ultrasonic treatment can enhance the solubility of MFGM (rich in milk phospholipids, MPL), improve the emulsifying stability of MPL-based emulsions [13], and retain more MFGM proteins compared to shear homogenisation [14]. These studies predominantly utilized commercial MFGM materials, where the native structure of fat globules was disrupted and MFGM existed in fragmented form. However, studies examining the impact of dairy processing units on MFGM derived from raw milk are limited. The gap underscores the importance of further investigations to better understand and optimize the processing of MFGs or MFGM ingredients in their most natural state.

In our previous study, we conducted a comparative analysis of the changes of interfacial and thermal-dynamic properties of MFGs/MFGM isolated from fresh milk exposed to ultrasound at varying intensities [15]. For this study, a follow-up research on the physicochemical and rheological properties, as well as the emulsions stability of MFGs/MFGM was investigated. To deepen our understanding of the technical functionalities of natural MFGs and MFGM, bovine raw milk was used as the raw material. Prior to the isolation of MFGs/MFGM materials, ultrasound at different intensities was applied to the raw milk. The changes in MFGM proteins and their interactions with non-membrane proteins were assessed using a combination of analytical techniques, including sodium dodecyl sulfate polyacrylamide gel electrophoresis (SDS-PAGE), Fourier transform infrared spectroscopy (FTIR), and confocal laser scanning microscopy (CLSM). Furthermore, shearing scanning was performed on all the MFGs/MFGM to characterize their rheological properties, while an accelerated centrifugation method was used to evaluate the stability of emulsion stabilized by MFGs/MFGM. The findings from this research may provide valuable insights into the innovative development of MFGs/MFGM products and their prospective uses in the dairy field.

## 2. Materials and methods

### 2.1. Materials and reagents

Fresh bovine milk samples were obtained from Teagasc animal & grassland research and innovation centre (Moorepark, Fermoy, Co. Cork, Ireland). Immediately after milking, the fresh milk samples were cooled down to 4 °C by plate heat exchanger and maintained at this temperature until further analysis. The compositions of the collected milk was analysed using the DairySpec FT–15 (Bentley Instruments Inc., Chaska, MN, USA), revealing the mean values of fat at 4.09 ± 0.01 %, protein at 3.36 ± 0.03 %, dry matter at 12.94 ± 0.03 %, pH at 6.68 ± 0.02.

Nile Red, Fast Green FCF, wheat germ agglutinin (WGA), Polyethylene glycol 200, and phosphate buffer saline (PBS) were purchased from Sigma–Aldrich® (Merck Life Science Ltd., Cork, Ireland). Thermo Scientific Inc. (Thermo Fisher Scientific Inc., Cork, Ireland) was the supplier of all the chemicals for gel electrophoresis.

### 2.2. Ultrasonic processing

Bovine raw milk was subjected to ultrasonic treatments of different intensities referring to the methodologies detailed in our previous research [15]. The procedure involved preheating the raw milk to 30–35 °C before subjecting it to sonication at frequencies of 20 kHz and 40 kHz, using both independent and synchronous operating models. An ultrasonic processor (WKS1200/2J, Jiangsu Jiangda Wukesong Biotechnology Co., LT, Zhenjiang, China) was employed, featuring a 2-cm diameter titanium probe. The durations of the ultrasonic treatments were 5 and 15 min using the 5 s: 3 s work/rest working model. Raw milk that did not undergo ultrasonic treatment served as the control groups.

### 2.3. Separation of MFGs/MFGM ingredients

The separation of MFGs/MFGM fractions was carried out using ultracentrifugation (10000 × g, 15 min at 4 °C) (Kendro Laboratory Products, Asheville, NC) following the method of Ren, et al. [16] with some modifications. The upper cream layer was collected and washed with 3 volumes of phosphate buffered saline (PBS, 0.1 mol/L, pH 6.80). This rinsing procedure was repeated 3 times. Subsequently, the upper layer obtained from the final centrifugation was freeze-dried for 72 h. The MFGs/MFGM were individually labelled according to the ultrasonic conditions: 20 kHz/ 5 min, 20 kHz/ 15 min, 40 kHz/ 5 min, 40 kHz/ 15 min, 20 + 40 kHz/ 5 min, and 20 + 40 kHz/ 15 min. The resulted total protein and fat content were noted in our previous study [15].

### 2.4. Fourier transform infrared spectroscopy (FTIR)

FTIR spectra was acquired using a Bruker Tensor 27 (Bruker Optik GmbH, Ettlingen, Germany) equipped with an Optics Platinum Attenuated Total Reflectance (ATR) cell (Pike Technology Inc., Madison, WI, USA). For the analysis, 20 mg of each sample was placed on the zinc ATR crystal aperture. Spectra were captured within the spectral range of 4000 to 900 $cm^{-1}$, averaging 120 scans at a resolution of 4 $cm^{-1}$. Each sample was analysed in triplicate. Prior to each determination, a background measurement was conducted under identical conditions. The collected spectral data was initially pre-processed using OPUS 7.5 software (Bruker Optik GmbH, Ettlingen, Germany) to eliminateatmospheric vapour and carbon dioxide interference, and vector normalization was applied to mitigate scaling effects.

Noise reduction, baseline subtraction, second derivation, and peaks fitting and deconvolution were performed using OriginPro 2023 (OriginLab, Northampton, MA, USA) to reveal hidden and overlapping bands. The Savityzky–Golay function was utilized for smoothing, and the baseline points were anchored using the 2nd derivative method. The fitting of peaks was carried out using Gaussian, Voigt, or Lorentz functions across various spectral regions to achieve the optimal fit. Parameters such as peaks widths and centres, along with baseline parameter, were adjusted until achieving a fit with $R^2 > 0.990$. Finally, unsupervised chemometric analysis, principal component analysis (PCA), was used to visually depict the variation within and between the spectra of all MFGs/MFGM and to classify samples according to treatments.

Namely, loading plots highlighted differentiated wavenumbers, and PCA plots illustrated distinct groups based on their spectral profiles.

### 2.5. Sodium dodecyl sulphate polyacrylamide gel electrophoresis (SDS-PAGE)

The protein profiles of control and ultrasonically-treated MFGs/MFGM isolates were characterized by SDS-PAGE with a modified method described by Sun, et al. [17]. The non-reducing SDS-PAGE was performed at 120 V for a duration of 45 min, after which the proteins were stained with Coomassie Blue. Subsequently, the gels were detained using a blend of 45 % ethanol and 5 % acetic acid until a clear background was achieved. Relative quantification of caseins, whey proteins, and specific MFGM proteins was performed to assess the impact of ultrasonic treatments. The densities of protein bands were analysed by ImageJ software 1.36b (Wayne Rasband, National Institutes of Health, Bethesda, MD, USA), and the results were normalized to a total of 100 %.

### 2.6. Rheological analysis

The rheological properties of both control and ultrasound-treated MFGs/MFGM were evaluated using an ARG 2 Rheometer (TA Instruments, Crawley, UK). Before analysis, the freeze-dried MFGs/MFGM was kept at 35–40 °C until melting into the liquid state. The measuring geometry consists a 60 mm diameter aluminium parallel plate. The gaps size was set to 300 μm during the analysis. The shear rate was increased from 0.1 $s^{-1}$ to 1000 $s^{-1}$, during which both shear (apparent) viscosity and normal stress were recorded as a function of shear rate. All measurements were conducted at a constant temperature of 25 °C. A lid was used to cover the MFGs/MFGM during the rheological analysis to reduce the moisture evaporation. Each analysis was replicated three times. Given that raw milk and cream predominantly exhibit non-Newtonian behaviour under conditions with temperature < 40 °C and at low shear rate, the experimental data were fitted using the power law model and Herschel-Bulkley to characterize the nonlinear behaviour of the MFGs/MFGM samples [18].

Power law,

$$\sigma = K\ddot{Y}^{n} \tag{1}$$

and Herschel-Bulkley,

$$\sigma = \sigma_0 + K\ddot{Y}^{n} \tag{2}$$

where σ is the shear stress (Pa), while $\ddot{Y}$ denotes the shear rate (1/s). The parameter $K$ (Pa $s^n$) serves as the consistency index, and n is the flow behavior index. Additionally, $\sigma_0$ refers to the yield stress (Pa). The power-law model is utilized to predict the rheological behaviour of fluids, characterizing them as shear-thinning for $0 < n < 1$, Newtonian for $n = 1$, and shear-thickening for $n > 1$.

### 2.7. Accelerated emulsion stability

Lumisizer was employed (LUM GmbH, Berlin, Germany) to investigate the impact of ultrasonic treatments on the physical stability of MFGs/MFGM. Freeze-dried MFGs/MFGM materials were initially preheated to a liquid phase at temperatures ranging from 35 °C to 40 °C. Subsequently, 400 μL of these liquid samples were loaded into a polyamide cell (2 mm light path) and subjected to a centrifugal force of 3000 rpm for 45 min at a controlled temperature of 37 ± 2 °C. The intensity of near-infrared (NIR) light (wavelength at 865 nm) transmitted through the length of samples was recorded every 10 s intervals during centrifugation. The SEP View software (SepView 4.1, LUM GmbH) was used for the data recording and instability calculation. To calculate the instability index, the clarity of the emulsion caused by phase separation was measured and then divided by the maximum possible transmission at the given centrifugal force. This dimensionless index spans from 0 to 1, where 0 means no alteration in NIR transmission and 1 means complete phase separation [19].

### 2.8. Confocal laser scanning microscopy (CLSM)

CLSM, as reported in the literature, provides reliable qualitative identification of protein adsorption on the surfaces of MFGs and has demonstrated the aggregation of protein and fat globules [20]. In this study, CLSM (Leica TCS SP5, Leica Microsystems, Germany) was used to examine the ultrasound-induced structural and surface compositional changes of the fat globules. Samples preparation and the instrument settings were based on our published report with modifications [17]. Generally, non-polar lipids, predominantly triglycerides, were stained with Nile Red, while non-membrane proteins and glycoproteins were labelled using Fast Green FCF and wheat germ agglutinin (WGA), respectively. All the MFGs/MFGM underwent dual staining by 10 μL mixture comprising 0.1 % (w/v) Nile Red in polyethylene glycol-200 and 0.1 % (w/v) Fast Green FCF in distilled water, at a ratio of 3:1 (v/v) (FCF: Nile Red). Additionally, 50 μL of 1 mg/mL WGA in PBS was combined with Nile Red at a 1:1 (v/v) ratio. All MFGs/MFGM were subsequently incubated in darkness for half an hour to ensure thorough staining. The excitation of Nile Red, Fast Green FCF, and WGA were performed with a helium–neon (He-Ne) laser at 565–625 nm, 632–719 nm, and 493–550 nm, respectively. For each sample, a minimum of 10 images were recorded, from which one representative image was selected for each experiment.

### 2.9. Statistical analysis

All analyses were conducted in triplicate, unless otherwise indicated. The tested results were expressed as mean value ± standard deviation (SD). The variant analysis was performed using Analysis of Varian (ANOVA), and the significance of mean differences was assessed using Fisher's test ($p < 0.05$). Additionally, Multivariate Statistical Analysis was executed in OriginPro, the results of which were visually represented through a heat map, derived from the Hierarchical Cluster analysis (HCA). All these statistical evaluation were conducted using the OriginPro 2023 software system (OriginPro 2023, OriginLab Corporation, Northampton, USA).

## 3. Results and discussion

### 3.1. General profiling of composition changes induced by ultrasonic treatment

The averaged FTIR spectra of MFGs/MFGM fractions extracted from bovine raw milk treated with ultrasound at varying intensities are depicted in Fig. 1A. Additionally, a second derivative analysis was conducted to search for the hidden peaks within each spectrum (Fig. 1B). The entire spectral range between 4000 and 900 $cm^{-1}$ has been classified into six regions based on different milk components referring to published articles. In particular, the region from 3000–2800 $cm^{-1}$ is attributed to the stretching modes of $CH_2$ groups of acyl chains in triglycerides and phospholipids [21] (Region 1); 1800–1700 $cm^{-1}$ represents the C═O stretching vibrations of ester, aldehydes and ketones [22] (Region 2); Protein secondary structure is commonly described by the Amide I (1700–1600 $cm^{-1}$) (Region 3), Amide II (1600–1500 $cm^{-1}$) (Region 4) and Amide III (1500–1200 $cm^{-1}$) [23] (Region 5); and the1200–900 $cm^{-1}$, known as the fingerprint region, corresponds to the lipid components of membranes, protein-lipid complexes, and lactose groups [24] (Region 6).

The original and 2nd deprivation spectra in regions numbered 1–3 show no noticeable differences, whereas more pronounced changes are observed in regions 4–6 for MFGs/MFGM treated for 5 min compared to those treated for 15 min and the control (Fig. 1A and B).

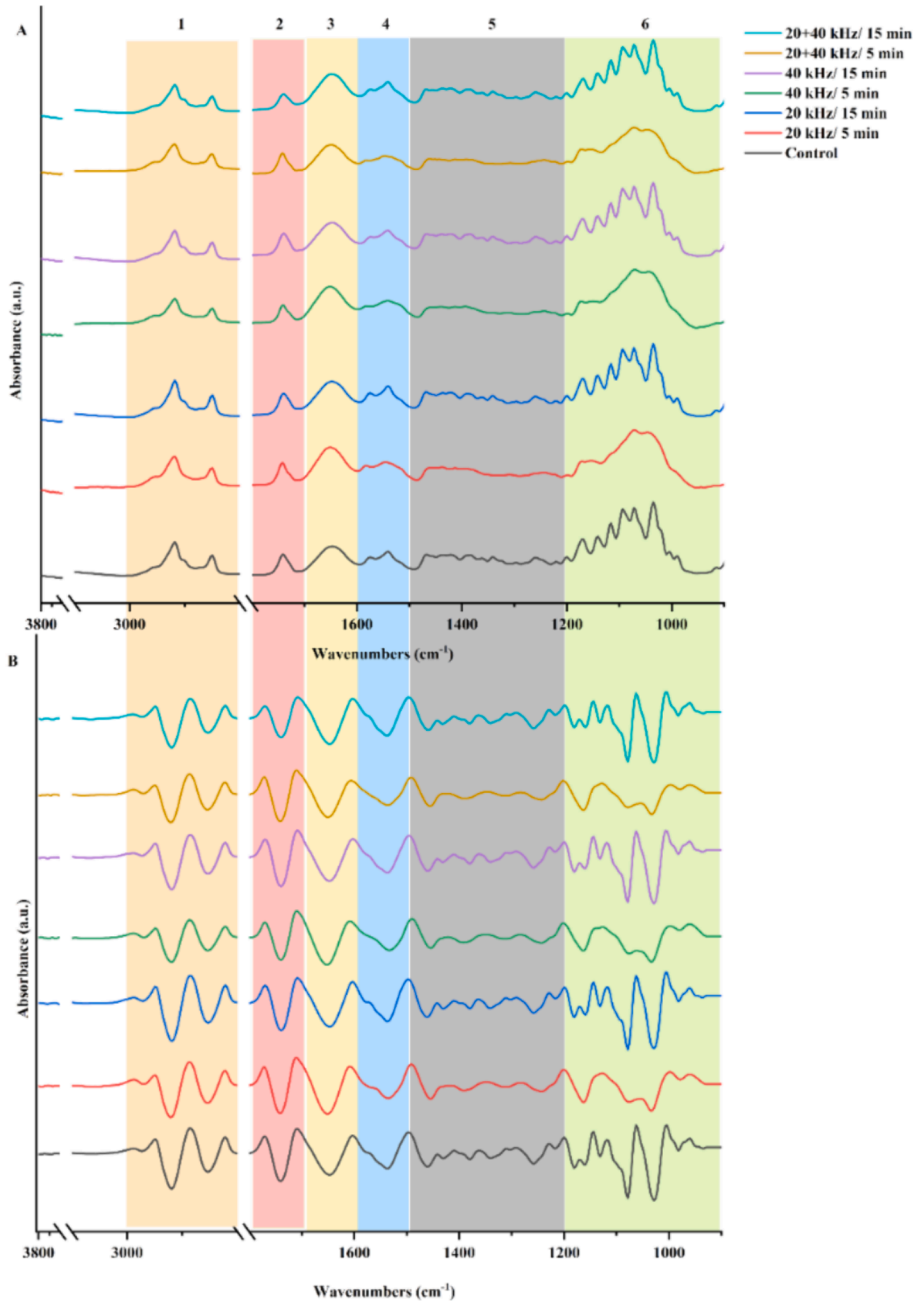



**Fig. 1.** FTIR spectra for MFGs/MFGM materials: original (A) and 2nd derivative (B). (Spectra between 2800 and 1800 $cm^{-1}$ are not shown as no peak was detected for any of the MFGs/MFGM, with all spectra displaying similar flat profiles). Numbers 1–6 above the figure indicate different wavenumber ranges: 1: 3000–2800 $cm^{-1}$; 2: 1800–1700 $cm^{-1}$; 3: Amide I, 1700–1600 $cm^{-1}$; 4: Amide II, 1600–1500 $cm^{-1}$; 5: Amide III, 1500–1200 $cm^{-1}$; 6: Finger print region, 1200–1900 $cm^{-1}$.

PCA conducted on the full spectra range from 4000–900 $cm^{-1}$ grouped the MFGs/MFGM into two distinct categories along the axis of Principle Component 1 (PC1), which accounts for 44.30 % of the variance (Fig. S1A). MFGs/MFGM treated for 5 min were differentiated from both control and 15 min ultrasonic treatment samples. This division is mainly due to different loadings for the wavenumber ranges of 3000–2800 $cm^{-1}$ and 1700–900 $cm^{-1}$ (Fig. S1B). Further PCA was performed on these specific wavenumber regions to explore the effects of ultrasonic treatments on the lipids, proteins, and the interactions of membrane proteins in the MFGs/MFGM materials. For the first region between 3000 $cm^{-1}$ and 2800 $cm^{-1}$, the control, 20 kHz/ 15 min, and 40 kHz/ 15 min MFGs/MFGM were separated from the 20 + 40 kHz/ 15 min and the 40 kHz/ 5 min ultra-sonicated MFGs/MFGM along the PC2 (Fig. S2A) with a variation of 9.2 %. This separation is due to peaks at 2916/2850 $cm^{-1}$ and 2900 $cm^{-1}$, which are ascribed to the methylene groups and C—H stretching of lipids, respectively (Fig. S2B) [21].

In the region of 1800–1700 $cm^{-1}$, the 20 + 40 kHz/ 15 min MFGs/MFGM were distinctly separated from other treatments along the direction of PC2 (9.1 %) (Fig. S3A). This division is primarily due to differences in the wavenumber at 1742 $cm^{-1}$, which is assigned to the ester functional group of lipids and their interactions with proteins via C═O stretching vibrations (Fig. S3B) [22]. In addition, hidden peaks at the wavenumber of 1726 $cm^{-1}$ in each sample were identified using a peak fitting function (Fig. S4A–G). The band at 1726 $cm^{-1}$ is typically indicative of the presence of hydrogen bonded carbonyl groups in esters [25]. Quantitative assessments of the respective corresponding groups at band of 1740 $cm^{-1}$ and 1727 $cm^{-1}$ in each MFGs/MFGM were conducted to elaborate on changes in lipids groups (Table 1). Bands

**Table 1**
Quantitative estimation of the functional ester group of lipids at the band of 1727–1726 $cm^{-1}$ and 1742–1739 $cm^{-1}$ in all MFGs/MFGM ingredients obtained from ultrasound-treated bovine raw milk (1800–1700 $cm^{-1}$).

| | 1727–1726 $cm^{-1}$ | 1742–1739 $cm^{-1}$ |
|---|---|---|
| Control | $94.29 \pm 0.22^{a}$ | $5.71 \pm 0.22^{b}$ |
| 20 kHz/ 5 min | $91.37 \pm 0.52^{ab}$ | $8.63 \pm 0.52^{ab}$ |
| 20 kHz/ 15 min | $87.41 \pm 0.10^{ab}$ | $12.59 \pm 0.10^{ab}$ |
| 40 kHz/ 5 min | $86.22 \pm 4.25^{ab}$ | $13.78 \pm 4.25^{ab}$ |
| 40 kHz/ 15 min | $91.94 \pm 0.92^{ab}$ | $8.06 \pm 0.92^{ab}$ |
| 20 + 40 kHz/ 5 min | $91.92 \pm 1.45^{ab}$ | $8.08 \pm 1.45^{ab}$ |
| 20 + 40 kHz/ 15 min | $81.38 \pm 17.19^{b}$ | $18.62 \pm 17.19^{a}$ |

Superscript letters that differ in the same column denote significant differences between MFGs/MFGM ($p < 0.05$). 'ns' stands for no significant difference ($p > 0.05$).

between 1727–1726 $cm^{-1}$ in control MFGs/MFGM were significantly higher than those in MFGs/MFGM fractions treated by 20 and 40 kHz for 15 min ($p < 0.05$), whereas the opposite trend was observed at 1742–1739 $cm^{-1}$, where a stronger spectrum was noted in the MFGs/MFGM sourced from 20 and 40 kHz ultra-sonicated raw milk for 15 min MFGs/MFGM compared to the control.

For the Amide I and Amide II regions, PC2 classified all of the MFGs/MFGM into two separate groups, respectively (Fig. S5B and S6B). MFGs/MFGM treated at 20 kHz/ 5 min and 40 kHz/ 5 min exhibited similar distributions, while the control and those treated for 15 min clustered into another group. Notably, MFGs/MFGM from the 20 + 40 kHz/ 5 min treatments demonstrated poor repeatability, as indicated by their dispersed distribution in both Fig. S5A and S6A. The separation observed in the Amide I region is due to the loading for the wavenumber at 1654 $cm^{-1}$, which can be associated with changes in the α-helix content of proteins. The loading for 1574 $cm^{-1}$ and 1540 $cm^{-1}$ is responsible for the group separation in the Amide II band, which has been reported to associate with the –COO-asymmetric stretching vibration of Asp and Glu residues and C—N and N—H stretching, respectively [26].

Peak fitting was applied to the Amide I region (Fig. S7A–G), the results of which demonstrated that the ultrasonic treatment had no significant effect on the structure of β-turn and side chain in all MFGs/MFGM ($p > 0.05$) (Table 2). Comparing with control, MFGs/MFGM exposed to 20 + 40 kHz for a duration of 15 min significantly reduced the intramolecular β-sheet content ($p < 0.05$). Additionally, more random coil were identified in MFGs/MFGM ingredients subjected to 40 kHz for 15 min than that in control. Under the same ultrasonic conditions, 15 min treatments significantly enhanced the random coil structure compared to 5 min treatments, except for the 20 kHz and 40 kHz concurrent treatment ($p < 0.05$). Conversely, α-helix structures were more prevalent in MFGs/MFGM treated for 5 min compared to those treated for 15 min. This finding is inconsistent with the PCA results for the band of Amide I, where differences in α-helix were a primary factor in grouping 5 min treated MFGs/MFGM separately from control and 15 treatments. Peak fitting in the spectrum of Amide II indicated an apparent band migration from 1582–1584 $cm^{-1}$ to 1572–1573 $cm^{-1}$ as the duration of ultrasonic treatment prolonged to 15 min (Fig. S8A–G). This supports the previous PCA results that distinguished 5 min MFGs/MFGM from those treated for 15 min and the control along the PC2 at the band at 1573 $cm^{-1}$.

**Table 2**
Relative content of secondary structures in Amide I region (1700–1600 $cm^{-1}$) in all MFGs/MFGM compounds sourced from bovine raw milk subjected to ultrasound treatment.

| | Intramolecular β-sheet | Random coil | α-helix | β-turn | Side chain |
|---|---|---|---|---|---|
| Control | $11.08 \pm 0.35^{a}$ | $36.26 \pm 6.00^{bcd}$ | $26.96 \pm 3.48^{b}$ | $17.78 \pm 7.70^{ns}$ | $7.92 \pm 1.82^{ns}$ |
| 20 kHz/ 5 min | $9.99 \pm 1.18^{ab}$ | $28.60 \pm 7.10^{d}$ | $43.13 \pm 10.46^{a}$ | $12.32 \pm 3.52$ | $5.96 \pm 1.07$ |
| 20 kHz/ 15 min | $8.69 \pm 4.53^{ab}$ | $41.18 \pm 6.77^{abc}$ | $26.90 \pm 3.37^{b}$ | $14.68 \pm 2.32$ | $8.54 \pm 1.86$ |
| 40 kHz/ 5 min | $7.39 \pm 2.87^{ab}$ | $31.67 \pm 5.46^{cd}$ | $40.00 \pm 6.32^{a}$ | $12.05 \pm 3.72$ | $8.88 \pm 2.56$ |
| 40 kHz/ 15 min | $6.24 \pm 2.85^{b}$ | $49.95 \pm 6.54^{a}$ | $20.18 \pm 5.88^{b}$ | $15.60 \pm 0.62$ | $8.03 \pm 3.64$ |
| 20 + 40 kHz/ 5 min | $8.53 \pm 3.09^{ab}$ | $35.62 \pm 10.68^{bcd}$ | $28.26 \pm 0.22^{b}$ | $17.19 \pm 2.69$ | $8.81 \pm 2.34$ |
| 20 + 40 kHz/ 15 min | $6.34 \pm 1.62^{b}$ | $45.70 \pm 2.59^{ab}$ | $23.72 \pm 2.52^{b}$ | $16.13 \pm 1.83$ | $8.11 \pm 1.20$ |

Superscript letters that differ in the same column denote significant differences between MFGs/MFGM ($p < 0.05$). 'ns' stands for no significant difference ($p > 0.05$).

Similar group distinctions observed in the Amide I and Amide II regions were also noted when analysing the fingerprint region of 1200–900 $cm^{-1}$ via PCA. The analysis demonstrated that MFGs/MFGM treated for 5 min were differentiated from control and 15 min treatment MFGs/MFGM (Fig. S9A). This differentiation was largely attributed to absorbance peaks at 987 $cm^{-1}$, 1035 $cm^{-1}$, and 1153 $cm^{-1}$ along the PC2 axis, which represented 80.40 % of the observed variance.

The band at 987 $cm^{-1}$ has been reported to be related to the release of colloidal calcium phosphate (CCP) from the phosphate residues due to pressure effects [27]. The bands around 1035 $cm^{-1}$ ascribes to $–CH_2$ bending, and peak around 1159 $cm^{-1}$ represents the C—O group (esters) [24]. Further insights were gained through peak fitting analysis of the region between 1200–900 $cm^{-1}$ (Fig. S10A–G), where peaks at bands 1003 $cm^{-1}$ and 1058 $cm^{-1}$ were absent in 5 min treatment MFGs/MFGM. Meanwhile, absorbance peaks positioned at 1035 $cm^{-1}$ and 1141 $cm^{-1}$ in both control and 15 min treatment MFGs/MFGM shifted to 1043 $cm^{-1}$ and 1153 $cm^{-1}$, respectively, in 5 min treatment MFGs/MFGM.

In summary, PCA analysis of the spectral bands from Amide I (1700–1600 $cm^{-1}$), Amide II (1600–1500 $cm^{-1}$), and 1200–900 $cm^{-1}$ revealed that all treatments could be categorized into two distinct groups: one compromising the 5 min treatment, and another encompassing the control and 15 min treatment, a finding further substantiated by the peak fitting results.

### 3.2. *Effect of ultrasonic treatments on the distribution of milk fat globule membrane proteins*

Non-reducing SDS-PAGE was conducted to illustrate the impact of varying ultrasound intensities on the MFGs/MFGM proteins, with the resulting SDS-PAGE patterns depicted in Fig. 2A. Notable non-membrane proteins identified included casein, β-lactoglobulin (β-LG), α-lactalbumin (α-LA), and six key membrane proteins: MUC1, the redox enzyme xanthin oxidase (XO), periodic acid Shciff 3 (PAS III), CD 36, butyrophilin (BTN), and periodic acid Schiff 6/7 (PAS 6/7). Generally, the intensity of PAS 6/7 bands was observed to be lower compared to other proteins, likely due to its classification as a peripheral protein, which is more susceptible to removal through mechanical shearing during sample preparation [17]. In contrast, casein, β-LG, and α-LA were distinctly present in the control, persisting through the centrifugation and rinsing processes (Fig. 2A), contrary to findings by Zhao, et al. [28] where more intensive centrifugation and rinsing were applied, resulting in the removal of most caseins and whey proteins during centrifugation. The concentration of MFGM proteins in MFGs/MFGM can further be improved by washing with SDS, followed by sonication [29].

The intensity of caseins in ultrasonically treated MFGs/MFGM increased dramatically, whereas a reduced intensity of β –LG bands was identified compared to control. From the quantitative analysis results in Fig. 2B, 20 kHz and 40 kHz treatments retained 55.44–63.28 % of caseins, compared to 36.53 % in the control. With prolonged ultrasonic durations, a higher retention of caseins was observed, except in the 40

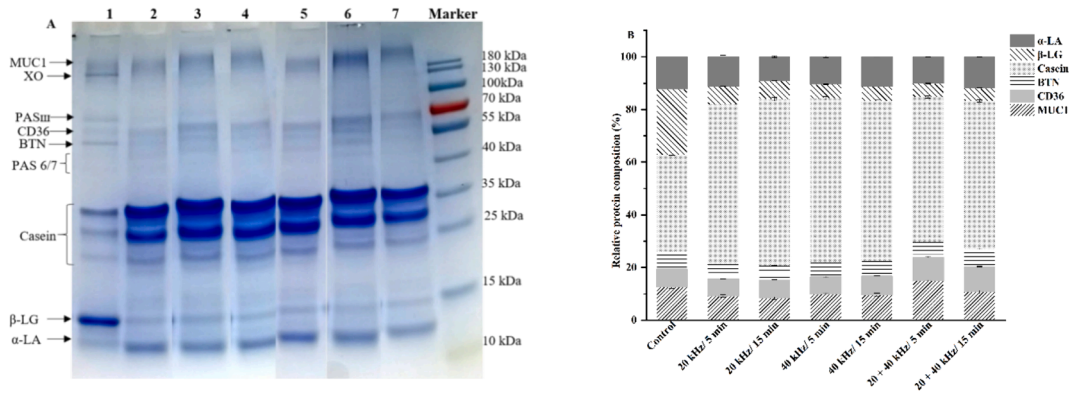



**Fig. 2.** SDS-PAGE patterns obtained under non-reducing conditions of fat globule materials from control and ultra-sonicated raw milk. (A) Lane 1–7, control, processed at 20 kHz for 5 min and 15 min, 40 kHz for 5 min and 15 min, 20 + 40 kHz for 5 min and 15 min.

kHz treatments, consistent with the study by Lu, et al. [29] which reported that homogenization damages MFGM while aqueous phase proteins like caseins and whey proteins adsorb onto the newly formed MFGM. Conversely, the reduction of β –LG intensity in ultrasonic MFGs/MFGM may be attributed to the formation of aggregates between β –LG and MFGM proteins via disulphide bands [30]. Subsequent centrifugation aided in the removal of these aggregates, concurrently removing the PAS III and XO. This accounts for the observed reductions in the intensities of PAS III and XO bands. Notably, treating at 20 + 40 kHz ultrasound for 15 min most efficiently facilitated the removal of β –LG from MFGs/MFGM ingredients, followed by 5-min treatments at 20 + 40 kHz, then 40 kHz, and lastly 20 kHz.

Additionally, the increased intensity of CD 36 in ultrasonic MFGs/MFGM, particularly in the 20 + 40 kHz treatments, suggests that ultrasonic treatment enhances the transfer of CD 36 into the rinsing phase from the MFGM structure. In contrast, lower amounts of BTN and MUC1 were detected in MFGs/MFGM after ultrasonic treatment compared to control. This variability in the effects of ultrasonic treatments on CD36, BTN, and MUC1 levels may be due to their distinct localizations within the three layers of membrane; CD 36 primarily localizes in the apical membrane [31], MUC1, characterized by its extended rod-like structure, forms part of the glycocalyx on various epithelial cell surfaces and milk membranes [32], and BTN is mainly found in a 'peripheral' cytoskeletal-like component [33]. Comparatively, the 20 kHz/ 15 min MFGs/MFGM contained fewer MFGM proteins but higher levels of non-membrane proteins than other MFGs/MFGM, indicating that more intensive ultrasonic treatment promotes greater loss of MFGM proteins.

### 3.3. Rheological properties

As shown in Fig. 3, the apparent viscosity of MFGs/MFGM consistently decreased with an increase in shear rate (0.1 $s^{-1}$ to 1000 $s^{-1}$) across all MFGs/MFGM, demonstrating shear-thinning behaviour (non-Newtonian), regardless of the ultrasonic treating intensities. There was a dramatic decrease in viscosity observed in the control, 20 kHz, and 20 + 40 kHz MFGs/MFGM within the shear rate range of 0.1 to 2 $s^{-1}$, with the exception of those treated at 40 kHz, suggesting a more pronounced degree of Newtonian behavior at higher shear rates. This observation of shear-thinning behaviour in the control is in disagreement with findings from Ayyash, et al. [34]. They demonstrated that non-fermented raw milk exhibited little or no shear-thinning behavior. This discrepancy in the magnitudes of viscosity could be due to differences in experimental conditions, particularly the higher shear rate range (10–1000 $s^{-1}$) used in their study.

The initial viscosity of the control was significantly lower compared to those treated at 20 kHz and 20 + 40 kHz, while the 40 kHz MFGs/MFGM exhibited the lowest viscosity. Additionally, a slight variation in the viscosity of 40 kHz MFGs/MFGM was observed throughout the

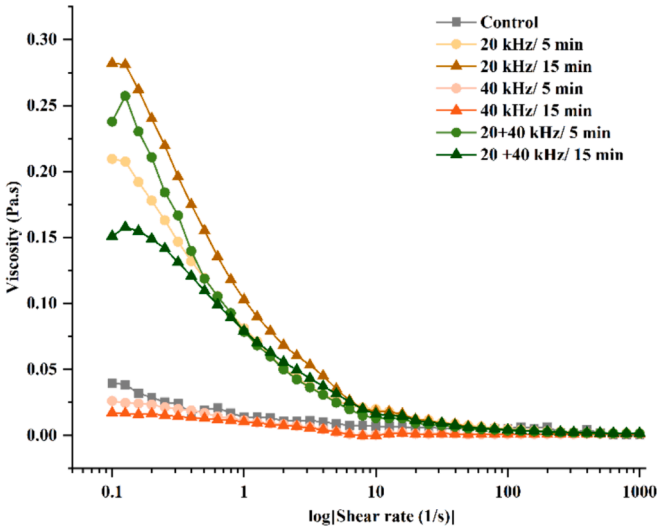



**Fig. 3.** Apparent viscosity of MFGs/MFGM components derived from bovine raw milk exposed to ultrasound with different intensities.

analysis. This trend is in accordance with the regression results in Table 3. The flow behavior indexes (n) for the 40 kHz MFGs/MFGM, derived from Herschel-Bulkley models, are 1 or close to 1, indicating Newtonian or shear thickening behaviour. This characteristic may be attributed to the increase in volume density (%) of larger particles observed at 40 kHz, as noted in the prior research [15]. A heterogeneous distribution of particles, induced by higher stresses, may lead to the shear thickening behavior observed in skim milk and 3.5 % fat milk at temperature of 25 and 40 °C [9]. Furthermore, the flow behavior indexes (n) of the control, fitted from the power law model, were higher

**Table 3**
Regressed parameters of the Herschel-Bulkley models used to describe the flow curve of MFGs/MFGM components derived from bovine raw milk exposed to ultrasound at different intensities.

| Samples | Herschel-Bulkley | | | |
|---|---|---|---|---|
| | $\sigma_0$ (Pa) | $K$(Pa $s^n$) | n | $R^2$ |
| Control | 0.013 | 0.002 | 0.950 | 0.999 |
| 20 kHz/ 5 min | 0.016 | 0.054 | 0.448 | 0.997 |
| 20 kHz/ 15 min | 0.070 | 0.032 | 0.529 | 0.990 |
| 40 kHz/ 5 min | 0.007 | 0.001 | 1.022 | 0.999 |
| 40 kHz/ 15 min | 0.008 | 0.000 | 1.096 | 0.999 |
| 20 + 40 kHz/ 5 min | 0.053 | 0.023 | 0.571 | 0.995 |
| 20 + 40 kHz/ 15 min | 0.064 | 0.021 | 0.608 | 0.988 |

than those exposed to 20 kHz or 20 kHz and 40 kHz combination treatment, indicating that ultrasonic treatment may enhance the shear thickening behaviour of MFGs/MFGM materials. Notably, the ultrasonicated treatment at 20 kHz for 15 min showed the highest consistency indexes (K, Pa $s^n$) among all ultrasonic treatments. As reported in our previous research, MFGs/MFGM isolates sourced from the bovine milk treated at 20 kHz with a duration of 15 min samples contained more protein content than other treatments [15]. This observation is opposite to findings by Kieferle, et al. [35], who reported the consistency indexes in fresh or reconstituted milk protein concentrates increased with rising protein content.

The flow curves of the control and MFGs/MFGM treated at 40 kHz exhibited the best fits, with $R^2 = 0.999$, followed by the 20 kHz/ 5 min MFGs/MFGM with an $R^2$ of 0.997 (Table 3). Our preliminary results showed that the Herschel-Bulkley model provided a better fit than the power law model across all MFGs/MFGM, with higher $R^2$ values ranging from 0.988 to 0.999. The predicted shear stress values from both the power law and Herschel-Bulkey models were higher than the expreimental values across the shear rate of 0–600 $s^{-1}$. Notably, the shear stress predicted by power law was higher than that predicted by the Herschel-Bulkey model in the shear rate of 0–600 $s^{-1}$, but was lower when the shear rate $>$ 600 $s^{-1}$ (Fig. S11). The differentiation in

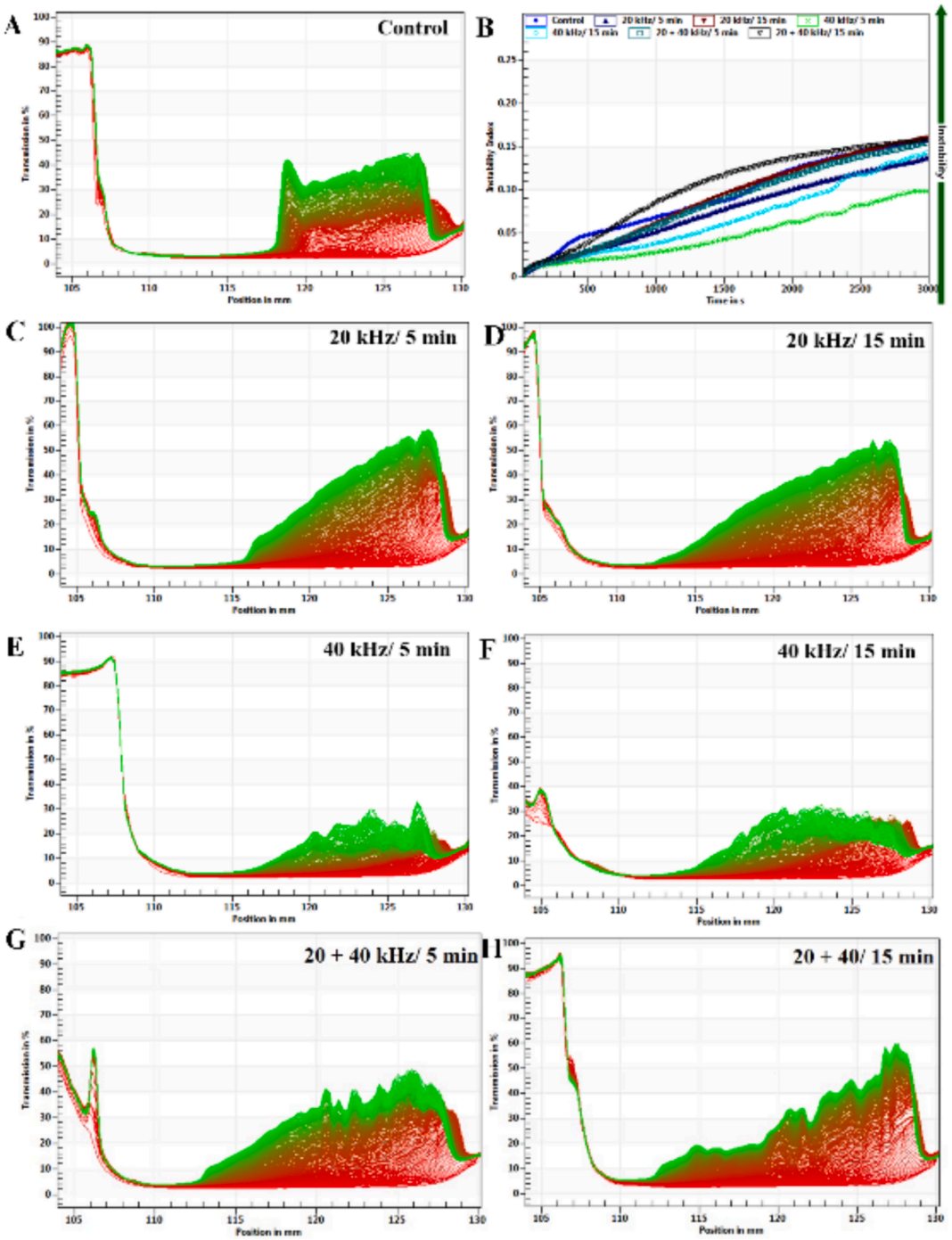



**Fig. 4.** Lumisizer phase separation near infrared (NIR) transmission profiles and instability index of MFGs/MFGM prepared from bovine raw milk treated by different ultrasonic intensities: A, control; B, instability index; C-D, 20 kHz treated for 5 min and 15 min; E-F, 40 kHz treated for 5 min and 15 min; G-H, Combined treatment using 20 kHz and 40 kHz for 5 min and 15 min.

predicted shear stress between these models can be explained by the absence of yield stress ($\sigma_0$) in the power law model [36].

### 3.4. Physical stability

Fig. 4 illustrates the transmission profiles of MFGs/MFGM as a function of time and space during an accelerated emulsion stability test. The red profile at the bottom of the image indicates the initial recorded profile, while the green profile layered on top shows the final transmitted profile. A noticeable shift from red to green profiles suggests the occurrence of creaming, characterized by the migration of the fat phase to the top of the cell, which implies phase separation in all MFGs/MFGM [37]. In the control, the larger and more distinct separation between the initial and final profiles indicates poorer cream stability compared to other MFGs/MFGM [38]. This observation is further confirmed by the visual evidence images in Fig. 5A, where a more pronounced cream layer was observed at the top of the control. Additionally, the final transmission profile of the control tended to be more horizontal, whereas the profiles of the ultrasonically treated MFGs/MFGM gradually inclined (Fig. 4C–H). This inferred that ultrasonic treatments decelerated the phase separation and resulted in a thinner cream layer at the top of the cell [39].

By comparison, the transmission profile area of 40 kHz treated MFGs/MFGM (Fig. 4E and 5F) was smaller than the control and MFGs/MFGM treated with other ultrasonic intensities. This suggested that 40 kHz treatments facilitated phase stability during the centrifugal process. This effect might be associated with decreased volume density (%) of particles sizes between 1 and 10 μm in the 40 kHz treated MFGMs/MFGM, as found in previous research [15]. The 40 kHz treatment likely caused the MFGs/MFGM to fragment into larger aggregates, decelerating their migration towards the top of the cell. Furthermore, the maximum transmission percentage in the control was 60 %, which decreased to 40 % following the 40 kHz treatments, reflecting lower droplet concentrations and improved cream stability. The duration of the ultrasonic treatments did not significantly affect the transmission profile for the 20 kHz and 40 kHz treatments, highlighting the impact of treatment intensity rather than duration.

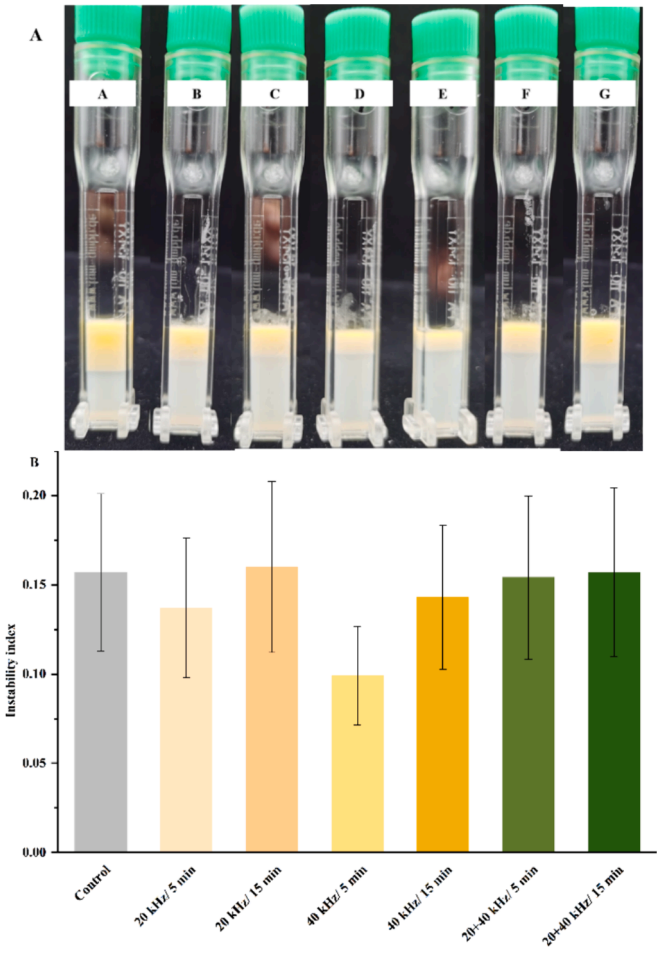



**Fig. 5.** (A) The visual cream layer of MFGs/MFGM after centrifugation by Lumisizer: A, control; B-C, 20 kHz treated for 5 min and 15 min; D-E, 40 kHz treated for 5 min and 15 min; F-G Combined treatment using 20 kHz and 40 kHz for 5 min and 15 min. (B) Instability indexes of all the MFGs/MFGM at the end of centrifugation (3000 s).

Except for the overall transmission profile, emulsion stability was quantitatively analysed and expressed as the instability index. The instability index is the slope of the integrated transmission time plots and is a dimensionless number between 0 and 1. A value of 0 signifies no change in NIR transmission, whereas 1 indicates total phase separation [19]. A significant decrease in the instability index for MFGs/MFGM treated at 40 kHz (0.099–0.143) by the end of the measurement period was observed compared to control (Fig. 5B). This result underscored the finding that 40 kHz treatments enhanced the emulsion stability under applied centrifugal forces, as evidenced by the reduced spacing between NIR transmission profile bands for 40 kHz treated MFGs/MFGM. This was in consist with the lower viscosity and Newtonian similar behaviour of the 40 kHz treatments, as discussed in section 3.3. Ultrasonic treatment at lower frequency (20 kHz) shows higher acoustic energy than at higher frequency (40 kHz) [15]. Based on the stability result from this study, we can speculate that ultrasound with moderate acoustic energy may promote the system stability. Contrarily, stringent shearing treatment induced by low frequency at 20 kHz, or 20 + 40 kHz may facilitate the formation of aggregates, which adversely affected the stability of the system.

From the start of the analysis until 700 s, the control exhibited the highest instability index, suggesting the greatest degree of phase separation during this initial period. However, from 700 s onward to the end of the analysis period at 3000 s, the concurrent treatment at 20 kHz and 40 kHz for 15 min displayed a consistently higher instability index compared to other treatments. Meanwhile, at the end of analysis period (3000 s), the instability index for the control equalized to levels similar to those observed in the MFGs/MFGM subjected to dual-frequency treatment at 20 kHz and 40 kHz for 5 min (0.154), 15 min (0.157), and 20 kHz independently for 5 min (0.154) (Fig. 5B). These data suggest that ultrasonic treatments, with the exception of 20 + 40 kHz/ 15 min treatment, generally enhanced the stability of MFGs/MFGM to varying extents compared to control given their wider transmission profiles and higher instability indexes. This observation was in agreement with the FTIR results in section 3.1 which highlighted the poor repeatability of sample distribution for the 20 + 40 kHz/ 15 min treatment. It can be inferred that phase separation may contribute to variations in sampling, thereby influencing the precision of the FTIR results.

### 3.5. Microstructure

The ultrasound-induced structural changes in MFGs/MFGM are evident in Fig. 6. Most MFGs maintained an intact spherical shape after ultrasonic treatments at different intensities, as seen by the stained triglyceride in green (Fig. 6A–D) or red (Fig. 6a–d) in the core of MFGs. However, 20 kHz independently or combined with 40 kHz ultrasonicated for 15 min caused the formation of irregular spheroids (Fig. 6B, D, and b). This observation may be associated with the disintegration of fat globules induced by acoustic stress, leading to the compromised MFGs integrity and release of triglycerides. More heterogeneous sizes of MFGs were observed in the ultrasonically treated MFGs/MFGM than that of control, especially noticeable in MFGs/MFGM treated with the combination of 20 kHz and 40 kHz for 15 min (Fig. 6D

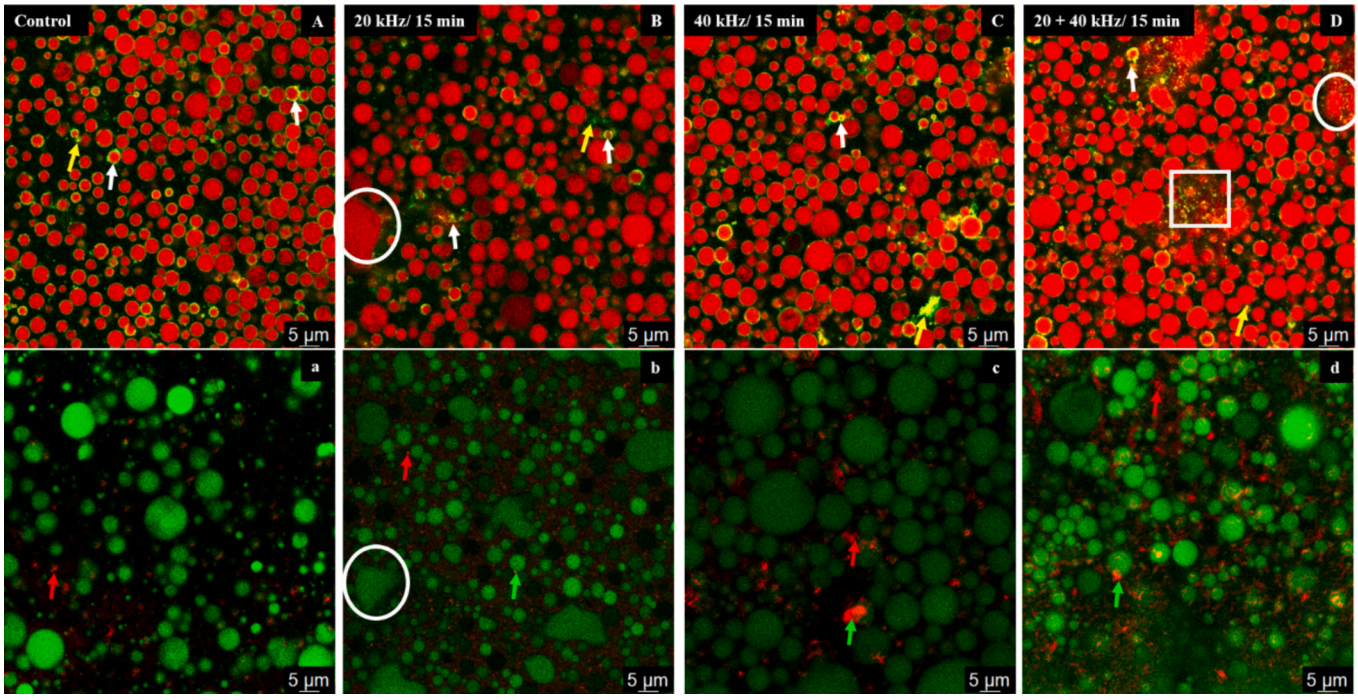



**Fig. 6.** Confocal laser scanning microscopy images of dual-stained MFGs/MFGM ingredients obtained from ultrasound-treated bovine raw milk at different ultrasonic intensities. A-D: control, 20 kHz/ 15 min, 40 kHz/ 15 min, and 20 + 40 kHz/ 15 min. Staining agents Nile Red and wheat germ agglutinin (WGA) were used to color neutral lipids (red) and membrane proteins (amber). White and yellow arrows highlight the membrane proteins present on the surface of MFGs/MFGM and within the whey phase. a-d: control, 20 kHz/ 15 min, 40 kHz/ 15 min, and 20 + 40 kHz/ 15 min. Staining of neutral lipids (green) and non-membrane proteins (red) was performed with Nile Red and fast green FCF. Green and red arrows indicate the non-membrane proteins on MFGs/MFGM surfaces and in the whey phase. The white circle highlights the flocculation of MFGs/MFGM fragments, and the white square marks the aggregated and unattached membrane proteins. (For interpretation of the references to color in this figure legend, the reader is referred to the web version of this article.)

and d). This further confirms our previous study, which indicated a the multimodal distribution of particle sizes [15]. Lee and Sherbon [40] reported similar findings, noting an increased surface area of MFGs and more pronounced non-uniformity in the MFGM structure in homogenized whole milk. The MFG was wrapped by a tri-layer structure which consisted of phospholipids and membrane proteins. Prior to ultrasonic treatment, most of the membrane proteins were evenly distributed around the fat globules (Fig. 6A). However, these proteins

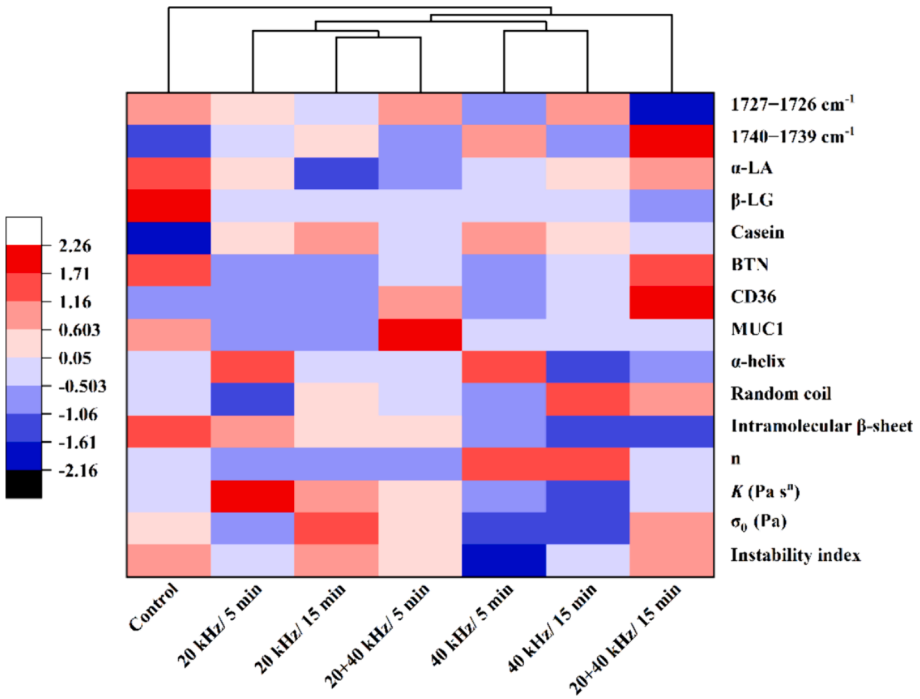



**Fig. 7.** Hierarchical cluster analysis of MFGs/MFGM ingredients obtained from ultrasound-treated bovine raw milk. The color scale differentiates values as high (red) to low (blue). (For interpretation of the references to color in this figure legend, the reader is referred to the web version of this article.)

were predominantly found in the whey phase after ultrasonic treatment, especially in samples processed at 20 kHz and 40 kHz for 15 min, with apparent flocculation of MFGM protein clusters evident in the while square. On the contrary, a significant amount of non-membrane proteins attached to the surface of ultrasonically treated fat globules, particularly in the MFGs/MFGM materials exposed to 20 kHz and 40 kHz concurrently ultra-sonicated for 15 min, whereas most of these proteins were randomly distributed in the whey phase of the control. This may be due to an increase in denatured non-membrane proteins adhering to the MFGs. The extent of protein coverage on MFGs, estimated by the surface fraction model ($\Phi_m$), showed that MFGs/MFGM treated by 20 + 40 kHz/ 15 min exhibited a higher $\Phi_m$ value than other MFGs/MFGM [15]. This observation may be linked to the increased ζ – potential due to the disruption of MFGs and subsequent membrane reorganization, exposing more negatively charged surface [17].

### 3.6. Hierarchical cluster analysis

The HCA results, illustrated in Fig. 7, reveal significant insights into the impact of ultrasonic treatments on the structural and compositional changes, rheological properties and instability indexes of MFGs/MFGM. The dendrogram generated by the HCA distinctly identified two main clusters: one encompassing the control sample and another grouping together the MFGs/MFGM under different ultrasonic intensities. Subsequently, 20 + 40 kHz/ 15 min treatment induced a notably differentiated impact on the analysed functionalities of MFGs/MFGM compared to other ultrasonic treatments. Additionally, the 40 kHz treatments formed a separated cluster, distinct from the 20 kHz and 20 + 40 kHz/ 5 min treatments. The latter group was further divided into two subclusters: one consisting solely of 20 kHz/ 5 min MFGs/MFGM, and another comprising MFGs/MFGM treated at both 20 kHz/ 15 min and 20 + 40 kHz/ 5 min.

The heat map associated with the HCA results clearly indicated that the ultrasonic treatments applied in this study significantly influenced the structure, composition, rheological properties, and emulsion stability of the MFGs/MFGM. Among all treatments, the 20 + 40 kHz/15 min treatment stood out as having a more pronounced effect compared to the others.

## 4. Conclusions

Milk fat globules/membrane (MFGs/MFGM) materials derived from bovine raw milk, treated by varying ultrasonic intensities, 20 kHz, 40 kHz, or a combination of 20 kHz and 40 kHz for duration of 5 min and 15 min, exhibited different physicochemical properties, rheological behaviour and emulsion stability compared to the control.

20 kHz and 40 kHz simultaneous processing for 15 min significantly influenced the ester groups of lipids and the interactions of hydrogen-bonded carbonyl groups in esters. The PCA results for Amide I grouped the 15 min with the controls, and the 5 min ultra-sonicated MFGs/MFGM into another group. Nevertheless, qualitative analysis of the protein secondary structures within Amide I revealed inconsistent results; notably, the 15 min treatments induced more significant changes in the intramolecular β-sheet, random coil, and α-helix structure compared to 5 min treatment. This discrepancy underscores the need for the further research to elucidate the underlying causes of these contradictory outcomes.

Ultrasonic treatment promoted the transfer of membrane proteins into the rinsing phase and facilitated the adsorption of non-membrane proteins onto the surfaces of fat globules. Moreover, all the MFGs/MFGM exhibited shear-thinning behaviour, except for the 40 kHz treated MFGs/MFGM, which displayed Newtonian behaviour at higher shear rate, as indicated by flow behaviour indexes (n), of 1 or close to 1, regressed from the Herschel-Bulkley model. Physical stability of MFGs/MFGM emulsions was generally enhanced by ultrasonic treatment with an exception of 20 + 40 kHz/ 15 min treatment, which led to the aggregated membrane proteins, as observed in CLSM images. This differentiation highlights the potential of specific ultrasonic treatment parameters to modify dairy product characteristics in targeted ways, which could be crucial for optimizing processing strategies in the dairy industry.

## CRediT authorship contribution statement

**Yanjun Sun:** Writing – original draft, Visualization, Validation, Methodology, Investigation, Funding acquisition, Formal analysis, Data curation, Conceptualization. **Yrjö H. Roos:** Writing – review & editing, Supervision. **Song Miao:** Writing – review & editing, Supervision, Project administration, Funding acquisition, Conceptualization.

## Declaration of competing interest

The authors declare that they have no known competing financial interests or personal relationships that could have appeared to influence the work reported in this paper.

## Acknowledgements

The project was supported by 'Teagasc-The Irish Agriculture and Food Development Authority (MDDT1392)', 'The China Scholarship Council (No.202008410212)', and 'The Open Project Program of State Key Laboratory of Dairy Biotechnology (No. SKLDB2022–007)'.

## Appendix A. Supplementary data

Supplementary data to this article can be found online at https://doi.org/10.1016/j.ultsonch.2024.107058.

## References

[1] B. Jiang, Y. Xia, L. Zhou, X. Liang, X. Chen, M. Chen, X. Li, S. Lin, N. Zhang, L. Zheng, M. Tao, P. Petocz, S. Gallier, A. Rowan, B. Wang, Safety and tolerance assessment of milk fat globule membrane- enriched infant formulas in healthy term chinese infants: a randomised multicenter controlled trial, BMC Pediatr. 22 (2022) 465.
[2] H.J.J. Mohamed, E.K.H. Lee, K.C.K. Woo, R. Sarvananthan, Y.Y. Lee, Z.A. Mohd Hussin, Brain-immune-gut benefits with early life supplementation of milk fat globule membrane, JGH Open 6 (2022) 454–461.
[3] Y. Sun, Y.H. Roos, S. Miao, A review of factors affecting the structure, compositions, and the techno-functionalities of bovine milk fat globule and membrane, Trends Food Sci. (2024) 104570.
[4] X. Wang, W. Wei, R. Wu, X. Zhu, F. Ren, L. Liu, Y. Su, N. Li, F. Li, Scientific consensus on milk fat globule membrane and its ingredients, J. Chin. Inst Food Sci. Technol. (2022) 1–6.
[5] Y. Pan, L. Liu, S. Tian, X. Li, M. Hussain, C. Li, L. Zhang, Q. Zhang, Y. Leng, S. Jiang, S. Liang, Comparative analysis of interfacial composition and structure of fat globules in human milk and infant formulas, Food Hydrocoll. 124 (2022) 107290.
[6] A. Garczewska-Murzyn, K. Kiełczewska, M. Smoczyński, The influence of buttermilk powder on the stability of emulsion and colloidal phases of homogenized milk, Eur. Food Res. Technol. 248 (2022) 2629–2636.
[7] C.C. Berton-Carabin, L. Sagis, K. Schroën, Formation, structure, and functionality of interfacial layers in food emulsions, Annu. Rev. Food Sci. Technol. 9 (2018) 551–587.
[8] J. Velez-Ruiz, G. Barbosa-Canovas, Effects of concentration and temperature on the rheology of concentrated milk, Trans. ASAE 40 (1997) 1113–1118.
[9] D. Kristensen, P.Y. Jensen, F. Madsen, K.S. Birdi, Rheology and surface tension of selected processed dairy fluids: influence of temperature, J. Dairy Sci. 80 (1997) 2282–2290.
[10] A. Bienvenue, R. Jiménez-Flores, H. Singh, Rheological properties of concentrated skim milk: importance of soluble minerals in the changes in viscosity during storage, J. Dairy Sci. 86 (2003) 3813–3821.
[11] L. Wiking, S.B. Gregersen, S.F. Hansen, M. Hammershøj, Heat-induced changes in milk fat and milk fat globules and its derived effects on acid dairy gelation – a review, Int. Dairy J. 127 (2022) 105213.
[12] A. Patist, D. Bates, Ultrasonic innovations in the food industry: from the laboratory to commercial production, Innov. Food Sci. Emerg. Technol. 9 (2008) 147–154.
[13] Y. Sun, X. Yu, M. Hussain, X. Li, L. Liu, Y. Liu, S. Ma, K.J.E. Kouame, C. Li, Y. Leng, S. Jiang, Influence of milk fat globule membrane and milk protein concentrate treated by ultrasound on the structural and emulsifying stability of mimicking human fat emulsions, Ultrason. Sonochem. 82 (2022) 105881.

[14] Y. Liu, S. Boeren, L. Zhang, P. Zhou, K. Hettinga, Ultrasonication retains more milk fat globule membrane proteins compared to equivalent shear-homogenization, Innov. Food Sci. Emerg. Technol. 70 (2021) 102703.
[15] Y. Sun, Y.H. Roos, S. Miao, Comparative study of interfacial properties and thermal behaviour of milk fat globules and membrane prepared from ultrasonicated bovine milk, Ultrason. Sonochem. 102 (2024) 106755.
[16] Q. Ren, F. Guo, F. Teng, Y. Ma, A novel approach for the reconstitution of bovine milk fat globules with different-melting-temperature triacylglycerol cores, Food Chem. 345 (2021) 128563.
[17] Y. Sun, Y.H. Roos, S. Miao, Changes in milk fat globules and membrane proteins prepared from ph-adjusted bovine raw milk, Foods 11 (2022) 4107.
[18] H. Randhahn, Flow properties of milk and milk concentrates, Milchwissenschaft 28 (1973) 620–628.
[19] M. Yerramilli, S. Ghosh, Long-term stability of sodium caseinate-stabilized nanoemulsions, J. Food Sci. Technol. 54 (2017) 82–92.
[20] A. Jukkola, R. Partanen, O.J. Rojas, A. Heino, Effect of heat treatment and pH on the efficiency of micro-diafiltration for the separation of native fat globules from cream in butter production, J. Membr. Sci. 548 (2018) 99–107.
[21] M.K. Grewal, J. Chandrapala, O. Donkor, V. Apostolopoulos, L. Stojanovska, T. Vasiljevic, Fourier transform infrared spectroscopy analysis of physicochemical changes in UHT milk during accelerated storage, Int. Dairy J. 66 (2017) 99–107.
[22] J. Vongsvivut, P. Heraud, W. Zhang, J.A. Kralovec, D. McNaughton, C.J. Barrow, Quantitative determination of fatty acid compositions in micro-encapsulated fish-oil supplements using Fourier transform infrared (FTIR) spectroscopy, Food Chem. 135 (2012) 603–609.
[23] A. Kher, P. Udabage, I. McKinnon, D. McNaughton, M.A. Augustin, FTIR investigation of spray-dried milk protein concentrate powders, Vib. Spectrosc. 44 (2007) 375–381.
[24] Q. Zhou, S.Q. Sun, L. Yu, C.-H. Xu, I. Noda, X.-R. Zhang, Sequential changes of main components in different kinds of milk powders using two-dimensional infrared correlation analysis, J. Mol. Struct. 799 (2006) 77–84.
[25] E. Dufour, A. Riaublanc, Potentiality of spectroscopic methods for the characterisation of dairy products. I. Front-face fluorescence study of raw, heated and homogenised milks, Le Lait 77 (1997) 657–670.
[26] C. Grelet, J.A. Fernandez Pierna, P. Dardenne, V. Baeten, F. Dehareng, Standardization of milk mid-infrared spectra from a European dairy network, J. Dairy Sci. 98 (2015) 2150–2160.
[27] R. Gebhardt, N. Takeda, U. Kulozik, W. Doster, Structure and stabilizing interactions of casein micelles probed by high-pressure light scattering and FTIR, J. Phys. Chem. b. 115 (2011) 2349–2359.
[28] L. Zhao, M. Du, X. Mao, Change in interfacial properties of milk fat globules by homogenization and thermal processing plays a key role in their in vitro gastrointestinal digestion, Food Hydrocoll. 96 (2019) 331–342.
[29] N. Lu, J. Wang, Z. Chen, X. Zhang, C. Chen, S. Wang, The effect of adding phospholipids before homogenization on the properties of milk fat globules, Lwt 146 (2021) 111659.
[30] S.F. Hansen, S.D. Nielsen, J.T. Rasmusen, L.B. Larsen, L. Wiking, Disulfide bond formation is not crucial for the heat-induced interaction between beta-lactoglobulin and milk fat globule membrane proteins, J. Dairy Sci. 103 (2020) 5874–5881.
[31] V.L. Spitsberg, E. Matitashvili, R.C. Gorewit, Association and coexpression of fatty-acid-binding protein and glycoprotein CD36 in the bovine mammary gland, Eur. J. Biochem. 230 (1995) 872–878.
[32] J.A. Peterson, C.D. Scallan, R.L. Ceriani, M. Hamosh, Structural and functional aspects of three major glycoproteins of the human milk fat globule membrane, Bioactive Components of Human Milk (2001) 179–187.
[33] L.R. Banghart, C.W. Chamberlain, J. Velarde, I.V. Korobko, S.L. Ogg, L.J. Jack, V. N. Vakharia, I.H. Mather, Butyrophilin is expressed in mammary epithelial cells from a single-sized messenger RNA as a type I membrane glycoprotein, J. Biol. Chem. 273 (1998) 4171–4179.
[34] M. Ayyash, A. Abdalla, B. Abu-Jdayil, T. Huppertz, R. Bhaskaracharya, S. Al-Mardeai, A. Mairpady, A. Ranasinghe, A. Al-Nabulsi, Rheological properties of fermented milk from heated and high pressure-treated camel milk and bovine milk, Lwt 156 (2022).
[35] I. Kieferle, K. Hiller, U. Kulozik, N. Germann, Rheological properties of fresh and reconstituted milk protein concentrates under standard and processing conditions, J. Colloid Interface Sci. 537 (2019) 458–464.
[36] N. Develi Isikli, M.N. Donmez, N. Kozan, E. Karababa, Rheological properties of salep powder-milk mixture, J. Food Sci. Technol. 52 (2015) 6556–6564.
[37] Y. Lin, H. Du, Y. Roos, S. Miao, Transglutaminase crosslinked fish gelatins for emulsion stabilization: from conventional to Pickering emulsions, Food Hydrocoll. 144 (2023).
[38] N. Ahn, J.H. Park, C. Chai, J.Y. Imm, The interaction of milk sphingomyelin and proteins on stability and microstructure of dairy emulsions, J. Dairy Sci. 105 (2022) 3832–3845.
[39] I. Dammak, P.J.d.A. Sobral, Effect of different biopolymers on the stability of hesperidin-encapsulating O/W emulsions, J. Food Eng. 237 (2018) 33–43.
[40] S.J. Lee, J.W. Sherbon, Chemical changes in bovine milk fat globule membrane caused by heat treatment and homogenization of whole milk, J. Dairy Res. 69 (2002) 555–567.